

AN OPTIMAL SCENARIO OF LAND USE AND LAND COVER
ALLOCATION TO MINIMIZE SEDIMENT AND NUTRIENT EXPORT,
UPPER ING WATERSHED, PHAYAO PROVINCE



A Thesis Submitted in Partial Fulfillment of the Requirements for the
Degree of Doctor of Philosophy in Geoinformatics
Suranaree University of Technology
Academic Year 2021

ภาพเหตุการณ์การจัดสรรการใช้ประโยชน์ที่ดินและสิ่งปกคลุมดินที่เหมาะสม
เพื่อลดการส่งออกตะกอนและธาตุอาหาร ลุ่มน้ำอิงตอนบน จังหวัดพะเยา



นางสาวจิราพร กุลสุนทรรัตน์

วิทยานิพนธ์นี้เป็นส่วนหนึ่งของการศึกษาตามหลักสูตรปริญญาวิทยาศาสตรดุษฎีบัณฑิต

สาขาวิชาภูมิสารสนเทศ

มหาวิทยาลัยเทคโนโลยีสุรนารี

ปีการศึกษา 2564

AN OPTIMAL SCENARIO OF LAND USE AND LAND COVER ALLOCATION
TO MINIMIZE SEDIMENT AND NUTRIENT EXPORT,
UPPER ING WATERSHED, PHAYAO PROVINCE

Suranaree University of Technology has approved this thesis submitted in partial fulfillment of the requirements for the Degree of Doctor of Philosophy.

Thesis Examining Committee

Sura Au

(Assoc. Prof. Dr. Sura Pattanakiat)

Chairperson

Suwit Ong.

(Assoc. Prof. Dr. Suwit Ongsomwang)

Member (Thesis Advisor)

S. Dasananda

(Assoc. Prof. Dr. Songkot Dasananda)

Member

Pantip Riyatadsananon

(Asst. Prof. Dr. Pantip Riyatadsananon)

Member

Tanakorn Sritarapipat

(Dr. Tanakorn Sritarapipat)

Member

Chatchai Jothityang

(Assoc. Prof. Dr. Chatchai Jothityangkoon)

Vice Rector for Academic Affairs

and Quality Assurance

Santi Maensiri

(Prof. Dr. Santi Maensiri)

Dean of Institute of Science

จิราพร กุศลสุนทรรัตน์ : ภาพเหตุการณ์การจัดสรรการใช้ประโยชน์ที่ดินและสิ่งปกคลุมดินที่เหมาะสมเพื่อลดการส่งออกตะกอนและธาตุอาหาร ลุ่มน้ำอิงตอนบน จังหวัดพะเยา (AN OPTIMAL SCENARIO OF LAND USE AND LAND COVER ALLOCATION TO MINIMIZE SEDIMENT AND NUTRIENT EXPORT, UPPER ING WATERSHED, PHAYAO PROVINCE)
อาจารย์ที่ปรึกษา : รองศาสตราจารย์ ดร.สุวิทย์ อ่องสมหวัง, 350 หน้า.

คำสำคัญ: การจัดสรรการใช้ประโยชน์ที่ดินและสิ่งปกคลุมดิน/การส่งออกตะกอนและธาตุอาหาร/
แบบจำลอง CLUE-S/ แบบจำลอง InVEST/ ลุ่มน้ำอิงตอนบน

กว๊านพะเยาเป็นแหล่งน้ำจืดขนาดใหญ่ที่สุดในภาคเหนือและถูกจัดให้เป็นพื้นที่ชุ่มน้ำที่มีความสำคัญระดับนานาชาติ กว๊านพะเยายังให้บริการทางระบบนิเวศต่างๆ รวมทั้ง การประปาเพื่อ การบริโภคในครัวเรือน การเกษตรและนันทนาการ อย่างไรก็ตาม กิจกรรมของมนุษย์และการเปลี่ยนแปลงการใช้ประโยชน์ที่ดินได้ส่งผลกระทบต่อคุณภาพน้ำในกว๊าน เนื่องจากปริมาณตะกอนที่สูงขึ้นและการเกิดปรากฏการณ์ยูโทรฟิเคชัน ฉะนั้น เป้าหมายการวิจัยในครั้งนี้คือ เพื่อระบุภาพ เหตุการณ์การ จัดสรรการใช้ประโยชน์ที่ดินและสิ่งปกคลุมดินที่เหมาะสมเพื่อลดการส่งออกตะกอน และธาตุอาหารสู่กว๊านให้น้อยที่สุด วัตถุประสงค์ของการวิจัยคือ (1) เพื่อจำแนกการใช้ประโยชน์ที่ดิน และสิ่งปกคลุมดินในปี พ.ศ. 2552 และ 2562 (2) เพื่อประเมินความต้องการที่ดินและคาดการณ์การใช้ประโยชน์ที่ดินและสิ่งปกคลุมดินของสามภาพเหตุการณ์ ในระหว่างปี พ.ศ. 2563 ถึง 2572 (3) เพื่อประมาณค่าการส่งออกตะกอนและธาตุอาหารของการใช้ประโยชน์ที่ดินและสิ่งปกคลุมดินจริงในปี พ.ศ. 2562 และการใช้ประโยชน์ที่ดินและสิ่งปกคลุมดินที่คาดการณ์ได้ของสามภาพเหตุการณ์ และ (4) เพื่อระบุภาพเหตุการณ์การจัดสรรการใช้ประโยชน์ที่ดินและสิ่งปกคลุมดินที่เหมาะสมเพื่อลดการ ส่งออกตะกอนและธาตุอาหารให้น้อยที่สุด การศึกษาในครั้งนี้เริ่มด้วยการประเมินสถานภาพและการ เปลี่ยนแปลงโดยอาศัยข้อมูลการใช้ประโยชน์ที่ดินและสิ่งปกคลุมดินในปี พ.ศ. 2552 และ 2562 ที่ได้ จากการจำแนกข้อมูลภาพถ่ายจากดาวเทียม Landsat ด้วยขั้นตอนวิธีซัพพอร์ตเวกเตอร์แมชชีน (SVM) จากนั้น ทำการประมาณค่าความต้องการที่ดินของสามภาพเหตุการณ์ ในระหว่างปี พ.ศ. 2563 ถึง 2572 โดยพิจารณาจากคุณลักษณะเฉพาะของแต่ละภาพเหตุการณ์ และนำข้อมูลที่ได้ไปใช้ คาดการณ์การเปลี่ยนแปลงการใช้ประโยชน์ที่ดินและสิ่งปกคลุมดินด้วยแบบจำลอง CLUE-S สำหรับการเปรียบเทียบแบบจำลอง SDR และ NDR จะนำพารามิเตอร์ที่ได้คัดเลือกสำหรับการส่งออกตะกอน และธาตุอาหารของชุดซอฟต์แวร์ InVEST ไปทำการเปรียบเทียบอย่างเป็นระบบเพื่อระบุค่าของ พารามิเตอร์ท้องถิ่นที่เหมาะสมที่สุดของแต่ละแบบจำลองโดยอาศัยการพิจารณาเปอร์เซ็นต์ความเอน เอียงของการประมาณ (PBIAS) และค่าสัมประสิทธิ์การตัดสินใจ (R^2) ในขั้นตอนสุดท้าย นำข้อมูลการ

ใช้ประโยชน์ที่ดินและสิ่งปกคลุมดินจริงในปี พ.ศ. 2562 และข้อมูลการใช้ประโยชน์ที่ดินและสิ่งปกคลุมดินที่ได้จากการคาดการณ์ของสามภาพเหตุการณ์ไปใช้ประมาณค่าการส่งออกตะกอนและธาตุอาหาร สำหรับการระบุการจัดสรรการใช้ประโยชน์ที่ดินและสิ่งปกคลุมดินที่เหมาะสมเพื่อลดการส่งออกตะกอนและธาตุอาหารให้น้อยที่สุดด้วยดัชนีการเปลี่ยนแปลงการให้บริการทางระบบนิเวศ

จากผลการศึกษาที่ได้รับ พบว่า ประเภทการใช้ประโยชน์ที่ดินและสิ่งปกคลุมดินที่เพิ่มขึ้นอย่างมีนัยสำคัญในระหว่างปี พ.ศ. 2552 ถึง 2562 ได้แก่ ไม้ยืนต้นและสวนผลไม้ ยางพาราและทุ่งหญ้า ประเภทของการใช้ประโยชน์ที่ดินและสิ่งปกคลุมดินที่ลดลงอย่างมีนัยสำคัญ ได้แก่ พื้นที่ป่าและนาข้าว ในขณะเดียวกัน ข้อมูลความต้องการที่ดินที่ได้จากประมาณและการใช้ประโยชน์ที่ดินและสิ่งปกคลุมดินที่ได้จากการคาดการณ์ของสามภาพเหตุการณ์ให้ผลลัพธ์ที่สมเหตุสมผลตามที่คาดหวัง โดยเฉพาะอย่างยิ่ง ภาพเหตุการณ์ที่ 2 ที่ใช้การโปรแกรมเชิงเส้น (LP) เพื่อคำนวณความต้องการที่ดินสำหรับเพิ่มมูลค่าการให้บริการทางระบบนิเวศให้มากที่สุด ค่า PBIAS และ R^2 สำหรับการเปรียบเทียบแบบจำลองมีค่าระหว่าง พอใช้ ถึง ดีมาก สำหรับการประมาณการส่งออกตะกอน ไนโตรเจน และฟอสฟอรัส จากผลการประมาณค่าการส่งออกตะกอนและธาตุอาหารของการใช้ประโยชน์ที่ดินและสิ่งปกคลุมดินจริงในปี พ.ศ. 2562 และการใช้ประโยชน์ที่ดินและสิ่งปกคลุมดินที่คาดการณ์ได้ของสามภาพเหตุการณ์ในระหว่างปี พ.ศ. 2563 ถึง 2572 พบว่า ภาพเหตุการณ์ที่ 2 (การเพิ่มมูลค่าการให้บริการทางระบบนิเวศสูงสุด) ส่งออกตะกอน ไนโตรเจน และฟอสฟอรัสน้อยที่สุด โดยมีค่าเฉลี่ยเท่ากับ 37,677.19 ตัน 196,135.56 กิโลกรัม และ 43,316.82 กิโลกรัม และให้ค่าดัชนีการเปลี่ยนแปลงการให้บริการทางระบบนิเวศเฉลี่ยต่ำที่สุด (0.1575) ในสามภาพเหตุการณ์ ดังนั้น การจัดสรรการใช้ประโยชน์ที่ดินและสิ่งปกคลุมดินของภาพเหตุการณ์ที่ 2 (การเพิ่มมูลค่าการให้บริการทางระบบนิเวศสูงสุด) จึงเป็นการจัดสรรการใช้ประโยชน์ที่ดินและสิ่งปกคลุมดินที่เหมาะสมสำหรับการลดการส่งออกตะกอนและธาตุอาหารไปสู่กัวนพะเยาให้น้อยที่สุด ผลการศึกษาที่ได้รับนี้สามารถใช้เป็นสารสนเทศสำคัญเพื่อลดการส่งออกตะกอนและธาตุอาหารให้น้อยที่สุดต่อนักวางแผนการใช้ที่ดิน ผู้จัดการที่ดิน และผู้มีอำนาจตัดสินใจ

จากผลการศึกษาที่ได้รับทั้งหมด สามารถสรุปได้ว่า การบูรณาการการรับรู้จากระยะไกลร่วมกับวิธีการจำแนกชั้นสูง ข้อมูลระบบสารสนเทศทางภูมิศาสตร์ร่วมกับการโปรแกรมเชิงเส้น และแบบจำลองเชิงพื้นที่ขั้นสูง สามารถนำมาใช้เป็นเครื่องมือเพื่อระบุภาพเหตุการณ์การจัดสรรการใช้ประโยชน์ที่ดินและสิ่งปกคลุมดินที่เหมาะสมเพื่อลดการส่งออกตะกอนและธาตุอาหารให้น้อยที่สุดได้อย่างมีประสิทธิภาพ

สาขาวิชาภูมิสารสนเทศ

ปีการศึกษา 2564

ลายมือชื่อนักศึกษา



ลายมือชื่ออาจารย์ที่ปรึกษา



JIRAPORN KULSOONTORN RAT : AN OPTIMAL SCENARIO OF LAND USE AND LAND COVER ALLOCATION TO MINIMIZE SEDIMENT AND NUTRIENT EXPORT, UPPER ING WATERSHED, PHAYAO PROVINCE. THESIS ADVISOR : ASSOC. PROF. SUWIT ONGSOMWANG, Dr. rer. Nat. 350 PP.

Keyword: LAND USE AND LAND COVER ALLOCATION/ SEDIMENT AND NUTRIENT EXPORT/ CLUE-S MODEL/ INVEST MODEL/ UPPER ING WATERSHED

Kwan Phayao Lake is the largest freshwater in the Northern region and is classified in the wetlands of international importance. It also provides various ecosystem services, including water supply for household consumption, agriculture, and recreation. However, the human activity and land use change have affected the lake's water quality due to high sediment load and eutrophication. Therefore, this research aims to identify the optimal LULC allocation scenario to minimize sediment and nutrient export into the lake. The research objectives were (1) to classify LULC data in 2009 and 2019, (2) to estimate the land requirement and predict LULC of three scenarios between 2020 and 2029, (3) to estimate sediment and nutrient export of actual LULC in 2019 and predicted LULC of three scenarios, and (4) to identify optimum LULC allocation to minimize sediment and nutrient export. This study first assessed LULC status and change based on classified LULC data in 2009 and 2019 from Landsat images using a support vector machine. Later, land requirements of three scenarios between 2020 and 2029 were estimated based on their characteristics and applied to predict LULC change by the CLUE-S model. For the calibration process of the SDR and NDR model, the selected parameters for sediment and nutrient export under the InVEST software suite were systematically calibrated to identify each model's optimum local parameters using the percent bias (PBIAS) and the coefficient of determination (R^2). Finally, actual LULC data in 2019 and predictive LULC data of three scenarios were used to estimate sediment and nutrient export for identifying suitable LULC allocation to minimize sediment and nutrient export by Ecosystems Services Change Index (ESCI).

As a result, the significantly increasing LULC types from 2009 to 2019 were perennial trees and orchards, para rubber, and rangeland. The critical decreasing LULC

types were forest land and paddy fields. Meanwhile, the derived land requirement and predictive LULC data of three scenarios provided reasonable results as expected, particularly Scenario II, which adopts the linear programming to calculate the land requirement for maximizing ecosystem services values. The PBIAS and R^2 values for the model calibration were between satisfactory and very good for sediment, nitrogen, and phosphorus export estimation. According to sediment and nutrient export estimation of actual LULC in 2019 and predicted LULC of three scenarios between 2020 and 2029, Scenario II (Maximization ecosystem service values) created the lowest yield of sediment, nitrogen, and phosphorus exports, with average values of 37,677.19 tons, 196,135.56 kg., and 43,316.82 kg. and provided the lowest average ESCI value (0.1575) among three scenarios. Thus, LULC allocation of Scenario II (Maximization ecosystem service value) was chosen as optimum LULC allocation for minimizing sediment and nutrient exports into Kwan Phayao Lake. These results can serve as crucial information to minimize sediment and nutrient loads for land use planners, land managers, and decision-makers.

In conclusion, integrating remote sensing with advanced classification methods, GIS data with linear programming, and advanced geospatial models can be used as an efficient tool to identify an optimum LULC allocation scenario to minimize sediment and nutrient export.

School of Geoinformatics
Academic Year 2021

Student's Signature Jiraporn k.
Advisor's Signature Savit Ong.

ACKNOWLEDGEMENTS

I would like to express my sincere gratitude to my advisor, Assoc. Prof. Dr. Suwit Ongsomwang, for his kindness, invaluable help, advice, constant encouragement throughout my study and thesis research, as well as many other life-living, mental suggestions. I would not have achieved this far, and this thesis would not have been completed without the support I have always received from him.

I would like to thank the chairman and committee members of this thesis defense: Assoc. Prof. Dr. Sura Pattanakiat, Asst. Prof. Dr. Pantip Piyatadsananon, Assoc. Prof. Dr. Songkot Dasananda, Dr. Tanakorn Sritarapipat, Dr. Siripon Kamontam and, Dr. Nobphadon Suksangpanya for all valuable suggestions and critical comments during the proposal and thesis defense.

I would like to special thank the University of Phayao for the opportunity to continue my education and the Suranaree University of Technology for providing a scholarship.

In addition, I am grateful to my colleagues for all their support and all of my friends in the School of Geoinformatics, especially Mr. Athiwat Phinyoyang, Mr. Nattapong Puangkaew, Miss Juthamas Noina, and Miss Wilawan Prasomsup, for all their help and encouragement throughout tough times.

Last but not least, I most gratefully acknowledge my family, who always believes in me. Thank you for all their love, support, and encouragement.

Jiraporn Kulsoontornrat

CONTENTS

	Page
ABSTRACT IN THAI.....	I
ABSTRACT IN ENGLISH.....	III
ACKNOWLEDGEMENTS	V
CONTENTS.....	VI
LIST OF TABLES	X
LIST OF FIGURES	XXI
LIST OF ABBREVIATIONS	XXX
CHAPTER	
I INTRODUCTION.....	1
1.1 Background problems and significance of the study.....	1
1.2 Research objectives	4
1.3 Scope and limitations of the study	5
1.3.1 Scope of the study	5
1.3.2 Limitation of the study	6
1.4 Study area.....	7
1.5 Benefit of the study.....	10
II BASIC CONCEPTS AND LITERATURE REVIEWS.....	11
2.1 LULC classification with support vector machine (SVM).....	11
2.1.1 Application of LULC classification with SVM.....	15
2.2 CLUE-S model	17
2.2.1 Application of the CLUE-S model.....	21
2.3 Linear programming	23
2.3.1 Application of Linear programming.....	25
2.4 Sediment Delivery Ratio model of InVEST software suite	27
2.4.1 Application of Sediment Delivery Ratio model of InVEST software.....	31

CONTENTS (Continued)

	Page
2.5 Nutrient Delivery Ratio model of InVEST software suite.....	32
2.5.1 Application of Nutrient Delivery Ratio model of InVEST software	37
III RESEARCH PROCEDURES.....	40
3.1 Data collection and preparation	40
3.2 Research Methodology.....	42
3.3.1 LULC evaluation and its change	42
3.3.2 Land requirement estimation of three different scenarios.....	47
3.3.3 LULC prediction of three different scenarios.....	52
3.3.4 Ecosystem service assessment: sediment and nutrient export	53
3.3.5 Optimum LULC allocation to minimize sediment and nutrient export.....	70
IV LAND USE AND LAND COVER CLASSIFICATION AND CHANGE DETECTION....	72
4.1 LULC classification in 2009.....	72
4.2 LULC classification in 2019	84
4.3 LULC change between 2009 and 2019	97
V LAND REQUIREMENT ESTIMATION AND LAND USE AND LAND COVER PREDICTION OF THREE DIFFERENT SCENARIOS	110
5.1 Driving force on LULC change.....	110
5.1.1 Driving force for urban and built-up area allocation.....	116
5.1.2 Driving force for paddy field allocation.....	116
5.1.3 Driving force for field crop allocation.....	117
5.1.4 Driving force for para rubber allocation	118
5.1.5 Driving force for perennial tree and orchard allocation	119
5.1.6 Driving force for forest land allocation.....	119
5.1.7 Driving force for water body allocation.....	120
5.1.8 Driving force for rangeland allocation	121
5.1.9 Driving force for wetland allocation.....	122
5.1.10 Driving force for miscellaneous land allocation.....	122

CONTENTS (Continued)

	Page
5.2 Local parameter of CLUE-S model for LULC prediction.....	124
5.3 Land requirement estimation and LULC prediction of Scenario I: Trend of LULC evolution	129
5.4 Land requirement estimation and LULC prediction of Scenario II: Maximization of ecosystem service values	139
5.5 Land requirement estimation and LULC prediction of Scenario III: Economic crop zonation.....	154
VI SEDIMENT EXPORT ESTIMATION OF THREE DIFFERENT SCENARIOS	169
6.1 Calibration of sediment delivery ratio model	169
6.2 Validation of sediment delivery ratio model.....	176
6.3 Sediment export estimation of actual LULC in 2019.....	182
6.4 Sediment export estimation of predictive LULC of Scenario I.....	186
6.5 Sediment export estimation of predictive LULC of Scenario II.....	198
6.6 Sediment export estimation of predictive LULC of Scenario III.....	211
6.7. Comparison of sediment export estimation among three different scenarios.....	223
VII NUTRIENT EXPORT ESTIMATION OF THREE DIFFERENT SCENARIOS	225
7.1 Calibration of nutrient delivery ratio model.....	225
7.2 Validation of nutrient delivery ratio model	235
7.3 Nutrient export estimation of actual LULC in 2019	244
7.4 Nutrient export estimation of predictive LULC of Scenario I	248
7.5 Nutrient export estimation of predictive LULC of Scenario II.	267
7.6 Nutrient export estimation of predictive LULC of Scenario III.	285
7.7 Comparison of nutrient export estimation among three different scenarios.....	303

CONTENTS (Continued)

	Page
VIII SUITABLE LAND USE AND LAND COVER ALLOCATION SCENARIOS TO MINIMIZE SEDIMENT AND NUTRIENT EXPORTS	306
8.1 Suitable LULC allocation scenario to minimize sediment export.....	307
8.1.1 Ecosystem service change on sediment export of Scenario I	307
8.1.2 Ecosystem service change on sediment export of Scenario II	309
8.1.3 Ecosystem service change on sediment export of Scenario III	311
8.1.4 Suitable LULC allocation scenario to minimize sediment export	313
8.2 Suitable LULC allocation scenario to minimize nutrient export.....	314
8.2.1 Ecosystem service change on Nutrient export of Scenario I	314
8.2.2 Ecosystem service change on nutrient export of Scenario II.....	318
8.2.3 Ecosystem service change on nutrient export of Scenario III.....	321
8.2.4 Suitable LULC allocation scenario to minimize nutrient export.....	324
8.3 Suitable LULC allocation scenario to minimize sediment and nutrient export	327
IX CONCLUSION AND RECOMMENDATIONS.....	330
9.1 Conclusion.....	330
9.1.1 Land use and land cover evaluation and its change	330
9.1.2 Land requirement estimation of three different scenarios.....	331
9.1.3 Land use and land cover prediction of three different scenarios.....	331
9.1.4 Ecosystem service assessment: sediment and nutrient export	333
9.1.5 Land use and land cover allocation scenario to minimize sediment and nutrient export	336
9.2 Recommendations.....	337
REFERENCES	338
CURRICULUM VITAE	350

LIST OF TABLES

Table	Page
1.1 The existing problem relates to Kwan Phayao Lake	4
3.1 List of data collection and preparation for analysis and modeling in the study	40
3.2 Description of LULC classification system	46
3.3 Coefficient value for different LULC types for ESV estimation.	48
3.4 The economic crop zonation by LDD.....	49
3.5 Basic statistics of rainfall erosivity factor between 2011 and 2019	59
3.6 Soil series and soil erodibility factor values.....	59
3.7 Geology unit and soil erodibility factor values.....	60
3.8 The values of the C and P factors corresponding to each LULC class in a biophysical table	60
3.9 Criteria for model performance	62
3.10 Basic statistics of annual rainfall between 2011 and 2019	63
3.11 Biophysical table containing data related to nitrogen, phosphorus and requires values of nutrients corresponding to each LULC class.....	66
4.1 Number of training sample points for LULC classification in 2009 using the SVM algorithm	76
4.2 Area and percentage of LULC data in 2009	79
4.3 Error matrix and accuracy assessment of LULC map in 2009	81
4.4 Characteristic of training sample points for LULC classification with the SVM algorithm	88
4.5 Number of training sample points for LULC classification in 2019 using the SVM algorithm	90
4.6 Area and percentage of LULC data in 2019	93

LIST OF TABLES (Continued)

Table	Page
4.7 Error matrix and accuracy assessment of LULC map in 2019	95
4.8 Comparison of LULC change between 2009 and 2019	97
4.9 The transitional matrix of LULC change between 2009 and 2019	99
5.1 Statistical data of multicollinearity test of driving factors effect on LULC type.....	114
5.2 Multiple linear equations of each LULC type location preference and AUC value by binary logistic regression analysis	115
5.3 Conversion matrix of possible LULC change between 2019 and 2029 for Scenario I: Trend of LULC evolution.....	125
5.4 Conversion matrix of possible LULC change between 2019 and 2029 for Scenario II: Maximization ecosystem service values.....	126
5.5 Conversion matrix of possible LULC change between 2019 and 2029 for Scenario III: Economic crop zonation.....	127
5.6 Transition probability matrix of LULC change between 2009 and 2019 by the Markov Chain model.....	128
5.7 Transition area matrix of LULC change between 2019 and 2029 from Markov Chain model.....	129
5.8 Annual land requirement of Scenario I (Trend of LULC evolution) by LULC type.....	129
5.9 Area of predicted LULC of Scenario I: Trend of LULC evolution between 2020 and 2029.....	133
5.10 Percentage of predicted LULC of Scenario I: Trend of LULC evolution between 2020 and 2029	134
5.11 Transition LULC change matrix between 2019 (Base year) and 2029 of Scenario I: Trend of LULC evolution.....	138
5.12 The constraint to maximize ecosystem service values of Scenario-II in a table form	143

LIST OF TABLES (Continued)

Table	Page
5.13 Allocated LULC area to maximize ecosystem service of Scenario II and annual change rate between 2019 and 2029	144
5.14 Annual land requirement of Scenario II (Maximization of ecosystem service values) for each LULC type	144
5.15 Area of predicted LULC of Scenario II: Maximization ecosystem service values between 2020 and 2029	149
5.16 Percentage of predicted LULC of Scenario II: Maximization ecosystem service values between 2020 and 2029.....	150
5.17 Transition matrix of LULC change between 2019 and 2029 of Scenario II: Maximization ecosystem service values	153
5.18 Annual land requirement for Scenario III: Economic crop zonation by each LULC type.....	155
5.19 Area of predicted LULC of Scenario III: Economic crop zonation between 2020 and 2029	160
5.20 Percentage of predicted LULC of Scenario III: Economic crop zonation between 2020 and 2029	161
5.21 Transition matrix of LULC change between 2019 and 2029 of Scenario III: Economic crop zonation	164
5.22 Comparison area of predicted LULC in three different scenarios and its change.....	166
6.1 Basic information of observed TSS data of PCD for model calibration.....	171
6.2 Sediment delivery ratio model parameters for model calibration	173
6.3 Observed and estimated sediment export and statistical measurement at default, initial and maximum value stages.....	174
6.4 Comparison of the observed and estimated sediment export with a statistical measurement under the calibration period	175
6.5 Basic information of observed TSS data of PCD for model validation.....	177

LIST OF TABLES (Continued)

Table	Page
6.6 Comparison of the observed and estimated sediment export with a statistical measurement under the validation period	179
6.7 Summary data on soil erosion, sediment retention, sediment deposition, and export of actual LULC data in 2019.....	183
6.8 Contribution of soil erosion, sediment retention, sediment deposition, and sediment export by LULC classes in 2019	184
6.9 Estimation of soil erosion, sediment retention, sediment deposition, and sediment export between 2020 and 2029 under Scenario I: Trend of LULC evolution.....	187
6.10 Basic statistics of predictive rainfall erosivity factor between 2020 and 2029	188
6.11 Contribution of soil erosion, sediment retention, sediment deposition, and sediment export by LULC classes in 2020 under Scenario I	189
6.12 Contribution of soil erosion, sediment retention, sediment deposition, and sediment export by LULC classes in 2021 under Scenario I	189
6.13 Contribution of soil erosion, sediment retention, sediment deposition, and sediment export by LULC classes in 2022 under Scenario I	190
6.14 Contribution of soil erosion, sediment retention, sediment deposition, and sediment export by LULC classes in 2023 under Scenario I	190
6.15 Contribution of soil erosion, sediment retention, sediment deposition, and sediment export by LULC classes in 2024 under Scenario I	191
6.16 Contribution of soil erosion, sediment retention, sediment deposition, and sediment export by LULC classes in 2025 under Scenario I	191
6.17 Contribution of soil erosion, sediment retention, sediment deposition, and sediment export by LULC classes in 2026 under Scenario I	192
6.18 Contribution of soil erosion, sediment retention, sediment deposition, and sediment export by LULC classes in 2027 under Scenario I	192

LIST OF TABLES (Continued)

Table	Page
6.19 Contribution of soil erosion, sediment retention, sediment deposition, and sediment export by LULC classes in 2028 under Scenario I	193
6.20 Contribution of soil erosion, sediment retention, sediment deposition, and sediment export by LULC classes in 2029 under Scenario I	193
6.21 Estimation of soil erosion, sediment retention, sediment deposition, and sediment export between 2020 and 2029 under Scenario II: Maximization of ecosystem service.....	200
6.22 Contribution of soil erosion, sediment retention, sediment deposition, and sediment export by LULC classes in 2020 under Scenario II	201
6.23 Contribution of soil erosion, sediment retention, sediment deposition, and sediment export by LULC classes in 2021 under Scenario II	201
6.24 Contribution of soil erosion, sediment retention, sediment deposition, and sediment export by LULC classes in 2022 under Scenario II	202
6.25 Contribution of soil erosion, sediment retention, sediment deposition, and sediment export by LULC classes in 2023 under Scenario II	202
6.26 Contribution of soil erosion, sediment retention, sediment deposition, and sediment export by LULC classes in 2024 under Scenario II	203
6.27 Contribution of soil erosion, sediment retention, sediment deposition, and sediment export by LULC classes in 2025 under Scenario II	203
6.28 Contribution of soil erosion, sediment retention, sediment deposition, and sediment export by LULC classes in 2026 under Scenario II	204
6.29 Contribution of soil erosion, sediment retention, sediment deposition, and sediment export by LULC classes in 2027 under Scenario II	204
6.30 Contribution of soil erosion, sediment retention, sediment deposition, and sediment export by LULC classes in 2028 under Scenario II	205
6.31 Contribution of soil erosion, sediment retention, sediment deposition, and sediment export by LULC classes in 2029 under Scenario II	205

LIST OF TABLES (Continued)

Table	Page
6.32 Estimation of soil erosion, sediment retention, sediment deposition, and sediment export between 2020 and 2029 under Scenario III: Economic crop zonation.....	212
6.33 Contribution of soil erosion, sediment retention, sediment deposition, and sediment export by LULC classes in 2020 under Scenario III.....	213
6.34 Contribution of soil erosion, sediment retention, sediment deposition, and sediment export by LULC classes in 2021 under Scenario III.....	213
6.35 Contribution of soil erosion, sediment retention, sediment deposition, and sediment export by LULC classes in 2022 under Scenario III.....	214
6.36 Contribution of soil erosion, sediment retention, sediment deposition, and sediment export by LULC classes in 2023 under Scenario III.....	214
6.37 Contribution of soil erosion, sediment retention, sediment deposition, and sediment export by LULC classes in 2024 under Scenario III.....	215
6.38 Contribution of soil erosion, sediment retention, sediment deposition, and sediment export by LULC classes in 2025 under Scenario III.....	215
6.39 Contribution of soil erosion, sediment retention, sediment deposition, and sediment export by LULC classes in 2026 under Scenario III.....	216
6.40 Contribution of soil erosion, sediment retention, sediment deposition, and sediment export by LULC classes in 2027 under Scenario III.....	216
6.41 Contribution of soil erosion, sediment retention, sediment deposition, and sediment export by LULC classes in 2028 under Scenario III.....	217
6.42 Contribution of soil erosion, sediment retention, sediment deposition, and sediment export by LULC classes in 2029 under Scenario III.....	217
6.43 Average sediment export (tons/km ²) between 2020 and 2029 of three different scenarios	223
7.1 Basic information of observed total nitrogen (TN) data of PCD for model calibration.....	227

LIST OF TABLES (Continued)

Table	Page
7.2 Basic information of observed total phosphorus (TP) data of PCD for model calibration.....	228
7.3 Nutrient delivery ratio model parameters for model calibration.....	229
7.4 Adjusted parameter of NDR model for nitrogen and phosphorus calibration.....	230
7.5 Observed and estimated TN export and statistical measurement at default, initial and maximum value stages.....	231
7.6 Observed and estimated TP export and statistical measurement at default, initial and maximum value stages.....	232
7.7 Comparison of the observed and estimated nitrogen export with a statistical measurement under the calibration period	233
7.8 Comparison of the observed and estimated phosphorus export with a statistical measurement under the calibration period	234
7.9 Basic information of observed total nitrogen (TN) data of PCD for model validation	236
7.10 Basic information of observed total phosphorus (TP) data of PCD for model validation	237
7.11 Comparison of the observed and estimated nitrogen export with a statistical measurement under the validation period	238
7.12 Comparison of the observed and estimated phosphorus export with a statistical measurement under the validation period	239
7.13 Summary data on nitrogen and phosphorus loads of actual LULC in 2019.....	244
7.14 Summary data on nitrogen and phosphorus export of actual LULC in 2019.....	244
7.15 Contribution of nutrient (nitrogen and phosphorus) load and export by LULC classes in 2019.....	246
7.16 Estimation of nitrogen and phosphorus export between 2020 and 2029 under Scenario I.....	248
7.17 Basic statistics of predictive annual rainfall between 2020 and 2029	249

LIST OF TABLES (Continued)

Table	Page
7.18 Contribution of nutrient (nitrogen and phosphorus) load and export by LULC classes in 2020 under Scenario I.....	251
7.19 Contribution of nutrient (nitrogen and phosphorus) load and export by LULC classes in 2021 under Scenario I.....	251
7.20 Contribution of nutrient (nitrogen and phosphorus) load and export by LULC classes in 2022 under Scenario I.....	252
7.21 Contribution of nutrient (nitrogen and phosphorus) load and export by LULC classes in 2023 under Scenario I.....	252
7.22 Contribution of nutrient (nitrogen and phosphorus) load and export by LULC classes in 2024 under Scenario I.....	253
7.23 Contribution of nutrient (nitrogen and phosphorus) load and export by LULC classes in 2025 under Scenario I.....	253
7.24 Contribution of nutrient (nitrogen and phosphorus) load and export by LULC classes in 2026 under Scenario I.....	254
7.25 Contribution of nutrient (nitrogen and phosphorus) load and export by LULC classes in 2027 under Scenario I.....	254
7.26 Contribution of nutrient (nitrogen and phosphorus) load and export by LULC classes in 2028 under Scenario I.....	255
7.27 Contribution of nutrient (nitrogen and phosphorus) load and export by LULC classes in 2029 under Scenario I.....	255
7.28 Estimation of nitrogen and phosphorus export between 2020 and 2029 under Scenario II.....	267
7.29 Contribution of nutrient (nitrogen and phosphorus) load and export by LULC classes in 2020 under Scenario II.....	269
7.30 Contribution of nutrient (nitrogen and phosphorus) load and export by LULC classes in 2021 under Scenario II.....	269
7.31 Contribution of nutrient (nitrogen and phosphorus) load and export by LULC classes in 2022 under Scenario II.....	270

LIST OF TABLES (Continued)

Table	Page
7.32 Contribution of nutrient (nitrogen and phosphorus) load and export by LULC classes in 2023 under Scenario II.....	270
7.33 Contribution of nutrient (nitrogen and phosphorus) load and export by LULC classes in 2024 under Scenario II.....	271
7.34 Contribution of nutrient (nitrogen and phosphorus) load and export by LULC classes in 2025 under Scenario II.....	271
7.35 Contribution of nutrient (nitrogen and phosphorus) load and export by LULC classes in 2026 under Scenario II.....	272
7.36 Contribution of nutrient (nitrogen and phosphorus) load and export by LULC classes in 2027 under Scenario II.....	272
7.37 Contribution of nutrient (nitrogen and phosphorus) load and export by LULC classes in 2028 under Scenario II.....	273
7.38 Contribution of nutrient (nitrogen and phosphorus) load and export by LULC classes in 2029 under Scenario II.....	273
7.39 Estimation of nitrogen and phosphorus export between 2020 and 2029 under Scenario III.....	285
7.40 Contribution of nutrient (nitrogen and phosphorus) load and export by LULC classes in 2020 under Scenario III.....	287
7.41 Contribution of nutrient (nitrogen and phosphorus) load and export by LULC classes in 2021 under Scenario III.....	287
7.42 Contribution of nutrient (nitrogen and phosphorus) load and export by LULC classes in 2022 under Scenario III.....	288
7.43 Contribution of nutrient (nitrogen and phosphorus) load and export by LULC classes in 2023 under Scenario III.....	288
7.44 Contribution of nutrient (nitrogen and phosphorus) load and export by LULC classes in 2024 under Scenario III.....	289
7.45 Contribution of nutrient (nitrogen and phosphorus) load and export by LULC classes in 2025 under Scenario III.....	289

LIST OF TABLES (Continued)

Table	Page
7.46 Contribution of nutrient (nitrogen and phosphorus) load and export by LULC classes in 2026 under Scenario III	290
7.47 Contribution of nutrient (nitrogen and phosphorus) load and export by LULC classes in 2027 under Scenario III	290
7.48 Contribution of nutrient (nitrogen and phosphorus) load and export by LULC classes in 2028 under Scenario III	291
7.49 Contribution of nutrient (nitrogen and phosphorus) load and export by LULC classes in 2029 under Scenario III	291
7.50 Average nitrogen and phosphorus export (kg/km ²) between 2020 and 2029 of three different scenarios	304
8.1 Ecosystem service on sediment export and its ESCI value under Scenario I.....	308
8.2 Ecosystem service on sediment export and its ESCI value under Scenario II.....	310
8.3 Ecosystem service on sediment export and its ESCI value under Scenario III	312
8.4 Sediment export and ESCI value and its average of three different scenarios	313
8.5 Details of t-Test for average ESCI values on sediment export among three different scenarios	314
8.6 Ecosystem service on nitrogen export and its ESCI value under Scenario I.....	316
8.7 Ecosystem service on phosphorus export and its ESCI value under Scenario I	316
8.8 Ecosystem service on nitrogen export and its ESCI value under Scenario II.....	319
8.9 Ecosystem service on phosphorus export and its ESCI value under Scenario II	319
8.10 Ecosystem service on nitrogen export and its ESCI value under Scenario III....	322
8.11 Ecosystem service on phosphorus export and its ESCI value under Scenario III	322
8.12 Nitrogen export and ESCI value and its average of three different scenarios	324
8.13 Phosphorus export and ESCI value and its average of three different scenarios	325

LIST OF TABLES (Continued)

Table	Page
8.14 Details of t-Test for average ESCI values on nitrogen export among three different scenarios	326
8.15 Details of t-Test for average ESCI values on phosphorus export among three different scenarios	326
8.16 Average ESCI values of sediment and nutrient export on ecosystem service among three different scenarios.....	329



LIST OF FIGURES

Figure	Page
1.1 Terrain and location map of the Upper Ing watershed, Mekong Basin	8
1.2 Spatial distribution of LULC by LDD in 2015.....	9
2.1 An example of a separable problem in a 2-dimensional space.....	12
2.2 Mapping of the data sets to the high-dimensional space with a Kernel function	14
2.3 Overview of the information flow in the CLUE-S model.....	18
2.4 Flow chart of the allocation module of the CLUE-S model	21
2.5 Conceptual approach applied in the sediment delivery ratio model.....	28
2.6 Relationship between the connectivity index IC and the SDR.....	30
2.7 Conceptual representation of the NDR model	33
2.8 Conceptual representation of nutrient delivery in the model	34
2.9 Illustration of the calculation of the retention efficiency along a simple flow path	36
3.1 Overview of the research framework	43
3.2 Schematic workflow of LULC evaluation and its change.....	45
3.3 Spatial distribution of economic crop zonation in Upper Ing watershed	50
3.4 Schematic workflow of land demand estimation of three different scenarios	51
3.5 Schematic workflow of LULC Prediction of three different scenarios	52
3.6 Schematic workflow of sediment export estimation	55
3.7 Digital elevation model (DEM) and soil erodibility (K).....	56
3.8 The rainfall erosivity factor for sediment export estimation: Data from 2011 to 2015 for model calibration, data from 2016 to 2018 for model validation, data in 2019 for actual sediment export estimation, and data from 2020 to 2029 for sediment export estimation under three scenarios	56

LIST OF FIGURES (Continued)

Figure	Page
3.9 Schematic workflow of nutrient export estimation.....	65
3.10 The annual rainfall as runoff proxy factor of NRD model: Data from 2011 to 2015 for model calibration, data from 2016 to 2018 for model validation, data in 2019 for actual nutrient export estimation, and data from 2020 to 2029 for nutrient export estimation under three scenarios	67
3.11 Schematic workflow of optimum LULC allocation to minimize sediment and nutrient export.	71
4.1 Surface reflectance and additional bands of Landsat 5 TM imagery	73
4.2 Spatial distribution of training sample points for LULC classification in 2009 using SVM algorithm	77
4.3 Spatial distribution of LULC classification in 2009	78
4.4 Spatial distribution of sampling points on Landsat 5-TM image for thematic accuracy assessment of classified LULC map in 2009.....	80
4.5 Ground photograph of harvested paddy fields (a), harvested field crop (b), and rangeland (c) from a field survey in 2020.....	83
4.6 Ground photograph of perennial trees and orchards nearby forest land from a field survey in 2020	83
4.7 Surface reflectance and additional bands of Landsat 8 OLI imagery	85
4.8 Distribution of training sample points for LULC classification in 2019.....	91
4.9 Spatial distribution of LULC classification in 2019	92
4.10 Spatial distribution of sampling points on Landsat 8-OLI image	94
4.11 Ground photograph of paddy fields (a,b) wetland (c,d) from field survey in 2020.....	96
4.12 Comparison of the annual change rate of LULC type between 2009 and 2019.....	98
4.13 Distribution of LULC change between 2009 and 2019	100

LIST OF FIGURES (Continued)

Figure	Page
4.14 Ground photograph of abandoned paddy field (a and b), perennial tree and orchards plots (c and d), and field crop (e) and perennial trees and orchards (f) in the natural forest from a field survey in 2020	102
4.15 Distribution of increased and unchanged area of perennial trees and orchards between 2009 and 2019	104
4.16 Distribution of increased and unchanged area of para rubber between 2009 and 2019	105
4.17 Distribution of increased and unchanged area of rangeland between 2009 and 2019	106
4.18 Spatial distribution of the decreased and unchanged area of paddy field between 2009 and 2019	107
4.19 Distribution of decreased and unchanged area of forest land between 2009 and 2019.	108
5.1 Driving factors on LULC change: (a) Soil drainage, (b) Distance to stream (m), (c) Distance to water body (m), (d) Distance to village (m), (e) Slope (%), (f) Distance to road (m), (g) Distance to fault (m), and (h) Annual rainfall (mm), (i) Elevation (m), (j) Income per capita at sub-district level (Baht), and (k) Population density at sub-district level (persons per km ²)	111
5.2 Spatial distribution of LULC prediction of Scenario I during 2020 to 2029	130
5.3 Spatial distribution of LULC prediction of Scenario II during 2020 to 2029	146
5.4 Spatial distribution of the economic crop zonation (a) para rubber, (b) perennial trees and orchards, (c) paddy field, and (d) field crop.....	156
5.5 Spatial distribution of LULC prediction of Scenario III during 2020 to 2029.....	157
5.6 Comparison of LULC type change between LULC in 2019 (base year) and the predicted LULC in 2029 of three different scenarios.....	167
6.1 The annual surface runoff data between 2011 and 2015 for model calibration.....	172

LIST OF FIGURES (Continued)

Figure	Page
6.2 Predicted LULC data between 2011 and 2015 for model calibration.....	172
6.3 Relationship between the estimated and observed sediment export under calibration period.....	175
6.4 The annual surface runoff data between 2016 and 2018 for model validation.....	178
6.5 Predicted LULC data between 2016 and 2018 for model validation.....	178
6.6 Relationship between the estimated and observed sediment export under validation period.....	179
6.7 Relationship between observed TSS data and annual surface runoff between 2011 and 2015	180
6.8 Relationship between average annual rainfall erosivity and the estimated sediment export under calibration period.	181
6.9 Spatial distribution of sediment export in 2019.....	183
6.10 Spatial distribution of sediment export in 2020, 2021, and 2022 under Scenario I	194
6.11 Spatial distribution of sediment export in 2023, 2024, and 2025 under Scenario I.....	195
6.12 Spatial distribution of sediment export in 2026, 2027, and 2028 under Scenario I	196
6.13 Spatial distribution of sediment export in 2029 under Scenario I.....	197
6.14 Spatial distribution of sediment export in 2020, 2021, and 2022 under Scenario II.	206
6.15 Spatial distribution of sediment export in 2023, 2024, and 2025 under Scenario II.	207
6.16 Spatial distribution of sediment export in 2026, 2027, and 2028 under Scenario II.	208
6.17 Spatial distribution of sediment export in 2029 under Scenario II.....	209

LIST OF FIGURES (Continued)

Figure	Page
6.18 Spatial distribution of sediment export in 2020, 2021, and 2022 under Scenario III.	218
6.19 Spatial distribution of sediment export in 2023, 2024, and 2025 under Scenario III.	219
6.20 Spatial distribution of sediment export in 2026, 2027, and 2028 under Scenario III.	220
6.21 Spatial distribution of sediment export in 2029 under Scenario III.	221
6.22 Comparison of sediment export between 2020 and 2029 of three different scenarios	224
7.1 Relationship between the observed and estimated nitrogen export under calibration process.....	233
7.2 Relationship between the observed and estimated phosphorus export under calibration period.....	234
7.3 Relationship between the observed and estimated nitrogen export under the validation period.....	238
7.4 Relationship between the observed and estimated phosphorus export under the validation period.....	239
7.5 Relationship between average annual rainfall and estimated total nitrogen data between 2011 and 2018.....	241
7.6 Relationship between average annual rainfall and estimated total phosphorus data between 2011 and 2018	241
7.7 Relationship between annual surface runoff and observed total nitrogen data under calibration period	243
7.8 Relationship between annual surface runoff and observed total phosphorus data under calibration period.....	243
7.9 Spatial distribution of nitrogen and phosphorus export in 2019.....	245
7.10 The relationship between average annual rainfall and estimated nutrient: (a) total nitrogen and (b) total phosphorus	250

LIST OF FIGURES (Continued)

Figure	Page
7.11 Spatial distribution of nitrogen and phosphorus export in 2020 under Scenario I	256
7.12 Spatial distribution of nitrogen and phosphorus export in 2021 under Scenario I	257
7.13 Spatial distribution of nitrogen and phosphorus export in 2022 under Scenario I	258
7.14 Spatial distribution of nitrogen and phosphorus export in 2023 under Scenario I	259
7.15 Spatial distribution of nitrogen and phosphorus export in 2024 under Scenario I	260
7.16 Spatial distribution of nitrogen and phosphorus export in 2025 under Scenario I	261
7.17 Spatial distribution of nitrogen and phosphorus export in 2026 under Scenario I	262
7.18 Spatial distribution of nitrogen and phosphorus export in 2027 under Scenario I	263
7.19 Spatial distribution of nitrogen and phosphorus export in 2028 under Scenario I	264
7.20 Spatial distribution of nitrogen and phosphorus export in 2029 under Scenario I	265
7.21 Spatial distribution of nitrogen and phosphorus export in 2020 under Scenario II	274
7.22 Spatial distribution of nitrogen and phosphorus export in 2021 under Scenario II	275
7.23 Spatial distribution of nitrogen and phosphorus export in 2022 under Scenario II	276
7.24 Spatial distribution of nitrogen and phosphorus export in 2023 under Scenario II	277

LIST OF FIGURES (Continued)

Figure	Page
7.25 Spatial distribution of nitrogen and phosphorus export in 2024 under Scenario II	278
7.26 Spatial distribution of nitrogen and phosphorus export in 2025 under Scenario II	279
7.27 Spatial distribution of nitrogen and phosphorus export in 2026 under Scenario II	280
7.28 Spatial distribution of nitrogen and phosphorus export in 2027 under Scenario II	281
7.29 Spatial distribution of nitrogen and phosphorus export in 2028 under Scenario II	282
7.30 Spatial distribution of nitrogen and phosphorus export in 2029 under Scenario II	283
7.31 Spatial distribution of nitrogen and phosphorus export in 2020 under Scenario III	292
7.32 Spatial distribution of nitrogen and phosphorus export in 2021 under Scenario III	293
7.33 Spatial distribution of nitrogen and phosphorus export in 2022 under Scenario III	294
7.34 Spatial distribution of nitrogen and phosphorus export in 2023 under Scenario III	295
7.35 Spatial distribution of nitrogen and phosphorus export in 2024 under Scenario III	296
7.36 Spatial distribution of nitrogen and phosphorus export in 2025 under Scenario III	297
7.37 Spatial distribution of nitrogen and phosphorus export in 2026 under Scenario III	298
7.38 Spatial distribution of nitrogen and phosphorus export in 2027 under Scenario III	299

LIST OF FIGURES (Continued)

Figure	Page
7.39 Spatial distribution of nitrogen and phosphorus export in 2028 under Scenario III	300
7.40 Spatial distribution of nitrogen and phosphorus export in 2029 under Scenario III	301
7.41 Comparison of nitrogen export between 2020 and 2029 of three different scenarios	304
7.42 Comparison of phosphorus export between 2020 and 2029 of three different scenarios	305
8.1 Ecosystem service on sediment export and its ESCI value under Scenario I	308
8.2 Ecosystem service on sediment export and its ESCI value under Scenario II	310
8.3 Ecosystem service on sediment export and its ESCI value under Scenario III	312
8.4 Comparison of ESCI on sediment export of three different scenarios	314
8.5 Ecosystem service on nitrogen export and its ESCI value under Scenario I	317
8.6 Ecosystem service on phosphorus export and its ESCI value under Scenario I	317
8.7 Ecosystem service on nitrogen export and its ESCI value under Scenario II	320
8.8 Ecosystem service on phosphorus export and its ESCI value under Scenario II	320
8.9 Ecosystem service on nitrogen export and its ESCI value under Scenario III	323
8.10 Ecosystem service on phosphorus export and its ESCI value under Scenario III	323
8.11 Comparison of ESCI on nitrogen export of three different scenarios	325

LIST OF FIGURES (Continued)

Figure	Page
8.12 Comparison of ESCI on phosphorus export of three different scenarios.....	326
8.13 Comparison of average ESCI value of sediment and nutrient export on ecosystem service among three scenarios.....	328



LIST OF ABBREVIATIONS

C	=	Cover factor
CLUE-S	=	Conversion of Land Use and Its Effects at Small regional extent
Crit_len_n	=	Critical length of nitrogen
Crit_len_p	=	Critical length of phosphorus
DEM	=	Digital Elevation Model
Eff_n	=	Maximum retention efficiency of nitrogen
Eff_p	=	Maximum retention efficiency of phosphorus
EnMAP	=	Environmental Mapping and Analysis Program
ESCI	=	Ecosystems Services Change Index
ESV	=	Ecosystem Service Values
InVEST	=	Integrated Valuation of Ecosystem Services and Tradeoffs
K	=	Soil erodibility
LDD	=	Land Development Department
LP	=	Linear Programming
LS	=	Slope length gradient factor
LULC	=	Land use and Land Cover
MNDWI	=	Modified Normalized Difference Water Index
MRC	=	Mekong River Commission
N_load	=	Nitrogen loads
NCAR	=	National Center for Atmospheric Research
NDMI	=	Normalized Difference Moisture Index
NDR	=	Nutrient Delivery Ratio
NIR	=	Near Infrared
P	=	Practice factor (erosion control practice)
P_load	=	Phosphorus loads

LIST OF ABBREVIATIONS (Continued)

PBIAS	=	Percent bias
PCD	=	Pollution Control Department
R	=	Rainfall erosivity
R ²	=	Coefficient of determination
RCPs	=	Representative Concentration Pathway
RID	=	Royal Irrigation Department
RP	=	Runoff proxy
RUSLE	=	Revised Universal Soil Loss Equation
SAVI	=	Soil Adjusted Vegetation Index
SDR	=	Sediment Delivery Ratio
SVM	=	Support Vector Machine
SWIR	=	Shortwave Infrared
TMD	=	Thai Meteorological Department
TN	=	Total nitrogen
TP	=	Total Phosphorus
TSS	=	Total Suspended solids

CHAPTER I

INTRODUCTION

1.1 Background problems and significance of the study

Freshwater ecosystems are considered as one of the essential natural resources for living organisms. The rate of deterioration of the water quality of freshwater resources, for example, lakes, ponds, rivers, etc., has become a global problem (Mushtaq and Pandey, 2013). Lakes are vital components of our planet's hydrological cycle, and they provide significant social and ecological functions while storing water and supporting significant aquatic biodiversity (Ballatore and Muhandiki, 2002). In the meantime, lakes are often the final recipients of nutrients discharged from adjacent uplands and wetlands. Although managing the lake means managing its watershed that needs proper management, they are probably mismanaged and challenged natural resources. Some problems originate in a lake itself, while most problems originate from activities on the surrounding land (ILEC, 2005). Several studies have shown that the variety of land uses plays an essential role in the water quality of lakes. Significantly, urban and built-up and cultivated areas influence the water quality within the lake basin (Huang, Zhan, Yan, Wu, and Deng, 2013; Hua, 2017). Also, land use and land cover changes are significant drivers for the accelerated eutrophication of surface waters due to soil loss and nutrient loads into water bodies. Besides, agricultural soil losses impact sediment deposition (Heathcote, Filstrup, and Downing, 2013).

Meanwhile, changes in land use have led to changes in ecosystem services (ESs). The impacts of several land use on ESs occur in three ways: major ESs are generated under different land use practices, land use patterns have a significant impact on ESs, and differing intensities of land use may have different impacts on the generation of ESs (Fu et al., 2015). Ecosystem services are the utilities people obtain from ecosystems. These include provisioning, regulating, cultural, and supporting services (Alcamo and Bennett, 2003). Therefore, the assessment of ecosystem services

and their relations to human well-being requires an integrated approach. For example, the modeling of land use changes is an effective method to estimate the impact on the environment and ecosystem services (Editorial, 2004; Yuan, 2008; Tolessaa, Senbetaa, and Kidaneb, 2017), and ecosystem services modeler such as the InVEST (Integrated Valuation of Ecosystem Services and Tradeoffs) has been used to assess and model ecosystem services quantitatively and analyze and map ecosystem services include GIS-based spatially explicit modeling tools. Additionally, it can also be used to estimate the monetary value of ecosystem services (Shoyamaa, Kamiyamaa, Morimotob, Oobac, and Okurod, 2017). For example, Srichaichana, Trisurat, and Ongsomwang (2019) applied toolsets of multiple ecosystem service evaluations, namely water yield and sediment delivery ratio models, to estimate water yield and sediment retention ecosystem services in the Klong U-Tapao watershed, Songkhla Province, Thailand, for identifying an optimum LULC scenario.

Kwan Phayao Lake is the largest freshwater in the Northern region and the fourth of Thailand as well as it was classified in the list of wetlands of international importance. This lake is an essential source of food security and species diversity conservation. Aquatic plants were found in the lake with about 36 species (Scott, 1989), and 44 fishes were identified by Rattanadaeng, Panboon, and Soe-been (2015). Furthermore, Kwan Phayao Lake provides various ecosystem services, including water supply for household consumption, agriculture, and recreation.

The Kwan Phayao Lake is situated in the Upper Ing watershed, where Nam Mae Ing River flows from Nong Leng Sai, located at the northern end and poured into the lake, while Nam Mae Tum River at the southern end also inflows to the lake. Primary cultivation practices in the watershed include paddy fields, field crops, perennial trees, and orchards. In the meantime, the extent of the Phayao Municipality was rapidly expanded due to the increase in population. These activities create many environmental problems, such as non-point sources (NPS) and soil erosion. Additionally, changing land use like urban and agriculture have affected the water quality of the lake. This effect has been caused by excessive amounts of nitrogen (N) and phosphorus (P) from agriculture practices and human activities. The nutrients flow into the lake have caused plankton bloom or eutrophication, such as the spread of

toxic algal diversity (Kaewsri and Traichaiyaporn, 2012), chlorophytic phytoplankton (Peerapornpisal, Suphan, Ngearnpat, and Pekkoh, 2008), and water hyacinth (Department of Public Works and Town & Country Planning, 2010). Also, the lake is becoming shallow as a result of the high sediment load from soil erosion.

Furthermore, the Department of Fisheries and Royal Irrigation Department (2017) summarized the recently existing problems related to Kwan Phayao Lake, as shown in Table 1.1. So, the Ministry of Agriculture and Cooperative spent about 134 million Baht for increasing water storage by sediment dredging, aquatic plant weeding, and flap-gate-weir building (Royal irrigation department, 2017).

Therefore, an optimal land use pattern identification to minimize sediment and nutrient export into Kwan Phayao Lake based on the ecosystem service change index is essential for sustainable development in the Upper Ing watershed.

Consequently, this study first assesses LULC and its change in the Upper Ing watershed in 2009 and 2019 using support vector machine algorithms (SVM) from the satellite data of Landsat 5 and Landsat 8. Then, the land requirements between 2020 and 2029 of three different scenarios are estimated for the CLUE-S model using the Markov Chain model for Scenario I (Trend of LULC evolution), linear programming for Scenario II (Maximization ecosystem service values), and based on economic crop zonation for Scenario III (Economic crop zonation). Next, the CLUE-S model simulates LULC change of three different scenarios in this period to account for the land use transformation. After that, sediment delivery ratio (SDR) and nutrient delivery ratio (NDR) models of the InVEST software suite and the LULC predicted between 2020 and 2029 of three different scenarios are used to assess the ecosystem service (sediment and nutrient export). Finally, optimum LULC allocation for minimizing sediment and nutrient export in the Kwan Phayao Lake is identified using the Ecosystems Services Change Index (ESCI) between the base year in 2019 and predicted years. The expected results will provide vital information to support land use planners, land managers, and decision-makers.

Table 1.1 The existing problem relates to Kwan Phayao Lake.

State of problems

1. Water flows into the lakes less than 33.84 million cubic meters.
 2. Total sediment is 134,459 tons per year (95,200 cubic meters per year).
 - 2.1 Sediment from water hyacinth and aquatic weed are 103,430 tons per year.
 - 2.2 Sediment from erosion is 31,029 tons per year.
 3. The expansion of the weed covers 4.414 square kilometers of the water surface or about 21.6 percent of the water surface.
 4. Water demand for irrigation is 15 million cubic meters per year.
-

Source: Department of Fisheries and Royal Irrigation Department (2017).

1.2 Research objectives

This research aims to identify the optimal scenario of LULC allocation to minimize sediment and nutrient export, Upper Ing Watershed, Phayao Province. Specific research objectives are set as follows:

- (1) To classify LULC in 2009 and 2019 from remotely sensed data by using a support vector machine algorithm;
- (2) To estimate land requirements between 2020 and 2029 of three different scenarios: Scenario I (Trend of LULC evolution) with Markov Chain model, Scenario II (Maximization ecosystem service values) with linear programming and Scenario III (Economic crop zonation) based on economic crop zonation;
- (3) To predict LULC of three different scenarios between 2020 and 2029 using CLUE-S model;
- (4) To estimate sediment and nutrient export of three different scenarios between 2019 and 2029 using SRD and NDR models;
- (5) To identify optimum LULC allocation to minimize sediment and nutrient export using the Ecosystems Services Change Index (ESCI).

1.3 Scope and limitations of the study

1.3.1 Scope of the study

The scope of the study can be summarized as follows:

(1) LULC data in 2009 and 2019 are classified from Landsat 5 (27 February 2009) and Landsat 8 (23 February 2019) by SVM algorithm with Gaussian radial basis function. This study uses ten LULC types that are modified from the standard land use classification of LDD include (1) urban and built-up area, (2) paddy field, (3) field crop, (4) para rubber, (5) perennial trees and orchards, (6) forest land, (7) water body, (8) rangeland, (9) wetland, and (10) miscellaneous land. Then, the post-classification comparison change detection algorithm is applied to extract LULC change for describing from-to-change information between 2009 and 2019.

(2) For land requirement estimation between 2020 and 2029 under Scenario I (Trend of LULC evolution), a transitional change area matrix that is extracted using the Markov Chain model based on classified LULC in 2009 and 2019 is applied to calculate annual decreasing and increasing areas of each LULC type between 2020 and 2029.

(3) For land requirement estimation between 2020 and 2029 under Scenario II (Maximization ecosystem service values), areas of each LULC type in 2029 are allocated to maximize ESV based on the coefficient value of different LULC types using Linear Programming (LP). They are further applied to calculate the annual decreasing and increasing areas of each LULC type between 2020 and 2029.

(4) Land requirement estimation between 2020 and 2029 for scenario III (Economic crop zonation) is determined based on land suitability zonation for economic crops of Agri-Map by the Land Development Department.

(5) Driving factors on LULC change, including physical and socio-economic, are applied to identify LULC type location preference using multicollinearity test and binary logistics regression analysis under the CLUE-S model.

(6) The sediment delivery ratio (SDR) model is applied to estimate soil erosion, sediment retention, sediment deposition, and sediment export in the base year (LULC in 2019) and the predicted LULC data between 2020 and 2029 of three different scenarios.

(7) The nutrient export in LULC 2019 and the predicted LULC between 2020 and 2029 of three different scenarios is estimated by the nutrient delivery ratio (NDR) model.

(8) Optimum LULC pattern to minimize sediment and nutrient export is identified by using average value ESCI value of ecosystem services (sediment and nutrient exports) between base year (2019) and predicted years (2020-2029).

1.3.2 Limitation of the study

The limitation of the study is summarized as follows:

(1) The parameters, namely nitrogen and phosphorus loads, maximum retention efficiency for the nutrient delivery ratio, were derived from the MRC (Mekong River Commission, 2017) report due to the lack of local data.

(2) The LULC data between 2011 and 2018 is predicted under the CLUE-S model based on the transitional change area of the Markov Chain model. Then, the predicted LULC as input is applied to calibrate and validate the SDR and NDR model.

(3) The observed sediment was calculated from the total suspended solids (TSS), which derived the data from the Pollution Control Department (PCD, 2019), and annual surface runoff data from RID. Then, the observed sediment is applied to calibrate and validate the SDR models.

(4) The observed nitrogen was calculated from the total nitrogen (sum of $\text{NO}_3\text{-N}$, $\text{NO}_2\text{-N}$, and $\text{NH}_3\text{-N}$), which derived the data from the Pollution Control Department (PCD, 2019), and annual surface runoff data RID. Then, the observed nitrogen is applied to calibrate and validate the NDR models.

(5) The observed phosphorus was calculated from the total phosphorus, which derived the data from the Pollution Control Department (PCD, 2019), and annual surface runoff data from RID. Then, the observed phosphorus is applied to calibrate and validate the NDR models.

(6) Monthly rainfall data between 2020 and 2029 for sediment and nutrient exports estimation are interpolated based on the simulated nine rainfall locations of the Global Products and Data Services of the National Center for Atmospheric Research (NCAR) over the study area using the Inverse Distance Weighted (IDW) method. The RCPs 8.5 simulation model of NCAR, which represents the highest

rising of radiative forcing pathway, population probability, economic trends, greenhouse gas emission level, and technological change (NCAR, 2004), is chosen in this study. Because this simulated rainfall characterizes the impact of climate change on water yield, as suggested by Riahi, Grubler and Nakicenovic (2007). The water yield is directly related to sediment and nutrient export in this study.

1.4 Study area

Upper Ing watershed is a part of the Mekong watershed where Ing River is the mainstream and flows backward into the Mekong River at Chiang Kong district, Chiang Rai province. The watershed area is about 891.35 sq. km, and it covers two whole districts (Mueang Phayao and Mae Chai) of Phayao province and some parts of two districts (Phan and Phadad) of Chiang Rai province. The watershed locates between 19° 01' 21" N to 19° 32' 53" N and 99° 41' 24" E to 99° 57' 32" E (Figure 1.1).

According to land use data of the Land Development Department in 2015, two main land use types were forest land, about 43% and agricultural land, about 32%, such as paddy fields, corn, lychee, and longan (Figure 1.2). In this watershed, there are two crucial wetland areas include Kwan Phayao and Nong Leng Sai. The highland and mountains are on the west side, while the areas between floodplain and highland are undulating and rolling plain. The lowest area in the study area is Kwan Phayao, which collects and stores water, sediments, and nutrients from the upstream in the northwest and west parts of the watershed.

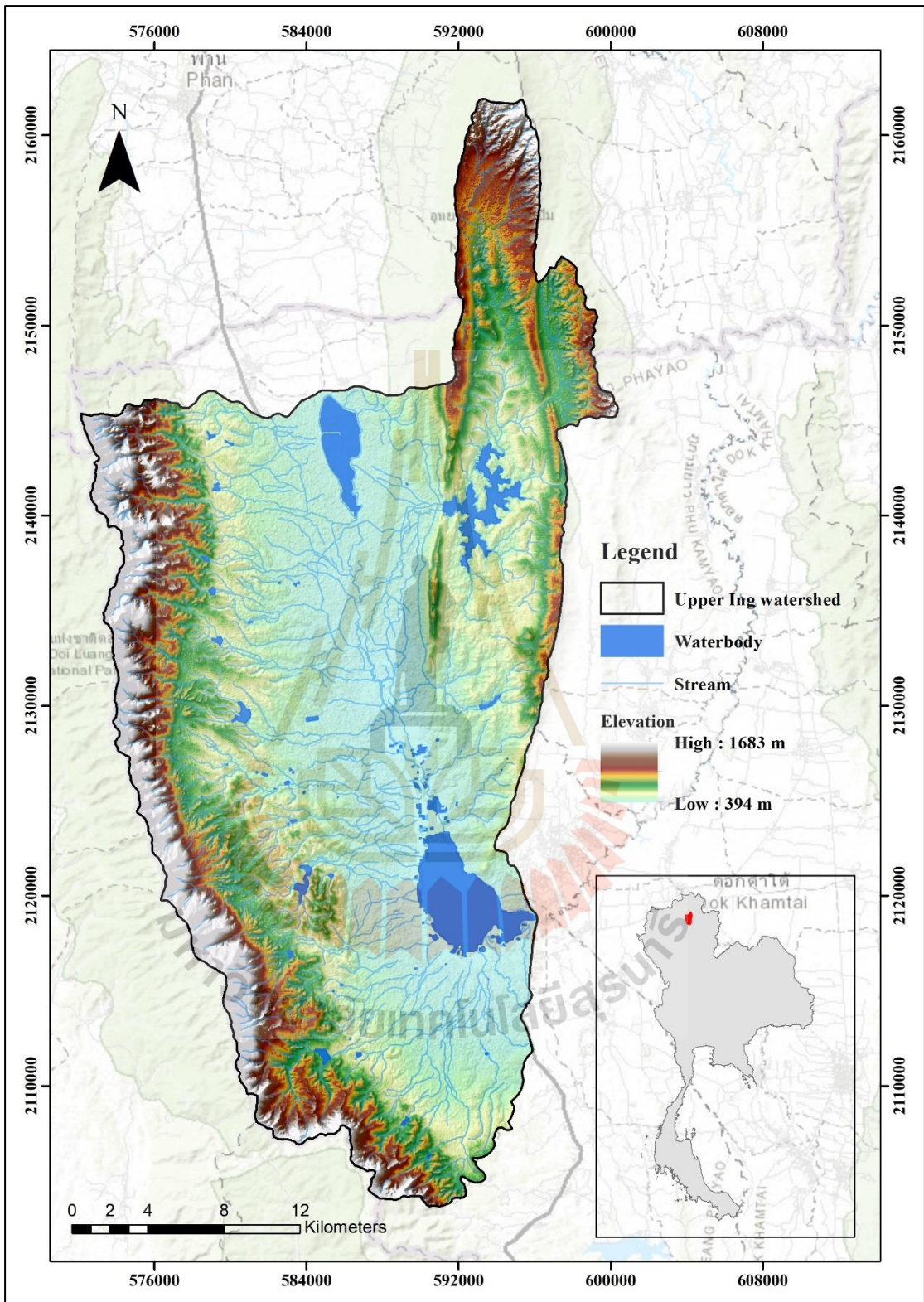


Figure 1.1 Terrain and location map of the Upper Ing watershed, Mekong Basin.

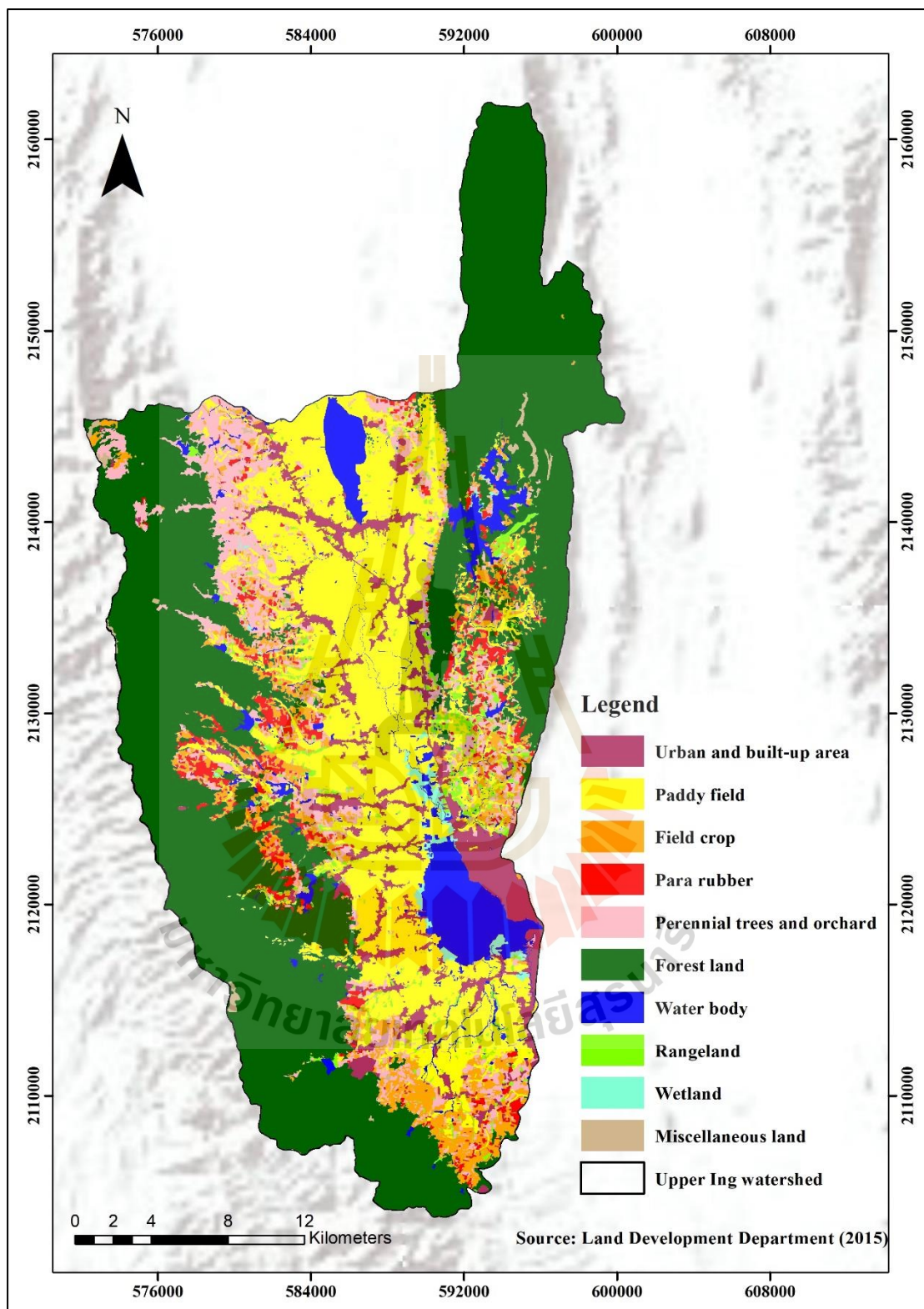


Figure 1.2 Spatial distribution of LULC by LDD in 2015.

1.5 Benefits of the study

The benefits of the study are summarized as follows:

- (1) LULC classification in 2009 and 2019,
- (2) LULC change map between 2009 and 2019,
- (3) Transition change area for land requirement between 2020 and 2029 for Scenario I (Trend of LULC evolution),
- (4) Land requirement between 2020 and 2029 for Scenario II (Maximization ecosystem service values) based on constraint and objective function to maximize ESV by linear programming,
- (5) Land requirement between 2020 and 2029 for Scenario III (Economic crop zonation) based on economic crop zonation of the LDD,
- (6) LULC prediction from 2020 to 2029 of three different scenarios.
- (7) Soil loss, sediment retention, and sediment export between 2020 and 2029 in three different scenarios,
- (8) Total phosphorus and nitrogen load in the watershed from different LULC,
- (9) Nitrogen and phosphorus export from the watershed between 2020 and 2029 in three different scenarios,
- (10) LULC pattern for optimum ecosystem services to minimize sediment and nutrient export in Upper Ing watershed.

CHAPTER II

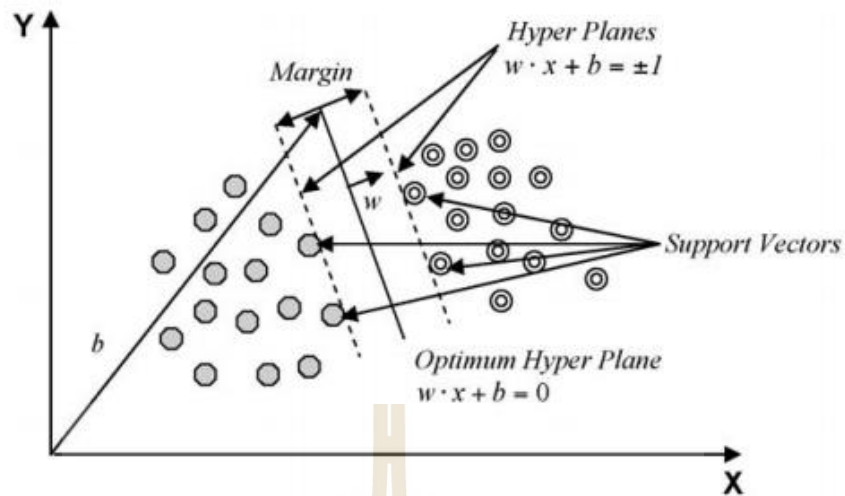
BASIC CONCEPTS AND LITERATURE REVIEWS

Basic concepts include (1) LULC classification with support vector machine (SVM), (2) Markov Chain model (3) CLUE-S model, (4) Linear programming, (5) Sediment Delivery Ratio model of InVEST software suite, (6) Nutrient Delivery Ratio model of InVEST software suite, and literature reviews are summarized in this chapter.

2.1 LULC classification with support vector machine (SVM)

Support Vector Machine (SVM) is a learning system that uses a hypothesis space of linear functions in an N-dimensional feature space, trained with a learning algorithm from optimization theory that carries out a learning bias derived from statistical learning theory (Cristianini and Shawe-Taylor, 2000). The SVM was rooted in the statistical learning theory developed by Vladimir Vapnik and co-workers at AT&T Bell Laboratories in 1995. The SVM training algorithm goals to find a hyperplane that separates the dataset into a discrete predefined number of classes in a model consistent with the training examples (Figure 2.1).

An optimal hyperplane is defined as the linear decision function with the maximal margin between the vectors of the two classes (see Figure 2.1). To construct such optimal hyperplanes, one only has to consider a small amount of the training data, which determines this margin (Cortes and Vapnik, 1995). The principle of the SVM-based solution for the learning process is very briefly described below (Vapnik, 1999; Zhu and Blumberg, 2002; Kavzoglu and Colkesen, 2009).



Source: Kavzoglu and Colkesen (2009).

Figure 2.1 An example of a separable problem in a 2-dimensional space. The support vectors define the margin of the largest separation between the two classes.

Consider the optimal separating hyperplanes. Suppose the training data

$$(x_1, y_1), \dots, (x_\lambda, y_\lambda), \quad x \in R^n, \quad y \in \{+1, -1\}, \quad (2.1)$$

Where $x \in R^n$ is an N-dimensional space, and $y \in \{+1, -1\}$ is a class label, and it can be separated by a hyperplane as:

$$(w \cdot x) + b = 0 \quad (2.2)$$

Where x is a point lying on the hyperplane, parameter w determines the orientation of the hyperplane in space, b is the bias that the distance of hyperplane from the origin.

In this case, this set of vectors is separated by the optimal hyperplane if it is split without error, and the distance between the closest vectors to the hyperplane is maximal. To describe the linear separating hyperplane, use the following form such that the inequalities:

$$\begin{aligned} (w \cdot x_i) + b &\geq +1 \quad \text{if } y_i = +1 \\ (w \cdot x_i) + b &\leq -1 \quad \text{if } y_i = -1 \end{aligned} \quad (2.3)$$

Among the separating hyperplanes, the one for which the distance to the closest point is maximal is called the optimal separating hyperplane. The learning

processing based on SVM aims to find the optimal separating hyperplane to separate the training data in n dimension by using the criteria described above and then to separate the real data in the same dimension (Zhu and Blumberg, 2002).

If α_i is denoted as $(\alpha_1, \dots, \alpha_\lambda)$. The λ , non-negative Lagrange multipliers associated with constraints Eq. (2.3), the optimization problem amounts to maximizing

$$w(\alpha) = \sum_{i=1}^{\lambda} \alpha_i - \frac{1}{2} \sum_{i,j=1}^{\lambda} \alpha_i \alpha_j y_i y_j x_i x_j \quad (2.4)$$

With $\alpha_i \geq 0$ and under the constraint $\sum_{i=1}^{\lambda} \alpha_i y_i = 0$. Once the vector $\alpha^0 = (\alpha_1^0, \dots, \alpha_\lambda^0)$ solution of the maximization problem Eq. (2.4) has been found, the optimal separating hyperplane (w_0, b_0) has an expansion, as shown in Eq. 2.5.

$$w_0 = \sum_{i=1}^{\lambda} \alpha_i^0 y_i x_i \quad (2.5)$$

The support vectors are the points for that $\alpha_i \geq 0$ and satisfy Eq. (2.3) with equality.

For a nonlinear situation, a support vector network tries to map the input vectors into a very high-dimensional feature space Z through some nonlinear mapping chosen *a priori*. In this space, the construction of an optimal separating hyperplane is completed. Therefore, x will be replaced by its mapping in the feature space $\Phi(x)$, as shown in Figure 2. Then, Eq. (2.4) will be changed to Eq. (2.6):

$$w(\alpha) = \sum_{i=1}^{\lambda} \alpha_i - \frac{1}{2} \sum_{i,j=1}^{\lambda} \alpha_i \alpha_j y_i y_j \Phi(x_i) \Phi(x_j) \quad (2.6)$$

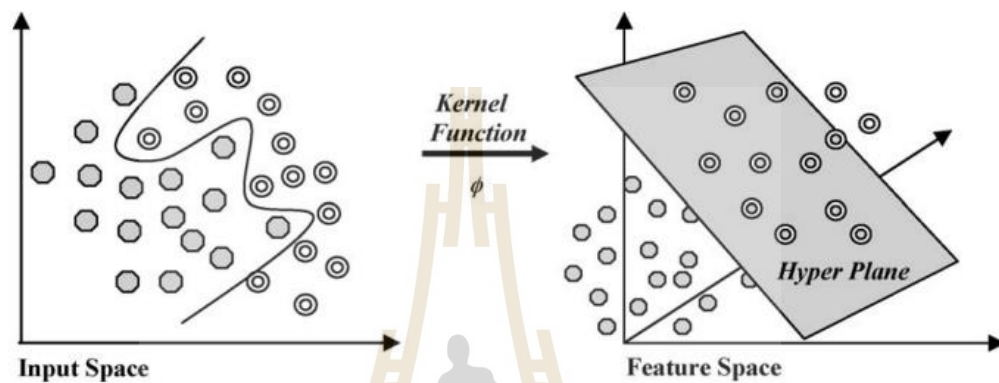
To prevent computational problems, arising from a rapid increase in the number of dimensions of mapped space Φ , an inner product between any two vectors in the feature space $\Phi(x_1)$ and $\Phi(x_2)$ is chosen as a function of two variables in the input space as:

$$\Phi(x) \cdot \Phi(x_i) = K(x, x_i) \quad (2.7)$$

Then, it will be possible to construct the solutions, which are equivalent to the optimal separating hyperplane in the feature space, and the nonlinear decision function changes the form to Eq. (2.8) as:

$$f(x) = \text{sign} \left(\sum_{\text{support_vector}} \alpha_i K(x_i \cdot x) + b_0 \right) \quad (2.8)$$

Where The $\alpha_i = (\alpha_1, \dots, \alpha_\lambda)$ is the λ non-negative Lagrange multipliers for the optimization process to look for the optimal separating hyperplane. $K(x, x_1)$ is an SVM type of kernel, which is chosen to replace the inner product (x_i, x_j) .



Source: Kavzoglu and Colkesen (2009).

Figure 2.2 Mapping of the data sets to the high-dimensional space with a Kernel function.

Kernel functions commonly used in SVMs can generally be aggregated into four groups: linear, polynomial, radial basis function, and sigmoid kernels (Patle and Chouhan, 2013).

Linear Kernel Function: Linear kernel function is commonly described as:

$$K(x, x_i) = x \cdot x_i^T \quad (2.9)$$

Polynomial Kernel Function: The polynomial kernel function is directional, i.e., the output depends on the direction of the two vectors in low dimensional space. This output is due to the dot product in the kernel. The magnitude of the output is also dependent on the magnitude of the vector x_i .

$$K(x, x_i) = (1 + x \cdot x_i^T)^d \quad (2.10)$$

Where 'd' is a degree of the kernel function.

Radial Basis Function: Radial basis function is one of the most popular kernel functions. RBF is implemented by using convolutions of the type.

$$K(x, x_i) = e^{-\gamma \|x - x_i\|^2} \quad (2.11)$$

Where kernel function parameter $\gamma > 0$

Sigmoid Function: The SVM with the Sigmoidal Kernel function is equivalent to the Multi-Layer Perceptron classifier in performance.

$$K(x, x_i) = \text{Tanh}(\gamma x_i^T x_j + r) \quad (2.12)$$

Here γ , r and d are kernel parameters. The selection of kernel function depends on the application. It is not fixed.

2.1.1 Application of LULC classification with SVM

Many review papers present that there has been a significant increase in SVM works on the classification of remote sensing because SVM-based classification has been known to strike the right balance between accuracy attained on a given finite amount of training patterns and the ability to generalize to unseen data (Mountrakis, Im, and Ogole, 2011). Also, the ability of SVMs in image classification is successfully used in small training data sets, often generating higher classification accuracy than the traditional methods (Mantero, Moser, and Serpico, 2005). However, some drawbacks of SVM classification have been reported by researchers. Nalepa and Kawulok (2019) found that the training and testing phase of the algorithm requires plenty of time, which depends on the training set size. Also, SVM with the kernel function still needs to find the appropriate kernel parameters to improve the highest classification accuracy (Zhang and Song, 2015).

Ustuner, Sanli, and Dixon (2015) investigated the sensitivity of SVM architecture, including internal parameters and kernel types, on land use classification accuracy of RapidEye imagery for the study area in Turkey. Four kernels (linear, polynomial, radial basis function, and sigmoid) were used for the SVM classification. The results suggested that the choice of model parameters and kernel types play an essential role in SVMs classification accuracy. The best model of polynomial kernel outperformed all SVMs models and gave the highest classification accuracy of 85.63% with RapidEye imagery.

Taati, Sarmadian, Mousavi, Pour, and Shahir (2015) classified land use using a support vector machine (SVM) in the case of linear separating hyperplane and maximum likelihood classifier (MLC) in Qazvin, Iran, by TM images of the Landsat 5 satellite. Land use classes were extracted: irrigated agricultural lands (including the irrigated land, fallow 1, and fallow 2), highway, hill, rainfed land, water channel, range, building, powerhouse, and saline land. The evaluation results verified that the SVM algorithm, with an overall accuracy of 86.67% and a kappa coefficient of 0.82, has higher accuracy than the MLC algorithm in land use mapping.

Likewise, Prasad, Savithri, and Krishna (2017) investigated the accuracy and reliability of the Support Vector Machine (SVM) classifier for classifying a multispectral image of Hyderabad and its surrounding area and also compared its performance with Artificial Neural Network (ANN) classifier. A hybrid technique, which was Fuzzy Incorporated Hierarchical clustering, was proposed for clustering the multispectral satellite images into LULC sectors. The classified results showed that the SVM yields an auspicious performance than the ANN in LULC classification. The overall accuracies of the LULC classification of Hyderabad and its surroundings area are approximately 93.159% for SVM and 89.925% for ANN. The corresponding kappa coefficient values are 0.893 and 0.843.

The integration of spectral and shape features, as well as the transformed spectral components in an SVM, were able to improve classification accuracy such as Wang, Jia, Yao, and Xu (2019) were used principal component analysis (PCA) and optimum index factor (OIF) to select the best band combination of Landsat TM images. The image extracted texture statistics, texture features, and spectral information of the homogeneity, contrast, entropy, and angular second moments using the gray level co-occurrence matrix. The land use classes of the study area were divided into eight classes, including cultivated land, forest land, grassland, water area, residential area, coal mine land, unused land, and transportation land. The results found that the support vector machine (SVM) and neural network (NN) classification techniques could classify all land use types in the coal mining area. The overall accuracy obtained was 92.40%, and the Kappa hat coefficient was 0.9126 for SVM, 90.90%, and 0.8930 for NN, respectively.

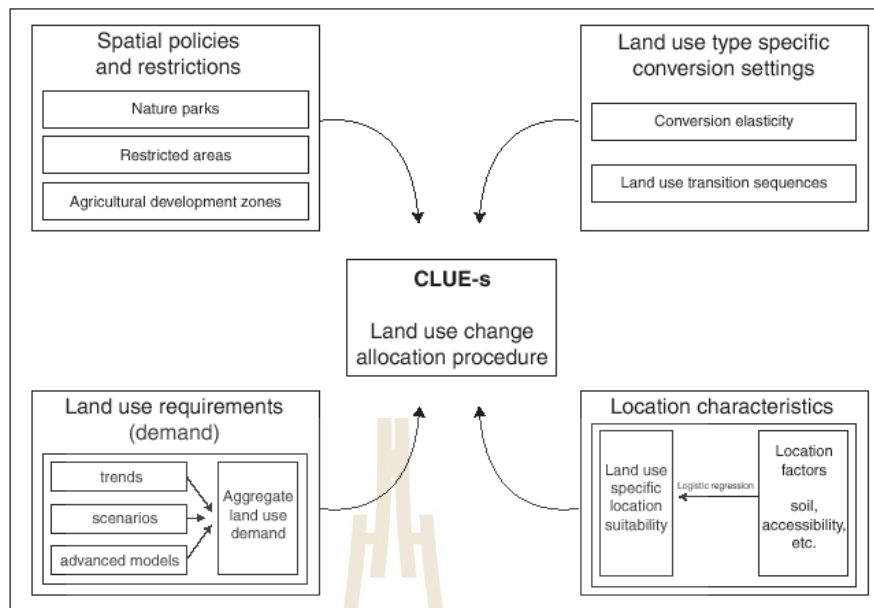
Moreover, SVMs have been used with object-based classification to achieve the best classification accuracy as Jia et al. (2019) investigated the capability and strategy of GF-2 multispectral data for land use and land cover (LULC) classification in a region of the North China Plain. The pixel-based and object-based classifications using maximum likelihood (MLC) and support vector machine (SVM) classifiers were evaluated to determine the classification strategy suitable for GF-2 multispectral data. The validation results indicated that GF-2 multispectral data achieved satisfactory LULC classification performance, and object-based classification using the SVM classifier succeeded the best classification accuracy with an overall classification accuracy of 94.33% and kappa coefficient of 0.911.

In summary, it can be observed that the SVM algorithm has been applied to classify LULC from moderate spatial resolution images by many researchers. This algorithm can provide an overall accuracy between 85% and 94%, and the Kappa hat coefficient ranges from 0.82-0.91.

2.2 CLUE-S model

The Conversion of Land Use and its Effects at Small regional extent (CLUE-S) model was developed to simulate land-use change using empirically quantified relations between land use and its driving factors combined with dynamic modeling for a small region. A multi-scale land-use change model is used to understand and predict the impact of biophysical and socio-economical forces driving land-use change. The model can simulate different land-use types simultaneously and the possibility to simulate different scenarios. Also, the model can easily be applied to a wide range of areas and land-use change situations. CLUE-S can simulate the future LULC map cartographically to continue the former CLUE model (Verburg and Overmars, 2007).

The CLUE-S model requires information to consider the following four components: (1) spatial policies and restrictions; (2) land use types specific conversion settings, (3) land (demand) requirements, and (4) location characteristics, as shown in Figure 2.3.



Source: Verburg and Lesschen (2014).

Figure 2.3 Overview of the information flow in the CLUE-S model.

A brief description of each component based on Verburg and Lesschen (2014) is summarized as follows.

(1) Spatial policies and restrictions

Spatial policies and land tenure indicate areas where land use changes are restricted through policies or tenure status. The conversions restricted by a specific spatial policy can be indicated in a land use conversion matrix.

(2) Land use type-specific conversion settings

Land use type-specific conversion settings determine the temporal dynamics of the simulations. Two parameters are required to characterize the individual land use types: conversion elasticities and land use transition sequences. The first parameter set, the conversion elasticities, is related to the reversibility of land use change. Land use types with high capital investment will not easily be converted to other uses as long as there is sufficient demand. Thus, each land use type value has to be specified to represent the relative elasticity to change, ranging from 0 (easy conversion) to 1 (irreversible change). Meanwhile, land use type characteristics needed to be specified are land use type, specific conversion settings, and temporal characteristics. These settings are designated in a conversion matrix.

(3) Land use requirements (demand)

Land use requirements are calculated at the aggregate level as part of a specific scenario. The land use requirements constrain the simulation by defining the required change in land use. In the approach, land use requirements are calculated independently from the CLUE-S model itself. The calculation of these land use requirements is based on various methods, depending on the case study and the scenario. The extrapolation of trends in land use change of the recent past into the near future is a common technique to calculate land use requirements.

(4) Location characteristics

Land use conversions are expected to occur at locations with the highest preference for the specific type of land use at that moment in time. The preference of a location is empirically estimated from a set of factors based on the different disciplinary understandings of the determinants of land-use change. The preference is calculated using the following equation:

$$R_{ki} = a_k X_{1i} + b_k X_{2i} + \dots \quad (2.13)$$

Where, R is the preference to devote location i to land use type k , $X_{1,2,..}$ are biophysical or socio-economical characteristics of location i and a_k and b_k the relative impact of these characteristics on the preference for land use type k .

A statistical model can be developed as a binomial logit model. The function that relates these probabilities with the biophysical and socio-economic location characteristics is defined as a logit model using the following equation:

$$\text{Log} \left(\frac{P_i}{1-P_i} \right) = \beta_0 + \beta_1 X_{1,i} + \beta_2 X_{2,i} + \dots + \beta_n X_{n,i} \quad (2.14)$$

Where, P_i is the probability of a grid cell for the occurrence of the considered land use type on location i and the X 's are the location factors. The coefficients (β) are estimated through logistic regression using the actual land use pattern as the dependent variable.

Allocation procedure

Allocation of land-use change is made in an iterative procedure given the probability maps, the decision rules in combination with the actual land-use map, and

the demand for the different land-use types (Figure 2.4). The following steps are followed in the calculation:

(1) The first step includes the determination of all grid cells that are allowed to change. Grid cells that are either part of a protected area or presently under a land use type that is not allowed to change are excluded from the further calculation.

(2) For each grid cell i , the total probability ($TPROP_{i,u}$) is calculated for each of the land use types u according to:

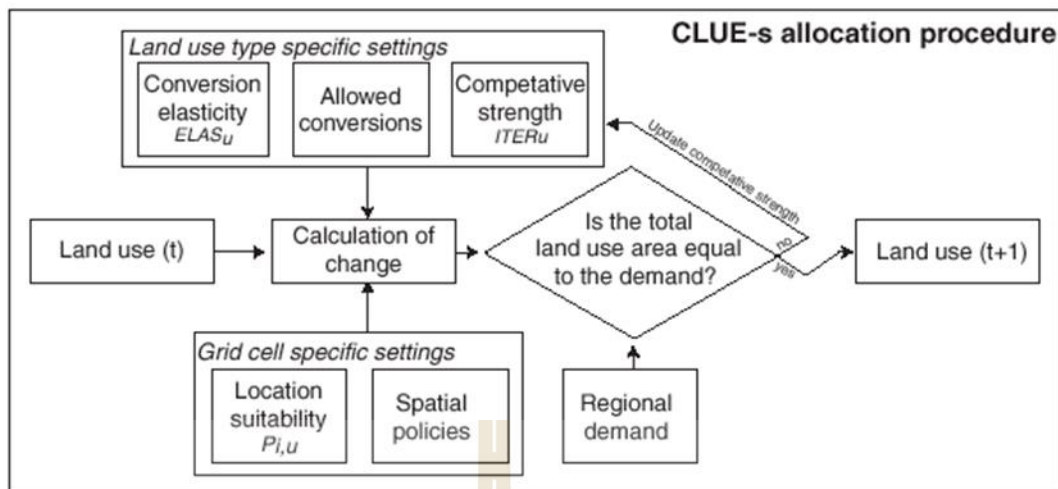
$$TPROP_{i,u} = P_{i,u} + ELAS_u + ITER_u \quad (2.15)$$

Where, $P_{i,u}$ are the suitability of location i for land use type u (based upon the logit model), $ELAS_u$ is the conversion elasticity for land use u and $ITER_u$ is an iteration variable that is specific for the land use type and indicative for the relative competitive strength of the land use type. $ELAS_u$, the land use type-specific elasticity to change the value, is only added if grid-cell i is already under land use type u in the year considered. $P_{i,u}$ consists of a part based on the biophysical and socio-economic factors and a neighborhood interaction part.

(3) A preliminary allocation is made with an equal value of the iteration variable ($ITER_u$) for all land use types by allocating the land use type with the highest total probability for the considered grid cell. This process will cause several grid cells to change land use.

(4) The total allocated area of each land use is now compared with the land use requirements (demand). For land-use types where the allocated area is smaller than the demanded area, the value of the iteration variable is increased. For land-use types for which too much is allocated, the value is decreased.

(5) Steps 2 to 4 are repeated as long as the demands are not correctly allocated. When allocation equals demand, the final map is saved, and the calculations can continue for the next timestep.



Source: Verburg and Lesschen (2014).

Figure 2.4 Flow chart of the allocation module of the CLUE-S model.

2.2.1 Application of the CLUE-S model

The CLUE-S model was applied to predict the spatial patterns of future land use. The model transfers and allocate land demand from the Markov chain model to improve LULC change projection to simulate different land-use scenarios. For instance, Ongsomwang and lamchuen (2015) assessed the historical and recent LULC and changes. The CLUE-S model was developed to simulate the land-use change in three different scenarios. Then, the three simulated scenarios from the LULC data in 2023 were used to assess soil erosion, water yield, and economic value and their changes. Finally, the optimum land use for three different scenarios was allocated. The results showed that the simulation of 3 LULC scenarios in 2023 by the CLUE-S model revealed that urban and built-up land, cassava, sugarcane, water body, and miscellaneous land would increase while maize, perennial tree/orchard, and forest land would decrease under Scenario I (Historical land use evolution). At the same time, the increase in cassava and sugarcane under Scenario II (Energy crop extension) came from maize, forest land, and miscellaneous land, while most of the increasing forest land under Scenario III (Forest conservation and prevention) was converted from maize, sugarcane, and miscellaneous land.

Han, Yang, and Song (2015) developed CLUE-S model that will transfer and allocate land demand from the Markov model to improve LULC change projection

to simulate future land use scenarios from 2010 to 2020, which comprise a development scenario (natural and rapid development) and protection scenarios (ecological and cultivated land protection). The results indicated that the conversion of cultivated land to urban built-up land would form the main features of LULC change in the future. The geographical environment restricted the expansion of urban built-up land, but the cultivated land will be converted to built-up land in mountainous areas and more widespread by 2020.

Guang Liu et al. (2017) investigated the relationship between government policy and land-use change to develop appropriate strategies for sustainable land use in the Lijiang River Basin, Guangxi Zhuang Autonomous Region in southern China. The predicted characteristics of land-use change were explored using the CLUE-S numerical model and logistic regression. The tendency of land-use changes from 1993 to 2020 under two scenarios: A Natural Growth Scenario (NS) and a Government Intervention Scenario (GS) was simulated. The CLUE-S model was applied to predict the spatial patterns of land use for 2020. It showed that construction and cultivated land areas increased under the NS while other land use areas decreased. Under the GS, the areas of the others declined, but the areas of construction land, woodland, cultivated land, and water all increased. Furthermore, a significant cultivated land area occurred in Lingchuan County under the NS and Xingan County under the GS. the woodland and water area decreased for every county under the NS. Under the GS, the areas of woodland expansion were located in Lingchuan and Lingui counties, while increases in water areas happened in Lingchuan and Guilin counties. Besides, construction land expanded in Lingchuan County under the NS and in Guilin County under the GS.

Zare, Samani, Mohammady, Salmani, and Bazrafshan (2017) evaluated land-use change effects on soil erosion in the north of Iran using five land-use scenarios. CLUE-S model was used to investigate land-use transition and to simulate land use for the year 2030. the reduction in land use degradation in the future was applied for the first three scenarios. Also, the new demand (% increase in demand) will be considered in the other scenario. In addition, the erosion and the effect of land-use change were estimated by the RUSLE model. The results showed that CLUE-S is suitable for modeling future land use transitions using the ROC curve. The soil loss

change ranges from 2% to 32% in the simulated period. Soil loss value was higher than the basis period in all scenarios.

Sun, Zhang, Shen, Randhir, and Cao (2019) assessed the effects of land use change on multiple ecosystem services in the Kaihua watershed of China based on the InVEST model and CLUE-S model. The modeling of land-use change was based on CLUE-S to simulate future land use patterns. Ecosystem services, namely, water yield, soil conservation, carbon storage, water purification, and habitat quality during 2000–2015, are evaluated and compared to future land use scenarios in 2025 (business-as-usual, strategic planning, environmental protection, and economic development). The strategic planning scenario is an optimal land use strategy to balance the requirements for urban development while providing higher ecosystem services.

2.3 Linear programming

Linear programming (LP) is a mathematical procedure for finding optimal solutions to problems expressed using linear constraints (equations and/or inequalities). A linear program includes a set of variables, a linear objective function indicating the contribution of each variable to the desired outcome, and a set of linear constraints describing the limits on the values of the variables. The “answer” to a linear program is a set of values for the problem variables that result in the objective function’s best - largest or smallest - a value and is consistent with all the constraints. Thus, solving a linear program is relatively easy. However, the most challenging part of applying linear programming is formulating the problem and interpreting the solution (McDill, 1999). LP is not explicitly spatial but can be used as a tool for spatial organization. Its application field ranges from business planning management to the problem of a spatial organization (Chuvieco, 1993). The primary feature of a linear programming problem is that all functions associated, the objective function, and the constraints must be linear. A single nonlinear function’s appearance, either on the objective or in the constraints, suffices to reject the problem as an LP problem (Pedregal, 2004).

In this study, LP is applied to maximize ecosystem service value because the coefficient value for ESV estimation has a linear relationship with LULC types. So, LP is here chosen to maximize ESV in this study.

The LP is an optimization problem of the general form as:

Maximize or minimize

$$Z = \sum_{i=1}^n c_i X_i \quad (2.16)$$

Where c_i = the objective function coefficient corresponding to the i th variable, and X_i = the i th decision variable.

The constraints explain the possible values that the variables of a linear programming problem may take. They typically represent resource constraints, or the minimum or maximum level of some activity or condition (McDill, 1999). The general form is the following:

subject to:

$$\begin{aligned} \sum_i a_{ji} X_i &\leq b_j, & j=1, \dots, p, \\ \sum_i a_{ji} X_i &\geq b_j, & j=p+1, \dots, q, \\ \sum_i a_{ji} X_i &= b_j, & j=q+1, \dots, m, \end{aligned} \quad (2.17)$$

Where a_{ji} = the coefficient on X_i in constraint j , and

b_j = the right-hand-side coefficient on constraint j .

c_i , b_j , a_{ji} are data of the problem. Depending on the particular values of p and q we may have inequality constraints of one type and/or the other, and equality restrictions.

The coefficients a_{ji} for $i=1,2,\dots,m$, $j=1,2,\dots,n$ are called the technological coefficients. The coefficients are usually expressed in a matrix form of A.

$$A = \begin{bmatrix} a_{11} & a_{12} & \dots & a_{1n} \\ a_{21} & a_{22} & \dots & a_{2n} \\ \vdots & \vdots & & \vdots \\ a_{m1} & a_{m2} & \dots & a_{mn} \end{bmatrix}$$

The column vector, whose i th component is b_i , which is referred to as the right-hand-side vector, represents the minimal requirement to be satisfied.

The non-negativity constraints: the constraints $x_1, x_2, \dots, x_n \geq 0$ are the non-negativity constraints. A set of variables x_1, \dots, x_n satisfying all the constraints is called a feasible point or vector. The set of all such points constitutes the feasible region or space. The variables of linear programs must always take non-negative values (i.e., greater than or equal to zero).

2.3.1 Application of Linear programming

Nikkami, Shabani, and Ahmadi (2009) optimized land allocation to different land uses like rangeland, orchard, irrigated farming, and dry farming to minimize soil erosion and maximize people's net income Kharestan watershed, Northwest of Eghlid in Fars province, Iran. Linear Programming (LP) model with multi-objective was applied in three different land-use scenarios, namely existing land uses plus land management (Scenario 1), existing land uses with some degree of land management (Scenario 2), and proper land uses plus land management (Scenario 3). The amount of soil loss and net benefit in each land use were computed and used as inputs to formulate the optimization problem's objective functions and governing constraints. The simplex method was used to solve the problem for finding the optimal solution. The results showed rangelands experience no change, the area of orchards should be increased, irrigated farms and dry farming lands should be decreased. Also, soil erosion decreases by 53%, and net income increases by 208% from proper land use and management. Sensitivity analysis displayed that the area of orchards and rangelands are the most sensitive parameters. Their changes have the highest consequence on the amount of net income and soil erosion.

Ying, Hongqi, Dongying, and Wei (2012) designed and developed agricultural land use by dividing zones and a pre-allocation for each land use. The spatial allocation module and land-use suitability and area optimization module were incorporated to constitute a whole agricultural land use optimal allocation (ALUOA) system. Land-use suitability on eight common crops was evaluated one by one using a linear weighted summation method in the land-use suitability model. The linear programming (LP) model in the area optimization model succeeds in giving out land area targets of each crop under three scenarios. At last, the land use targets are

allotted in space, both with a six-subzone file and without a subzone file. The results show that the land use maps with a subzone not only ensure every part has enough land for every crop but also gives a more fragmental land use pattern, with about 87.99% and 135.92% more patches than the one without, while at the expense of loss between 15.30% and 19.53% in the overall suitability at the same time.

Zhang et al. (2016) adopted the linear programming (LP) model to consider Abandoned Mining Land (AML) dynamics and calculate future land requirements for all land-use types. The map of the spatial transformations of AML for 2020 in the Mentougou District (Beijing, China) was created by the CLUE-S model. Three scenarios are generated to map the spatial distribution of land-use types using 2007 as a baseline: Scenario 1: the planning scenario based on the general land-use plan in Mentougou District, Scenario 2: maximal comprehensive benefits, and Scenario 3: maximal ecosystem service value (ESV). Next, landscape pattern changes are analyzed by using several landscape-scale metrics. The results displayed that the coupled model could simulate the dynamics of AML effectively, and the spatially explicit transformations of AML were different. Reclaiming AML by transformation into more forests can reduce the variability and maintain the stability of the landscape ecological system in the study area.

Sokouti and Nikkami (2017) determined the optimal land use to reduce erosion and increase the resident's income of the Qushchi watershed in West Azerbaijan province, Iran. The optimizing land use pattern problem was solved by linear programming. The Simplex Method was used for three different conditions, including the current status of land uses without and with land management, the standard status of land uses with soil and water conservation practices inputs and high land use outputs. Finally, the best land use option was determined by comparing each scenario's erosion rate and cost. Then, the circumstances and the recommended conditions were compared. The results indicated that the current surface area of current land uses is not suitable to minimize erosion and increase the income of residents and should change in the optimum conditions. Conversion of rangeland area not indispensable. Besides, the results showed that high decreased soil erosion and high increased profitability in the standard conditions. The sensitivity analysis results

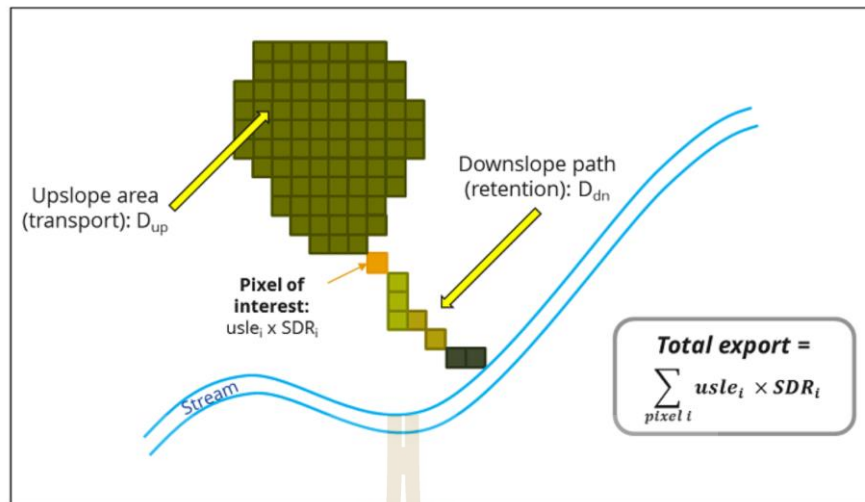
showed that the changes in the horticulture and rangeland areas have the most significant impact on increasing profitability and reducing soil erosion of the Qushchi watershed.

Pokhrel and Paudel (2019) proceeded biophysical simulations using MapShed to assign the effects of adopting best management practices (BMPs) to decrease nutrients and sediment pollution in a watershed dominated by poultry production at Saline Bayou Watershed, Louisiana, USA. The reduction of three water pollutants, nitrogen, phosphorus, and sediment, from adopting different BMPs, was estimated using a linear programming model to maximize pollution reduction at the lowest cost. Three weather scenarios (dry, normal, and wet) were considered, and BMP parameter efficiencies were received from linear regression models. The results showed that nutrient management and agricultural land retirement reduced most phosphorus runoff at the lowest cost in the watershed. Also, results were robust to alternative weather (dry, normal, and wet) scenarios.

2.4 Sediment Delivery Ratio model of InVEST software suite

Primary sediment sources comprise overland erosion, gullies, bank erosion, and mass erosion. Sinks include on-slope, floodplain or instream deposition, and reservoir retention. However, the SDR model only focuses on overland erosion processes (Sharp et al., 2020).

The sediment delivery module is a spatially explicit model working at the spatial resolution of the input digital elevation model raster. The model first computes the annual soil loss from each pixel, then computes the sediment delivery ratio (SDR), the proportion of soil loss reaching the stream. Once sediment reaches the stream, it ends up at the catchment outlet; thus, no in-stream processes are modeled (Borselli, Cassi, and Torri, 2008), as illustrated in Figure 2.5.



Source: Sharp et al. (2020).

Figure 2.5 Conceptual approach applied in the sediment delivery ratio model.

The amount of annual soil loss on pixel i , A_i is given by the Revised Universal Soil Loss Equation (RUSLE) by Renard and Freimund (1994) as:

$$A_i = R_i \cdot K_i \cdot LS_i \cdot C_i \cdot P_i, \quad (2.18)$$

Where A_i is annual soil erosion ($\text{ton} \cdot \text{ha}^{-1} \cdot \text{yr}^{-1}$),
 R_i is rainfall erosivity ($\text{MJ} \cdot \text{mm} \cdot \text{ha}^{-1} \cdot \text{h}^{-1} \cdot \text{y}^{-1}$),
 K_i is soil erodibility ($\text{ton} \cdot \text{ha} \cdot \text{hr} \cdot (\text{MJ} \cdot \text{ha} \cdot \text{mm})^{-1}$),
 LS_i is slope length-gradient factor,
 C_i is crop-management factor, and
 P_i is a support practice factor for erosion control.

The LS_i factor is given from the method for the two-dimension surface as:

$$LS_i = S_i \frac{(A_{i-in} + D^2)^{m+1} \cdot A_{i-in}^{m+1}}{D^{m+2} \cdot x_i^m \cdot (22.13)^m} \quad (2.19)$$

Where

S_i the slope factor for grid cell calculated as a function of slope radians θ ,

$$S = 10.8 \cdot \sin \theta + 0.03, \text{ where } \theta < 9\%,$$

$$S = 16.8 \cdot \sin \theta - 0.50, \text{ where } \theta \geq 9\%.$$

Where, A_{i-in} is the contributing area (m^2) at the inlet of a grid cell which is computed from the d -infinity flow direction method, D is the grid cell linear dimension $x_i = | \sin$

$\alpha_i / + / \cos \alpha_i /$ where α_i is the aspect direction for grid cell_{*i*}, m is the RUSLE length exponent factor.

To avoid overestimation of the LS factor in heterogeneous landscapes, long slope lengths are capped to a value of 333 m. The value of m , the length exponent of LS factor, is based on the classical USLE, as discussed in as:

$$m = 0.2 \quad m = 0.2 \text{ for slope } \leq 1\%,$$

$$m = 0.3 \quad m = 0.3 \text{ for } 1\% < \text{slope} \leq 3.5\%,$$

$$m = 0.4 \quad m = 0.4 \text{ for } 3.5\% < \text{slope} \leq 5\%,$$

$$m = 0.5 \quad m = 0.5 \text{ for } 5\% < \text{slope} \leq 9\%,$$

$$m = \beta / (1 + \beta) \text{ where } \beta = \sin \theta / 0.0986 / (3 \sin \theta + 0.8 + 0.56) \text{ for slope } \geq 9\%.$$

Meanwhile, sediment delivery ratio (SDR) is estimated using connectivity index (IC) that reflecting the attributes of each LULC based on the work by Borselli, Cassi, and Torri (2008) as:

$$IC = \log_{10} \left(\frac{D_{up}}{D_{dn}} \right) \quad (2.20)$$

The sediment delivery ratio (SDR) for each pixel is a function of the upslope area (D_{up}) and downslope flow path. D_{up} is the upslope component defined as:

$$D_{up} = \overline{CS} \sqrt{A} \quad (2.21)$$

Where, \overline{CS} is the average C factor of the upslope contributing area, S is the average slope gradient of the upslope contributing area and \sqrt{A} is the upslope contributing area (m^2). Meanwhile, the downslope contributing area (D_{dn}) is delineated from the equation type, D-infinity flow algorithm. The D_{dn} is given by:

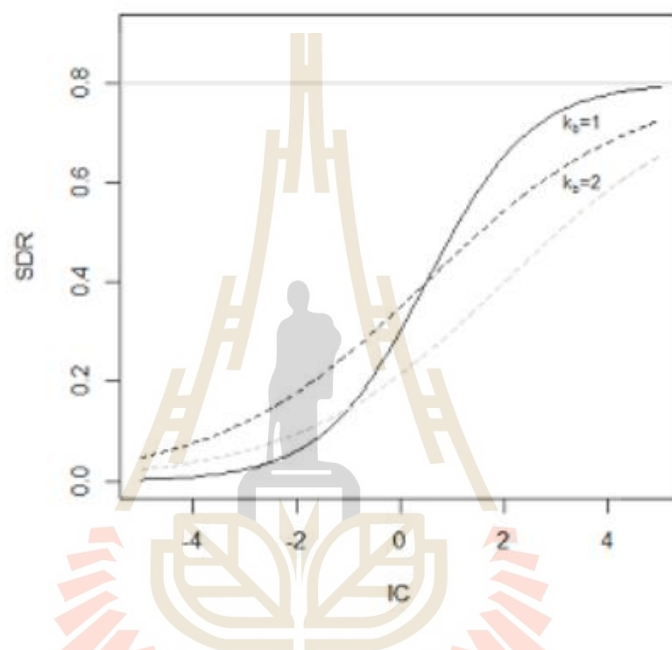
$$D_{dn} = \sum_i \frac{d_i}{C_i S_i} \quad (2.22)$$

Where d_i is the length of the flow path along with the i cell according to the steepest downslope direction (m), C_i and S_i are the C factor and the slope gradient of the i^{th} cell, respectively. Again, the downslope flow path is determined by the D-infinity flow algorithm.

The SDR ratio for a pixel i is then derived from the connectivity index IC (Vigiak, Borselli, Newham, McInnes, and Roberts, 2012) as:

$$SDR_i = \frac{SDR_{max}}{1 + \exp\left(\frac{IC_0 - IC_i}{k}\right)} \quad (2.23)$$

Where, SDR_{max} is the maximum theoretical SDR , set to an average value of 0.8 and IC_0 and k are calibration parameters that define the shape of the SDR_{IC} relationship increasing function. The effect of IC_0 and k on the SDR is illustrated in Figure 2.6.



Source: Sharp et al. (2020).

Figure 2.6 Relationship between the connectivity index IC and the SDR .

Sediment Export: The sediment export from a given pixel i E_i (units: $tons \cdot ha^{-1} yr^{-1}$), is the amount of sediment eroded from that pixel that reaches the stream. Sediment export is given by:

$$E_i = rusle_i \cdot SDR_i \quad (2.24)$$

The total catchment sediment export E (units: $tons \cdot ha^{-1} yr^{-1}$) is given by:

$$E = \sum_i E_i \quad (2.25)$$

E is the value used for calibration/validation purposes, in combination with other sediment sources, if data are available.

2.4.1 Application of Sediment Delivery Ratio model of InVEST software

Arunyawat and Shrestha (2016) analyzed the impact of change in land use on ecosystem services using the InVEST model to map and quantify a set of ecosystem services, namely sediment retention, water yield, carbon stock, and habitat quality. Also, assessing the changes in land use from 1989 to 2013 and their impact on overall ecosystem services were using GIS in Northern Thailand. The results confirmed that rubber plantation cultivation and built-up areas resulting in reduced forest cover. Moreover, a general decrease in ecosystem services for the study period in the watershed, particularly a negative effect on ecosystem services, was observed in agricultural areas.

Similarly, Shicheng, Zhaofeng, and Yili (2017) estimated crop cover reconstruction and its effects on sediment retention in the Tibetan Plateau by using historical population data as a proxy in the provincial cropland areas of Qinghai province, the Tibet Autonomous Region for 1900, 1930, and 1950. For the 20th century, the provincial cropland areas were converted into crop cover datasets with a 1 × 1 km resolution. The sediment delivery ratio module of the InVEST model assessed changes in sediment retention due to crop cover change. The result found that sediment export increased rapidly in the Minhe autonomous county of the Yellow River-Huangshui River Valley (YHRV) and in the Nianchu River and Lhasa River basins, the Yarlung Zangbo River and its two tributaries valley (YRTT), which means that sediment retention clearly decreased in these regions over this period in 1950–1980.

Also, the model provides scientific support for conservation planning, development planning, or restoration activities. For example, Srichaichana, Trisurat, and Ongsomwang (2019) assessed ecosystem services as water yield and sediment retention using the InVEST model. The results found that the optimum water yield and sediment retention ecosystem services in Klong U-Tapao watershed, Songkhla, Thailand was Scenario II: Forest conservation and prevention between 2018 and 2024.

Bogdan, Pătru-Stupariu, and Zaharia (2016) assessed The link between the sediment retention service and land cover change. The analysis concentrates on a mountain landscape from the upper catchment of Râul Târgului, the Iezer Mountains, in the Romanian Carpathians. Three scenarios (Business-as-Usual, Conservation, and

Development) were developed to compare the supply of sediment retention services using the InVEST model. Results show the highest increase for the Conservation scenario and the highest decrease in the sediment retention service for the Development scenario.

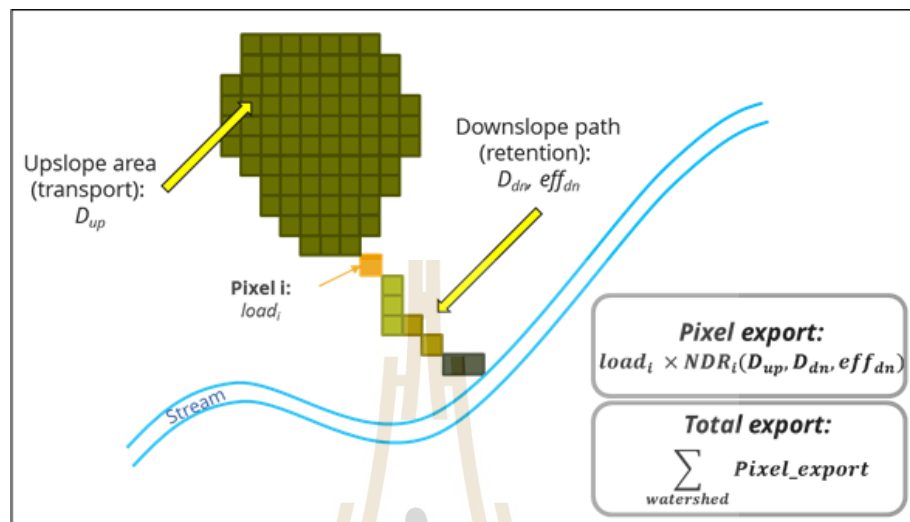
Furthermore, the explicit spatial approach to ES modeling enables an informed discussion with stakeholders and may be used to implement, monitor effectively, and communicate future planning policies similar to Pedro, Clément, Harold, Mélodie, and Damien (2016) examined multiple ES provided by the landscape of the Urban Community of Bordeaux (CUB), in France, between 1990 and 2006. The selected ES were (1) food provisioning, (2) flood regulation: water yield, (3) water quality: nutrient retention, (4) erosion regulation: sediment retention, (5) recreation, (6) climate regulation and (7) biodiversity, and were computed using a spatially explicit modeling approach with InVEST and own-produced models. All ES, except erosion regulation, have decreased as a consequence of LUCC. The results also suggest that LUCC change decisions that do not consider policy measures for ES protection tend to generate land-use patterns providing lower levels of ES.

2.5 Nutrient Delivery Ratio model of InVEST software suite

The nutrient delivery and retention model provide information for non-point source pollutants from water flows over the landscape carrying pollutants from surfaces into streams, rivers, lakes, and the ocean. The model was designed for nutrients (nitrogen and phosphorous) and used a simple mass balance approach, describing the movement of a mass of nutrients through space (Figure 2.7).

The model represents the long-term, steady-state flow of nutrients through empirical relationships. The nutrient loads are determined based on a map of land use/land cover (LULC) and associated loading rates. Nutrient loads can be divided into sediment-bound and dissolved parts, transported through surface and subsurface flow, respectively, stopping when they reach a stream. In a second step, delivery factors are computed for each pixel based on the properties of pixels belonging to the same flow path (particularly their slope and retention efficiency of the land use). At the

watershed/sub-watershed outlet, the nutrient export is computed as the sum of the pixel-level contributions (Sharp et al., 2020).



Source: Sharp et al. (2020).

Figure 2.7 Conceptual representation of the NDR model.

From Figure 2.7, each pixel i is characterized by its nutrient load, $load_i$, and nutrient delivery ratio (NDR), which is a function of the upslope area, and downslope flow path. Pixel-level export is computed based on these two factors, and the nutrient export at the watershed level is the sum of pixel-level nutrient exports.

Nutrient Loads: Loads are the sources of nutrients associated with each pixel of the landscape. Consistent with the export coefficient literature, load values for each LULC class are derived from empirical measures of nutrient export (e.g., nutrient export running off urban areas, crops, etc.).

Next, each pixel's load is modified to account for the local runoff potential. The LULC-based loads defined above are averages for the region, but each pixel's contribution will depend on the amount of runoff transporting nutrients. As a simple approximation, the loads can be modified as follows:

$$modified.load_{xi} = load_{xi} \cdot RPI_{xi} \quad (2.26)$$

Where RPI_i is the runoff potential index on pixel i . It is defined as $RPI_i = RP_i / RP_{o,v}$, where RP_i is the nutrient runoff proxy for the runoff on pixel i , and $RP_{o,v}$ is the average

RP over the raster. In practice, the raster RP is defined either as a quick flow index (e.g., from the InVEST Seasonal Water Yield model) or as annual precipitation.

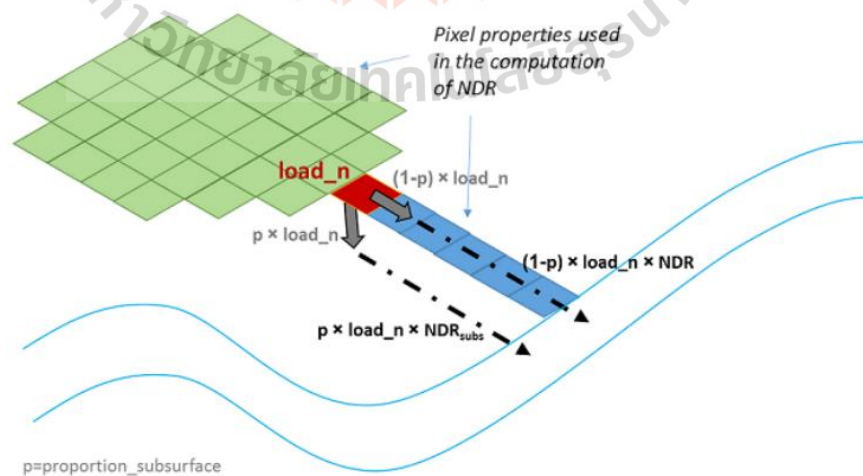
For each pixel, modified loads can be divided into sediment-bound and dissolved nutrient portions. Conceptually, the former represents nutrients transported by surface or shallow subsurface runoff, while the latter represents nutrients transported by groundwater. Because phosphorus particles are usually sediment-bound and less likely to be transported via subsurface flow, the model uses the subsurface option only for nitrogen. The ratio between these two nutrient sources is given by the parameter $proportion_subsurface_n$, which quantifies the ratio of dissolved nutrients over the total amount of nutrients. For a pixel i :

$$load_{surf,i} = (1 - proportion_subsurface_n) * modified.load_n_i \quad (2.27)$$

$$load_{subsurf,i} = proportion_subsurface_n * modified.load_n_i \quad (2.28)$$

If the value of $proportion_subsurface_n$ is zero, it means that all nutrients are reaching the stream via surface flow.

Nutrient Delivery: Nutrient delivery is based on the concept of nutrient delivery ratio (NDR). The concept is similar to the risk-based index approaches that are popular for nutrient modeling. However, it provides quantitative values of nutrient export (e.g., the proportion of the nutrient load that will reach the stream). Two delivery ratios are computed, one for nutrient transported by surface flow and subsurface flow.



Source: Sharp et al. (2020).

Figure 2.8 Conceptual representation of nutrient delivery in the model.

Figure 2.8, if the user chooses to represent subsurface flow, the load on each pixel, $load_n$, is divided into two parts. The total nutrient export is the sum of the surface and subsurface contributions.

Surface NDR: The surface NDR is the product of a delivery factor, representing the ability of downstream pixels to transport nutrients without retention, and a topographic index, representing the position on the landscape. For a pixel i :

$$NDR_i = NDR_{0,i} \left(1 + \exp \left(\frac{IC_i - IC_0}{k} \right) \right)^{-1} \quad (2.29)$$

Where IC_0 and k are calibration parameters, IC_i is a topographic index, and $NDR_{0,i}$ is the proportion of a nutrient not retained by downstream pixels (irrespective of the pixel's position on the landscape). The details on the computation of each factor are shown below.

$NDR_{0,i}$ is based on the maximum retention efficiency of the land between a pixel and the stream (downslope path, in Figure 2.7):

$$NDR_{0,i} = 1 - eff'_i \quad (2.30)$$

Moving along a flow path, the algorithm computes the additional retention provided by each pixel, taking into account the total distance traveled across each LULC type. Each additional pixel from the same LULC type will contribute a smaller value to the total retention until the maximum retention efficiency for the given LULC is reached (Figure 7). The total retention is capped by the maximum retention value that LULC types along the flow path can provide, eff_{LULC_i} . In mathematical terms:

$$eff'_i = \begin{cases} eff_{LULC_i} \cdot (1 - s_i) & \text{if } down_i \text{ is a stream pixel} \\ eff_{down_i} \cdot s_i + eff_{LULC_i} \cdot (1 - s_i) & \text{if } eff_{LULC_i} > eff_{down_i} \\ eff_{down_i} & \text{Otherwise} \end{cases} \quad (2.31)$$

Where:

- eff'_{down_i} is the effective downstream retention on the pixel directly downstream from i
- eff_{LULC_i} is the maximum retention efficiency that LULC type i can reach, and
- s_i is the step factor defined as:

$$s_i = \exp\left(\frac{-5l_{i\text{down}}}{l_{LULC_i}}\right) \quad (2.32)$$

With:

- $l_{i\text{down}}$ is the length of the flow path from pixel i to its downstream neighbor
- l_{LULC_i} is the LULC retention length of the land cover type on pixel i

In equation (2.32), factor 5 is based on the assumption that maximum efficiency is reached when 99% of its value is reached (assumption due to the exponential form of the efficiency function, which implies that the maximum value cannot be reached with a finite flow path length) as shown in Figure 2.9.

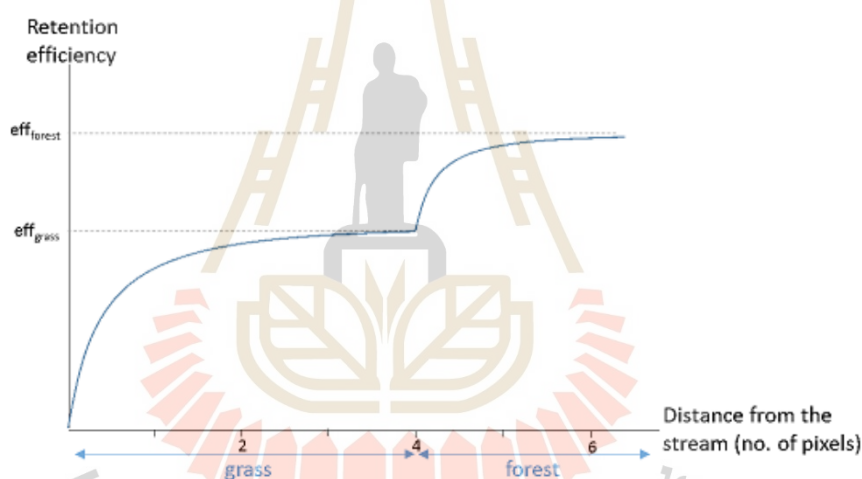


Figure 2.9 Illustration of the calculation of the retention efficiency along a simple flow path.

Figure 2.9 shows that each additional pixel of the grass LULC contributes to a smaller percentage toward the maximum efficiency provided by grass. The shape of the exponential curves is determined by the maximum efficiency and retention length.

IC , the index of connectivity, represents the hydrological connectivity, i.e., how likely nutrient on a pixel is likely to reach the stream. In this model, IC is a function of topography only:

$$IC = \log_{10}\left(\frac{D_{up}}{D_{dn}}\right) \quad (2.33)$$

Where:

- $D_{up} = \bar{S}\sqrt{A}$ and,
- $D_{dn} = \sum_i \frac{d_i}{S_i}$

where $D_{up} = \bar{S}$ is the average slope gradient of the upslope contributing area (m/m), A is the upslope contributing area (m²); d_i is the length of the flow path along with the i^{th} cell according to the steepest downslope direction (m) (see details in sediment model), and S_i is the slope gradient of the i^{th} cell, respectively.

Subsurface NDR: The expression for the subsurface NDR is a simple exponential decay with distance to stream, plateauing at the value corresponding to the user-defined maximum subsurface nutrient retention:

$$NDR_{subs,i} = 1 - eff_{subs} \left(1 - e^{\frac{-5 \cdot l}{l_{subs}}} \right) \quad (2.34)$$

Where:

- eff_{subs} is the maximum nutrient retention efficiency that can be reached through subsurface flow (i.e., retention due to biochemical degradation in soils),
- l_{subs} is the subsurface flow retention length, i.e., the distance after which it can be assumed that soil retains nutrient at its maximum capacity,
- l_i is the distance from the pixel to the stream.

Nutrient export: Nutrient export from each pixel i is calculated as the product of the load and the NDR:

$$x_{exp_i} = load_{surf,i} \cdot NDR_{surf,i} + load_{subs,i} \cdot NDR_{subs,i} \quad (2.35)$$

Total nutrient at the outlet of each user-defined watershed is the sum of the contributions from all pixels within that watershed:

$$x_{exp_{tot}} = \sum_i x_{exp_i} \quad (2.36)$$

2.5.1 Application of Nutrient Delivery Ratio model of InVEST software

Redhead et al. (2018) found that the InVEST model can provide valuable information on nutrient fluxes to decision-makers, especially relative differences among catchments. The model performed well regarding the relative magnitude of

nutrient export among catchments (best Spearman's rank correlation for N and P, respectively: 0.81 and 0.88). However, wide variation among catchments in the model's accuracy and absolute values of nutrient exports frequently showed a high percentage of differences between modeled and empirically derived exports (best median absolute percentage difference for N and P, respectively: $\pm 64\%$, $\pm 44\%$). The model also showed a high degree of sensitivity to nutrient loads and hydrologic routing input parameters, and these sensitivities varied among catchments.

Mei, Kong, Ke, and Yang (2017) explored the impacts of implementing a strict cropland protection policy on ecological lands and the ecosystem services, specifically water purification, for the city of Wuhan, and explored the critical mechanism of these impacts. The InVEST model was used to estimate the amount of nutrient export from land use under two different scenarios and analyze the main factors for the impacts of policy on ecosystem service of water purification. The results show that the scenario with strict cropland protection (CP) will lead to more ecological lands losses than those without cropland protection (NCP). Besides, the nitrogen export in the CP scenario is an average of 8.6% higher than the NCP scenario, which indicates that the Cropland Balance Policy has a negative impact on water purification. Also, the nitrogen export is transported mainly by subsurface, which is 1.73 times higher than the surface averaged over the two scenarios.

Salata, Garnero, Barbieri, and Giaimo (2017) investigated the nutrient retention model through its spatial distribution and quantitative value. The model was examined by testing its response to changes in input parameters: (1) the digital terrain elevation model; and (2) different LULC attribute configurations. Besides, the model increased attention to specific ES models that use water runoff as a proxy of nutrient delivery. This study shows that many factors, including the DEM characteristics and its interaction with LULC, highly influence the spatial distribution of biophysical values. The biophysical value of ES is still affected by a high degree of uncertainty which encourages an expert field campaign as the only solution to use ES mapping for a regulative land use framework.

Gurung, Yang, and Fang (2018) assessed ecosystem services from the forestry-based reclamation of surface-mined areas in the North Fork, the Kentucky River

watershed. The result from InVEST model, namely carbon storage and sequestration, water yield and reservoir hydropower production, sediment delivery ratio (SDR), and nutrient delivery ratio (NDR), indicate that barren and grassland land covers provide less carbon storage, yield more water, and export more sediments and nutrients than forests.

Yang et al. (2019) simulated the nitrogen and phosphorus exports of the Bosten Lake basin using the InVEST model. The spatial and temporal dynamics of N and P exports and the response of N and P exports to land use and precipitation change were analyzed between 2000 and 2015. The results show that N and P exports increased from 2000 to 2015, and the N and P exports are primarily distributed around Bosten Lake. Cultivated land, built-up areas, and grassland greatly impacted the N and P exports, while other land use types had fewer effects. The high precipitation areas with small exports of N and P are mainly distributed in mountain areas. In contrast, small precipitation areas with significant exports of N and P are distributed in plains where the cultivated land and built-up areas are intensive.

CHAPTER III

RESEARCH PROCEDURES

The research procedures comprise data collection and preparation and six significant components. Summary of collected and prepared data and details of methodology including (1) data collection and preparation, (2) LULC evaluation and its change, (3) land demand estimation of three different scenarios, (4) LULC prediction of three different scenarios, (5) ecosystem services assessment: sediment and nutrient export, and (6) optimum LULC allocation to minimize sediment and nutrient export are described in this chapter.

3.1 Data collection and preparation

The required input data for data analysis included GIS data, remotely sensed data, and relevant data were collected and prepared for (1) LULC classification, (2) land requirement estimation of three scenarios, (3) driving factors, (4) the models of sediment and nutrient delivery ratio, and (5) the model calibration and validation. The list of data collection and preparation are summarized in Table 3.1.

Table 3.1 List of data collection and preparation for analysis and modeling in the study.

Data	Data collection	Data Preparation	Source	Component
GIS	LULC data in 2009 and 2015	-	LDD (2009, 2015)	1
	Watershed boundary	Raster	RID (2018)	1, 2, 3 and 4
	SRTM DEM	-	USGS	3 and 4
	Elevation (m)	Create from SRTM DEM	-	3
	Slope (%)	Create from SRTM DEM	-	3
	Soil drainage (m)	Raster	LDD	3
	Distance to stream (m)	Euclidean distance	DEQP	3
	Distance to waterbody (m)	Euclidean distance	DEQP	3

Table 3.1 (Continued).

Data	Data collection	Data Preparation	Source	Component
	Distance to village (m)	Euclidean distance	LDD	3
	Distance to road (m)	Euclidean distance	LDD	3
	Distance to fault (m)	Euclidean distance	DMR	3
	Income per capita at sub-district level	Calculation from income	NSO	3
	Population density at sub-district level	Calculation from personal income by sub-district area	DOPA	3
	Slope length gradient factor (LS-factor) calculation	Create from SRTM DEM	-	4
	Soil series and Geology unit	Soil erodibility, Rasterization	LDD (2000)	4
Remote Sensing	Landsat 5 TM 2009	Layer stacking images	USGS	1
	Landsat 8 OLI 2019	Subset images		
Secondary data	Google Image 2009 and 2010	-	Google Earth (2009)	
	Agri-Map	Modified based on LULC types, Overlay by Updating	LDD (2017, 2018)	2
	Annual rainfall	IDW interpolation	TMD (2020)	3 and 4
	Monthly rainfall	Rainfall erosivity index calculation	Wischmeier and Smith (1978)	4
	C-factor and P-factor	Modified based on LULC types	LDD (2000)	4
	Predictive rainfall	IDW interpolation	NCAR (2020)	4
	Nitrogen (N) loads	-	MRC (2017)	4
	Phosphorus (P) loads	-	MRC (2017)	4
	Nitrogen retention efficiency (eff_n)	-	MRC (2017)	4
	Phosphorus retention efficiency (eff_p)	-	MRC (2017)	4
	Total suspended solids (TSS)	Convert to tons/yr. Convert to kg/yr.	PCD (2018)	4
	Total phosphorus (TP)	Convert to kg/yr.		
	Total nitrogen (TN)			
	Annual surface runoff	Modified based on the year of rainfall data	RID (2019)	4

Note: DEQP: Department of Environmental Quality Promotion; DMR: Department of Mineral Resources; DOPA: Department of Provincial Administration; LDD: Land Development Department; MRC: Mekong River Commission; NCAR: National Center for Atmospheric Research; NSO: National Statistical Office of Thailand; PCD: Pollution Control Department; RID: Royal Irrigation Department; TMD: Thai Meteorological Department; USGS: United States Geological Survey.

3.2 Research Methodology

The overview framework of research methodology and linkage is schematically illustrated in Figure 3.1. It consists of data collection and preparation and five main components, which include: (1) LULC evaluation and its change, (2) Land requirement estimation of three different scenarios, (3) LULC prediction of three different scenarios, (4) Ecosystem services assessment: sediment and nutrient exports, and (5) Optimum LULC allocation to minimize sediment and nutrient export. The information on each component is separately summarized in the following sections.

3.3.1 LULC evaluation and its change

Landsat 5 TM data in 2009 and Landsat OLI data in 2019 were downloaded from the USGS website (www.earthexplorer.usgs.gov) for LULC classification using the support vector machines (SVM) algorithm. Then, the thematic accuracy of LULC maps in 2009 and 2019 was assessed using the high spatial resolution imagery from the Google Earth in 2009, 2010 and field survey in 2020, respectively. Finally, LULC maps in 2009 and 2019 were applied to detect LULC change using a post-classification comparison algorithm (Figure 3.2). The final LULC maps in 2009 and 2019 are further applied for LULC change prediction between 2020 and 2029 in three different scenarios using the CLUE-S model in the next component.

The main tasks under this component include (1) LULC Classification using SVM algorithms, (2) accuracy assessment, and (3) LULC change detection, which are summarized in the following sections.

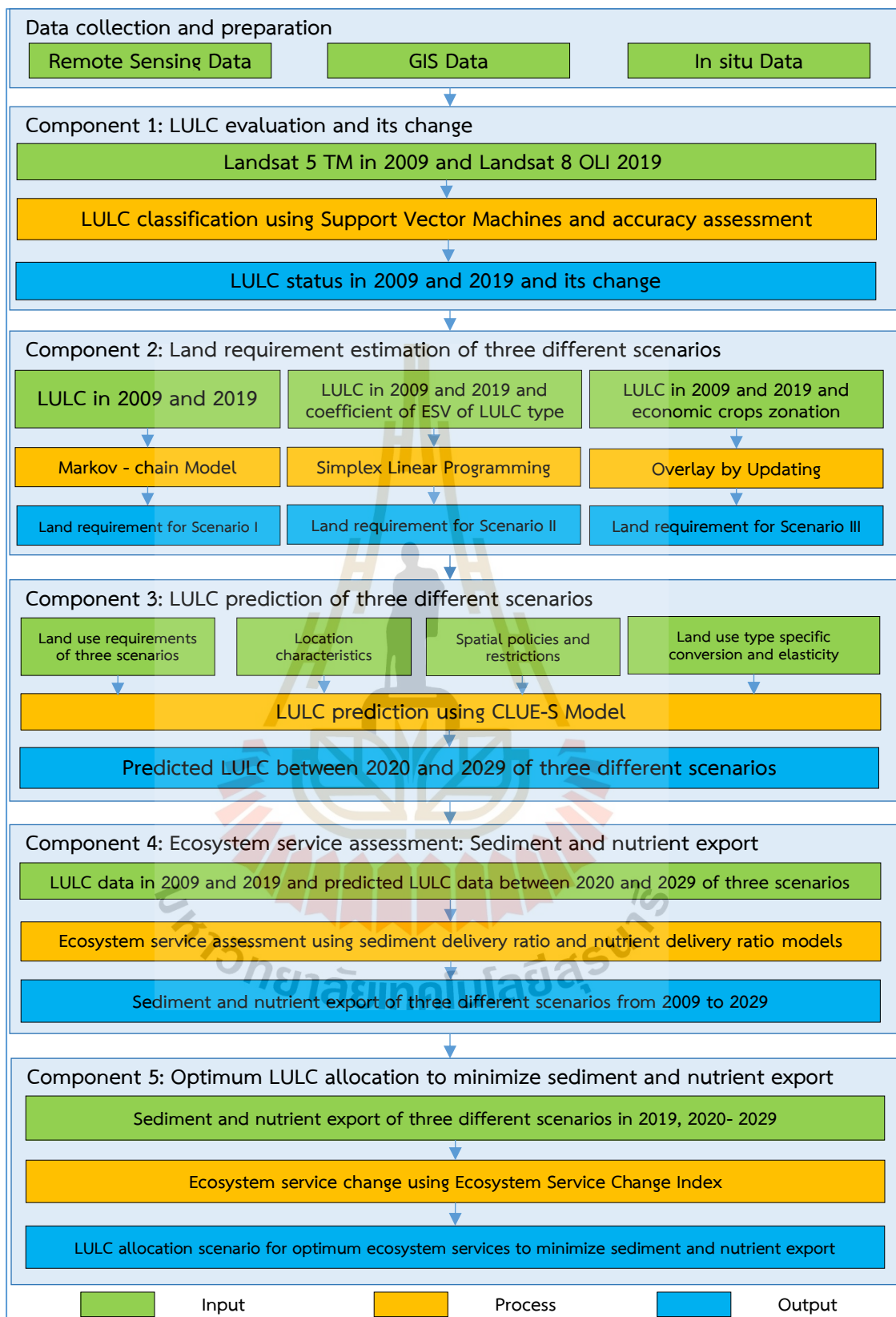


Figure 3.1 Overview of the research framework.

(1) LULC Classification using SVM algorithms.

Two datasets of training areas based on ten LULC types for two Landsat images were separately prepared to define an optimal hyperplane for LULC classification using SVM algorithms of EnMap-Box software. The optimized model parameter from the EnMap-Box for both images provided by grid search, namely Gaussian radial basis function kernel, which required the gamma (γ) that defines the width of Gaussian and the regularization parameter (C), which controls the trade-off between the maximization of the margin between the training data vectors and the decision boundary plus the penalization of training errors (Van der Linden et al., 2014). In this study, the γ was 0.01 in 2009 and 0.1 in 2019, and C was 10. The standard product of scaled reflectance of Landsat 5-TM at Level 2: band 1, 2, 3, 4, 5, 7, and additional bands (Normalized Difference Vegetation Index (NDVI), Normalized Difference Moisture Index (NDMI), Soil Adjusted Vegetation Index (SAVI), Modified Normalized Difference Wetness Index (MNDWI), and DEM) were applied to classify LULC in 2009, while standard product scaled reflectance of Landsat 8-OLI at Level 2: band 2, 3, 4, 5, 6, 7, and additional bands (NDVI, NDMI, SAVI, MNDWI, and DEM) were used to classify LULC in 2019. These additional bands can enhance specific features in the study area. For example, NDVI and SAVI enhance vegetation features, NDMI and MNDWI enhance wetness regimes. DEM stratifies geographical regions for specific LULC types.

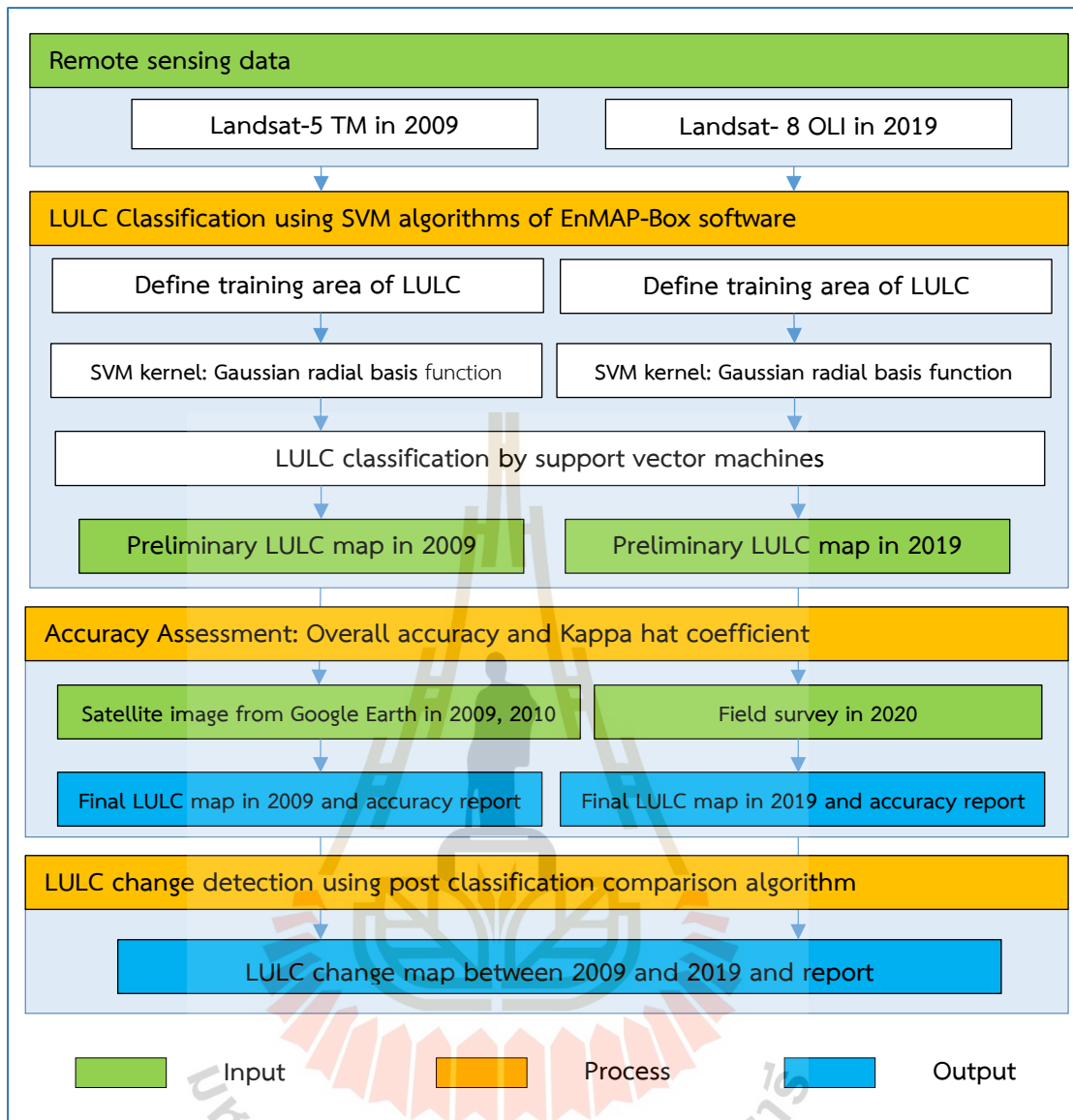


Figure 3.2 Schematic workflow of LULC evaluation and its change.

In this study, the LULC classification system was modified from the standard land use classification system of the Land Development Department included (1) urban and built-up area (UR), (2) paddy field (PD), (3) field crop (FC), (4) para rubber (RB), (5) perennial trees and orchards (PO), (6) forest land (FO), (7) water body (WB), and (8) rangeland (RL), (9) wetland (WL), and (10) miscellaneous land (ML).

Besides, ten LULC types were adapted subject to the ecosystem service value of each LULC type which was modified from Mamat, Halik, and Rouzi (2018) for Scenario II. The description of the LULC type was summarized in Table 3.2.

Table 3.2 Description of LULC classification system.

Code	Modified LULC type for SVM	Modified LULC type for ESV	LDD land use class
1	Urban and built-up area	Construction land	Urban and built-up area
2	Paddy field	Cultivated land	Paddy field
3	Field crop	Cultivated land	Field crops
4	Para rubber	Forest land	Para rubber
5	Perennial trees and orchards	Forest land	Mixed perennial trees and orchards which exclude para rubber
6	Forest land	Forest land	Natural forest and man-made forest
7	Water body	Water body	River, canal, natural water resource, reservoir, pond, irrigation canal
8	Rangeland	Rangeland	Scrub, grass, and pasture
9	Wetland	Wetland	Marsh and swamp
10	Miscellaneous land	Unused land	Bush fallow, mine, laterite pit, soil pit, garbage dump, landfill, rock outcrop

(2) Accuracy assessment

The preliminary LULC maps in 2009 and 2019 were assessed overall accuracy and Kappa hat coefficient based on reference LULC data from very high spatial resolution image of Google Earth in 2009/2010 and field survey in 2020, respectively. In this study, the classified LULC maps in 2009 and 2019 were assessed the accuracy with several sampling points based on multinomial distribution and allocated sample points using the stratified random sampling technique as suggested by Congalton and Green (2009). The number of sample points for accuracy assessment was 788, with a confidence level of 95 percent.

(3) LULC change detection

Final LULC maps in 2009 and 2019 were applied to detect LULC change using a post-classification comparison algorithm to describe from-to-change information among LULC classes between 2009 and 2019, as suggested by Jensen (2015).

3.3.2 Land requirement estimation of three different scenarios

In this study, the land requirement was estimated corresponding to three different scenarios: Scenario I (Trend of LULC evolution), Scenario II (Maximization of ecosystem service values), and Scenario III (Economic crop zonation), to predict LULC between 2020 and 2029. The explanations of the land requirement for each scenario are defined as follows.

Land requirement estimation for Scenario I. The land requirements between 2020 and 2029 were calculated based on the annual change rate of LULC between 2009 and 2019 from the transition area matrix using the Markov Chain model. The Markov stochastic process generally describes the probability of change from one state to another, i.e., from one land use type to another, using a transition probability matrix. In this study, the transition probability matrix of land use change derived from LULC in 2009 and 2019, which applied to provide estimations of the probability that a land cover type in each pixel at the state i in T_m changes to another land cover type or remain in the same class in the state j in T_{m+1} (Zhang et al., 2011). The transition probability matrix is:

$$P=P_{ij} = \begin{bmatrix} P_{00} & P_{01} & \dots & P_{0m} \\ P_{10} & P_{11} & \dots & P_{1m} \\ \dots & \dots & \dots & \dots \\ P_{m1} & P_{m2} & \dots & P_{mm} \end{bmatrix} \quad (3.1)$$

Where, P_{ij} is the probability of transition from one land use to another, m is the type within land use of the area studied, P_{ij} values are within the range between zero and one.

Land requirement estimation for Scenario II. The allocated LULC areas between 2020 and 2029 were performed by linear programming with the simplex method of What's Best software under MS-Excel software. This scenario applied a simple benefit transfer method to estimate economic values for ecosystem service values (Costanza et al., 1997). Thus, the ecosystem service value of each LULC type (USD/ha/year) by Mamat, Halik, and Rouzi (2018) was used as the coefficient values for ESV estimation (Table 3.3). In this study, the objective function aimed to maximize ecosystem service values subject to constraints that define the possible values that

the variables of a linear programming problem may take in each LULC type of Scenario II.

Table 3.3 Coefficient value for different LULC types for ESV estimation.

Ecosystem services category	Ecosystem services function	Ecosystem service value of each LULC type (USD/ha/year)						
		Constructi on land	Cultivate d land	Forest land	Water body	Range land	Wet land	Unused land
1. Regulating services	1.1 Gas regulation	0.0	74.7	299.4	0.0	104.0	268.9	4.2
	1.2 Climate regulation	0.0	133.0	282.1	68.7	108.0	2,554.7	9.0
	1.3 Waste treatment	0.0	245.0	119.2	2,719.0	91.5	2,716.0	18.0
2. Supporting services	2.1 Soil formation	0.0	218.1	278.6	1.5	155.0	255.5	11.8
	2.2 Biodiversity protection	0.0	106.1	312.6	372.0	130.0	373.5	27.7
3. Provision services	3.1 Water supply	0.0	89.6	283.5	3,047.7	105.0	2,315.6	4.8
	3.2 Food production	0.0	149.4	22.9	14.9	29.8	44.8	1.4
	3.3 Raw materials	0.0	14.9	206.5	1.5	25.0	10.5	2.8
4. Cultural services	4.1 Recreation and culture	12.7	1.5	144.2	648.4	60.3	829.2	16.6
Total		12.7	1,032.3	1,949.0	6,873.7	808.6	9,368.7	96.3

Source: Modified from Mamat, Halik, and Rouzi (2018).

The objective function and constraints for scenario II were solved to maximize ecosystem service values, as shown in Equation 3.2.

$$Z_{Max} = [12.7(X_1) + 1,032.3(X_2) + 1,032.3(X_3) + 1,949.0(X_4) + 1,949.0(X_5) + 1,949.0(X_6) + 6,873.7(X_7) + 808.6(X_8) + 9,368.7(X_9) + 96.3(X_{10})] \quad (3.2)$$

Where Z_{max} is the objective function of scenario II for ESV maximization, X_1 is urban and built-up area (UR), X_2 is paddy field (PD), X_3 is field crop (FC), X_4 is para rubber (RP), X_5 is perennial trees and orchards (PO) X_6 is forest land (FO), X_7 is water body (WB), X_8 is rangeland (RL), X_9 is wetland (WL), and X_{10} is miscellaneous land (ML). The decision variables are the set of quantities determined to solve the problem and take on a range of values within limits assigned by the constraints.

Land requirement estimation for Scenario III. The land requirements between 2020 and 2029 of Scenario III were estimated based on areas of suitability

classes for economic crops by the LDD and Markov Chain model. In this study, areas of three suitability classes (S1, S2, and S3) of nine economic crops (Table 3.4 and Figure 3.3) were combined according to the modified LULC classification system and then applied to estimate the land requirement for each LULC type. Meanwhile, land requirements for non-agricultural LULC types include urban and built-up areas, forest land, waterbody, rangeland, wetland, and miscellaneous land, were first estimated based on the Markov Chain model. Then, those areas were updated by the land requirement of regrouped economic crops.

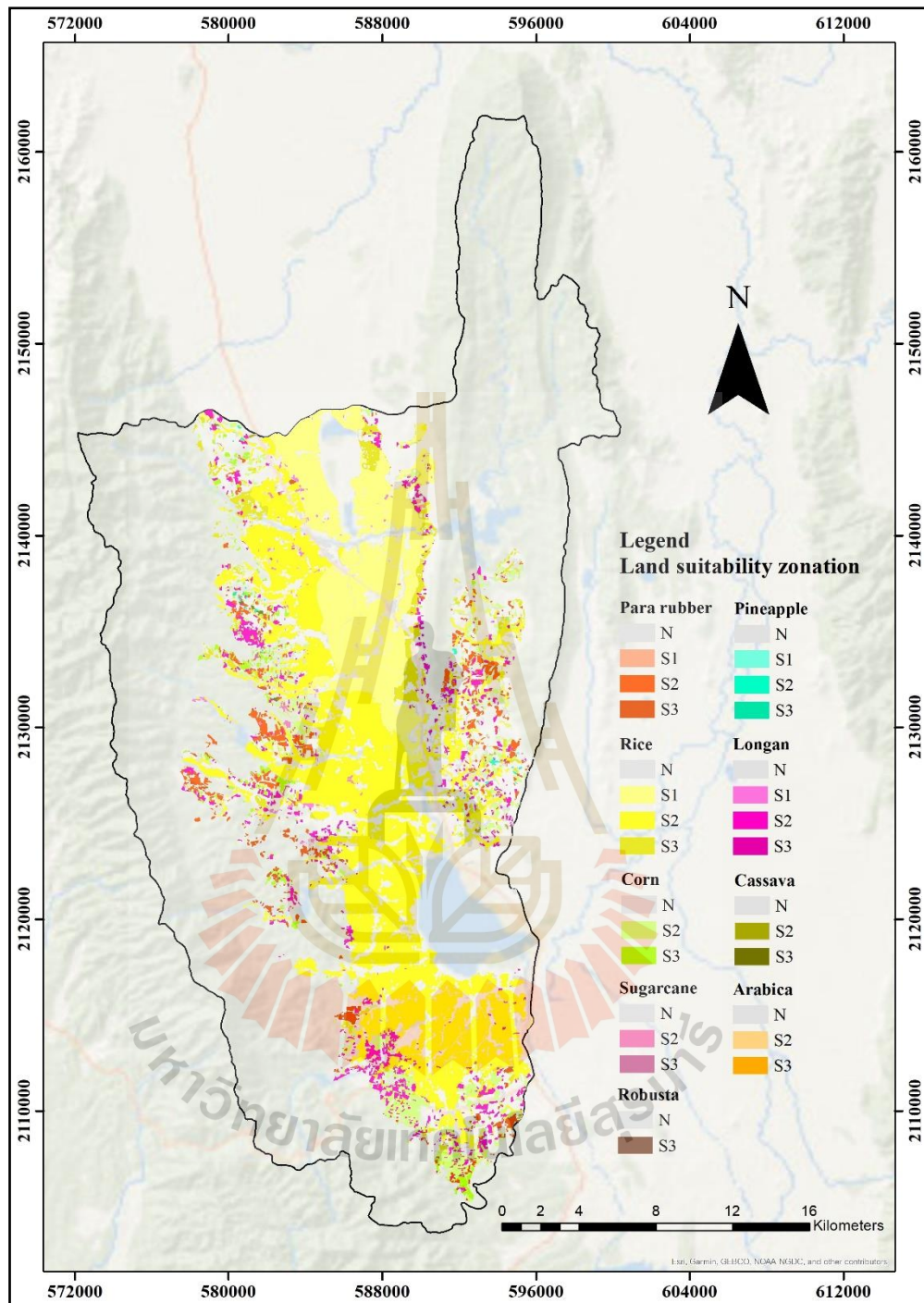
Table 3.4 The economic crop zonation by LDD.

Code	Economic crop types	Land suitability zonation			
1	Para rubber	S1	S2	S3	N
2	Pineapple	S1	S2	S3	N
3	Rice	S1	S2	S3	N
4	Corn	-	S2	S3	N
5	Longan	S1	S2	S3	N
6	Cassava	-	S2	S3	N
7	Sugarcane	-	S2	S3	N
8	Arabica	-	S2	S3	N
9	Robusta	-	-	S3	N

Note: S1: high suitability area, S2: moderate suitability area, S3: low suitability area; and N: Not suitable

Source: Land Development Department (2017, 2018).

The derived results of three different Scenarios were applied for LULC prediction between 2020 and 2029 in the next component. The schematic workflow of land demand estimation of three different scenarios is displayed in Figure 3.4.



Source: Land Development Department (2017, 2018).

Figure 3.3 Spatial distribution of economic crop zonation in Upper Ing watershed.

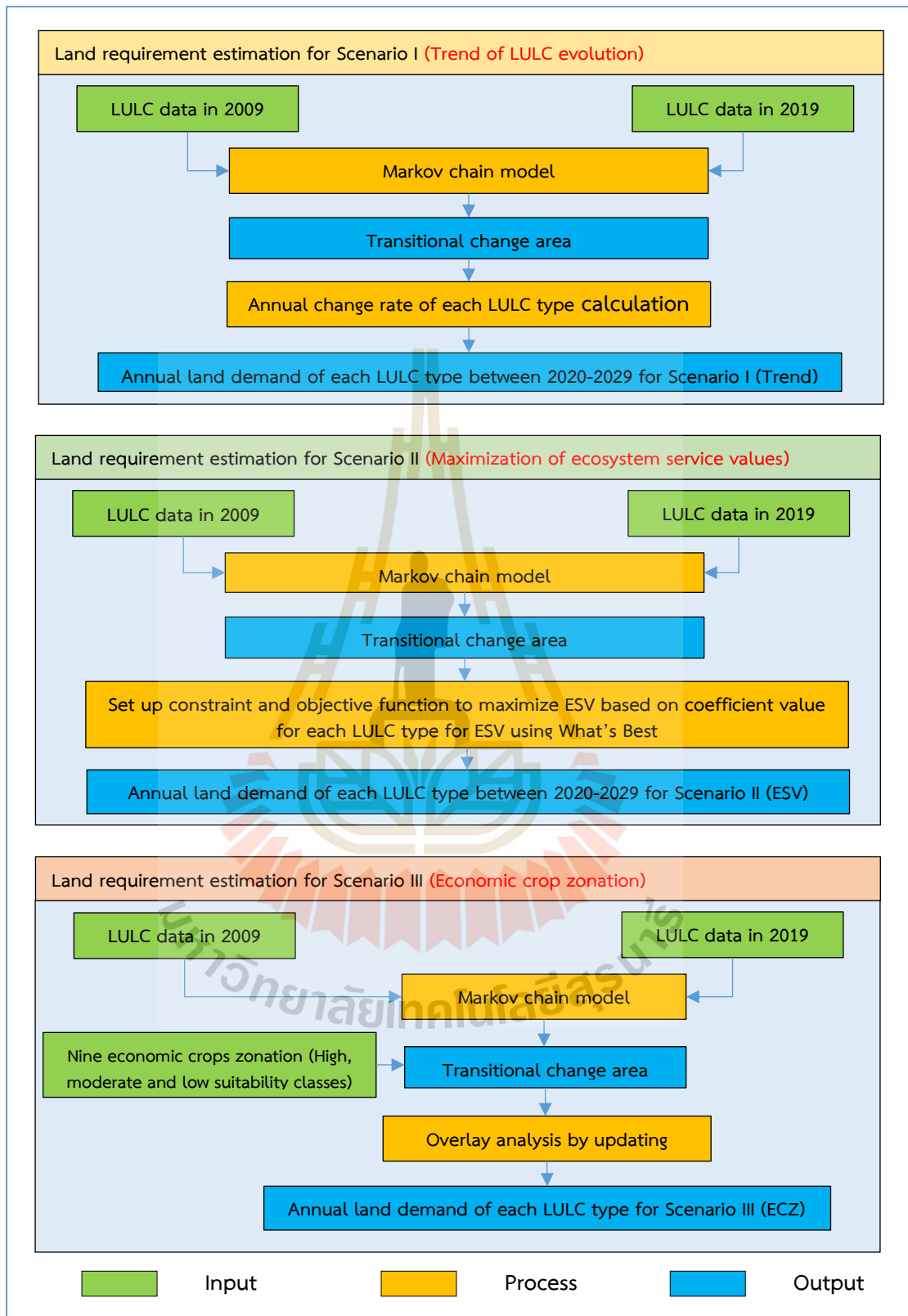


Figure 3.4 Schematic workflow of land demand estimation of three different scenarios.

3.3.3 LULC prediction of three different scenarios

The required parameters for the CLUE-S model include (1) spatial policies and restrictions, (2) land-use type-specific conversion setting, which includes conversion matrix and elasticity of LULC change, (3) land requirement which derives from the previous component in three different scenarios, and (4) LULC type location preference (driving factors). LULC type location preference according to driving force on LULC change was identified by performing logistic regression analysis. The driving factors include physical (soil drainage, distance to stream, distance to waterbody, distance to village, slope, distance to road, distance to fault, annual rainfall, elevation), and socio-economic data (income per capita and population density at sub-district level), were modified based on Iamchuen and Thepwong (2020). In this study, the multicollinearity test was examined using the variance inflation factor (VIF) value to prevent the correlation among driving factors. The general rule of thumb, the VIF values should not exceed 10 (Traore and Watanabe, 2017; Kamwi et al., 2018). Then, logistic regression analysis proceeded to identify the significant driving factors for specific LULC type allocation.

The dynamics of LULC change between 2020 and 2029 were simulated under the CLUE-S model (Figure 3.5).

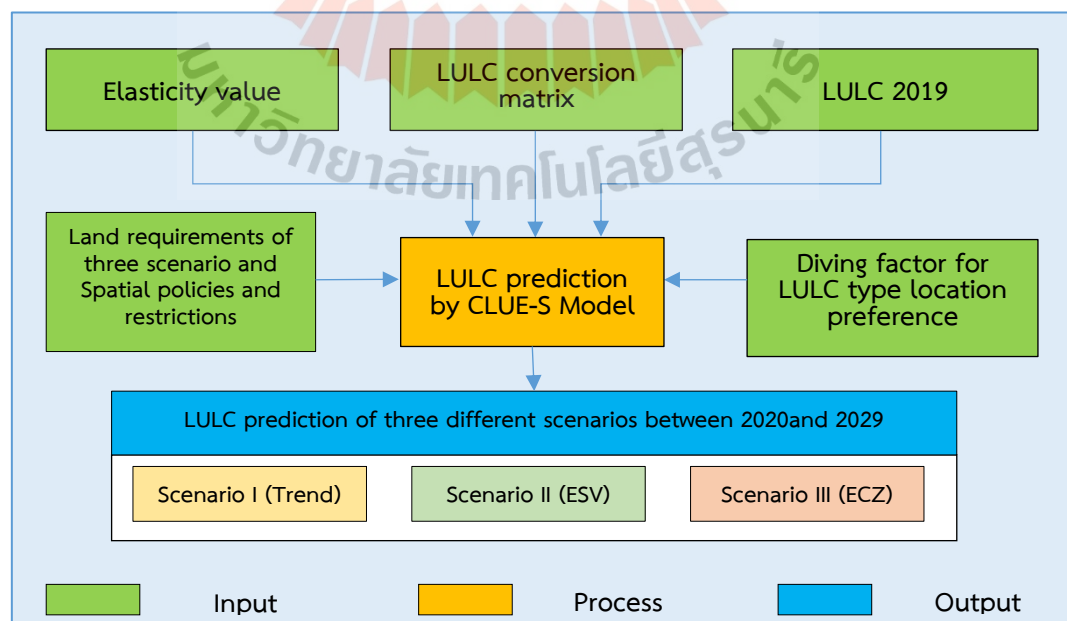


Figure 3.5 Schematic workflow of LULC Prediction of three different scenarios.

3.3.4 Ecosystem service assessment: Sediment and nutrient export

Under this component, the base year LULC in 2019 and the predicted LULC between 2020 and 2029 of three different scenarios as primary input data were applied to estimate sediment and nutrient exports based on the required data and parameters. In practice, the sediment delivery ratio (SDR) model and nutrient delivery ratio (NDR) model under the InVEST software Version 3.8.9 were applied to estimate sediment and nutrient exports over the study period of three different scenarios.

3.3.4.1 Sediment export estimation

The sediment export is the amount of sediment eroded in the watershed from overland sources and delivered to the stream. In principle, the sediment delivery ratio (SDR) model in the InVEST toolset is firstly applied to calculate the amount of annual soil loss using the Revised Universal Soil Loss Equation (RUSLE). The schematic workflow of sediment export estimation is displayed in Figure 3.6. The required factors for soil erosion estimation are summarized below.

(1) **Digital elevation model (DEM).** DEM was downloaded from the USGS web service (<https://earthexplorer.usgs.gov>), filled up the holes, and cut outlier data using the Hydrology tool in ESRI ArcGIS as shown in Figure 3.7.

(2) **Rainfall erosivity (R).** The rainfall erosivity factor was calculated based on monthly rainfall data, as suggested by Wischmeier and Smith (1978) using Eq. 3.3. Rainfall data collected from the Thailand Meteorological Department (TMD, 2020) were used to calculate the R factor for the calibration years (2011 to 2015) and validation years (2016 to 2018) of the SDR model. Besides, the predicted rainfall data between 2020 and 2029 from the National Center for Atmospheric Research (NCAR, 2020) were used to compute the R for the SDR of three different scenarios. The rainfall erosivity factor for calibration years, validation years, the base year, and predicted years of the SDR model are shown in Figure 3.8 and Table 3.5.

$$R = \sum_{i=1}^{12} 1.735 \times 10^4 \left(1.5 \log_{10} \left(\frac{P_i^2}{P} \right) - 0.08188 \right) \quad (3.3)$$

Where R is the rainfall erosivity factor ($\text{MJ mm ha}^{-1} \text{ h}^{-1} \text{ y}^{-1}$), P_i is the monthly rainfall (mm), and P is the annual rainfall (mm).

(3) Soil erodibility (K). Soil erodibility was mainly applied from standard values of LDD (2000), which were extracted from soil series data, whereas its value under slope complex was extracted from the geology unit as a summary in Tables 3.6 and 3.7, and Figure 3.7.

(4) Slope length gradient factor (LS). The LS factor was calculated from the Digital Elevation Model (DEM) with a method developed by Desmet and Desmet and Govers (1996), as mentioned in Section 2.4.

(5) Land use and land cover (LULC). LULC data for calibration year (2011 to 2015), LULC data for validation (2016 to 2018), LULC 2019 for the base year, and LULC data for three scenarios (2020 to 2029) were used as input data to assign C and P factor values based on the standard assignment of LDD in 2000. In practice, values of C and P factors were prepared as a biophysical table, as shown in Table 3.8.



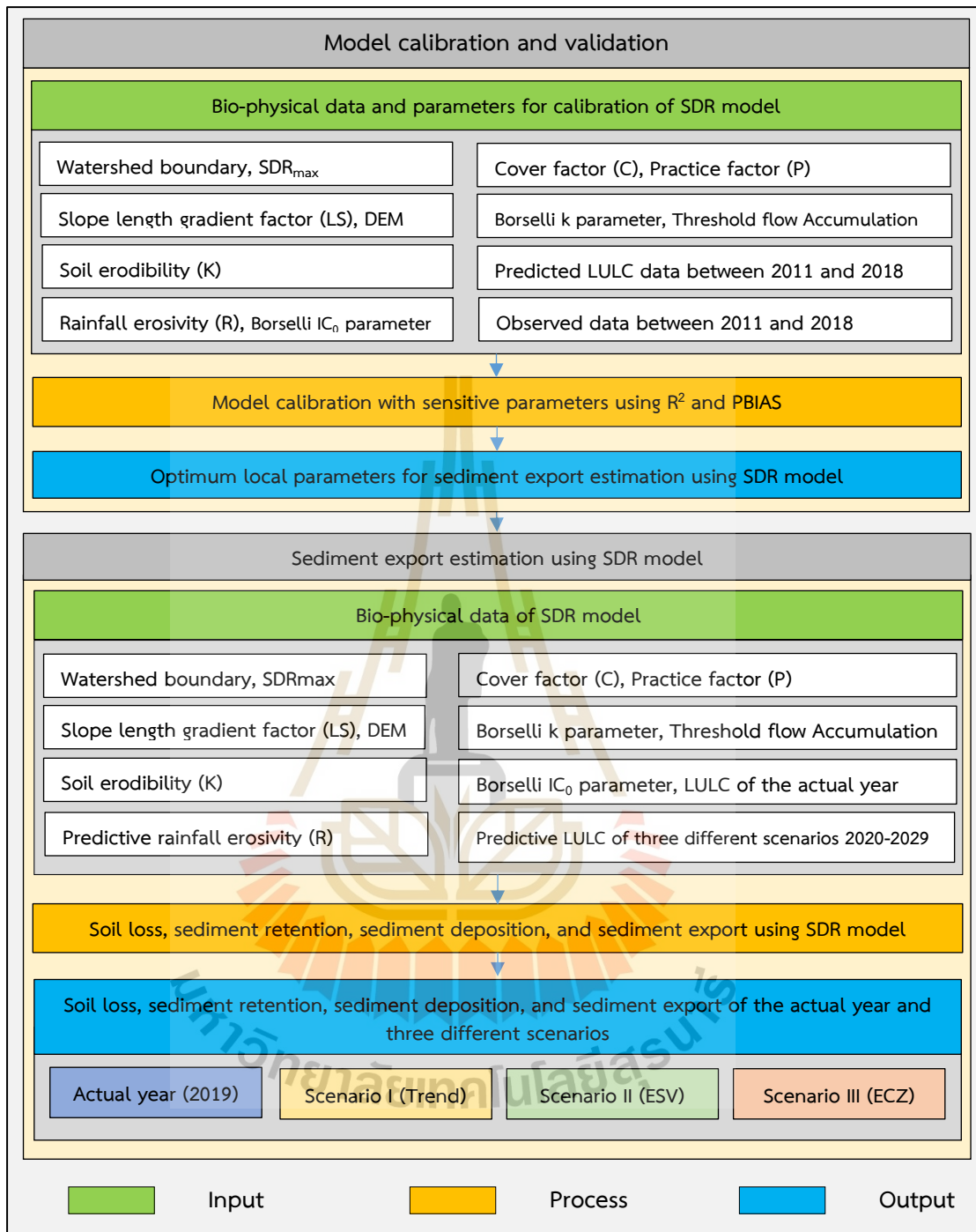


Figure 3.6 Schematic workflow of sediment export estimation.

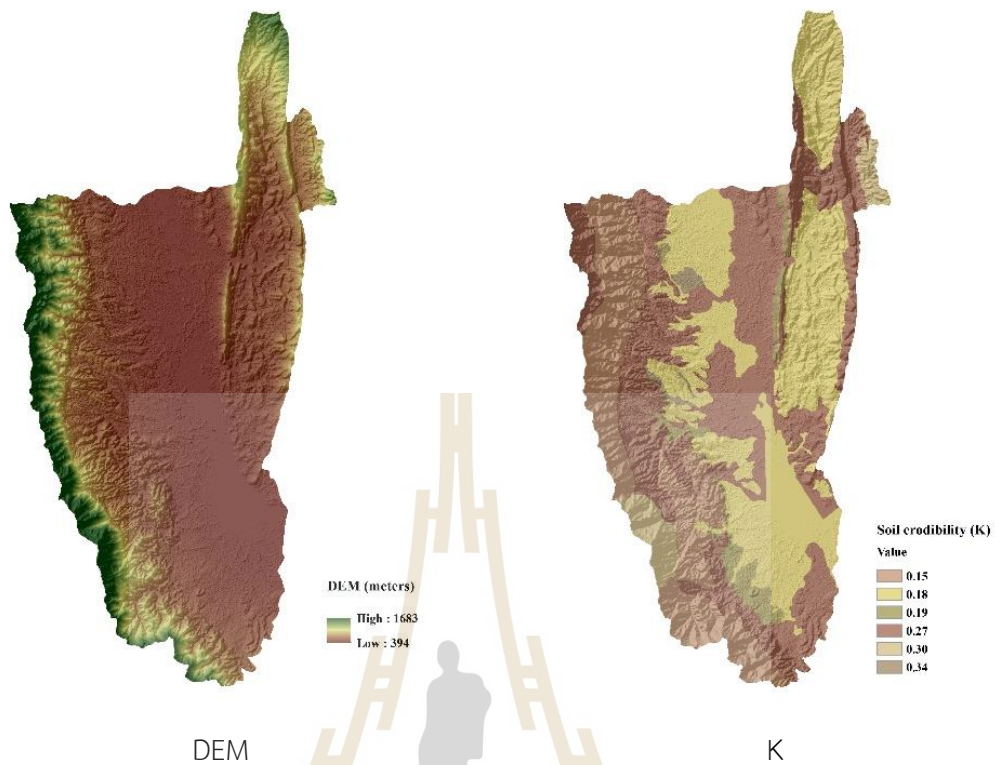


Figure 3.7 Digital elevation model (DEM) and soil erodibility (K).



Figure 3.8 The rainfall erosivity factor for sediment export estimation: Data from 2011 to 2015 for model calibration, data from 2016 to 2018 for model validation, data in 2019 for actual sediment export estimation, and data from 2020 to 2029 for sediment export estimation under three scenarios.

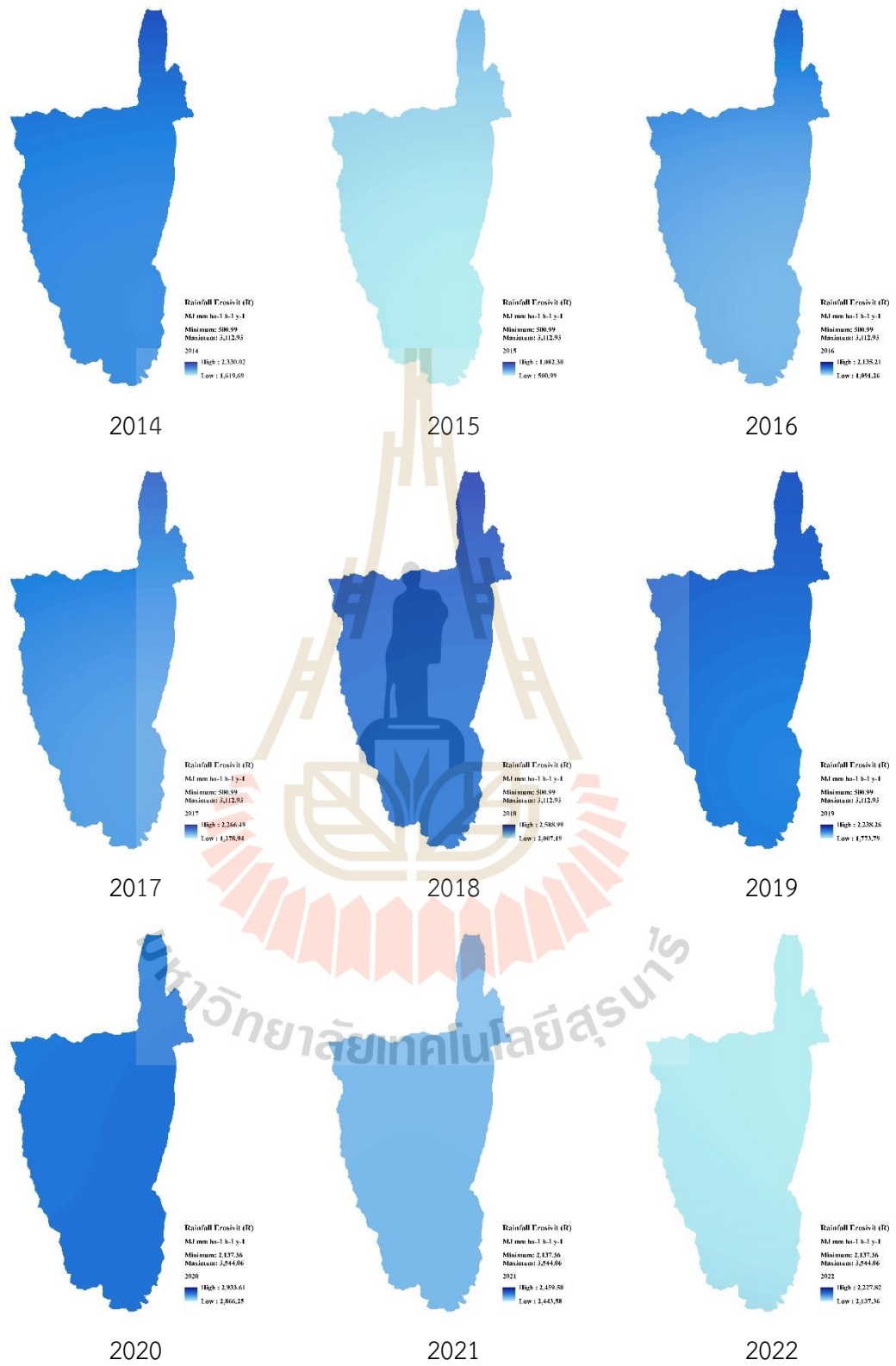


Figure 3.8 (Continued).

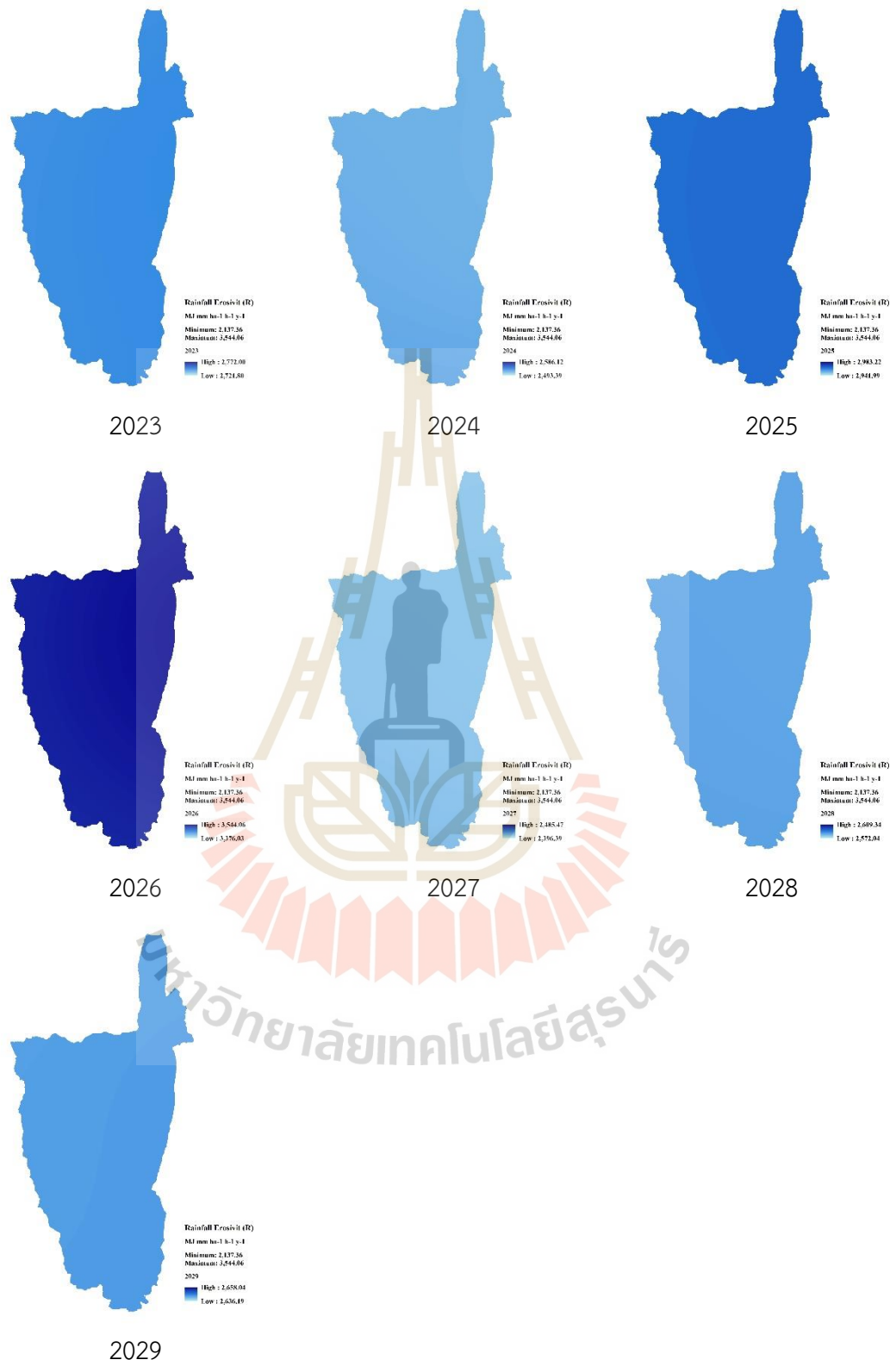


Figure 3.8 (Continued).

Table 3.5 Basic statistics of rainfall erosivity factor between 2011 and 2019.

Year	Rainfall erosivity (MJ mm ha ⁻¹ h ⁻¹ y ⁻¹)				
	MIN	MAX	MEAN	RANGE	STD
2011	1,513.31	4,815.35	2,821.01	3,302.04	1,290.48
2012	1,797.22	3,716.74	2,415.87	1,919.52	805.14
2013	1,127.41	3,936.73	2,079.30	2,809.32	1,094.11
2014	1,254.66	3,305.54	1,827.60	2,050.88	849.18
2015	500.99	1,705.82	970.27	1,204.83	471.52
2016	1,005.97	3,264.81	1,930.66	2,258.83	926.72
2017	1,378.94	3,218.46	2,104.00	1,839.52	720.09
2018	1,347.06	3,467.88	2,027.64	2,120.82	855.87
2019	1,773.79	4,663.38	2,944.67	2,889.59	1,115.96

Table 3.6 Soil series and soil erodibility factor values.

Soil series	Erodibility factor value
Chaing Rai series	0.27
Hang Chat series	0.27
Hang Chat/Renu association	0.27
Hang Dong series	0.18
Lampang series	0.34
Mae Rim/Hang Chat Association	0.27
Mae Sai series	0.27
Nan series	0.27
Phan series	0.18
Phayao series	0.18
Phimai series	0.18
Pran Buri, mottle Variant	0.27
Tha Muang/Sanphaya Association	0.27
Tha Yang/Lat Ya Association	0.27

Source: LDD, 2000.

Table 3.7 Geology unit and soil erodibility factor values.

Geology units	Erodibility factor value
Jurassic (J)	0.15
Jurassic- Cretaceous (JK)	0.27
Cretaceous (K)	0.27
Permian (P)	0.15
Quaternary Alluvium (Qa)	0.19
Quaternary (Qc)	0.27
Pleistocene (Qt)	0.27
Triassic (Trhh)	0.27
Igneous rock	0.30

Source: LDD, 2000.

Table 3.8 The values of the C and P factors corresponding to each LULC class in a biophysical table.

LULC code	LULC type	C factor of RUSLE	P factor of RUSLE
1	Urban	0.000	0.000
2	Paddy field	0.280	0.100
3	Field crop	0.340	1.000
4	Para rubber	0.150	1.000
5	Perennial tree and orchard	0.150	1.000
6	Forest land	0.001	1.000
7	Water body	0.000	0.000
8	Rangeland	0.032	1.000
9	Wetland	0.000	0.000
10	Miscellaneous land	0.800	1.000

Source: LDD, 2000.

After that, the model calculates the sediment delivery ratio using a connectivity index (*IC*), threshold flow accumulation, and maximum SDR to indicate sediment retention. The SDR value was calculated as suggested by Borselli et al. (2008) as:

$$SDR_i = \frac{SDR_{max}}{1 + \exp\left(\frac{IC_0 - IC_i}{k}\right)} \quad (3.4)$$

Where, SDR_{max} is the maximum theoretical SDR, set to an average value of 0.8 (Vigiak et al., 2012), and IC_0 and k are calibration parameters that define the shape of the SDR-IC relationship (Sigmoid function).

Finally, the sediment reaches the stream at the outlet of the Upper Ing watershed. The sediment export was calculated from the amount of annual soil loss multiply by sediment delivery ratio as:

$$E_i = RUSLE_i \cdot SDR_i \quad (3.5)$$

Where, E_i is the sediment export erodes from any LULC.

In this study, the observed sediment data from 2011 to 2015 from the PCD were applied to calibrate the SDR model based on the selected parameters, namely, TFA, k_b , and IC_0 as suggested by Vigiak et al. (2012). Meanwhile, the observed sediment data from 2016 to 2018 from the PCD were applied to validate the model. The coefficient of determination (R^2) and percent bias ($PBIAS$) were applied for the calibration and validation process using Equations 3.6 and 3.7, respectively.

$$R^2 = \left\{ \frac{\sum_{i=1}^n (X_s - \bar{X}_s) (X_o - \bar{X}_o)}{[\sum_{i=1}^n (X_s - \bar{X}_s)^2 \sum_{i=1}^n (X_o - \bar{X}_o)^2]^{0.5}} \right\}^2 \quad (3.6)$$

Where \bar{X}_o is the observed export value at station i , \bar{X}_o is the average of observed export value over the validation period, X_s is the simulated export value at station i , and \bar{X}_s is the average simulated export value over the validation period. i is the number of stations, and n is the total count of the data pair. The value of R^2 varies from 0 to 1.

$$PBIAS = \frac{\sum_{i=1}^n (X_i^o - X_i^s)}{\sum_{i=1}^n (X_i^o)} \times 100 \quad (3.7)$$

Where X_i^o is an observed export value at time step i , and X_i^s simulated export value at time step i .

The calibration process could be accepted if the values from two different performance ratings were satisfied, as suggested by Moriasi et al. (2007) and

Me, Abell, and Hamilton (2015) (Table 3.9). Then, the parameter can be used for the validation process, actual sediment export estimation, and sediment export estimation under three scenarios.

Table 3.9 Criteria for model performance.

Model evaluation	Constituent	Performance ratings			
		Unsatisfactory	Satisfactory	Good	Very good
R^2	SS	< 0.5	0.5-0.6	0.6-0.7	0.7-1
	TP, TN				
<i>PBIAS</i>	SS	> 55	30-55	15-30	< 15
	TP, TN	> 70	40-70	25-40	< 25

Note: SS: suspended sediment, TP: total phosphorus and TN: total nitrogen.

Source: Moriasi, Arnold, Liew, Bingner, Harmel, and Veith (2007) and Me, Abell, and Hamilton (2015).

3.3.4.2 Nutrient export estimation

Nutrient export is nutrient sources from watersheds and their transport to the stream and end at the outlet. The nutrient delivery ratio (NDR) model required a specific factor and parameter to run the model. Some factors in this model were used the same as the SDR model, including DEM, LULC, *TFA*, and K_b . Other parameters, i.e., nitrogen and phosphorus loads, nutrient runoff proxy, maximum retention efficiency, and critical length, were added. The schematic workflow of nutrient export estimation is displayed in Figure 3.9. The required factors for nitrogen export estimation are summarized below.

(1) Nutrient runoff proxy (RP). The nutrient runoff proxy is used for calculating the runoff potential index. The runoff proxy was interpolated by inverse distance weighted using annual precipitation between 2011 and 2019 (Table 3.10). Annual rainfall was collected from five rain gauge stations surrounding the study area from the Thailand Meteorological Department (TMD, 2020). In addition, the predicted rainfall data between 2020 and 2029 from the National Center for Atmospheric Research (NCAR, 2020) were used to obtain annual rainfall for the NDR of three

different scenarios. The annual rainfall for calibration year, validation year, base year, and predicted year of the NDR model are shown in Figure 3.10.

(2) Land use and land cover (LULC). LULC data represents the influence of the nutrient delivery to the stream. LULC data were used as input data to assign the nutrient loading for each LULC class (load_n, load_p), as a summary in Table 3.11.

Table 3.10 Basic statistics of annual rainfall between 2011 and 2019.

Year	Annual Rainfall (mm.)				
	MIN	MAX	MEAN	RANGE	STD
2011	1,398.90	2,042.60	1,761.70	643.70	275.08
2012	1,133.40	1,904.50	1,360.10	771.10	319.47
2013	1,053.20	2,141.50	1,323.54	1,088.30	459.56
2014	1,046.10	1,470.00	1,170.30	423.90	174.36
2015	814.80	1,350.80	1,030.86	536.00	212.76
2016	1,080.00	1,875.80	1,363.30	795.80	321.03
2017	1,205.30	2,244.70	1,531.90	1,039.40	415.34
2018	1,039.50	1,939.30	1,337.00	899.80	376.22
2019	712.40	1,275.00	1,047.80	562.60	225.92

(3) Maximum retention efficiency (eff_n, eff_p). The maximum retention efficiency indicates the proportion of the amount of nutrient retention by vegetation. The value for each LULC class varied between zero and one (Table 3.11).

(4) Critical length (crit_{len}_n, crit_{len}_p). The distance that a patch of LULC retains nutrients in its maximum capacity. The value of critical lengths ranges from 10 to 300 meters (Mayer et al., 2007; Zhang et al., 2010). In this study, the value was firstly set to pixel resolution, with a value of 30 meters (Table 3.11).

(5) Proportion subsurface (proportion_{subsurface}_n, or p). The proportion of dissolved nutrients that travels via surface and subsurface flow. This study set the value to zero, which indicates that all nutrients are delivered via surface flow (See Table 3.11).

All of the values above were applied to the biophysical table. In this study, $load_n$, $load_p$, eff_n , eff_p values were derived from the Mekong River Commission (2017). Moreover, values of subsurface critical length and subsurface maximum retention efficiency were assigned to zero because the proportion of the nutrient was set to zero.

In the NDR model, the nutrient loads are defined based on the LULC map and associated loading rates. Then, the model calculates LULC-based loads and runoff potential index to approximate modified loads, which are divided into sediment-bound (surface flow) and dissolved parts (subsurface flow). After that, nutrient delivery is computed for surface NDR and subsurface NDR based on the properties of pixels belonging to the same flow path (particularly their slope and retention efficiency of the land use).

In this study, the model was computed for nutrients transported by surface flow. The surface nutrient delivery ratio is the product of a delivery factor, representing the ability of downstream pixels to transport nutrients without retention. A topographic index represents the position on the landscape. The surface NDR value was calculated as:

$$NDR_i = \frac{NDR_{0,i}}{1 + \exp\left(\frac{IC_i - IC_0}{k}\right)} \quad (3.8)$$

Where, $NDR_{0,i}$ is the proportion of a nutrient that is not retained by downstream pixels, which is based on the maximum retention efficiency of the land between a pixel and the stream, IC_i is a topographic index, and IC_0 and k are calibration parameters that define the shape of the NDR-IC relationship.

Finally, the total nutrient export at the outlet of the watershed is estimated by-product of the load and the NDR as:

$$x_{expi} = load_{surf, i} \cdot NDR_{surf, i} \quad (3.9)$$

Where, x_{expi} is the nutrient export from any LULC.

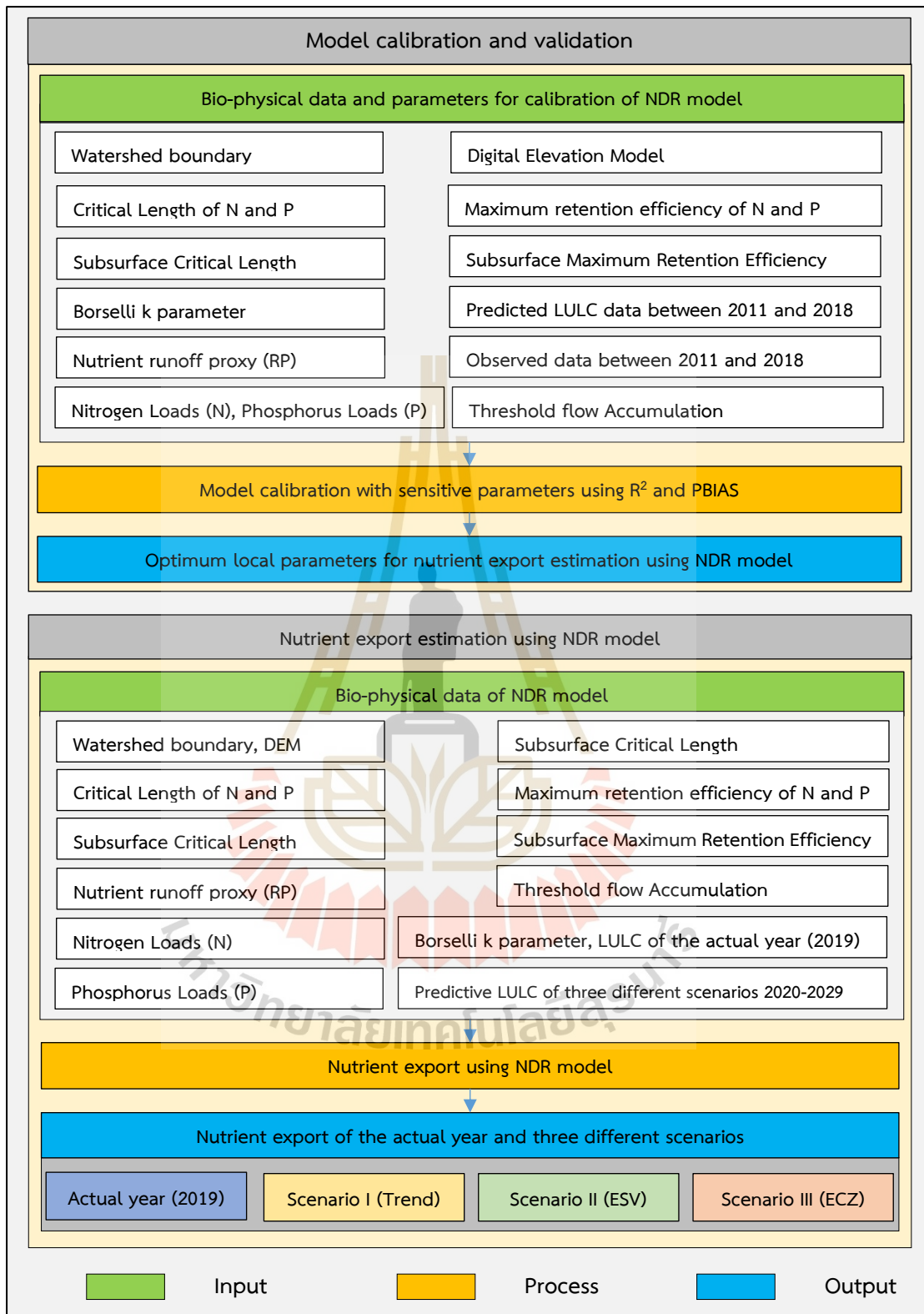
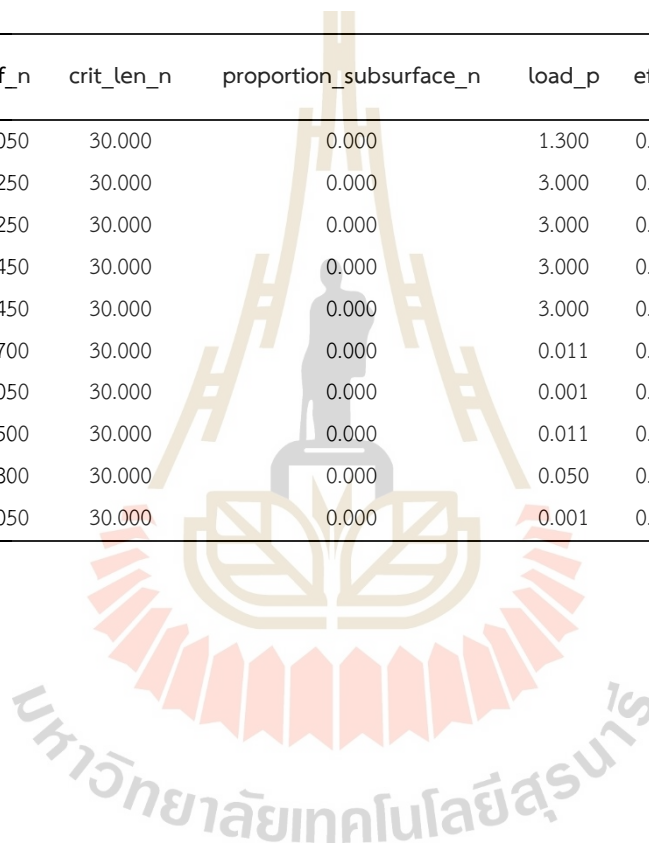


Figure 3.9 Schematic workflow of nutrient export estimation.

Table 3.11 Biophysical table containing data related to nitrogen, phosphorus and requires values of nutrients corresponding to each LULC class.

LULC code	LULC type	load_n	eff_n	crit_len_n	proportion_subsurface_n	load_p	eff_p	crit_len_p	proportion_subsurface_p
1	Urban	7.750	0.050	30.000	0.000	1.300	0.050	30.000	0.000
2	Paddy field	11.000	0.250	30.000	0.000	3.000	0.250	30.000	0.000
3	Field crop	11.000	0.250	30.000	0.000	3.000	0.250	30.000	0.000
4	Para rubber	10.000	0.450	30.000	0.000	3.000	0.450	30.000	0.000
5	Perennial tree and orchard	10.000	0.450	30.000	0.000	3.000	0.450	30.000	0.000
6	Forest area	1.800	0.700	30.000	0.000	0.011	0.700	30.000	0.000
7	Waterbody	0.001	0.050	30.000	0.000	0.001	0.050	30.000	0.000
8	Rangeland	2.000	0.500	30.000	0.000	0.011	0.500	30.000	0.000
9	Wetland	2.000	0.800	30.000	0.000	0.050	0.800	30.000	0.000
10	Miscellaneous land	4.000	0.050	30.000	0.000	0.001	0.050	30.000	0.000

Source: Mekong River Commission (2017).



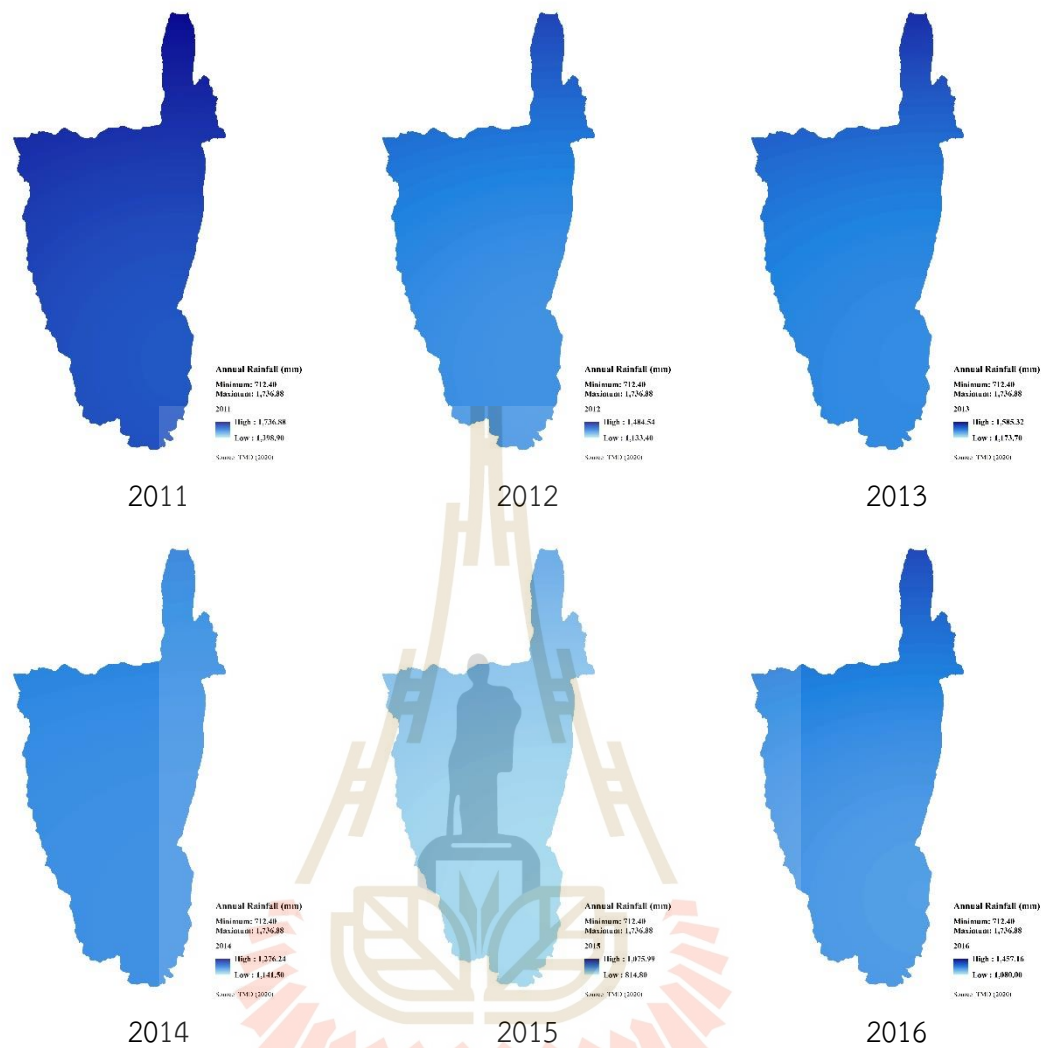


Figure 3.10 The annual rainfall as runoff proxy factor of NDR model: Data from 2011 to 2015 for model calibration, data from 2016 to 2018 for model validation, data in 2019 for actual nutrient export estimation, and data from 2020 to 2029 for nutrient export estimation under three scenarios.

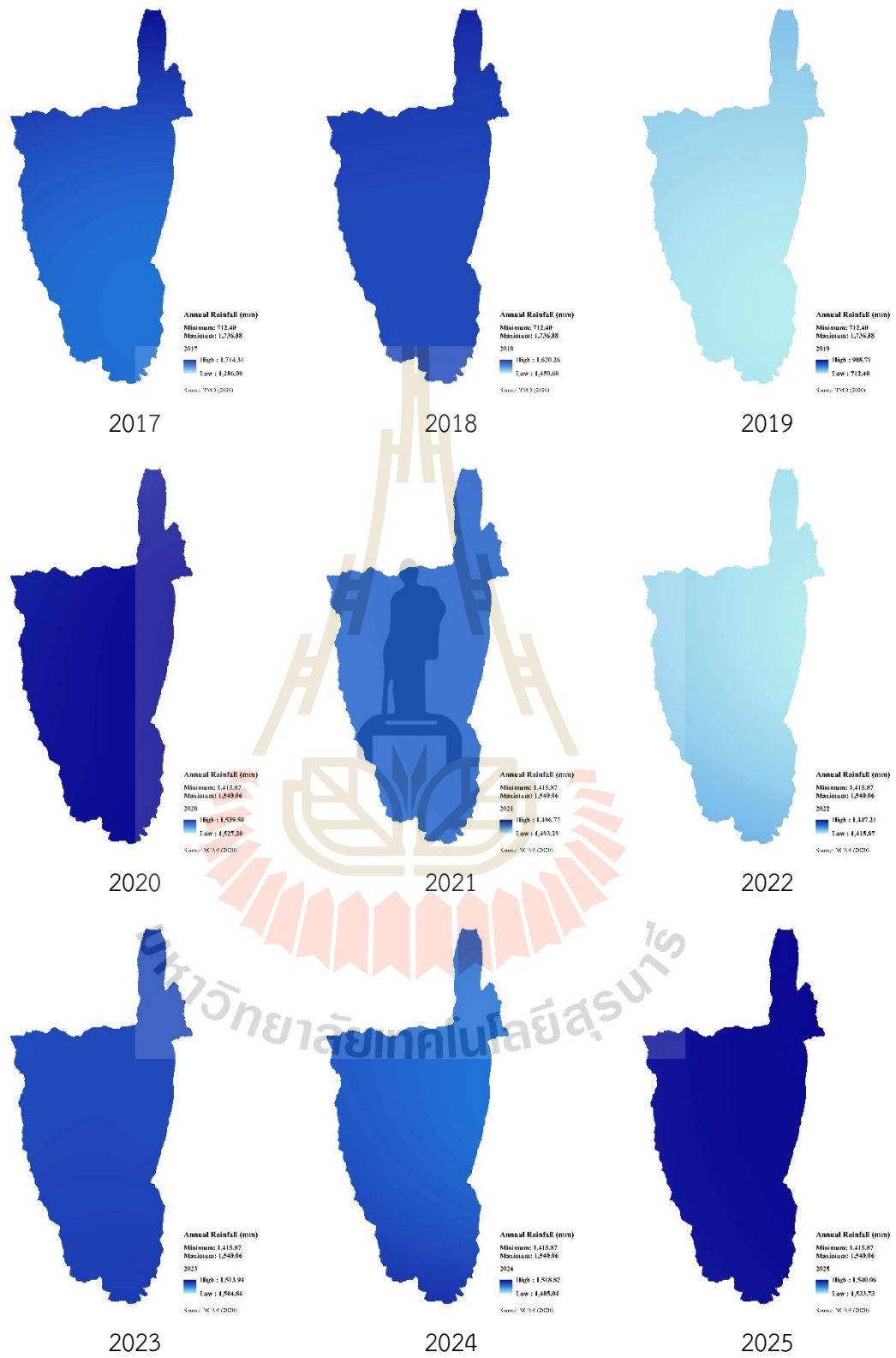


Figure 3.10 (Continued).

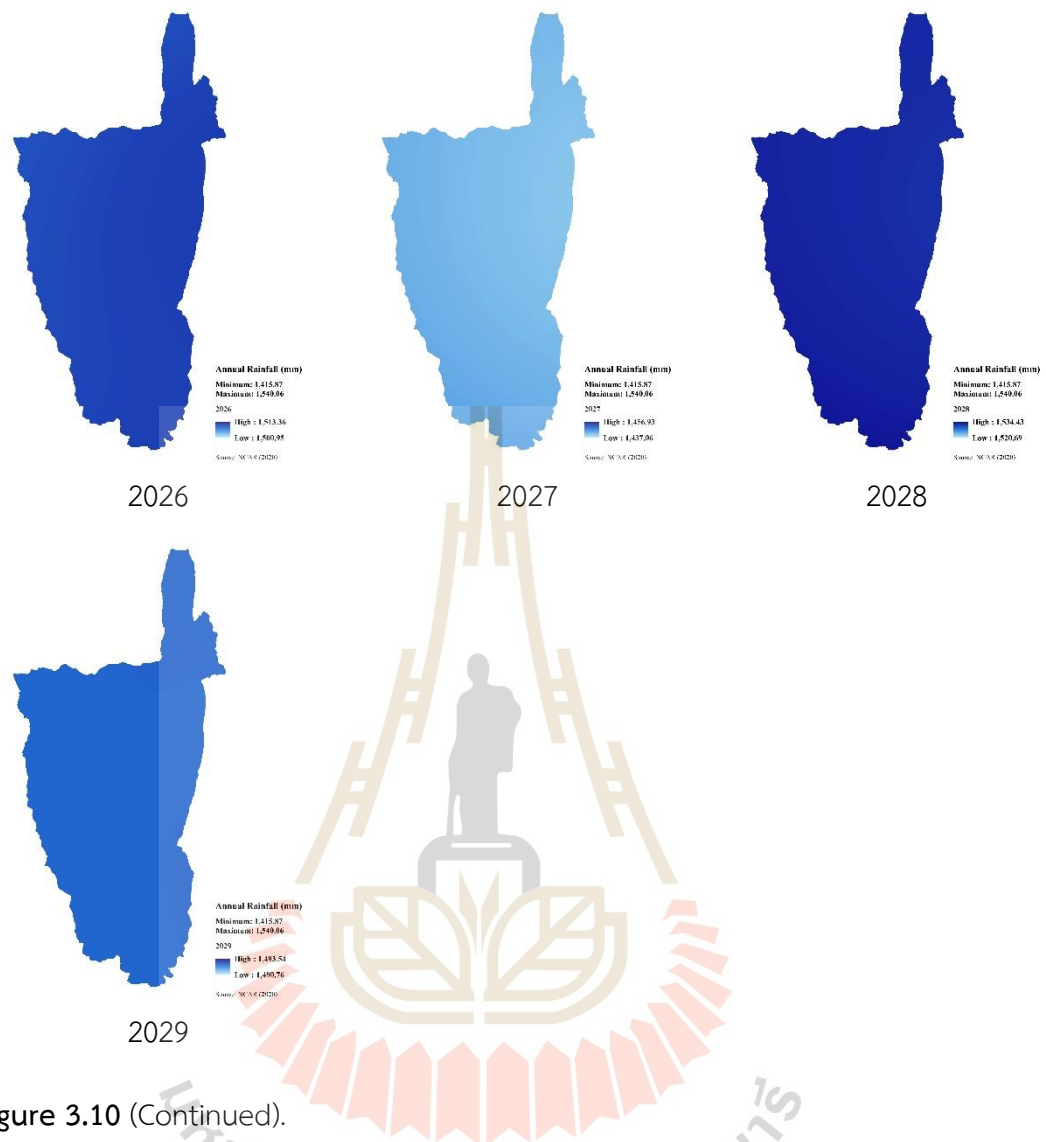


Figure 3.10 (Continued).

In this study, the observed nutrient (TN, TP) data from 2011 to 2015 from the PCD were applied to calibrate the NDR model based on the selected parameters, namely *load_n*, *load_p*, *eff_n*, *eff_p*, *crit_len_n*, and *crit_len_p* as suggested by Griffin et al. (2020). Meanwhile, the observed nutrient data from 2016 to 2018 from the PCD were applied to validate the model. The coefficient of determination (R^2) and percent bias (*PBIAS*) were applied for the calibration and validation process using Equations 3.25 and 3.26, respectively.

Similar to the SDR model, the calibration process could be accepted if the values from two different performance ratings were satisfied, as

suggested by Moriasi et al. (2007) and Me, Abell, and Hamilton (2015) (see Table 3.9). Then, the parameter can be used for the validation process, actual nutrient export estimation, and nutrient export estimation under three scenarios.

3.3.5 Optimum LULC allocation to minimize sediment and nutrient export

To assess the state of change in ecosystem services, i.e., sediment and nutrient export due to LULC change, the ecosystem services change index (ESCI) as Equation 3.10 was applied to assess the ecosystem services states (ES) as proposed by Leh, Matlock, Cummings, and Nalley (2013).

$$ESCI_x = \left[\frac{ES_{CURx_j} - ES_{HISx_i}}{ES_{HISx_i}} \right] \quad (3.10)$$

Where, $ESCI_x$ is the Ecosystems Services Change Index of service X , ES_{CURx_j} and ES_{HISx_i} are the current and historic ecosystem service state values of service X at times j and i , respectively.

In this study, sediment and nutrient export ecosystem service values were assessed based on the base year in 2019 and the predictive LULC between 2020 and 2029. The ecosystem service values in 2019 and annual ecosystem services values between 2020 and 2029 were separately calculated pair by pair using the $ESCI$. The derived results were then averaged to identify the LULC scenario for optimum LULC allocation to minimize sediment and nutrient export (Figure 3.11).

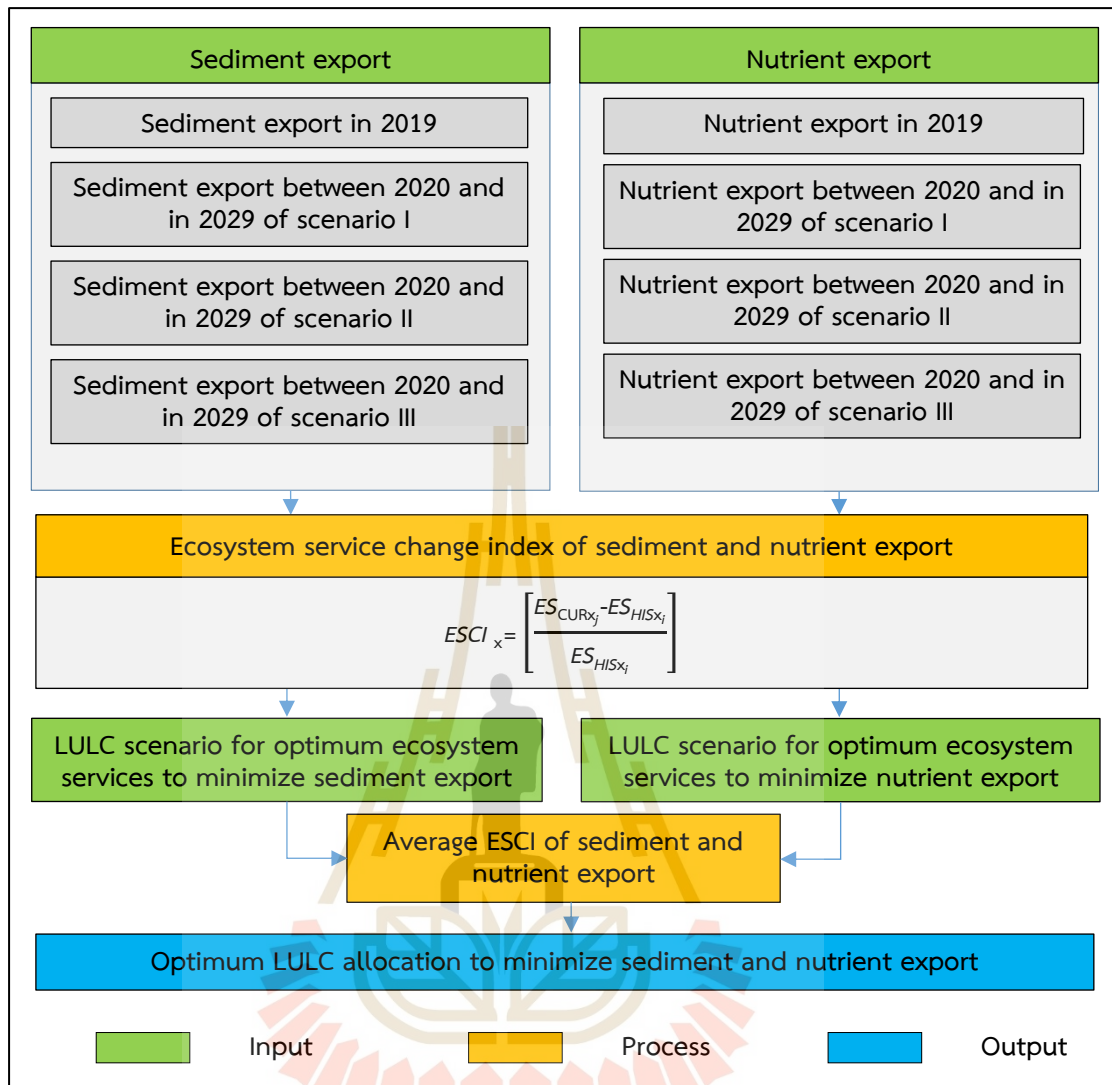


Figure 3.11 Schematic workflow of optimum LULC allocation to minimize sediment and nutrient export.

CHAPTER IV

LAND USE AND LAND COVER CLASSIFICATION AND CHANGE DETECTION

This chapter reports the first objective results, focusing on the classification of LULC in 2009 and 2019 using the support vector machines (SVM) algorithm and change detection between 2009 and 2019 using the post-classification comparison algorithm. The results cover (1) LULC classification in 2009, (2) LULC classification in 2019, and (3) LULC change between 2009 and 2019 are described and discussed in detail.

4.1 LULC classification in 2009

The input data for LULC classification in 2009 as a historical record using the SVM algorithm consisted of surface reflectance Landsat 5 TM data (27 February 2009) and additional bands, including NDVI, NDMI, SAVI, MNDWI and elevation (DEM) is displayed in Figure 4.1. The training sample points were visually selected based on the homogeneity of spectral reflectance bands (4, 5 and 3). The number of training sample points rapidly estimated from LULC data in 2009 of LDD is summarized in Table 4.1 and displayed in Figure 4.2. The sample points indicate a proportional area of each LULC type in 2009 of the reference data. The result of the LULC classification in 2009 is spatially displayed in Figure 4.3. Area and the percentage of LULC data are summarized in Table 4.2.

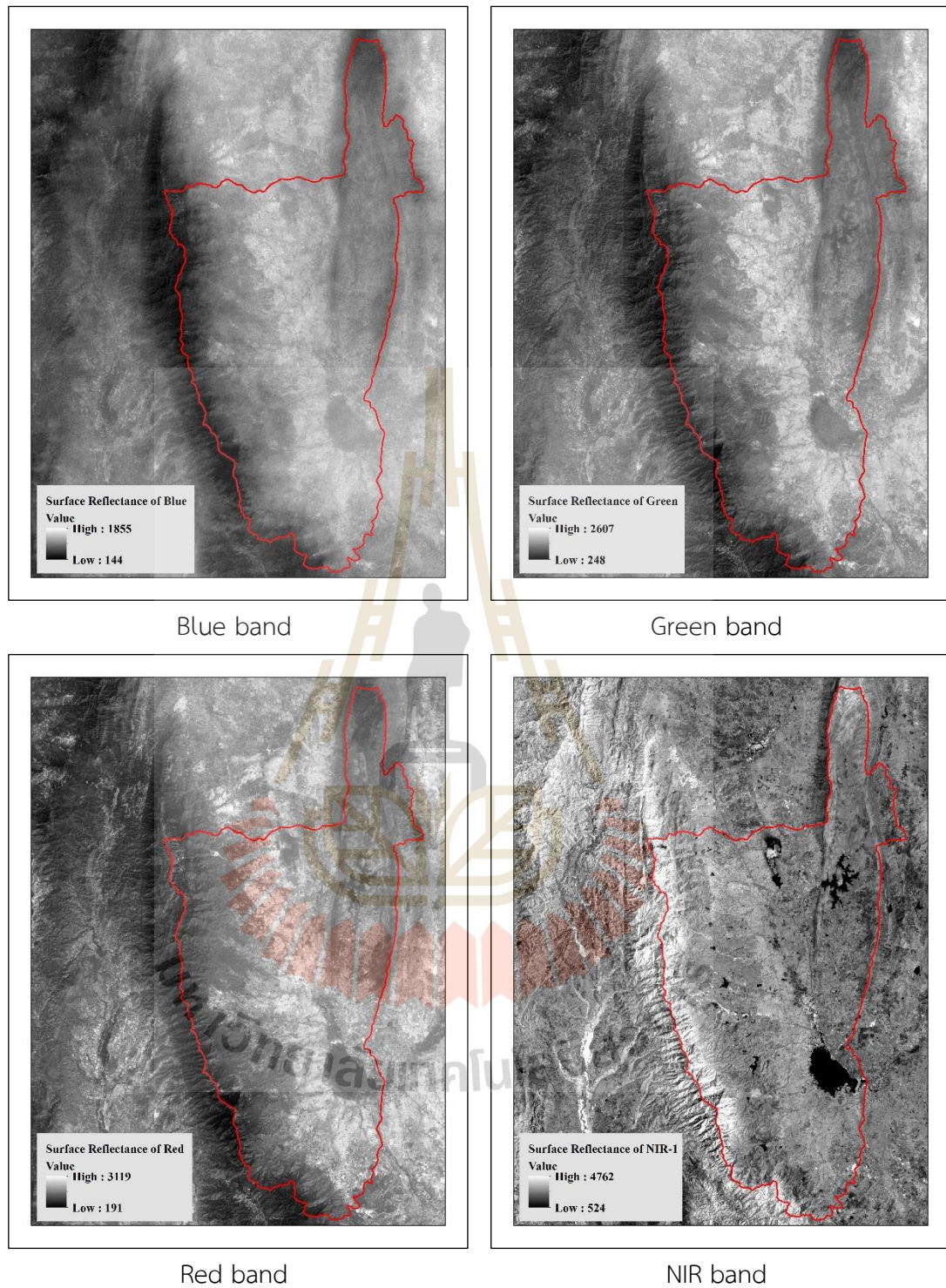


Figure 4.1 Surface reflectance and additional bands of Landsat 5 TM imagery.

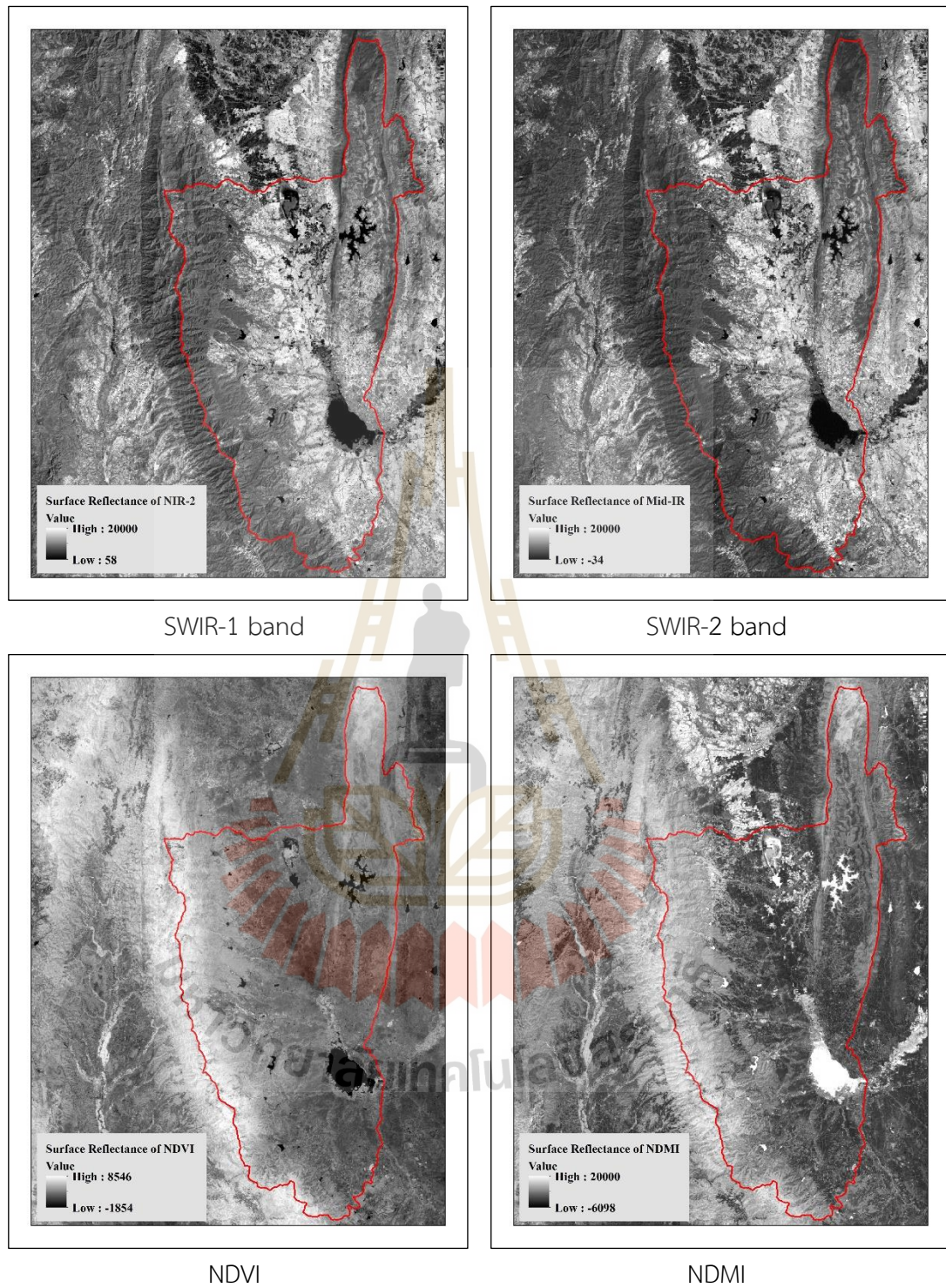


Figure 4.1 (Continued).

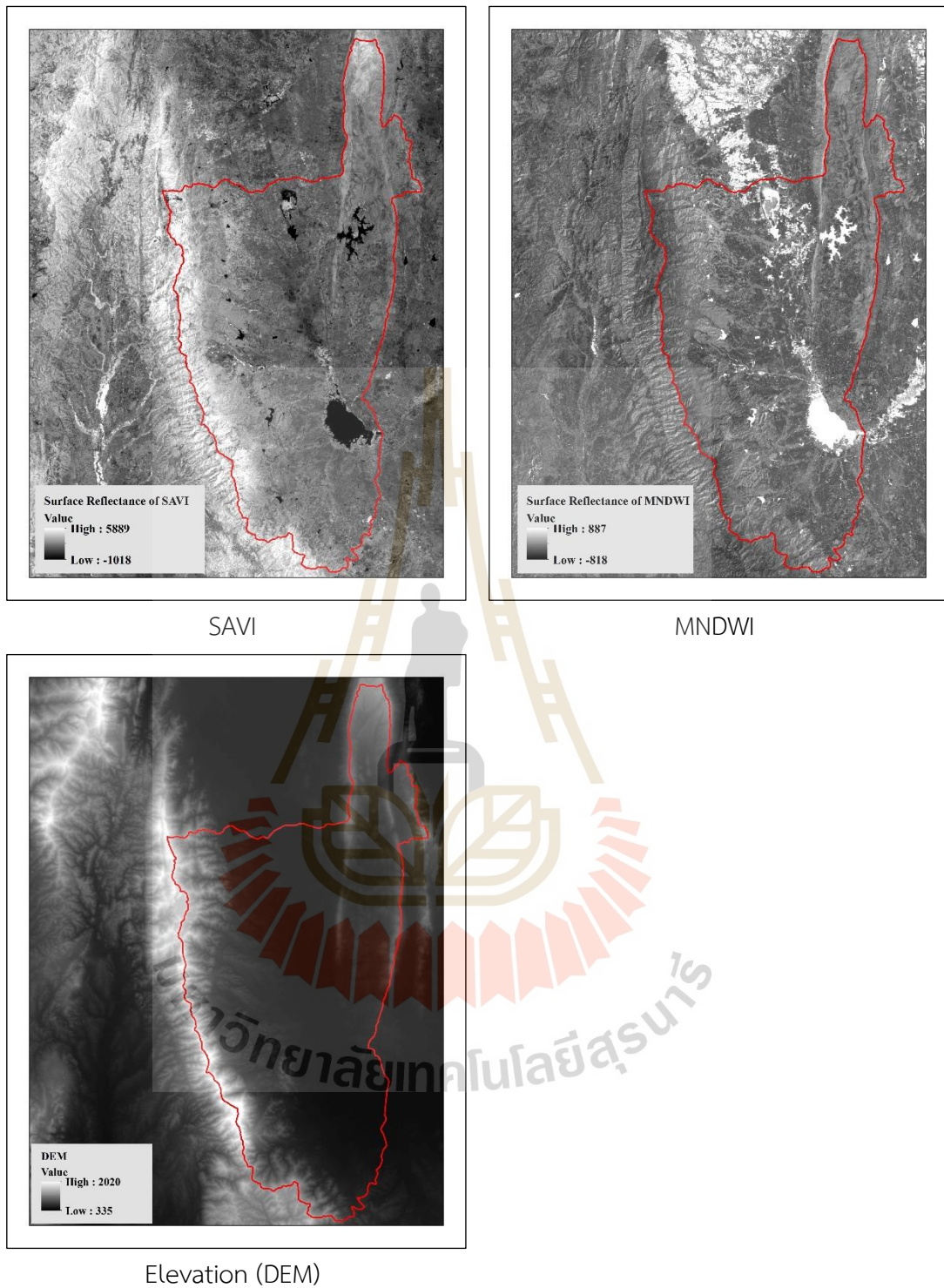


Figure 4.1 (Continued).

Table 4.1 Number of training sample points for LULC classification in 2009 using the SVM algorithm.

No	LULC type	Number of training point
1	Urban and built-up area	78
2	Paddy field	303
3	Field crop	22
4	Para rubber	32
5	Perennial trees and Orchard	59
6	Forest land	510
7	Water body	64
8	Rangeland	3
9	Wetland	9
10	Miscellaneous land	2
Total		1,082

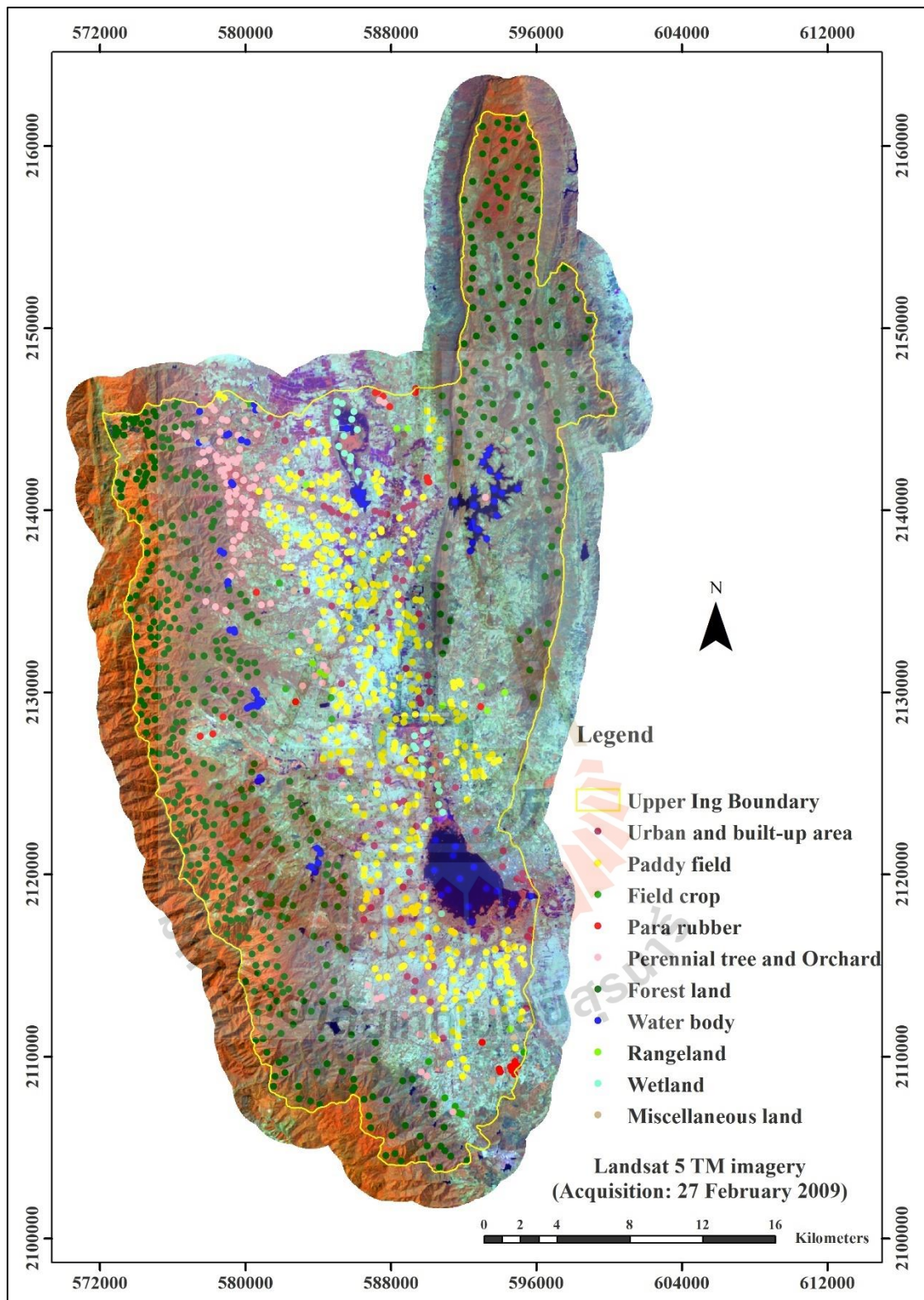


Figure 4.2 Spatial distribution of training sample points for LULC classification in 2009 using SVM algorithm.

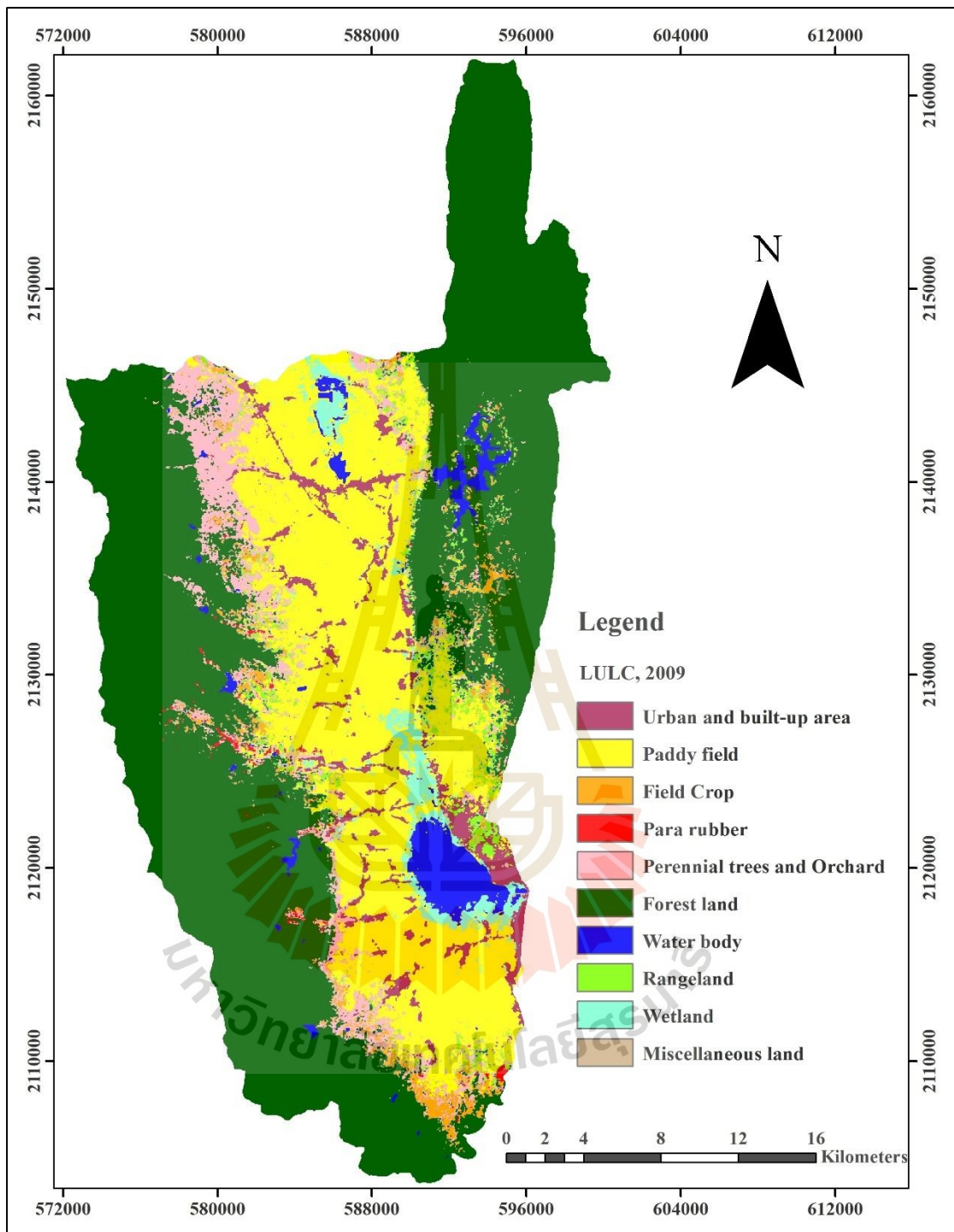


Figure 4.3 Spatial distribution of LULC classification in 2009.

Table 4.2 Area and percentage of LULC data in 2009.

No	LULC type	Area	
		Km ²	Percent
1	Urban and built-up area	29.78	3.34
2	Paddy field	241.14	27.05
3	Field crop	17.49	1.96
4	Para rubber	3.35	0.38
5	Perennial trees and Orchard	59.71	6.70
6	Forest land	476.73	53.48
7	Water body	26.06	2.92
8	Rangeland	16.75	1.88
9	Wetland	19.47	2.18
10	Miscellaneous land	0.87	0.10
Total		891.35	100.00

The results reveal that the top three dominant LULC types are forest land, paddy field, perennial trees and orchard, which cover 476.73 km² (53.48%), 241.14 km² (27.05%), and 59.71 km² (6.70%), respectively. Conversely, the top three least LULC types in 2009 are rangeland, para rubber and miscellaneous land and cover area of 16.75 km² (1.88%), 3.35 km² (0.38%), and 0.87 km² (0.10%), respectively.

Besides, the classified LULC map in 2009 was further assessed the thematic accuracy with 788 sampling points. In this study, a very high spatial resolution image from Google Earth in 2009 and 2010 was used as ground reference information to check the accuracy of the classified LULC map in 2009 (Figure 4.4). The error matrix and accuracy assessment of the thematic LULC map is reported in Table 4.3.

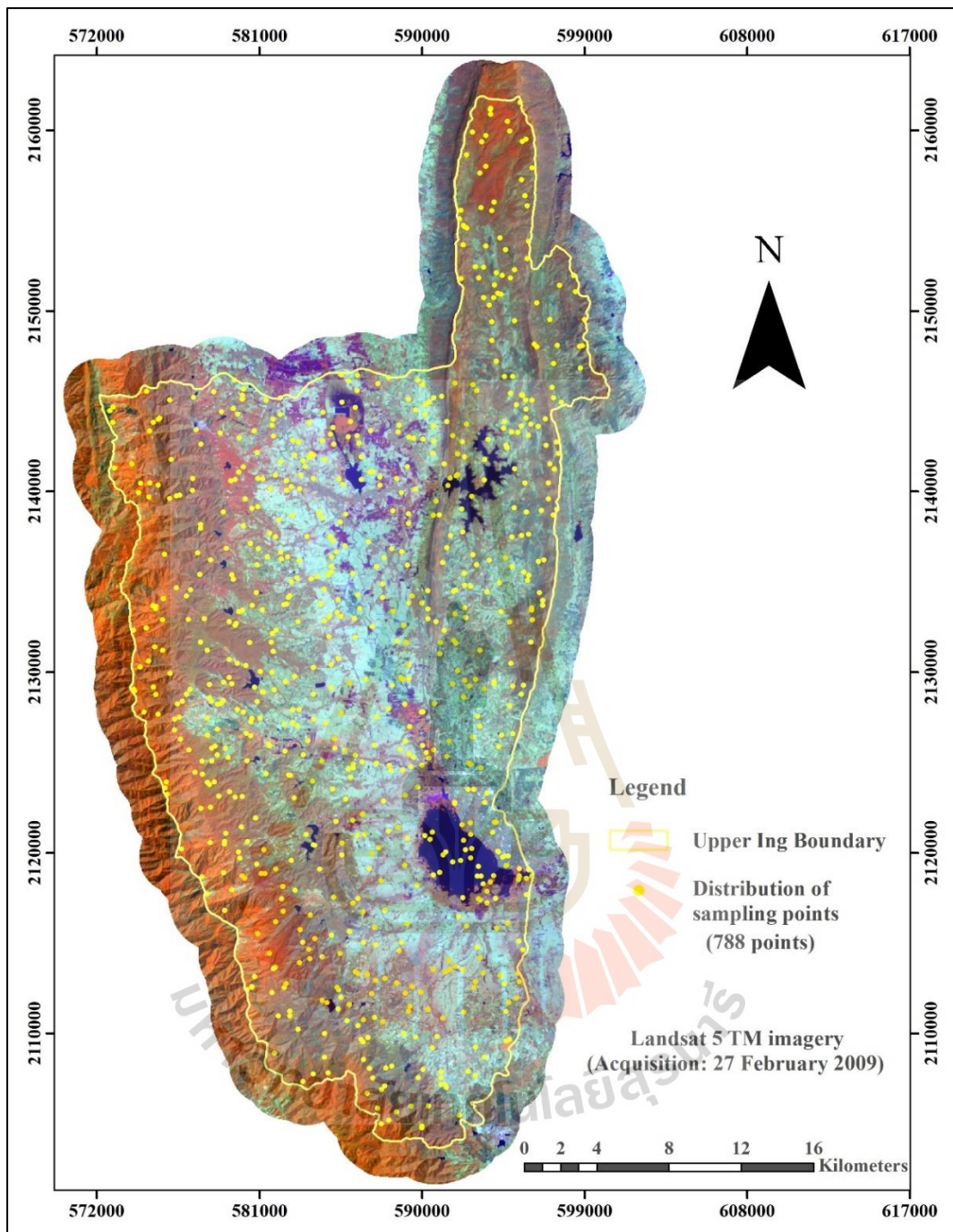


Figure 4.4 Spatial distribution of sampling points on Landsat 5-TM image for thematic accuracy assessment of classified LULC map in 2009.

Table 4.3 Error matrix and accuracy assessment of LULC map in 2009.

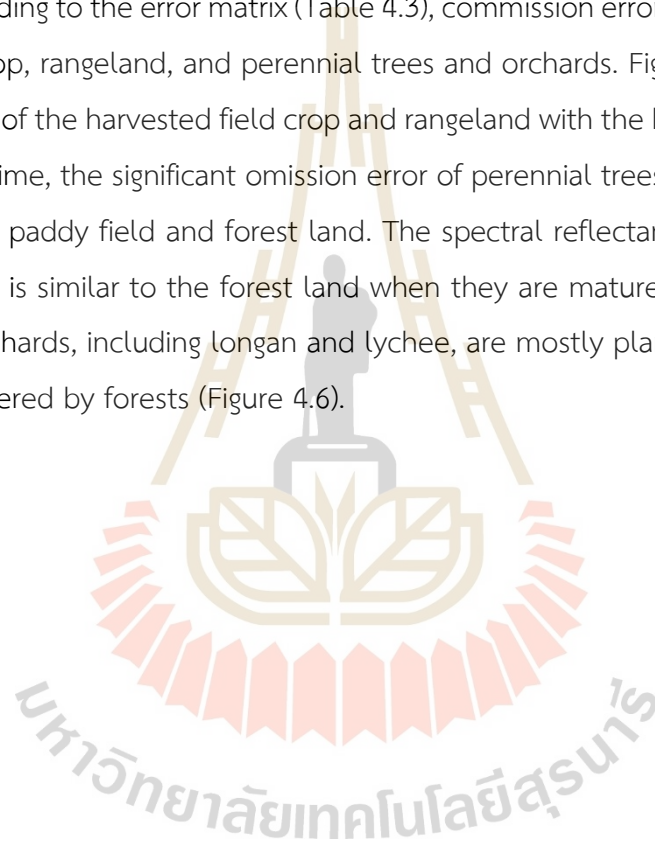
LULC types	Ground reference data from Google Earth in 2009										Total
	UR	PD	FC	RB	PO	FO	WB	RL	WL	ML	
Urban and built-up area (UR)	33										33
Paddy field (PD)		173	9	1	4	2	2	5	1		197
Field crop (FC)		4	16	2				1			23
Para rubber (RB)		3	1	6	1			1			12
Perennial trees and Orchard (PO)		3		1	51	1					56
Forest land (FO)		3	3	2	7	363		3			381
Water body (WB)							30				30
Rangeland (RL)			1	3	2			16			22
Wetland (WL)		4			1		1		18		24
Miscellaneous land (ML)										10	10
Total	33	190	30	15	66	366	33	26	19	10	788
Producer's accuracy	100.00	91.05	53.33	40.00	77.27	99.18	90.91	61.54	94.74	100.00	
User's accuracy	100.00	87.82	69.57	50.00	91.07	95.28	100.00	72.73	75.00	100.00	
Overall accuracy	90.86										
Kappa hat coefficient	87.00										

The results reveal that overall accuracy is 90.86%, and the Kappa hat coefficient is 87.00%. Meanwhile, producer's accuracy (PA), which indicates the probability of a reference ground information being correctly classified and is a measure of omission error (Congalton and Green, 2009), varies between 40.00% for para rubber and 100% for the urban and built-up area and miscellaneous land. The user's accuracy (UA), which is the probability that a pixel classified on the map represents that category on the ground and is a measure of the commission (Congalton and Green, 2009), varies between 50.00 % for para rubber and 100% for the urban and built-up area and miscellaneous land and water body.

As a result, the Kappa hat coefficient value, which is more than 80%, represents the substantial agreement between the classification map and the reference data (Rosenfield and Fitzpatrick-Lins, 1986). Meanwhile, the overall accuracy with a value of more than 85% of the LULC map in 2009 can provide an acceptable result (Anderson, Hardy, Roach, and Witmer, 1976). Besides, the overall accuracy and Kappa hat coefficient from this study are similar to Al-doski, Mansor, and Shafri (2013) research. They applied the SVM to classify land cover from Landsat 5 TM images over four years

to spot land cover changes in Halabja City, Iraq. This algorithm can provide the output with an average overall accuracy of 93% and the Kappa hat coefficient of 0.85. Also, Taati, Sarmadian, Mousavi, Pour, and Shahir (2014) confirmed that the SVM algorithm was performed well for land use classification by Landsat 5 TM images by giving 86.67% of overall accuracy and 0.82 of kappa coefficient. Thus, the classified LULC map in 2009 can be accepted and further applied for LULC change detection and prediction in this study.

According to the error matrix (Table 4.3), commission error of paddy field comes from field crop, rangeland, and perennial trees and orchards. Figure 4.5 demonstrates the similarity of the harvested field crop and rangeland with the harvested paddy field. In the meantime, the significant omission error of perennial trees and orchards mostly come from a paddy field and forest land. The spectral reflectance of perennial trees and orchards is similar to the forest land when they are mature. Moreover, perennial trees and orchards, including longan and lychee, are mostly planted near the hillside, primarily covered by forests (Figure 4.6).



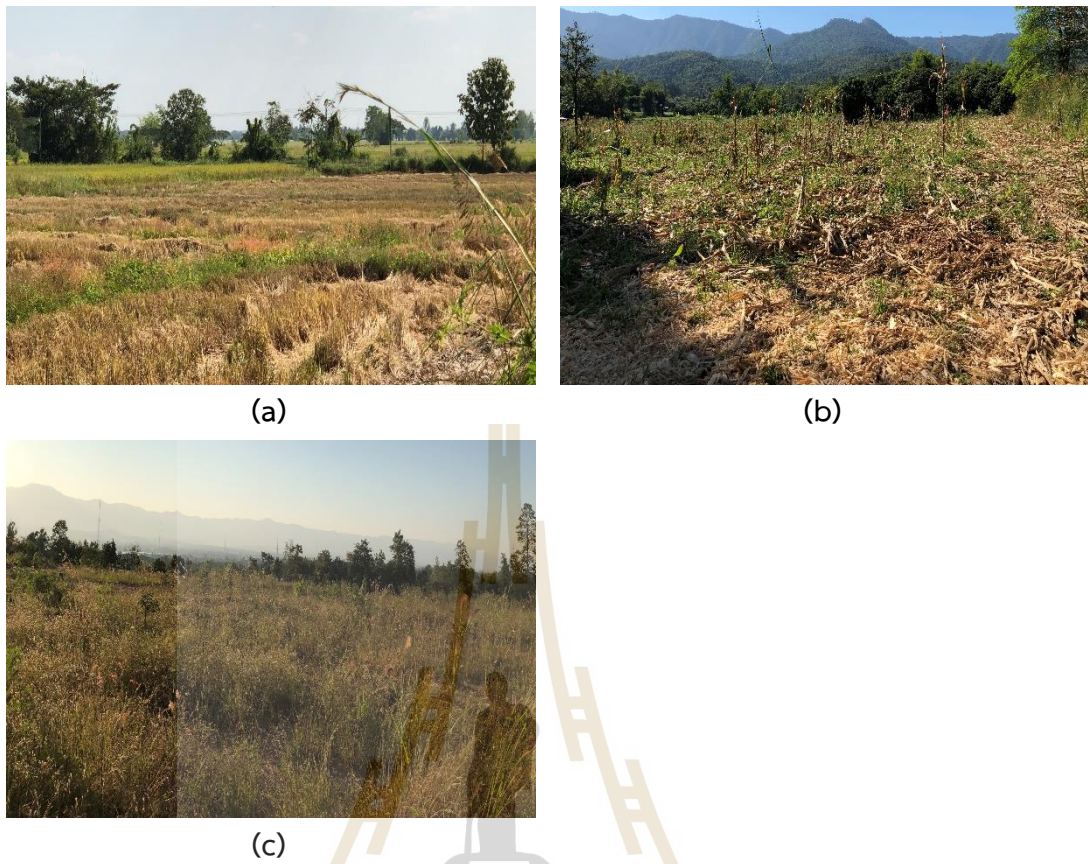


Figure 4.5 Ground photograph of harvested paddy fields (a), harvested field crop (b), and rangeland (c) from a field survey in 2020.



Figure 4.6 Ground photograph of perennial trees and orchards nearby forest land from a field survey in 2020.

4.2 LULC classification in 2019

The input data for LULC classification in 2019 as a recent record by the SVM algorithm were composed of surface reflectance of Landsat 8 OLI imagery (23 February 2019), additional spectral bands (NDVI, NDMI, SAVI, MNDWI) and elevation (DEM) is shown in Figure 4.7. The training sample points were visually chosen based on the similarity of the spectral signature of each LULC type. The characteristic of training sample points for each LULC type is presented in Table 4.4. As a result, it can be observed that the spectral profile patterns of para rubber, perennial trees and orchards, and forest land are similar, but spectral reflectance values are different. In the meantime, spectral plot patterns and reflectance value of paddy field and miscellaneous land (bush follow) or field crop and rangeland are similar. These spectral plots represent average spectral reflectance values from each LULC type training point. Hence, additional spectral bands show a significant role in this LULC classification using the SVM algorithm in this study.

Like the LULC classification in 2009, the number of points estimated from the LULC proportion coverage of LDD in 2015 is summarized in Table 4.5. The spatial distribution of training sample points is presented in Figure 4.8. Simultaneously, the spatial distribution of the LULC map in 2019 is shown in Figure 4.9, and the area and the percentage of LULC data in 2019 are summarized in Table 4.6.

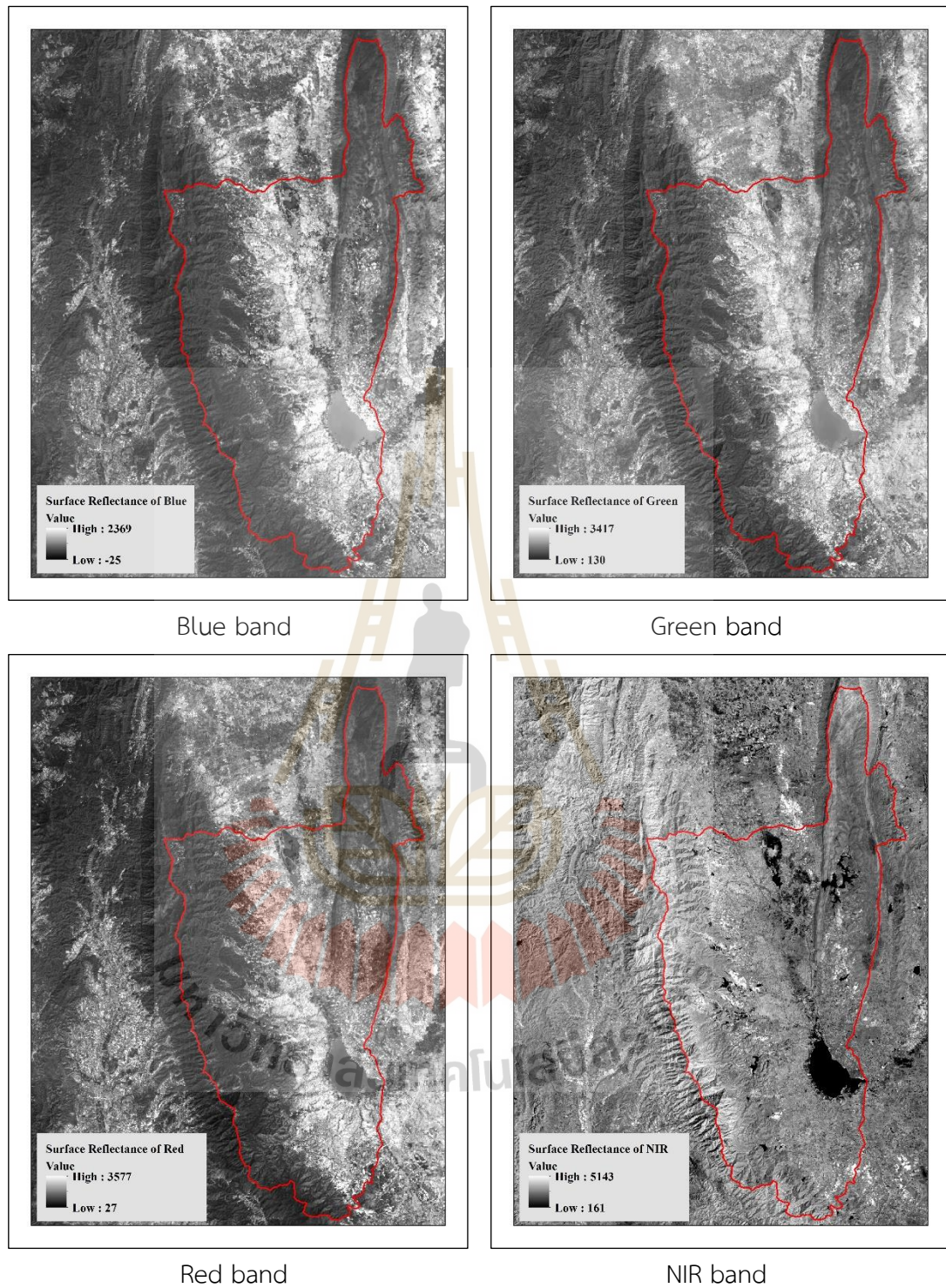


Figure 4.7 Surface reflectance and additional bands of Landsat 8 OLI imagery.

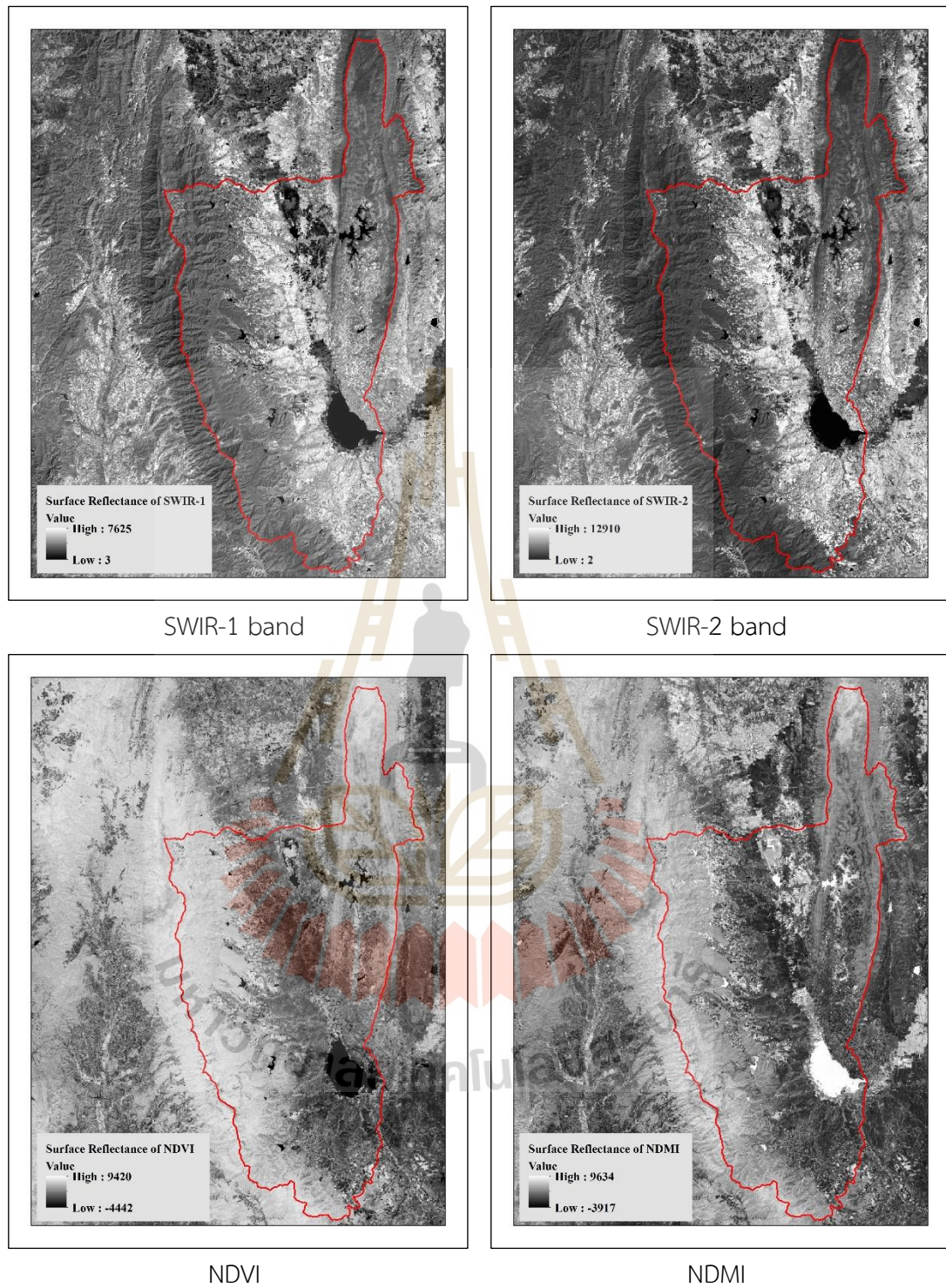


Figure 4.7 (Continued).

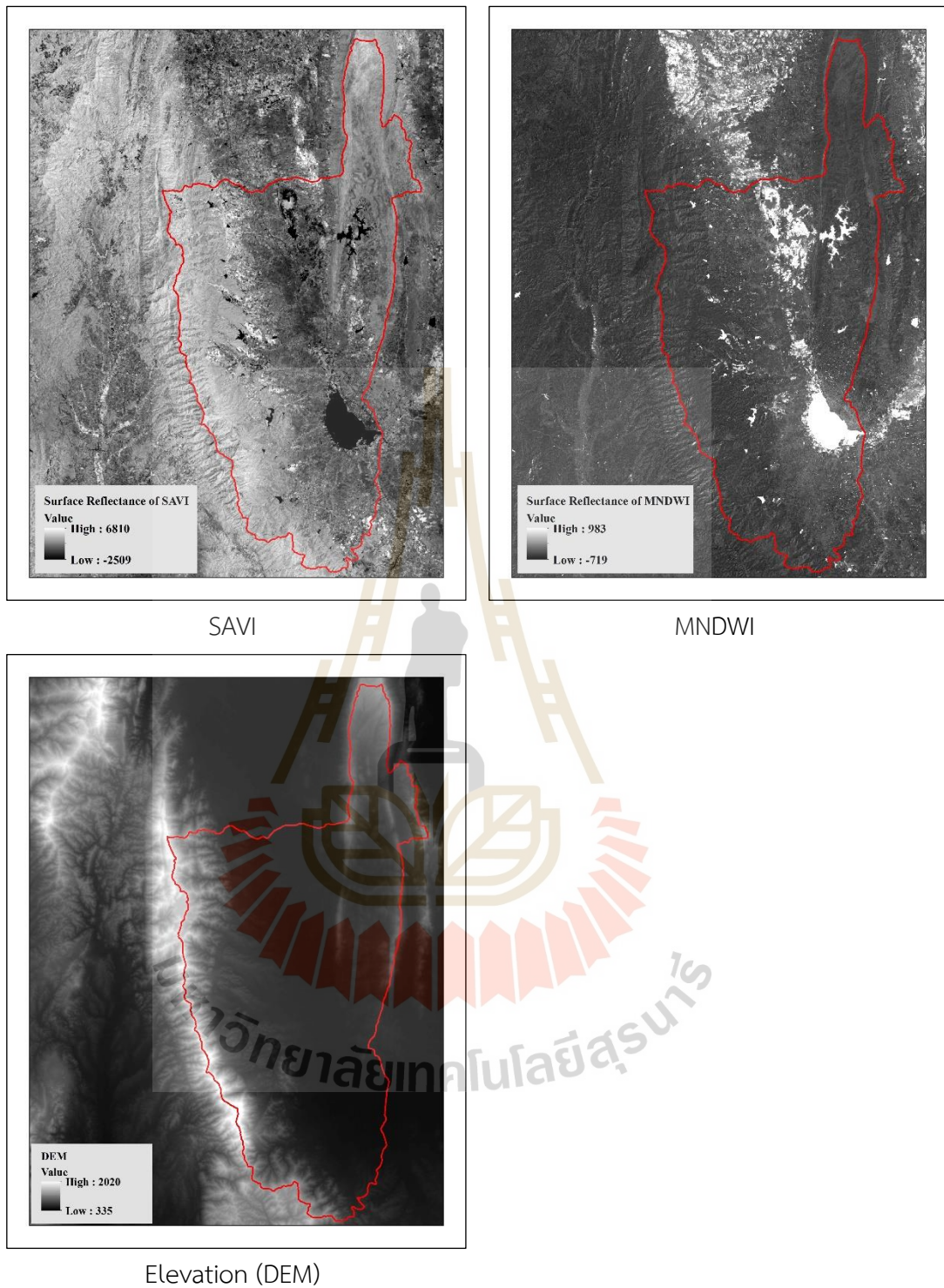


Figure 4.7 (Continued).

Table 4.4 Characteristic of training sample points for LULC classification with the SVM algorithm.

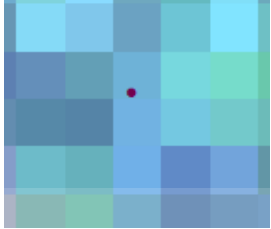
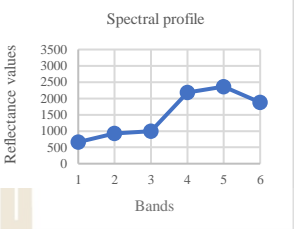

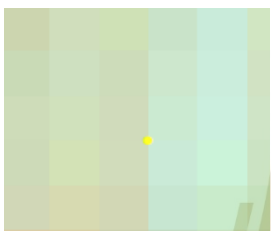
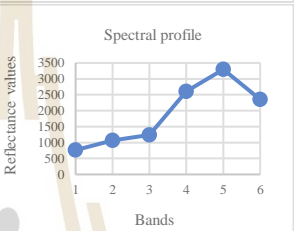


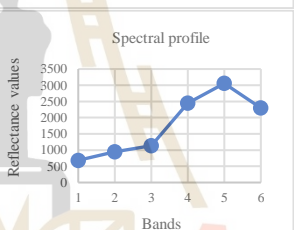


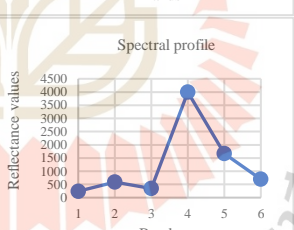


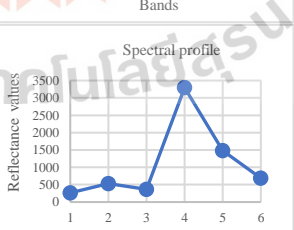


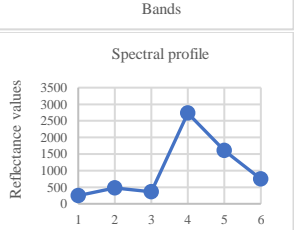

LULC type	Composite Landsat image	Spectral plot	Ground photographs														
Urban and built-up area		<p>Spectral profile</p>  <table border="1"> <caption>Spectral profile data for Urban and built-up area</caption> <thead> <tr> <th>Bands</th> <th>Reflectance values</th> </tr> </thead> <tbody> <tr><td>1</td><td>500</td></tr> <tr><td>2</td><td>1000</td></tr> <tr><td>3</td><td>1000</td></tr> <tr><td>4</td><td>2200</td></tr> <tr><td>5</td><td>2500</td></tr> <tr><td>6</td><td>1800</td></tr> </tbody> </table>	Bands	Reflectance values	1	500	2	1000	3	1000	4	2200	5	2500	6	1800	
Bands	Reflectance values																
1	500																
2	1000																
3	1000																
4	2200																
5	2500																
6	1800																
Paddy field		<p>Spectral profile</p>  <table border="1"> <caption>Spectral profile data for Paddy field</caption> <thead> <tr> <th>Bands</th> <th>Reflectance values</th> </tr> </thead> <tbody> <tr><td>1</td><td>500</td></tr> <tr><td>2</td><td>1000</td></tr> <tr><td>3</td><td>1200</td></tr> <tr><td>4</td><td>2500</td></tr> <tr><td>5</td><td>3200</td></tr> <tr><td>6</td><td>2200</td></tr> </tbody> </table>	Bands	Reflectance values	1	500	2	1000	3	1200	4	2500	5	3200	6	2200	
Bands	Reflectance values																
1	500																
2	1000																
3	1200																
4	2500																
5	3200																
6	2200																
Field crop		<p>Spectral profile</p>  <table border="1"> <caption>Spectral profile data for Field crop</caption> <thead> <tr> <th>Bands</th> <th>Reflectance values</th> </tr> </thead> <tbody> <tr><td>1</td><td>500</td></tr> <tr><td>2</td><td>1000</td></tr> <tr><td>3</td><td>1000</td></tr> <tr><td>4</td><td>2500</td></tr> <tr><td>5</td><td>3200</td></tr> <tr><td>6</td><td>2200</td></tr> </tbody> </table>	Bands	Reflectance values	1	500	2	1000	3	1000	4	2500	5	3200	6	2200	
Bands	Reflectance values																
1	500																
2	1000																
3	1000																
4	2500																
5	3200																
6	2200																
Para rubber		<p>Spectral profile</p>  <table border="1"> <caption>Spectral profile data for Para rubber</caption> <thead> <tr> <th>Bands</th> <th>Reflectance values</th> </tr> </thead> <tbody> <tr><td>1</td><td>500</td></tr> <tr><td>2</td><td>1000</td></tr> <tr><td>3</td><td>1000</td></tr> <tr><td>4</td><td>4000</td></tr> <tr><td>5</td><td>1500</td></tr> <tr><td>6</td><td>1000</td></tr> </tbody> </table>	Bands	Reflectance values	1	500	2	1000	3	1000	4	4000	5	1500	6	1000	
Bands	Reflectance values																
1	500																
2	1000																
3	1000																
4	4000																
5	1500																
6	1000																
Perennial trees and Orchard		<p>Spectral profile</p>  <table border="1"> <caption>Spectral profile data for Perennial trees and Orchard</caption> <thead> <tr> <th>Bands</th> <th>Reflectance values</th> </tr> </thead> <tbody> <tr><td>1</td><td>500</td></tr> <tr><td>2</td><td>1000</td></tr> <tr><td>3</td><td>1000</td></tr> <tr><td>4</td><td>3000</td></tr> <tr><td>5</td><td>1500</td></tr> <tr><td>6</td><td>1000</td></tr> </tbody> </table>	Bands	Reflectance values	1	500	2	1000	3	1000	4	3000	5	1500	6	1000	
Bands	Reflectance values																
1	500																
2	1000																
3	1000																
4	3000																
5	1500																
6	1000																
Forest land		<p>Spectral profile</p>  <table border="1"> <caption>Spectral profile data for Forest land</caption> <thead> <tr> <th>Bands</th> <th>Reflectance values</th> </tr> </thead> <tbody> <tr><td>1</td><td>500</td></tr> <tr><td>2</td><td>1000</td></tr> <tr><td>3</td><td>1000</td></tr> <tr><td>4</td><td>2800</td></tr> <tr><td>5</td><td>1500</td></tr> <tr><td>6</td><td>1000</td></tr> </tbody> </table>	Bands	Reflectance values	1	500	2	1000	3	1000	4	2800	5	1500	6	1000	
Bands	Reflectance values																
1	500																
2	1000																
3	1000																
4	2800																
5	1500																
6	1000																

Table 4.4 (Continued).


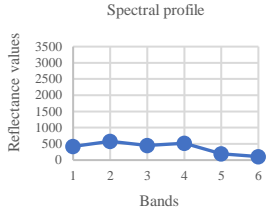

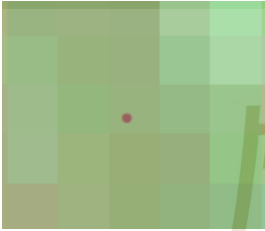
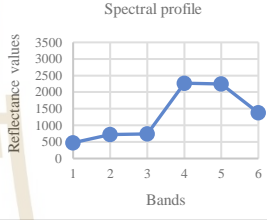


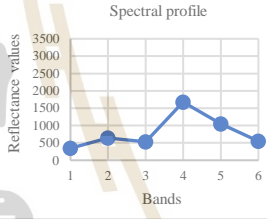


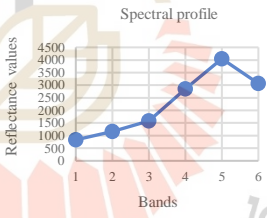

LULC type	Composite Landsat image	Spectral plot	Ground photographs														
Water body		<p>Spectral profile</p>  <table border="1"> <caption>Reflectance values for Water body</caption> <thead> <tr> <th>Bands</th> <th>Reflectance values</th> </tr> </thead> <tbody> <tr><td>1</td><td>500</td></tr> <tr><td>2</td><td>600</td></tr> <tr><td>3</td><td>500</td></tr> <tr><td>4</td><td>600</td></tr> <tr><td>5</td><td>400</td></tr> <tr><td>6</td><td>300</td></tr> </tbody> </table>	Bands	Reflectance values	1	500	2	600	3	500	4	600	5	400	6	300	
Bands	Reflectance values																
1	500																
2	600																
3	500																
4	600																
5	400																
6	300																
Rangeland		<p>Spectral profile</p>  <table border="1"> <caption>Reflectance values for Rangeland</caption> <thead> <tr> <th>Bands</th> <th>Reflectance values</th> </tr> </thead> <tbody> <tr><td>1</td><td>500</td></tr> <tr><td>2</td><td>600</td></tr> <tr><td>3</td><td>700</td></tr> <tr><td>4</td><td>2200</td></tr> <tr><td>5</td><td>2200</td></tr> <tr><td>6</td><td>1300</td></tr> </tbody> </table>	Bands	Reflectance values	1	500	2	600	3	700	4	2200	5	2200	6	1300	
Bands	Reflectance values																
1	500																
2	600																
3	700																
4	2200																
5	2200																
6	1300																
Wetland		<p>Spectral profile</p>  <table border="1"> <caption>Reflectance values for Wetland</caption> <thead> <tr> <th>Bands</th> <th>Reflectance values</th> </tr> </thead> <tbody> <tr><td>1</td><td>500</td></tr> <tr><td>2</td><td>600</td></tr> <tr><td>3</td><td>500</td></tr> <tr><td>4</td><td>1600</td></tr> <tr><td>5</td><td>1000</td></tr> <tr><td>6</td><td>500</td></tr> </tbody> </table>	Bands	Reflectance values	1	500	2	600	3	500	4	1600	5	1000	6	500	
Bands	Reflectance values																
1	500																
2	600																
3	500																
4	1600																
5	1000																
6	500																
Miscellaneous land		<p>Spectral profile</p>  <table border="1"> <caption>Reflectance values for Miscellaneous land</caption> <thead> <tr> <th>Bands</th> <th>Reflectance values</th> </tr> </thead> <tbody> <tr><td>1</td><td>1000</td></tr> <tr><td>2</td><td>1200</td></tr> <tr><td>3</td><td>1500</td></tr> <tr><td>4</td><td>2800</td></tr> <tr><td>5</td><td>4000</td></tr> <tr><td>6</td><td>3000</td></tr> </tbody> </table>	Bands	Reflectance values	1	1000	2	1200	3	1500	4	2800	5	4000	6	3000	
Bands	Reflectance values																
1	1000																
2	1200																
3	1500																
4	2800																
5	4000																
6	3000																

Table 4.5 Number of training sample points for LULC classification in 2019 using the SVM algorithm.

No	LULC type	Number of training point
1	Urban and built-up area	88
2	Paddy field	397
3	Field crop	11
4	Para rubber	109
5	Perennial trees and Orchard	101
6	Forest land	510
7	Water body	103
8	Rangeland	11
9	Wetland	28
10	Miscellaneous land	14
Total		1,372

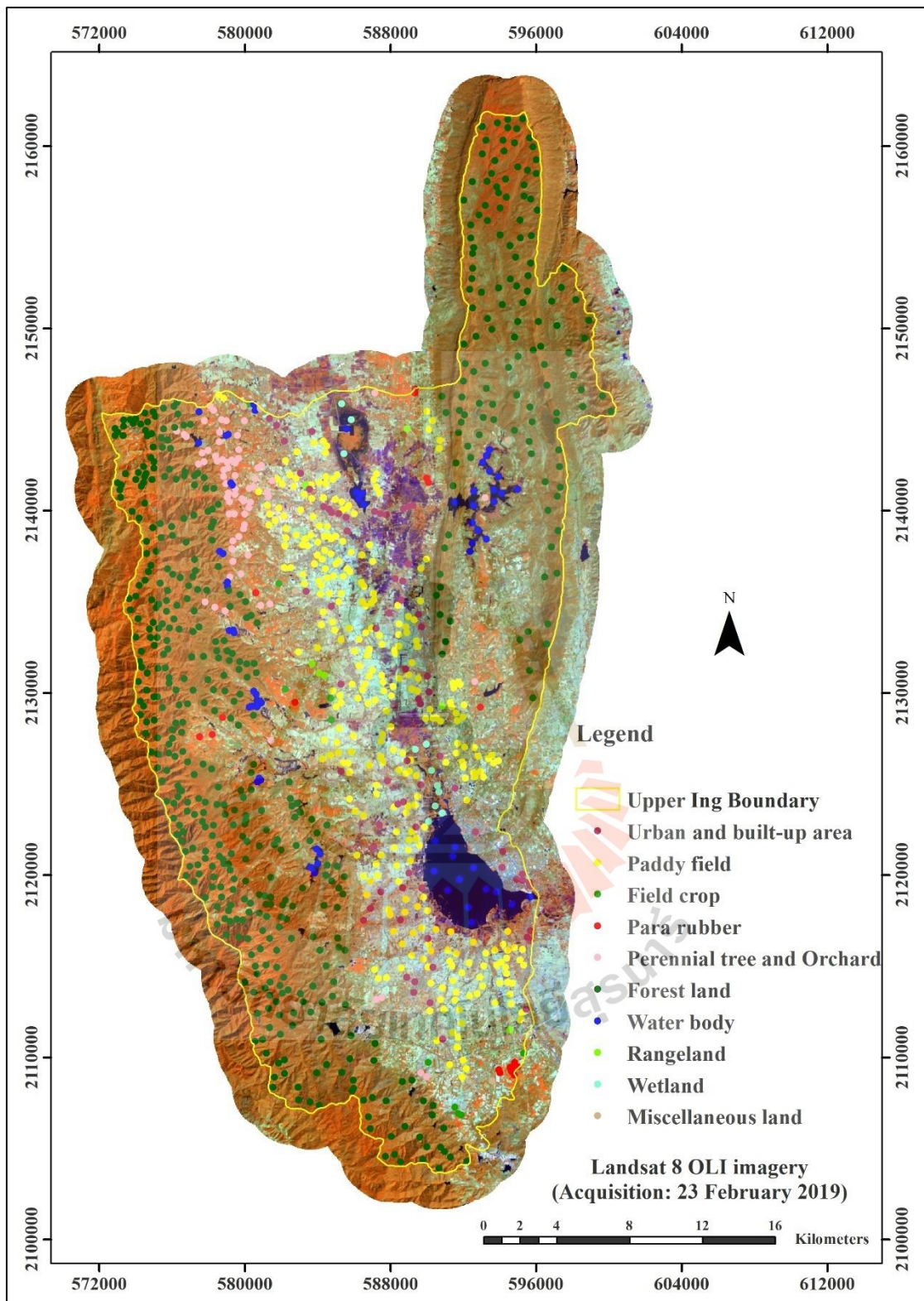


Figure 4.8 Distribution of training sample points for LULC classification in 2019.

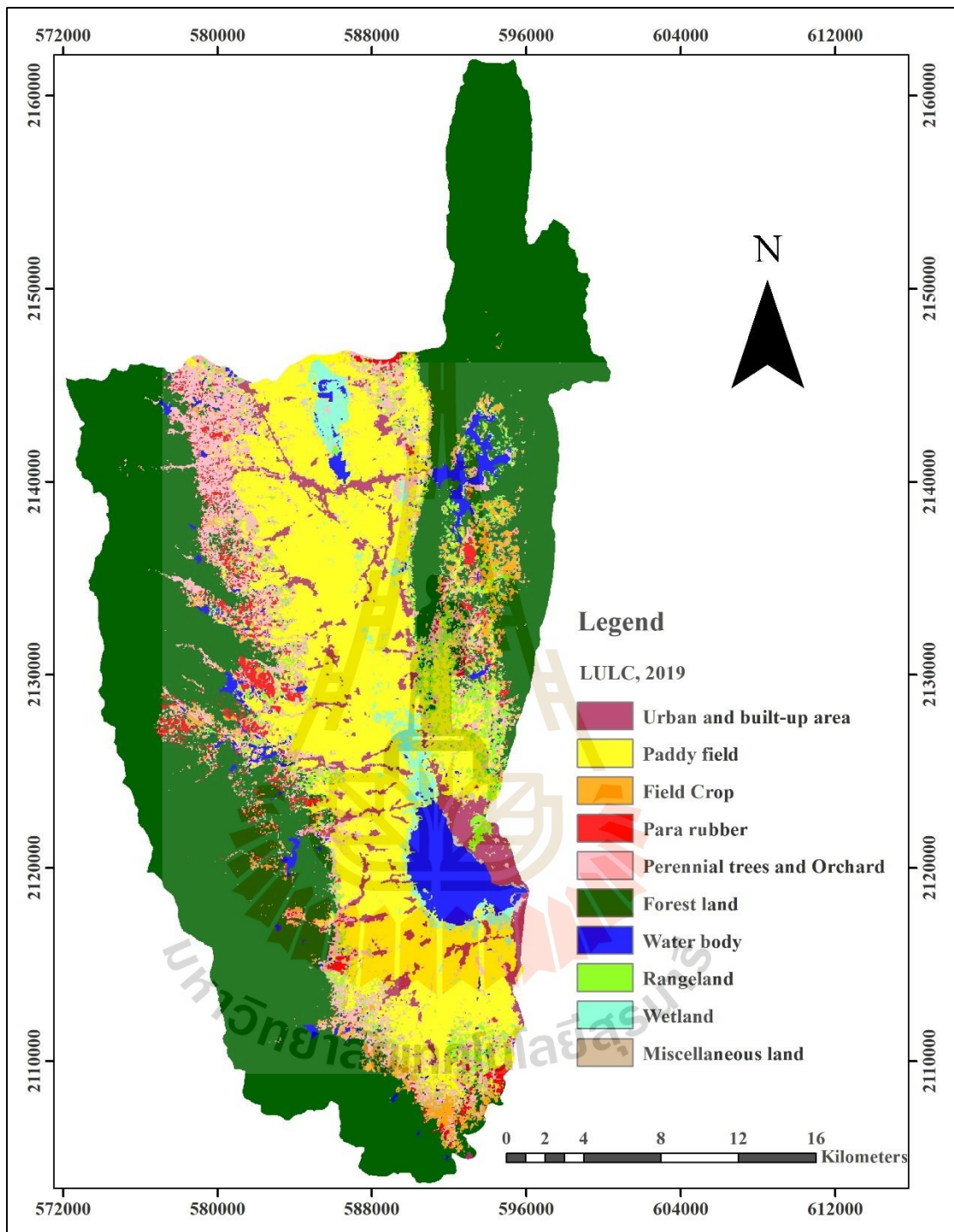


Figure 4.9 Spatial distribution of LULC classification in 2019.

Table 4.6 Area and percentage of LULC data in 2019.

No	LULC type	Area	
		km ²	Percent
1	Urban and built-up area	33.10	3.71
2	Paddy field	220.74	24.76
3	Field crop	21.84	2.45
4	Para rubber	19.78	2.22
5	Perennial trees and Orchard	79.22	8.89
6	Forest land	436.91	49.02
7	Water body	33.37	3.74
8	Rangeland	27.26	3.06
9	Wetland	16.41	1.84
10	Miscellaneous land	2.71	0.30
Total		891.35	100.00

Like LULC data in 2009, the top three dominant LULC types are still forest land, paddy field, and perennial trees and orchards, which cover an area of 436.91 km² (49.02%), 220.74 km² (24.76%), and 79.22 km² (8.89%), respectively. Conversely, the top three least areas of LULC types in 2019 are para rubber, wetland and miscellaneous land and cover area of 19.78 km² (2.22%), 16.41 km² (1.84%), and 2.71 km² (0.30%), respectively. This finding implies that the LULC change pattern in both years is similar with a bit of change.

Also, the classified LULC map in 2019 was assessed the thematic accuracy with 788 sampling points using high spatial image resolution from Google Earth and field survey in 2020 (Figure 4.10). The error matrix and accuracy assessment of the LULC map in 2019 is reported in Table 4.7.

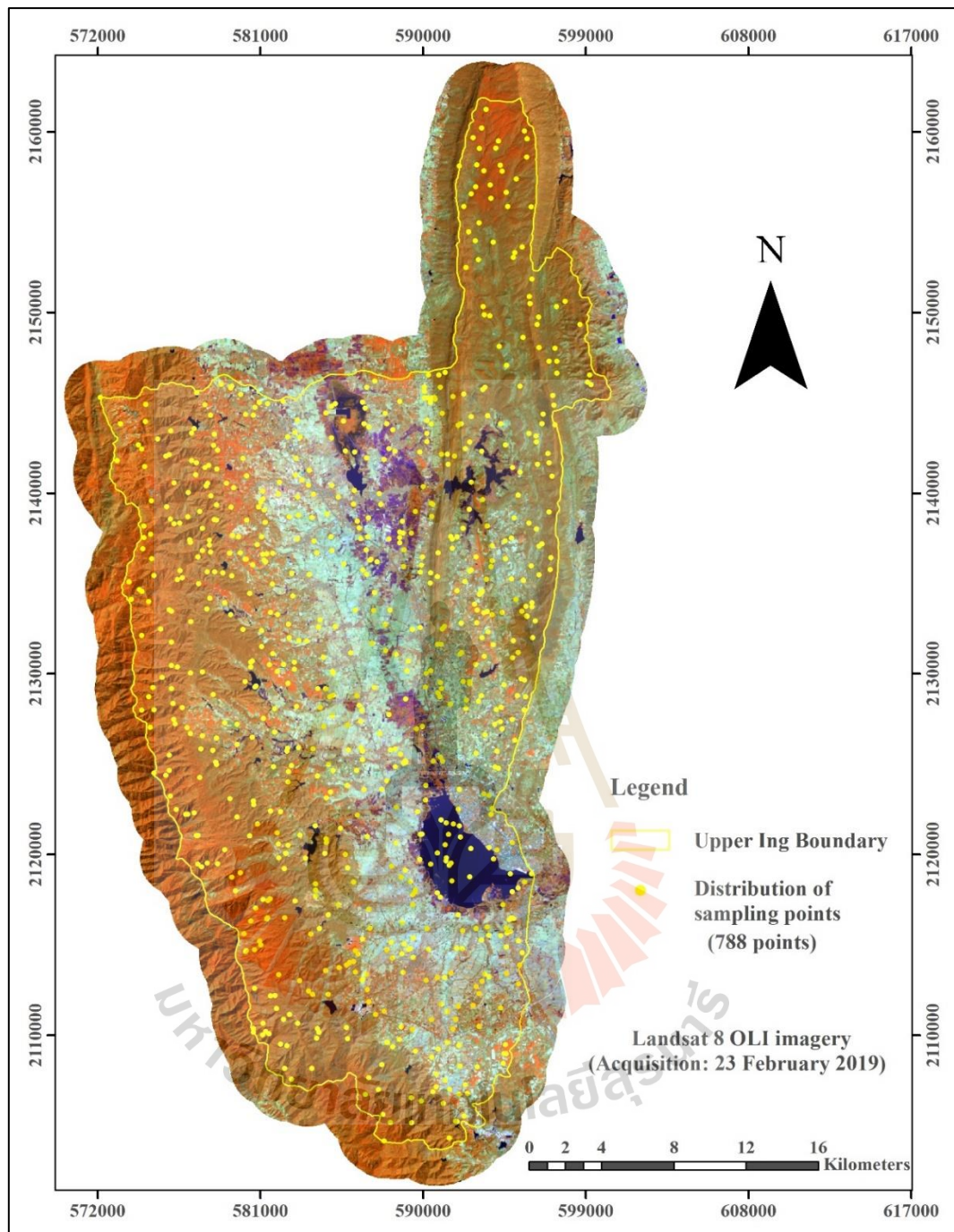


Figure 4.10 Spatial distribution of sampling points on Landsat 8-OLI image (23 February 2019) for accuracy assessment of thematic LULC map in 2019.

Table 4.7 Error matrix and accuracy assessment of LULC map in 2019.

LULC types	Ground reference data from Google Earth in 2019 and field survey in 2020										Total
	UR	PD	FC	RB	PO	FO	WB	RL	WL	ML	
Urban and built-up area (UR)	34										34
Paddy field (PD)		164	5		4		1	6	1	2	183
Field crop (FC)		1	22			1		1			25
Para rubber (RB)		1		19	4						24
Perennial trees and Orchard (PO)		3	4	6	54	2		1		1	71
Forest land (FO)		1	2	8	7	337		1			356
Water body (WB)							34				34
Rangeland (RL)		3			4			23			30
Wetland (WL)		5					2	1	13		21
Miscellaneous land (ML)			4							6	10
Total	34	178	37	33	73	340	37	33	14	9	788
Producer's accuracy	100.00	92.13	59.46	57.58	73.97	99.12	91.89	69.70	92.86	66.67	
User's accuracy	100.00	89.62	88.00	79.17	76.06	94.66	100.00	76.67	61.90	60.00	
Overall accuracy	89.59										
Kappa hat coefficient	85.85										

The results display that the overall accuracy is 89.59%, and the Kappa hat coefficient is 85.85%. Meanwhile, the producer's accuracy (PA) varies between 57.58% for para rubber and 100% for the urban and built-up area. The user's accuracy (UA) varies between 60.00 % for miscellaneous land and 100% for the urban and built-up area.

According to the value of the kappa hat coefficient of the agreement, which is more than 80%, it represents a substantial agreement between the classification map and the reference data (Rosenfield and Fitzpatrick-Lins, 1986). Additionally, the overall accuracy of the LULC map in 2019, more than 85%, can provide an acceptable result (Anderson et al., 1976). In this study, the overall accuracy and Kappa hat coefficient are similar to the previous research. Bouaziz, Eisold, and Guermazi (2017) classified LULC from Landsat 8 imagery at arid semi-arid areas in southeastern Tunisia. Their results confirmed that the SVM with radial basis function affords the highest overall accuracy of 91.20% and a kappa coefficient of 0.87. Likewise, Mandal and Saha (2018) applied SVM algorithms to classify land use from Landsat5 TM and Landsat8 OLI to quantify and analyze the spatial-temporal relationships between land use change

and urban growth in Kurseong and surrounding Darjeeling Himalaya. The overall classification Kappa statistics were 0.8630 for 1991 and 0.8927 for 2017. Hence, the classified LULC in 2019 in this current study can be accepted and further applied for LULC change detection and prediction in this study.

Besides, it can be observed that the significant omission error of the paddy field is caused by wetland, perennial trees and orchards, rangeland, field crop, para rubber and forest land. Figure 4.11 displays the similarity of active paddy fields and wetlands. In the meantime, the significant commission error of perennial trees and orchards come from various LULC types, including para rubber, field crop, paddy field, forest land, rangeland and miscellaneous land. As mentioned earlier, mature perennial trees and orchards' reflectance value is similar to para rubber and forest.

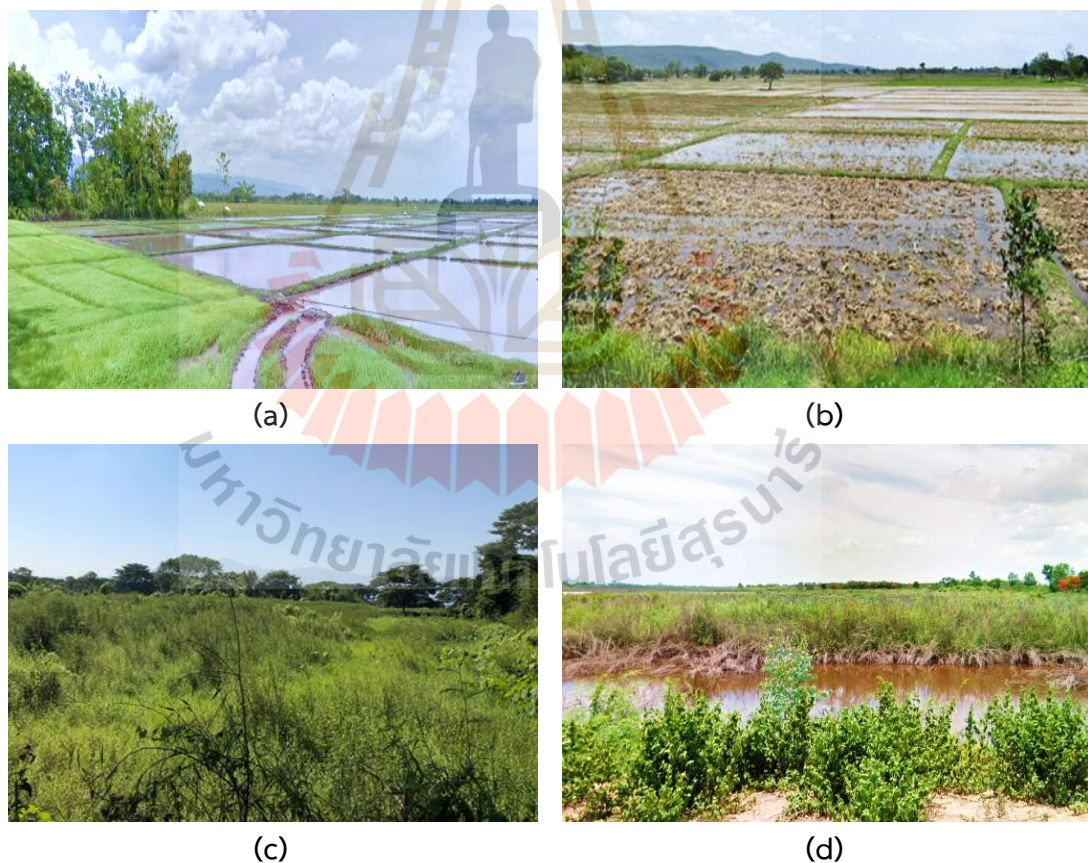


Figure 4.11 Ground photograph of paddy fields (a,b) wetland (c,d) from field survey in 2020.

In summary, the SVM classifier with a kernel of Gaussian radial basis function can be used as a helpful tool to classify LULC from remote sensing imagery because it can provide high accuracy since it aims to define an optimal hyperplane and give a maximum margin between two cases. Moreover, the kernels that turn non-linear boundaries into linear ones in the high-dimensional space define optimal hyperplane and determine complex decision boundaries between classes (Cortes and Vapnik, 1995). Under the EnMap BOX software, the SVM algorithm can be processed as semi-automated by offering a grid search for the optimized model parameter (kernel parameter, γ and penalization parameter, C). The K- Cross-validation is also tested to estimate the model's ability to avoid overfitting or selecting bias data (training and testing datasets) (Van der Linden et al., 2015).

In this study, the SVM algorithm can provide overall accuracy of 89.59% and the Kappa hat coefficient of 85.85% for LULC classification in 2009. Besides, it delivers overall accuracy of 90.86% and the Kappa hat coefficient of 87.00% for LULC classification in 2019. However, selecting suitable training points for LULC classification under the EnMap BOX software requires time and skill.

4.3 LULC change between 2009 and 2019

The comparison of LULC change area and its change rate between 2009 and 2019 are summarized in Table 4.8 and Figure 4.12

Table 4.8 Comparison of LULC change between 2009 and 2019.

LULC	LULC type (Area in km ²)									
	UR	PD	FC	RP	PO	FO	WB	RL	WL	ML
In 2009	29.78	241.14	17.49	3.35	59.71	476.73	26.06	16.75	19.47	0.87
In 2019	33.10	220.74	21.84	19.78	79.22	436.91	33.37	27.26	16.41	2.71
Change area	3.32	-20.40	4.35	16.43	19.51	-39.82	7.31	10.51	-3.06	1.84
Annual change rate	0.33	-2.04	0.44	1.64	1.95	-3.98	0.73	1.05	-0.31	0.18
Percentage of change	0.37	-2.29	0.49	1.84	2.19	-4.47	0.82	1.18	-0.34	0.21

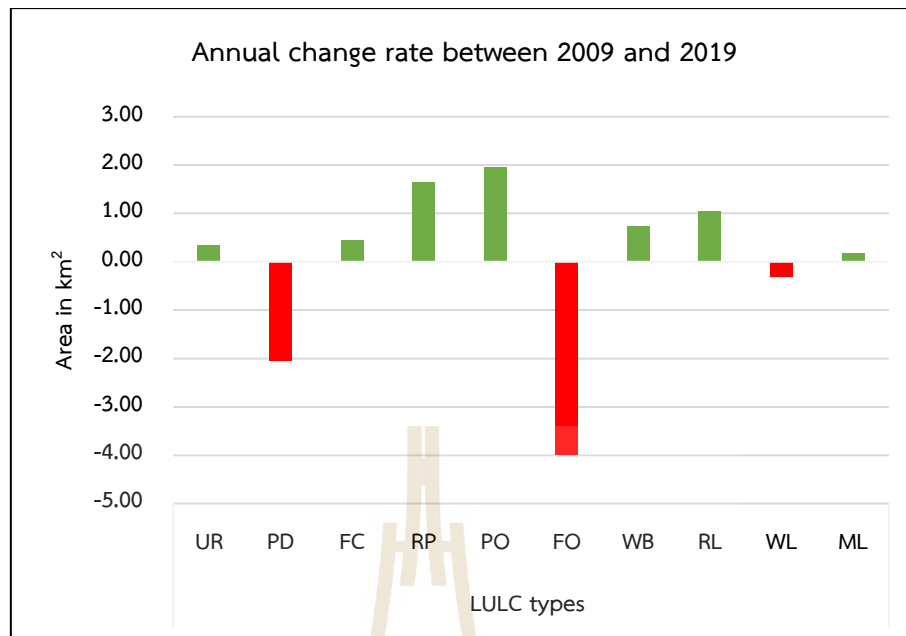


Figure 4.12 Comparison of the annual change rate of LULC type between 2009 and 2019.

As a result, the substantially increasing LULC types between 2009 and 2019 are perennial trees and orchards, para rubber, and rangeland with an annual change rate of 1.95, 1.64 and 1.05 km² per year, respectively. Slight increasing LULC types in this period are water body, field crop, urban and built-up area, and miscellaneous land with the annual change rate of 0.73, 0.44, 0.33, and 0.18 km² per year, respectively. On the contrary, the significantly decreasing LULC types in this period are forest land and paddy fields with an annual change rate of 3.98 and 2.04 km² per year, respectively, and the slightly decreasing LULC type in this period is a wetland with an annual change rate of 0.31 km² per year.

A transitional change matrix of LULC between 2009 and 2019, which provides from-to-change class information, is summarized in Table 4.9, and the LULC change map is displayed in Figure 4.13.

As a result, urban and built-up areas in 2009 were not converted into other LULC classes in 2019, and the increasing area of urban and built areas in 2019 mainly comes from paddy fields (1.30 km²) and rangeland (0.95 km²) in 2009.

Table 4.9 The transitional matrix of LULC change between 2009 and 2019.

LULC types		LULC data in 2019 (km ²)										
		UR	PD	FC	RP	PO	FO	WB	RL	WL	ML	Total
LULC data in 2009 (km ²)	Urban and built-up area (UR)	29.78	-	-	-	-	-	-	-	-	-	29.78
	Paddy field (PD)	1.30	202.88	0.16	2.80	16.41	-	2.33	8.79	5.99	0.48	241.14
	Field crop (FC)	0.03	1.58	3.80	2.56	4.63	-	0.09	3.58	-	1.22	17.49
	Para rubber (RP)	-	0.63	0.11	1.25	1.01	-	0.27	0.07	-	0.01	3.35
	Perennial trees and Orchard (PO)	0.11	5.12	1.71	5.90	39.63	-	1.68	5.27	0.03	0.26	59.71
	Forest land (FO)	0.60	1.35	15.72	6.16	11.13	436.91	1.42	2.91	0.44	0.08	476.73
	Water body (WB)	-	0.08	-	-	0.63	-	24.21	0.07	1.05	0.02	26.06
	Rangeland (RL)	0.95	4.11	0.25	1.00	3.84	-	0.10	6.41	0.01	0.08	16.75
	Wetland (WL)	0.22	4.87	-	0.03	1.82	-	3.23	0.13	8.89	0.28	19.47
	Miscellaneous land (ML)	0.11	0.12	0.09	0.08	0.12	-	0.04	0.03	-	0.28	0.87
Total		33.10	220.74	21.84	19.78	79.22	436.91	33.37	27.26	16.41	2.71	891.35

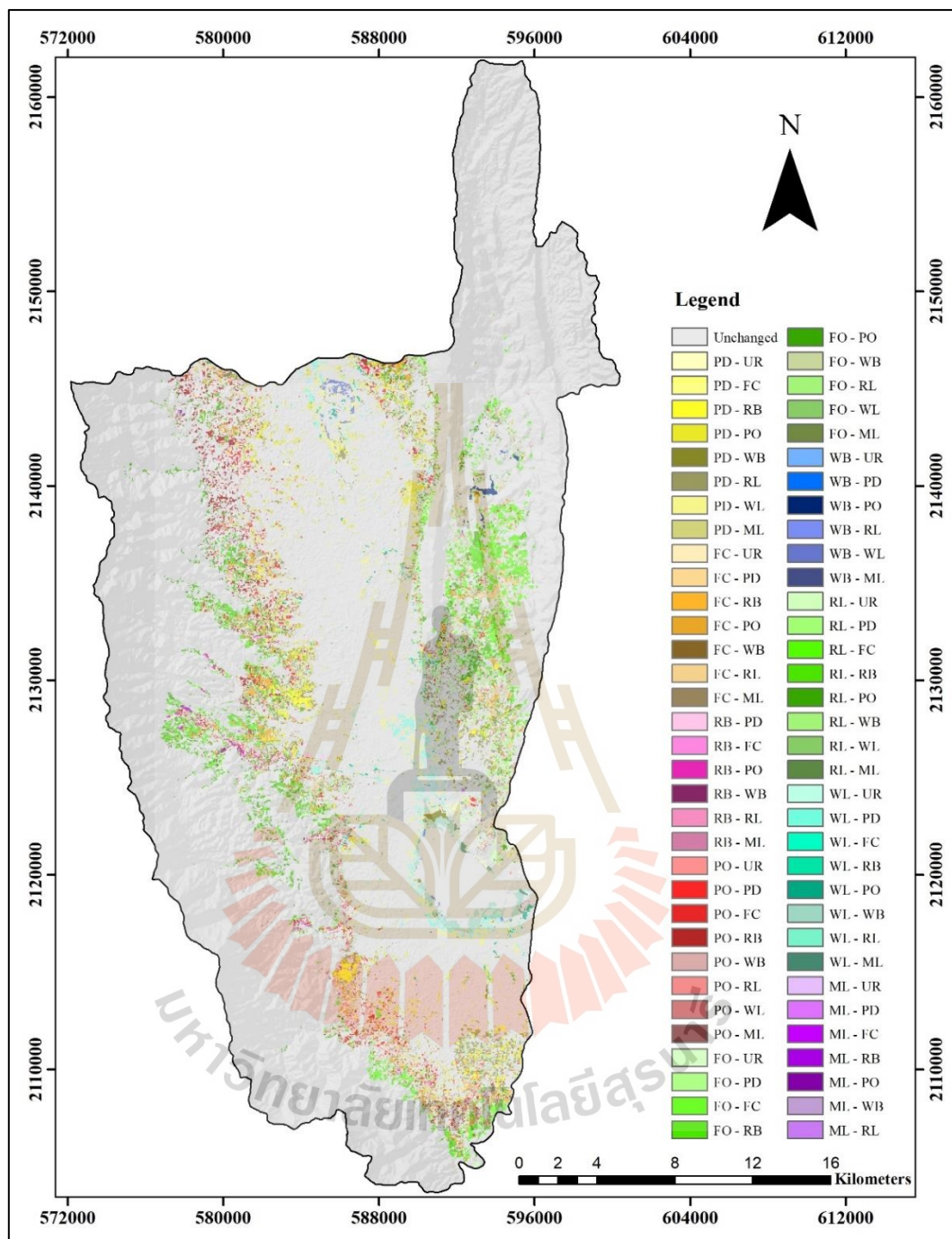


Figure 4.13 Distribution of LULC change between 2009 and 2019.

According to a transitional change matrix of LULC between 2009 and 2019 in Table 4.9, the considerable increasing area of LULC types between 2009 and 2019 are perennial trees and orchard (19.51 km² or 1.95 km² per year), para rubber (16.43 km² or 1.64 km² per year) and rangeland (10.51 km² or 1.05 km² per year). The significant increase of perennial trees and orchard areas mainly comes from paddy fields (16.41 km²) and forest land (11.13 km²) in 2009. These findings indicate the conversion of paddy fields into perennial trees and orchards and the expansion of perennial trees and orchards into forests by farmers, as shown in Figure 4.6.

Meanwhile, the significant increase of para rubber mainly comes from forest land (6.16 km²) and perennial trees and orchards (5.90 km²) in 2009. These phenomena show the expansion of para rubber into forests and farmers' conversion of perennial trees and orchards into para rubber. As the statistical report of the existing forest area by the Royal Forest Department, the existing forest area in Phayao province decreased by 105.20 km² from 2008 to 2019 (Forest Land Management Office, 2019). Due to the trend of field Latex price increased, especially in 2011, which it reached 122.33 baths per kg. from 56.10 baths per kg. in 2009 (Thailand Rubber Statistics, 2020) that led to deforestation and change the perennial tree and orchard area to para rubber area by the farmers own the land without title documents which encroaching on forest areas to plant para rubber, accounted for 20.97% (Kreoungsanu, C. and Suksard, S., 2014). In the meantime, the increased area of rangeland mainly comes from paddy fields (8.79 km²) and perennial trees and orchards (5.27 km²) in 2009. These findings indicate the existing temporal abandoned paddy fields or perennial tree and orchards plots in the study area, as shown in Figure 4.14 (a, b, c, and d).

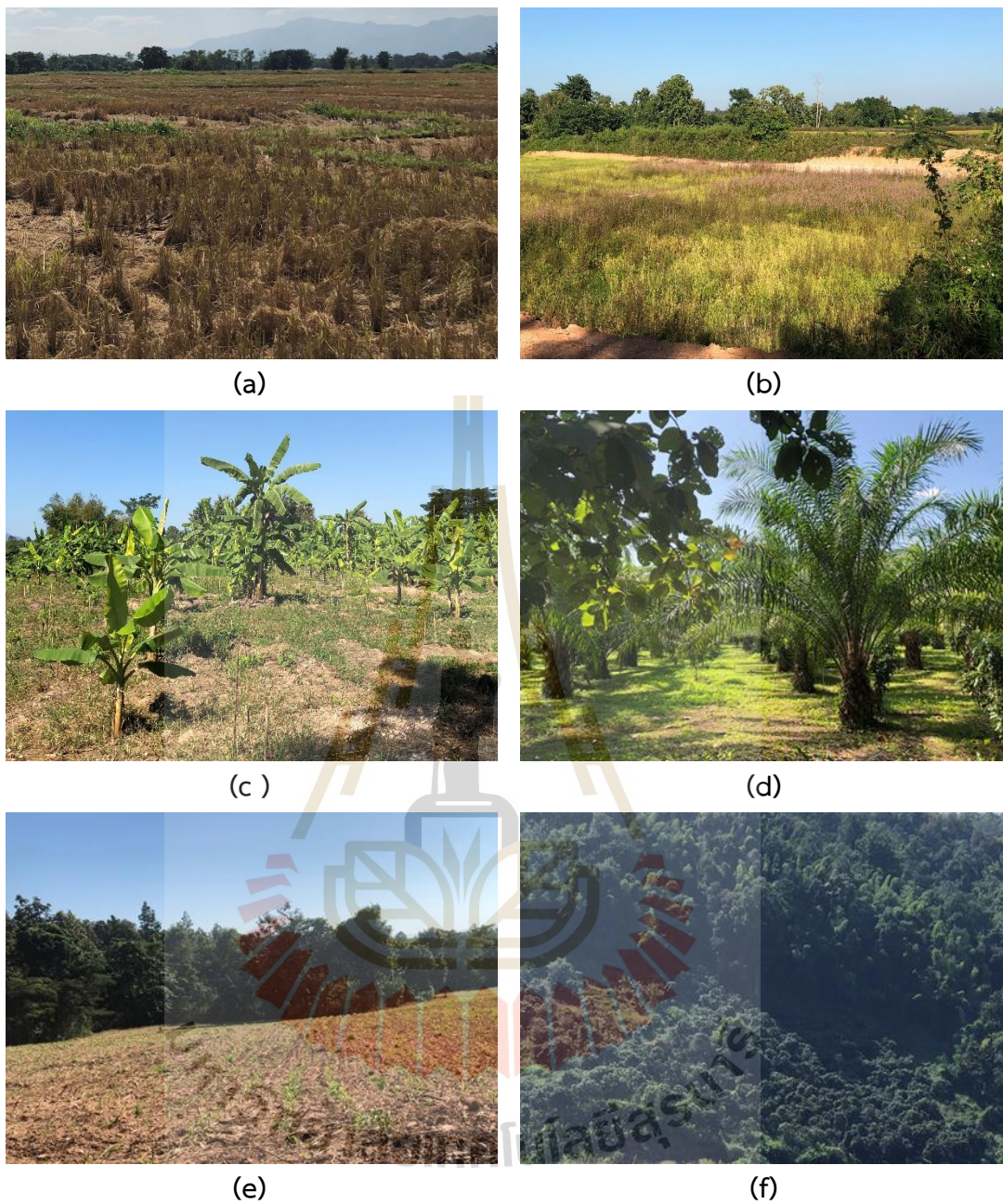


Figure 4.14 Ground photograph of abandoned paddy field (a and b), perennial tree and orchards plots (c and d), and field crop (e) and perennial trees and orchards (f) in the natural forest from a field survey in 2020.

Details for the irrelevant increasing area of LULC types between 2009 and 2019 are reported in Table 4.9. Spatial distribution of significantly increased areas of perennial trees and orchard, para-rubber and rangeland between 2009 and 2019 is displayed in Figures 4.15 to 4.17, respectively.

In contrast, the significant decreasing area of LULC types between 2009 and 2019 are forest land (39.82 km² or 3.98 km² per year) and paddy field (20.40 km² or 2.04 km² per year). The significantly decreasing forest land in 2009 was mainly converted into field crop (15.72 km²), perennial trees and orchard (11.13 km²) and para rubber (6.16 km²) in 2019. The possible reasons to describe these phenomena are the expansion of the agricultural area into the natural forest as mentioned in many studies in the area, as shown in Figure 4.14 (e and f). Meanwhile, the considerable decreasing area of paddy fields in 2009 was most converted into perennial trees and orchards (16.41 km²), rangeland (8.79 km²), and wetland (5.99 km²). These phenomena indicate the conversion of paddy fields into perennial trees and orchards and abandoned paddy fields in rangeland and wetland.

Details for the irrelevant decreasing area of LULC types between 2009 and 2019 are reported in Table 4.9. The spatial distribution of significant decrease in forest land and paddy field between 2009 and 2019 is displayed in Figures 4.18 to 4.19, respectively.

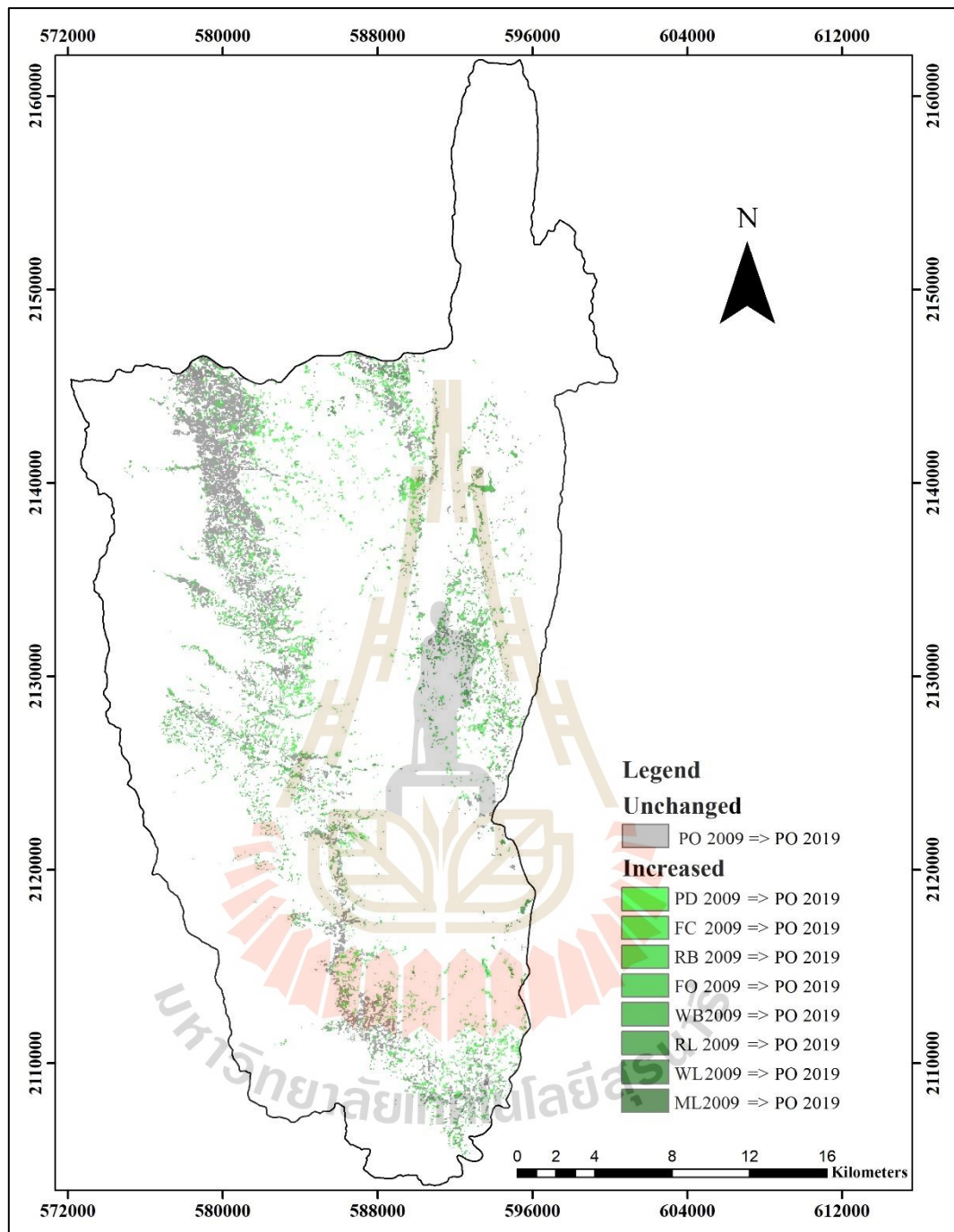


Figure 4.15 Distribution of increased and unchanged area of perennial trees and orchards between 2009 and 2019.

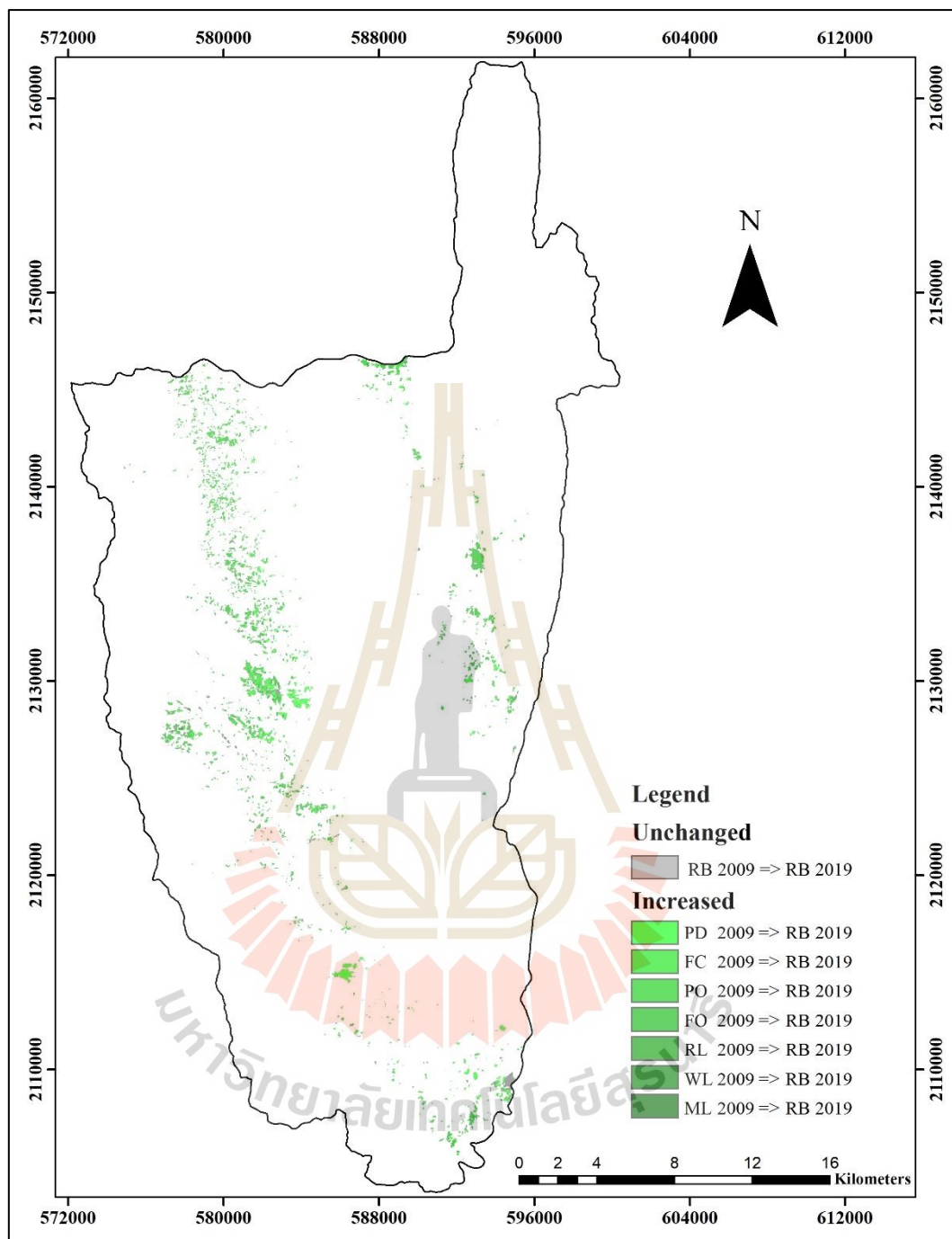


Figure 4.16 Distribution of increased and unchanged area of para rubber between 2009 and 2019.

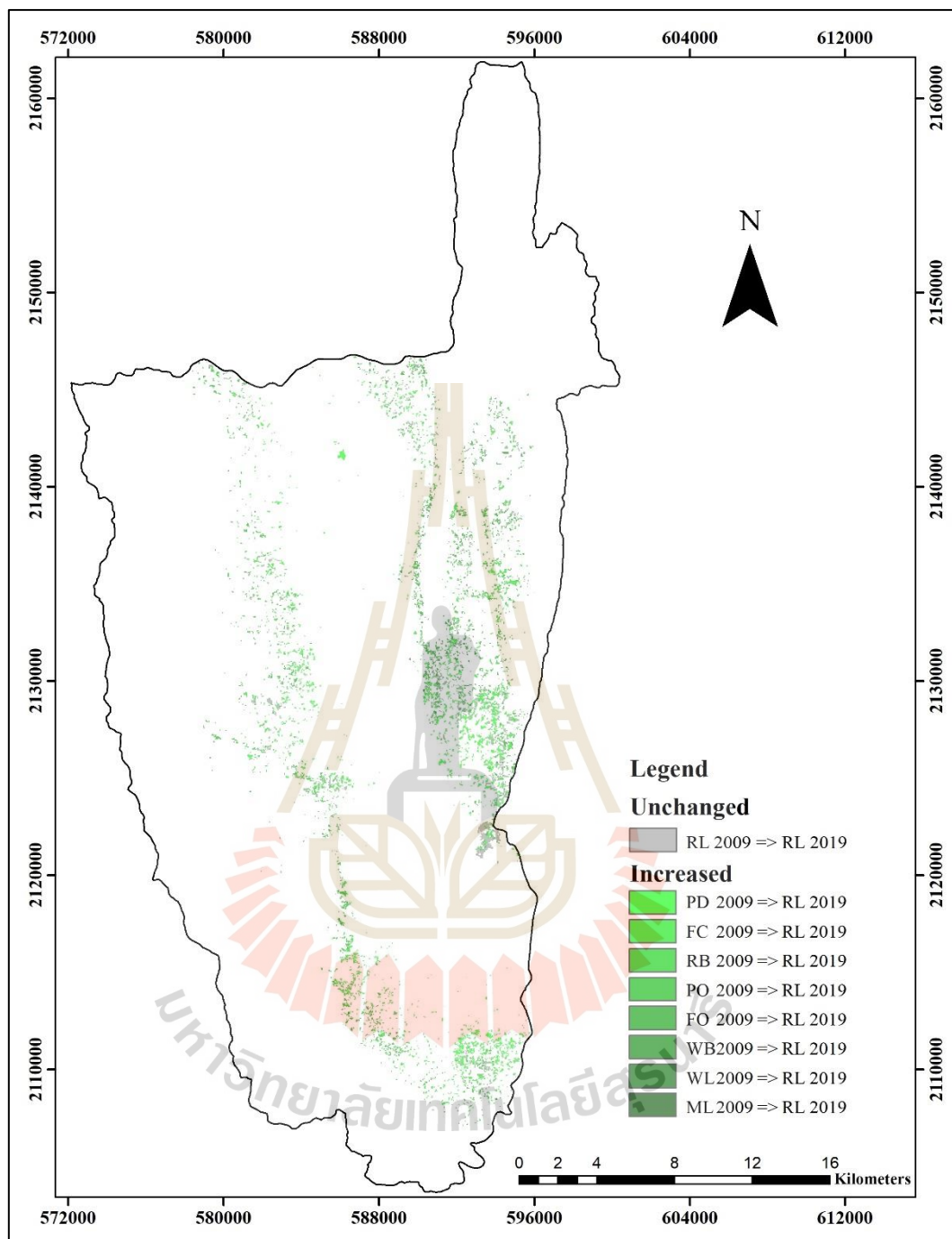


Figure 4.17 Distribution of increased and unchanged area of rangeland between 2009 and 2019.

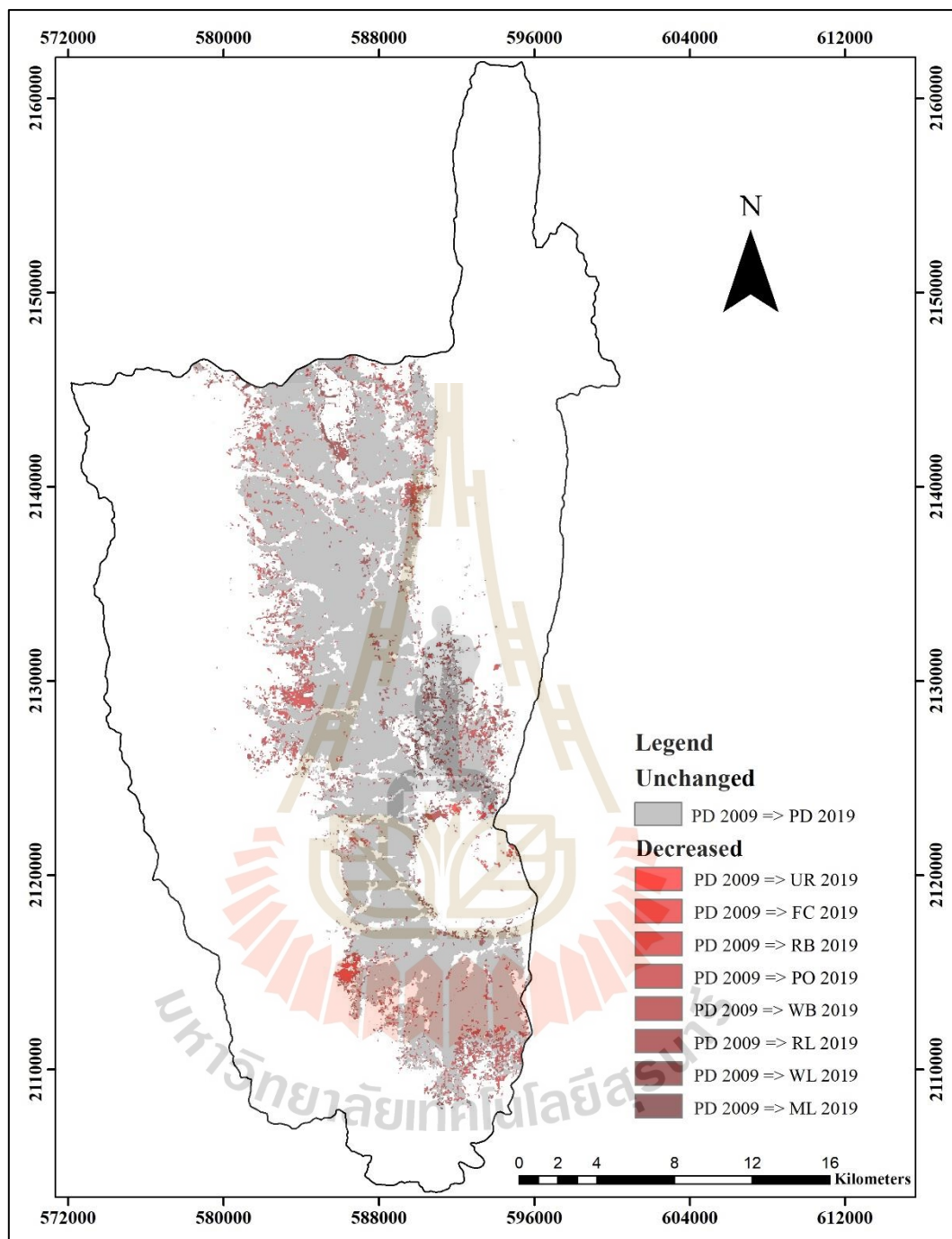


Figure 4.18 Spatial distribution of the decreased and unchanged area of paddy field between 2009 and 2019.

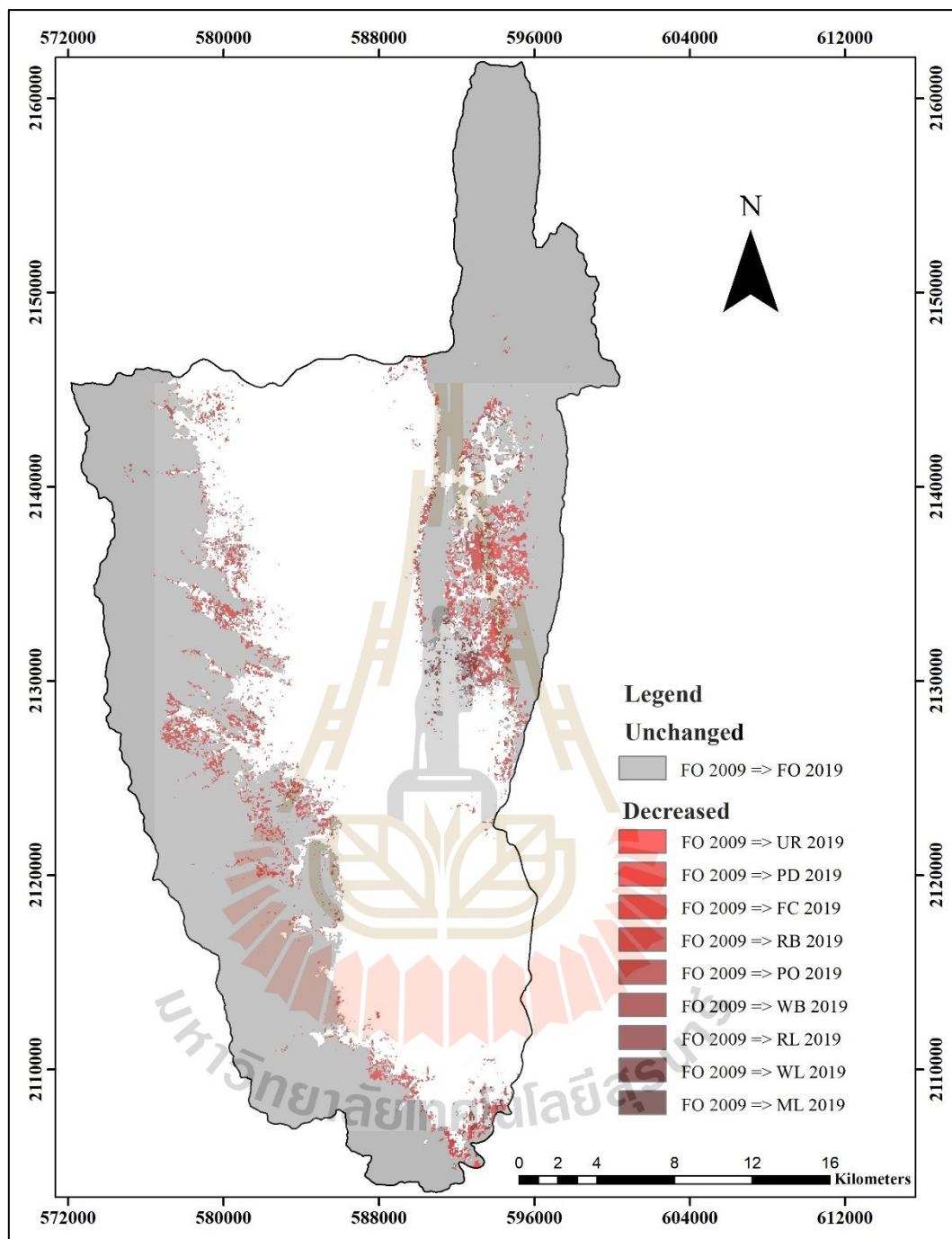
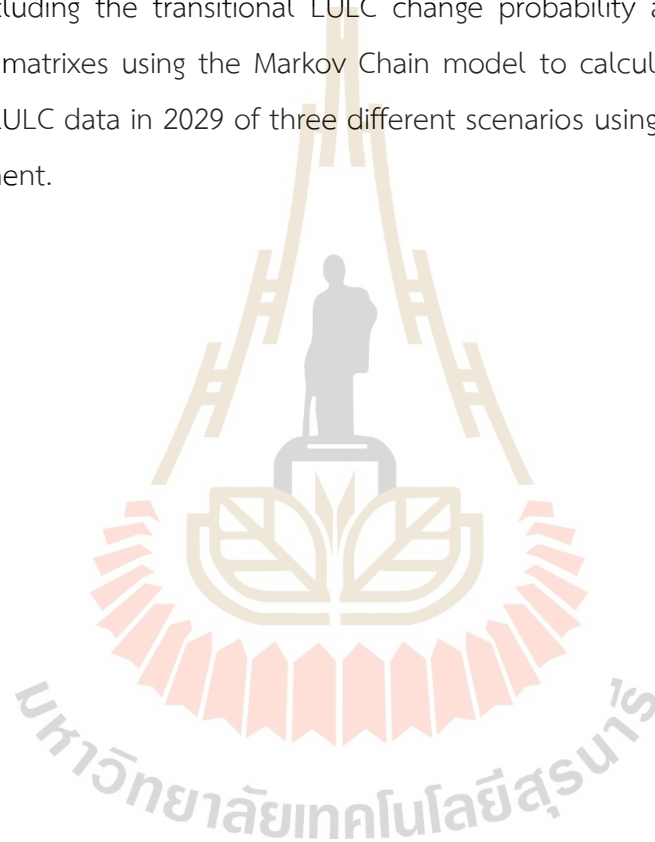


Figure 4.19 Distribution of decreased and unchanged area of forest land between 2009 and 2019.

In summary, the classified LULC maps in 2009 and 2019, applied to detect LULC change, are acceptable results as mentioned in Sections 4.1 and 4.2. A post-classification comparison change detection algorithm could provide detailed from-to-change class information between 2009 and 2019. However, reliable information depends on LULC maps' accuracy, as Coppin, Jonckheere, Nackaerts, Muys, and Lambin (2004) mentioned.

This study will apply the classified maps in 2009 and 2019 with derivative products, including the transitional LULC change probability and transitional LULC change area matrixes using the Markov Chain model to calculate land requirement and predict LULC data in 2029 of three different scenarios using the CLUE-S model in next component.



CHAPTER V

LAND REQUIREMENT ESTIMATION AND LAND USE AND LAND COVER PREDICTION OF THREE DIFFERENT SCENARIOS

This chapter presents the second and third objectives' results focusing on land requirement estimation and prediction of LULC of three different scenarios. The main results consist of (1) driving force on LULC change, (2) local parameter of CLUE-S model for LULC prediction, (3) land requirement estimation and prediction of Scenario I: Trend of LULC evolution, (4) land requirement estimation and prediction of Scenario II: Maximization ecosystem service values, and (5) land requirement estimation and prediction of Scenario III: Economic crop zonation are here described and discussed in details

5.1 Driving force on LULC change

According to the CLUE-S model's first step, LULC type location preference according to driving force on LULC change was identified by performing logistic regression analysis. In this study, eleven driving factors on LULC change, modified based on lamchuen and Thepwong (2020), were examined to identify a specific LULC type preference using multicollinearity test and logistics regression analysis. These factors include soil drainage, distance to stream, distance to water body, distance to village, slope, distance to road, distance to fault, annual rainfall, elevation, income per capita at sub-district level, and population density at sub-district level (Figure 5.1). The multicollinearity test among the physical and socio-economic factors (independent available) using the VIF (variance inflation factor) is summarized in Table 5.1. The general rule of thumb, the VIF values should not exceed 10 (Traore and Watanabe, 2017; Kamwi et al., 2018). As a result, all selected driving factors are insignificantly correlated among variables. The multiple linear regression equation of each specific

LULC type location preference with AUC value by logistic regression analysis is summarized in Table 5.2.

The details of the driving force for each LULC type allocation using logistic regression analysis are separately explained and discussed in the following section.

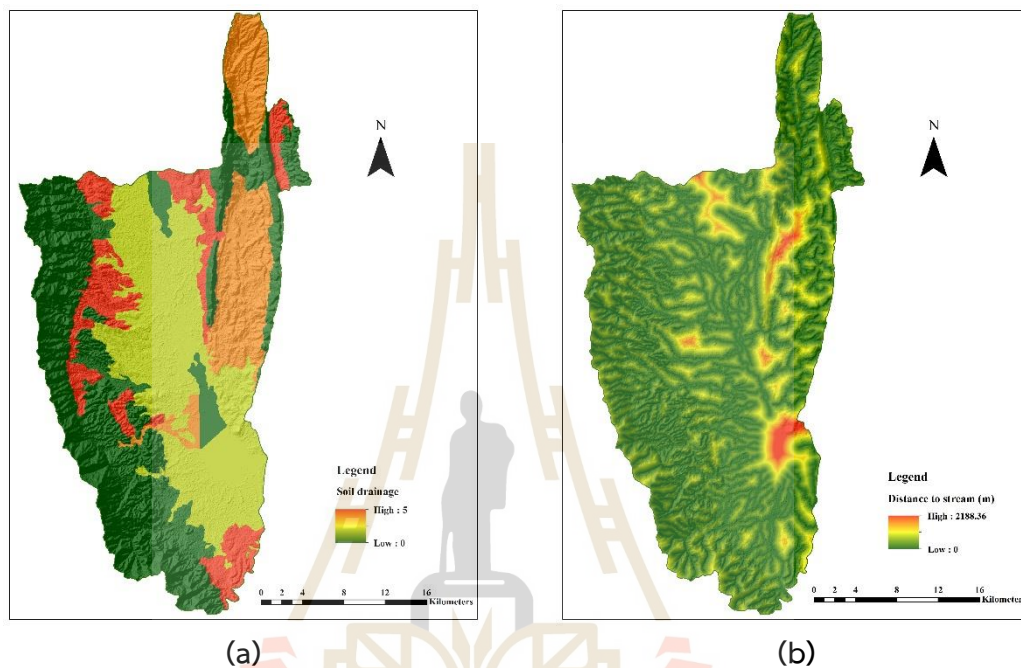


Figure 5.1 Driving factors on LULC change: (a) Soil drainage, (b) Distance to stream (m), (c) Distance to water body (m), (d) Distance to village (m), (e) Slope (%), (f) Distance to road (m), (g) Distance to fault (m), and (h) Annual rainfall (mm), (i) Elevation (m), (j) Income per capita at sub-district level (Baht), and (k) Population density at sub-district level (persons per km²).

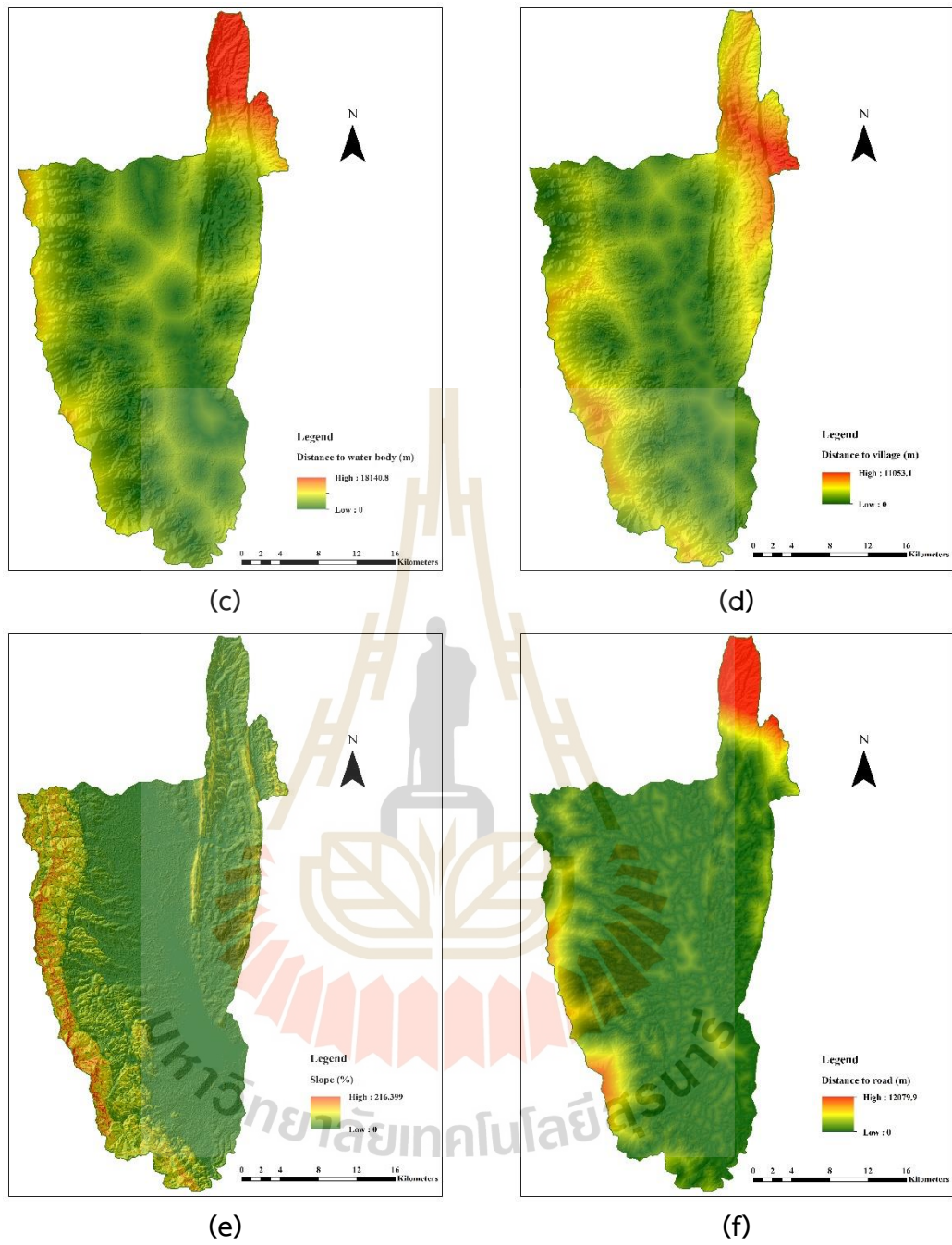


Figure 5.1 (Continued).

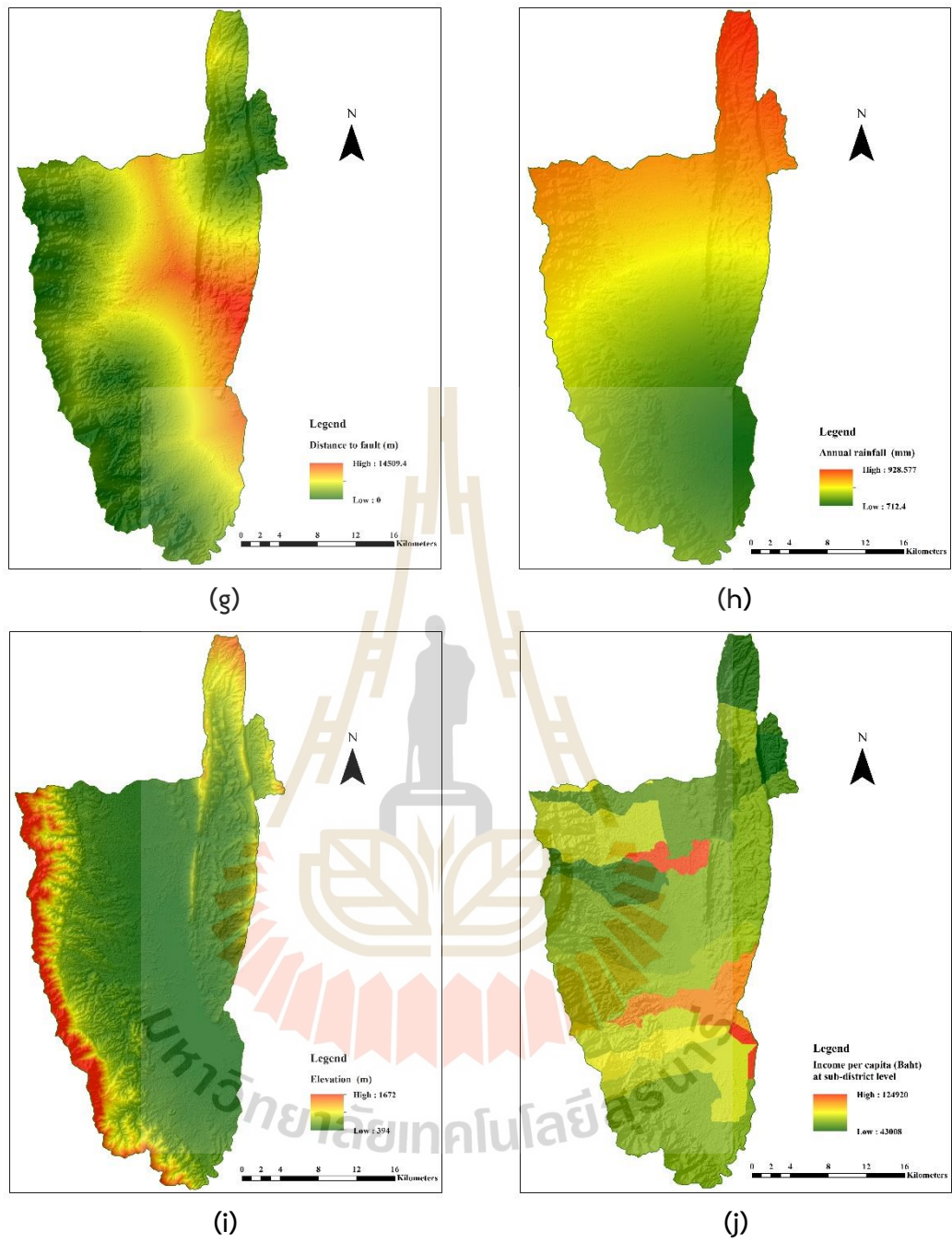
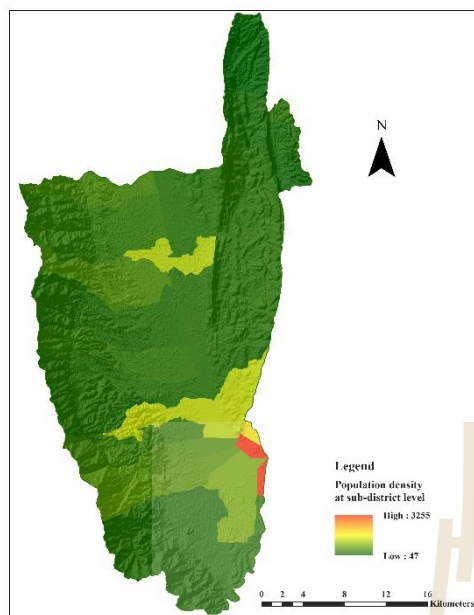


Figure 5.1 (Continued).



(k)

Figure 5.1 (Continued).

Table 5.1 Statistical data of multicollinearity test of driving factors effect on LULC type.

No.	Driving factor	Unstandardized Coefficients		Standardized Coefficient	t-test	Sig.	VIF
		Beta	Std. error				
1	Soil drainage (X_1)	-0.0229	.0056	-.0207	-4.1086	.0000	1.4736
2	Distance to stream (X_2)	0.0011	.0000	.1476	33.5946	.0000	1.1226
3	Distance to water body (X_3)	-0.0002	.0000	-.3006	-29.9464	.0000	5.8550
4	Distance to village (X_4)	0.0003	.0000	.3579	66.7967	.0000	1.6688
5	Slope (X_5)	0.0142	.0008	.1225	17.8190	.0000	2.7464
6	Distance to road (X_6)	0.0003	.0000	.2327	26.3178	.0000	4.5438
7	Distance to fault (X_7)	-0.0001	.0000	-.0991	-18.5922	.0000	1.6527
8	Annual rainfall (X_8)	0.0015	.0001	.0737	12.3901	.0000	2.0576
9	Elevation (X_9)	0.0011	.0001	.0966	12.5618	.0000	3.4356
10	Income per capita at sub-district level (X_{10})	0.0000	.0000	.0271	3.1387	.0017	4.3486
11	Population density at sub-district level (X_{11})	-0.0005	.0001	-.0576	-7.0590	.0000	3.8632

Table 5.2 Multiple linear equations of each LULC type location preference and AUC value by binary logistic regression analysis.

Driving forces	UR	PD	FC	RB	PO	FO	WA	RL	WL	ML
Constant	12.85642	39.00502	4.95668	-3.06218	-4.42909	-29.41296	3.26850	3.67703	26.40860	4.77505
Soil drainage (X ₁)	-0.07307	0.00050	0.33867	0.32365	0.19337	0.02614	n. s.	0.34216	-0.64019	0.40240
Distance to stream (X ₂)	0.00099	-0.00193	n. s.	n. s.	n. s.	n. s.	0.00144	0.00113	n. s.	n. s.
Distance to water body (X ₃)	0.00020	n. s.	n. s.	-0.00025	n. s.	n. s.	-0.00225	n. s.	-0.00148	n. s.
Distance to village (X ₄)	-0.00110	n. s.	0.00044	n. s.	n. s.	n. s.	n. s.	n. s.	n. s.	n. s.
Slope (X ₅)	n. s.	-0.02408	-0.02545	n. s.	-0.00531	0.08870	-0.13605	0.01579	-0.09618	-0.06799
Distance to road (X ₆)	-0.02255	-0.00103	-0.00329	-0.00220	-0.00332	n. s.	0.00342	-0.00388	n. s.	n. s.
Distance to fault (X ₇)	n. s.	n. s.	n. s.	n. s.	n. s.	n. s.	n. s.	n. s.	n. s.	n. s.
Annual rainfall (X ₈)	n. s.	0.00151	-0.00921	n. s.	0.00366	0.00222	-0.00288	-0.00398	0.00719	-0.01191
Elevation (X ₉)	-0.03247	-0.09496	n. s.	n. s.	-0.00222	0.05739	-0.00715	-0.00860	-0.08387	n. s.
Income per capita at sub-district level (X ₁₀)	n. s.	n. s.	n. s.	n. s.	n. s.	n. s.	n. s.	n. s.	n. s.	n. s.
Population density at sub-district level (X ₁₁)	0.00166	-0.00313	-0.00923	-0.00543	n. s.	n. s.	n. s.	-0.00146	n. s.	n. s.
AUC	0.95856	0.95724	0.85819	0.79793	0.79656	0.99081	0.94559	0.83176	0.95208	0.80433

Remark: All explanatory variables are significant at $p < 0.05$ error level; n. s. is not significant at 0.05 level; AUC, area under the curve.



5.1.1 Driving force for urban and built-up area allocation

The multiple linear equation of the binomial logit regression model for urban and built-up area allocation after multicollinearity test is as follows:

$$\text{Log} \left(\frac{P_i}{1-P_i} \right) = 12.85642 - 0.07307X_1 + 0.00099X_2 + 0.00020X_3 - 0.00110X_4 - 0.02255X_6 - 0.03247X_9 + 0.00166X_{11} \quad (5.1)$$

Where

- X_1 is Soil drainage (m);
- X_2 is Distance to stream (m);
- X_3 is Distance to water body (m);
- X_4 is Distance to village (m);
- X_6 is Distance to road (m);
- X_9 is Elevation (m); and
- X_{11} is Population density at sub-district level (persons per km²).

According to Eq. 5.1, four driving factors, including soil drainage, distance to the village, distance to the road, and elevation, negatively correlate with the urban and built-up area. Still, three driving factors, the distance to the stream, distance to water body, and population density at sub-district level, positively correlate with the probability of urban and built-up area allocation. All significant driving factors truly play a major role in urban and built-up area allocation. These results indicate that urban and built-up areas like to situate at poor soil drainage, far from stream and water body, close to village and road, low elevation, and high population density at sub-district level.

The AUC value for urban and built-up area allocation with a value of 0.959 is more than 0.9, suggesting an excellent fit between the predicted and actual LULC transition (Chen, Zhang, Gao, and Nie, 2018).

5.1.2 Driving force for paddy field allocation

The multiple linear equation of the binomial logit regression model for paddy field allocation after multicollinearity test is as follows:

$$\begin{aligned} \text{Log} \left(\frac{P_i}{1-P_i} \right) = & 39.00502 + 0.00050X_1 - 0.00193X_2 - 0.02408X_5 \\ & - 0.00103X_6 + 0.00151X_8 - 0.09496X_9 - 0.00313X_{11} \end{aligned} \quad (5.2)$$

Where

- X_1 is Soil drainage (m);
- X_2 is Distance to stream (m);
- X_5 is Slope (%);
- X_6 is Distance to road (m);
- X_8 is Annual rainfall (mm);
- X_9 is Elevation (m); and
- X_{11} is Population density at sub-district level (persons per km²).

According to Eq. 5.2, five driving factors include the distance to the stream, slope, distance to the road, elevation, and population density at sub-district level have a negative relationship with the probability of paddy field allocation, but two driving factors include soil drainage and annual rainfall, which positively correlate with the probability of paddy field allocation. All significant driving factors play a crucial role in paddy field allocation. These results indicate that paddy field prefers to locate at close to stream and road, flat terrain and gentle slope, proper soil drainage and rainfall, and low population density.

The AUC value for paddy field allocation with a value of 0.957 is more than 0.9; it suggests an excellent fit between the predicted and real LULC transition (Chen et al., 2018).

5.1.3 Driving force for field crop allocation

The multiple linear equation of the binomial logit regression model for field crop allocation after multicollinearity test is as follows:

$$\begin{aligned} \text{Log} \left(\frac{P_i}{1-P_i} \right) = & 4.95668 + 0.33867X_1 + 0.00044X_4 - 0.02545X_5 \\ & - 0.00329X_6 - 0.00921X_8 - 0.00923X_{11} \end{aligned} \quad (5.3)$$

Where

- X_1 is Soil drainage (m);
- X_4 is Distance to village (m);

- X_5 is Slope (%);
 X_6 is Distance to road (m);
 X_8 is Annual rainfall (mm); and
 X_{11} is Population density at sub-district level (persons per km²).

Referring to Eq. 5.3, four driving factors, including slope, distance to the road, annual rainfall, and population density at sub-district level, negatively correlate with the probability of field crop allocation. While two driving factors include soil drainage and distance to the village, have a positive relationship with the probability of field crop allocation. All significant driving factors play a significant role in field crop allocation. These results show that field crop occurs at an area with moderate to well soil drainage, far from the village, gentle slope, close to the road network, less rainfall, and low population density.

The AUC value for field crop allocation has a value of 0.858, between 0.8 and 0.9. it suggests a good fit between the predicted and real LULC transition (Chen et al., 2018).

5.1.4 Driving force for para rubber allocation

The multiple linear equation of the binomial logit regression model for para rubber allocation after multicollinearity test is as follows:

$$\text{Log} \left(\frac{P_i}{1-P_i} \right) = -3.06218 + 0.32365X_1 - 0.00025X_3 - 0.00220X_6 - 0.00543X_{11} \quad (5.4)$$

Where

- X_1 is Soil drainage (m);
 X_3 is Distance to water body (m);
 X_6 is Distance to road (m); and
 X_{11} is Population density at sub-district level (persons per km²).

According to Eq. 5.4, three driving factors, including the distance to the water body and road and population density at the sub-district level, negatively correlate with the probability of para rubber allocation. On the contrary, only one driving factor, soil drainage, has a positive relationship with the probability of para rubber allocation. All significant driving factors play an essential role in para rubber allocation. These

results demonstrate that para rubber prefers to situate at moderate to well soil drainage, close to water body and road, and few population densities at sub-district level.

The AUC value for para rubber allocation is 0.798, suggesting a fair fit between the predicted and real LULC transition (Chen et al., 2018).

5.1.5 Driving force for perennial tree and orchard allocation

The multiple linear equation of the binomial logit regression model for perennial tree and orchard allocation after multicollinearity test is as follows:

$$\begin{aligned} \text{Log} \left(\frac{P_i}{1-P_i} \right) = & -4.42909 + 0.19337X_1 - 0.00531X_5 - 0.00332X_6 \\ & + 0.00366X_8 - 0.00222X_9 \end{aligned} \quad (5.5)$$

Where

- X_1 is Soil drainage (m);
- X_5 is Slope (%);
- X_6 is Distance to road (m);
- X_8 is Annual rainfall (mm); and
- X_9 is Elevation (m).

According to Eq. 5.5, three driving factors, including slope, distance to the road, and elevation, have a negative relationship with the probability of perennial tree and orchard allocation, but two driving factors, namely soil drainage and annual rainfall, have a positive relationship with the probability of perennial tree and orchard allocation. All significant driving factors play a crucial role in the perennial tree and orchard allocation. These results reveal that perennial trees and orchards prefer to be located at good soil drainage, high rainfall, gentle slope, flat terrain, and close to the road.

The AUC value for perennial tree and orchard allocation is 0.797, suggesting a fair fit between the predicted and actual LULC transition (Chen et al., 2018).

5.1.6 Driving force for forest land allocation

The multiple linear equation of the binomial logit regression model for forest land allocation after multicollinearity test is as follows:

$$\text{Log} \left(\frac{P_i}{1-P_i} \right) = -29.41296 + 0.02614X_1 + 0.08870X_5 + 0.00222X_8 + 0.05739X_9 \quad (5.6)$$

Where

- X_1 is Soil drainage (m);
- X_5 is Slope (%);
- X_8 is Annual rainfall (mm); and
- X_9 is Elevation (m).

According to Eq. 5.6, all driving factors, including soil drainage, slope, annual rainfall, and elevation, positively correlate with the probability of forest land allocation. All significant driving factors play a critical role in forest land allocation. These results expose that forest land is mainly located at good soil drainage, high rainfall, steep gradient, and high altitude.

The AUC value for forest land allocation with a value of 0.991 is more than 0.9; it suggests an excellent fit between the predicted and real LULC transition (Chen, Zhang, Gao, and Nie, 2018).

5.1.7 Driving force for water body allocation

The multiple linear equation of the binomial logit regression model for water body allocation after multicollinearity test is as follows:

$$\text{Log} \left(\frac{P_i}{1-P_i} \right) = 3.26850 + 0.00144X_2 - 0.00225X_3 - 0.13605X_5 + 0.00342X_6 - 0.00288X_8 - 0.00715X_9 \quad (5.7)$$

Where

- X_2 is Distance to stream (m);
- X_3 is Distance to water body (m);
- X_5 is Slope (%);
- X_6 is Distance to road (m);
- X_8 is Annual rainfall (mm); and
- X_9 is Elevation (m).

According to Eq. 5.7, four driving factors, which include the distance to the water body, slope, annual rainfall, and elevation, have a negative relationship with the

probability of water body allocation, but two driving factors, including the distance to stream and road, have a positive relationship with the probability of water body allocation. All significant driving factors play a crucial role in water body allocation. These results express that the water body primarily situates far from stream and road, close to the water body, gentle slope, low rainfall, and low elevation.

The AUC value for water body allocation with a value of 0.946 is more than 0.9; it suggests an excellent fit between the predicted and actual LULC transition (Chen et al., 2018).

5.1.8 Driving force for rangeland allocation

The multiple linear equation of the binomial logit regression model for rangeland allocation after multicollinearity test is as follows:

$$\text{Log} \left(\frac{P_i}{1-P_i} \right) = 3.67703 + 0.34216X_1 + 0.00113X_2 + 0.01579X_5 - 0.00388X_6 - 0.00398X_8 - 0.00860X_9 - 0.00146X_{11} \quad (5.8)$$

Where

- X_1 is Soil drainage (m);
- X_2 is Distance to stream (m);
- X_5 is Slope (%);
- X_6 is Distance to road (m);
- X_8 is Annual rainfall (mm);
- X_9 is Elevation (m); and
- X_{11} is Population density at sub-district level (persons per km²).

According to Eq. 5.8, four driving factors, including the distance to the road, annual rainfall, elevation, and population density at sub-district level, negatively correlate with the probability of rangeland allocation. Still, three driving factors, including soil drainage, distance to the stream, and slope, have positively correlated with the probability of rangeland allocation. All significant driving factors play an important role in rangeland allocation. These results show that rangeland is mainly located at good soil drainage, far from the stream, steep slope, close to the road, low precipitation, and low population density.

The AUC value for field crop allocation with a value of 0.832 is between values 0.8 and 0.9. it suggests a good fit between the predicted and real LULC transition (Chen et al., 2018).

5.1.9 Driving force for wetland allocation

The multiple linear equation of the binomial logit regression model for wetland allocation after multicollinearity test is as follows:

$$\begin{aligned} \text{Log} \left(\frac{P_i}{1-P_i} \right) = & 26.40860 - 0.64019X_1 - 0.00148X_3 - 0.09618X_5 \\ & + 0.00719X_8 - 0.08387X_9 \end{aligned} \quad (5.9)$$

Where

- X_1 is Soil drainage (m);
- X_3 is Distance to water body (m);
- X_5 is Slope (%);
- X_8 is Annual rainfall (mm); and
- X_9 is Elevation (m).

According to Eq. 5.9, four driving factors include soil drainage, distance to water body, slope, and elevation, have a negative relationship with the probability of wetland allocation, but only one driving factor, annual rainfall, has a positive relationship with the probability of wetland allocation. All significant driving factors play a significant role in wetland allocation. These results indicate that wetland is mainly situated at poor soil drainage, close to the water body, high precipitation, and a low slope with flat terrain.

The AUC value for wetland allocation with a value of 0.952 is more than 0.9; it suggests an excellent fit between the predicted and real LULC transition (Chen et al., 2018).

5.1.10 Driving force for miscellaneous land allocation

The multiple linear equation of the binomial logit regression model for miscellaneous land allocation after multicollinearity test is as follows:

$$\text{Log} \left(\frac{P_i}{1-P_i} \right) = 4.77505 + 0.40240X_1 - 0.06799X_5 - 0.01191X_8 \quad (5.10)$$

Where

- X_1 is Soil drainage (m);
 X_5 is Slope (%); and
 X_8 is Annual rainfall (mm).

According to Eq. 5.10, two driving factors, slope and annual rainfall, have a negative relationship with the probability of miscellaneous land allocation, but only one factor, namely soil drainage, has a positive relationship with the probability of miscellaneous land allocation. All significant driving factors play a vital role in miscellaneous land allocation. These results reveal that miscellaneous land mainly situates at moderate to well soil drainage, low slope, and low rainfall.

The AUC value for miscellaneous land allocation is 0.804, suggesting a fair fit between the predicted and real LULC transition (Chen et al., 2018).

In summary, the most significant driving factor for all LULC type allocation in the study area is soil drainage. The second vital driving factors for LULC type allocation are slope and annual rainfall. The third crucial driving factor for the LULC type allocation area is the distance to the road and elevation. While, population density at the sub-district level plays a vital role in the land allocation of urban and built-up areas, paddy fields, field crops, para rubber, and rangeland. Likewise, the distance to the stream plays a crucial role in the land allocation of urban and built-up areas, paddy fields, water bodies, and rangeland. Also, the distance to water body plays a significant role in the land allocation of built-up area, para rubber, water body, and wetland. Moreover, distance to village plays an essential role in urban and built-up areas and field crops. Nevertheless, the distance to fault and the income per capita at sub-district level are insignificant driving factors for all LULC type allocations in the study area. The significant driving factors of each LULC type are further used by the CLUE-S model for LULC allocation during the simulation process.

These findings are similar to the previous works of lamchuen and Thepwong (2020). They applied the CLUMondo model, the previous version of the CLUE-S model, to predict LULC type in the Upper Ing watershed, Phayao province. They found that the top two driving factors for thirteen LULC types allocations by logistic regression

analysis were annual rainfall and elevation. Moreover, soil drainage was a crucial driving factor for nine LULC Types in agriculture.

Furthermore, using logistic regression analysis, the derived AUC values varying from 0.79656 to 0.99081 for each LULC type allocation show primarily good and excellent fits between the predicted and actual LULC allocation.

5.2 Local parameter of CLUE-S model for LULC prediction

Two sets of local parameters for LULC prediction of three different scenarios by the CLUE-S model are conversion matrix and elasticity of LULC change. These are considered and set up based on the transitional and probability change matrix of LULC data between 2009 and 2019. The conversion matrix, which shows LULC change opportunity among LULC types, is assigned as 1 when it is allowed or as 0 when it is not allowed. Meanwhile, elasticity values imply the probability of land use change. It ranges from 0 (easy conversion) to 1 (irreversible change) and is set up according to the transitional probability change matrix in the past period.

The conversion matrix of LULC change between 2019 and 2029 for LULC prediction in 2029 of three scenarios was assigned according to characteristics of each scenario as follows:

(1) Scenario I: Trend of LULC evolution. The transitional change matrix between LULC data in 2009 and 2019, as shown in Table 4.9, extracted by the Markov Chain model, was used as basic information to assign the conversion matrix of this scenario, as a summary in Table 5.3. As a result, the urban and built-up areas in 2019 cannot be converted into other LULC classes from 2020 to 2029. Meanwhile, other LULC classes in 2019 can be converted into specific LULC classes between 2020 and 2029. For instance, the paddy field in 2019 allows converting into an urban and built-up area, rangeland, and miscellaneous land between 2020 and 2029. Likewise, forest land in 2019 allows converting into an urban and built-up area, field crop, para rubber, water body, rangeland, and miscellaneous land between 2020 and 2029.

Table 5.3 Conversion matrix of possible LULC change between 2019 and 2029 for Scenario I: Trend of LULC evolution.

LULC Types	Possible change in 2029									
	UR	PD	FC	RB	PO	FO	WB	RL	WL	ML
Urban and built-up area (UR)	1	0	0	0	0	0	0	0	0	0
Paddy field (PD)	1	1	0	0	0	0	0	1	0	1
Field crop (FC)	1	0	1	1	1	0	0	1	0	1
Para rubber (RB)	0	0	0	1	0	0	0	0	0	0
Perennial tree and orchard (PO)	0	0	0	1	1	0	0	0	0	0
Forest land (FO)	1	0	1	1	0	1	1	1	0	1
Water body (WB)	0	0	0	0	0	0	1	0	1	0
Rangeland (RL)	1	1	0	1	1	0	0	1	0	0
Wetland (WL)	0	1	0	0	0	0	1	0	1	1
Miscellaneous land (ML)	1	0	1	1	0	0	0	0	0	1

Note 0 is not allowed and 1 is allowed

(2) Scenario II: Maximization ecosystem service values. The conversion matrix of Scenario II is subject to maximizing ecosystem service values using a simple benefit transfer method (Costanza et al., 1997) by increasing wetland and decreasing paddy field, rangeland, and miscellaneous land. According to scenario characteristics, paddy fields, rangeland, and miscellaneous land are allowed to convert into the wetland to increase the wetland's ecosystem service function to retain sediment and nutrient export. Meanwhile, the conversion of urban and built-up area, field crop, para rubber, perennial tree and orchard, and forest land into other LULC types is based on the transitional LULC change matrix between 2009 and 2019 by the Markov Chain model same as Scenario I. In contrast, the water body does not convert into other LULC classes, as a summary in Table 5.4.

Table 5.4 Conversion matrix of possible LULC change between 2019 and 2029 for Scenario II: Maximization ecosystem service values.

LULC Types	Possible change in 2029									
	UR	PD	FC	RB	PO	FO	WB	RL	WL	ML
Urban and built-up area (UR)	1	0	0	0	0	0	0	0	0	0
Paddy field (PD)	1	1	0	0	0	0	0	1	1	1
Field crop (FC)	1	0	1	1	1	0	0	1	0	1
Para rubber (RB)	0	0	0	1	0	0	0	0	0	0
Perennial tree and orchard (PO)	0	0	0	1	1	0	0	0	0	0
Forest land (FO)	1	0	1	1	0	1	1	1	0	1
Water body (WB)	0	0	0	0	0	0	1	0	0	0
Rangeland (RL)	1	1	0	1	1	0	0	1	1	0
Wetland (WL)	0	1	0	0	0	0	0	0	1	1
Miscellaneous land (ML)	1	0	1	1	0	0	0	0	1	1

Note 0 is not allowed and 1 is allowed

(3) Scenario III: Economic crop zonation. The conversion matrix of Scenario III is assigned based on areas of suitability classes for economic crops (paddy field, field crop, para rubber, and perennial tree and orchard) from Agri-Map by the LDD and Markov Chain model. According to scenario characteristics, existing LULC types as non-economic crops include forest land, rangeland and miscellaneous land, excluding urban and built-up area, water body and wetland are allowed to convert into economic crops (paddy field, field crop, para rubber, and perennial tree and orchard) according to their zonation by updating with the existing LULC data in 2019. Meanwhile, the conversion of urban and built-up area, water body and wetland into other LULC types are based on transitional change matrix between LULC data in 2009 and 2019 by the Markov Chain model, same as Scenario I. The conversion matrix of Scenario III is reported in Table 5.5.

Table 5.5 Conversion matrix of possible LULC change between 2019 and 2029 for Scenario III: Economic crop zonation.

LULC Types	Possible change in 2029									
	UR	PD	FC	RB	PO	FO	WB	RL	WL	ML
Urban and built-up area (UR)	1	0	0	0	0	0	0	0	0	0
Paddy field (PD)	1	1	0	0	0	0	0	1	0	1
Field crop (FC)	1	0	1	0	0	0	0	1	0	1
Para rubber (RB)	0	0	1	1	0	0	0	0	0	0
Perennial tree and orchard (PO)	0	0	1	1	1	0	0	0	0	0
Forest land (FO)	1	1	1	1	1	1	1	1	0	1
Water body (WB)	0	0	0	0	0	0	1	0	1	0
Rangeland (RL)	1	1	1	0	0	0	0	1	0	0
Wetland (WL)	0	1	0	0	0	0	1	0	1	1
Miscellaneous land (ML)	1	1	1	0	0	0	0	1	0	1

Note 0 is not allowed and 1 is allowed

Besides, elasticity values, which are applied to three different scenarios in LULC prediction using the CLUE-S model, were assigned according to the transition probability matrix of LULC change between 2009 and 2019 by the Markov Chain model suggested by Ongsomwang and lamchuen (2015), which is presented in Table 5.6. As a result, the elasticity values as probability value for the urban and built-up area, paddy field, field crop, para rubber, perennial tree and orchard, forest land, water body, rangeland, wetland, and miscellaneous land are 1.00, 0.84, 0.22, 0.37, 0.67, 0.92, 0.93, 0.38, 0.45, and 0.29 respectively.

Table 5.6 Transition probability matrix of LULC change between 2009 and 2019 by the Markov Chain model.

LULC Types		LULC in 2019									
		UR	PD	FC	RB	PO	FO	WB	RL	WL	ML
LULC in 2009	Urban and built-up area (UR)	1.000	0.000	0.000	0.000	0.000	0.000	0.000	0.000	0.000	0.000
	Paddy field (PD)	0.005	0.842	0.001	0.012	0.068	0.000	0.010	0.037	0.025	0.002
	Field crop (FC)	0.002	0.085	0.216	0.146	0.269	0.000	0.005	0.207	0.000	0.071
	Para rubber (RB)	0.000	0.187	0.026	0.371	0.308	0.000	0.081	0.022	0.000	0.005
	Perennial tree and orchard (PO)	0.002	0.086	0.029	0.096	0.667	0.000	0.029	0.087	0.000	0.004
	Forest land (FO)	0.001	0.003	0.033	0.013	0.023	0.916	0.003	0.006	0.001	0.000
	Water body (WB)	0.000	0.003	0.000	0.000	0.023	0.000	0.930	0.002	0.040	0.001
	Rangeland (RL)	0.055	0.255	0.014	0.059	0.224	0.000	0.006	0.382	0.000	0.006
	Wetland (WL)	0.010	0.253	0.000	0.002	0.095	0.000	0.166	0.007	0.452	0.016
	Miscellaneous land (ML)	0.123	0.140	0.094	0.100	0.165	0.000	0.043	0.048	0.000	0.288



5.3 Land requirement estimation and LULC prediction of Scenario I: Trend of LULC evolution

The land requirement (demand) estimation of Scenario I: Trend of LULC evolution was calculated based on the annual rate of LULC change from the transition area matrix between 2019 and 2029 using the Markov Chain model, as shown in Table 5.7. The annual land requirement of Scenario I between 2019 and 2029 are presented in Table 5.8.

Table 5.7 Transition area matrix of LULC change between 2019 and 2029 from Markov Chain model.

LULC in 2019	LULC Change									
	UR	PD	FC	RB	PO	FO	WB	RL	WL	ML
Urban and built-up area (UR)	33.10	0.00	0.00	0.00	0.00	0.00	0.00	0.00	0.00	0.00
Paddy field (PD)	1.19	185.84	0.15	2.59	14.93	0.00	2.15	8.05	5.41	0.43
Field crop (FC)	0.05	1.86	4.71	3.18	5.88	0.00	0.11	4.51	0.00	1.54
Para rubber (RB)	0.00	3.71	0.50	7.34	6.10	0.00	1.60	0.43	0.00	0.10
Perennial trees and Orchard (PO)	0.18	6.76	2.31	7.63	52.84	0.00	2.30	6.85	0.02	0.33
Forest land (FO)	0.41	1.10	14.48	5.79	10.11	400.38	1.16	2.79	0.62	0.07
Water body (WB)	0.01	0.11	0.00	0.00	0.78	0.00	31.03	0.07	1.33	0.04
Rangeland (RL)	1.48	6.95	0.38	1.62	6.10	0.00	0.15	10.42	0.01	0.15
Wetland (WL)	0.17	4.15	0.00	0.03	1.55	0.00	2.73	0.11	7.41	0.26
Miscellaneous land (ML)	0.33	0.38	0.26	0.27	0.45	0.00	0.11	0.13	0.00	0.78

Table 5.8 Annual land requirement of Scenario I (Trend of LULC evolution) by LULC type.

Year	Area in km ²									
	UR	PD	FC	RB	PO	FO	WB	RL	WL	ML
2019	33.10	220.74	21.84	19.78	79.22	436.91	33.37	27.26	16.41	2.71
2020	33.48	219.75	21.94	20.65	81.18	433.26	34.16	27.87	16.25	2.81
2021	33.86	218.77	22.03	21.52	83.13	429.61	34.96	28.48	16.09	2.91
2022	34.24	217.78	22.13	22.38	85.08	425.96	35.76	29.09	15.93	3.01
2023	34.63	216.79	22.22	23.25	87.03	422.30	36.56	29.70	15.77	3.11
2024	35.01	215.80	22.32	24.12	88.98	418.65	37.35	30.31	15.60	3.21
2025	35.39	214.82	22.41	24.98	90.93	415.00	38.15	30.92	15.44	3.30
2026	35.77	213.83	22.51	25.85	92.89	411.34	38.95	31.53	15.28	3.40
2027	36.16	212.84	22.60	26.71	94.84	407.69	39.75	32.14	15.12	3.50
2028	36.54	211.85	22.70	27.58	96.79	404.04	40.54	32.75	14.96	3.60
2029	36.92	210.86	22.79	28.45	98.74	400.38	41.34	33.36	14.80	3.70
Annual rate	0.38	-0.99	0.10	0.87	1.95	-3.65	0.80	0.61	-0.16	0.10

As a result, the increased LULC classes in 2029 are perennial trees and orchards, para rubber, water body, rangeland, urban and built-up area, field crop, and miscellaneous land with an increasing annual rate of 1.95, 0.87, 0.80, 0.61, 0.38, 0.10, and 0.10 km², respectively. In contrast, the decreased LULC classes in 2029 are forest land, paddy field, and wetland, with a decreasing annual rate of 3.65, 0.99, and 0.16 km², respectively.

For LULC prediction of Scenario I: Trend of LULC evolution, conversion matrix and elasticity of LULC change (Tables 5.3 and 5.6) and estimated land requirement between 2020 and 2029 (Table 5.8) were simultaneously combined to allocate LULC data between 2020 and 2029 based on the driving factors on LULC change for specific LULC type location preference (Table 5.2). The spatial distribution of the predicted LULC maps of Scenario I between 2020 and 2029 is presented in Figure 5.2. The area and percentage of LULC classes of Scenario I between 2020 and 2029 are summarized in Tables 5.9 and 5.10, respectively.

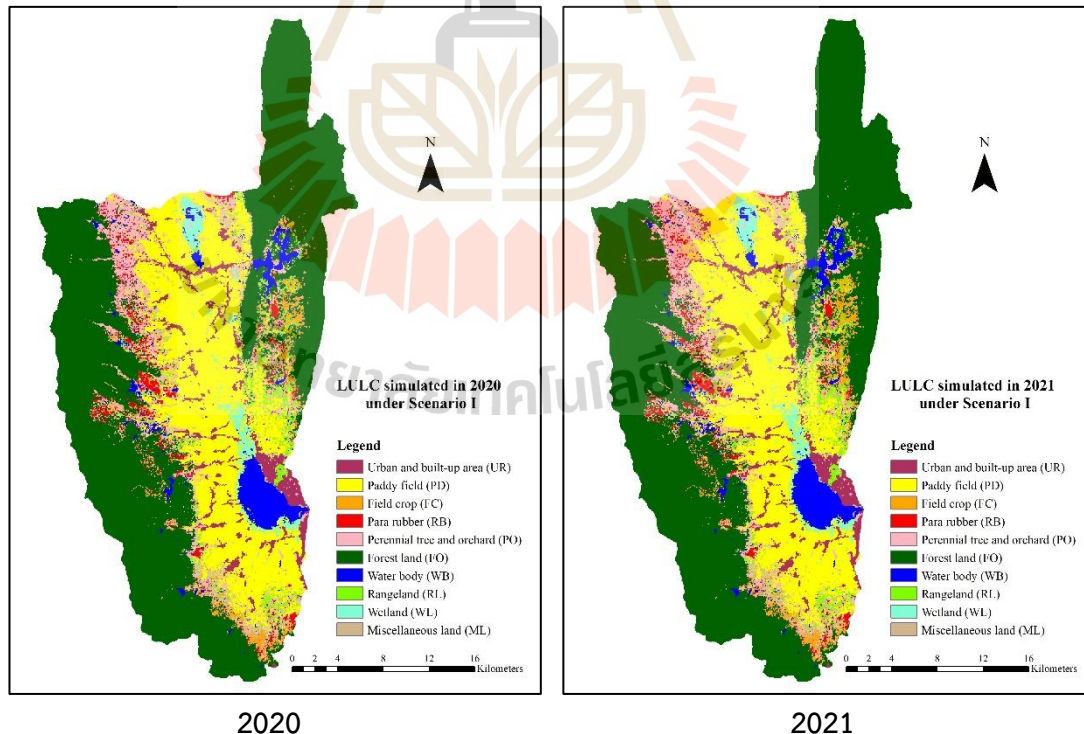


Figure 5.2 Spatial distribution of LULC prediction of Scenario I during 2020 to 2029.

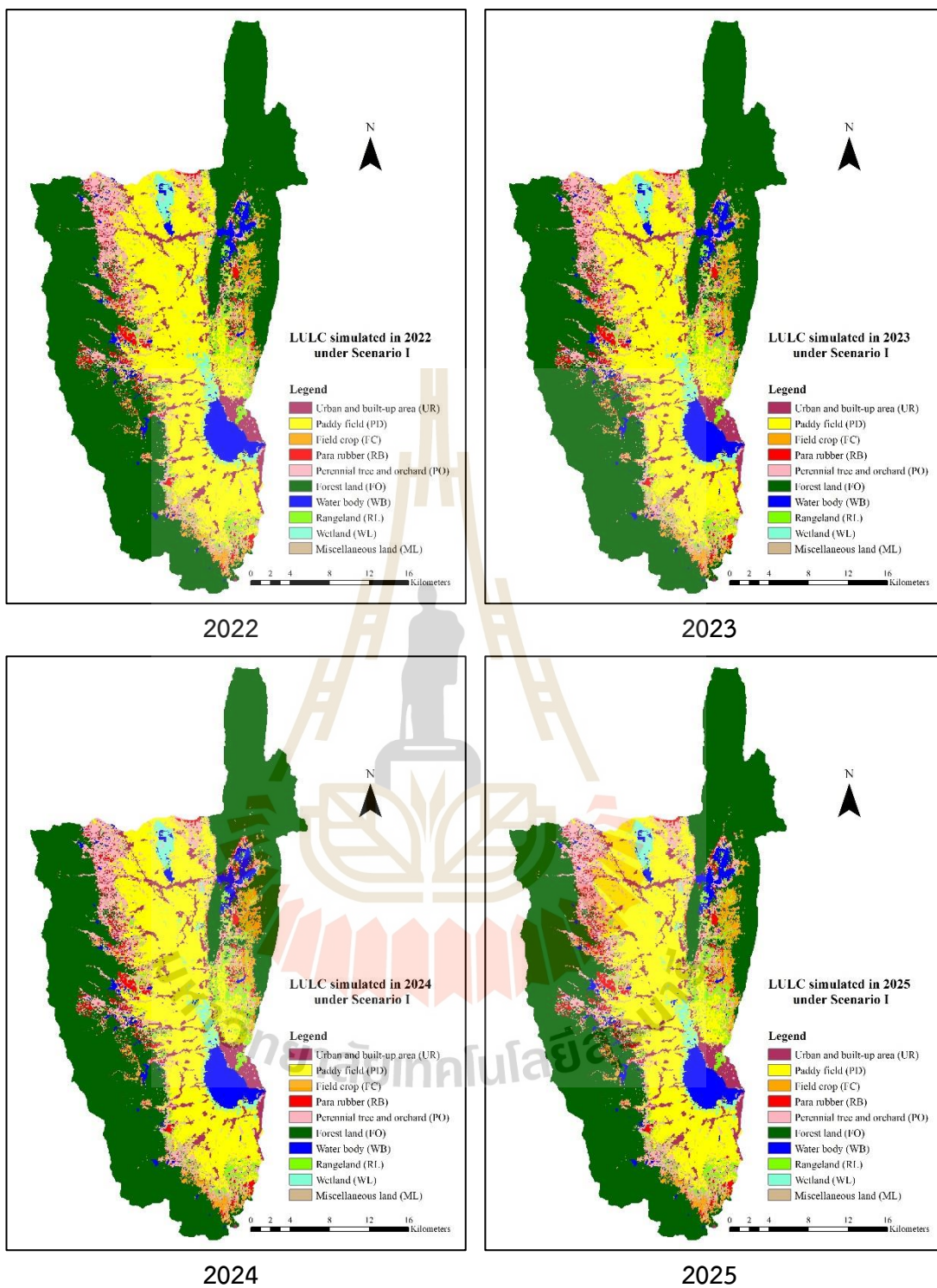


Figure 5.2 (Continued).

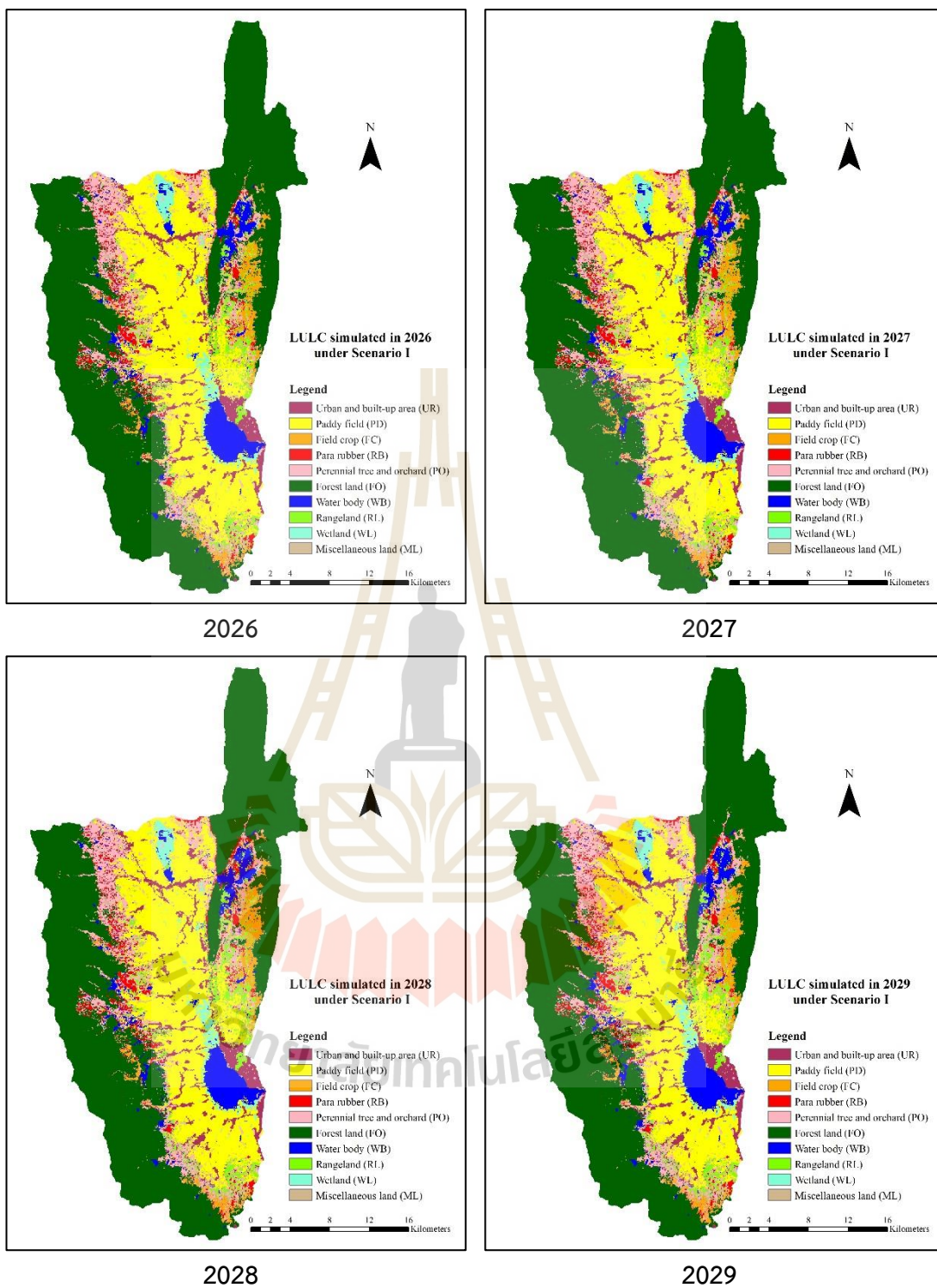


Figure 5.2 (Continued).

Table 5.9 Area of predicted LULC of Scenario I: Trend of LULC evolution between 2020 and 2029.

LULC types	Area in km ²									
	2020	2021	2022	2023	2024	2025	2026	2027	2028	2029
Urban and built-up area (UR)	33.45	33.83	34.19	34.61	34.99	35.39	35.76	36.15	36.50	36.90
Paddy field (PD)	219.73	218.73	217.73	216.77	215.77	214.81	213.81	212.79	211.82	210.84
Field crop (FC)	21.94	22.04	22.13	22.23	22.31	22.43	22.51	22.58	22.69	22.81
Para rubber (RB)	20.65	21.53	22.42	23.26	24.10	24.99	25.86	26.69	27.57	28.45
Perennial trees and Orchard (PO)	81.17	83.14	85.12	87.04	88.95	90.94	92.89	94.82	96.77	98.75
Forest land (FO)	433.27	429.62	425.96	422.30	418.63	415.00	411.35	407.68	404.03	400.39
Water body (WB)	34.18	34.99	35.78	36.57	37.36	38.16	38.97	39.76	40.58	41.35
Rangeland (RL)	27.86	28.48	29.10	29.70	30.29	30.91	31.52	32.13	32.72	33.36
Wetland (WL)	16.31	16.10	15.95	15.79	15.76	15.44	15.30	15.27	15.10	14.82
Miscellaneous land (ML)	2.79	2.88	2.98	3.08	3.19	3.28	3.38	3.48	3.57	3.68
Total	891.35	891.35	891.35	891.35	891.35	891.35	891.35	891.35	891.35	891.35

Table 5.10 Percentage of predicted LULC of Scenario I: Trend of LULC evolution between 2020 and 2029.

LULC types	Percent									
	2020	2021	2022	2023	2024	2025	2026	2027	2028	2029
Urban and built-up area (UR)	3.75	3.80	3.84	3.88	3.93	3.97	4.01	4.06	4.09	4.14
Paddy field (PD)	24.65	24.54	24.43	24.32	24.21	24.10	23.99	23.87	23.76	23.65
Field crop (FC)	2.46	2.47	2.48	2.49	2.50	2.52	2.53	2.53	2.55	2.56
Para rubber (RB)	2.32	2.42	2.52	2.61	2.70	2.80	2.90	2.99	3.09	3.19
Perennial trees and Orchard (PO)	9.11	9.33	9.55	9.76	9.98	10.20	10.42	10.64	10.86	11.08
Forest land (FO)	48.61	48.20	47.79	47.38	46.97	46.56	46.15	45.74	45.33	44.92
Water body (WB)	3.83	3.93	4.01	4.10	4.19	4.28	4.37	4.46	4.55	4.64
Rangeland (RL)	3.13	3.20	3.26	3.33	3.40	3.47	3.54	3.61	3.67	3.74
Wetland (WL)	1.83	1.81	1.79	1.77	1.77	1.73	1.72	1.71	1.69	1.66
Miscellaneous land (ML)	0.31	0.32	0.33	0.35	0.36	0.37	0.38	0.39	0.40	0.41
Total	100.00	100.00	100.00	100.00	100.00	100.00	100.00	100.00	100.00	100.00

As a result of the predicted LULC for Scenario I, areas of seven LULC types are increased in 2029 according to the rate of LULC change from the transition area matrix between LULC in 2019 and 2029 composed of urban and built-up area, field crop, para rubber, perennial trees and orchards, water body, rangeland, and miscellaneous land, which the areas cover 36.90 km² (4.14%), 22.81 km² (2.56%), 28.45 km² (3.19%), 98.75 km² (11.08%), 41.35 km² (4.64%), 33.36 km² (3.74%) and 3.68 km² (0.41%), respectively. On the contrary, the areas of paddy fields, forest land, and wetland are decreased in 2029, which the areas cover 210.84 km² (23.65%), 400.39 km² (44.92%), and 14.82 km² (1.66%), respectively.

Moreover, the transition LULC change matrix between 2019 and 2029 of Scenario I is displayed in Table 5.11. The result shows that urban and built-up area in 2019 is not converted in other LULC types in 2029, and its area is increased from 33.10 km² in 2019 to 36.90 km² in 2029. The increased areas of urban and built-up area in 2029 come from paddy field (2.62 km²), field crop (0.02 km²), forest land (1.08 km²), rangeland (0.01 km²), and miscellaneous land (0.08 km²) in 2019. Likewise, para rubber in 2019 is not converted into other LULC classes in 2029, and its area is increased from 19.78 km² in 2019 to 28.45 km² in 2029. The increased areas of para rubber in 2029 come from forest lands (8.67 km²) in 2019. Similarly, perennial trees and orchards in 2019 are not converted into other LULC classes in 2029. Its area increased from 79.22 km² in 2019 to 98.75 km² in 2029. The increased areas in 2029 come from paddy fields (0.45 km²), field crops (11.27 km²), forest lands (5.14 km²), and rangeland (2.67 km²) in 2019. Also, the water body in 2019 is not converted into other LULC classes in 2029. Its area increased from 33.37 km² in 2019 to 41.35 km² in 2029. The water body's increased areas in 2029 come from forest lands (6.40 km²) and wetlands (1.59 km²) in 2019. Similarly, the increased areas of rangeland come from paddy field (5.70 km²), field crop (0.01 km²), and forest land (3.07 km²) in 2019. Also, a wetland in 2019 is converted into a water body (1.59 km²) in 2029, and its area is decreased from 16.41 km² in 2019 to 14.82 km² in 2029.

On the opposite, paddy field in 2019 is converted into the urban and built-up area (2.62 km²), field crop (0.01 km²), perennial tree and orchards (0.45 km²), rangeland

(5.70 km²), and miscellaneous land (1.13 km²) in 2029 and its area is decreased from 220.74 km² in 2019 to 210.84 km² in 2029. Likewise, field crop in 2019 is converted into the urban and built-up areas (0.02 km²), perennial trees and orchards (11.27 km²), and rangeland (0.01 km²) in 2029, but its area is increased from 21.84 km² in 2019 to 22.81 km² in 2029. The increased areas of field crop come from paddy fields (0.01 km²), forest land (12.11 km²), and miscellaneous land (0.14 km²) in 2019. Similarly, forest land in 2019 is converted into the urban and built-up area (1.08 km²), field crop (12.11 km²), para rubber (8.67 km²), perennial tree and orchard (5.14 km²), water body (6.40 km²), rangeland (3.07 km²), and miscellaneous land (0.05 km²) in 2029 and its area is decreased from 436.91 km² in 2019 to 400.39 km² in 2029. Besides, rangeland in 2019 is converted into the urban and built-up area (0.01 km²), and perennial tree and orchard (2.67 km²) in 2029, and rangeland areas are increased from 27.26 km² in 2019 to 33.36 km² in 2029. Furthermore, miscellaneous land in 2019 is converted into urban and built-up areas (0.08 km²) and field crops (0.14 km²) in 2029, but its area is increased from 2.71 km² in 2019 to 3.68 km² in 2029. The increased areas of miscellaneous land come from paddy fields (1.13 km²) and forest lands (0.05 km²) in 2019.

As a result, the characteristics of the from-to change among LULC types between 2019 and 2029 are determined by driving factors on LULC change, their local parameters (conversion matrix and elasticity values), and their land requirements, which are applied for LULC prediction of Scenario I (Trend of LULC evolution) under the CLUE-S model. The derived predictive LULC data between 2020 and 2029 correspond with the definition of Scenario I, which allows LULC change (decreased or increased area) according to the trend of LULC evaluation between 2009 and 2019 by the Markov Chain model.

Scenario I shows a slight difference between the required land area and the predicted area of each LULC type in 2029. Even land requirement generally dictates the final area of each LULC type under of CLUE-S model. For example, the required area of paddy field in 2029 is 210.86 km², but it is allocated only 210.84 km², whereas the required area of wetland in 2029 is 14.80 km², but it is allocated over requirement with a value of 14.82 km². In this study, the deviation values between the required

area and each LULC type's predicted area under Scenario I vary between -0.0002% (0.02 km²), as underestimation to 0.0002% (0.02 km²), as overestimation. The summation of deviation values, which are a trade-off between overestimation and underestimation among LULC types, is 0.00% (see Table 5.11). Hence, the deviation values depend on the iterative driving factor that determines the highest probability that each spatial will be converted to specific land-use types in the following year (Xu, L., Li, Z., Song, H., and Yin, H., 2013; Zhang et al., 2016). Therefore, the LULC prediction under Scenario I using the CLUE-S model can be validated and accepted for estimating sediment and nutrient export in this study.



Table 5.11 Transition LULC change matrix between 2019 (Base year) and 2029 of Scenario I: Trend of LULC evolution.

LULC types	LULC in 2029 (km ²)										
	UR	PD	FC	RB	PO	FO	WB	RL	WL	ML	Total
Urban and built-up area (UR)	33.10	-	-	-	-	-	-	-	-	-	33.10
Paddy field (PD)	2.62	210.84	0.01	-	0.45	-	-	5.70	-	1.13	220.74
Field crop (FC)	0.02	-	10.55	-	11.27	-	-	0.01	-	-	21.84
Para rubber (RB)	-	-	-	19.78	-	-	-	-	-	-	19.78
Perennial trees and Orchard (PO)	-	-	-	-	79.22	-	-	-	-	-	79.22
Forest land (FO)	1.08	-	12.11	8.67	5.14	400.39	6.40	3.07	-	0.05	436.91
Water body (WB)	-	-	-	-	-	-	33.37	-	-	-	33.37
Rangeland (RL)	0.01	-	-	-	2.67	-	-	24.58	-	-	27.26
Wetland (WL)	-	-	-	-	-	-	1.59	-	14.82	-	16.41
Miscellaneous land (ML)	0.08	-	0.14	-	-	-	-	-	-	2.49	2.71
Total	36.90	210.84	22.81	28.45	98.75	400.39	41.35	33.36	14.82	3.68	891.35
Land use requirement	36.92	210.86	22.79	28.45	98.74	400.38	41.34	33.36	14.80	3.70	891.35
Deviation value (%)	-0.0002	-0.0002	0.0002	-	0.0001	0.0001	0.0001	-	0.0002	-0.0002	-
Deviation value (km ²)	-0.02	-0.02	0.02	-	0.01	0.01	0.01	-	0.02	-0.02	-

5.4 Land requirement estimation and LULC prediction of Scenario II: Maximization of ecosystem service values

Land requirement estimation for Scenario II: Maximization of ecosystem service values was calculated based on allocated LULC type area after maximization ecosystem service value with a simple benefit transfer method using linear programming with the simplex method of What's Best under MS-Excel software.

The objective functions for ecosystem service value maximization was formulated in the following equation:

$$Z_{Max} = [12.7(X_1) + 1,032.3(X_2) + 1,032.3(X_3) + 1,949.0(X_4) + 1,949.0(X_5) + 1,949.0(X_6) + 6,873.7(X_7) + 808.6(X_8) + 9,368.7(X_9) + 96.3(X_{10})] \quad (5.11)$$

Where Z_{max} is the objective function of scenario II for ESV maximization, X_1 is urban and built-up area (UR), X_2 is paddy field (PD), X_3 is field crop (FC), X_4 is para rubber (RP), X_5 is perennial trees and orchards (PO), X_6 is forest land (FO), X_7 is water body (WB), X_8 is rangeland (RL), X_9 is wetland (WL), and X_{10} is miscellaneous land (ML).

The constraints to maximize ecosystem service values in this study are presented below.

The first constraint is the area of all land use types must be equal to the allowable area of 89,135.00 ha, as expressed in Equation 5.12.

$$X_1 + X_2 + X_3 + X_4 + X_5 + X_6 + X_7 + X_8 + X_9 + X_{10} = 89,135.00 \quad (5.12)$$

The second constraint is the urban and built-up area should be equal to 3,692.29 ha based on transitional change area between 2009 and 2019 using the Markov Chain model, as expressed in Equation 5.13.

$$X_1 = 3,692.29 \quad (5.13)$$

The third constraint is the paddy field that should be less than or equal to 22,074.23 ha based on classified LULC in 2019, as expressed in Equation 5.14.

$$X_2 \leq 22,074.23 \quad (5.14)$$

The fourth constraint is the paddy field that should be more than or equal to 21,086.41 ha based on transitional change area between 2009 and 2019 using the Markov Chain model, as expressed in Equation 5.15.

$$X_2 \geq 21,086.41 \quad (5.15)$$

The fifth constraint is field crop that should be less than or equal to 2,279.25 ha based on transitional change area between 2009 and 2019 using the Markov Chain model, as expressed in Equation 5.16.

$$X_3 \leq 2,279.25 \quad (5.16)$$

The sixth constraint is field crop that should be more than or equal to 2,184.17 ha based on classified LULC in 2019, as expressed in Equation 5.17.

$$X_3 \geq 2,184.17 \quad (5.17)$$

The seventh constraint is para rubber that should be less than or equal to 2,844.72 ha based on transitional change area between 2009 and 2019 using the Markov Chain model, as expressed in Equation 5.18.

$$X_4 \leq 2,844.72 \quad (5.18)$$

The eighth constraint is para rubber that should be more than or equal to 1,978.41 ha based on classified LULC in 2019, as expressed in Equation 5.19.

$$X_4 \geq 1,978.41 \quad (5.19)$$

The ninth constraint is perennial trees and orchards that should be less than or equal to 9,874.03 ha based on transitional change area between 2009 and 2019 using the Markov Chain model, as expressed in Equation 5.20.

$$X_5 \leq 9,874.03 \quad (5.20)$$

The tenth constraint is perennial trees and orchards that should be more than or equal to 7,922.37 ha based on classified LULC in 2019, as expressed in Equation 5.21.

$$X_5 \geq 7,922.37 \quad (5.21)$$

The eleventh constraint is forest land that should be less than or equal to 43,691.43 ha based on classified LULC in 2019, as expressed in Equation 5.22.

$$X_6 \leq 43,691.43 \quad (5.22)$$

The twelfth constraint is forest land that should be more than or equal to 40,038.00 ha based on transitional change area between 2009 and 2019 using the Markov Chain model, as expressed in Equation 5.23.

$$X_6 \geq 40,038.00 \quad (5.23)$$

The thirteenth constraint is water body should be equal to 3,336.76 ha based on classified LULC in 2019, as expressed in Equation 5.24.

$$X_7 = 3,336.76 \quad (5.24)$$

The fourteenth constraint is rangeland that should be less than or equal to 2,726.21 ha based on classified LULC in 2019, as expressed in Equation 5.25.

$$X_8 \leq 2,726.21 \quad (5.25)$$

The fifteenth constraint is rangeland that should be more than or equal to 1,363.11 ha, as expressed in Equation 5.26. This constraint was set by decreasing 50% based on classified LULC in 2019.

$$X_8 \geq 1,363.11 \quad (5.26)$$

The sixteenth constraint is a wetland that should be less than or equal to 2,985.48 ha, expressed in Equation 5.27. This constraint was set by considering the reclaimed areas (decreased rangeland and miscellaneous land by 50%) and other LULC types.

$$X_9 \leq 2,985.48 \quad (5.27)$$

The seventeenth constraint is a wetland that should be more than or equal to 1,640.63 ha based on classified LULC in 2019, as expressed in Equation 5.28.

$$X_9 \geq 1,640.63 \quad (5.28)$$

The eighteenth constraint is miscellaneous land that should be less than or equal to 271.27 ha based on classified LULC in 2019, as expressed in Equation 5.29.

$$X_{10} \leq 271.27 \quad (5.29)$$

The nineteenth constraint is miscellaneous land that should be more than or equal to 135.64 ha, as expressed in Equation 5.30. This constraint was set by decreasing 50% based on classified LULC in 2019.

$$X_{10} \geq 135.64 \quad (5.30)$$

Meanwhile, constraints of the objective function to maximize ecosystem service value from each LULC type in tabular form are summarized in Table 5.12. These decision variables are the set of quantities determined to solve the problem and take on a range of values within limits assigned by the constraints. The result of optimized LULC allocation to maximize ecosystem service values in 2029 of each LULC type was

further applied to calculate the annual change rate for the annual land requirement of Scenario II, as shown in Tables 5.13 and 5.14.



Table 5.12 The constraint to maximize ecosystem service values of Scenario-II in a table form.

Constraints	UR (X1)	PD (X2)	FC (X3)	RP (X4)	PO (X5)	FO (X6)	WB (X7)	RL (X8)	WL (X9)	ML (X10)	Operator	Area (ha)	Remark
Constraint 1	1	1	1	1	1	1	1	1	1	1	=	89,135.00	Total area
Constraint 2 (UR)	1	0	0	0	0	0	0	0	0	0	=	3,692.29	Markov Chain Model
Constraint 3 (PD)	0	1	0	0	0	0	0	0	0	0	<=	22,074.23	Classified LULC in 2019
Constraint 4 (PD)	0	1	0	0	0	0	0	0	0	0	>=	21,086.41	Markov Chain Model
Constraint 5 (FC)	0	0	1	0	0	0	0	0	0	0	<=	2,279.25	Markov Chain Model
Constraint 6 (FC)	0	0	1	0	0	0	0	0	0	0	>=	2,184.17	Classified LULC in 2019
Constraint 7 (RP)	0	0	0	1	0	0	0	0	0	0	<=	2,844.72	Markov Chain Model
Constraint 8 (RP)	0	0	0	1	0	0	0	0	0	0	>=	1,978.41	Classified LULC in 2019
Constraint 9 (PO)	0	0	0	0	1	0	0	0	0	0	<=	9,874.03	Markov Chain Model
Constraint 10 (PO)	0	0	0	0	1	0	0	0	0	0	>=	7,922.37	Classified LULC in 2019
Constraint 11 (FO)	0	0	0	0	0	1	0	0	0	0	<=	43,691.43	Markov Chain Model
Constraint 12 (FO)	0	0	0	0	0	1	0	0	0	0	>=	40,038.00	Markov Chain Model
Constraint 13 (WB)	0	0	0	0	0	0	1	0	0	0	=	3,336.76	Classified LULC in 2019
Constraint 14 (RL)	0	0	0	0	0	0	0	1	0	0	<=	2,726.21	Classified LULC in 2019
Constraint 15 (RL)	0	0	0	0	0	0	0	1	0	0	>=	1,363.11	Decrease by 50% from classified LULC in 2019
Constraint 16 (WL)	0	0	0	0	0	0	0	0	1	0	<=	2,985.48	Increased by the reclaimed areas and other LULC types
Constraint 17 (WL)	0	0	0	0	0	0	0	0	1	0	>=	1640.63	Classified LULC in 2019
Constraint 18 (ML)	0	0	0	0	0	0	0	0	0	1	<=	271.27	Classified LULC in 2019
Constraint 19 (ML)	0	0	0	0	0	0	0	0	0	1	>=	135.64	Decrease by 50% from classified LULC in 2019

Table 5.13 Allocated LULC area to maximize ecosystem service of Scenario II and annual change rate between 2019 and 2029

No	LULC Types	Area in km ²		
		2019 ¹	2029 ²	Annual rate
1	Urban and built-up area (UR)	33.10	36.92	0.38
2	Paddy field (PD)	220.74	210.86	-0.99
3	Field crop (FC)	21.84	21.84	0
4	Para rubber (RB)	19.78	28.45	0.87
5	Perennial trees and Orchard (PO)	79.22	98.74	1.95
6	Forest land (FO)	436.91	416.32	-2.06
7	Water body (WB)	33.37	33.37	0
8	Rangeland (RL)	27.26	13.63	-1.36
9	Wetland (WL)	16.41	29.85	1.34
10	Miscellaneous land (ML)	2.71	1.36	-0.14

Note: 1 Classified LULC by SVM

2 Allocated LULC area to maximize ecosystem service by LP

Table 5.14 Annual land requirement of Scenario II (Maximization of ecosystem service values) for each LULC type.

Year	Area in km ²									
	UR	PD	FC	RB	PO	FO	WA	RL	WL	ML
2019	33.10	220.74	21.84	19.78	79.22	436.91	33.37	27.26	16.41	2.71
2020	33.48	219.75	21.84	20.65	81.18	434.86	33.37	25.90	17.75	2.58
2021	33.86	218.77	21.84	21.52	83.13	432.80	33.37	24.54	19.10	2.44
2022	34.24	217.78	21.84	22.38	85.08	430.74	33.37	23.17	20.44	2.31
2023	34.63	216.79	21.84	23.25	87.03	428.68	33.37	21.81	21.79	2.17
2024	35.01	215.80	21.84	24.12	88.98	426.62	33.37	20.45	23.13	2.03
2025	35.39	214.82	21.84	24.98	90.93	424.56	33.37	19.08	24.48	1.90
2026	35.77	213.83	21.84	25.85	92.89	422.50	33.37	17.72	25.82	1.76
2027	36.16	212.84	21.84	26.71	94.84	420.44	33.37	16.36	27.17	1.63
2028	36.54	211.85	21.84	27.58	96.79	418.38	33.37	14.99	28.51	1.49
2029	36.92	210.86	21.84	28.45	98.74	416.32	33.37	13.63	29.85	1.36
Annual Change	0.38	-0.99	0.00	0.87	1.95	-2.06	0.00	-1.36	1.34	-0.14

The land requirement characteristics of each LULC type under this scenario can be described in five categories below.

(1) Historical rate of LULC change. The land requirement of urban and built-up areas was calculated based on the historical rate of LULC change between 2009 and 2019 using the Markov Chain model.

(2) Unchanged area. The land requirement of the water body was assigned based on its area from the classified map in 2019.

(3) Decreased area. The land requirement of rangeland and miscellaneous land, as reclaimed areas, was reduced to half of the areas received from the classified map in 2019 because these areas provided low ecosystem service values. The areas were reclaimed and allocated to wetland areas by linear programming. The total area of rangeland and miscellaneous land in 2029 is about 13.63 km² and 1.36 km², respectively.

(4) Increased area. The wetland land requirement was allocated from the reclaimed areas (rangeland and miscellaneous land) and other LULC types by linear programming. The total area of wetland in 2029 is about 29.85 km².

(5) Allocated area. The land requirement of paddy fields, field crops, para rubber, perennial trees and orchards, and forest land were allocated from linear programming. The areas of each LULC were increased not over the area from the Markov Chain model in 2029.

As a result, in Table 5.14, the increased LULC classes in 2029 under this scenario are urban and built-up area, para rubber, perennial trees and orchards and wetland with an increasing annual rate of 0.38, 0.87, 1.95, and 1.34 km², respectively. In contrast, the decreased LULC classes in 2029 are paddy fields, forest land, rangeland, and miscellaneous land, with a decreasing annual rate of 0.99, 2.06, 1.36 and 0.14 km², respectively. Meanwhile, field crops and water bodies are unchanged.

Consequently, the annual land requirement of Scenario II (Maximization of ecosystem service values) by linear programming to maximize ESV (Table 5.14) with conversion matrix and elasticity of LULC change (Tables 5.4 and 5.6) were simultaneously combined to predict LULC data between 2020 and 2029 of this scenario based on the driving factors on LULC change for specific LULC type location

preference (Table 5.2) under the CLUE-S model. The spatial distribution of the predicted LULC of Scenario II between 2020 and 2029 is presented in Figure 5.3. The area and percentage of LULC classes of Scenario II between 2020 and 2029 are displayed in Tables 5.15 and 5.16, respectively.

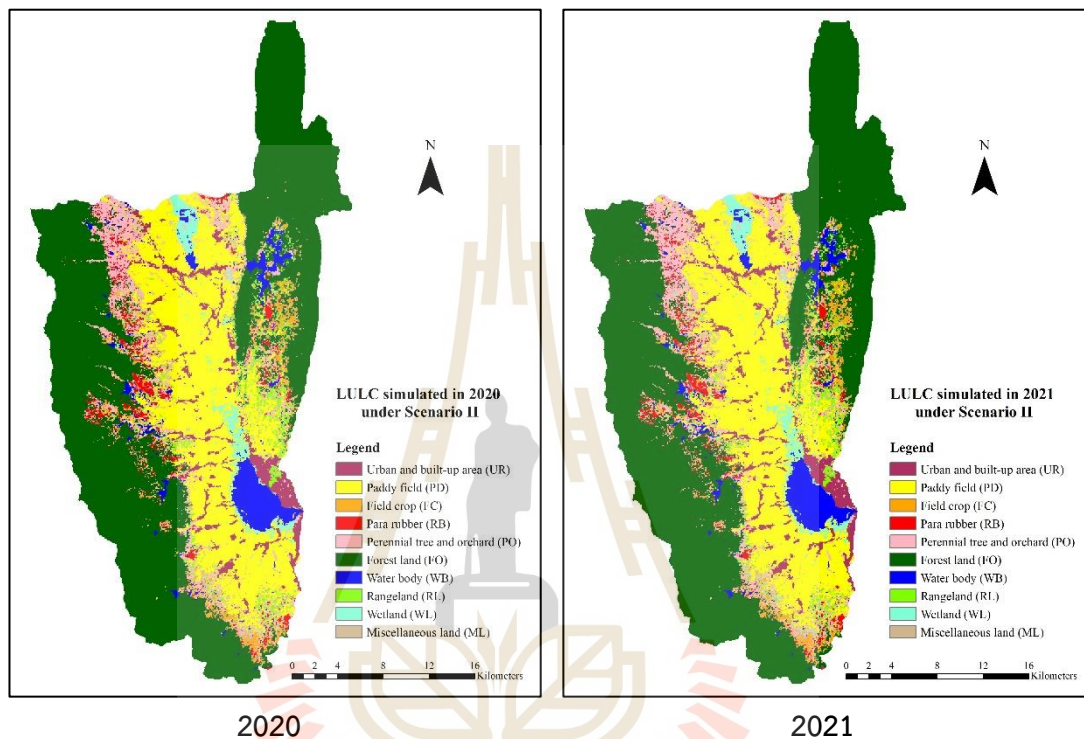


Figure 5.3 Spatial distribution of LULC prediction of Scenario II during 2020 to 2029.

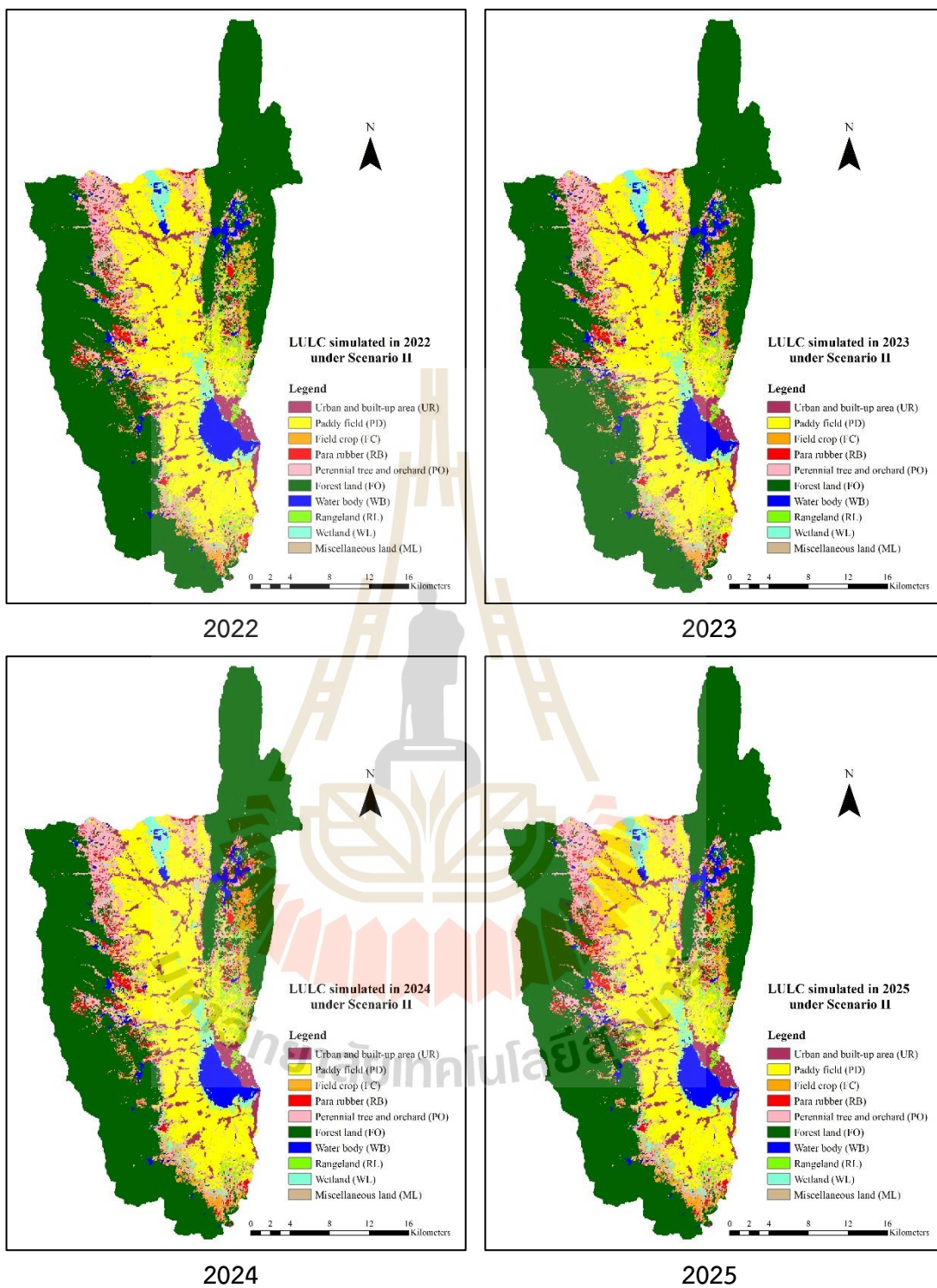


Figure 5.3 (Continued).

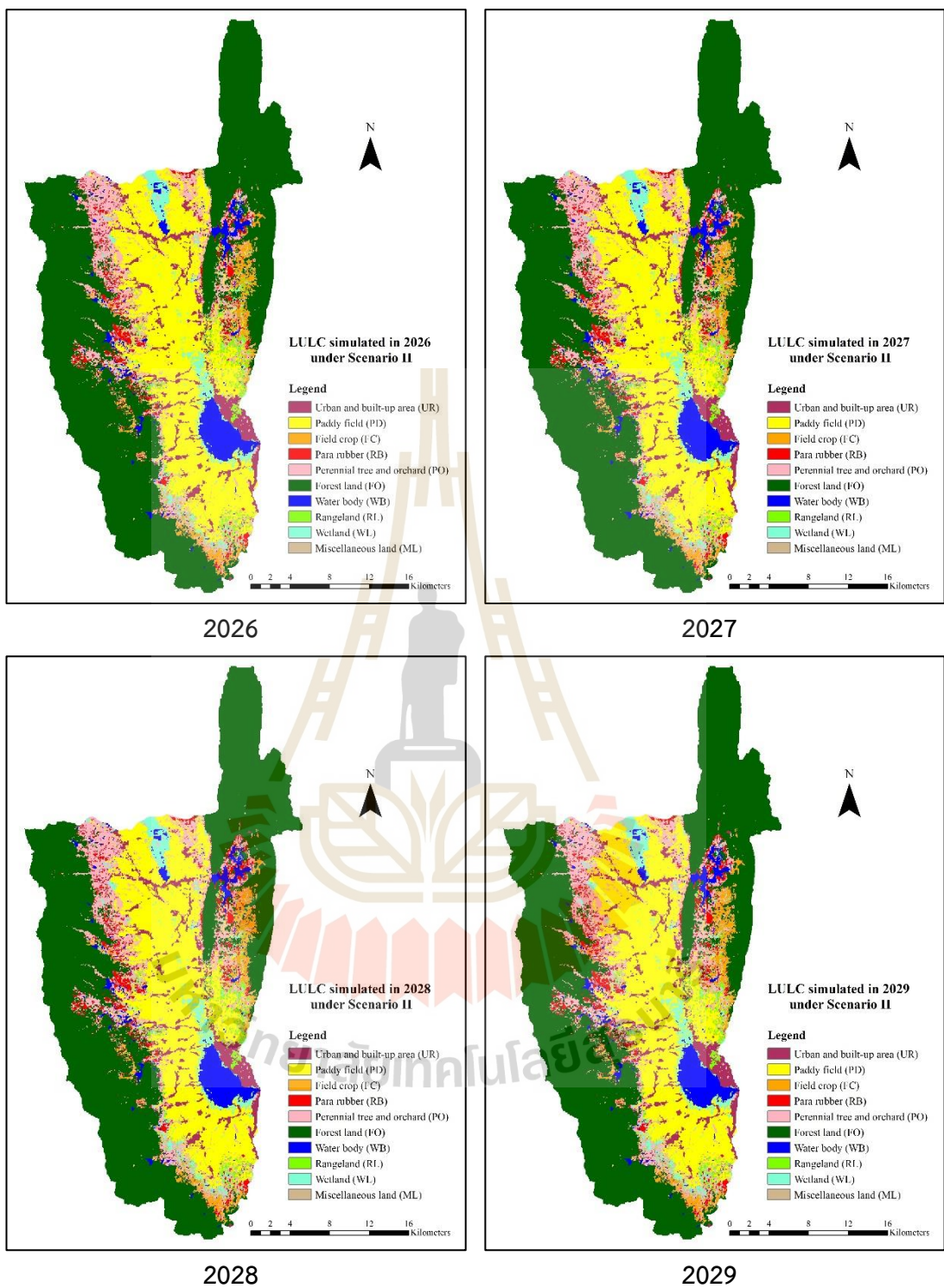


Figure 5.3 (Continued).

Table 5.15 Area of predicted LULC of Scenario II: Maximization ecosystem service values between 2020 and 2029.

LULC types	Area in km ²									
	2020	2021	2022	2023	2024	2025	2026	2027	2028	2029
Urban and built-up area (UR)	33.36	33.84	34.22	34.60	34.99	35.39	35.42	36.17	36.47	36.94
Paddy field (PD)	219.74	218.73	217.75	216.77	215.78	214.77	213.82	212.74	211.81	210.78
Field crop (FC)	21.85	21.82	21.82	21.81	21.81	21.86	21.85	21.84	21.86	21.80
Para rubber (RB)	20.67	21.50	22.37	23.23	24.09	24.98	25.87	26.74	27.56	28.46
Perennial trees and Orchard (PO)	81.16	83.12	85.05	87.01	88.96	90.81	92.90	94.81	96.70	98.68
Forest land (FO)	434.86	432.77	430.71	428.65	426.61	424.52	422.49	420.45	418.34	416.34
Water body (WB)	33.57	33.57	33.57	33.57	33.57	33.70	33.70	33.70	33.70	33.70
Rangeland (RL)	25.87	24.51	23.16	21.78	20.43	19.14	17.72	16.35	14.97	13.57
Wetland (WL)	17.72	19.07	20.42	21.76	23.10	24.27	25.82	26.93	28.44	29.72
Miscellaneous land (ML)	2.56	2.42	2.29	2.15	2.02	1.89	1.77	1.62	1.48	1.36
Total	891.35	891.35	891.35	891.35	891.35	891.35	891.35	891.35	891.35	891.35

Table 5.16 Percentage of predicted LULC of Scenario II: Maximization ecosystem service values between 2020 and 2029.

LULC types	Percent									
	2020	2021	2022	2023	2024	2025	2026	2027	2028	2029
Urban and built-up area (UR)	3.74	3.80	3.84	3.88	3.93	3.97	3.97	4.06	4.09	4.14
Paddy field (PD)	24.65	24.54	24.43	24.32	24.21	24.09	23.99	23.87	23.76	23.65
Field crop (FC)	2.45	2.45	2.45	2.45	2.45	2.45	2.45	2.45	2.45	2.45
Para rubber (RB)	2.32	2.41	2.51	2.61	2.70	2.80	2.90	3.00	3.09	3.19
Perennial trees and Orchard (PO)	9.11	9.32	9.54	9.76	9.98	10.19	10.42	10.64	10.85	11.07
Forest land (FO)	48.79	48.55	48.32	48.09	47.86	47.63	47.40	47.17	46.93	46.71
Water body (WB)	3.77	3.77	3.77	3.77	3.77	3.78	3.78	3.78	3.78	3.78
Rangeland (RL)	2.90	2.75	2.60	2.44	2.29	2.15	1.99	1.83	1.68	1.52
Wetland (WL)	1.99	2.14	2.29	2.44	2.59	2.72	2.90	3.02	3.19	3.33
Miscellaneous land (ML)	0.29	0.27	0.26	0.24	0.23	0.21	0.20	0.18	0.17	0.15
Total	100.00	100.00	100.00	100.00	100.00	100.00	100.00	100.00	100.00	100.00

As a result of the predicted LULC for Scenario II (Maximization of ecosystem service values), areas of five LULC types are increased in 2029 consist of urban and built-up area, para rubber, perennial trees and orchards, water body, and wetland which areas cover 36.94 km² (4.14%), 28.46 km² (3.19%), 98.68 km² (11.07%), 33.70 km² (3.78%), and 29.72 km² (3.33%) respectively. On the contrary, the areas of paddy field, field crop, forest land, rangeland, and miscellaneous land are decreased in 2029, which the areas cover 210.78 km² (23.65%), 21.80 km² (2.45%), 416.34 km² (46.71%), 13.57 km² (1.52%), and 1.36 km² (0.15%), respectively.

Additionally, the transition LULC change matrix between 2019 and 2029 of Scenario II is displayed in Table 5.17. As a result, urban and built-up in 2019 is not converted in other LULC types in 2029, and its area is increased as a trend of LULC change from 33.10 km² in 2019 to 36.94 km² in 2029. The increased urban and built-up areas in 2029 mainly come from forest land (2.78 km²) in 2019. Likewise, para rubber in 2019 is not converted into other LULC classes in 2029, and its area is increased from 19.78 km² in 2019 to 28.46 km² in 2029. The increased areas of para rubber in 2029 come from forest land (8.68 km²) in 2019. Similarly, perennial trees and orchards in 2019 are not converted into other LULC classes in 2029. Its area increased from 79.22 km² in 2019 to 98.68 km² in 2029. The increased areas in 2029 come from field crops (8.05 km²), forest land (1.02 km²), and rangeland (10.39 km²) in 2019. Likewise, a wetland in 2019 is an increased area under Scenario II as expected, which is not converted into other LULC types in 2029, and its area is increased from 16.41 km² in 2019 to 29.72 km² in 2029. The increased areas of the wetland in 2029 come from paddy fields (9.50 km²), rangeland (2.83 km²), and miscellaneous land (0.98 km²) in 2019. This result implies the efficacy of linear programming for reclaimed and changing other areas into the wetland.

On the contrary, the paddy field in 2019 is mainly converted into wetland (9.50 km²) in 2029, and its area is decreased from 220.74 km² in 2019 to 210.78 km² in 2029. Likewise, field crop is mainly converted into perennial trees and orchards (8.05 km²), and its area is decreased from 21.84 km² in 2019 to 21.80 km² in 2029. Also, forest land is primarily converted into the urban and built-up area (2.78 km²), field crop (7.75 km²),

and para rubber (8.68 km²), and its area is decreased from 436.91 km² in 2019 to 416.34 km² in 2029. Similarly, rangeland is a decreased area under Scenario II as expected in 2029, mainly converted into perennial trees and Orchards (10.39 km²) and wetland (2.83 km²). Its area decreased from 27.26 km² in 2019 to 13.57 km² in 2029. Also, miscellaneous land is decreased in 2029 as desired, mostly converted into wetland (0.98 km²). The area decreased of its from 2.71 km² in 2019 to 1.36 km² in 2029. Meanwhile, under Scenario II, the water body is a fixed land requirement area between 2019 and 2029, which is not converted into other LULC classes in 2029. However, the water body area increased from 33.37 km² in 2019 to 33.70 km² in 2029. Most of the increased water body areas in 2029 are scattered in undulated areas.

In summary, linear programming with an objective function to maximize ecosystem services values can be used to allocate specific LULC areas using the simple benefit transfer method. Similar to Scenario I, there is a slight difference between the required land area and the predicted area of each LULC type in 2029 under Scenario II. For instance, the required wetland area in 2029 is 29.85 km², but it is allocated only 29.72 km², while the required area of the water body in 2029 is 33.37 km², but it is allocated over the requirement, with a value of 33.70 km². The deviation values between the required and the predicted area of each LULC type under Scenario II vary from -0.0013% to 0.0033% or from -0.13 km² (underestimation) to 0.33 km² (overestimation). The summation of deviation values, which are trade-offs between overestimation and underestimation among LULC types, is 0.00% (see Table 5.17). The deviation values depend on the iterative driving factor that determines the highest probability that each spatial will be converted to specific land-use types in the following year (Xu et al., 2013; Zhang et al., 2016). Therefore, the LULC prediction using the CLUE-S model can be validated and accepted for estimating sediment and nutrient export under Scenario II.

Table 5.17 Transition matrix of LULC change between 2019 and 2029 of Scenario II: Maximization ecosystem service values.

LULC types	LULC in 2029 (km ²)										
	UR	PD	FC	RB	PO	FO	WB	RL	WL	ML	Total
Urban and built-up area (UR)	33.10	-	-	-	-	-	-	-	-	-	33.10
Paddy field (PD)	0.46	210.78	-	-	-	-	-	-	9.50	-	220.74
Field crop (FC)	0.06	-	13.73	-	8.05	-	-	-	-	-	21.84
Para rubber (RB)	-	-	-	19.78	-	-	-	-	-	-	19.78
Perennial trees and Orchard (PO)	-	-	-	-	79.22	-	-	-	-	-	79.22
Forest land (FO)	2.78	-	7.75	8.68	1.02	416.34	0.33	0.01	-	-	436.91
Water body (WB)	-	-	-	-	-	-	33.37	-	-	-	33.37
Rangeland (RL)	0.48	-	-	-	10.39	-	-	13.56	2.83	-	27.26
Wetland (WL)	-	-	-	-	-	-	-	-	16.41	-	16.41
Miscellaneous land (ML)	0.06	-	0.32	-	-	-	-	-	0.98	1.36	2.71
Total	36.94	210.78	21.80	28.46	98.68	416.34	33.70	13.57	29.72	1.36	891.35
Land use requirement	36.92	210.86	21.84	28.45	98.74	416.32	33.37	13.63	29.85	1.36	891.35
Deviation value (%)	0.0002	-0.0008	-0.0004	0.0001	-0.0006	0.0002	0.0033	-0.0006	-0.0013	-	-
Deviation value (km²)	0.02	-0.08	-0.04	0.01	-0.06	0.02	0.33	-0.06	-0.13	-	-

5.5 Land requirement estimation and LULC prediction of Scenario III: Economic crop zonation

The land requirement is estimated based on the LULC change rate between 2009 and 2019 under this scenario using the Markov chain model and suitability classes (highly, moderate, and low suitability) for economic crops zonation in 2017 and 2018 from Land Department Development. In this scenario, the suitability zonation of four economic crops (paddy field, field crop, para rubber and perennial tree and orchard) was updated with existing LULC data in 2019 for estimating land requirement. The result of the annual land requirement of Scenario III (Economic crop zonation) between 2020 and 2029 is presented in Table 5.18. The characteristics of the land requirement of each LULC type under this scenario can be described in three categories below.

(1) Historical rate of LULC change. The land requirement of urban and built-up area, forest land, water body, rangeland, wetland, and miscellaneous land was calculated based on the historical rate of LULC change between 2009 and 2019 using the Markov Chain model.

(2) Decreased area. The land requirement of para rubber was reduced following their suitability zonation from LDD. The land requirement of para rubber was estimated by updating its existing area with the area of para rubber suitability zonation (highly, moderate, and low suitability). The total area of para rubber in 2029 is about 19.66 km² (See Figure 5.4a). Simultaneously, land requirements of perennial tree and orchard were estimated based on the updating longan and coffee zonation with existing perennial tree and orchard in 2019. The perennial tree and orchard area in 2029 is about 26.88 km² (See Figure 5.4b).

(3) Increased area. The land requirement of paddy fields and field crops was increased based on updating their suitability zonation (highly, moderate, and low suitability) from LDD with the existing LULC in 2019. The total required areas of the paddy field and field crops in 2029 are about 280.34 km² and 33.96 km². See Figures 5.4(c) and 5.4(d).

Table 5.18 Annual land requirement for Scenario III: Economic crop zonation by each LULC type.

Year	Area in km ²									
	UR	PD	FC	RB	PO	FO	WA	RL	WL	ML
2019	33.10	220.74	21.84	19.78	79.22	436.91	33.37	27.26	16.41	2.71
2020	33.48	226.70	23.05	19.77	73.99	433.26	34.16	27.87	16.25	2.81
2021	33.86	232.66	24.26	19.76	68.76	429.61	34.96	28.48	16.09	2.91
2022	34.24	238.62	25.48	19.75	63.52	425.96	35.76	29.09	15.93	3.01
2023	34.63	244.58	26.69	19.74	58.29	422.30	36.56	29.70	15.77	3.11
2024	35.01	250.54	27.90	19.72	53.05	418.65	37.35	30.31	15.60	3.21
2025	35.39	256.50	29.11	19.71	47.82	415.00	38.15	30.92	15.44	3.30
2026	35.77	262.46	30.32	19.70	42.58	411.34	38.95	31.53	15.28	3.40
2027	36.16	268.42	31.53	19.69	37.35	407.69	39.75	32.14	15.12	3.50
2028	36.54	274.38	32.74	19.68	32.12	404.04	40.54	32.75	14.96	3.60
2029	36.92	280.34	33.96	19.66	26.88	400.38	41.34	33.36	14.80	3.70
Annual Change	0.38	5.96	1.21	-0.01	-5.23	-3.65	0.80	0.61	-0.16	0.10

As a result of the annual land requirement for Scenario III (Economic crop zonation) for each LULC type between 2019 and 2029, the increased LULC classes are paddy field, field crop, water body, rangeland, urban and built-up area, and miscellaneous land with an annual increased rate of 5.96, 1.21, 0.80, 0.61, 0.38 and 0.10 km², respectively. In contrast, the decreased LULC classes are perennial trees and orchards, forest land, wetland, and para rubber with an annual decreased rate of 5.23, 3.65, 0.16, and 0.01 km², respectively.

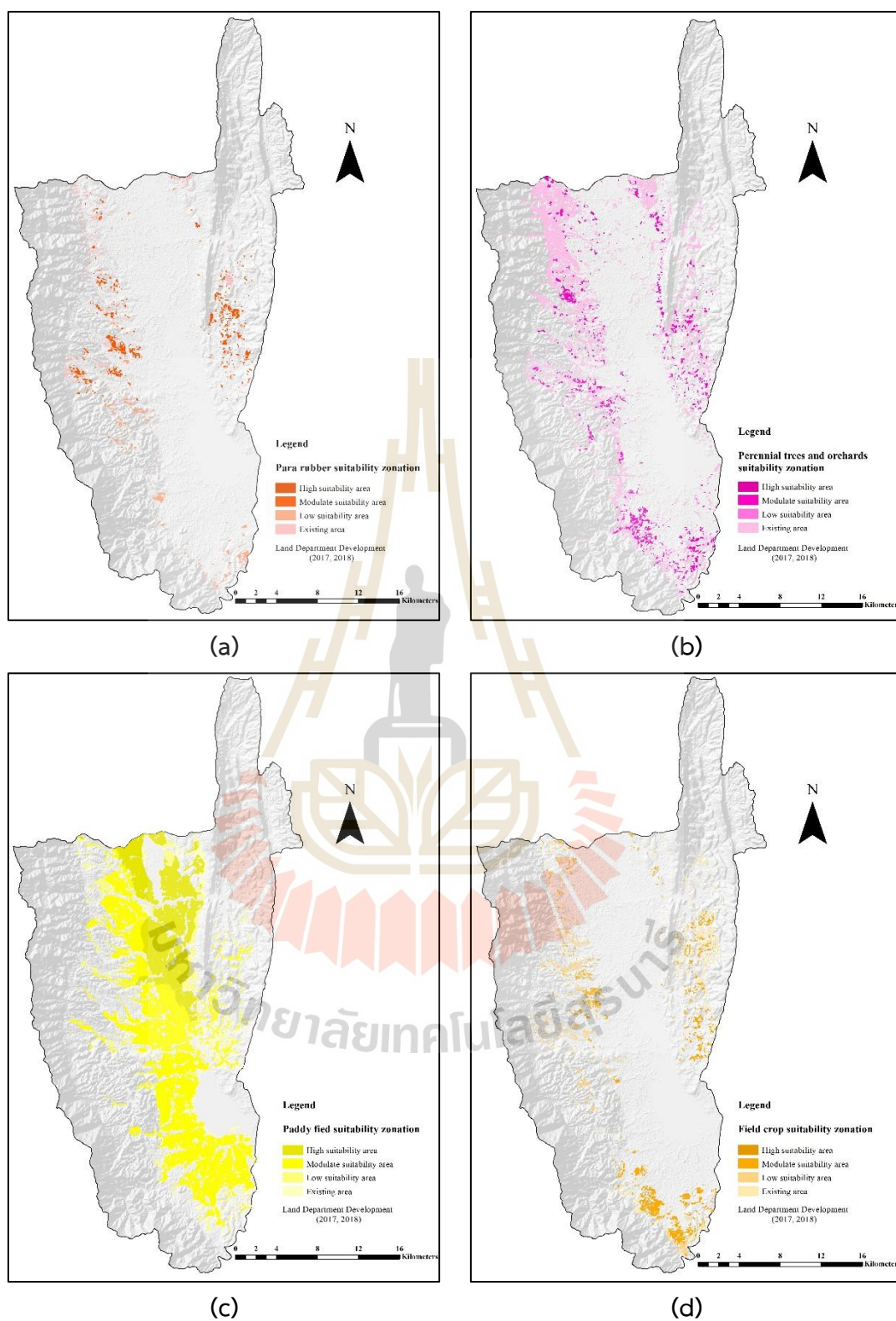


Figure 5.4 Spatial distribution of the economic crop zonation (a) para rubber, (b) perennial trees and orchards, (c) paddy field, and (d) field crop.

Subsequently, the annual land requirement of Scenario III (Economic crop zonation) (Table 5.18) with conversion matrix and elasticity of LULC change (Tables 5.5 and 5.6) were simultaneously combined to predict LULC data between 2020 and 2029 of this scenario based on the driving factors on LULC change for specific LULC type location preference (Table 5.2) under the CLUE-S model. The spatial distribution of the predicted LULC of Scenario III between 2020 and 2029 is presented in Figure 5.5. The area and percentage of LULC classes of Scenario III between 2020 and 2029 are displayed in Tables 5.19 and 5.20, respectively.

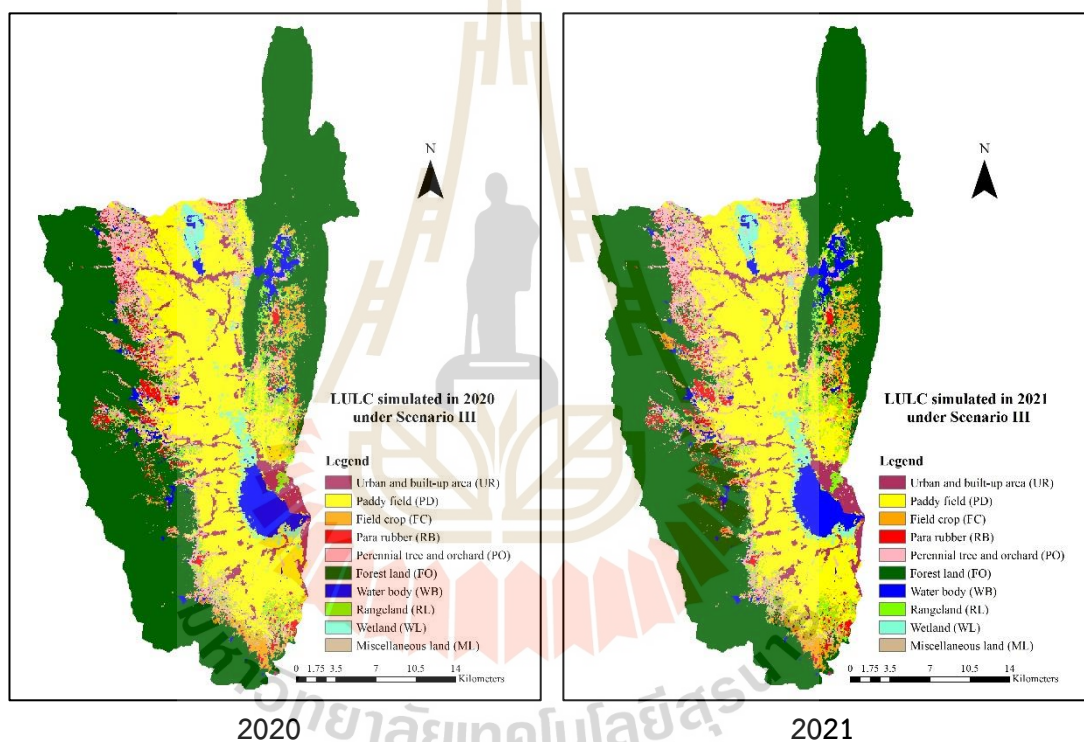


Figure 5.5 Spatial distribution of LULC prediction of Scenario III during 2020 to 2029.

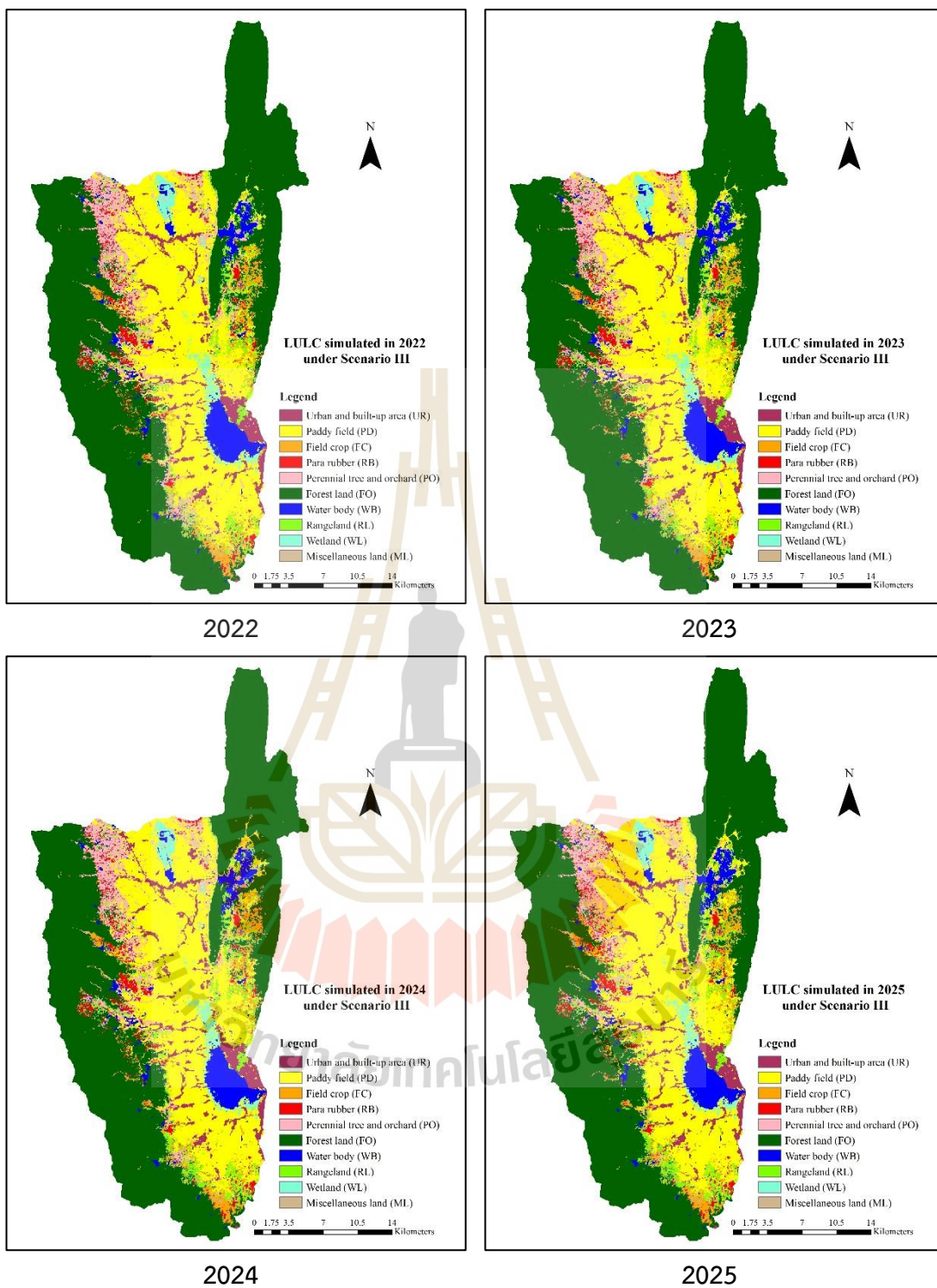


Figure 5.5 (Continued).

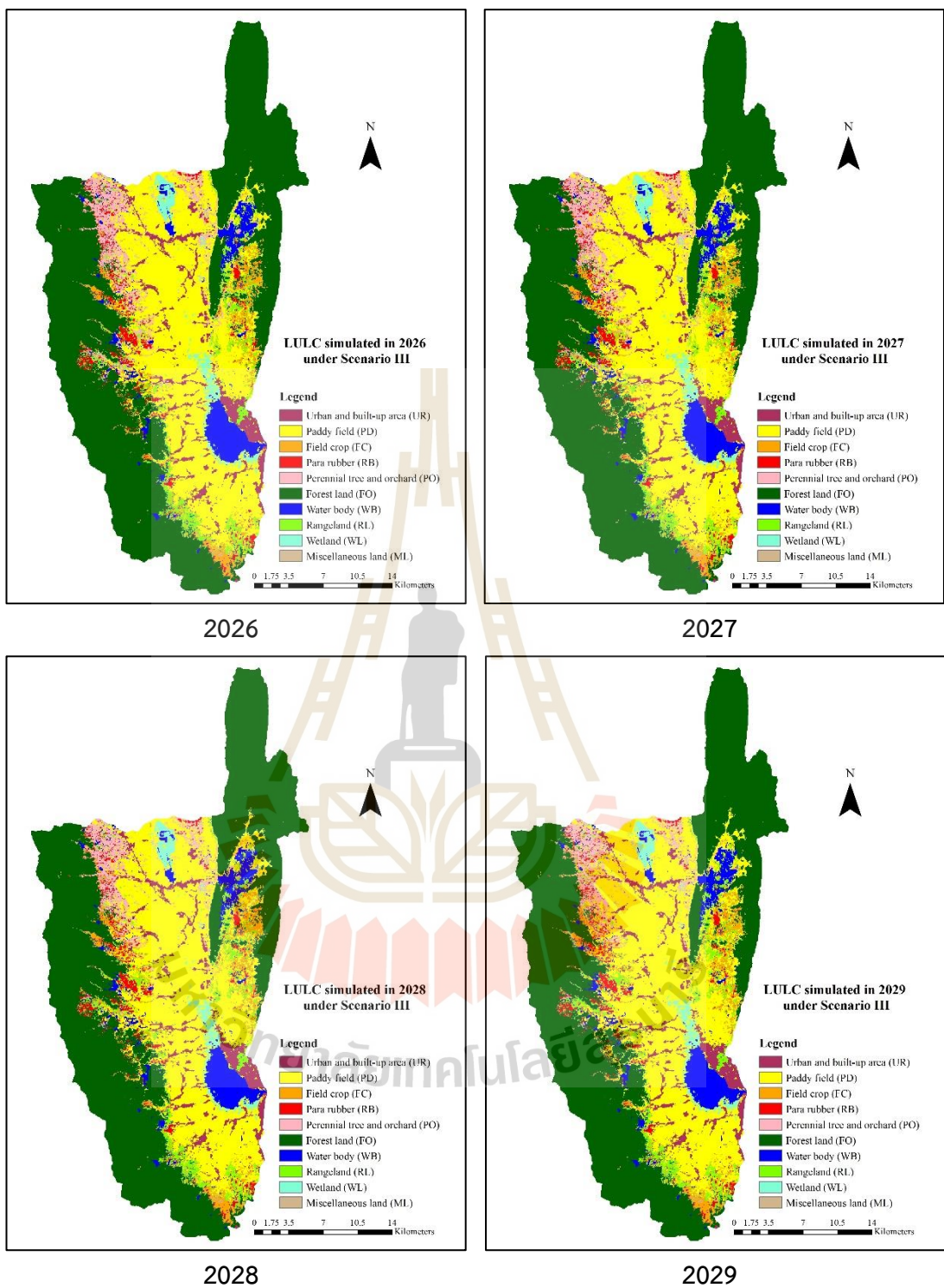


Figure 5.5 (Continued).

Table 5.19 Area of predicted LULC of Scenario III: Economic crop zonation between 2020 and 2029.

LULC types	Area in km ²									
	2020	2021	2022	2023	2024	2025	2026	2027	2028	2029
Urban and built-up area (UR)	33.20	33.78	33.94	34.56	34.76	35.41	35.75	36.10	36.65	36.96
Paddy field (PD)	226.72	232.67	238.65	244.54	250.55	256.39	262.42	268.46	274.37	280.20
Field crop (FC)	23.08	24.26	25.54	26.74	27.93	29.15	30.40	31.62	32.79	34.11
Para rubber (RB)	19.78	19.83	19.85	19.87	19.89	19.89	19.89	19.88	19.59	19.78
Perennial trees and Orchard (PO)	74.06	68.78	63.62	58.31	53.13	47.91	42.65	37.46	32.17	26.94
Forest land (FO)	433.30	429.61	425.98	422.30	418.60	414.93	411.24	407.57	403.96	400.22
Water body (WB)	34.34	34.93	35.73	36.43	37.07	37.96	38.71	39.48	40.47	41.11
Rangeland (RL)	27.86	28.46	29.06	29.68	30.61	30.94	31.56	32.14	32.78	33.44
Wetland (WL)	16.22	16.10	15.97	15.78	15.63	15.43	15.29	15.11	14.96	14.85
Miscellaneous land (ML)	2.79	2.92	3.00	3.14	3.18	3.34	3.44	3.53	3.61	3.73
Total	891.35	891.35	891.35	891.35	891.35	891.35	891.35	891.35	891.35	891.35

Table 5.20 Percentage of predicted LULC of Scenario III: Economic crop zonation between 2020 and 2029.

LULC types	Percent									
	2020	2021	2022	2023	2024	2025	2026	2027	2028	2029
Urban and built-up area (UR)	3.72	3.79	3.81	3.88	3.90	3.97	4.01	4.05	4.11	4.15
Paddy field (PD)	25.44	26.10	26.77	27.44	28.11	28.76	29.44	30.12	30.78	31.44
Field crop (FC)	2.59	2.72	2.87	3.00	3.13	3.27	3.41	3.55	3.68	3.83
Para rubber (RB)	2.22	2.23	2.23	2.23	2.23	2.23	2.23	2.23	2.20	2.22
Perennial trees and Orchard (PO)	8.31	7.72	7.14	6.54	5.96	5.37	4.79	4.20	3.61	3.02
Forest land (FO)	48.61	48.20	47.79	47.38	46.96	46.55	46.14	45.72	45.32	44.90
Water body (WB)	3.85	3.92	4.01	4.09	4.16	4.26	4.34	4.43	4.54	4.61
Rangeland (RL)	3.13	3.19	3.26	3.33	3.43	3.47	3.54	3.61	3.68	3.75
Wetland (WL)	1.82	1.81	1.79	1.77	1.75	1.73	1.72	1.70	1.68	1.67
Miscellaneous land (ML)	0.31	0.33	0.34	0.35	0.36	0.37	0.39	0.40	0.41	0.42
Total	100.00	100.00	100.00	100.00	100.00	100.00	100.00	100.00	100.00	100.00

As a result of the predicted LULC for Scenario III (Economic crop zonation), areas of six LULC types are increased in 2029, including urban and built-up areas, paddy fields, field crops, water body, rangeland, and miscellaneous land. The areas are 36.96 km² or 4.15%, 280.20 km² or 31.44%, 34.11 km² or 3.83%, 41.11 km² or 4.61%, 33.44 km² or 3.75%, and 3.73 km² or 0.42% respectively. Conversely, para rubber, perennial trees and orchard, forest land, and wetland are decreased in 2029, which the areas are 19.78 km² 2.22or %, 26.94 km² or 3.02%, 400.22 km² or 44.90%, and 14.85 km² or 1.67%, respectively.

The transition LULC change matrix between 2019 and 2029 of Scenario III (Economic crop zonation) is displayed in Table 5.21. The result shows that urban and built-up areas will increase as expected in 2029. The area is not converted to other LULC types in 2029, and its area is increased from 33.10 km² in 2019 to 36.96 km² in 2029, and the increased areas in 2029 mainly come from perennial trees and orchards (3.09 km²) in 2019. Likewise, the water body in 2019 is not converted into other LULC classes in 2029, and its area is increased from 33.37 km² in 2019 to 41.11 km² in 2029. The increased water body areas in 2029 mainly come from forest land (7.73 km²) in 2019. Besides, the rangeland area increased from 27.26 km² in 2019 to 33.44 in 2029 km², and the increased areas of the rangeland in 2029 mainly come from field crop (7.65 km²) and perennial trees and orchards (13.95 km²) in 2019. Similarly, the miscellaneous land area increased from 2.71 km² in 2019 to 3.73 in 2029 km², and the increased areas of the miscellaneous land in 2029 generally come from perennial trees and orchards (2.22 km²) in 2019. In contrast, forest land was mainly converted into paddy fields (28.26 km²) and water bodies (7.73 km²) in 2029. The forest land decreased from 436.91 km² in 2019 to 400.22 km² in 2029. Likewise, the wetland decreased from 16.41 km² in 2019 to 14.85 km² in 2029, mainly converted into paddy fields (1.55 km²).

As a result, economic crop areas in Scenario III: Economic crop zonation, specifically paddy field, field crop, para rubber, perennial tree and orchard, are located based on suitability classes of economic crop zonation. According to the land suitability, the paddy field and field crop areas will increase in 2029. Paddy field areas are not converted to other LULC types in 2029, expanded from 220.74 km² in 2019 to 280.20 km² in 2029, and they come from perennial trees and orchard (10.25 km²),

forest land (28.26 km²), and rangeland (16.11 km²) in 2019. Likewise, field crop areas increased from 21.84 km² in 2019 to 34.11 km² in 2029. Their areas mostly come from perennial trees and orchards (22.47 km²). However, some field crop areas are converted into rangeland (7.65 km²) and paddy field (1.51 km²). Conversely, para rubber areas are decreased in 2029. Some para rubber areas in 2019 are converted into field crop (0.31 km²) in 2029, and some areas are gained from perennial trees and orchards (0.30 km²) in 2019. Consequently, areas of para rubber will be unchanged in 2029, with areas of 19.78 km². In the meantime, areas of perennial trees and orchards in 2019 are converted into the urban and built-up area (3.09 km²), paddy field (10.25 km²), field crop (22.47 km²), rangeland (13.95 km²), and miscellaneous land (2.22 km²) in 2029 and their area are decreased from 79.22 km² in 2019 to 26.94 km² in 2029. This result indicates the influence of economic crop zonation on LULC prediction under Scenario III.

Similar to Scenario I and II, there are slight differences between the required land area and the predicted area of each LULC type in 2029 under Scenario III. For example, the required area of the water body in 2029 is 41.34 km², but it is allocated only 41.11 km², while the required area of the field crop in 2029 is 33.96 km², but it is allocated over requirement (34.11 km²). In this study, the deviation values between the required land area and each LULC type's predicted area under Scenario III vary from -0.0023% to 0.0015% or from -0.23 km² (underestimation) to 0.15 km² (overestimation). The summation of deviation values, which are trade-offs between over and underestimation among LULC types, is 0.00% (see Table 5.21). Therefore, the deviation values depend on the iterative driving factor that determines the highest probability that each spatial will be converted to specific land-use types in the following year (Xu et al., 2013; Zhang et al., 2016). Therefore, the LULC prediction under Scenario II using the CLUE-S model can be validated and accepted for estimating sediment and nutrient export under Scenario III.

Table 5.21 Transition matrix of LULC change between 2019 and 2029 of Scenario III: Economic crop zonation.

LULC types	LULC in 2029 (km ²)										
	UR	PD	FC	RB	PO	FO	WB	RL	WL	ML	Total
Urban and built-up area (UR)	33.10	-	-	-	-	-	-	-	-	-	33.10
Paddy field (PD)	-	220.74	-	-	-	-	-	-	-	-	220.74
Field crop (FC)	0.68	1.51	11.31	-	-	-	-	7.65	-	0.69	21.84
Para rubber (RB)	-	-	0.31	19.48	-	-	-	-	-	-	19.78
Perennial trees and Orchard (PO)	3.09	10.25	22.47	0.30	26.94	-	-	13.95	-	2.22	79.22
Forest land (FO)	0.05	28.26	0.02	-	-	400.22	7.73	0.63	-	-	436.91
Water body (WB)	-	-	-	-	-	-	33.37	-	-	-	33.37
Rangeland (RL)	-	16.11	-	-	-	-	-	11.15	-	-	27.26
Wetland (WL)	-	1.55	-	-	-	-	0.01	-	14.85	-	16.41
Miscellaneous land (ML)	0.04	1.78	-	-	-	-	-	0.06	-	0.82	2.71
Total	36.96	280.20	34.11	19.78	26.94	400.22	41.11	33.44	14.85	3.73	891.35
Land use requirement	36.92	280.34	33.96	19.66	26.88	400.38	41.34	33.36	14.80	3.70	891.35
Deviation value (%)	0.0004	-0.0014	0.0015	0.0012	0.0006	-0.0016	-0.0023	0.0008	0.0005	0.0003	-
Deviation value (km ²)	0.04	-0.14	0.15	0.12	0.06	-0.16	-0.23	0.08	0.05	0.03	-

In summary, the predicted LULC data between 2020 and 2029 of three different scenarios (trend of LULC evolution, maximization ecosystem service values, and economic crop zonation) for estimating sediment and nutrient export are compared and characterized in this section. Table 5.22 shows the area of the predicted LULC types of three different scenarios between 2019 and 2029 and its change, and Figure 5.6 displays a comparison of LULC type change between actual LULC in 2019 and the predicted LULC in 2029 of three different scenarios.

As a result, it reveals that the significant LULC types with an increased area between 2019 and 2020 under Scenario I: Trend of LULC evolution is the urban and built-up area, field crop, para rubber, perennial trees and orchards, water body, rangeland, and miscellaneous land. In contrast, the dominant LULC types with the decreased area in the same period are paddy fields, forest land, and wetlands. The LULC change under this scenario is set out by historical LULC change between 2009 and 2019, representing socio-economic development in the study area.

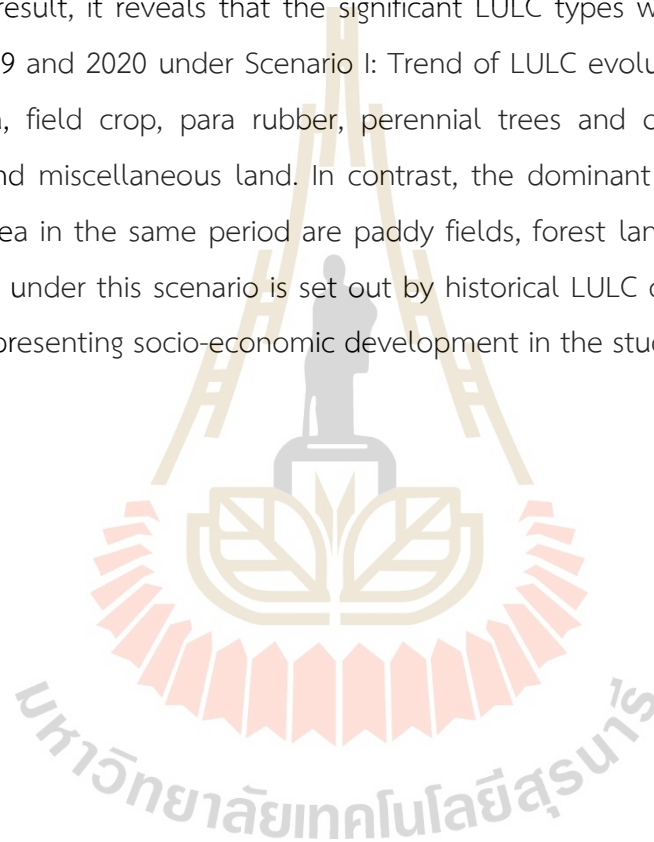


Table 5.22 Comparison area of predicted LULC in three different scenarios and its change.

LULC type and scenario	LULC in 2019 (base year)	LULC in 2029 (predicted year)	Change
UR-Scenario-I	33.1	36.90	3.80
UR-Scenario-II	33.1	36.94	3.84
UR-Scenario-III	33.1	36.96	3.86
PD-Scenario-I	220.74	210.84	-9.90
PD-Scenario-II	220.74	210.78	-9.96
PD-Scenario-III	220.74	280.20	59.46
FC-Scenario-I	21.84	22.81	0.97
FC-Scenario-II	21.84	21.80	-0.04
FC-Scenario-III	21.84	34.11	12.27
RB-Scenario-I	19.78	28.45	8.67
RB-Scenario-II	19.78	28.46	8.68
RB-Scenario-III	19.78	19.78	0.00
PO-Scenario-I	79.22	98.75	19.53
PO-Scenario-II	79.22	98.68	19.46
PO-Scenario-III	79.22	26.94	-52.28
FO-Scenario-I	436.91	400.39	-36.52
FO-Scenario-II	436.91	416.34	-20.57
FO-Scenario-III	436.91	400.22	-36.69
WB-Scenario-I	33.37	41.35	7.98
WB-Scenario-II	33.37	33.70	0.33
WB-Scenario-III	33.37	41.11	7.74
RL-Scenario-I	27.26	33.36	6.10
RL-Scenario-II	27.26	13.57	-13.69
RL-Scenario-III	27.26	33.44	6.18
WL-Scenario-I	16.41	14.82	-1.59
WL-Scenario-II	16.41	29.72	13.31
WL-Scenario-III	16.41	14.85	-1.56
ML-Scenario-I	2.71	3.68	0.97
ML-Scenario-II	2.71	1.36	-1.35
ML-Scenario-III	2.71	3.73	1.02

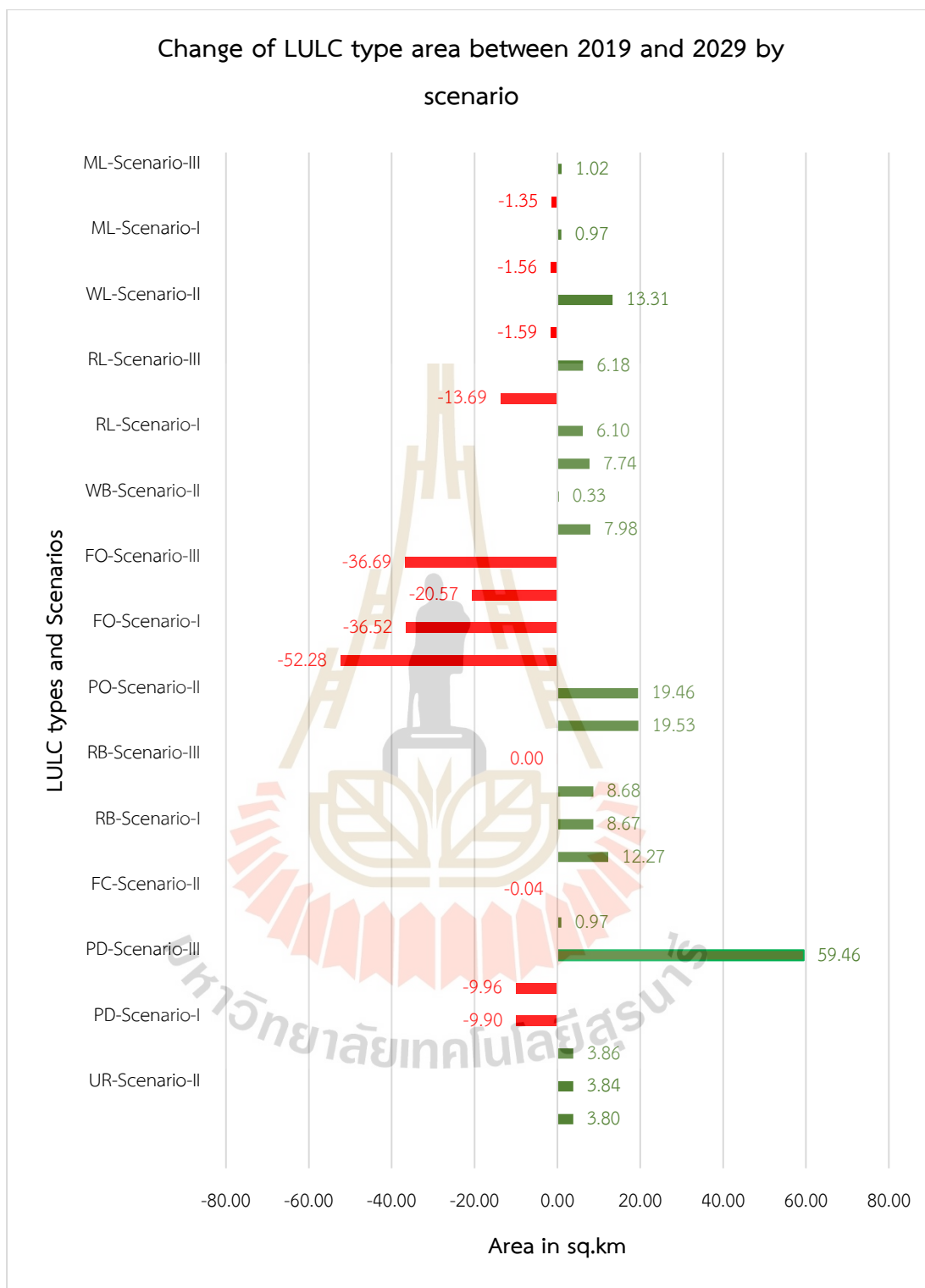


Figure 5.6 Comparison of LULC type change between LULC in 2019 (base year) and the predicted LULC in 2029 of three different scenarios.

In the meantime, the significant LULC types with the increased area between 2019 and 2029 under Scenario II: Maximization ecosystem service values are urban and built-up area, para rubber, perennial trees/orchards, water body, and wetlands. However, the several LULC types with the decreased area in the same period are paddy fields, field crops, forest land, rangeland, and miscellaneous land. Under this scenario, the LULC change is mainly determined by linear programming to maximize ecosystem services values, significantly increasing wetland. This scenario is reasonable for reducing sediment and nutrient export to the water due to wetland efficiency that can retain sediment and nutrient when receiving inflows (Wetland for Thai, 2018).

Meanwhile, the significant LULC types with the increased area between 2019 and 2029 under Scenario III: economic crop zonation is the urban and built-up area, paddy field, field crop, water body, rangeland, and miscellaneous land. In contrast, the prominent LULC types with the decreased area in the same period are perennial trees and orchards, Forest land, wetland, while the para rubber is stable. Under this scenario, the LULC change is mainly dictated by suitability classes (highly, moderate, and low suitability) for economic crops zonation by Agri-Map, particularly paddy field, field crop, para rubber, and perennial tree and orchard. This scenario represents the government's policy on an agricultural extension to reduce cost, increase production, and provide agriculture competition opportunities.

Moreover, the predicted LULC data in three different scenarios using the CLUE-S model furnish the results as expected objectives of this study. It was found that the CLUE-S model is an efficient tool to predict LULC in different specific scenarios. The deviation values between the required and predicted area of each LULC type vary from -0.23 km^2 (underestimation) to 0.33 km^2 (overestimation). Nevertheless, the CLUE-S model requires an optimum conversion matrix and elasticity of land use change, land requirement and driving factors on LULC change.

CHAPTER VI

SEDIMENT EXPORT ESTIMATION OF THREE DIFFERENT SCENARIOS

This chapter presents the results of the fourth objective focusing on sediment export assessment using the sediment delivery ratio (SDR) model of the InVEST software suite from LULC in 2019 and predictive LULC between 2020 and 2029 of three different scenarios. The main results consist of (1) calibration and validation of sediment delivery ratio model, (2) sediment export estimation of actual LULC in 2019, (3) sediment export estimation of predictive LULC of Scenario I: Trend of LULC evolution, (4) sediment export estimation of predictive LULC of Scenario II: Maximization ecosystem service values, (5) sediment export estimation of predictive LULC of Scenario III: Economic crop zonation, and (6) comparison of sediment export estimation among three different scenarios are here described and discussed in details.

6.1 Calibration of sediment delivery ratio model

In general, a calibration process is firstly required to identify optimum model parameters using available observed data in the study. Then, the optimum parameters are applied to validate the model. In this study, the available data between 2011 and 2018 were systematically separated into two datasets: calibration and validation. Thus, observed data between 2011 and 2015 were applied for model calibration, while observed data in 2016, 2017 and 2018 were applied for model validation.

The required input data for SDR model calibration are total suspended solids (TSS) data, runoff and LULC data. Due to this study using the past data, the correlation of TSS data and the surface runoff that provides the highest correlation was first analyzed to estimate the observed data. Therefore, the observed maximum daily total suspended solids data collected three or four times per year between 2011 and 2015 from six locations in Kwan Phayao Lake by the PCD (Table 6.1) were applied to calculate annual observed TSS data with the annual surface runoff. Meanwhile, the

daily surface runoff data from the RID were applied to calculate annual surface runoff in the same period (Figure 6.1). The required LULC data in the same period were predicted based on the classified LULC in 2009 and 2019 using the CLUE-S model (Figure 6.2).

For model calibration, this study applies the guideline from the InVEST documentation and the reviewed paper by Griffin et al. (2020) to calibrate essential parameters of the SDR model. The critical model parameters, namely K_b , IC_0 , and TFA, were systematically adjusted until the satisfied fit was obtained between the modeled and observed sediment export based on statistical measurement using R^2 and *PBIAS*.

In principle, the Borselli K (K_b) is a sensitivity parameter as the slight increase of K_b value increases sediment export. On the other hand, reducing the Borselli IC (IC_0) value affects sediment export by increasing export, which both parameters (K_b and IC_0) define the relationship between the index of connectivity and the sediment delivery ratio (SDR). Moreover, the increase of threshold flow accumulation (TFA) value has also decreased the sediment export.



Table 6.1 Basic information of observed TSS data of PCD for model calibration.

Year	Date	KP01			KP05			KP06			KP07			KP09			KP010		
		Time	Depth (m)	TSS (mg/l)	Time	Depth (m)	TSS (mg/l)	Time	Depth (m)	TSS (mg/l)	Time	Depth (m)	TSS (mg/l)	Time	Depth (m)	TSS (mg/l)	Time	Depth (m)	TSS (mg/l)
2011	2011-12-07	09:53	2.90	7.00	10:10	1.80	5.00	10:21	2.60	4.00	11:17	0.80	10.00	10:31	3.00	4.00	10:44	3.00	12.00
	2011-09-01	09:10	3.60	37.00	09:25	2.60	15.00	09:40	3.00	13.00	10:50	1.30	18.00	09:46	3.60	12.00	10:01	3.20	14.00
	2011-06-16	09:00	2.80	15.00	09:18	2.30	10.00	09:25	2.50	16.00	15:20	-	37.00	09:35	3.00	10.00	09:47	1.60	18.00
	2011-03-18	10:52	2.00	25.00	11:08	1.50	42.00	11:18	1.60	36.00	13:10	1.00	4.00	11:25	2.00	34.00	11:37	1.50	10.00
2012	2012-11-30	09:20	2.90	20.00	09:40	2.30	16.00	10:00	2.50	13.00	07:50	0.60	11.00	10:10	3.00	13.00	10:25	1.70	16.00
	2012-08-30	09:20	1.80	27.00	09:36	2.60	21.00	09:49	2.50	19.00	08:00	1.60	22.00	10:00	2.90	20.00	10:16	3.00	42.00
	2012-05-30	09:43	2.30	25.00	-	1.80	25.00	-	2.00	23.00	11:19	1.60	73.00	-	2.60	17.00	-	2.00	9.00
	2012-03-01	09:15	2.00	12.00	09:30	14.00	5.00	09:45	1.90	55.00	08:00	1.70	7.00	09:50	2.50	9.00	10:05	2.30	11.00
2013	2013-12-13	-	3.30	8.00	-	1.80	3.00	-	2.70	4.00	-	1.60	5.00	-	3.20	2.00	-	1.40	4.00
	2013-05-30	10:27	1.40	21.00	10:47	0.80	54.00	11:00	1.20	31.00	12:51	0.70	29.00	11:10	1.60	55.00	11:22	0.20	14.00
	2013-02-21	11:30	2.40	18.00	11:55	2.10	19.00	12:05	2.00	11.00	13:15	0.40	11.00	12:15	2.20	12.00	12:25	2.50	8.00
2014	2014-11-20	10:06	3.20	6.00	10:21	2.00	5.00	10:32	2.70	6.00	11:47	2.20	8.00	10:47	3.30	2.00	11:00	1.20	9.00
	2014-08-22	09:29	3.40	17.00	09:42	1.80	19.00	09:50	2.50	16.00	07:58	1.80	13.00	09:59	2.90	31.00	10:14	1.00	11.00
	2014-06-04	08:37	1.20	17.00	08:52	0.20	25.00	09:01	1.10	20.00	07:18	0.80	12.00	09:09	1.50	15.00	09:21	0.10	4.00
2015	2015-12-23	10:25	1.10	39.52	10:40	0.40	34.33	10:50	0.75	21.79	11:10	0.15	20.16	11:30	0.75	15.90	11:50	0.35	33.68
	2015-09-10	08:50	2.15	17.00	09:05	0.30	24.00	09:15	1.15	14.40	09:35	0.80	15.00	10:00	1.00	21.78	10:15	1.05	7.20
	2015-05-29	09:35	1.95	38.00	09:50	0.30	20.00	10:00	1.30	6.00	10:25	0.65	55.00	10:40	1.20	4.00	11:00	0.15	28.00
	2015-03-12	09:21	2.70	4.00	09:42	1.10	3.00	09:51	2.00	52.00	11:26	1.30	26.00	10:05	2.20	5.00	10:24	0.60	10.00

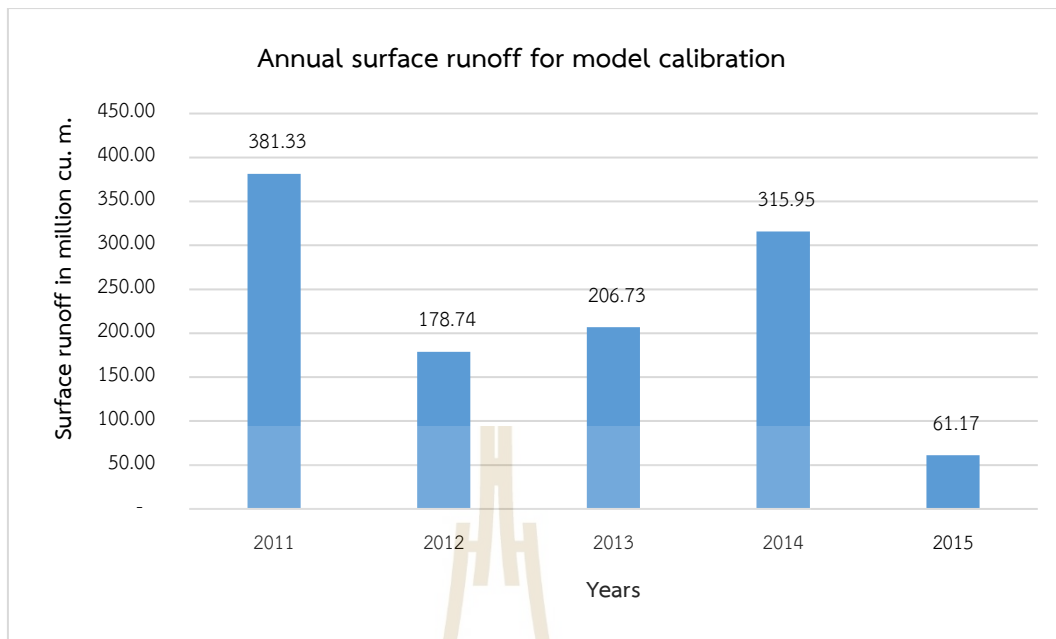


Figure 6.1 The annual surface runoff data between 2011 and 2015 for model calibration.

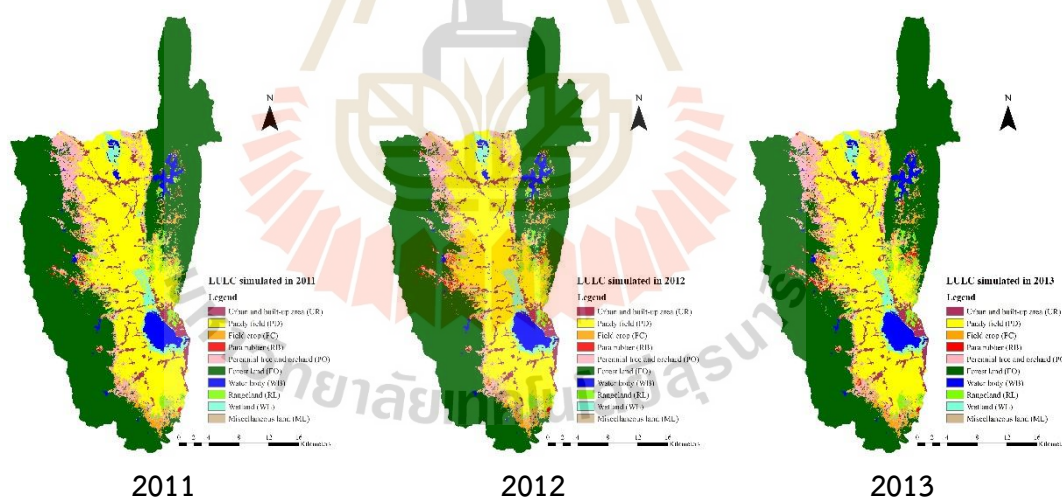


Figure 6.2 Predicted LULC data between 2011 and 2015 for model calibration.

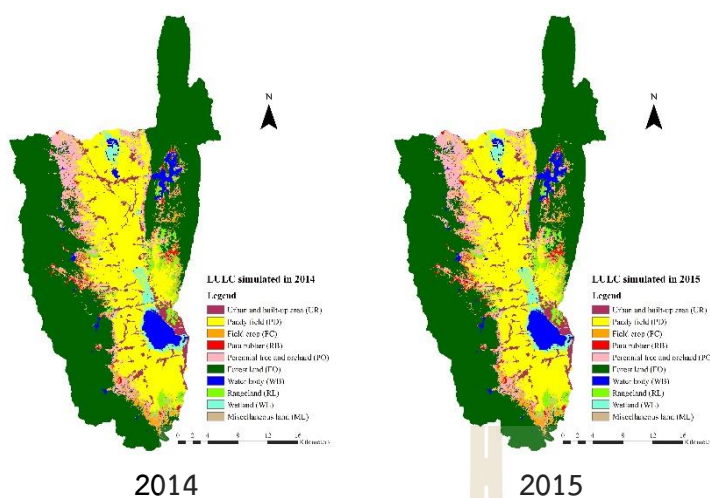


Figure 6.2 (Continued).

In practice, the default values of selected parameters of the SDR model were first applied to examine the sensitivity of each parameter on sediment export. Then, systematic adjustment was conducted from the initial to the maximum value to identify an optimum local parameter based on R^2 and $PBIAS$. (See detail in Table 6.2).

Table 6.2 Sediment delivery ratio model parameters for model calibration.

Parameter	Default value	Initial value	Maximum value	Adjusted value	Optimum value
K_b	2	1	2	0.5	1
IC_0	0.5	0.1	1	0.1	1
TFA	1000	1000	1800	200	1800

Table 6.3 compares the results and statistical measurement at default, initial and maximum value stages. As a result of Table 6.3, it can be observed that results of sediment export estimation between 2010 and 2015 with a default value, initial value, and maximum value provide overestimated value with $PBIAS$ values varying from -1,216.30 to -225.64 and the R^2 values ranging from 0.69 to 0.70. This finding indicates that the systematic adjustment for optimum model parameters identification is required to minimize the $PBIAS$ value with the expected overestimate, as shown in

Table 6.2. The comparison of the observed and estimated sediment export and statistical measurement values under the calibration period is reported in Table 6.4 and Figure 6.3.

Table 6.3 Observed and estimated sediment export and statistical measurement at default, initial and maximum value stages.

Default setting: $K_b = 2$, $IC_0 = 0.5$, $TFA = 1000$				
Year	Observed (tons/km ²)	Estimated (tons/km ²)	R ²	PBIAS (%)
2011	21.56	218.69		
2012	17.57	241.31		
2013	15.31	175.51	0.69	-1,216.30
2014	13.19	229.28		
2015	4.52	85.00		
Initial setting: $K_b = 1$, $IC_0 = 0.1$, $TFA = 1000$				
Year	Observed (tons/km ²)	Estimated (tons/km ²)	R ²	PBIAS (%)
2011	21.56	54.10		
2012	17.57	59.65		
2013	15.31	43.44	0.69	-225.64
2014	13.19	56.59		
2015	4.52	21.19		
Maximum setting: $K_b = 2$, $IC_0 = 1$, $TFA = 1800$				
Year	Observed (tons/km ²)	Estimated (tons/km ²)	R ²	PBIAS (%)
2011	21.56	172.53		
2012	17.57	189.85		
2013	15.31	137.80	0.70	-934.47
2014	13.19	179.68		
2015	4.52	66.57		

Table 6.4 Comparison of the observed and estimated sediment export with a statistical measurement under the calibration period.

Year	Sediment export in tons/km ²		Statistical measurement		
	Observed data	Estimated data	PBIAS	R ²	Adjusted R ²
2011	21.56	21.18			
2012	17.57	23.32			
2013	15.31	16.88	-27.03%	0.697	0.60
2014	13.19	22.02			
2015	4.52	8.26			

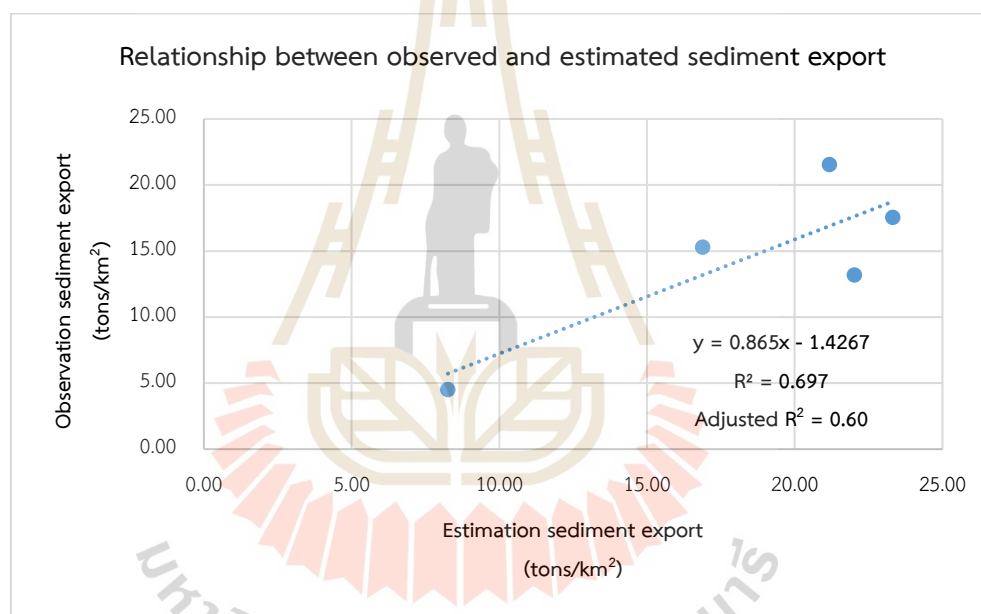


Figure 6.3 Relationship between the observed and estimated sediment export under calibration period.

As a result of Table 6.4, the estimated sediment export between 2011 and 2015 is overestimated, as mentioned earlier. However, the *PBIAS* value was reduced until an acceptable result, with a value of -27.03% and the R^2 value of 0.697, which can provide a good fit for sediment export estimation, as suggested by Moriasi et al. (2007) and Me, Abell, and Hamilton (2015). This finding is similar to Bouguerra, Jebari, and Tarhouni (2019) previous study, which applied the SDR of the InVEST model to analyze sediment production and control in the Rmel river basin. They found that the

correlation between estimated and observed sediment export in the calibration process was high, with R^2 value of 0.84. Additionally, the k_b parameter showed large variability when varied values. Therefore, an optimum local parameter of the SDR model of the InVEST software suite can be accepted and further applied to validate the model in the next step.

6.2 Validation of sediment delivery ratio model

The identified optimum local parameters of the SDR model were applied here to estimate sediment export between 2016 and 2018 for model validation. Like the calibration process, the required input data are the observed TSS data, runoff and LULC data. The observed daily TSS data collected four times per year from 2016 to 2018 from six locations in Kwan Phayao Lake by the PCD were applied to calculate annual TSS data (Table 6.5). Meanwhile, the daily surface runoff data from the RID were applied to calculate annual surface runoff in the same period (Figure 6.4). Besides, the required LULC data in the same period were predicted based on the classified LULC in 2009 and 2019 using the CLUE-S model (Figure 6.5). The derived results of the model validation with an optimum SDR model parameter are reported in Table 6.6 and Figures 6.6.

Table 6.5 Basic information of observed TSS data of PCD for model validation.

Year	Date	KP01		KP05		KP06		KP07		KP09		KP10							
		Time	Depth (m)	TSS (mg/l)	Time	Depth (m)	TSS (mg/l)	Time	Depth (m)	TSS (mg/l)	Time	Depth (m)	TSS (mg/l)						
2016	2016-11-21	10:00	3.50	15.00	10:20	2.00	16.00	10:31	4.50	12.00	13:00	1.00	11.00	10:46	3.50	9.00	11:10	2.30	12.00
	2016-08-22	09:05	2.00	119.00	09:25	1.00	52.00	09:35	1.80	40.00	11:25	0.50	10.00	09:50	1.40	44.00	10:10	1.60	26.00
	2016-06-16	09:15	0.90	47.00	09:38	0.50	112.00	09:48	1.00	174.00	12:05	0.30	82.00	10:08	1.50	101.00	10:30	1.00	56.00
	2016-03-01	10:15	1.30	62.66	10:55	0.30	42.85	10:45	0.80	25.96	13:00	0.50	37.71	11:00	1.00	26.02	11:15	1.00	40.87
2017	2017-11-23	08:50	3.10	9.40	09:15	1.80	14.00	09:35	3.00	8.80	11:30	1.40	20.00	09:40	3.10	6.20	10:00	2.00	22.00
	2017-07-06	-	2.50	25.00	-	1.50	40.00	-	3.00	37.00	-	1.00	19.00	-	2.20	20.00	-	1.70	60.00
	2017-05-18	09:05	2.50	32.00	09:10	1.00	56.00	09:15	2.00	60.00	11:05	1.80	95.00	09:30	3.00	24.00	09:50	1.50	140.00
	2017-01-26	10:13	3.50	8.80	10:00	2.00	12.00	09:35	1.00	14.00	09:20	1.00	6.60	-	-	0.00	08:30	1.50	19.00
2018	2018-11-22	09:50	4.20	6.80	10:15	2.00	7.30	10:30	3.40	5.30	10:50	2.40	5.60	11:00	3.00	13.00	11:20	2.00	3.60
	2018-08-06	08:30	2.50	21.00	08:45	1.20	25.00	09:00	2.30	22.00	10:10	1.30	53.00	09:30	3.00	18.00	10:40	2.50	39.00
	2018-05-24	08:30	3.00	21.00	08:45	1.50	21.00	09:00	4.50	18.00	10:20	1.50	42.00	09:20	2.50	20.00	09:45	2.20	222.00
	2018-02-24	09:30	2.50	15.00	09:40	1.20	26.00	09:50	2.50	22.00	08:10	1.20	14.00	10:00	2.70	10.00	10:10	1.50	10.00



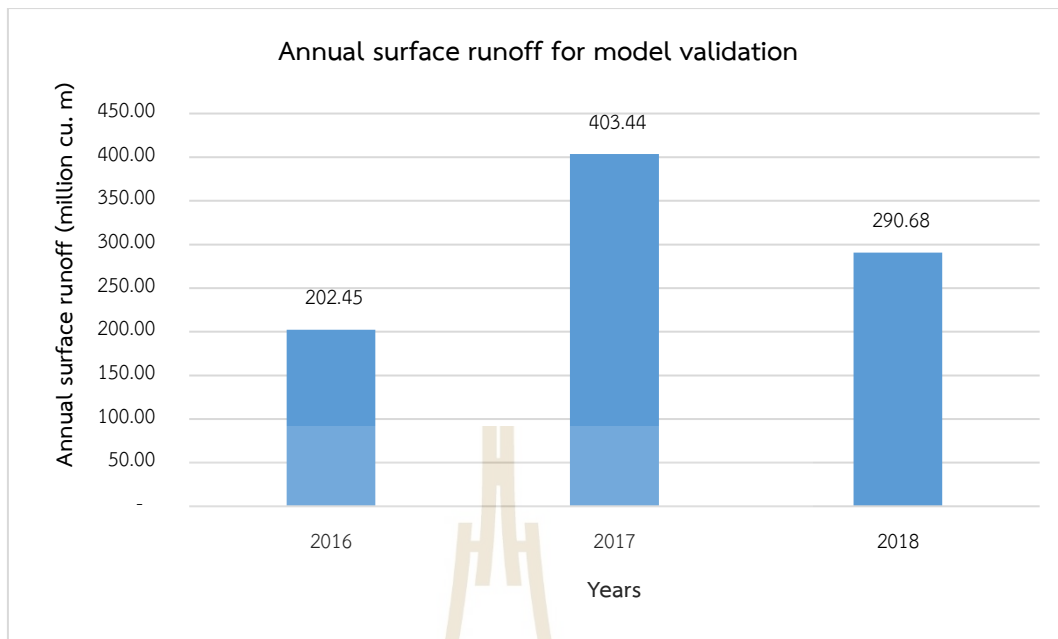


Figure 6.4 The annual surface runoff data between 2016 and 2018 for model validation.

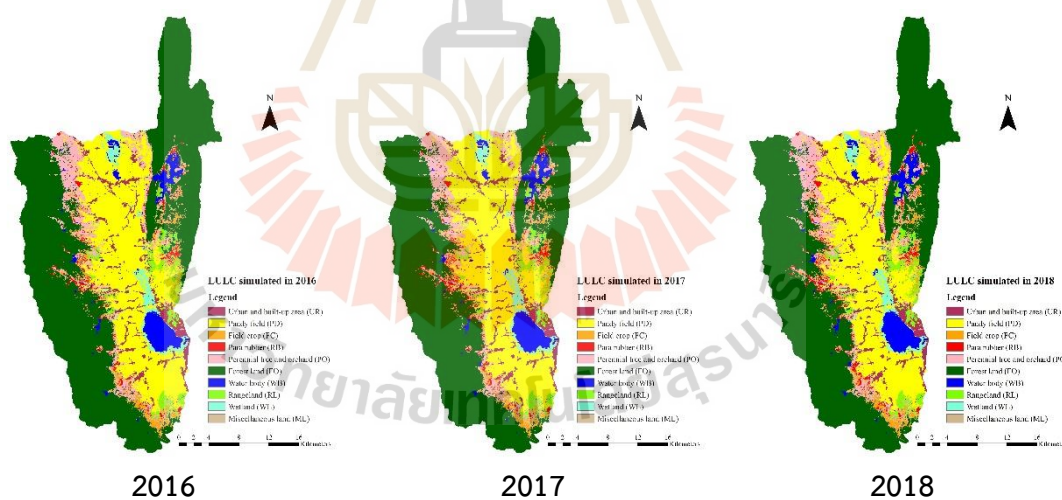


Figure 6.5 Predicted LULC data between 2016 and 2018 for model validation.

Table 6.6 Comparison of the observed and estimated sediment export with a statistical measurement under the validation period.

Year	Sediment export in tons/km ²		Statistical measurement		
	Observed data	Estimated data	PBIAS	R ²	Adjusted R ²
2016	47.42	18.14			
2017	76.04	22.73	65.60%	0.824	0.65
2018	86.88	31.50			

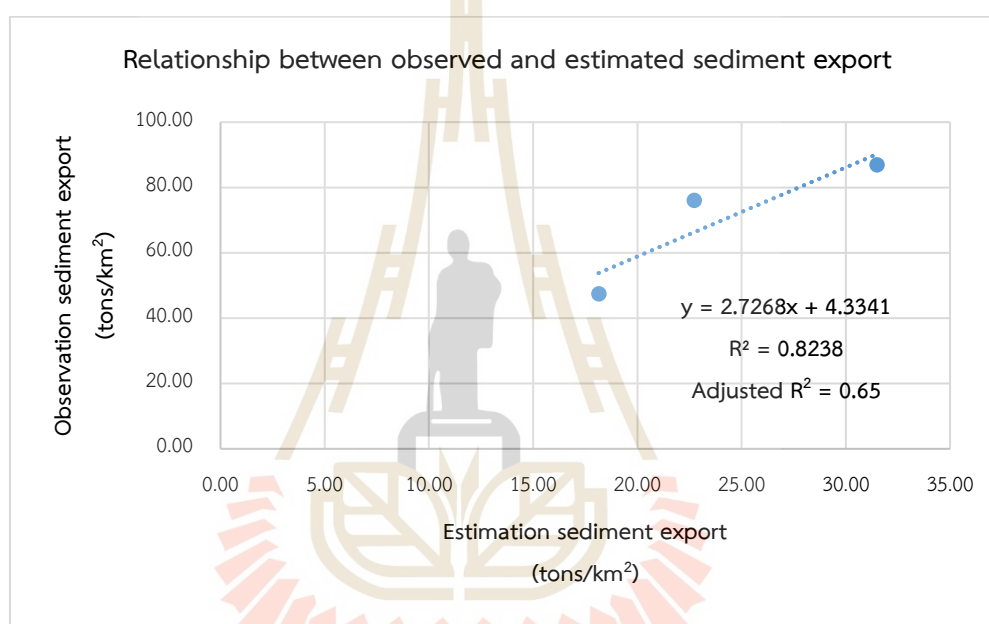


Figure 6.6 Relationship between the estimated and observed sediment export under validation period.

As a validation result, the *PBIAS* value is 65.59%, which provides an unsatisfactory model validation in sediment export estimation. However, the coefficient of determination between the observed and estimated sediment export is very good, with a value of about 0.824 as suggested by Moriasi et al. (2007) and Me, Abell, and Hamilton (2015). However, the ranges of observed and estimated sediment in the validation period were quite different. The possible reason for this phenomenon was the data uncertainty, which came from several sources such as location and frequency of sample collection, instrument variability, and different observers. These

effects were associated with the result of observed data. Conversely, the estimated data were systematically adjusted in the calibration process for optimal local parameters and applied in the validation process. Therefore, the sediment delivery ratio model of the InVEST software suite can be validated and further applied to estimate soil loss, sediment retention, sediment deposition, and sediment export in an actual year and the three different scenarios between 2020 and 2029.

In summary, the calibration of the SDR model exposed that the annual surface runoff influences the observed TSS data because it was applied to calculate the total suspended solids in units of tons per year. In this study, the relationship between annual surface runoff and the observed TSS data under calibration periods shows a positive correlation as the expected result, with the R^2 value of 0.6079 (Figure 6.7). It suggests a good fit between the actual and predicted data, as suggested by Moriasi et al. (2007) and Me, Abell, and Hamilton (2015). This finding implies that the annual surface runoff of the RID and the observed TSS data of the PCD can be accepted for sediment export estimation in this study.

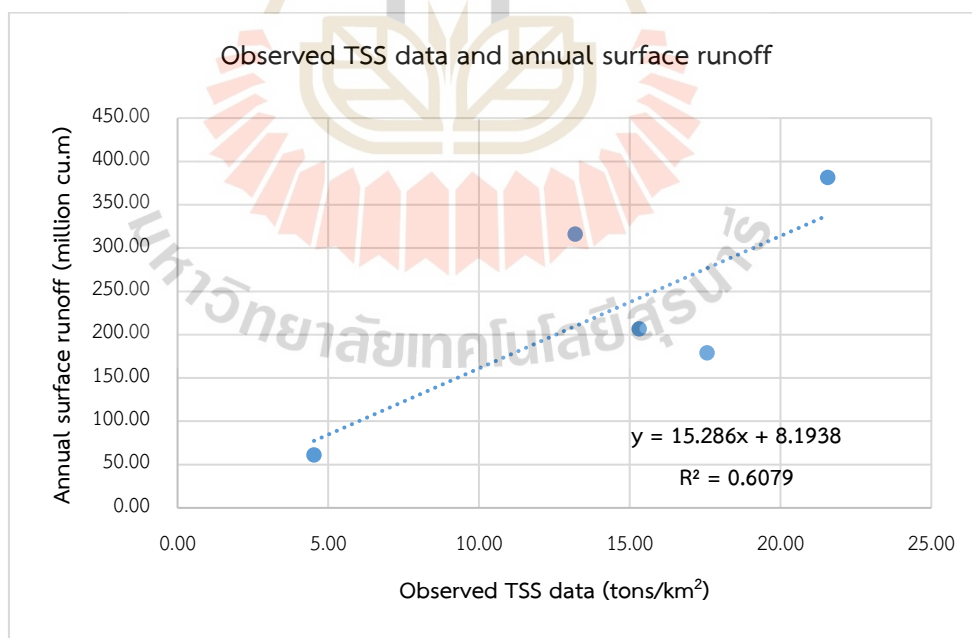


Figure 6.7 Relationship between observed TSS data and annual surface runoff between 2011 and 2015.

Moreover, annual rainfall erosivity has affected estimated sediment export using the SDR model. It is applied under the RUSLE equation to calculate total soil loss and deliver sediment to the streams (See Eq. 2.18). In general, annual rainfall erosivity and sediment yield have a positive correlation; as rainfall erosivity increases, sediment yield increases. So, the average annual rainfall erosivity data under the calibration period were here applied to confirm the relationship with the estimated sediment export data, as shown in Figure 6.8. As a result, it disclosed that average rainfall erosivity data, which interpolated using the IDW method, as shown in Figure 3.8, have a positive with the estimated sediment export as the expected result, with the R^2 value of 0.6758. It suggests a good fit between the actual and predicted data, as suggested by Moriasi et al. (2007) and Me, Abell, and Hamilton (2015).

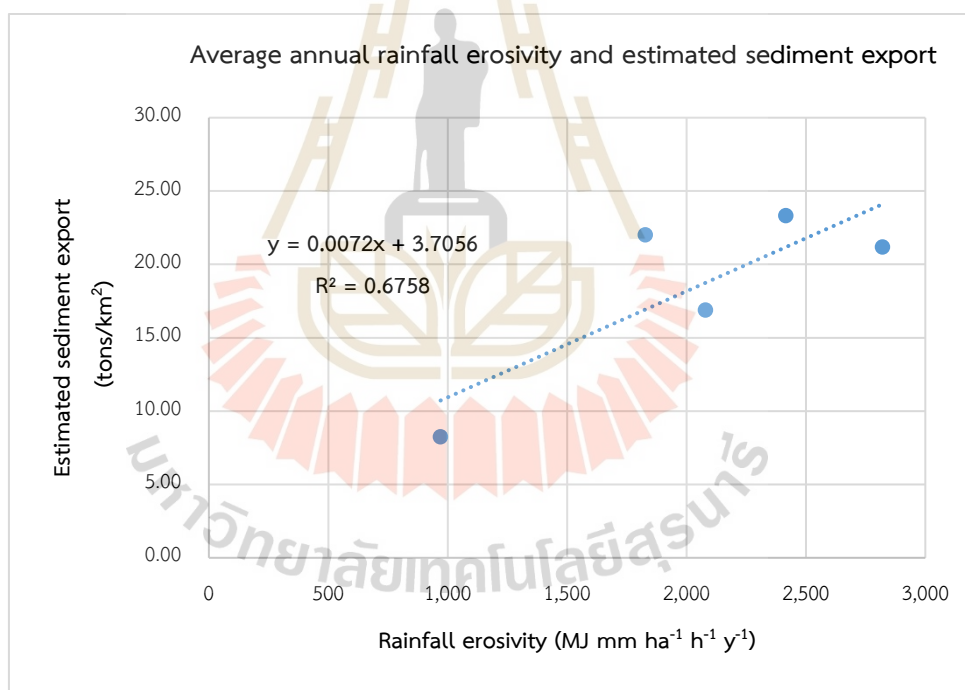


Figure 6.8 Relationship between average annual rainfall erosivity and the estimated sediment export under calibration period.

This finding is consistent with the previous work of Guesri, Megnounif, and Ghenim (2020), who examine the relationship between rainfall erosivity and sediment yield at the K'sob watershed, Northeast Algeria. They found a positive relationship

between annual rainfall erosivity and sediment yield between 1973 and 1994, with an R^2 value of 0.47. Additionally, the seasonal rainfall erosivity data (autumn, winter, spring, and summer) positively correlated with sediment yield, with R^2 values varying from 0.42 to 0.68.

Liu et al. (2018) studied spatial-temporal changes of rainfall erosivity in the loess plateau, Jing River Basin (JRB), China. They found that rainfall erosivity shows statistically positive correlations with sediment discharge variations in the JRB with 1–2 years rainfall patterns in 1963–1966. They also stated that rainfall erosivity was closely associated with sediment load in the JRB. As the observed decreasing rainfall erosivity, sediment load may have reduced in the JRB to a certain extent.

Similarly, Yao, Yu, Jiang, Sun, and Li (2016) evaluated the factors affecting soil erosion in Lushi Basin, and they found that rainfall erosivity in annual mean, monthly, and seasonal scales have a very good correlation with sediment yield with $R^2 = 0.81$, $R^2 = 0.90$, and $R^2 = 0.92$ respectively. Thus, these review papers confirm that sediment yield is driven mainly by rainfall erosivity.

Consequently, an optimum parameter of the SDR model can be further applied to estimate sediment export of actual LULC data in 2019 and predictive LULC data of three scenarios between 2020 and 2029 in this study.

6.3 Sediment export estimation of actual LULC in 2019

The estimation of total and average soil erosion, sediment retention, sediment deposition, and sediment export of actual LULC in 2019 is presented in Table 6.7. The results found that the total of soil erosion, sediment retention, sediment deposition, and sediment export in 2019 is about 4,559,886.82 tons (5,115.71 tons/km²), 63,637,227.03 tons (71,394.21 tons/km²), 4,518,235.50 (5,068.98 tons/km²), and 26,421.41 tons (29.64 tons/km²), respectively. The spatial distribution of sediment export in 2019 is shown in Figure 6.9. Moreover, the amount of soil erosion, sediment retention, sediment deposition, and sediment export from each LULC type in 2019 are presented in Table 6.8.

Table 6.7 Summary data on soil erosion, sediment retention, sediment deposition and export of actual LULC data in 2019.

Area (km²)	891.35
Soil loss (tons)	4,559,886.82
Soil loss (tons/km²)	5,115.71
Sediment retention (tons)	63,637,227.03
Sediment retention (tons/km²)	71,394.21
Sediment deposition (tons)	4,518,235.50
Sediment deposition (tons/km²)	5,068.98
Sediment export (tons)	26,421.41
Sediment export (tons/km²)	29.64

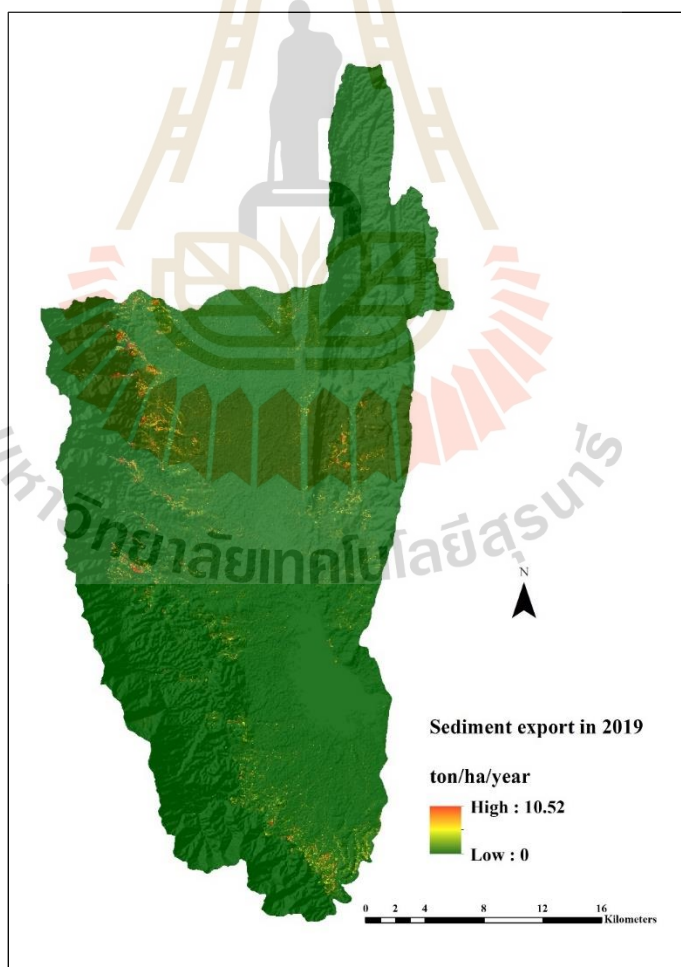


Figure 6.9 Spatial distribution of sediment export in 2019.

Table 6.8 Contribution of soil erosion, sediment retention, sediment deposition, and sediment export by LULC classes in 2019.

LULC types	Area km ²	Soil erosion			Sediment retention			Sediment deposition			Sediment export		
		Total (tons)	Average (tons/km ²)	%	Total (tons)	Average (tons/km ²)	%	Total (tons)	Average (tons/km ²)	%	Total (tons)	Average (tons/km ²)	%
Urban and built-up area (UR)	33.10	-	-	-	40,101.19	1,211.70	0.59	23,568.28	712.14	0.98	-	-	-
Paddy field (PD)	220.74	267,650.35	1,212.50	0.63	387,120.22	1,753.72	0.86	1,413,987.86	6,405.60	8.78	2,471.12	11.19	0.80
Field crop (FC)	21.84	1,170,319.04	53,581.83	27.71	256,492.49	11,743.24	5.76	262,229.50	12,005.90	16.46	7,169.79	328.26	23.57
Para rubber (RB)	19.78	548,984.27	27,748.83	14.35	254,470.68	12,862.41	6.31	156,049.37	7,887.63	10.82	2,555.61	129.18	9.27
Perennial tree and orchard (PO)	79.22	1,782,917.30	22,504.84	11.64	976,358.61	12,324.07	6.05	1,251,519.57	15,797.28	21.66	11,578.36	146.15	10.49
Forest land (FO)	436.91	473,171.45	1,082.98	0.56	61,133,624.65	139,921.31	68.68	872,640.83	1,997.28	2.74	246.47	0.56	0.04
Water body (WB)	33.37	-	-	-	442,048.34	13,247.82	6.50	308,728.98	9,252.35	12.69	-	-	-
Rangeland (RL)	27.26	89,011.80	3,265.03	1.69	117,943.11	4,326.26	2.12	173,766.84	6,373.93	8.74	323.29	11.86	0.85
Wetland (WL)	16.41	-	-	-	14,252.10	868.70	0.43	26,165.81	1,594.86	2.19	-	-	-
Miscellaneous land (ML)	2.71	227,832.60	83,986.99	43.43	14,815.64	5,461.56	2.68	29,578.46	10,903.64	14.95	2,076.77	765.57	54.97
Total	891.35	4,559,886.82		100.00	63,637,227.03		0.59	4,518,235.50		100.00	26,421.41		100.00



According to zonal statistic operation between soil erosion, sediment retention, sediment deposition, and sediment export with LULC data in 2019, it revealed that the highest soil erosion was found on miscellaneous land with an average value of 83,986.99 tons/km² (43.43%) while the lowest average soil loss occurred on forest land with the value of 1,082.98 tons/km² (0.56%). In the meantime, sediment retention concerning a watershed where all LULC types are converted to the bare ground, the highest average sediment retention is forest land with the value of 139,921.31 tons/km² (68.68%). In comparison, the lowest average sediment retention is a wetland with a value of 868.70 tons/km² (0.43%). Meanwhile, the highest sediment deposition appears on perennial trees and orchards with an average value of 15,797.28 tons/km² (21.66%), whereas the lowest sediment deposition occurs on the urban and built-up area with the value of 712.14 ton/km² (0.98%). At the same time, the highest sediment export appears on miscellaneous land with an average value of 765.57 tons/km² (54.97%), while the lowest sediment export comes from forest land with the value of 0.56 ton/km² (0.04%).

As a result, the intensity of monthly rainfall affects soil loss, sediment retention, sediment deposition, and sediment export due to an average rainfall erosivity from monthly rainfall data from 5 meteorological stations. It was found that an average rainfall erosivity in 2019 was about 2,944.67 MJ mm. ha⁻¹ h⁻¹ y⁻¹, which was over than mean of rainfall erosivity from every year (See Table 3.7). Even though the average annual rainfall in 2019 was 1,047.80 mm., which is lower than the mean annual rainfall from every year, which was about 1,352.17 mm. (See Table 3.12). This finding suggests the influence of LULC types and rainfall erosivity on soil loss, sediment retention, sediment deposition, and sediment export.

In this study, the highest sediment export occurs in miscellaneous land, while the lowest is forest land. Additionally, urban and built-up areas, water bodies, and wetland do not create soil erosion and sediment export according to the C and P coefficient in the biophysical table. In contrast, the sediment retention is modeled concerning a watershed where all LULC types are cleared to the bare ground. The value of the retention service is then based on the difference between the sediment export from this bare soil catchment and that of the scenario of interest. At the same

time, sediment deposition is the total amount of sediment deposited on the pixel from upstream sources due to retention (Sharp et al.,2020).

6.4 Sediment export estimation of predictive LULC of Scenario I

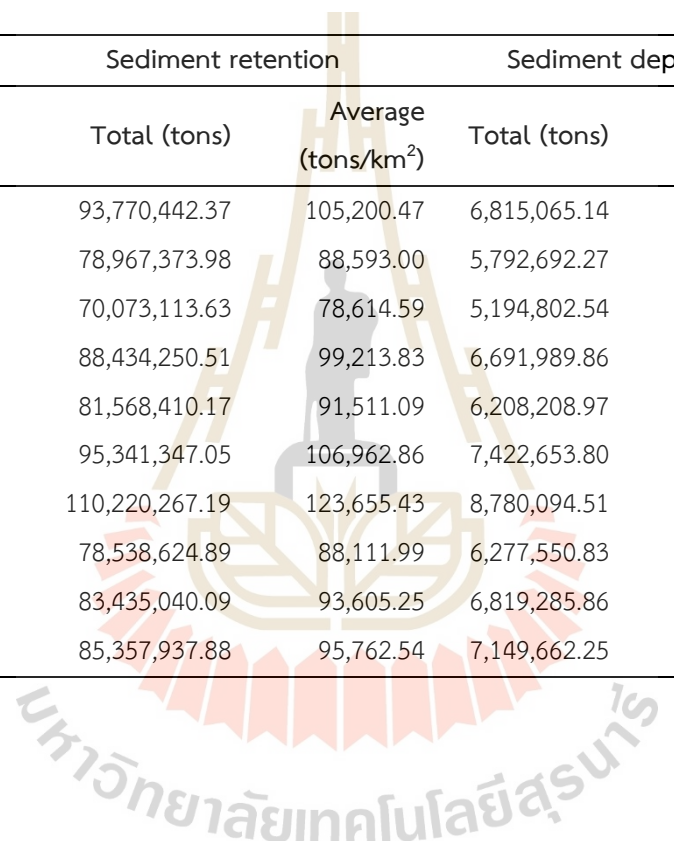
Estimation of total and average soil loss, sediment retention, sediment deposition, and sediment export of predictive LULC between 2020 and 2029 under Scenario I: Trend of LULC evolution is presented in Table 6.9.

As a result, it was found that the highest total and average soil erosion under Scenario I (Trend of LULC evolution) are about 8.87 million tons and 9,955.88 tons/km² occurring in 2026, while the lowest total and average soil erosion are about 5.24 million tons and 5,883.34 tons/km² occurring in 2022. Likewise, the highest total and average sediment exports are about 0.06 million tons and 65.97 tons/km² in 2026. The lowest total and average sediment exports are about 0.03 million tons and 36.32 tons/km² in 2022.

Meanwhile, the highest total and average sediment retention under Scenario I are about 110.22 million tons and 123,655.43 tons/km² occurring in 2026. The lowest total and average sediment retention are about 70.07 million tons and 78,614.59 tons/km² occurring in 2022. Simultaneously, the highest total and average sediment deposition will be about 8.78 million tons and 9,850.33 tons/km² in 2026. The lowest total and average sediment deposition are about 5.19 million tons and 5,828.02 tons/km² in 2022.

Table 6.9 Estimation of soil erosion, sediment retention, sediment deposition, and sediment export between 2020 and 2029 under Scenario I: Trend of LULC evolution.

Year	Area km ²	Soil erosion		Sediment retention		Sediment deposition		Sediment export	
		Total (tons)	Average (tons/km ²)	Total (tons)	Average (tons/km ²)	Total (tons)	Average (tons/km ²)	Total (tons)	Average (tons/km ²)
2020	891.35	6,878,528.82	7,716.98	93,770,442.37	105,200.47	6,815,065.14	7,645.78	41,445.02	46.50
2021	891.35	5,847,404.62	6,560.17	78,967,373.98	88,593.00	5,792,692.27	6,498.79	35,685.45	40.04
2022	891.35	5,244,119.47	5,883.34	70,073,113.63	78,614.59	5,194,802.54	5,828.02	32,373.49	36.32
2023	891.35	6,756,574.63	7,580.16	88,434,250.51	99,213.83	6,691,989.86	7,507.70	41,954.52	47.07
2024	891.35	6,272,703.02	7,037.31	81,568,410.17	91,511.09	6,208,208.97	6,964.95	39,669.68	44.51
2025	891.35	7,500,767.58	8,415.06	95,341,347.05	106,962.86	7,422,653.80	8,327.43	48,329.18	54.22
2026	891.35	8,874,175.32	9,955.88	110,220,267.19	123,655.43	8,780,094.51	9,850.33	58,797.97	65.97
2027	891.35	6,345,432.93	7,118.90	78,538,624.89	88,111.99	6,277,550.83	7,042.75	42,549.03	47.74
2028	891.35	6,893,185.82	7,733.42	83,435,040.09	93,605.25	6,819,285.86	7,650.51	46,867.05	52.58
2029	891.35	7,227,180.35	8,108.13	85,357,937.88	95,762.54	7,149,662.25	8,021.16	49,558.85	55.60



These results indicate that the primary influence of LULC types and the rainfall erosivity factor in the RUSLE model affect soil erosion, sediment retention, sediment deposition, and sediment export. Table 6.10 shows the basic statistics of the predictive rainfall erosivity factor between 2020 and 2029, calculated from the equation (see Equation 3.3).

Table 6.10 Basic statistics of predictive rainfall erosivity factor between 2020 and 2029.

Year	Rainfall erosivity (MJ mm ha ⁻¹ h ⁻¹ y ⁻¹)				
	MIN	MAX	MEAN	RANGE	STD
2020	2,200.46	3,628.76	2,854.33	1,428.30	491.39
2021	1,985.90	3,249.31	2,490.34	1,263.41	344.98
2022	1,837.56	2,753.87	2,239.93	916.31	348.57
2023	2,297.64	3,532.87	2,711.93	1,235.23	370.98
2024	2,148.41	3,085.24	2,601.06	936.83	367.02
2025	2,456.77	4,221.46	2,992.66	1,764.69	520.98
2026	2,711.94	3,791.71	3,130.43	1,079.77	349.27
2027	1,923.79	3,161.59	2,456.18	1,237.80	401.79
2028	2,213.24	2,855.04	2,588.82	641.80	204.96
2029	2,282.63	3,403.08	2,640.18	1,120.46	344.94

The contribution of the predictive LULC of Scenario I (Trend of LULC evolution) on soil erosion, sediment retention, sediment deposition, and sediment export between 2020 and 2029 are summarized in Tables 6.11 to 6.20, and the spatial distribution of sediment export of the predictive LULC between 2020 and 2029 of Scenario I is displayed in Figures 6.10 to 6.13.

Table 6.11 Contribution of soil erosion, sediment retention, sediment deposition, and sediment export by LULC classes in 2020 under Scenario I.

LULC types	Area	Soil erosion			Sediment retention			Sediment deposition			Sediment export		
	km ²	Total (tons)	Average (tons/km ²)	%	Total (tons)	Average (tons/km ²)	%	Total (tons)	Average (tons/km ²)	%	Total (tons)	Average (tons/km ²)	%
Urban and built-up area (UR)	33.45	-	-	-	66,911.39	2,000.20	0.67	34,261.16	1,024.18	0.92	-	-	-
Paddy field (PD)	219.73	404,682.22	1,841.76	0.64	579,913.86	2,639.27	0.88	2,002,731.04	9,114.70	8.19	3,717.20	16.92	0.83
Field crop (FC)	21.94	1,742,970.30	79,455.12	27.81	379,796.81	17,313.43	5.78	481,272.15	21,939.29	19.71	11,871.85	541.19	26.40
Para rubber (RB)	20.65	844,623.82	40,899.01	14.32	394,281.68	19,092.21	6.37	299,270.69	14,491.51	13.02	4,241.10	205.37	10.02
Perennial tree and orchard (PO)	81.17	2,705,661.88	33,331.96	11.67	1,412,504.02	17,401.11	5.81	1,857,974.38	22,889.01	20.57	17,819.11	219.52	10.71
Forest land (FO)	433.27	697,397.51	1,609.62	0.56	90,108,946.96	207,975.14	69.42	1,308,423.69	3,019.90	2.71	366.17	0.85	0.04
Water body (WB)	34.18	-	-	-	606,042.65	17,729.67	5.92	481,126.11	14,075.26	12.65	-	-	-
Rangeland (RL)	27.86	139,103.16	4,992.14	1.75	178,851.19	6,418.61	2.14	283,279.49	10,166.34	9.13	510.48	18.32	0.89
Wetland (WL)	16.31	-	-	-	21,846.30	1,339.35	0.45	31,523.23	1,932.62	1.74	-	-	-
Miscellaneous land (ML)	2.79	344,089.93	123,542.48	43.25	21,347.49	7,664.63	2.56	35,203.19	12,639.40	11.36	2,919.11	1,048.08	51.12
Total	891.35	6,878,528.82		100.00	93,770,442.37		100.00	6,815,065.14		100.00	41,445.02		100.00

Table 6.12 Contribution of soil erosion, sediment retention, sediment deposition, and sediment export by LULC classes in 2021 under Scenario I.

LULC types	Area	Soil erosion			Sediment retention			Sediment deposition			Sediment export		
	km ²	Total (tons)	Average (tons/km ²)	%	Total (tons)	Average (tons/km ²)	%	Total (tons)	Average (tons/km ²)	%	Total (tons)	Average (tons/km ²)	%
Urban and built-up area (UR)	33.83	-	-	-	57,767.61	1,707.72	0.68	29,011.31	857.63	0.87	-	-	-
Paddy field (PD)	218.73	336,585.46	1,538.83	0.64	483,582.49	2,210.89	0.87	1,699,310.36	7,769.06	7.90	3,120.75	14.27	0.82
Field crop (FC)	22.04	1,450,810.85	65,814.18	27.57	317,800.15	14,416.60	5.70	493,740.13	22,397.89	22.77	10,164.20	461.09	26.63
Para rubber (RB)	21.53	726,543.20	33,751.09	14.14	337,486.01	15,677.69	6.20	296,362.73	13,767.34	14.00	3,689.39	171.39	9.90
Perennial tree and orchard (PO)	83.14	2,327,746.56	27,997.63	11.73	1,208,744.17	14,538.51	5.75	1,560,532.77	18,769.75	19.08	15,413.32	185.39	10.71
Forest land (FO)	429.62	586,519.89	1,365.20	0.57	75,860,227.17	176,574.10	69.86	990,796.67	2,306.20	2.34	309.63	0.72	0.04
Water body (WB)	34.99	-	-	-	513,493.70	14,674.41	5.81	425,009.67	12,145.75	12.35	-	-	-
Rangeland (RL)	28.48	119,122.50	4,182.38	1.75	151,351.68	5,313.94	2.10	242,388.07	8,510.22	8.65	443.25	15.56	0.90
Wetland (WL)	16.10	-	-	-	18,157.86	1,127.56	0.45	26,065.07	1,618.58	1.65	-	-	-
Miscellaneous land (ML)	2.88	300,076.16	104,095.45	43.60	18,763.14	6,508.87	2.58	29,475.50	10,224.96	10.39	2,544.90	882.82	50.99
Total	891.35	5,847,404.62		100.00	78,967,373.98		100.00	5,792,692.27		100.00	35,685.45		100.00

Table 6.13 Contribution of soil erosion, sediment retention, sediment deposition, and sediment export by LULC classes in 2022 under Scenario I.

LULC types	Area	Soil erosion			Sediment retention			Sediment deposition			Sediment export		
	km ²	Total (tons)	Average (tons/km ²)	%	Total (tons)	Average (tons/km ²)	%	Total (tons)	Average (tons/km ²)	%	Total (tons)	Average (tons/km ²)	%
Urban and built-up area (UR)	34.19	-	-	-	52,795.41	1,544.18	0.69	25,545.13	747.15	0.83	-	-	-
Paddy field (PD)	217.73	293,207.94	1,346.69	0.64	421,831.50	1,937.45	0.86	1,518,430.09	6,974.06	7.74	2,737.49	12.57	0.80
Field crop (FC)	22.13	1,290,639.61	58,329.90	27.74	278,805.35	12,600.49	5.60	473,096.80	21,381.41	23.72	9,165.41	414.23	26.27
Para rubber (RB)	22.42	666,474.30	29,728.01	14.14	309,599.29	13,809.64	6.14	273,180.48	12,185.18	13.52	3,404.13	151.84	9.63
Perennial tree and orchard (PO)	85.12	2,094,492.07	24,605.34	11.70	1,086,565.62	12,764.58	5.68	1,398,346.11	16,427.27	18.22	13,940.68	163.77	10.39
Forest land (FO)	425.96	519,452.85	1,219.47	0.58	67,296,569.64	157,986.20	70.25	822,811.17	1,931.64	2.14	275.06	0.65	0.04
Water body (WB)	35.78	-	-	-	457,745.97	12,795.13	5.69	413,087.66	11,546.82	12.81	-	-	-
Rangeland (RL)	29.10	107,651.43	3,699.74	1.76	136,353.65	4,686.17	2.08	217,217.45	7,465.28	8.28	408.25	14.03	0.89
Wetland (WL)	15.95	-	-	-	15,635.46	980.36	0.44	23,146.55	1,451.32	1.61	-	-	-
Miscellaneous land (ML)	2.98	272,201.26	91,336.30	43.44	17,211.73	5,775.34	2.57	29,941.10	10,046.64	11.14	2,442.47	819.56	51.98
Total	891.35	5,244,119.47		100.00	70,073,113.63		100.00	5,194,802.54		100.00	32,373.49		100.00

Table 6.14 Contribution of soil erosion, sediment retention, sediment deposition, and sediment export by LULC classes in 2023 under Scenario I.

LULC types	Area	Soil erosion			Sediment retention			Sediment deposition			Sediment export		
	km ²	Total (tons)	Average (tons/km ²)	%	Total (tons)	Average (tons/km ²)	%	Total (tons)	Average (tons/km ²)	%	Total (tons)	Average (tons/km ²)	%
Urban and built-up area (UR)	34.61	-	-	-	71,711.79	2,071.85	0.72	34,393.82	993.68	0.84	-	-	-
Paddy field (PD)	216.77	370,649.24	1,709.89	0.64	532,546.17	2,456.76	0.86	1,949,781.55	8,994.80	7.61	3,468.57	16.00	0.79
Field crop (FC)	22.23	1,620,047.66	72,871.53	27.38	330,178.40	14,851.79	5.19	621,399.75	27,951.24	23.64	11,205.02	504.01	24.84
Para rubber (RB)	23.26	881,129.51	37,879.09	14.23	411,909.09	17,707.66	6.19	360,094.45	15,480.19	13.09	4,603.54	197.90	9.75
Perennial tree and orchard (PO)	87.04	2,730,250.55	31,369.17	11.79	1,422,950.50	16,348.97	5.72	1,803,657.21	20,723.09	17.53	18,459.97	212.10	10.45
Forest land (FO)	422.30	655,935.32	1,553.25	0.58	84,851,457.76	200,927.15	70.25	1,010,499.78	2,392.85	2.02	347.43	0.82	0.04
Water body (WB)	36.57	-	-	-	588,817.47	16,099.98	5.63	547,564.20	14,971.99	12.66	-	-	-
Rangeland (RL)	29.70	141,360.59	4,759.68	1.79	179,338.67	6,038.42	2.11	287,969.88	9,696.09	8.20	543.28	18.29	0.90
Wetland (WL)	15.79	-	-	-	19,960.05	1,264.21	0.44	30,016.48	1,901.15	1.61	-	-	-
Miscellaneous land (ML)	3.08	357,201.76	115,966.47	43.58	25,380.60	8,239.88	2.88	46,612.75	15,132.95	12.80	3,326.71	1,080.02	53.23
Total	891.35	6,756,574.63		100.00	88,434,250.51		100.00	6,691,989.86		100.00	41,954.52		100.00

Table 6.15 Contribution of soil erosion, sediment retention, sediment deposition, and sediment export by LULC classes in 2024 under Scenario I.

LULC types	Area km ²	Soil erosion			Sediment retention			Sediment deposition			Sediment export		
		Total (tons)	Average (tons/km ²)	%	Total (tons)	Average (tons/km ²)	%	Total (tons)	Average (tons/km ²)	%	Total (tons)	Average (tons/km ²)	%
Urban and built-up area (UR)	34.99	-	-	-	68,049.37	1,944.55	0.73	31,176.54	890.89	0.81	-	-	-
Paddy field (PD)	215.77	334,706.64	1,551.24	0.64	479,250.25	2,221.14	0.84	1,792,306.41	8,306.65	7.54	3,128.76	14.50	0.74
Field crop (FC)	22.31	1,464,172.30	65,631.27	26.88	292,624.62	13,116.85	4.95	571,767.05	25,629.36	23.28	10,619.53	476.02	24.38
Para rubber (RB)	24.10	839,897.93	34,844.48	14.27	396,815.92	16,462.53	6.22	343,633.88	14,256.19	12.95	4,412.44	183.06	9.38
Perennial tree and orchard (PO)	88.95	2,555,960.07	28,734.40	11.77	1,331,399.73	14,967.75	5.65	1,683,880.23	18,930.37	17.19	17,272.01	194.17	9.95
Forest land (FO)	418.63	603,355.59	1,441.25	0.59	78,235,266.44	186,882.10	70.55	912,596.14	2,179.94	1.98	320.92	0.77	0.04
Water body (WB)	37.36	-	-	-	553,907.21	14,828.15	5.60	522,314.74	13,982.41	12.70	-	-	-
Rangeland (RL)	30.29	131,890.49	4,354.31	1.78	168,227.67	5,553.97	2.10	273,847.42	9,040.96	8.21	518.33	17.11	0.88
Wetland (WL)	15.76	-	-	-	18,176.41	1,153.43	0.44	28,683.07	1,820.15	1.65	-	-	-
Miscellaneous land (ML)	3.19	342,719.98	107,596.85	44.07	24,692.55	7,752.22	2.93	48,003.49	15,070.68	13.69	3,397.69	1,066.70	54.64
Total	891.35	6,272,703.02		100.00	81,568,410.17		100.00	6,208,208.97		100.00	39,669.68		100.00

Table 6.16 Contribution of soil erosion, sediment retention, sediment deposition, and sediment export by LULC classes in 2025 under Scenario I.

LULC types	Area km ²	Soil erosion			Sediment retention			Sediment deposition			Sediment export		
		Total (tons)	Average (tons/km ²)	%	Total (tons)	Average (tons/km ²)	%	Total (tons)	Average (tons/km ²)	%	Total (tons)	Average (tons/km ²)	%
Urban and built-up area (UR)	35.39	-	-	-	86,14-	2,433.85	0.78	37,676.71	1,064.54	0.79	-	-	-
Paddy field (PD)	214.81	391,103.27	1,820.74	0.64	558,156.78	2,598.43	0.83	2,128,721.17	9,910.01	7.38	3,657.99	17.03	0.73
Field crop (FC)	22.43	1,721,569.12	76,764.70	26.95	342,369.28	15,266.23	4.89	720,960.02	32,147.58	23.93	13,155.40	586.60	25.08
Para rubber (RB)	24.99	1,034,332.93	41,391.11	14.53	491,487.14	19,667.94	6.30	420,778.80	16,838.39	12.54	5,561.65	222.56	9.52
Perennial tree and orchard (PO)	90.94	3,081,252.45	33,880.81	11.89	1,594,890.22	17,537.08	5.62	1,999,583.67	21,987.01	16.37	20,814.64	228.87	9.79
Forest land (FO)	415.00	705,243.10	1,699.37	0.60	91,350,249.13	220,120.23	70.56	1,039,050.84	2,503.73	1.86	375.08	0.90	0.04
Water body (WB)	38.16	-	-	-	663,025.57	17,373.67	5.57	643,966.88	16,874.26	12.56	-	-	-
Rangeland (RL)	30.91	160,440.36	5,189.78	1.82	204,352.08	6,610.20	2.12	333,109.31	10,775.12	8.02	625.53	20.23	0.87
Wetland (WL)	15.44	-	-	-	21,310.02	1,380.53	0.44	32,963.42	2,135.48	1.59	-	-	-
Miscellaneous land (ML)	3.28	406,826.35	124,118.33	43.57	29,366.83	8,959.50	2.87	65,842.97	20,087.98	14.95	4,138.89	1,262.73	53.99
Total	891.35	7,500,767.58		100.00	95,341,347.05		100.00	7,422,653.80		100.00	48,329.18		100.00

Table 6.17 Contribution of soil erosion, sediment retention, sediment deposition, and sediment export by LULC classes in 2026 under Scenario I.

LULC types	Area km ²	Soil erosion			Sediment retention			Sediment deposition			Sediment export		
		Total (tons)	Average (tons/km ²)	%	Total (tons)	Average (tons/km ²)	%	Total (tons)	Average (tons/km ²)	%	Total (tons)	Average (tons/km ²)	%
Urban and built-up area (UR)	35.76	-	-	-	105,466.50	2,949.49	0.81	45,131.74	1,262.16	0.78	-	-	-
Paddy field (PD)	213.81	452,996.62	2,118.71	0.64	643,383.36	3,009.17	0.83	2,492,233.81	11,656.44	7.21	4,223.68	19.75	0.70
Field crop (FC)	22.51	1,995,289.67	88,624.09	26.91	396,056.76	17,591.52	4.83	921,764.60	40,941.70	25.32	16,624.44	738.40	26.20
Para rubber (RB)	25.86	1,258,865.01	48,686.01	14.78	612,381.27	23,683.56	6.51	504,974.71	19,529.66	12.08	6,880.22	266.09	9.44
Perennial tree and orchard (PO)	92.89	3,678,918.91	39,605.53	12.03	1,893,849.73	20,388.31	5.60	2,363,628.64	25,445.73	15.74	24,809.63	267.09	9.48
Forest land (FO)	411.35	815,446.13	1,982.35	0.60	105,474,964.12	256,409.33	70.44	1,144,372.63	2,781.97	1.72	432.36	1.05	0.04
Water body (WB)	38.97	-	-	-	788,343.23	20,231.97	5.56	776,771.55	19,934.99	12.33	-	-	-
Rangeland (RL)	31.52	191,977.68	6,090.24	1.85	246,150.92	7,808.81	2.15	409,614.09	12,994.46	8.04	750.72	23.82	0.85
Wetland (WL)	15.30	-	-	-	24,855.83	1,624.18	0.45	38,404.09	2,509.49	1.55	-	-	-
Miscellaneous land (ML)	3.38	480,681.30	142,203.43	43.18	34,815.48	10,299.72	2.83	83,198.65	24,613.26	15.22	5,076.93	1,501.94	53.30
Total	891.35		329,310.36	100.00	110,220,267.19		100.00	8,780,094.51		100.00	58,797.97		100.00

Table 6.18 Contribution of soil erosion, sediment retention, sediment deposition, and sediment export by LULC classes in 2027 under Scenario I.

LULC types	Area km ²	Soil erosion			Sediment retention			Sediment deposition			Sediment export		
		Total (tons)	Average (tons/km ²)	%	Total (tons)	Average (tons/km ²)	%	Total (tons)	Average (tons/km ²)	%	Total (tons)	Average (tons/km ²)	%
Urban and built-up area (UR)	36.15	-	-	-	77,383.29	2,140.76	0.82	32,768.02	906.51	0.77	-	-	-
Paddy field (PD)	212.79	312,907.13	1,470.52	0.63	443,815.16	2,085.72	0.80	1,760,277.56	8,272.47	7.02	2,920.67	13.73	0.68
Field crop (FC)	22.58	1,397,106.66	61,883.00	26.70	275,086.44	12,184.59	4.68	705,160.57	31,234.16	26.49	12,004.80	531.74	26.41
Para rubber (RB)	26.69	918,434.73	34,405.56	14.85	441,987.43	16,557.33	6.36	360,382.38	13,500.31	11.45	5,083.55	190.44	9.46
Perennial tree and orchard (PO)	94.82	2,652,292.18	27,971.38	12.07	1,369,340.04	14,441.22	5.55	1,707,813.63	18,010.80	15.28	17,963.91	189.45	9.41
Forest land (FO)	407.68	578,490.83	1,418.99	0.61	75,130,976.04	184,289.73	70.84	699,233.21	1,715.16	1.45	308.26	0.76	0.04
Water body (WB)	39.76	-	-	-	581,514.77	14,627.36	5.62	619,468.23	15,582.03	13.22	-	-	-
Rangeland (RL)	32.13	136,997.35	4,263.21	1.84	176,196.91	5,483.06	2.11	305,012.53	9,491.67	8.05	543.27	16.91	0.84
Wetland (WL)	15.27	-	-	-	17,305.57	1,133.04	0.44	26,786.08	1,753.75	1.49	-	-	-
Miscellaneous land (ML)	3.48	349,204.05	100,338.95	43.30	25,019.25	7,188.93	2.76	60,648.60	17,426.54	14.78	3,724.55	1,070.20	53.16
Total	891.35		231,751.61	100.00	78,538,624.89		100.00	6,277,550.83		100.00	42,549.03		100.00

Table 6.19 Contribution of soil erosion, sediment retention, sediment deposition, and sediment export by LULC classes in 2028 under Scenario I.

LULC types	Area km ²	Soil erosion			Sediment retention			Sediment deposition			Sediment export		
		Total (tons)	Average (tons/km ²)	%	Total (tons)	Average (tons/km ²)	%	Total (tons)	Average (tons/km ²)	%	Total (tons)	Average (tons/km ²)	%
Urban and built-up area (UR)	36.50	-	-	-	85,826.32	2,351.40	0.85	35,53-	973.42	0.76	-	-	-
Paddy field (PD)	211.82	330,156.83	1,558.69	0.63	466,999.38	2,204.73	0.79	1,889,911.10	8,922.36	6.95	3,082.15	14.55	0.67
Field crop (FC)	22.69	1,517,436.05	66,872.17	27.11	294,947.98	12,998.12	4.67	802,965.55	35,386.04	27.57	13,490.08	594.50	27.23
Para rubber (RB)	27.57	1,025,420.43	37,187.36	15.08	488,110.42	17,701.56	6.36	397,030.56	14,398.50	11.22	5,672.85	205.73	9.42
Perennial tree and orchard (PO)	96.77	2,882,644.75	29,788.84	12.08	1,484,911.13	15,344.86	5.51	1,887,380.74	19,503.92	15.20	19,619.48	202.74	9.29
Forest land (FO)	404.03	613,529.15	1,518.53	0.62	79,739,664.64	197,361.57	70.93	704,188.67	1,742.92	1.36	326.89	0.81	0.04
Water body (WB)	40.58	-	-	-	638,142.97	15,727.36	5.65	683,881.25	16,854.60	13.13	-	-	-
Rangeland (RL)	32.72	148,835.69	4,548.10	1.84	191,358.55	5,847.51	2.10	322,920.66	9,867.77	7.69	584.57	17.86	0.82
Wetland (WL)	15.10	-	-	-	18,315.11	1,212.84	0.44	28,315.40	1,875.06	1.46	-	-	-
Miscellaneous land (ML)	3.57	375,162.91	105,153.92	42.64	26,763.59	7,501.53	2.70	67,161.92	18,824.73	14.67	4,091.02	1,146.67	52.53
Total	891.35	6,893,185.82		100.00	83,435,040.09		100.00	6,819,285.86		100.00	46,867.05		100.00

Table 6.20 Contribution of soil erosion, sediment retention, sediment deposition, and sediment export by LULC classes in 2029 under Scenario I.

LULC types	Area km ²	Soil erosion			Sediment retention			Sediment deposition			Sediment export		
		Total (tons)	Average (tons/km ²)	%	Total (tons)	Average (tons/km ²)	%	Total (tons)	Average (tons/km ²)	%	Total (tons)	Average (tons/km ²)	%
Urban and built-up area (UR)	36.90	-	-	-	92,714.70	2,512.42	0.87	37,124.09	1,006.00	0.75	-	-	-
Paddy field (PD)	210.84	336,124.96	1,594.22	0.63	475,036.51	2,253.07	0.78	1,930,485.13	9,156.17	6.81	3,136.28	14.88	0.66
Field crop (FC)	22.81	1,597,127.07	70,021.49	27.63	317,178.27	13,905.78	4.84	859,804.91	37,695.70	28.05	14,632.98	641.54	28.55
Para rubber (RB)	28.45	1,104,439.65	38,814.24	15.31	521,838.52	18,339.41	6.39	417,857.54	14,685.12	10.93	6,096.94	214.27	9.54
Perennial tree and orchard (PO)	98.75	3,015,108.92	30,533.70	12.05	1,544,737.86	15,643.40	5.45	1,986,115.79	20,113.19	14.97	20,528.58	207.89	9.25
Forest land (FO)	400.39	626,804.06	1,565.48	0.62	81,487,963.97	203,521.18	70.87	716,284.11	1,788.96	1.33	334.25	0.83	0.04
Water body (WB)	41.35	-	-	-	670,373.27	16,211.03	5.64	735,919.78	17,796.09	13.24	-	-	-
Rangeland (RL)	33.36	157,205.71	4,712.78	1.86	201,933.76	6,053.65	2.11	366,000.33	10,972.11	8.17	605.15	18.14	0.81
Wetland (WL)	14.82	-	-	-	18,610.69	1,255.69	0.44	29,631.28	1,999.27	1.49	-	-	-
Miscellaneous land (ML)	3.68	390,369.99	106,215.68	41.91	27,550.34	7,496.17	2.61	70,439.30	19,165.81	14.26	4,224.68	1,149.49	51.16
Total	891.35	7,227,180.35		100.00	85,357,937.88		100.00	7,149,662.25		100.00	49,558.85		100.00

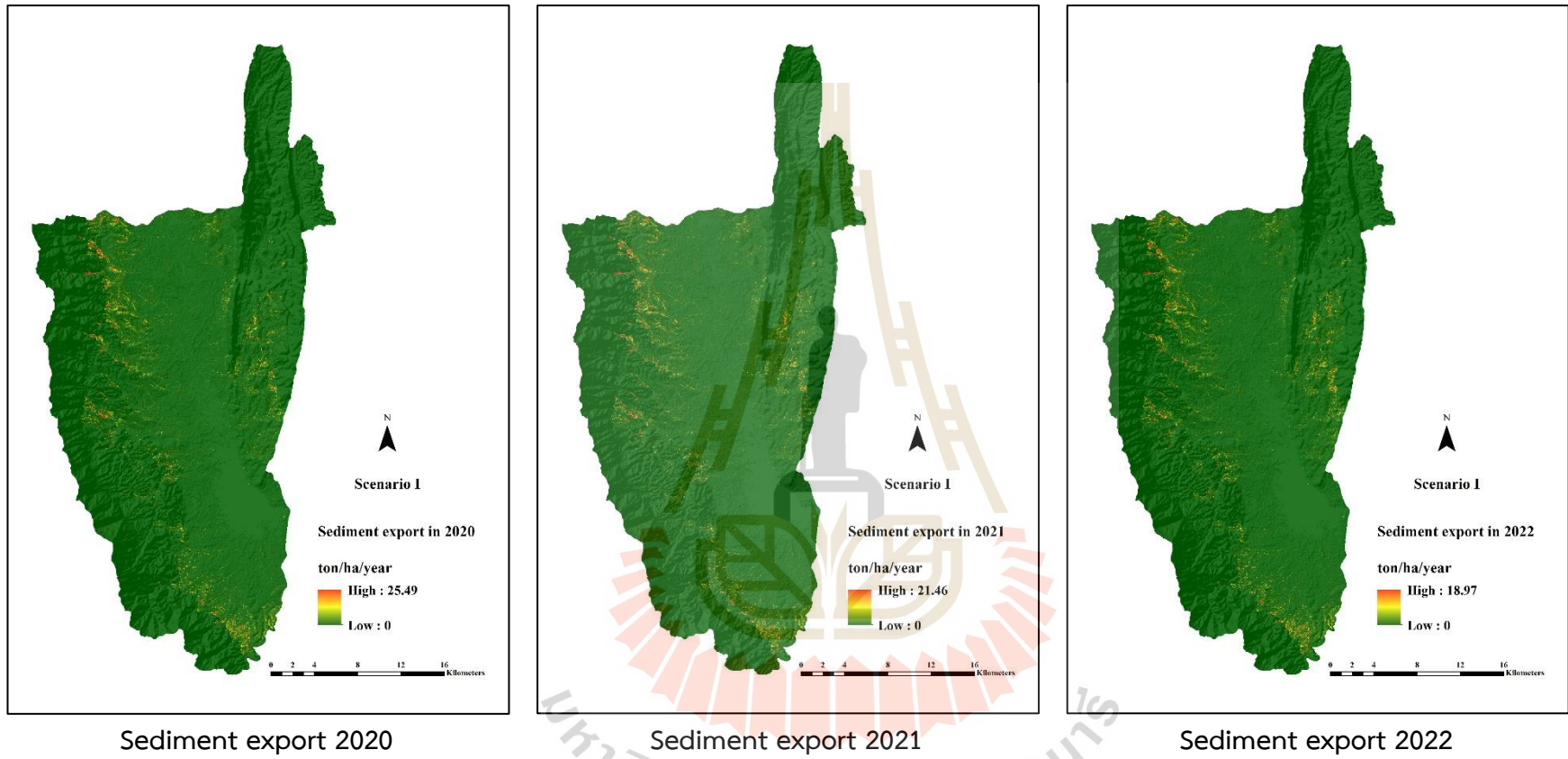


Figure 6.10 Spatial distribution of sediment export in 2020, 2021, and 2022 under Scenario I.

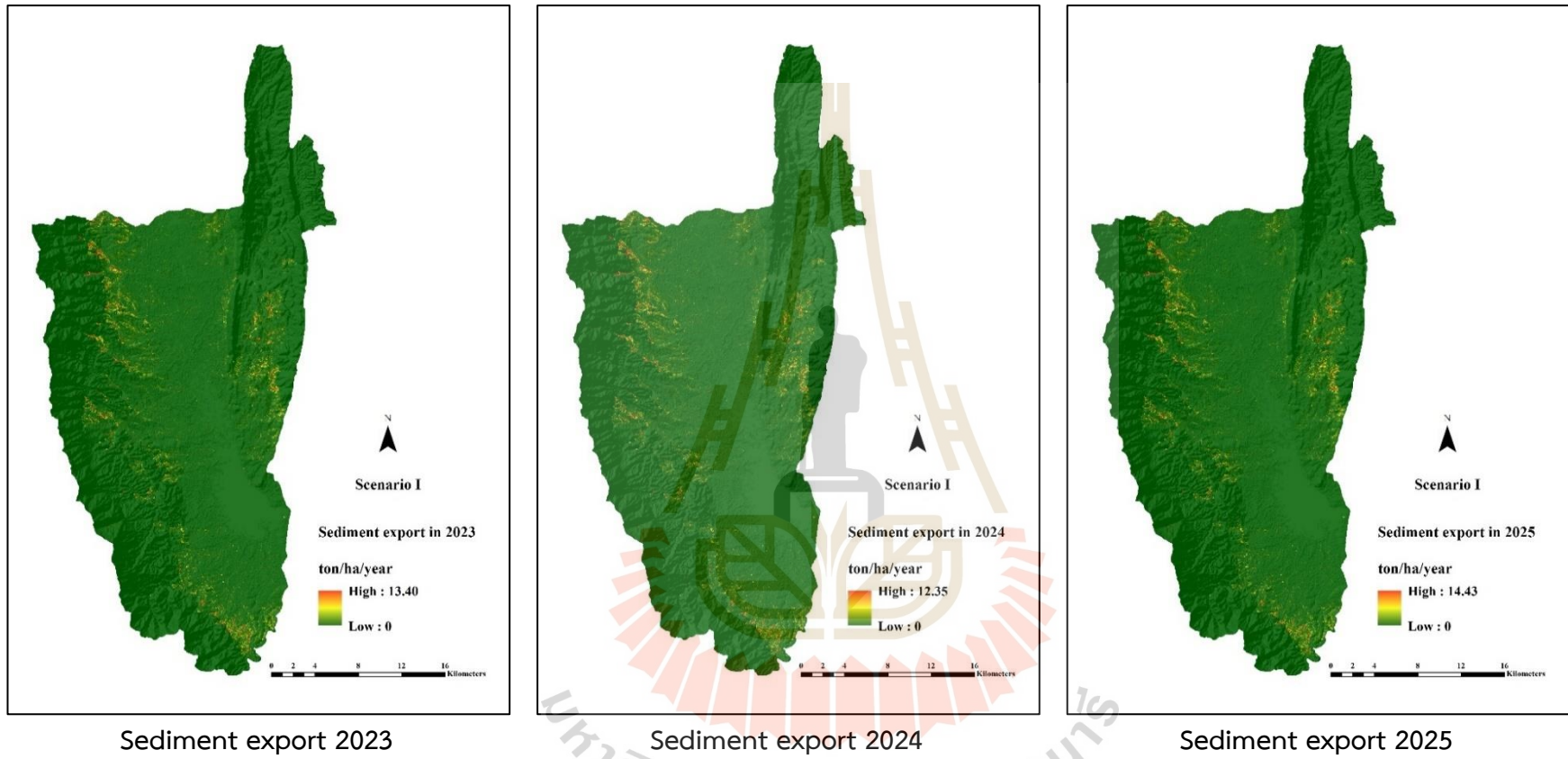


Figure 6.11 Spatial distribution of sediment export in 2023, 2024, and 2025 under Scenario I.

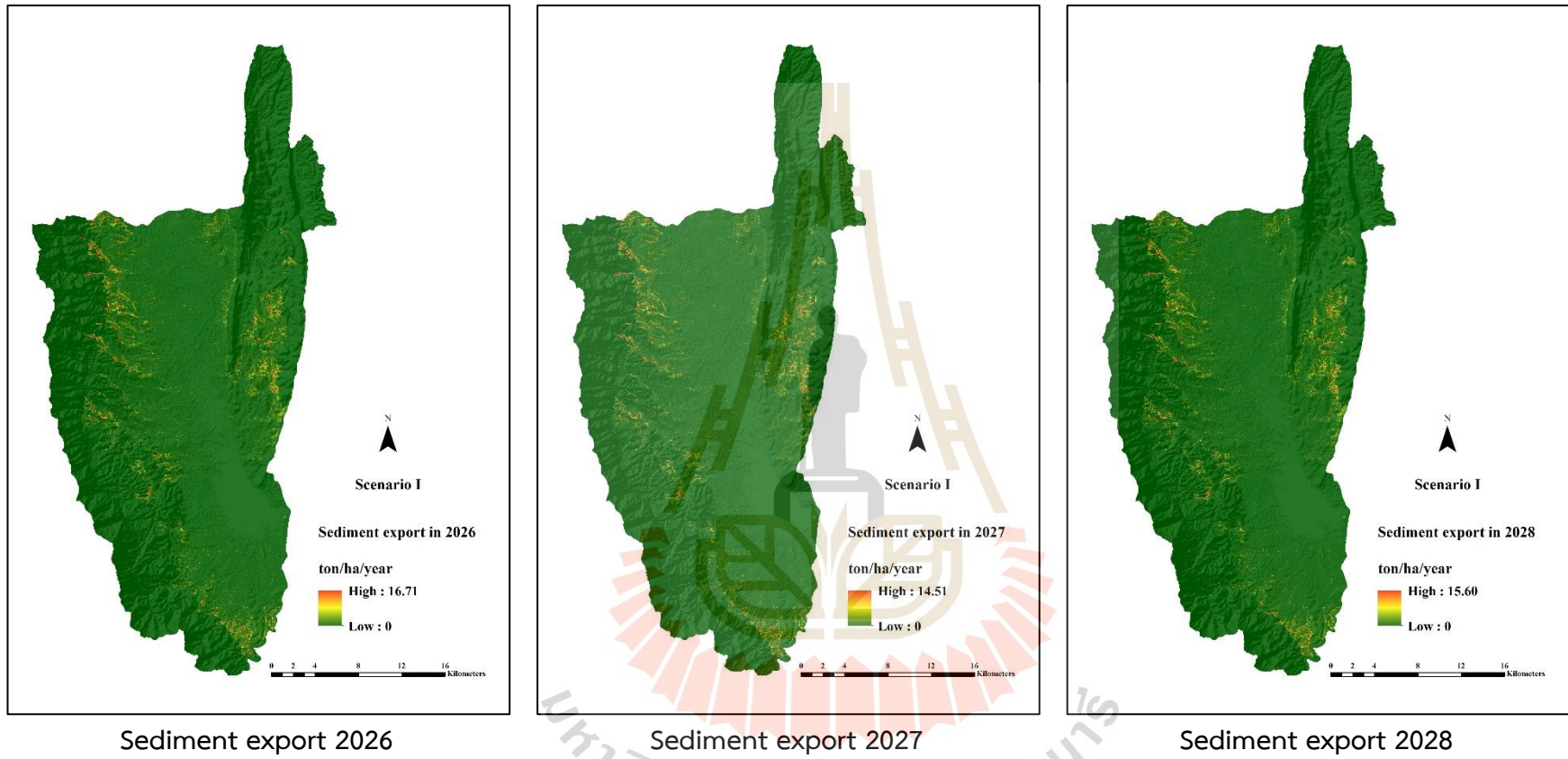
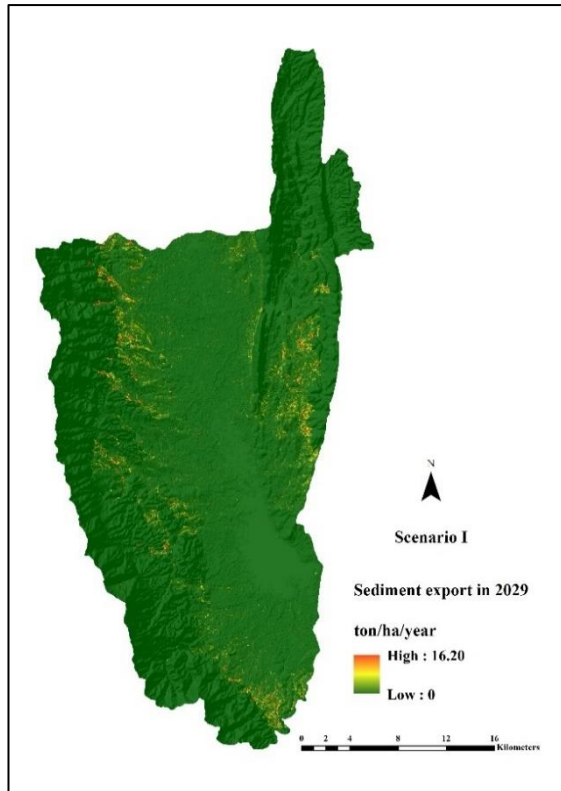
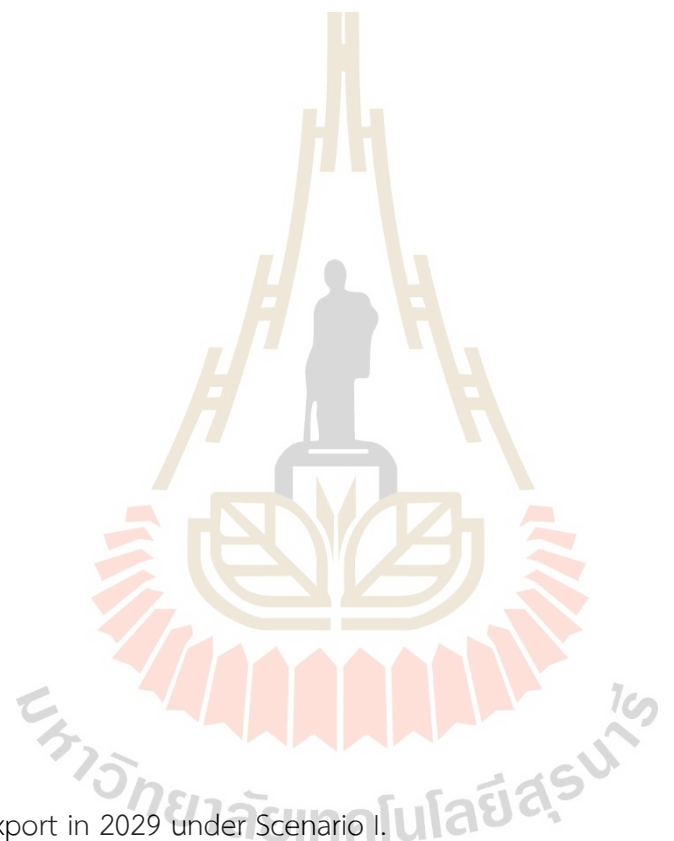


Figure 6.12 Spatial distribution of sediment export in 2026, 2027, and 2028 under Scenario I.



Sediment export 2029

Figure 6.13 Spatial distribution of sediment export in 2029 under Scenario I.



As results from 2020 to 2029 (Tables 6.11 to 6.20), miscellaneous land causes the highest average soil erosion with values between 91,336.30 tons/km² in 2022 and 142,203.43 tons/km² in 2026, while forest land generates the lowest average soil erosion with values between 1,219.47 tons/km² in 2022 and 1,982.35 tons/km² in 2026. Meanwhile, the highest average sediment retention is forest land with values between 256,409.33 in 2026 and 157,986.20 tons/km² in 2022, while the lowest average sediment retention is a wetland with values between 980.36 tons/km² in 2022 and 1,624.18 tons/km² in 2026.

In the meantime, the highest sediment deposition appears on field crops with values between 40,941.70 in 2026 and 21,381.41 tons/km² in 2022, while the lowest average sediment deposition is the urban and built-up area with values between 747.15 tons/km² in 2022 and 1,262.16 tons/km² in 2026. At the same time, miscellaneous land causes the highest average sediment export with values between 819.56 tons/km² in 2022 and 1,501.94 tons/km² in 2026 and, while the forest land generates the lowest average sediment export with values between 0.65 tons/km² in 2022 and 1.05 tons/km² in 2026.

This finding suggests that variation of predicted rainfall erosivity from 2020 to 2029 has a direct effect on sediment export, while the LULC data under this scenario has low influences due to LULC data of Scenario I (Trend of LULC evolution) is simulated based on the annual rate of LULC change from the transition area matrix between 2009 and 2019, which does not represent dramatically change under this scenario.

6.5 Sediment export estimation of predictive LULC of Scenario II

Estimation of total and average soil loss, sediment retention, sediment deposition, and sediment export of predictive LULC between 2020 and 2029 under Scenario II (Maximization of ecosystem service values) is presented in Table 6.21.

As a result, it was found that the highest total and average soil erosion under Scenario II (Maximization of ecosystem service values) are about 8.46 million tons and 9,490.50 tons/km² occurring in 2026, while the lowest total and average soil erosion are about 5.17 million tons and 5,796.56 tons/km² occurring in 2022. Likewise, the

highest total and average sediment export under this scenario are about 0.05 million tons and 53.98 tons/km² occurring in 2026. The lowest total and average sediment exports are about 0.03 million tons and 33.87 tons/km² in 2022. Meanwhile, the highest total and average sediment retention under this scenario are about 110.23 million tons and 123,667.41 tons/km² in 2026. The lowest total and average sediment retention are about 70.08 million tons and 78,617.03 tons/km² occurring in 2022. Simultaneously, the highest total and average sediment deposition are about 8.38 million tons and 9,406.58 tons/km² in 2026. The lowest total and average sediment deposition are about 5.12 million tons and 5,744.13 tons/km² occurring in 2022. These results indicate that the primary influence of LULC types and the rainfall erosivity factor in the RUSLE model affect soil erosion, sediment retention, sediment deposition, and sediment export.

The contribution of the predictive LULC of Scenario II (Maximization of ecosystem service values) on soil erosion, sediment retention, sediment deposition, and sediment export between 2020 and 2029 is summarized in Tables 6.22 to 6.31. The spatial distribution of sediment export of the predictive LULC between 2020 and 2029 of Scenario II is displayed in Figures 6.14 to 6.17.

Table 6.21 Estimation of soil erosion, sediment retention, sediment deposition, and sediment export between 2020 and 2029 under Scenario II: Maximization of ecosystem service values.

Year	Area km ²	Soil erosion		Sediment retention		Sediment deposition		Sediment export	
		Total (tons)	Average (tons/km ²)	Total (tons)	Average (tons/km ²)	Total (tons)	Average (tons/km ²)	Total (tons)	Average (tons/km ²)
2020	891.35	6,856,106.69	7,691.82	93,770,910.15	105,201.00	6,793,134.04	7,621.17	40,979.13	45.97
2021	891.35	5,804,322.37	6,511.83	78,968,909.15	88,594.73	5,751,535.65	6,452.61	34,149.06	38.31
2022	891.35	5,166,761.22	5,796.56	70,075,293.08	78,617.03	5,120,030.04	5,744.13	30,190.61	33.87
2023	891.35	6,615,079.56	7,421.42	88,437,718.65	99,217.72	6,555,364.05	7,354.42	38,483.96	43.17
2024	891.35	6,099,038.63	6,842.47	81,572,423.10	91,515.59	6,043,806.45	6,780.51	35,659.13	40.01
2025	891.35	7,219,372.95	8,099.37	95,348,148.66	106,970.49	7,154,800.25	8,026.93	41,526.64	46.59
2026	891.35	8,459,357.14	9,490.50	110,230,950.08	123,667.41	8,384,556.65	9,406.58	48,115.01	53.98
2027	891.35	5,983,939.89	6,713.34	78,547,323.01	88,121.75	5,932,154.50	6,655.25	33,851.75	37.98
2028	891.35	6,404,707.69	7,185.40	83,445,689.76	93,617.20	6,351,218.30	7,125.39	36,216.79	40.63
2029	891.35	6,617,327.19	7,423.94	85,369,894.18	95,775.95	6,563,157.11	7,363.16	37,599.82	42.18

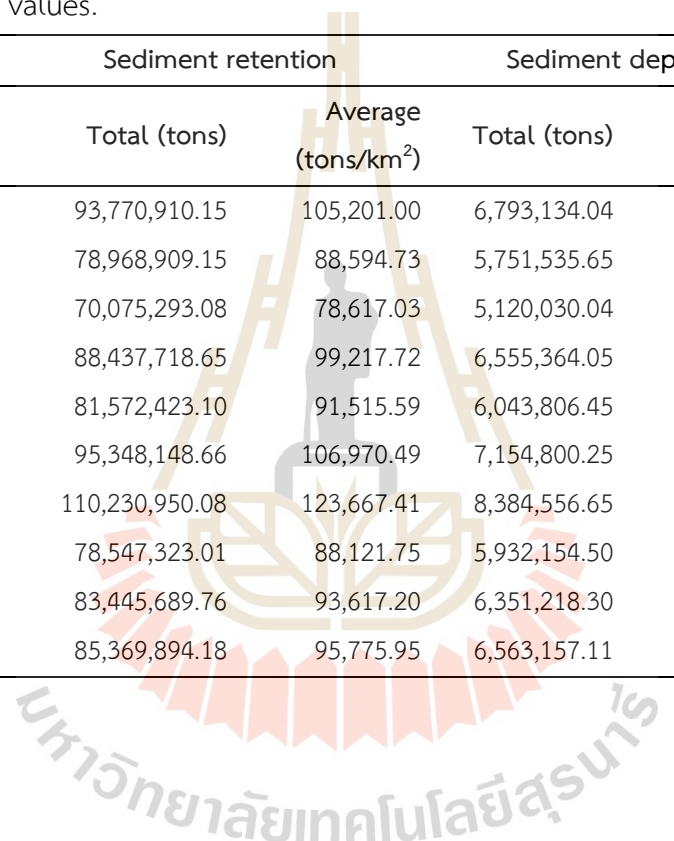


Table 6.22 Contribution of soil erosion, sediment retention, sediment deposition, and sediment export by LULC classes in 2020 under Scenario II.

LULC types	Area km ²	Soil erosion			Sediment retention			Sediment deposition			Sediment export		
		Total (tons)	Average (tons/km ²)	%	Total (tons)	Average (tons/km ²)	%	Total (tons)	Average (tons/km ²)	%	Total (tons)	Average (tons/km ²)	%
Urban and built-up area (UR)	33.36	-	-	-	66,315.50	1,987.59	0.66	34,202.18	1,025.10	0.93	-	-	-
Paddy field (PD)	219.74	406,955.65	1,852.00	0.64	582,844.87	2,652.45	0.89	2,080,832.78	9,469.61	8.61	3,742.08	17.03	0.82
Field crop (FC)	21.85	1,755,912.74	80,374.90	27.66	376,905.87	17,252.44	5.76	464,393.61	21,257.09	19.34	11,605.33	531.22	25.54
Para rubber (RB)	20.67	844,630.49	40,869.65	14.06	394,175.16	19,073.19	6.37	301,784.26	14,602.62	13.28	4,242.79	205.30	9.87
Perennial tree and orchard (PO)	81.16	2,695,020.42	33,205.98	11.43	1,407,814.15	17,346.01	5.79	1,853,793.91	22,841.03	20.78	17,775.67	219.02	10.53
Forest land (FO)	434.86	697,662.23	1,604.35	0.55	90,125,988.80	207,255.03	69.22	1,314,810.41	3,023.56	2.75	365.69	0.84	0.04
Water body (WB)	33.57	-	-	-	602,847.35	17,958.00	6.00	474,409.54	14,132.01	12.86	-	-	-
Rangeland (RL)	25.87	129,626.65	5,010.34	1.72	168,024.61	6,494.50	2.17	199,677.72	7,717.96	7.02	466.32	18.02	0.87
Wetland (WL)	17.72	-	-	-	25,728.62	1,451.85	0.48	33,527.96	1,891.96	1.72	-	-	-
Miscellaneous land (ML)	2.56	326,298.50	127,700.83	43.94	20,265.20	7,931.03	2.65	35,701.68	13,972.28	12.71	2,781.25	1,088.47	52.33
Total	33.36	6,856,106.69		100.00	93,770,910.15		100.00	6,793,134.04		100.00	40,979.13		100.00

Table 6.23 Contribution of soil erosion, sediment retention, sediment deposition, and sediment export by LULC classes in 2021 under Scenario II.

LULC types	Area km ²	Soil erosion			Sediment retention			Sediment deposition			Sediment export		
		Total (tons)	Average (tons/km ²)	%	Total (tons)	Average (tons/km ²)	%	Total (tons)	Average (tons/km ²)	%	Total (tons)	Average (tons/km ²)	%
Urban and built-up area (UR)	33.84	-	-	-	58,382.98	1,725.27	0.68	28,861.24	852.88	0.87	-	-	-
Paddy field (PD)	218.73	338,563.01	1,547.86	0.62	481,992.57	2,203.59	0.87	1,698,535.19	7,765.43	7.92	3,100.14	14.17	0.86
Field crop (FC)	21.82	1,458,034.45	66,808.67	26.82	318,836.50	14,609.42	5.77	426,057.64	19,522.41	19.90	9,722.21	445.48	27.11
Para rubber (RB)	21.50	726,199.66	33,782.22	13.56	337,780.09	15,713.25	6.20	290,995.45	13,536.87	13.80	3,670.05	170.73	10.39
Perennial tree and orchard (PO)	83.12	2,316,787.34	27,874.20	11.19	1,198,927.66	14,424.78	5.69	1,567,164.35	18,855.19	19.22	14,998.04	180.45	10.98
Forest land (FO)	432.77	586,924.60	1,356.20	0.54	75,883,064.51	175,342.57	69.19	1,046,033.83	2,417.06	2.46	308.37	0.71	0.04
Water body (WB)	33.57	-	-	-	507,113.60	15,106.22	5.96	407,387.14	12,135.51	12.37	-	-	-
Rangeland (RL)	24.51	103,339.87	4,215.94	1.69	134,230.60	5,476.18	2.16	164,322.76	6,703.84	6.83	376.15	15.35	0.93
Wetland (WL)	19.07	-	-	-	31,244.01	1,638.06	0.65	94,745.11	4,967.28	5.06	-	-	-
Miscellaneous land (ML)	2.42	274,473.44	113,528.11	45.57	17,336.64	7,170.81	2.83	27,432.94	11,346.85	11.57	1,974.11	816.53	49.68
Total	891.35	5,804,322.37		100.00	78,968,909.15		100.00	5,751,535.65		100.00	34,149.06		100.00

Table 6.24 Contribution of soil erosion, sediment retention, sediment deposition, and sediment export by LULC classes in 2022 under Scenario II.

LULC types	Area	Soil erosion			Sediment retention			Sediment deposition			Sediment export		
	km ²	Total (tons)	Average (tons/km ²)	%	Total (tons)	Average (tons/km ²)	%	Total (tons)	Average (tons/km ²)	%	Total (tons)	Average (tons/km ²)	%
Urban and built-up area (UR)	34.22	-	-	-	53,897.89	1,574.93	0.70	24,776.55	723.99	0.81	-	-	-
Paddy field (PD)	217.75	295,175.55	1,355.57	0.60	417,389.43	1,916.83	0.85	1,498,540.91	6,881.92	7.72	2,697.17	12.39	0.84
Field crop (FC)	21.82	1,284,630.17	58,869.85	26.16	282,140.34	12,929.45	5.73	417,332.68	19,124.81	21.45	8,711.65	399.22	27.23
Para rubber (RB)	22.37	656,331.95	29,341.05	13.04	304,162.99	13,597.48	6.03	273,987.97	12,248.52	13.74	3,239.04	144.80	9.88
Perennial tree and orchard (PO)	85.05	2,082,678.29	24,488.86	10.88	1,072,359.40	12,609.17	5.59	1,398,309.11	16,441.80	18.44	13,267.93	156.01	10.64
Forest land (FO)	430.71	520,093.34	1,207.54	0.54	67,334,943.88	156,336.50	69.31	882,711.48	2,049.46	2.30	274.26	0.64	0.04
Water body (WB)	33.57	-	-	-	448,337.14	13,355.35	5.92	369,675.16	11,012.12	12.35	-	-	-
Rangeland (RL)	23.16	85,455.78	3,689.14	1.64	110,285.04	4,761.03	2.11	132,387.11	5,715.18	6.41	309.93	13.38	0.91
Wetland (WL)	20.42	-	-	-	36,448.10	1,785.23	0.79	99,258.01	4,861.67	5.45	-	-	-
Miscellaneous land (ML)	2.29	242,396.15	106,074.03	47.14	15,328.88	6,708.01	2.97	23,051.08	10,087.29	11.32	1,690.63	739.83	50.46
Total	891.35	5,166,761.22		100.00	70,075,293.08		100.00	5,120,030.04		100.00	30,190.61		100.00

Table 6.25 Contribution of soil erosion, sediment retention, sediment deposition, and sediment export by LULC classes in 2023 under Scenario II.

LULC types	Area	Soil erosion			Sediment retention			Sediment deposition			Sediment export		
	km ²	Total (tons)	Average (tons/km ²)	%	Total (tons)	Average (tons/km ²)	%	Total (tons)	Average (tons/km ²)	%	Total (tons)	Average (tons/km ²)	%
Urban and built-up area (UR)	34.60	-	-	-	74,189.32	2,144.05	0.75	42,245.37	1,220.88	1.06	-	-	-
Paddy field (PD)	216.77	373,909.14	1,724.91	0.61	527,321.33	2,432.63	0.85	1,912,467.01	8,822.56	7.64	3,411.36	15.74	0.86
Field crop (FC)	21.81	1,626,674.03	74,578.63	26.23	355,929.98	16,318.43	5.71	570,587.49	26,159.90	22.67	10,901.17	499.79	27.47
Para rubber (RB)	23.23	863,640.76	37,171.21	13.07	397,947.68	17,127.72	5.99	357,865.20	15,402.57	13.35	4,297.19	184.95	10.16
Perennial tree and orchard (PO)	87.01	2,703,784.91	31,074.02	10.93	1,384,268.40	15,909.10	5.57	1,797,479.51	20,658.05	17.90	17,211.74	197.81	10.87
Forest land (FO)	428.65	657,107.26	1,532.96	0.54	84,924,405.34	198,119.44	69.32	1,071,059.55	2,498.67	2.16	346.35	0.81	0.04
Water body (WB)	33.57	-	-	-	569,294.00	16,958.49	5.93	487,838.31	14,532.04	12.59	-	-	-
Rangeland (RL)	21.78	102,858.33	4,721.73	1.66	132,208.02	6,069.03	2.12	130,767.82	6,002.92	5.20	373.94	17.17	0.94
Wetland (WL)	21.76	-	-	-	54,496.99	2,503.99	0.88	157,347.65	7,229.71	6.26	-	-	-
Miscellaneous land (ML)	2.15	287,105.12	133,527.90	46.96	17,657.60	8,212.26	2.87	27,706.15	12,885.68	11.16	1,942.22	903.29	49.64
Total	891.35	6,615,079.56		100.00	88,437,718.65		100.00	6,555,364.05		100.00	38,483.96		100.00

Table 6.26 Contribution of soil erosion, sediment retention, sediment deposition, and sediment export by LULC classes in 2024 under Scenario II.

LULC types	Area	Soil erosion			Sediment retention			Sediment deposition			Sediment export		
	km ²	Total (tons)	Average (tons/km ²)	%	Total (tons)	Average (tons/km ²)	%	Total (tons)	Average (tons/km ²)	%	Total (tons)	Average (tons/km ²)	%
Urban and built-up area (UR)	34.99	-	-	-	73,121.05	2,089.92	0.79	42,888.48	1,225.82	1.15	-	-	-
Paddy field (PD)	215.78	338,118.12	1,566.94	0.61	475,913.08	2,205.52	0.84	1,746,137.75	8,092.11	7.60	3,079.97	14.27	0.85
Field crop (FC)	21.81	1,489,780.19	68,318.08	26.42	322,740.78	14,800.19	5.61	526,953.19	24,164.93	22.69	10,069.14	461.75	27.40
Para rubber (RB)	24.09	816,032.15	33,871.94	13.10	379,355.79	15,746.33	5.97	335,776.20	13,937.43	13.08	4,111.28	170.65	10.13
Perennial tree and orchard (PO)	88.96	2,518,816.38	28,315.23	10.95	1,288,032.56	14,479.40	5.49	1,678,504.31	18,868.88	17.71	16,070.22	180.65	10.72
Forest land (FO)	426.61	604,781.65	1,417.65	0.55	78,326,534.28	183,602.24	69.60	968,609.89	2,270.48	2.13	319.28	0.75	0.04
Water body (WB)	33.57	-	-	-	522,308.84	15,557.71	5.90	460,302.44	13,710.76	12.87	-	-	-
Rangeland (RL)	20.43	87,830.78	4,299.33	1.66	111,948.12	5,479.88	2.08	94,477.91	4,624.71	4.34	310.56	15.20	0.90
Wetland (WL)	23.10	-	-	-	57,693.83	2,497.93	0.95	164,966.44	7,142.45	6.71	-	-	-
Miscellaneous land (ML)	2.02	243,679.35	120,774.35	46.71	14,774.76	7,322.79	2.78	25,189.84	12,484.80	11.72	1,698.69	841.92	49.96
Total	891.35	6,099,038.63		100.00	81,572,423.10		100.00	6,043,806.45		100.00	35,659.13		100.00

Table 6.27 Contribution of soil erosion, sediment retention, sediment deposition, and sediment export by LULC classes in 2025 under Scenario II.

LULC types	Area	Soil erosion			Sediment retention			Sediment deposition			Sediment export		
	km ²	Total (tons)	Average (tons/km ²)	%	Total (tons)	Average (tons/km ²)	%	Total (tons)	Average (tons/km ²)	%	Total (tons)	Average (tons/km ²)	%
Urban and built-up area (UR)	35.39	-	-	-	95,975.68	2,711.56	0.88	50,655.74	1,431.16	1.13	-	-	-
Paddy field (PD)	214.77	395,637.96	1,842.15	0.61	556,529.98	2,591.28	0.84	2,064,980.62	9,614.84	7.62	3,608.14	16.80	0.92
Field crop (FC)	21.86	1,742,509.80	79,706.66	26.30	365,602.79	16,723.57	5.42	625,962.38	28,633.05	22.70	11,197.81	512.22	27.91
Para rubber (RB)	24.98	984,723.72	39,421.67	13.01	454,592.99	18,198.82	5.89	423,141.44	16,939.66	13.43	4,937.60	197.67	10.77
Perennial tree and orchard (PO)	90.81	3,023,003.75	33,287.91	10.99	1,549,132.05	17,058.32	5.52	2,001,759.07	22,042.44	17.47	19,408.09	213.71	11.64
Forest land (FO)	424.52	707,477.21	1,666.53	0.55	91,499,494.05	215,535.21	69.79	1,099,308.24	2,589.52	2.05	373.06	0.88	0.05
Water body (WB)	33.70	-	-	-	614,629.76	18,239.70	5.91	558,824.74	16,583.63	13.15	-	-	-
Rangeland (RL)	19.14	97,245.51	5,079.73	1.68	121,685.27	6,356.37	2.06	105,581.23	5,515.15	4.37	343.83	17.96	0.98
Wetland (WL)	24.27	-	-	-	74,722.48	3,078.27	1.00	196,788.50	8,106.90	6.43	-	-	-
Miscellaneous land (ML)	1.89	268,775.00	142,011.18	46.87	15,783.62	8,339.51	2.70	27,799.74	14,688.40	11.64	1,658.10	876.08	47.73
Total	891.35	7,219,372.95		100.00	95,348,148.66		100.00	7,154,800.25		100.00	41,526.64		100.00

Table 6.28 Contribution of soil erosion, sediment retention, sediment deposition, and sediment export by LULC classes in 2026 under Scenario II.

LULC types	Area	Soil erosion			Sediment retention			Sediment deposition			Sediment export		
	km ²	Total (tons)	Average (tons/km ²)	%	Total (tons)	Average (tons/km ²)	%	Total (tons)	Average (tons/km ²)	%	Total (tons)	Average (tons/km ²)	%
Urban and built-up area (UR)	35.42	-	-	-	113,219.53	3,196.71	0.89	58,459.07	1,650.57	1.15	-	-	-
Paddy field (PD)	213.82	458,869.48	2,146.00	0.61	643,574.53	3,009.82	0.84	2,405,099.36	11,247.98	7.83	4,151.43	19.42	0.96
Field crop (FC)	21.85	1,993,708.13	91,259.71	25.81	409,445.01	18,741.88	5.23	752,115.71	34,427.24	23.95	12,801.55	585.98	28.83
Para rubber (RB)	25.87	1,185,288.66	45,818.33	12.96	550,101.28	21,264.63	5.94	510,897.62	19,749.18	13.74	5,937.73	229.53	11.29
Perennial tree and orchard (PO)	92.90	3,600,121.86	38,754.11	10.96	1,847,753.61	19,890.45	5.56	2,357,811.52	25,381.05	17.66	22,779.03	245.21	12.06
Forest land (FO)	422.49	818,757.19	1,937.95	0.55	105,713,953.57	250,218.17	69.89	1,254,073.21	2,968.31	2.07	431.55	1.02	0.05
Water body (WB)	33.70	-	-	-	714,420.37	21,201.08	5.92	668,790.23	19,846.96	13.81	-	-	-
Rangeland (RL)	17.72	105,885.50	5,976.75	1.69	121,733.10	6,871.27	1.92	105,660.46	5,964.04	4.15	366.24	20.67	1.02
Wetland (WL)	25.82	-	-	-	99,432.71	3,850.35	1.08	248,868.52	9,636.99	6.70	-	-	-
Miscellaneous land (ML)	1.77	296,726.30	167,630.22	47.42	17,316.36	9,782.57	2.73	22,780.95	12,869.69	8.95	1,647.47	930.71	45.79
Total	891.35	8,459,357.14		100.00	110,230,950.08		100.00	8,384,556.65		100.00	48,115.01		100.00

Table 6.29 Contribution of soil erosion, sediment retention, sediment deposition, and sediment export by LULC classes in 2027 under Scenario II.

LULC types	Area	Soil erosion			Sediment retention			Sediment deposition			Sediment export		
	km ²	Total (tons)	Average (tons/km ²)	%	Total (tons)	Average (tons/km ²)	%	Total (tons)	Average (tons/km ²)	%	Total (tons)	Average (tons/km ²)	%
Urban and built-up area (UR)	36.17	-	-	-	90,853.95	2,512.20	0.99	54,873.77	1,517.32	1.55	-	-	-
Paddy field (PD)	212.74	316,842.73	1,489.31	0.60	442,922.44	2,081.94	0.82	1,679,676.69	7,895.26	8.07	2,871.40	13.50	1.05
Field crop (FC)	21.84	1,399,022.42	64,067.98	25.74	286,055.95	13,099.88	5.14	523,255.06	23,962.37	24.49	9,075.53	415.61	32.29
Para rubber (RB)	26.74	858,305.51	32,095.94	12.90	396,666.86	14,833.17	5.82	364,068.32	13,614.17	13.91	4,258.82	159.26	12.37
Perennial tree and orchard (PO)	94.81	2,567,181.22	27,076.64	10.88	1,319,572.99	13,917.84	5.47	1,711,621.62	18,052.86	18.45	16,287.69	171.79	13.35
Forest land (FO)	420.45	581,369.52	1,382.73	0.56	75,343,049.48	179,195.37	70.37	874,260.31	2,079.33	2.12	307.18	0.73	0.06
Water body (WB)	33.70	-	-	-	504,035.23	14,956.60	5.87	474,413.91	14,077.62	14.39	-	-	-
Rangeland (RL)	16.35	69,184.30	4,232.45	1.70	76,303.42	4,667.98	1.83	46,444.58	2,841.32	2.90	220.73	13.50	1.05
Wetland (WL)	26.93	-	-	-	77,308.83	2,870.53	1.13	192,741.37	7,156.62	7.31	-	-	-
Miscellaneous land (ML)	1.62	192,034.19	118,531.31	47.63	10,553.88	6,514.29	2.56	10,798.88	6,665.51	6.81	830.38	512.54	39.83
Total	891.35	5,983,939.89		100.00	78,547,323.01		100.00	5,932,154.50		100.00	33,851.75		100.00

Table 6.30 Contribution of soil erosion, sediment retention, sediment deposition, and sediment export by LULC classes in 2028 under Scenario II.

LULC types	Area	Soil erosion			Sediment retention			Sediment deposition			Sediment export		
	km ²	Total (tons)	Average (tons/km ²)	%	Total (tons)	Average (tons/km ²)	%	Total (tons)	Average (tons/km ²)	%	Total (tons)	Average (tons/km ²)	%
Urban and built-up area (UR)	36.47	-	-	-	102,761.89	2,817.71	1.04	63,060.66	1,729.11	1.68	-	-	-
Paddy field (PD)	211.81	334,746.37	1,580.37	0.61	467,825.43	2,208.65	0.82	1,759,871.46	8,308.54	8.08	3,029.52	14.30	1.13
Field crop (FC)	21.86	1,473,854.17	67,417.70	25.85	294,908.97	13,489.86	4.99	566,399.73	25,908.51	25.21	9,782.23	447.46	35.37
Para rubber (RB)	27.56	944,127.12	34,254.75	13.13	438,613.06	15,913.73	5.89	399,355.16	14,489.37	14.10	4,694.94	170.34	13.46
Perennial tree and orchard (PO)	96.70	2,786,053.38	28,810.03	11.05	1,434,948.88	14,838.52	5.49	1,831,294.93	18,937.06	18.42	17,534.96	181.33	14.33
Forest land (FO)	418.34	617,255.32	1,475.48	0.57	80,003,434.88	191,239.38	70.75	914,575.32	2,186.19	2.13	326.16	0.78	0.06
Water body (WB)	33.70	-	-	-	536,071.88	15,907.24	5.89	519,036.08	15,401.73	14.99	-	-	-
Rangeland (RL)	14.97	67,275.98	4,492.99	1.72	67,487.33	4,507.10	1.67	40,947.69	2,734.67	2.66	202.60	13.53	1.07
Wetland (WL)	28.44	-	-	-	90,484.15	3,181.08	1.18	250,348.97	8,801.32	8.56	-	-	-
Miscellaneous land (ML)	1.48	181,395.36	122,763.21	47.07	9,153.28	6,194.68	2.29	6,328.30	4,282.81	4.17	646.37	437.45	34.58
Total	891.35	6,404,707.69		100.00	83,445,689.76		100.00	6,351,218.30		100.00	36,216.79		100.00

Table 6.31 Contribution of soil erosion, sediment retention, sediment deposition, and sediment export by LULC classes in 2029 under Scenario II.

LULC types	Area	Soil erosion			Sediment retention			Sediment deposition			Sediment export		
	km ²	Total (tons)	Average (tons/km ²)	%	Total (tons)	Average (tons/km ²)	%	Total (tons)	Average (tons/km ²)	%	Total (tons)	Average (tons/km ²)	%
Urban and built-up area (UR)	36.94	-	-	-	112,114.84	3,034.84	1.09	73,187.48	1,981.11	1.87	-	-	-
Paddy field (PD)	210.78	340,351.62	1,614.73	0.60	474,203.25	2,249.76	0.81	1,804,512.88	8,561.13	8.08	3,072.99	14.58	1.13
Field crop (FC)	21.80	1,507,974.83	69,176.24	25.71	303,308.62	13,913.86	5.01	599,690.11	27,509.95	25.95	10,248.97	470.16	36.37
Para rubber (RB)	28.46	997,929.01	35,067.97	13.03	460,395.26	16,178.63	5.83	416,594.73	14,639.45	13.81	4,975.09	174.83	13.53
Perennial tree and orchard (PO)	98.68	2,903,080.23	29,418.56	10.93	1,485,265.08	15,051.04	5.42	1,889,381.53	19,146.18	18.06	18,197.16	184.40	14.27
Forest land (FO)	416.34	631,382.15	1,516.52	0.56	81,814,892.20	196,511.37	70.82	927,080.62	2,226.76	2.10	333.37	0.80	0.06
Water body (WB)	33.70	-	-	-	549,403.24	16,302.83	5.88	540,556.36	16,040.31	15.13	-	-	-
Rangeland (RL)	13.57	63,002.17	4,641.57	1.72	60,135.28	4,430.36	1.60	35,062.81	2,583.19	2.44	181.31	13.36	1.03
Wetland (WL)	29.72	-	-	-	101,500.12	3,415.26	1.23	271,388.79	9,131.65	8.61	-	-	-
Miscellaneous land (ML)	1.36	173,607.17	127,643.38	47.44	8,676.28	6,379.17	2.30	5,701.82	4,192.22	3.95	590.93	434.48	33.61
Total	891.35	6,617,327.19		100.00	85,369,894.18		100.00	6,563,157.11		100.00	37,599.82		100.00

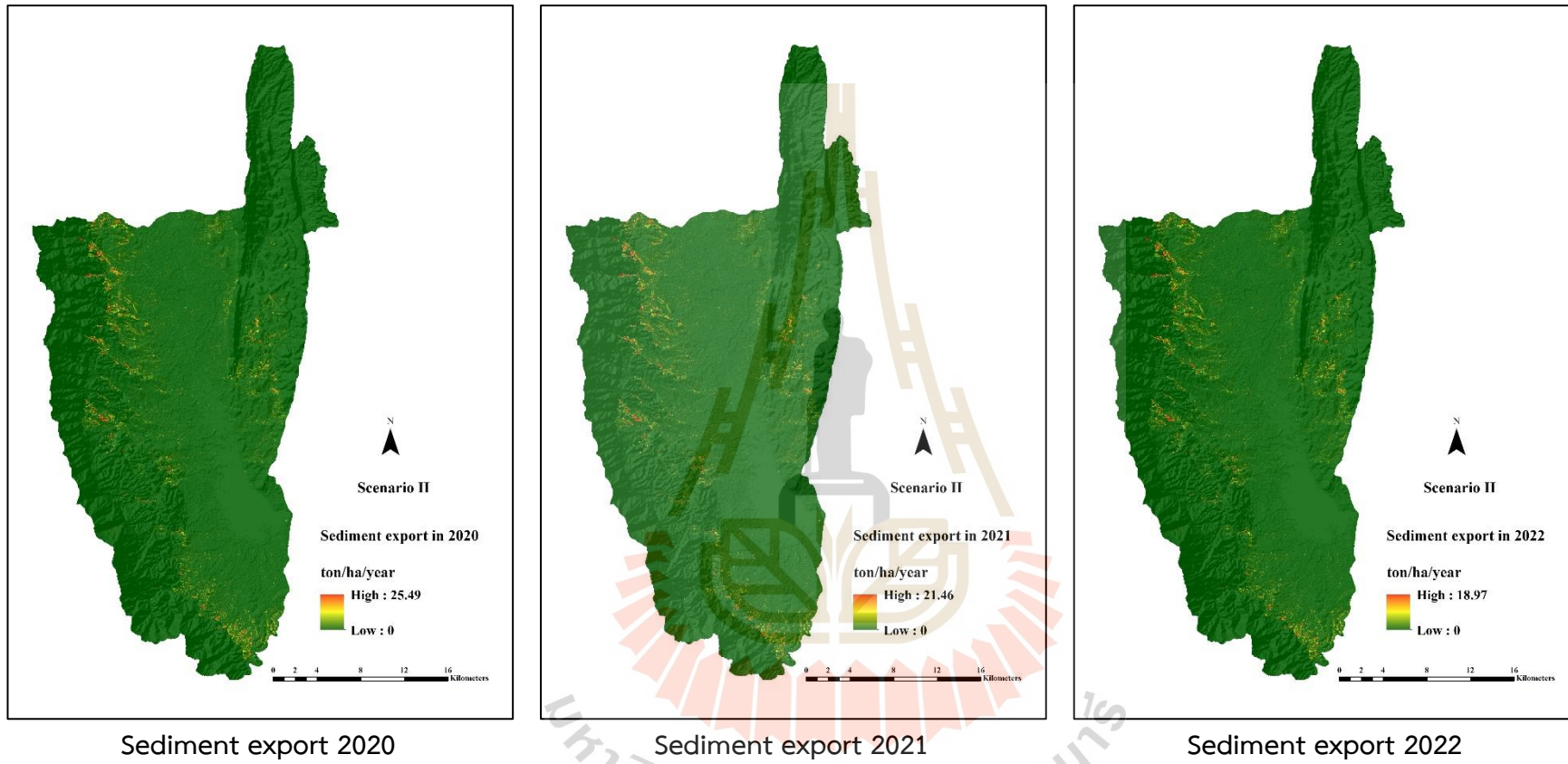


Figure 6.14 Spatial distribution of sediment export in 2020, 2021, and 2022 under Scenario II.

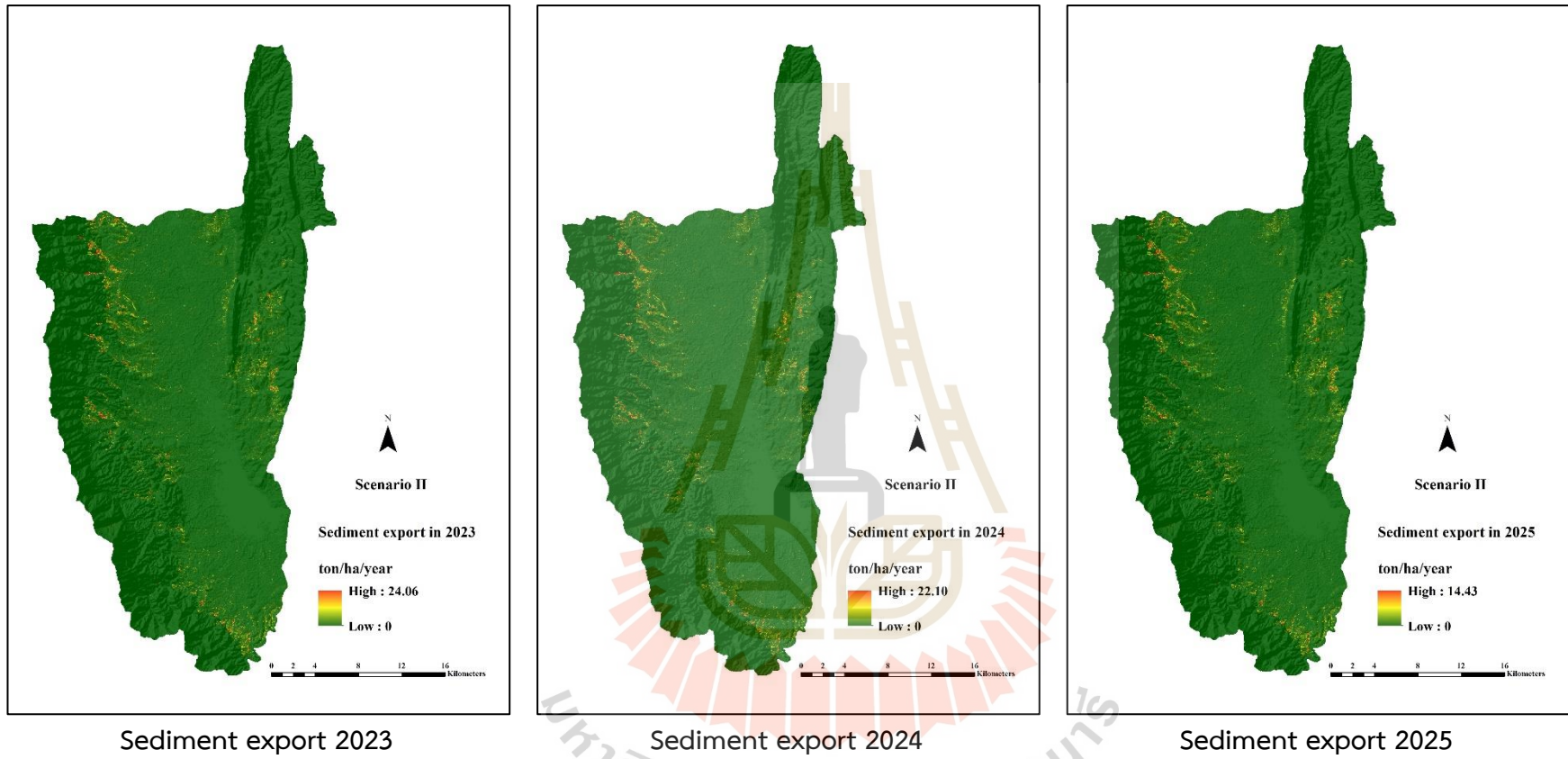


Figure 6.15 Spatial distribution of sediment export in 2023, 2024, and 2025 under Scenario II.

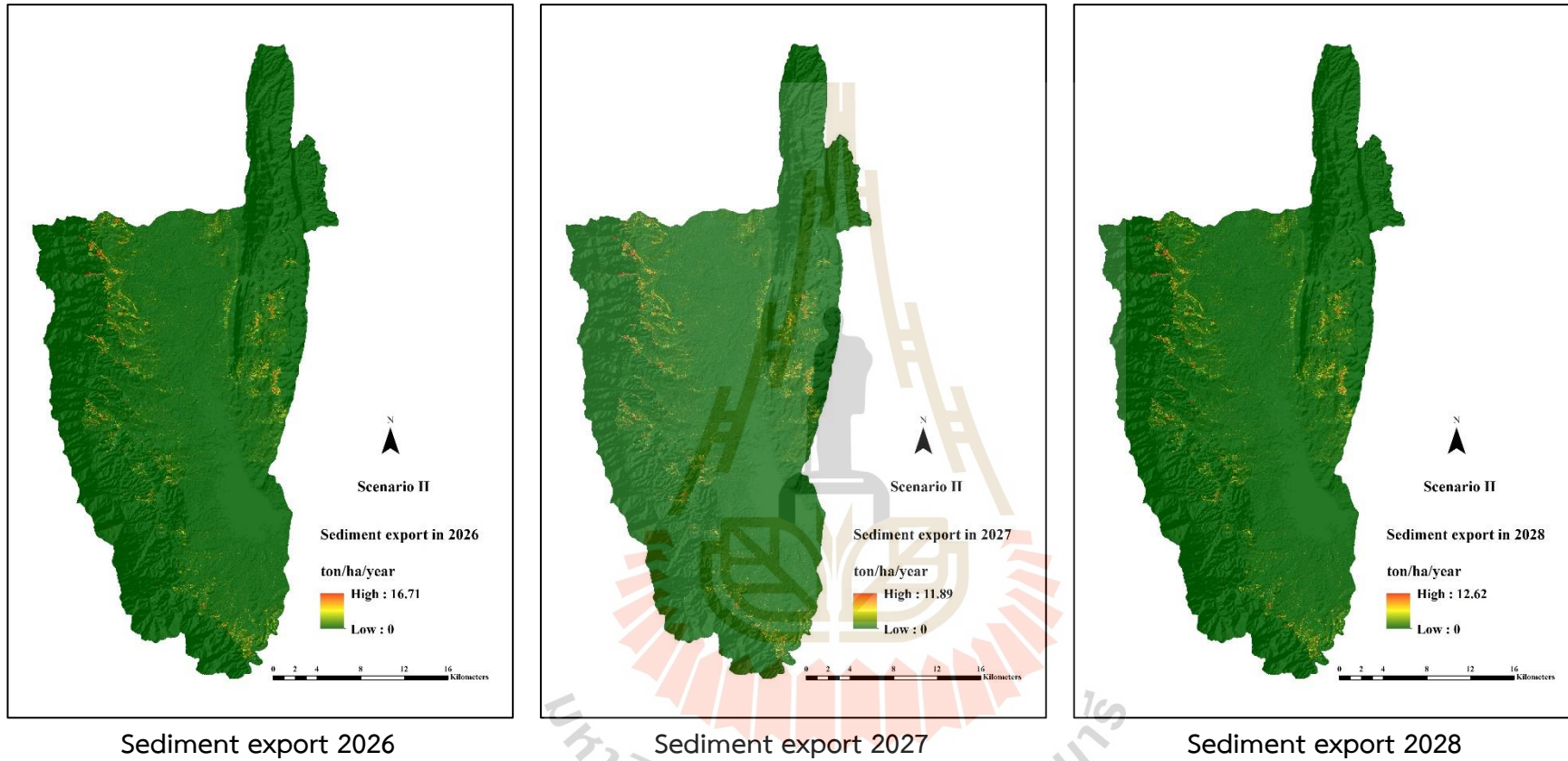
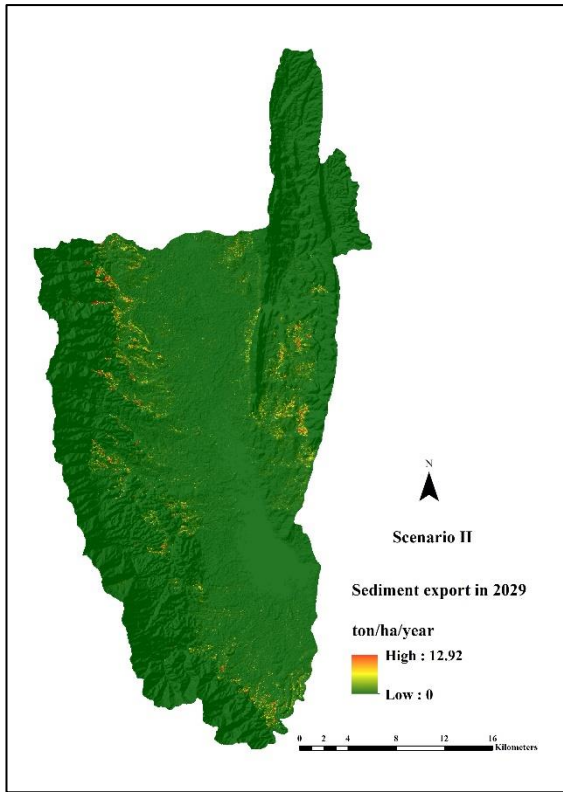


Figure 6.16 Spatial distribution of sediment export in 2026, 2027, and 2028 under Scenario II.



Sediment export 2029

Figure 6.17 Spatial distribution of sediment export in 2029 under Scenario II.



As results (Tables 6.22 to 6.31) disclosed that from 2020 to 2029, miscellaneous land causes the highest average soil erosion with values between 106,074.03 tons/km² in 2022 and 167,630.22 tons/km² in 2026, while forest land generates the lowest average soil erosion with values between 1,207.54 tons/km² in 2022 and 1,937.95 tons/km² in 2026. Meanwhile, the highest average sediment retention is forest land, with values between 156,336.50 tons/km² in 2022 and 250,218.17 tons/km² in 2026. On the other hand, the lowest average sediment retention is a wetland with a value of 1,451.85 tons/km² in 2020. However, the wetland area increases between 2020 and 2029, affecting its higher retention with an average value of 3,415.26 tons/km² in 2029, whereas the paddy field was the lowest retention, with an average value of 2,249.76 tons/km² in 2029.

In the meantime, the highest sediment deposition appears on field crops with values between 34,427.24 in 2026 and 19,124.81 tons/km² in 2022, while the lowest average sediment deposition is the urban and built-up area with values between 723.99 tons/km² in 2022 and 1,981.11 tons/km² in 2029. Although the area of miscellaneous land is decreased every year in this scenario, still it causes the highest average sediment export until 2027 with values between 1,088.47 tons/km² in 2020 and 512.54 tons/km² in 2027, then the field crop turns into the highest average sediment export in 2028 and 2029 with values between 447.46 tons/km² and 470.16 tons/km², respectively. In contrast, the forest land generates the lowest average sediment export with values between 0.64 tons/km² in 2022 and 1.02 tons/km² in 2026.

This finding suggests that variation of predicted rainfall erosivity from 2020 to 2029 directly affects sediment export. Furthermore, the LULC data under this scenario has influences sediment export due to the LULC data of Scenario II (Maximization of ecosystem service values) simulated based on the annual rate of LULC change from transition area matrix between 2009 and 2019 for some LULC types and the linear programming to maximize ecosystem service values by reclaiming the area for wetland with its function to retain the sediment. Therefore, it shows significant LULC change under this scenario.

6.6 Sediment export estimation of predictive LULC of Scenario III

Estimation of total and average soil loss, sediment retention, sediment deposition, and sediment export of predictive LULC between 2020 and 2029 under Scenario III: Economic crop zonation is presented in Table 6.32.

As a result, it was found that the highest total and average soil erosion under Scenario III (Economic crop zonation) are about 8.52 million tons and 9,556.45 tons/km² occurring in 2026, while the lowest total and average soil erosion are about 5.05 million tons and 5,670.51 tons/km² occurring in 2022. Similarly, the highest total and average sediment exports are about 0.08 million tons and 85.34 tons/km² in 2026. On the other hand, the lowest total and average sediment exports in 2022 are about 0.03 million tons 38.73 tons/km². Meanwhile, the highest total and average sediment retention are about 110.20 million tons and 123,636.05 tons/km² in 2026. The lowest total and average sediment retention are about 70.07 million tons 78,612.18 tons/km² occurring in 2022. Simultaneously, the highest total and average sediment deposition are about 8.43 million tons and 9,452.05 tons/km² occurring in 2026. The lowest total and average sediment deposition are about 5.01 million tons and 5,616.50 tons/km² occurring in 2022.

These results reveal that the primary influence of LULC types and the rainfall erosivity factor in the RUSLE model affect soil erosion, sediment retention, sediment deposition, and sediment export like Scenario I and II. The contribution of the predictive LULC of Scenario III (Economic crop zonation) on soil erosion, sediment retention, sediment deposition, and sediment export between 2020 and 2029 is summarized in Tables 6.33 to 6.42. The spatial distribution of soil erosion, sediment retention, sediment deposition, and sediment export of the predictive LULC between 2020 and 2029 of Scenario III (Economic crop zonation) is displayed in Figures 6.18 to 6.21.

Table 6.32 Estimation of soil erosion, sediment retention, sediment deposition, and sediment export between 2020 and 2029 under Scenario III (Economic crop zonation).

Year	Area km ²	Soil erosion		Sediment retention		Sediment deposition		Sediment export	
		Total (tons)	Average (tons)	Total (tons)	Average (tons)	Total (tons)	Average (tons)	Total (tons)	Average (tons)
2020	891.35	6,827,549.33	7,659.78	93,768,757.96	105,198.58	6,760,994.35	7,585.12	43,130.50	48.39
2021	891.35	5,710,383.07	6,406.44	78,965,730.32	88,591.16	5,655,705.11	6,345.10	37,330.55	41.88
2022	891.35	5,054,407.78	5,670.51	70,070,965.95	78,612.18	5,006,268.60	5,616.50	34,520.48	38.73
2023	891.35	6,506,030.31	7,299.07	88,429,750.45	99,208.78	6,445,336.33	7,230.98	46,451.16	52.11
2024	891.35	6,025,279.69	6,759.72	81,560,632.57	91,502.36	5,965,026.50	6,692.13	47,447.38	53.23
2025	891.35	7,203,860.23	8,081.97	95,330,148.57	106,950.30	7,130,036.54	7,999.14	59,526.42	66.78
2026	891.35	8,518,141.02	9,556.45	110,202,993.74	123,636.05	8,425,084.43	9,452.05	76,068.33	85.34
2027	891.35	6,142,602.94	6,891.35	78,522,081.78	88,093.43	6,070,245.92	6,810.17	59,092.34	66.30
2028	891.35	6,586,200.48	7,389.02	83,414,531.34	93,582.24	6,503,508.42	7,296.25	67,376.26	75.59
2029	891.35	6,835,243.67	7,668.42	85,332,754.97	95,734.29	6,744,804.46	7,566.95	74,740.75	83.85

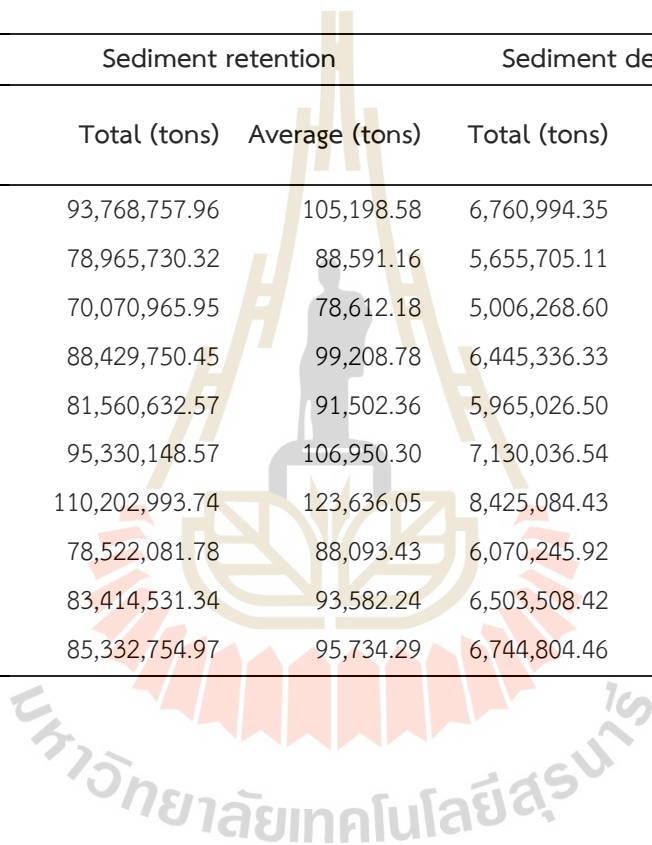


Table 6.33 Contribution of soil erosion, sediment retention, sediment deposition, and sediment export by LULC classes in 2020 under Scenario III.

LULC types	Area	Soil erosion			Sediment retention			Sediment deposition			Sediment export		
	km ²	Total (tons)	Average (tons/km ²)	%	Total (tons)	Average (tons/km ²)	%	Total (tons)	Average (tons/km ²)	%	Total (tons)	Average (tons/km ²)	%
Urban and built-up area (UR)	33.20	0.00	0.00	0.00	65,876.57	1,984.24	0.63	31,550.14	950.31	0.67	0.00	0.00	0.00
Paddy field (PD)	226.72	435,388.41	1,920.37	0.53	640,570.09	2,825.37	0.90	2,223,695.72	9,808.08	6.89	4,054.83	17.88	0.59
Field crop (FC)	23.08	1,654,120.71	71,656.22	19.80	347,102.36	15,036.41	4.78	695,104.74	30,111.82	21.16	11,372.04	492.63	16.23
Para rubber (RB)	19.78	817,490.30	41,321.01	11.42	380,965.84	19,256.37	6.12	282,182.84	14,263.27	10.02	4,190.99	211.84	6.98
Perennial tree and orchard (PO)	74.06	2,489,332.17	33,613.42	9.29	1,322,741.42	17,860.96	5.68	1,444,340.72	19,502.91	13.71	16,820.16	227.12	7.48
Forest land (FO)	433.30	697,299.90	1,609.28	0.44	90,104,541.92	207,949.37	66.10	1,267,659.24	2,925.59	2.06	366.96	0.85	0.03
Water body (WB)	34.34	0.00	0.00	0.00	607,799.40	17,699.51	5.63	472,148.65	13,749.27	9.66	0.00	0.00	0.00
Rangeland (RL)	27.86	158,663.40	5,695.65	1.57	213,394.66	7,660.37	2.44	199,356.84	7,156.45	5.03	562.26	20.18	0.66
Wetland (WL)	16.22	0.00	0.00	0.00	21,677.39	1,336.78	0.42	27,411.63	1,690.39	1.19	0.00	0.00	0.00
Miscellaneous land (ML)	2.79	575,254.44	206,169.93	56.96	64,088.31	22,969.11	7.30	117,543.85	42,127.46	29.61	5,763.26	2,065.54	68.03
Total	891.35	6,827,549.33		100.00	93,768,757.96		100.00	6,760,994.35		100.00	43,130.50		100.00

Table 6.34 Contribution of soil erosion, sediment retention, sediment deposition, and sediment export by LULC classes in 2021 under Scenario III.

LULC types	Area	Soil erosion			Sediment retention			Sediment deposition			Sediment export		
	km ²	Total (tons)	Average (tons/km ²)	%	Total (tons)	Average (tons/km ²)	%	Total (tons)	Average (tons/km ²)	%	Total (tons)	Average (tons/km ²)	%
Urban and built-up area (UR)	33.78	0.00	0.00	0.00	64,190.06	1,900.11	0.71	37,749.27	1,117.43	0.91	0.00	0.00	0.00
Paddy field (PD)	232.67	393,959.62	1,693.18	0.56	610,622.62	2,624.37	0.98	1,938,886.95	8,333.07	6.82	3,690.07	15.86	0.61
Field crop (FC)	24.26	1,435,552.65	59,169.50	19.40	297,849.26	12,276.52	4.58	673,837.44	27,773.71	22.73	10,782.61	444.43	17.19
Para rubber (RB)	19.83	691,767.32	34,878.04	11.43	321,668.23	16,218.11	6.05	230,971.23	11,645.28	9.53	3,590.53	181.03	7.00
Perennial tree and orchard (PO)	68.78	1,948,836.34	28,332.36	9.29	1,050,906.11	15,278.17	5.70	1,077,835.48	15,669.67	12.82	13,387.94	194.64	7.53
Forest land (FO)	429.61	586,158.04	1,364.40	0.45	75,820,595.01	176,486.98	65.84	1,010,084.75	2,351.17	1.92	309.97	0.72	0.03
Water body (WB)	34.93	0.00	0.00	0.00	514,907.08	14,741.13	5.50	394,031.21	11,280.61	9.23	0.00	0.00	0.00
Rangeland (RL)	28.46	144,843.35	5,089.46	1.67	208,265.25	7,317.95	2.73	162,063.68	5,694.54	4.66	519.61	18.26	0.71
Wetland (WL)	16.10	0.00	0.00	0.00	18,123.27	1,125.94	0.42	22,459.54	1,395.34	1.14	0.00	0.00	0.00
Miscellaneous land (ML)	2.92	509,265.75	174,543.29	57.21	58,603.43	20,085.46	7.49	107,785.57	36,941.91	30.23	5,049.82	1,730.75	66.94
Total	891.35	5,710,383.07		100.00	78,965,730.32		100.00	5,655,705.11		100.00	37,330.55		100.00

Table 6.35 Contribution of soil erosion, sediment retention, sediment deposition, and sediment export by LULC classes in 2022 under Scenario III.

LULC types	Area	Soil erosion			Sediment retention			Sediment deposition			Sediment export		
	km ²	Total (tons)	Average (tons/km ²)	%	Total (tons)	Average (tons/km ²)	%	Total (tons)	Average (tons/km ²)	%	Total (tons)	Average (tons/km ²)	%
Urban and built-up area (UR)	33.94	0.00	0.00	0.00	57,379.13	1,690.74	0.70	33,885.75	998.48	0.90	0.00	0.00	0.00
Paddy field (PD)	238.65	370,315.95	1,551.68	0.56	589,016.94	2,468.08	1.02	1,785,516.97	7,481.61	6.73	3,476.83	14.57	0.59
Field crop (FC)	25.54	1,341,948.03	52,539.31	18.84	300,991.13	11,784.26	4.86	645,844.72	25,285.80	22.76	10,721.26	419.75	17.11
Para rubber (RB)	19.85	614,077.53	30,933.73	11.09	287,438.50	14,479.51	5.97	201,046.05	10,127.55	9.11	3,292.44	165.85	6.76
Perennial tree and orchard (PO)	63.62	1,582,703.93	24,876.69	8.92	844,854.02	13,279.28	5.48	876,501.66	13,776.72	12.40	11,296.12	177.55	7.24
Forest land (FO)	425.98	519,075.71	1,218.54	0.44	67,253,004.97	157,877.44	65.12	850,881.47	1,997.46	1.80	275.89	0.65	0.03
Water body (WB)	35.73	0.00	0.00	0.00	459,489.43	12,859.14	5.30	379,523.80	10,621.25	9.56	0.00	0.00	0.00
Rangeland (RL)	29.06	137,717.63	4,739.56	1.70	202,827.40	6,980.32	2.88	105,708.51	3,637.97	3.27	486.73	16.75	0.68
Wetland (WL)	15.97	0.00	0.00	0.00	15,878.17	994.02	0.41	19,542.76	1,223.44	1.10	0.00	0.00	0.00
Miscellaneous land (ML)	3.00	488,569.01	162,980.73	58.45	60,086.25	20,044.05	8.27	107,816.91	35,966.42	32.37	4,971.20	1,658.33	67.59
Total	891.35	5,054,407.78		100.00	70,070,965.95		100.00	5,006,268.60		100.00	34,520.48		100.00

Table 6.36 Contribution of soil erosion, sediment retention, sediment deposition, and sediment export by LULC classes in 2023 under Scenario III.

LULC types	Area	Soil erosion			Sediment retention			Sediment deposition			Sediment export		
	km ²	Total (tons)	Average (tons/km ²)	%	Total (tons)	Average (tons/km ²)	%	Total (tons)	Average (tons/km ²)	%	Total (tons)	Average (tons/km ²)	%
Urban and built-up area (UR)	34.56	0.00	0.00	0.00	112,927.42	3,267.11	1.04	45,204.82	1,307.82	0.92	0.00	0.00	0.00
Paddy field (PD)	244.54	507,163.63	2,073.91	0.55	844,453.83	3,453.17	1.10	2,388,416.06	9,766.79	6.90	4,809.79	19.67	0.60
Field crop (FC)	26.74	1,854,017.97	69,330.14	18.29	427,604.83	15,990.08	5.11	800,425.39	29,931.54	21.15	15,832.91	592.06	18.16
Para rubber (RB)	19.87	781,603.94	39,333.12	10.38	365,211.12	18,378.74	5.87	265,342.53	13,352.99	9.43	4,352.70	219.04	6.72
Perennial tree and orchard (PO)	58.31	1,808,366.62	31,012.13	8.18	945,733.02	16,218.61	5.18	1,054,814.30	18,089.27	12.78	13,674.88	234.51	7.19
Forest land (FO)	422.30	655,369.51	1,551.92	0.41	84,775,147.02	200,747.64	64.15	1,061,101.95	2,512.69	1.78	349.15	0.83	0.03
Water body (WB)	36.43	0.00	0.00	0.00	591,066.72	16,226.93	5.19	497,572.07	13,660.16	9.65	0.00	0.00	0.00
Rangeland (RL)	29.68	178,478.23	6,013.50	1.59	257,366.14	8,671.49	2.77	164,085.25	5,528.56	3.91	612.35	20.63	0.63
Wetland (WL)	15.78	0.00	0.00	0.00	20,142.73	1,276.79	0.41	24,591.37	1,558.77	1.10	0.00	0.00	0.00
Miscellaneous land (ML)	3.14	721,030.41	229,794.38	60.61	90,097.63	28,714.36	9.18	143,782.59	45,823.91	32.38	6,819.38	2,173.36	66.67
Total	891.35	6,506,030.31		100.00	88,429,750.45		100.00	6,445,336.33		100.00	46,451.16		100.00

Table 6.37 Contribution of soil erosion, sediment retention, sediment deposition, and sediment export by LULC classes in 2024 under Scenario III.

LULC types	Area	Soil erosion			Sediment retention			Sediment deposition			Sediment export		
	km ²	Total (tons)	Average (tons/km ²)	%	Total (tons)	Average (tons/km ²)	%	Total (tons)	Average (tons/km ²)	%	Total (tons)	Average (tons/km ²)	%
Urban and built-up area (UR)	34.76	0.00	0.00	0.00	103,731.27	2,984.00	0.99	44,253.59	1,273.03	0.84	0.00	0.00	0.00
Paddy field (PD)	250.55	491,914.70	1,963.36	0.50	835,594.24	3,335.07	1.11	2,234,789.25	8,919.62	5.90	4,692.39	18.73	0.44
Field crop (FC)	27.93	1,735,025.40	62,121.70	15.95	395,722.11	14,168.63	4.72	750,903.89	26,885.73	17.77	15,674.86	561.23	13.22
Para rubber (RB)	19.89	717,253.23	36,058.47	9.26	335,569.29	16,870.07	5.62	245,936.46	12,363.96	8.17	4,114.65	206.86	4.87
Perennial tree and orchard (PO)	53.13	1,492,602.03	28,094.07	7.21	785,371.39	14,782.42	4.92	922,196.65	17,357.78	11.47	11,815.46	222.39	5.24
Forest land (FO)	418.60	602,747.38	1,439.91	0.37	78,162,112.33	186,721.85	62.20	968,905.78	2,314.62	1.53	324.33	0.77	0.02
Water body (WB)	37.07	0.00	0.00	0.00	546,998.01	14,755.77	4.92	448,375.07	12,095.33	8.00	0.00	0.00	0.00
Rangeland (RL)	30.61	177,954.09	5,814.14	1.49	259,850.27	8,489.86	2.83	121,418.71	3,967.01	2.62	596.21	19.48	0.46
Wetland (WL)	15.63	0.00	0.00	0.00	18,239.69	1,166.88	0.39	22,650.11	1,449.04	0.96	0.00	0.00	0.00
Miscellaneous land (ML)	3.18	807,782.87	254,001.96	65.21	117,443.97	36,929.48	12.30	205,596.99	64,648.61	42.74	10,229.47	3,216.59	75.75
Total	891.35	6,025,279.69		100.00	81,560,632.57		100.00	5,965,026.50		100.00	47,447.38		100.00

Table 6.38 Contribution of soil erosion, sediment retention, sediment deposition, and sediment export by LULC classes in 2025 under Scenario III.

LULC types	Area	Soil erosion			Sediment retention			Sediment deposition			Sediment export		
	km ²	Total (tons)	Average (tons/km ²)	%	Total (tons)	Average (tons/km ²)	%	Total (tons)	Average (tons/km ²)	%	Total (tons)	Average (tons/km ²)	%
Urban and built-up area (UR)	35.41	0.00	0.00	0.00	123,685.23	3,492.95	0.97	52,137.37	1,472.39	0.79	0.00	0.00	0.00
Paddy field (PD)	256.39	617,210.01	2,407.33	0.49	1,067,396.68	4,163.21	1.16	2,676,797.56	10,440.42	5.59	5,935.18	23.15	0.43
Field crop (FC)	29.15	2,136,169.26	73,283.11	14.86	513,104.18	17,602.48	4.90	973,567.41	33,399.06	17.88	20,817.25	714.15	13.24
Para rubber (RB)	19.89	844,533.24	42,451.88	8.61	395,274.04	19,869.11	5.53	309,528.45	15,558.97	8.33	5,041.37	253.41	4.70
Perennial tree and orchard (PO)	47.91	1,570,639.18	32,784.24	6.65	812,093.04	16,950.97	4.72	1,055,527.80	22,032.23	11.79	12,927.27	269.83	5.00
Forest land (FO)	414.93	704,485.90	1,697.85	0.34	91,267,020.70	219,958.11	61.22	1,099,163.23	2,649.04	1.42	380.29	0.92	0.02
Water body (WB)	37.96	0.00	0.00	0.00	652,923.28	17,199.09	4.79	535,035.15	14,093.72	7.54	0.00	0.00	0.00
Rangeland (RL)	30.94	218,993.45	7,077.51	1.44	315,793.88	10,205.94	2.84	129,874.48	4,197.33	2.25	720.66	23.29	0.43
Wetland (WL)	15.43	0.00	0.00	0.00	21,263.26	1,377.95	0.38	27,576.24	1,787.06	0.96	0.00	0.00	0.00
Miscellaneous land (ML)	3.34	1,111,829.18	333,358.69	67.61	161,594.29	48,450.66	13.49	270,828.86	81,202.36	43.46	13,704.40	4,108.98	76.18
Total	891.35	7,203,860.23		100.00	95,330,148.57		100.00	7,130,036.54		100.00	59,526.42		100.00

Table 6.39 Contribution of soil erosion, sediment retention, sediment deposition, and sediment export by LULC classes in 2026 under Scenario III.

LULC types	Area	Soil erosion			Sediment retention			Sediment deposition			Sediment export		
	km ²	Total (tons)	Average (tons/km ²)	%	Total (tons)	Average (tons/km ²)	%	Total (tons)	Average (tons/km ²)	%	Total (tons)	Average (tons/km ²)	%
Urban and built-up area (UR)	35.75	0.00	0.00	0.00	144,697.61	4,047.20	0.95	65,581.87	1,834.33	0.81	0.00	0.00	0.00
Paddy field (PD)	262.42	769,083.24	2,930.72	0.48	1,351,018.93	5,148.29	1.21	3,169,732.16	12,078.81	5.32	7,345.63	27.99	0.38
Field crop (FC)	30.40	2,603,114.74	85,636.86	13.92	630,540.94	20,743.44	4.87	1,397,765.09	45,983.45	20.23	28,158.62	926.36	12.70
Para rubber (RB)	19.89	982,006.82	49,380.84	8.03	458,862.63	23,074.20	5.42	382,269.81	19,222.68	8.46	6,104.53	306.97	4.21
Perennial tree and orchard (PO)	42.65	1,608,703.39	37,716.07	6.13	810,277.39	18,996.97	4.46	1,025,374.16	24,039.91	10.58	13,593.58	318.70	4.37
Forest land (FO)	411.24	814,449.49	1,980.49	0.32	105,384,737.23	256,263.20	60.20	1,243,866.63	3,024.70	1.33	442.83	1.08	0.01
Water body (WB)	38.71	0.00	0.00	0.00	773,708.21	19,987.18	4.70	593,435.52	15,330.21	6.75	0.00	0.00	0.00
Rangeland (RL)	31.56	266,300.87	8,436.66	1.37	408,438.55	12,939.72	3.04	178,817.08	5,665.09	2.49	903.45	28.62	0.39
Wetland (WL)	15.29	0.00	0.00	0.00	24,648.65	1,611.70	0.38	31,576.83	2,064.71	0.91	0.00	0.00	0.00
Miscellaneous land (ML)	3.44	1,474,482.46	429,222.44	69.76	216,063.60	62,896.20	14.77	336,665.28	98,003.40	43.13	19,519.69	5,682.19	77.92
Total	891.35	8,518,141.02		100.00	110,202,993.74		100.00	8,425,084.43		100.00	76,068.33		100.00

Table 6.40 Contribution of soil erosion, sediment retention, sediment deposition, and sediment export by LULC classes in 2027 under Scenario III.

LULC types	Area	Soil erosion			Sediment retention			Sediment deposition			Sediment export		
	km ²	Total (tons)	Average (tons/km ²)	%	Total (tons)	Average (tons/km ²)	%	Total (tons)	Average (tons/km ²)	%	Total (tons)	Average (tons/km ²)	%
Urban and built-up area (UR)	36.10	0.00	0.00	0.00	102,865.87	2,849.67	0.92	44,582.30	1,235.05	0.69	0.00	0.00	0.00
Paddy field (PD)	268.46	570,213.86	2,124.01	0.45	1,024,183.73	3,815.01	1.23	2,253,866.63	8,395.50	4.66	5,435.61	20.25	0.33
Field crop (FC)	31.62	1,950,403.79	61,678.27	13.06	499,821.34	15,806.02	5.10	1,016,423.80	32,142.71	17.84	22,730.31	718.81	11.68
Para rubber (RB)	19.88	691,677.64	34,790.20	7.37	323,812.51	16,287.21	5.25	295,688.70	14,872.63	8.26	4,371.47	219.88	3.57
Perennial tree and orchard (PO)	37.46	956,191.91	25,523.89	5.40	446,819.11	11,927.06	3.85	697,597.30	18,621.15	10.34	8,052.51	214.95	3.49
Forest land (FO)	407.57	577,834.20	1,417.76	0.30	75,074,511.02	184,200.93	59.42	881,477.73	2,162.77	1.20	316.57	0.78	0.01
Water body (WB)	39.48	0.00	0.00	0.00	552,201.50	13,987.66	4.51	414,605.62	10,502.26	5.83	0.00	0.00	0.00
Rangeland (RL)	32.14	193,248.76	6,013.23	1.27	302,486.22	9,412.32	3.04	139,818.56	4,350.67	2.42	674.62	20.99	0.34
Wetland (WL)	15.11	0.00	0.00	0.00	16,818.36	1,112.98	0.36	20,979.23	1,388.34	0.77	0.00	0.00	0.00
Miscellaneous land (ML)	3.53	1,203,032.77	340,778.59	72.15	178,562.11	50,580.62	16.32	305,206.05	86,454.57	48.00	17,511.25	4,960.35	80.58
Total	891.35	6,142,602.94		100.00	78,522,081.78		100.00	6,070,245.92		100.00	59,092.34		100.00

Table 6.41 Contribution of soil erosion, sediment retention, sediment deposition, and sediment export by LULC classes in 2028 under Scenario III.

LULC types	Area	Soil erosion			Sediment retention			Sediment deposition			Sediment export		
	km ²	Total (tons)	Average (tons/km ²)	%	Total (tons)	Average (tons/km ²)	%	Total (tons)	Average (tons/km ²)	%	Total (tons)	Average (tons/km ²)	%
Urban and built-up area (UR)	36.65	0.00	0.00	0.00	110,999.06	3,028.82	0.90	44,777.50	1,221.84	0.62	0.00	0.00	0.00
Paddy field (PD)	274.37	642,785.57	2,342.75	0.45	1,172,360.54	4,272.89	1.27	2,455,887.92	8,950.95	4.56	6,168.35	22.48	0.30
Field crop (FC)	32.79	2,141,941.22	65,318.42	12.43	546,230.77	16,657.29	4.94	1,121,506.71	34,200.31	17.41	25,281.36	770.95	10.13
Para rubber (RB)	19.59	726,948.59	37,100.81	7.06	342,266.43	17,468.03	5.18	316,092.38	16,132.20	8.21	4,804.38	245.20	3.22
Perennial tree and orchard (PO)	32.17	850,122.53	26,426.14	5.03	358,403.36	11,141.00	3.30	696,046.83	21,636.68	11.01	7,154.86	222.41	2.92
Forest land (FO)	403.96	612,856.37	1,517.14	0.29	79,675,562.75	197,238.31	58.47	932,899.95	2,309.41	1.18	336.66	0.83	0.01
Water body (WB)	40.47	0.00	0.00	0.00	600,913.39	14,850.08	4.40	421,175.82	10,408.31	5.30	0.00	0.00	0.00
Rangeland (RL)	32.78	217,892.99	6,646.16	1.27	373,007.65	11,377.46	3.37	148,343.74	4,524.77	2.30	802.50	24.48	0.32
Wetland (WL)	14.96	0.00	0.00	0.00	17,702.58	1,183.44	0.35	21,470.28	1,435.32	0.73	0.00	0.00	0.00
Miscellaneous land (ML)	3.61	1,393,653.21	386,026.45	73.48	217,084.81	60,130.08	17.82	345,307.28	95,646.28	48.68	22,828.15	6,323.14	83.10
Total	891.35	6,586,200.48		100.00	83,414,531.34		100.00	6,503,508.42		100.00	67,376.26		100.00

Table 6.42 Contribution of soil erosion, sediment retention, sediment deposition, and sediment export by LULC classes in 2029 under Scenario III.

LULC types	Area	Soil erosion			Sediment retention			Sediment deposition			Sediment export		
	km ²	Total (tons)	Average (tons/km ²)	%	Total (tons)	Average (tons/km ²)	%	Total (tons)	Average (tons/km ²)	%	Total (tons)	Average (tons/km ²)	%
Urban and built-up area (UR)	36.96	0.00	0.00	0.00	115,227.46	3,117.83	0.88	46,301.37	1,252.82	0.60	0.00	0.00	0.00
Paddy field (PD)	280.20	701,203.68	2,502.49	0.45	1,300,386.27	4,640.89	1.31	2,583,781.41	9,221.13	4.38	6,770.19	24.16	0.28
Field crop (FC)	34.11	2,250,767.94	65,980.95	11.77	559,127.71	16,390.75	4.62	1,230,363.43	36,067.93	17.14	28,250.12	828.15	9.49
Para rubber (RB)	19.78	760,063.55	38,428.02	6.85	356,415.56	18,020.00	5.07	328,134.11	16,590.12	7.89	5,186.06	262.20	3.00
Perennial tree and orchard (PO)	26.94	702,090.24	26,059.43	4.65	256,626.29	9,525.18	2.68	585,919.70	21,747.54	10.34	5,796.18	215.14	2.46
Forest land (FO)	400.22	626,024.18	1,564.19	0.28	81,416,902.87	203,428.81	57.29	963,930.96	2,408.48	1.14	344.84	0.86	0.01
Water body (WB)	41.11	0.00	0.00	0.00	628,353.18	15,284.54	4.30	436,317.39	10,613.31	5.04	0.00	0.00	0.00
Rangeland (RL)	33.44	232,565.13	6,954.21	1.24	416,894.15	12,466.06	3.51	150,879.14	4,511.62	2.14	911.95	27.27	0.31
Wetland (WL)	14.85	0.00	0.00	0.00	18,114.46	1,219.54	0.34	22,287.85	1,500.51	0.71	0.00	0.00	0.00
Miscellaneous land (ML)	3.73	1,562,528.95	419,160.13	74.76	264,707.01	71,009.65	20.00	396,889.11	106,468.49	50.61	27,481.40	7,372.09	84.45
Total	891.35	6,835,243.67		100.00	85,332,754.97		100.00	6,744,804.46		100.00	74,740.75		100.00

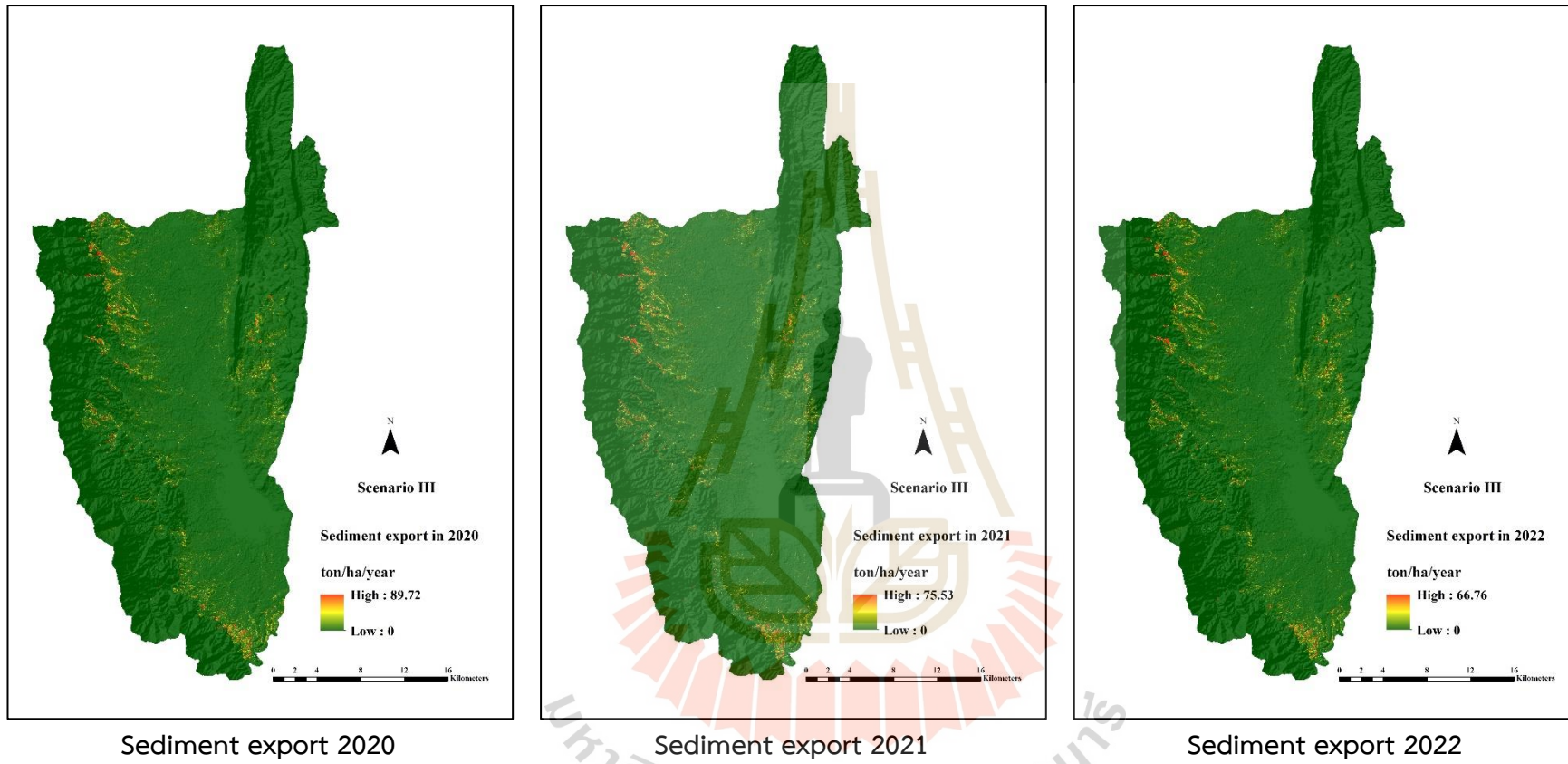


Figure 6.18 Spatial distribution of sediment export in 2020, 2021, and 2022 under Scenario III.

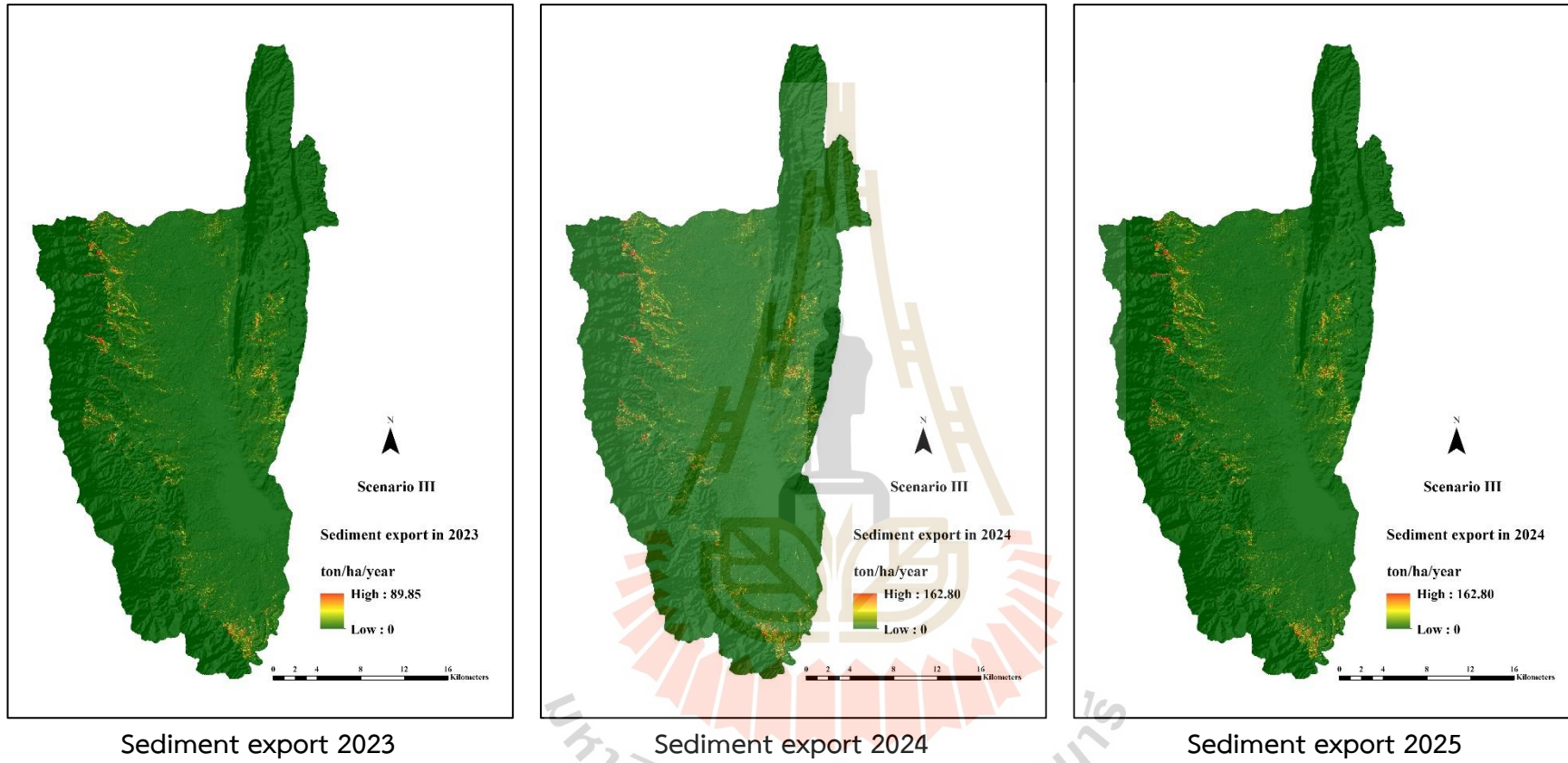


Figure 6.19 Spatial distribution of sediment export in 2023, 2024, and 2025 under Scenario III.

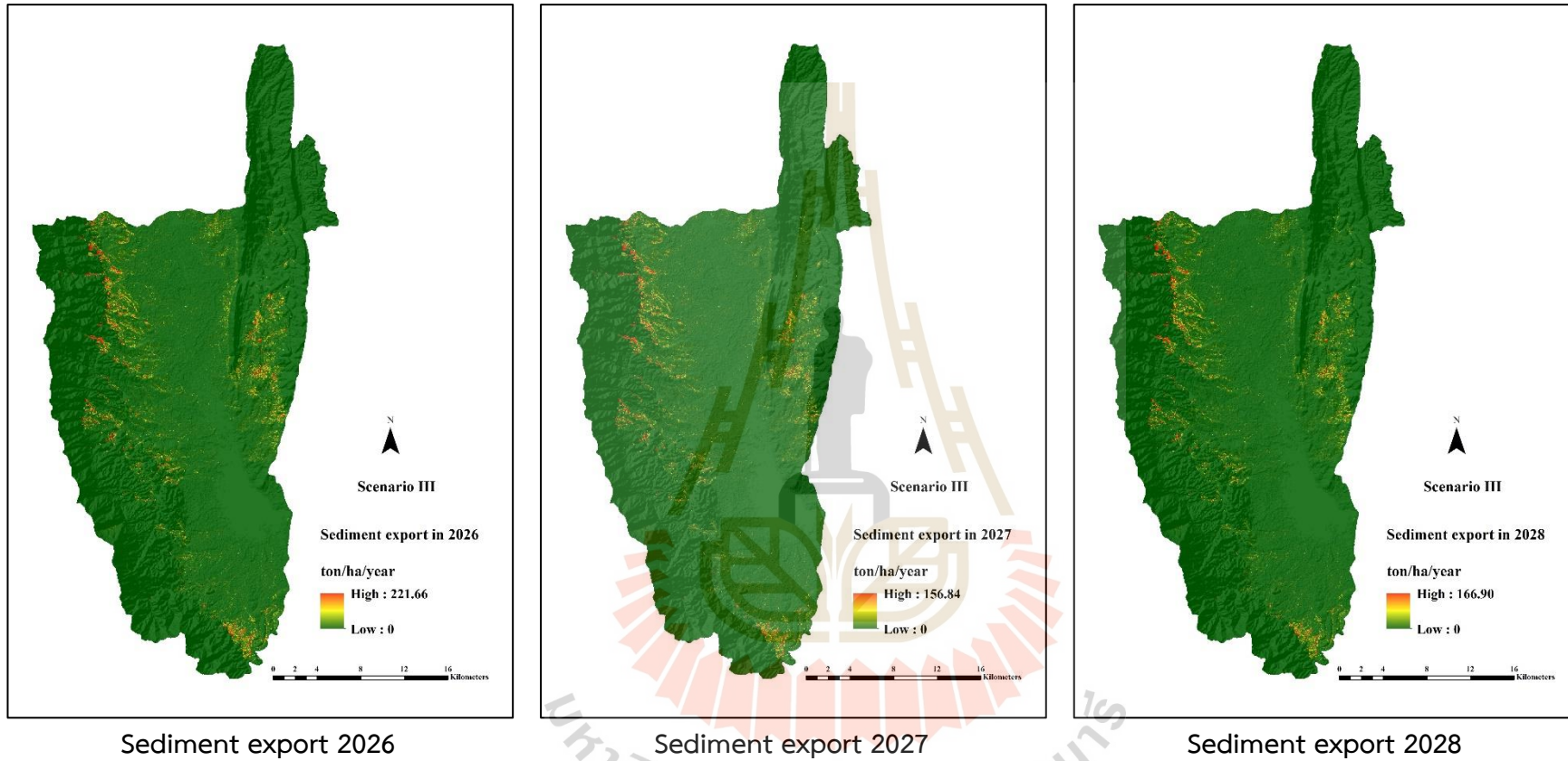
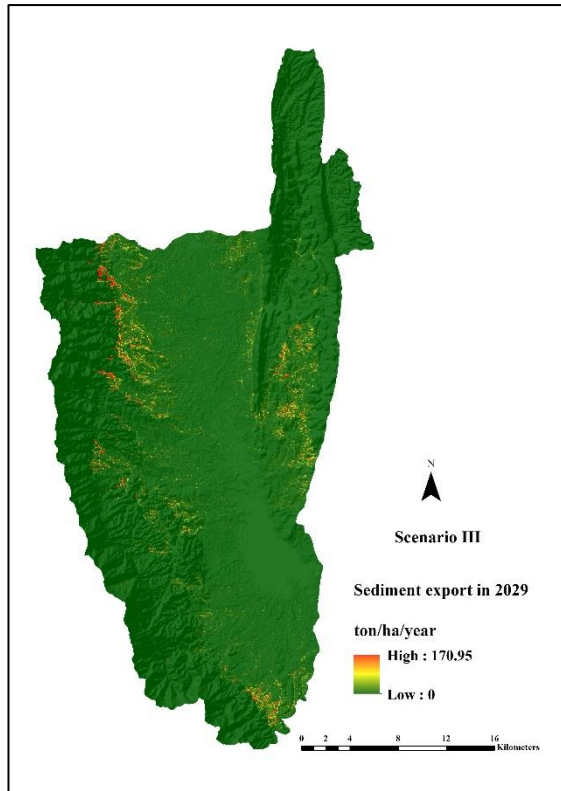
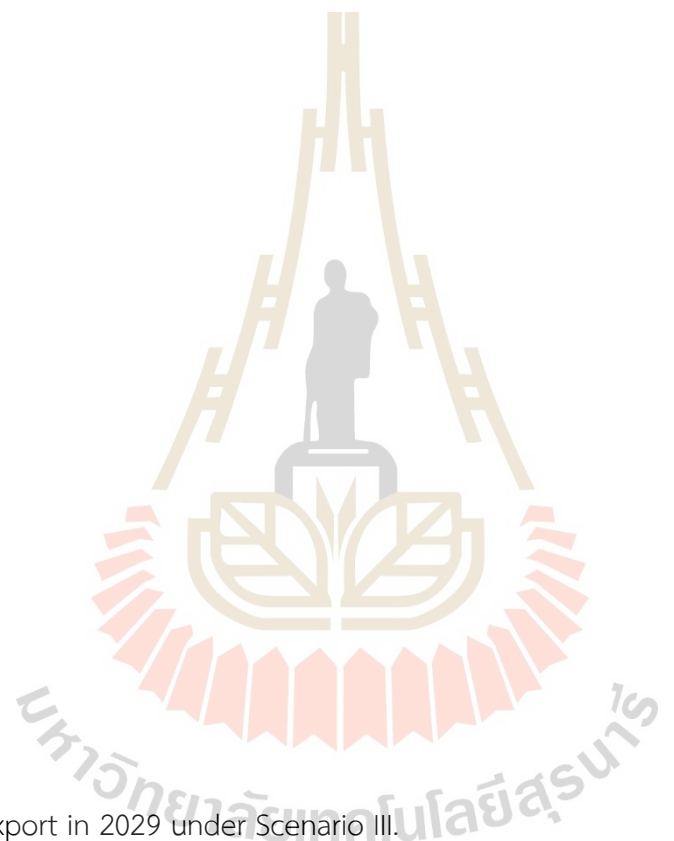


Figure 6.20 Spatial distribution of sediment export in 2026, 2027, and 2028 under Scenario III.



Sediment export 2029

Figure 6.21 Spatial distribution of sediment export in 2029 under Scenario III.



As results from 2020 to 2029 (Tables 6.33 to 6.42), miscellaneous land causes the highest average soil erosion with values between 162,980.73 tons/km² in 2022 and 429,222.44 tons/km² in 2026, while forest land generates the lowest average soil erosion with values between 1,218.54 tons/km² in 2022 and 1,980.49 tons/km² in 2026.

Meanwhile, the highest average sediment retention is forest land with values between 256,263.20 tons/km² in 2026 and 157,877.44 tons/km² in 2022, while the lowest average sediment retention is a wetland with values between 994.02 tons/km² in 2022 and 1,611.70 tons/km² in 2026.

In the meantime, the highest sediment deposition appears on miscellaneous land with values between 106,468.49 in 2029 and 35,966.42 tons/km² in 2022, while the lowest average sediment deposition is the urban and built-up area with values between 950.31 tons/km² in 2020 and 1,834.33 tons/km² in 2026.

At the same time, miscellaneous land causes the highest average sediment export with values between 1,658.33 tons/km² in 2022 and 7,372.09 tons/km² in 2029, while the forest land generates the lowest average sediment export with values between 0.65 tons/km² in 2022 and 1.08 tons/km² in 2026. Even though the paddy field and field crop do not generate the highest sediment export, increasing paddy field and field crop area by updating the area from zonation generates more sediment export and soil erosion.

This finding suggests that variation of predicted rainfall erosivity from 2020 to 2029 directly affects sediment export. Besides, the LULC data under this scenario has influences sediment export due to the LULC data of Scenario III (Economic crop zonation) simulated based on the annual rate of LULC change from transition area matrix between 2009 and 2019 for some LULC types and the economic crop zonation, particularly the increase of paddy field and field crop areas and decrease of the perennial tree and orchard areas. Hence, it shows significant LULC change under this scenario.

6.7 Comparison of sediment export estimation among three different scenarios

Under this section, the summary on sediment export between 2020 and 2029 of three different scenarios was compared and discussed. Table 6.43 summarizes the average sediment export between 2020 and 2029 of three scenarios and is displayed in Figures 6.22.

Table 6.43 Average sediment export (tons/km²) between 2020 and 2029 of three different scenarios.

Year	Sediment export		
	Scenario I (Trend of LULC evolution)	Scenario II (Maximization of ecosystem service values)	Scenario III (Economic crop zonation)
2020	46.50	45.97	48.39
2021	40.04	38.31	41.88
2022	36.32	33.87	38.73
2023	47.07	43.17	52.11
2024	44.51	40.01	53.23
2025	54.22	46.59	66.78
2026	65.97	53.98	85.34
2027	47.74	37.98	66.30
2028	52.58	40.63	75.59
2029	55.60	42.18	83.85
Average	49.05	42.27	61.22

As a result, it disclosed that the predictive LULC between 2020 and 2029 of Scenario II (Maximization of ecosystem service values) delivers the lowest annual sediment export than Scenario I and III, with an average value of 42.27 tons/km². Due to the increasing areas of wetland and decreasing areas of rangeland and miscellaneous land under this scenario can reduce soil loss and sediment export. The increase of wetland and decrease of rangeland or miscellaneous land are caused by

linear programming to maximize the ecosystem service values. In contrast, the areas of miscellaneous land of scenarios I and III were increased based on the annual change rate of the Markov chain model. Though the miscellaneous land is a minor increase, it caused much soil loss and sediment export.

Moreover, Scenario III (Economic crop zonation) delivers the highest annual sediment export than other scenarios since the paddy field and field crop areas increase according to their suitability classes by the LDD. This finding is similar to Zhou et al. (2019), who found that the decreases in miscellaneous land (bare land) significantly contributed to the reductions in sediment export. In contrast, increases in agricultural land, such as cropland and garden plots, were increased sediment export in the watershed.

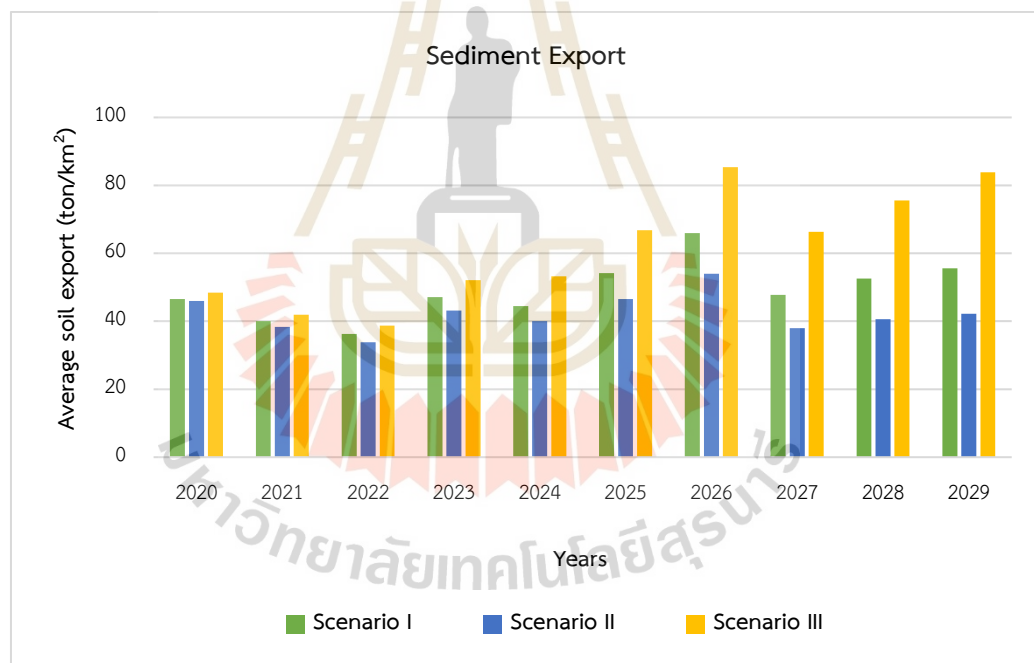


Figure 6.22 Comparison of sediment export between 2020 and 2029 of three different scenarios.

CHAPTER VII

NUTRIENT EXPORT ESTIMATION OF THREE DIFFERENT SCENARIOS

This chapter presents the results of the fourth objective focusing on nutrient export assessment using the nutrient delivery ratio (NDR) model of the InVEST software suite from LULC in 2019 and predictive LULC between 2020 and 2029 of three different scenarios. The main results consist of (1) calibration of nutrient delivery ratio model, (2) validation of nutrient delivery ratio model, (3) nutrient export estimation of actual LULC in 2019, (4) nutrient export estimation of predictive LULC of Scenario I, (5) nutrient export estimation of predictive LULC of Scenario II, (6) nutrient export estimation of predictive LULC of Scenario III, and (7) comparison of nutrient export estimation among three different scenarios are here described and discussed in details.

7.1 Calibration of nutrient delivery ratio model

As mentioned in the previous chapter, this study's calibration and validation process is processed on the observed data between 2011 and 2015 for model calibration, while observed data between 2016 and 2018 were applied for model validation.

The required input data for NDR model calibration were total phosphorus and nitrogen, annual surface runoff, and LULC data. Due to this study using the past data, the correlation of TP and TN data and the surface runoff that provides the highest correlation was first analyzed to estimate the observed data. Herein, the observed maximum daily nutrient data collected three or four times per year between 2011 and 2015 from six locations in Kwan Phayao Lake by the PCD (Tables 7.1 and 7.2) were applied to calculate annual observed total nitrogen data (sum of nitrate-nitrogen, $\text{NO}_3\text{-N}$, nitrite-nitrogen, $\text{NO}_2\text{-N}$, ammonia – nitrogen, $\text{NH}_3\text{-N}$) and total phosphorus data. Meanwhile, annual runoff in the same years was calculated from daily surface runoff data of the RID (See Figure 6.1). The required LULC data in the same period were predicted based on the classified LULC in 2009 and 2019 using the CLUE-S model (See

Figure 6.2).

Besides, the guideline from the InVEST documentation and the review paper by Griffin et al. (2020) were applied to calibrate critical parameters of the NDR model. Herein, the significant model parameters, namely loading N and P (*load_n*, *load_p*), maximum retention efficiency (*eff_n*, *eff_p*), and critical length (*crit_len_n*, *crit_len_p*), were systematically adjusted until the satisfied fit was obtained between the modeled and observed nutrient export based on statistical measurement using R^2 and *PBIAS*, as a summary in Table 7.3. In addition, other parameters as K_b and *TFA* were applied similarly to the SDR model. Moreover, the wastewater treatment facilities (WWTF) are relevant to the NDR model parameters by affecting the retention and treatment of nutrients of that area before export to the streams. Hence, the area within and outside the WWTF was adjusted by adding values differently. In this study, urban and built-up areas are within the management of water treatment (The 2017 Industrial Census Basic Information, Phayao Province), and wetland which is the wastewater treatment by nature (PWQMP-P2 in 2017), are considered within the WWTF. Other LULC areas are outside the WWTF.

Table 7.1 Basic information of observed total nitrogen (TN) data of PCD for model calibration.

Year	Date	KP01		KP05		KP06		KP07		KP09		KP010							
		Time	Depth (m)	TN (mg/l)	Time	Depth (m)	TN (mg/l)	Time	Depth (m)	TN (mg/l)	Time	Depth (m)	TN (mg/l)						
2011	2011-12-07	09:53	2.90	0.27	10:10	1.80	0.22	10:21	2.60	0.10	11:17	0.80	0.04	10:31	3.00	0.04	10:44	3.00	0.05
	2011-09-01	09:10	3.60	0.00	09:25	2.60	0.11	09:40	3.00	0.00	10:50	1.30	0.00	09:46	3.60	0.06	10:01	3.20	0.00
	2011-06-16	09:00	2.80	0.36	09:18	2.30	0.44	09:25	2.50	0.47	15:20	-	0.39	09:35	3.00	0.28	09:47	1.60	0.31
	2011-03-18	10:52	2.00	0.21	11:08	1.50	0.21	11:18	1.60	0.11	13:10	1.00	0.21	11:25	2.00	0.21	11:37	1.50	0.21
2012	2012-11-30	09:20	2.90	0.12	09:40	2.30	0.15	10:00	2.50	0.21	07:50	0.60	0.06	10:10	3.00	0.04	10:25	1.70	0.04
	2012-08-30	09:20	1.80	0.10	09:36	2.60	0.10	09:49	2.50	0.10	08:00	1.60	0.10	10:00	2.90	0.10	10:16	3.00	0.10
	2012-05-30	09:43	2.30	0.21	-	1.80	0.10	-	2.00	0.10	11:19	1.60	0.22	-	2.60	0.10	-	2.00	0.16
	2012-03-01	09:15	2.00	0.31	09:30	14.00	0.20	09:45	1.90	0.20	08:00	1.70	0.21	09:50	2.50	0.20	10:05	2.30	0.11
2013	2013-12-13	-	3.30	0.11	-	1.80	0.11	-	2.70	0.11	-	1.60	0.11	-	3.20	0.11	-	1.40	0.11
	2013-05-30	10:27	1.40	0.48	10:47	0.80	1.06	11:00	1.20	1.41	12:51	0.70	0.53	11:10	1.60	0.82	11:22	0.20	0.47
	2013-02-21	11:30	2.40	0.41	11:55	2.10	0.11	12:05	2.00	0.31	13:15	0.40	0.11	12:15	2.20	0.11	12:25	2.50	0.11
2014	2014-11-20	10:06	3.20	0.20	10:21	2.00	0.81	10:32	2.70	0.19	11:47	2.20	0.15	10:47	3.30	0.14	11:00	1.20	0.12
	2014-08-22	09:29	3.40	0.11	09:42	1.80	0.11	09:50	2.50	0.11	07:58	1.80	0.12	09:59	2.90	0.11	10:14	1.00	0.11
	2014-06-04	08:37	1.20	0.11	08:52	0.20	0.11	09:01	1.10	0.28	07:18	0.80	0.56	09:09	1.50	0.28	09:21	0.10	0.17
2015	2015-12-23	10:25	1.10	0.11	10:40	0.40	0.11	10:50	0.75	0.11	11:10	0.15	0.11	11:30	0.75	0.11	11:50	0.35	0.12
	2015-09-10	08:50	2.15	0.12	09:05	0.30	0.10	09:15	1.15	0.10	09:35	0.80	0.11	10:00	1.00	0.11	10:15	1.05	0.10
	2015-05-29	09:35	1.95	0.11	09:50	0.30	0.11	10:00	1.30	0.11	10:25	0.65	0.11	10:40	1.20	0.11	11:00	0.15	0.11
	2015-03-12	09:21	2.70	0.40	09:42	1.10	0.40	09:51	2.00	0.40	11:26	1.30	0.20	10:05	2.20	0.40	10:24	0.60	0.40

Table 7.2 Basic information of observed total phosphorus (TP) data of PCD for model calibration.

Year	Date	KP01		KP05		KP06		KP07		KP09		KP010							
		Time	Depth (m)	TP (mg/l)	Time	Depth (m)	TP (mg/l)	Time	Depth (m)	TP (mg/l)	Time	Depth (m)	TP (mg/l)						
2011	2011-12-07	09:53	2.90	0.06	10:10	1.80	0.09	10:21	2.60	0.13	11:17	0.80	0.11	10:31	3.00	0.14	10:44	3.00	0.08
	2011-09-01	09:10	3.60	0.01	09:25	2.60	0.01	09:40	3.00	0.01	10:50	1.30	0.01	09:46	3.60	0.01	10:01	3.20	0.01
	2011-06-16	09:00	2.80	0.04	09:18	2.30	0.04	09:25	2.50	0.03	15:20	-	0.07	09:35	3.00	0.05	09:47	1.60	0.05
	2011-03-18	10:52	2.00	0.02	11:08	1.50	0.02	11:18	1.60	0.02	13:10	1.00	0.02	11:25	2.00	0.02	11:37	1.50	0.01
2012	2012-11-30	09:20	2.90	0.03	09:40	2.30	0.00	10:00	2.50	0.04	07:50	0.60	0.01	10:10	3.00	0.00	10:25	1.70	0.03
	2012-08-30	09:20	1.80	0.06	09:36	2.60	0.06	09:49	2.50	0.06	08:00	1.60	0.06	10:00	2.90	0.07	10:16	3.00	0.04
	2012-05-30	09:43	2.30	0.03	-	1.80	0.03	-	2.00	0.03	11:19	1.60	0.06	-	2.60	0.03	-	2.00	0.05
	2012-03-01	09:15	2.00	0.06	09:30	14.00	0.06	09:45	1.90	0.05	08:00	1.70	0.04	09:50	2.50	0.06	10:05	2.30	0.04
2013	2013-12-13	-	3.30	0.04	-	1.80	0.04	-	2.70	0.02	-	1.60	0.03	-	3.20	0.02	-	1.40	0.02
	2013-05-30	10:27	1.40	0.12	10:47	0.80	0.09	11:00	1.20	0.15	12:51	0.70	0.13	11:10	1.60	0.15	11:22	0.20	0.06
	2013-02-21	11:30	2.40	0.04	11:55	2.10	0.05	12:05	2.00	0.04	13:15	0.40	0.03	12:15	2.20	0.04	12:25	2.50	0.03
2014	2014-11-20	10:06	3.20	0.06	10:21	2.00	0.11	10:32	2.70	0.06	11:47	2.20	0.08	10:47	3.30	0.06	11:00	1.20	0.06
	2014-08-22	09:29	3.40	0.06	09:42	1.80	0.07	09:50	2.50	0.07	07:58	1.80	0.09	09:59	2.90	0.05	10:14	1.00	0.11
	2014-06-04	08:37	1.20	0.18	08:52	0.20	0.15	09:01	1.10	0.14	07:18	0.80	0.22	09:09	1.50	0.14	09:21	0.10	0.08
2015	2015-12-23	10:25	1.10	0.05	10:40	0.40	0.04	10:50	0.75	0.03	11:10	0.15	0.04	11:30	0.75	0.03	11:50	0.35	0.03
	2015-09-10	08:50	2.15	0.05	09:05	0.30	0.05	09:15	1.15	0.03	09:35	0.80	0.04	10:00	1.00	0.04	10:15	1.05	0.03
	2015-05-29	09:35	1.95	0.21	09:50	0.30	0.11	10:00	1.30	0.08	10:25	0.65	0.12	10:40	1.20	0.03	11:00	0.15	0.06
	2015-03-12	09:21	2.70	0.10	09:42	1.10	0.10	09:51	2.00	0.09	11:26	1.30	1.26	10:05	2.20	0.10	10:24	0.60	0.09

Table 7.3 Nutrient delivery ratio model parameters for model calibration.

Parameter	Default value	Initial value	Maximum value	Adjusted value	Calibrated value
K_b	2	1	2	0.5	1
TFA	1000	1000	1800	200	1800
$load_n$	by LULC ¹ (See Table 3.11)	0.5x	3x	0.5x	by LULC (Table 7.4)
eff_n	by LULC ² (See Table 3.11)	0.5x	1x	0.5x	by LULC (Table 7.4)
$crit_len_n$	30 meters ³	30	10x	5x	150
$load_p$	by LULC ² (See Table 3.11)	0.5x	3x	0.5x	by LULC (Table 7.4)
eff_p	by LULC ² (See Table 3.11)	0.5x	1x	0.5x	by LULC (Table 7.4)
$crit_len_p$	30 meters ³	30	10x	5x	150

Note

1. $load_n$ can be added from default values of all LULC types;
2. eff_n , eff_p , $load_p$, can be added from default values only LULC types outside WWTF
3. $crit_len_n$ and $crit_len_p$ can be added from default values only LULC types outside WWTF.

According to selected parameters for the model calibration process, the K_b value and TFA were used the same as the SDR model. In general, the K_b parameter determines the relationship between hydrologic connectivity and the nutrient delivery ratio. At the same time, TFA is used to delineate the stream network that the model assumes no data at stream pixels, which means where retention stops and the remaining pollutant will be exported to stream. However, the change of TFA also changes the number of pixels that contribute to nutrient loading and retention (Redhead et al., 2018).

Additionally, the nutrient load and maximum retention efficiency are significant drivers because the nutrient export is calculated as the product of nutrient load and the NDR, which is proportional to nutrient retention parameters from the downslope. In addition, the critical length is the distance that it travels across each land cover type

to retain nutrients at its maximum retention efficiency, viz., the increase of nutrient load and the critical length has increased the nutrient export. In contrast, the increase of maximum retention efficiency has decreased nutrient export. So, *load_n*, *eff_n*, *crit_len_n*, *load_p*, *eff_p*, and *crit_len_p* were adjusted according to LULC type and location (inside or outside wastewater treatment facilities) (Table 7.4).

Table 7.4 Adjusted parameter of NDR model for nitrogen and phosphorus calibration.

LULC types	load_n	eff_n	crit_len_n	load_p	eff_p	crit_len_p
Urban and built-up area (UR)	23.25	0.05	30	1.3	0.05	30
Paddy field (PD)	33	0.25	150	9	0.25	150
Field crop (FC)	33	0.25	150	9	0.25	150
Para rubber (RP)	30	0.45	150	9	0.45	150
Perennial trees and Orchard (PO)	30	0.45	150	9	0.45	150
Forest area (FO)	5.4	0.7	150	0.033	0.7	150
Waterbody (WB)	0.003	0.05	150	0.003	0.05	150
Rangeland (RL)	6	0.5	150	0.033	0.5	150
Wetland (WL)	6	0.8	30	0.05	0.8	30
Miscellaneous land (ML)	12	0.05	150	0.003	0.05	150

Under model calibration, the default values of selected parameters of the NDR model were first applied to examine each parameter's sensitivity on nutrient export. Then, systematic adjustment was conducted from the initial to the maximum value to identify an optimum local parameter based on R^2 and $PBIAS$. (See detail in Table 7.3 and 7.4).

Tables 7.5 and 7.6 compare the results and statistical measurement of TN and TP at default, initial, and maximum value stages under model calibration. As a result of Table 7.5, it can be observed that results of the estimated TN export between 2010 and 2015 with a default value, initial value, and maximum value provide overestimated and underestimated value with $PBIAS$ values varying from -25.56% to 77.63% and the R^2 values ranging from 0.00 to 0.01. Meanwhile, according to Table 7.6, the estimated

TP export results between 2010 and 2015 with a default value, initial value, and maximum value provide overestimated and underestimated value with *PBIAS* values varying from 9.74% to 82.59% and the R^2 values ranging from 0.48 to 0.52.

These findings indicate that the systematic adjustment for optimum parameters identification for TN and TP estimation is required to minimize *PBIAS* value and maximize the R^2 value, as reported in Tables 7.2 and 7.3.

The comparison of the observed and estimated nitrogen exports and statistical measurement values under the calibration period is reported in Table 7.7 and Figure 7.1. Meanwhile, the comparison of the observed and estimated phosphorus exports and statistical measurement values under the calibration period is reported in Table 7.8 and Figure 7.2.

Table 7.5 Observed and estimated TN export and statistical measurement at default, initial and maximum value stages.

Default setting for Nitrogen: by LULC (See Table 3.11)				
Year	Observed (kg/km ²)	Estimated TN (kg/km ²)	R ²	PBIAS (%)
2011	201.07	69.80		
2012	62.16	70.08		
2013	327.02	70.46	0.00	60.99
2014	287.12	71.32		
2015	27.45	71.35		
Initial setting for Nitrogen: load_n = 0.5x, eff_n = 0.5x, crit_len_n = 30 meters				
Year	Observed (kg/km ²)	Estimated TN (kg/km ²)	R ²	PBIAS (%)
2011	201.07	40.02		
2012	62.16	40.18		
2013	327.02	40.38	0.01	77.63
2014	287.12	40.88		
2015	27.45	40.96		
Maximum setting for Nitrogen: load_n = 3x, eff_n = 1x, crit_len_n = 300 meters				
Year	Observed (kg/km ²)	Estimated TN (kg/km ²)	R ²	PBIAS (%)
2011	201.07	224.61		
2012	62.16	225.59		
2013	327.02	226.81	0.00	-25.56
2014	287.12	229.50		
2015	27.45	229.60		

Table 7.6 Observed and estimated TP export and statistical measurement at default, initial and maximum value stages.

Default setting for phosphorus: by LULC (See Table 3.11)				
Year	Observed (kg/km ²)	Estimated TP (kg/km ²)	R ²	PBIAS (%)
2011	59.89	15.35		
2012	14.04	15.44		
2013	34.79	15.57	0.50	71.42
2014	77.98	15.85		
2015	86.47	15.86		
Initial setting for phosphorus: load_p = 0.5x, eff_p = 0.5x, crit_len_p = 30 meters				
Year	Observed (kg/km ²)	Estimated TP (kg/km ²)	R ²	PBIAS (%)
2011	59.89	9.36		
2012	14.04	9.41		
2013	34.79	9.48	0.52	82.59
2014	77.98	9.65		
2015	86.47	9.67		
Maximum setting for phosphorus: load_p = 3x, eff_p = 1x, crit_len_p = 300 meters				
Year	Observed (kg/km ²)	Estimated TP (kg/km ²)	R ²	PBIAS (%)
2011	59.89	48.47		
2012	14.04	48.79		
2013	34.79	49.18	0.48	9.74
2014	77.98	50.05		
2015	86.47	50.08		

Table 7.7 Comparison of the observed and estimated nitrogen export with a statistical measurement under the calibration period.

Year	Nitrogen export in kg/km ²		Statistical measurement		
	Observed data	Estimated data	PBIAS	R ²	Adjusted R ²
2011	201.07	220.04			
2012	62.16	216.84			
2013	327.02	218.01	-20.42%	0.5746	0.43
2014	287.12	220.63			
2015	27.45	214.04			

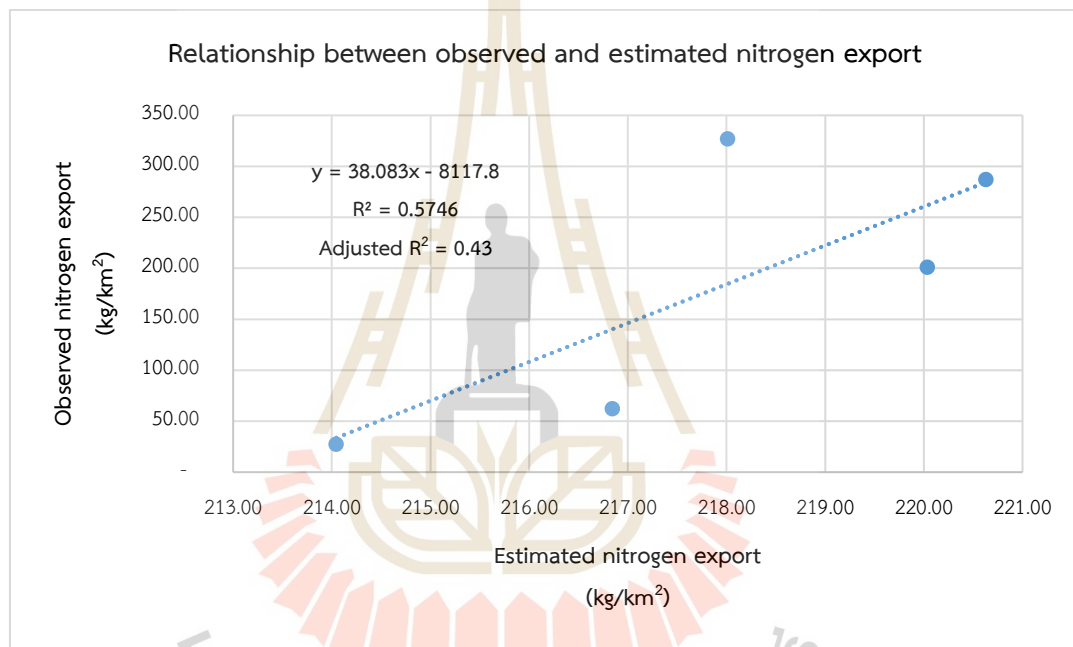


Figure 7.1 Relationship between the observed and estimated nitrogen export under calibration process.

Table 7.8 Comparison of the observed and estimated phosphorus export with a statistical measurement under the calibration period.

Year	Phosphorus export in kg/km ²		Statistical measurement		
	Observed data	Estimated data	PBIAS	R ²	Adjusted R ²
2011	59.89	47.50			
2012	14.04	46.89			
2013	34.79	47.26	12.57%	0.8279	0.77
2014	77.98	48.10			
2015	86.47	49.08			

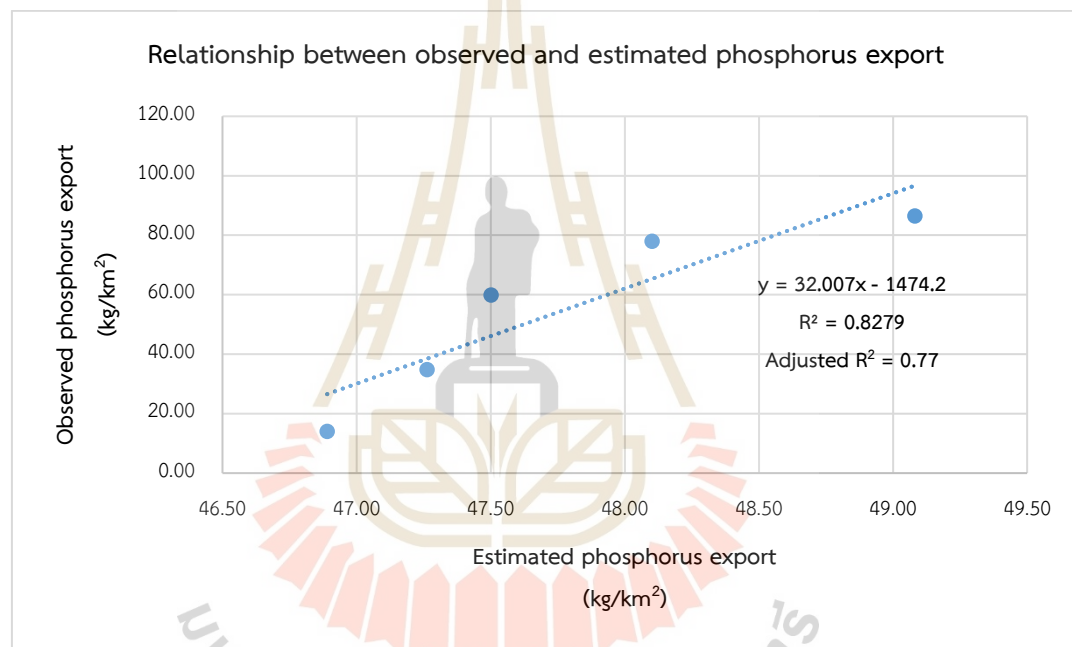


Figure 7.2 Relationship between the observed and estimated phosphorus export under calibration period.

As a result of nitrogen export, the *PBIAS* value is -20.42% which provide a very good fit for calibrate the model in term of nitrogen export estimation as suggested by Moriasi et al. (2007) and Me, Abell, and Hamilton (2015), with a satisfactory coefficient of determination between the observed and estimated nitrogen export with the value is 0.57. Likewise, in the case of phosphorus export, the *PBIAS* value is 12.57% which provide a very good fit for calibrating the model in term of phosphorus export estimation as suggested by Moriasi et al. (2007) and Me, Abell, and Hamilton (2015),

with a very good coefficient of determination between the observed and estimated phosphorus export with the value is 0.83. Therefore, the nutrient delivery ratio model of the InVEST software suite can be accepted and applied to validate nitrogen and phosphorus export between 2016 and 2018.

7.2 Validation of nutrient delivery ratio model

The identified optimum local parameters of the NDR model were applied here to estimate nutrient export between 2016 and 2018 for model validation. Like the calibration process, the required input data are the observed TN and TP data, runoff and LULC data. The observed daily TN and TP data collected four times per year from 2016 to 2018 from six locations in Kwan Phayao Lake by the PCD were applied to calculate annual TN and TP data (Tables 7.9 and 7.10). Meanwhile, the daily surface runoff data from the RID were applied to calculate annual surface runoff in the same period (See Figure 6.4). Besides, the required LULC data in the same period were predicted based on the classified LULC in 2009 and 2019 using the CLUE-S model (See Figure 6.5). The derived results of the model validation with an optimum NDR model parameter for nitrogen and phosphorus estimation are separately reported in Table 7.11 and Figure 7.3 and Table 7.12 and Figure 7.4, respectively.

Table 7.9 Basic information of observed total nitrogen (TN) data of PCD for model validation.

Year	Date	KP01		KP05		KP06		KP07		KP09		KP10							
		Time	Depth (m)	TN (mg/l)	Time	Depth (m)	TN (mg/l)	Time	Depth (m)	TN (mg/l)	Time	Depth (m)	TN (mg/l)						
2016	2016-11-21	10:00	3.50	0.41	10:20	2.00	0.57	10:31	4.50	0.47	13:00	1.00	0.48	10:46	3.50	0.47	11:10	2.30	0.47
	2016-08-22	09:05	2.00	0.90	09:25	1.00	0.85	09:35	1.80	0.76	11:25	0.50	0.76	09:50	1.40	0.77	10:10	1.60	0.68
	2016-06-16	09:15	0.90	1.31	09:38	0.50	0.80	09:48	1.00	0.78	12:05	0.30	1.38	10:08	1.50	1.01	10:30	1.00	1.14
	2016-03-01	10:15	1.30	0.11	10:55	0.30	0.11	10:45	0.80	0.11	13:00	0.50	0.11	11:00	1.00	0.11	11:15	1.00	0.13
2017	2017-11-23	08:50	3.10	0.43	09:15	1.80	0.41	09:35	3.00	0.44	11:30	1.40	0.38	09:40	3.10	0.40	10:00	2.00	0.44
	2017-07-06	-	2.50	0.35	-	1.50	0.46	-	3.00	0.47	-	1.00	0.55	-	2.20	0.40	-	1.70	0.58
	2017-05-18	09:05	2.50	1.06	09:10	1.00	0.72	09:15	2.00	0.54	11:05	1.80	1.03	09:30	3.00	0.40	09:50	1.50	0.72
	2017-01-26	10:13	3.50	0.14	10:00	2.00	0.18	09:35	1.00	0.26	09:20	1.00	0.42	-	-	0.00	08:30	1.50	0.44
2018	2018-11-22	09:50	4.20	0.22	10:15	2.00	0.24	10:30	3.40	0.17	10:50	2.40	0.30	11:00	3.00	0.21	11:20	2.00	0.13
	2018-08-06	08:30	2.50	0.25	08:45	1.20	0.25	09:00	2.30	0.30	10:10	1.30	0.54	09:30	3.00	0.27	10:40	2.50	0.52
	2018-05-24	08:30	3.00	0.11	08:45	1.50	0.31	09:00	4.50	0.34	10:20	1.50	0.71	09:20	2.50	0.24	09:45	2.20	0.82
	2018-02-24	09:30	2.50	0.09	09:40	1.20	0.22	09:50	2.50	0.11	08:10	1.20	0.14	10:00	2.70	0.10	10:10	1.50	0.31



Table 7.10 Basic information of observed total phosphorus (TP) data of PCD for model validation.

Year	Date	KP01			KP05			KP06			KP07			KP09			KP10		
		Time	Depth (m)	TP (mg/l)	Time	Depth (m)	TP (mg/l)	Time	Depth (m)	TP (mg/l)	Time	Depth (m)	TP (mg/l)	Time	Depth (m)	TP (mg/l)	Time	Depth (m)	TP (mg/l)
2016	2016-11-21	10:00	3.50	0.08	10:20	2.00	0.07	10:31	4.50	0.06	13:00	1.00	0.07	10:46	3.50	0.06	11:10	2.30	0.06
	2016-08-22	09:05	2.00	0.33	09:25	1.00	0.20	09:35	1.80	0.14	11:25	0.50	0.07	09:50	1.40	0.12	10:10	1.60	0.10
	2016-06-16	09:15	0.90	0.10	09:38	0.50	0.11	09:48	1.00	0.13	12:05	0.30	0.19	10:08	1.50	0.13	10:30	1.00	0.10
	2016-03-01	10:15	1.30	0.06	10:55	0.30	0.05	10:45	0.80	0.03	13:00	0.50	0.03	11:00	1.00	0.03	11:15	1.00	0.04
2017	2017-11-23	08:50	3.10	0.08	09:15	1.80	0.12	09:35	3.00	0.09	11:30	1.40	0.16	09:40	3.10	0.09	10:00	2.00	0.13
	2017-07-06	-	2.50	0.10	-	1.50	0.13	-	3.00	0.11	-	1.00	0.09	-	2.20	0.07	-	1.70	0.13
	2017-05-18	09:05	2.50	0.15	09:10	1.00	0.14	09:15	2.00	0.14	11:05	1.80	0.25	09:30	3.00	0.07	09:50	1.50	0.27
	2017-01-26	10:13	3.50	0.09	10:00	2.00	0.07	09:35	1.00	0.07	09:20	1.00	0.06	-	-	0.00	08:30	1.50	0.07
2018	2018-11-22	09:50	4.20	0.01	10:15	2.00	0.00	10:30	3.40	0.01	10:50	2.40	0.03	11:00	3.00	0.01	11:20	2.00	0.02
	2018-08-06	08:30	2.50	0.08	08:45	1.20	0.09	09:00	2.30	0.07	10:10	1.30	0.03	09:30	3.00	0.08	10:40	2.50	0.05
	2018-05-24	08:30	3.00	0.06	08:45	1.50	0.08	09:00	4.50	0.07	10:20	1.50	0.06	09:20	2.50	0.03	09:45	2.20	0.09
	2018-02-24	09:30	2.50	0.03	09:40	1.20	0.00	09:50	2.50	0.01	08:10	1.20	0.03	10:00	2.70	0.00	10:10	1.50	0.00



Table 7.11 Comparison of the observed and estimated nitrogen export with a statistical measurement under the validation period.

Year	Nitrogen export in kg/km ²		Statistical measurement		
	Observed data	Estimated data	PBIAS	R ²	Adjusted R ²
2016	313.43	222.04			
2017	479.78	257.68	33.39%	0.8951	0.79
2018	267.41	226.77			

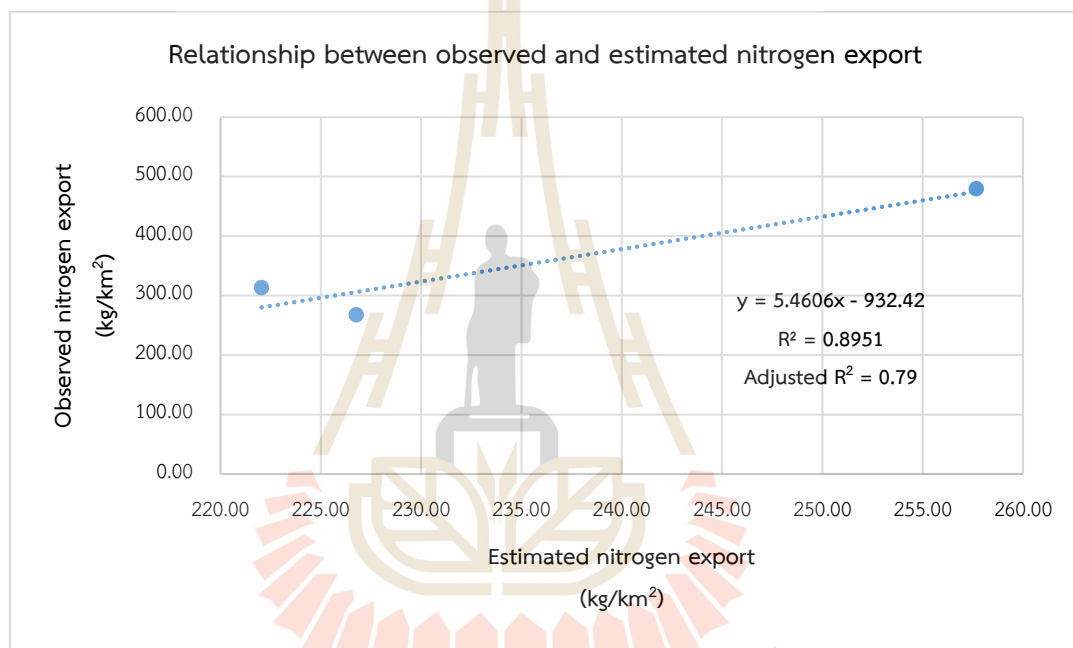


Figure 7.3 Relationship between the observed and estimated nitrogen export under the validation period.

Table 7.12 Comparison of the observed and estimated phosphorus export with a statistical measurement under the validation period.

Year	Phosphorus export in kg/km ²		Statistical measurement		
	Observed data	Estimated data	PBIAS	R ²	Adjusted R ²
2016	74.95	48.55			
2017	122.21	59.48	30.21%	0.643	0.29
2018	29.35	50.05			

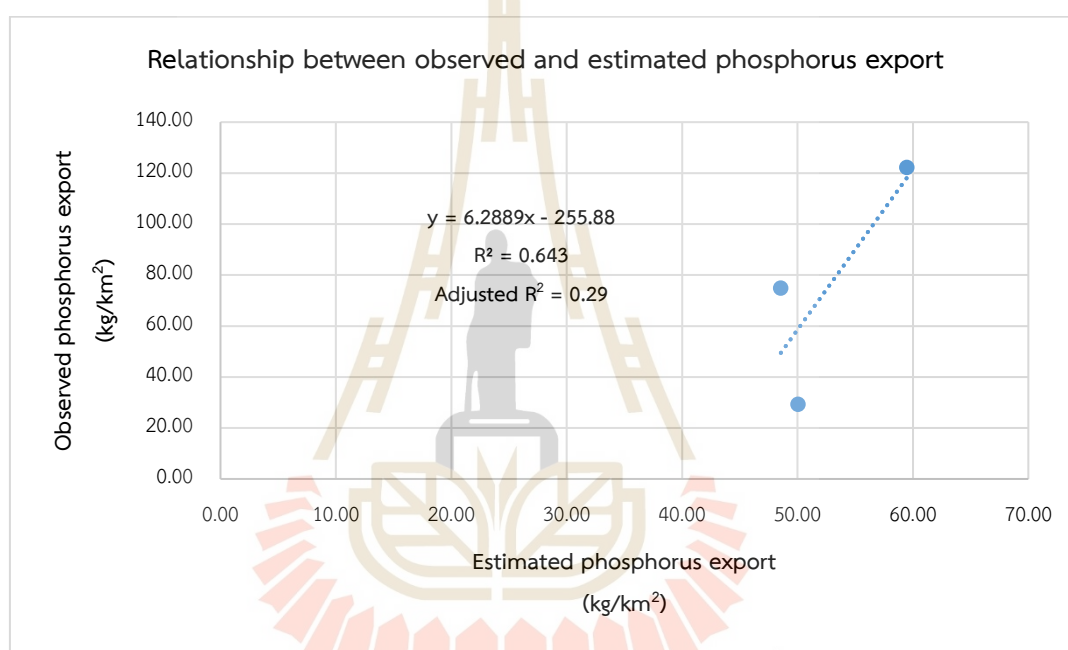


Figure 7.4 Relationship between the observed and estimated phosphorus export under the validation period.

As a result of nitrogen export, the PBIAS value is 33.39, which provide a good fit for calibrating the model in term of nitrogen export estimation as suggested by Moriasi et al. (2007) and Me, Abell, and Hamilton (2015), with a very good coefficient of determination between the observed and estimated nitrogen export with the value of 0.90. Likewise, in the case of phosphorus export, the PBIAS value is 30.21, which provide a good fit for calibrating the model in term of phosphorus export estimation as suggested by Moriasi et al. (2007) and Me, Abell, and Hamilton (2015), with a good coefficient of determination between the observed and estimated phosphorus export

with the value of 0.64.

However, the result values of observed and estimated nutrients in the calibration and validation period have fluctuated. The possible reason for this occurrence is the data uncertainty, which comes from several sources such as location and frequency of sample collection, instrument variability, and different observers. These effects were associated with the result of observed data. In contrast, the estimated data were systematically adjusted in the calibration process for optimal local parameters and applied in the validation process. Therefore, according to the statistical measurement, the nutrient delivery ratio model of the InVEST software suite can be accepted and further applied to estimate nitrogen and phosphorus export in an actual year and the three different scenarios between 2020 and 2029.

During the calibration and validation phases, it was observed that the precipitation data or runoff proxy is not presented as sensitive to the estimated data due to its calculation to modify load to account runoff potential by relating the precipitation per cell to the average over the raster, as suggested by Redhead et al. (2018). This finding is similar to the work of Benez-Secanho and Dwivedi (2019). They tested to verify the influence of rainfall modeling nutrient exports using the NDR model using three precipitation grids. They found that the precipitation grid had no significant effect when other grids replaced it for all watersheds combined, which means all precipitation grids used in their study yielded overall similar results.

In this study, the relationship between average annual rainfall data and the estimated total nitrogen and phosphorus data between 2011 and 2018 positively correlates with the R^2 value of 0.1492 and 0.0477, respectively (Figures 7.5 and 7.6). These values suggest an unsatisfactory fit between the average annual rainfall data and estimated total nitrogen and phosphorus data predicted data, as Moriasi et al. (2007) and Me, Abell, and Hamilton (2015) suggested. So, these findings reconfirm the insensitivity of rainfall on nutrient export, as mentioned earlier by quoted researchers.

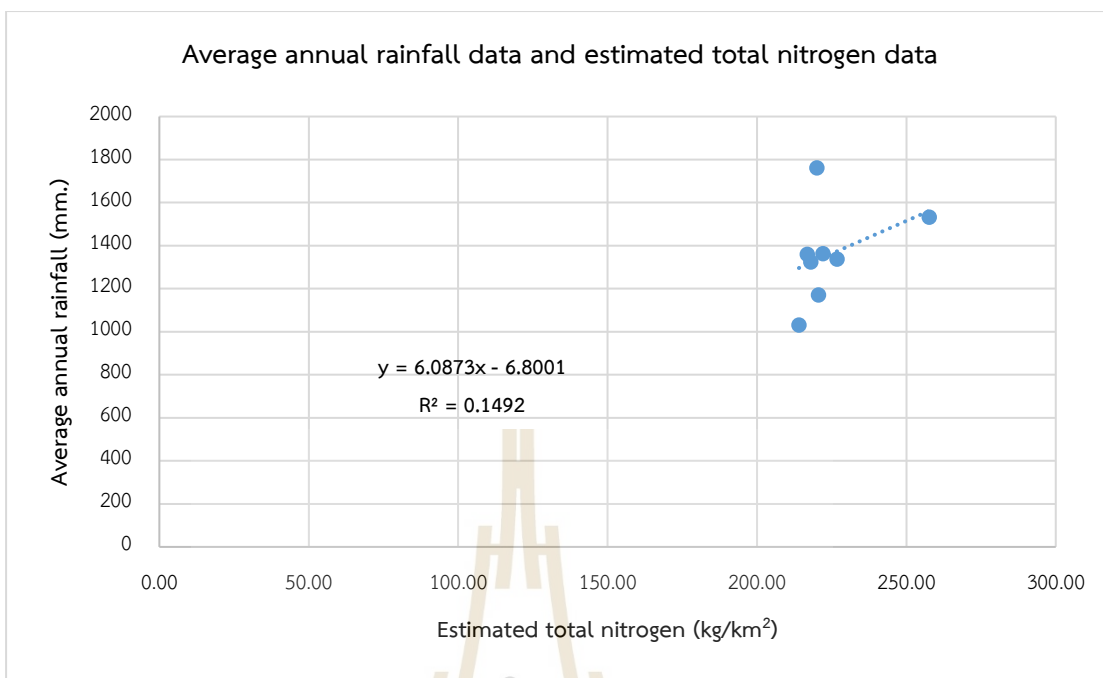


Figure 7.5 Relationship between average annual rainfall and estimated total nitrogen data between 2011 and 2018.

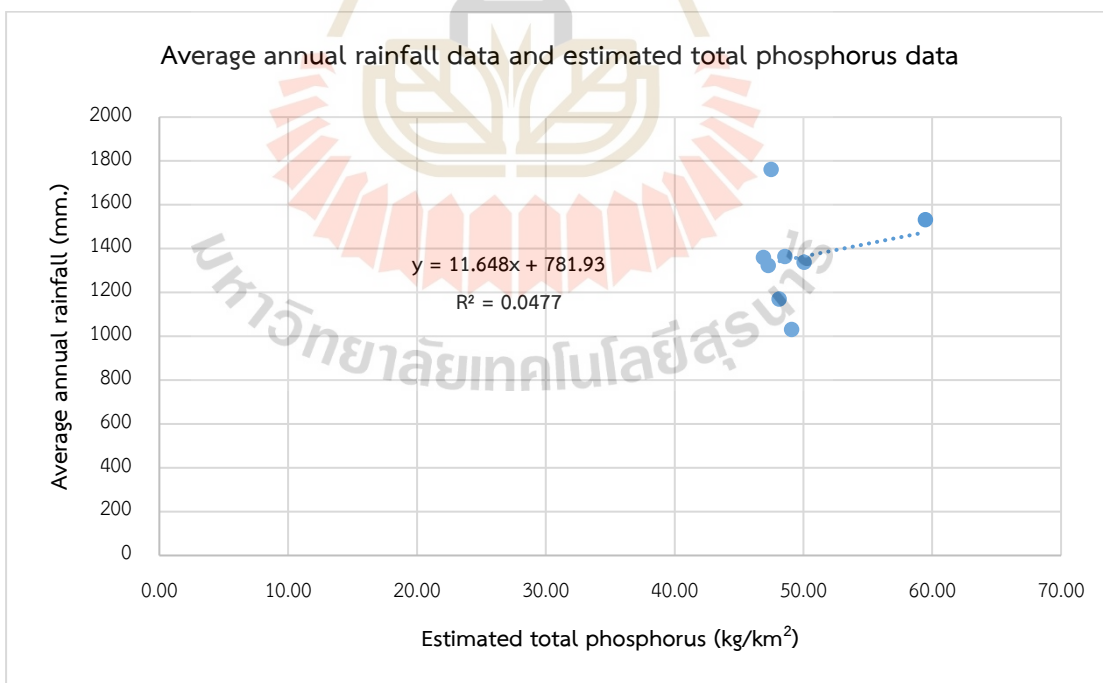
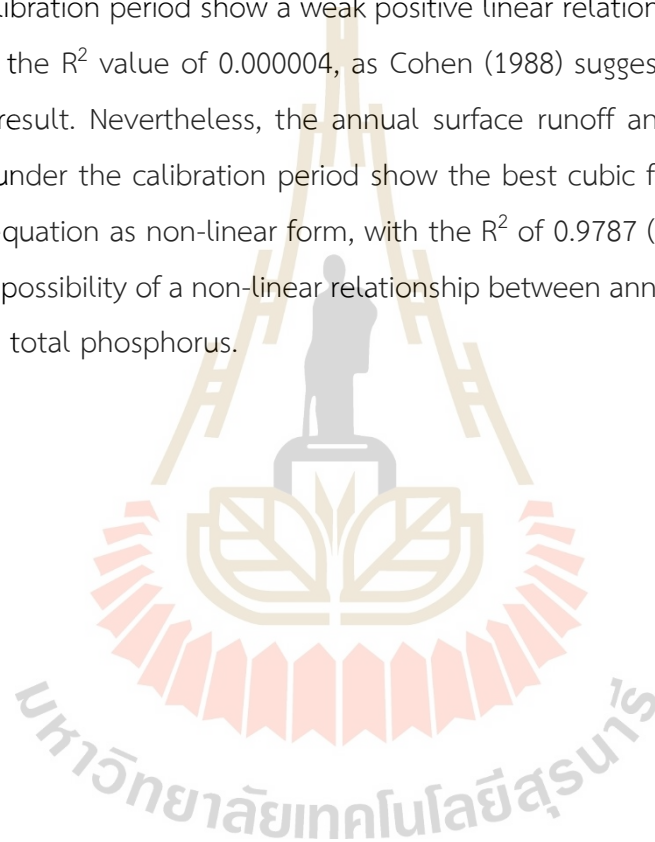


Figure 7.6 Relationship between average annual rainfall and estimated total phosphorus data between 2011 and 2018.

In addition, annual surface runoff, which was used to calculate the total nitrogen and phosphorus observed data under calibration period (2011-2015), was examined the linear relationship with both observed data, like total suspended solids (TSS) in the previous chapter. It was found that annual surface runoff and the observed total nitrogen show a strong positive linear relationship, with the R value of 0.6162 and the R^2 value of 0.3797, as suggested by Cohen (1988) (Figure 7.7). This finding shows an expected result. However, annual surface runoff and the observed total phosphorus under the calibration period show a weak positive linear relationship, with the R value of 0.002 and the R^2 value of 0.000004, as Cohen (1988) suggested. This finding is an unexpected result. Nevertheless, the annual surface runoff and the observed total phosphorus under the calibration period show the best cubic fit with the third-order polynomial equation as non-linear form, with the R^2 of 0.9787 (Figure 7.8). This result shows a high possibility of a non-linear relationship between annual surface runoff and the observed total phosphorus.



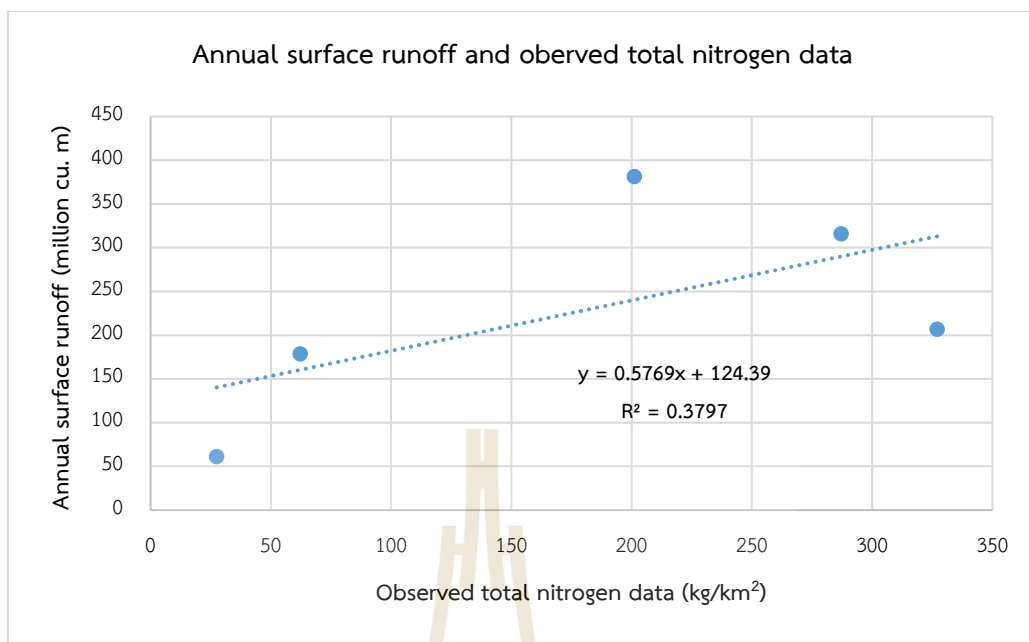


Figure 7.7 Relationship between annual surface runoff and observed total nitrogen data under calibration period.

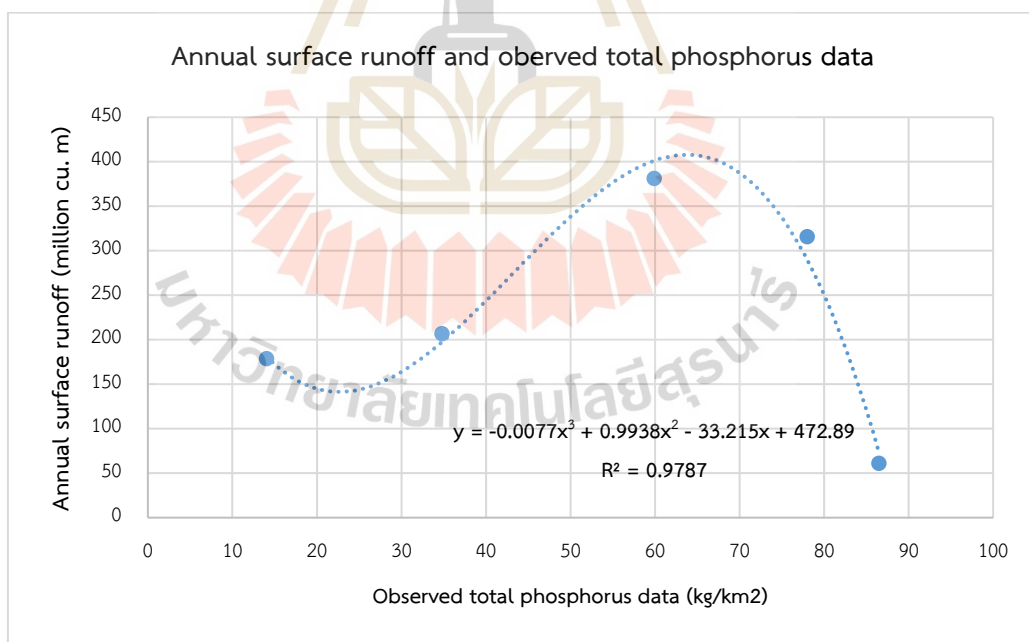


Figure 7.8 Relationship between annual surface runoff and observed total phosphorus data under calibration period.

7.3 Nutrient export estimation of actual LULC in 2019

The estimated total and average nutrient (nitrogen and phosphorus) load and export of actual LULC in 2019 are presented in Tables 7.13 and 7.14. The spatial distribution of nitrogen and phosphorus export in 2019 is shown in Figure 7.8. Moreover, the amount of nutrient load and export from each LULC type in 2019 are presented in Table 7.15.

As a result, the total nitrogen and phosphorus load in 2019 are about 1,422,800.13 kg (1,596.23 kg/km²) and 308,267.70 (345.84 kg/km²) and the total nitrogen and phosphorus export is about 193,307.56 kg. (216.87 kg/km²), and 41,978.66 kg. (47.10 kg/km²), respectively.

Table 7.13 Summary data on nitrogen and phosphorus loads of actual LULC in 2019.

(km ²)	(kg/year)		Average (kg/watershed in km ²)	
	Nitrogen load	Phosphorus load	Nitrogen load	Phosphorus load
891.35	1,422,800.13	308,267.70	1,596.23	345.84

Table 7.14 Summary data on nitrogen and phosphorus export of actual LULC in 2019.

(km ²)	(kg/year)		Average (kg/watershed in km ²)	
	Nitrogen export	Phosphorus export	Nitrogen export	Phosphorus export
891.35	193,307.56	41,978.66	216.87	47.10

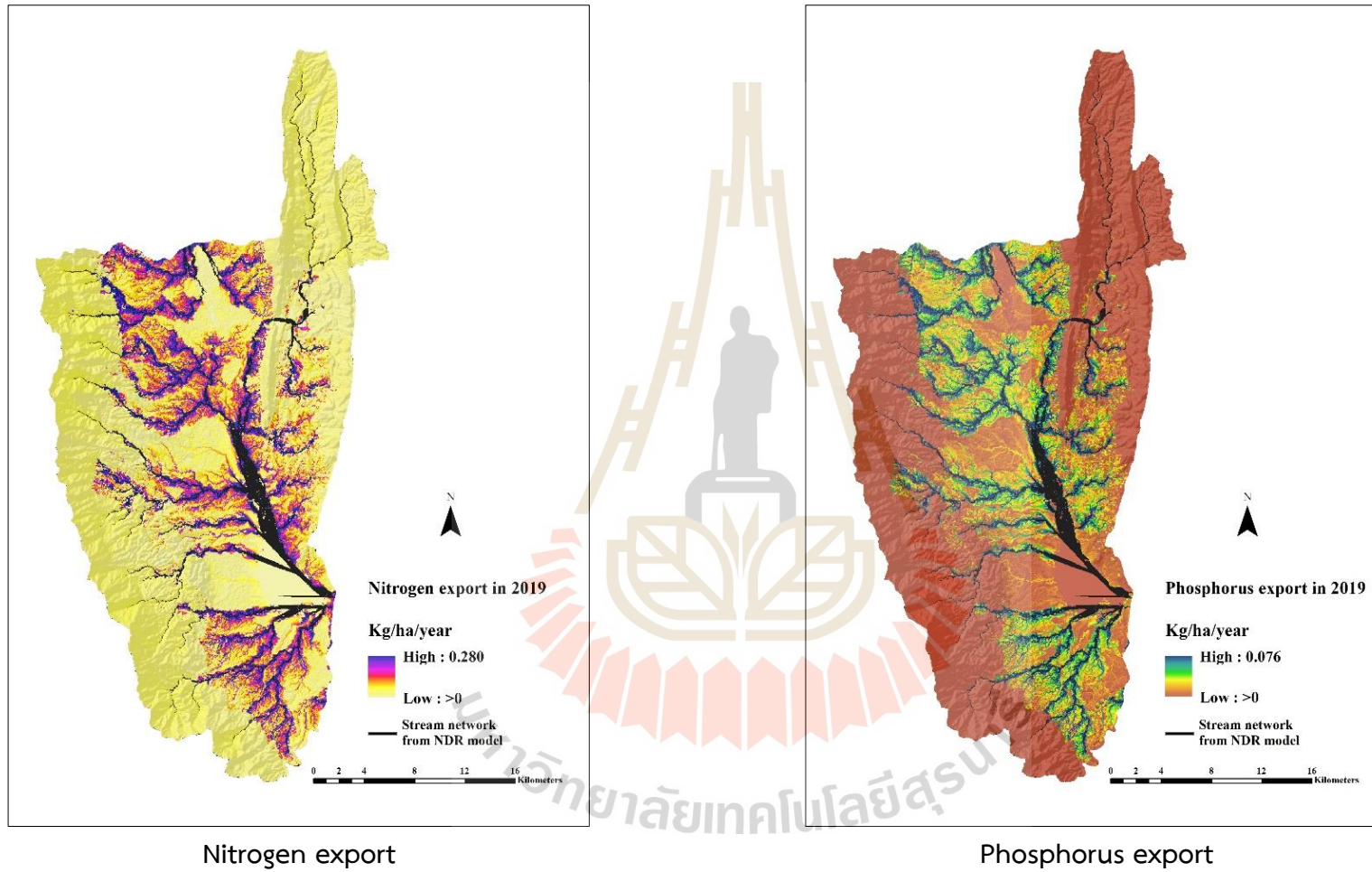


Figure 7.9 Spatial distribution of nitrogen and phosphorus export in 2019.

Table 7.15 Contribution of nutrient (nitrogen and phosphorus) load and export by LULC classes in 2019.

LULC types	Area	Nitrogen loads			Phosphorus loads			Nitrogen export			Phosphorus export		
	km ²	Total (kg.)	Average (kg/km ²)	%	Total (kg.)	Average (kg/km ²)	%	Total (kg.)	Average (kg/km ²)	%	Total (kg.)	Average (kg/km ²)	%
Urban and built-up area (UR)	33.10	75,731.67	2,288.30	12.95	4,216.32	127.40	3.46	8,965.07	270.89	11.54	501.27	15.15	3.02
Paddy field (PD)	220.74	719,516.10	3,259.53	18.44	195,391.18	885.15	24.02	95,828.98	434.12	18.49	26,135.18	118.40	23.59
Field crop (FC)	21.84	71,513.28	3,274.16	18.52	19,420.08	889.13	24.13	9,919.11	454.14	19.34	2,705.21	123.86	24.68
Para rubber (RB)	19.78	58,667.80	2,965.41	16.78	17,524.96	885.81	24.04	7,613.26	384.82	16.39	2,283.98	115.45	23.00
Perennial tree and orchard (PO)	79.22	234,719.25	2,962.74	16.76	70,114.17	885.01	24.02	33,756.21	426.09	18.15	10,126.86	127.83	25.47
Forest land (FO)	436.91	233,258.91	533.88	3.02	1,419.37	3.25	0.09	34,402.68	78.74	3.35	210.24	0.48	0.10
Water body (WB)	33.37	9.85	0.30	0.00	9.80	0.29	0.01	2.22	0.07	0.00	2.22	0.07	0.01
Rangeland (RL)	27.26	16,281.58	597.22	3.38	89.17	3.27	0.09	1,860.71	68.25	2.91	10.23	0.38	0.07
Wetland (WL)	16.41	9,863.64	601.21	3.40	81.84	4.99	0.14	398.40	24.28	1.03	3.32	0.20	0.04
Miscellaneous land (ML)	2.71	3,238.06	1,193.66	6.75	0.81	0.30	0.01	560.91	206.77	8.81	0.14	0.05	0.01
Total	891.35	1,422,800.13		100.00	308,267.70		100.00	193,307.56		100.00	41,978.66		100.00



According to zonal statistic operation between nitrogen and phosphorus loads with LULC data in 2019, it revealed that the highest total nitrogen and phosphorus load are found on paddy field with a value of 719,516.10 kg. (3,259.53 kg/km²) and 195,391.18 kg. (885.15 kg/km²), respectively, while the lowest total nitrogen load occurs on the waterbody with the value of 9.85 kg. (0.30 kg/km²) and the lowest total phosphorus load occurs on miscellaneous land with the value of 0.81 (0.30 kg/km²), respectively. However, the highest average nitrogen and phosphorus load appear on field crop with values of 3,274.16 kg/km² (18.52%) and 889.13 kg/km² (24.13%).

In the meantime, the highest total nitrogen and phosphorus exports appear on the paddy field with a value of 95,828.98 kg. (434.12 kg/km²) and 26,135.18 kg. (118.40 kg/km²), respectively. In contrast, the lowest total nitrogen export comes from waterbody with a value of 2.22 (0.07 kg/km²), and the lowest total phosphorus export comes from miscellaneous land with a value of 0.14 (0.05 kg/km²). However, the highest average nitrogen and phosphorus export appeared on field crop and perennial trees and orchard with values of 454.14 kg/km² (19.34%) and 127.83 kg/km² (25.47%), respectively. This result is similar to Raji, Odunuga, and Fasona (2020), who found that cropland and agroforestry influenced roughly 90% of the nutrient exported while water bodies were identified as sinks. This finding suggests that the change of LULC types associated with the parameters in the biophysical table affects nitrogen and phosphorus export.

7.4 Nutrient export estimation of predictive LULC of Scenario I

Estimating total and average nitrogen and phosphorus export of predictive LULC between 2020 and 2029 under Scenario I: Trend of LULC evolution is presented in Table 7.16.

Table 7.16 Estimation of nitrogen and phosphorus export between 2020 and 2029 under Scenario I.

Year	Area km ²	Nitrogen export		Phosphorus export	
		Total (kg)	Average (kg/km ²)	Total (kg)	Average (kg/km ²)
2020	891.35	197,972.93	222.10	43,358.11	48.64
2021	891.35	199,580.02	223.91	43,832.43	49.18
2022	891.35	200,858.16	225.34	44,196.29	49.58
2023	891.35	202,275.64	226.93	44,619.00	50.06
2024	891.35	203,395.90	228.19	44,951.18	50.43
2025	891.35	205,172.77	230.18	45,494.30	51.04
2026	891.35	206,743.37	231.94	45,966.11	51.57
2027	891.35	207,795.18	233.12	46,273.02	51.91
2028	891.35	209,325.14	234.84	46,740.48	52.44
2029	891.35	210,907.86	236.62	47,221.47	52.98

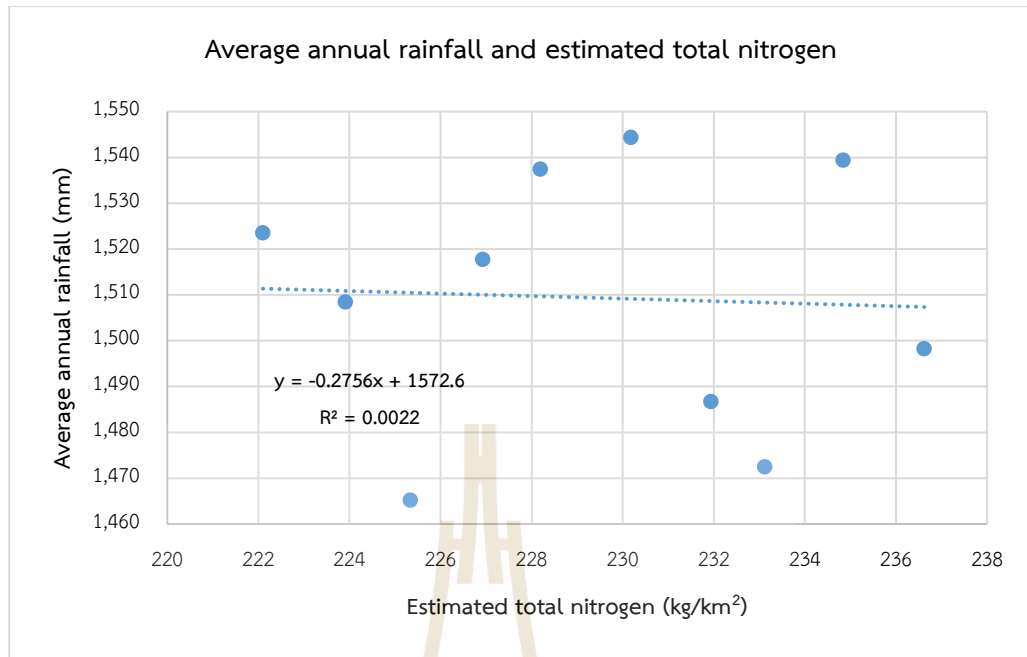
As a result, it was found that the highest total and average nitrogen export under Scenario I (Trend of LULC evolution) are 210,907.86 kg. and 236.62 kg/km² occurring in 2029, while the lowest total and average nitrogen export are 197,972.93 kg. and 222.10 kg/km² occurring in 2020. Likewise, the highest total and average phosphorus export under this scenario are 47,221.47 kg. and 52.98 kg/km² occurring in 2029, while the lowest total and average phosphorus export are 43,358.11 kg. and 48.64 kg/km² occurring in 2020. These results indicate that the change of LULC types and areas affects parameters in the biophysical table, which leads to different nitrogen and phosphorus export. In contrast, the annual rainfall as runoff proxy is not major influencing nitrogen and phosphorus export. Table 7.17 shows the basic statistics of the predictive annual rainfall between 2020 and 2029, while Figure 7.10 shows the

relationship between average annual rainfall and estimated total nitrogen and phosphorus. As a result, they indicate a poor fit between average rainfall and an estimated nutrient (TN and TP) with the R^2 value of 0.0022 and 0.0021, as expected.

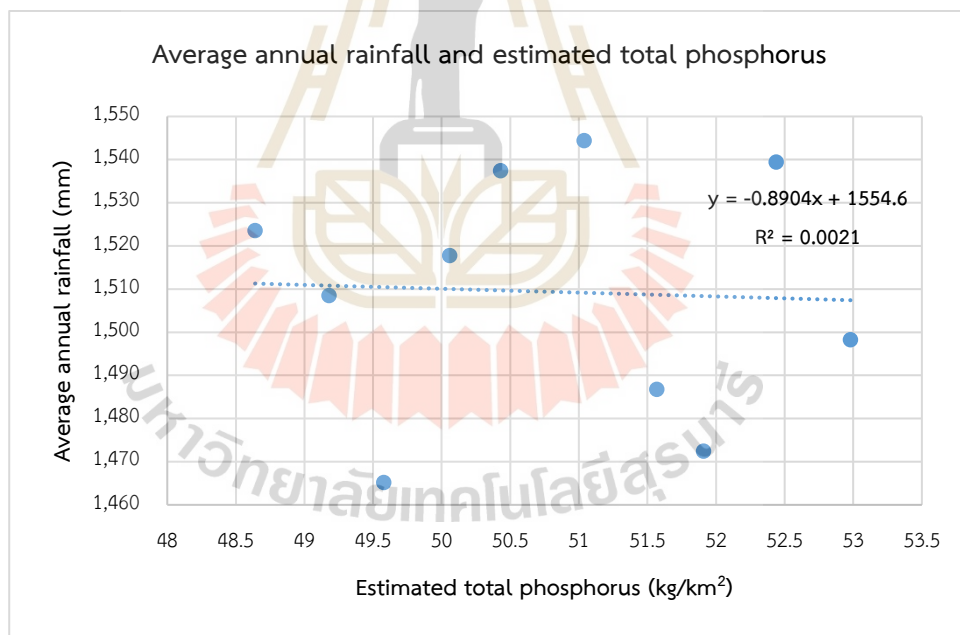
Table 7.17 Basic statistics of predictive annual rainfall between 2020 and 2029.

Year	Annual rainfall (mm.)				
	MIN	MAX	MEAN	RANGE	STD
2020	1,357.40	1,734.31	1,523.53	376.91	107.30
2021	1,345.67	1,748.02	1,508.50	402.34	111.35
2022	1,365.92	1,579.98	1,465.20	214.05	84.68
2023	1,371.04	1,712.94	1,517.76	341.90	93.16
2024	1,405.15	1,668.42	1,537.45	263.27	101.91
2025	1,434.30	1,774.74	1,544.38	340.44	99.52
2026	1,338.02	1,607.98	1,486.75	269.95	78.62
2027	1,387.74	1,572.54	1,472.48	184.80	55.14
2028	1,471.20	1,629.70	1,539.43	158.50	50.77
2029	1,426.87	1,679.65	1,498.28	252.77	73.75

The contribution of the predictive LULC type of Scenario I (Trend of LULC evolution) on nutrient (nitrogen and phosphorus) load and export between 2020 and 2029 are summarized in Tables 7.18 to 7.27 and the spatial distribution of nitrogen and phosphorus export of the predictive LULC between 2020 and 2029 of Scenario I (Trend of LULC evolution) is displayed in Figures 7.11 to 7.20.



(a)



(b)

Figure 7.10 The relationship between average annual rainfall and estimated nutrient: (a) total nitrogen and (b) total phosphorus.

Table 7.18 Contribution of nutrient (nitrogen and phosphorus) load and export by LULC classes in 2020 under Scenario I.

LULC types	Area	Nitrogen loads			Phosphorus loads			Nitrogen export			Phosphorus export		
	km ²	Total (kg.)	Average (kg/km ²)	%	Total (kg.)	Average (kg/km ²)	%	Total (kg.)	Average (kg/km ²)	%	Total (kg.)	Average (kg/km ²)	%
Urban and built-up area (UR)	33.45	77,838.24	2,326.84	13.02	4,352.65	130.12	3.47	9,569.74	286.07	11.82	535.08	16.00	3.09
Paddy field (PD)	219.73	724,853.82	3,298.91	18.46	197,705.89	899.79	24.00	98,331.00	447.52	18.49	26,817.54	122.05	23.57
Field crop (FC)	21.94	72,578.96	3,308.59	18.51	19,796.11	902.43	24.07	10,367.46	472.61	19.53	2,827.49	128.89	24.90
Para rubber (RB)	20.65	62,140.48	3,009.01	16.84	18,643.89	902.79	24.08	8,307.62	402.28	16.62	2,492.29	120.68	23.31
Perennial tree and orchard (PO)	81.17	244,016.62	3,006.12	16.82	73,211.83	901.92	24.06	34,879.74	429.70	17.76	10,463.92	128.91	24.90
Forest land (FO)	433.27	234,014.02	540.11	3.02	1,430.22	3.30	0.09	33,570.02	77.48	3.20	205.15	0.47	0.09
Water body (WB)	34.18	10.26	0.30	0.00	10.26	0.30	0.01	2.39	0.07	0.00	2.39	0.07	0.01
Rangeland (RL)	27.86	16,686.56	598.85	3.35	91.78	3.29	0.09	1,969.50	70.68	2.92	10.83	0.39	0.08
Wetland (WL)	16.31	9,772.76	599.15	3.35	81.45	4.99	0.13	391.79	24.02	0.99	3.26	0.20	0.04
Miscellaneous land (ML)	2.79	3,299.18	1,184.54	6.63	0.82	0.30	0.01	583.68	209.56	8.66	0.15	0.05	0.01
Total	891.35	1,445,210.91		100.00	315,324.91		100.00	197,972.93		100.00	43,358.11		100.00

Table 7.19 Contribution of nutrient (nitrogen and phosphorus) load and export by LULC classes in 2021 under Scenario I.

LULC types	Area	Nitrogen loads			Phosphorus loads			Nitrogen export			Phosphorus export		
	km ²	Total (kg.)	Average (kg/km ²)	%	Total (kg.)	Average (kg/km ²)	%	Total (kg.)	Average (kg/km ²)	%	Total (kg.)	Average (kg/km ²)	%
Urban and built-up area (UR)	33.83	78,703.18	2,326.61	13.03	4,400.70	130.09	3.47	9,681.35	286.20	11.73	541.32	16.00	3.06
Paddy field (PD)	218.73	721,333.22	3,297.86	18.47	196,731.19	899.43	24.02	98,030.19	448.18	18.38	26,735.51	122.23	23.35
Field crop (FC)	22.04	72,881.80	3,306.19	18.52	19,877.25	901.71	24.08	10,666.96	483.89	19.84	2,909.17	131.97	25.21
Para rubber (RB)	21.53	64,576.69	2,999.87	16.80	19,373.40	899.98	24.03	8,770.41	407.42	16.70	2,631.12	122.23	23.35
Perennial tree and orchard (PO)	83.14	249,787.81	3,004.39	16.83	74,937.85	901.34	24.07	35,979.95	432.76	17.74	10,793.98	129.83	24.80
Forest land (FO)	429.62	232,044.50	540.11	3.02	1,418.08	3.30	0.09	33,428.80	77.81	3.19	204.29	0.48	0.09
Water body (WB)	34.99	10.50	0.30	0.00	10.50	0.30	0.01	2.47	0.07	0.00	2.47	0.07	0.01
Rangeland (RL)	28.48	17,081.12	599.72	3.36	93.95	3.30	0.09	2,039.13	71.59	2.94	11.22	0.39	0.08
Wetland (WL)	16.10	9,646.00	599.00	3.35	80.38	4.99	0.13	383.03	23.79	0.98	3.19	0.20	0.04
Miscellaneous land (ML)	2.88	3,405.42	1,181.33	6.62	0.85	0.30	0.01	597.73	207.35	8.50	0.15	0.05	0.01
Total	891.35	1,449,470.27		100.00	316,924.14		100.00	199,580.02		100.00	43,832.43		100.00

Table 7.20 Contribution of nutrient (nitrogen and phosphorus) load and export by LULC classes in 2022 under Scenario I.

LULC types	Area	Nitrogen loads			Phosphorus loads			Nitrogen export			Phosphorus export		
	km ²	Total (kg.)	Average (kg/km ²)	%	Total (kg.)	Average (kg/km ²)	%	Total (kg.)	Average (kg/km ²)	%	Total (kg.)	Average (kg/km ²)	%
Urban and built-up area (UR)	34.19	79,535.60	2,326.29	13.03	4,446.12	130.04	3.48	9,833.99	287.63	11.72	549.86	16.08	3.06
Paddy field (PD)	217.73	717,606.19	3,295.93	18.47	195,665.53	898.68	24.02	97,562.67	448.10	18.26	26,608.00	122.21	23.23
Field crop (FC)	22.13	73,268.62	3,311.34	18.55	19,977.73	902.88	24.13	10,691.71	483.21	19.69	2,915.92	131.78	25.05
Para rubber (RB)	22.42	67,142.17	2,994.87	16.78	20,137.99	898.25	24.00	9,275.57	413.74	16.86	2,782.67	124.12	23.60
Perennial tree and orchard (PO)	85.12	255,450.58	3,000.94	16.81	76,617.46	900.07	24.05	37,062.78	435.40	17.74	11,118.83	130.62	24.83
Forest land (FO)	425.96	229,950.69	539.83	3.02	1,404.93	3.30	0.09	33,317.33	78.22	3.19	203.61	0.48	0.09
Water body (WB)	35.78	10.73	0.30	0.00	10.73	0.30	0.01	2.53	0.07	0.00	2.53	0.07	0.01
Rangeland (RL)	29.10	17,443.47	599.49	3.36	95.92	3.30	0.09	2,101.78	72.23	2.94	11.56	0.40	0.08
Wetland (WL)	15.95	9,547.79	598.66	3.35	79.55	4.99	0.13	377.08	23.64	0.96	3.14	0.20	0.04
Miscellaneous land (ML)	2.98	3,516.87	1,180.07	6.61	0.88	0.29	0.01	632.70	212.30	8.65	0.16	0.05	0.01
Total	891.35	1,453,472.70		100.00	318,436.83		100.00	200,858.16		100.00	44,196.29		100.00

Table 7.21 Contribution of nutrient (nitrogen and phosphorus) load and export by LULC classes in 2023 under Scenario I.

LULC types	Area	Nitrogen loads			Phosphorus loads			Nitrogen export			Phosphorus export		
	km ²	Total (kg.)	Average (kg/km ²)	%	Total (kg.)	Average (kg/km ²)	%	Total (kg.)	Average (kg/km ²)	%	Total (kg.)	Average (kg/km ²)	%
Urban and built-up area (UR)	34.61	80,569.31	2,327.76	13.03	4,504.93	130.15	3.47	10,050.75	290.38	11.73	561.98	16.24	3.06
Paddy field (PD)	216.77	714,882.98	3,297.92	18.47	194,967.35	899.43	24.01	97,212.58	448.46	18.12	26,512.52	122.31	23.07
Field crop (FC)	22.23	73,636.84	3,312.27	18.55	20,082.70	903.34	24.11	10,838.85	487.54	19.70	2,956.05	132.97	25.08
Para rubber (RB)	23.26	69,769.55	2,999.34	16.79	20,930.79	899.80	24.02	9,772.02	420.09	16.97	2,931.61	126.03	23.77
Perennial tree and orchard (PO)	87.04	261,422.50	3,003.61	16.82	78,426.45	901.08	24.05	38,123.14	438.02	17.70	11,436.94	131.40	24.79
Forest land (FO)	422.30	228,068.34	540.06	3.02	1,393.75	3.30	0.09	33,076.31	78.32	3.16	202.13	0.48	0.09
Water body (WB)	36.57	10.97	0.30	0.00	10.97	0.30	0.01	2.61	0.07	0.00	2.61	0.07	0.01
Rangeland (RL)	29.70	17,799.88	599.33	3.36	97.90	3.30	0.09	2,161.67	72.78	2.94	11.89	0.40	0.08
Wetland (WL)	15.79	9,456.69	598.96	3.35	78.81	4.99	0.13	373.01	23.63	0.95	3.11	0.20	0.04
Miscellaneous land (ML)	3.08	3,634.28	1,179.88	6.61	0.91	0.29	0.01	664.69	215.79	8.72	0.17	0.05	0.01
Total	891.35	1,459,251.35		100.00	320,494.56		100.00	202,275.64		100.00	44,619.00		100.00

Table 7.22 Contribution of nutrient (nitrogen and phosphorus) load and export by LULC classes in 2024 under Scenario I.

LULC types	Area	Nitrogen loads			Phosphorus loads			Nitrogen export			Phosphorus export		
	km ²	Total (kg.)	Average (kg/km ²)	%	Total (kg.)	Average (kg/km ²)	%	Total (kg.)	Average (kg/km ²)	%	Total (kg.)	Average (kg/km ²)	%
Urban and built-up area (UR)	34.99	81,426.01	2,326.79	13.04	4,551.78	130.07	3.47	10,185.97	291.07	11.70	569.54	16.27	3.05
Paddy field (PD)	215.77	711,331.96	3,296.75	18.47	193,953.88	898.90	24.01	96,668.91	448.02	18.01	26,364.25	122.19	22.92
Field crop (FC)	22.31	73,786.80	3,307.48	18.53	20,118.93	901.83	24.09	10,978.76	492.12	19.78	2,994.21	134.21	25.17
Para rubber (RB)	24.10	72,306.29	2,999.74	16.81	21,686.77	899.71	24.04	10,231.68	424.48	17.06	3,069.50	127.34	23.89
Perennial tree and orchard (PO)	88.95	267,063.45	3,002.36	16.82	80,100.14	900.49	24.06	39,114.33	439.73	17.67	11,734.30	131.92	24.74
Forest land (FO)	418.63	225,963.36	539.76	3.02	1,380.56	3.30	0.09	32,943.41	78.69	3.16	201.32	0.48	0.09
Water body (WB)	37.36	11.21	0.30	0.00	11.20	0.30	0.01	2.66	0.07	0.00	2.66	0.07	0.01
Rangeland (RL)	30.29	18,133.65	598.68	3.35	99.71	3.29	0.09	2,205.54	72.82	2.93	12.13	0.40	0.08
Wetland (WL)	15.76	9,433.04	598.60	3.35	78.59	4.99	0.13	371.57	23.58	0.95	3.10	0.20	0.04
Miscellaneous land (ML)	3.19	3,744.72	1,175.65	6.59	0.94	0.29	0.01	693.06	217.59	8.74	0.17	0.05	0.01
Total	891.35	1,463,200.49		100.00	321,982.50		100.00	203,395.90		100.00	44,951.18		100.00

Table 7.23 Contribution of nutrient (nitrogen and phosphorus) load and export by LULC classes in 2025 under Scenario I.

LULC types	Area	Nitrogen loads			Phosphorus loads			Nitrogen export			Phosphorus export		
	km ²	Total (kg.)	Average (kg/km ²)	%	Total (kg.)	Average (kg/km ²)	%	Total (kg.)	Average (kg/km ²)	%	Total (kg.)	Average (kg/km ²)	%
Urban and built-up area (UR)	35.39	82,415.42	2,328.61	13.04	4,608.51	130.21	3.48	10,365.65	292.88	11.65	579.58	16.38	3.03
Paddy field (PD)	214.81	708,612.41	3,298.86	18.48	193,271.98	899.76	24.02	96,384.95	448.71	17.85	26,286.80	122.38	22.68
Field crop (FC)	22.43	74,150.52	3,306.37	18.52	20,224.34	901.80	24.07	11,268.05	502.44	19.99	3,073.10	137.03	25.39
Para rubber (RB)	24.99	74,989.83	3,000.88	16.81	22,498.58	900.33	24.04	10,794.93	431.98	17.19	3,238.48	129.59	24.02
Perennial tree and orchard (PO)	90.94	273,294.70	3,005.09	16.83	81,994.37	901.59	24.07	40,327.26	443.43	17.64	12,098.18	133.03	24.65
Forest land (FO)	415.00	224,148.15	540.11	3.03	1,369.89	3.30	0.09	32,679.39	78.75	3.13	199.71	0.48	0.09
Water body (WB)	38.16	11.46	0.30	0.00	11.46	0.30	0.01	2.74	0.07	0.00	2.74	0.07	0.01
Rangeland (RL)	30.91	18,523.18	599.17	3.36	101.88	3.30	0.09	2,272.42	73.51	2.92	12.50	0.40	0.07
Wetland (WL)	15.44	9,244.85	598.91	3.35	77.05	4.99	0.13	363.29	23.53	0.94	3.03	0.20	0.04
Miscellaneous land (ML)	3.28	3,854.14	1,175.86	6.59	0.96	0.29	0.01	714.09	217.86	8.67	0.18	0.05	0.01
Total	891.35	1,469,244.65		100.00	324,159.03		100.00	205,172.77		100.00	45,494.30		100.00

Table 7.24 Contribution of nutrient (nitrogen and phosphorus) load and export by LULC classes in 2026 under Scenario I.

LULC types	Area	Nitrogen loads			Phosphorus loads			Nitrogen export			Phosphorus export		
	km ²	Total (kg.)	Average (kg/km ²)	%	Total (kg.)	Average (kg/km ²)	%	Total (kg.)	Average (kg/km ²)	%	Total (kg.)	Average (kg/km ²)	%
Urban and built-up area (UR)	35.76	83,230.15	2,327.63	13.04	4,654.23	130.16	3.48	10,500.25	293.65	11.56	587.11	16.42	3.01
Paddy field (PD)	213.81	705,411.97	3,299.29	18.48	192,405.95	899.90	24.03	95,970.54	448.86	17.67	26,173.78	122.42	22.42
Field crop (FC)	22.51	74,351.62	3,302.45	18.50	20,279.91	900.77	24.05	11,660.16	517.91	20.39	3,180.04	141.25	25.87
Para rubber (RB)	25.86	77,563.65	2,999.74	16.80	23,271.62	900.02	24.03	11,296.48	436.89	17.20	3,388.94	131.07	24.00
Perennial tree and orchard (PO)	92.89	279,244.27	3,006.21	16.84	83,782.37	901.96	24.08	41,396.47	445.66	17.54	12,418.94	133.70	24.48
Forest land (FO)	411.35	222,229.71	540.24	3.03	1,358.22	3.30	0.09	32,479.05	78.96	3.11	198.48	0.48	0.09
Water body (WB)	38.97	11.70	0.30	0.00	11.70	0.30	0.01	2.80	0.07	0.00	2.80	0.07	0.01
Rangeland (RL)	31.52	18,878.44	598.89	3.35	103.84	3.29	0.09	2,332.40	73.99	2.91	12.83	0.41	0.07
Wetland (WL)	15.30	9,161.58	598.66	3.35	76.35	4.99	0.13	359.08	23.46	0.92	2.99	0.20	0.04
Miscellaneous land (ML)	3.38	3,986.35	1,179.31	6.61	1.00	0.29	0.01	746.14	220.73	8.69	0.19	0.06	0.01
Total	891.35	1,474,069.44		100.00	325,945.20		100.00	206743.37		100.00	45,966.11		100.00

Table 7.25 Contribution of nutrient (nitrogen and phosphorus) load and export by LULC classes in 2027 under Scenario I.

LULC types	Area	Nitrogen loads			Phosphorus loads			Nitrogen export			Phosphorus export		
	km ²	Total (kg.)	Average (kg/km ²)	%	Total (kg.)	Average (kg/km ²)	%	Total (kg.)	Average (kg/km ²)	%	Total (kg.)	Average (kg/km ²)	%
Urban and built-up area (UR)	36.15	84,067.10	2,325.67	13.04	4,699.44	130.01	3.48	10,652.06	294.68	11.56	595.60	16.48	3.01
Paddy field (PD)	212.79	701,546.95	3,296.94	18.48	191,286.86	898.96	24.03	95,339.54	448.05	17.58	26,001.69	122.20	22.30
Field crop (FC)	22.58	74,642.44	3,306.19	18.53	20,352.34	901.48	24.10	11,760.67	520.92	20.44	3,207.45	142.07	25.92
Para rubber (RB)	26.69	79,906.10	2,993.37	16.78	23,966.30	897.80	24.00	11,729.97	439.42	17.25	3,518.99	131.83	24.05
Perennial tree and orchard (PO)	94.82	284,744.75	3,002.95	16.83	85,403.72	900.68	24.08	42,441.34	447.59	17.57	12,732.40	134.28	24.50
Forest land (FO)	407.68	220,064.80	539.80	3.03	1,344.53	3.30	0.09	32,364.94	79.39	3.12	197.79	0.49	0.09
Water body (WB)	39.76	11.93	0.30	0.00	11.93	0.30	0.01	2.84	0.07	0.00	2.84	0.07	0.01
Rangeland (RL)	32.13	19,231.98	598.48	3.36	105.75	3.29	0.09	2,378.75	74.02	2.91	13.08	0.41	0.07
Wetland (WL)	15.27	9,138.06	598.29	3.35	76.13	4.98	0.13	357.62	23.41	0.92	2.98	0.20	0.04
Miscellaneous land (ML)	3.48	4,093.26	1,176.14	6.59	1.02	0.29	0.01	767.43	220.51	8.65	0.19	0.06	0.01
Total	891.35	1,477,447.37		100.00	327,248.02		100.00	207,795.18		100.00	46,273.02		100.00

Table 7.26 Contribution of nutrient (nitrogen and phosphorus) load and export by LULC classes in 2028 under Scenario I.

LULC types	Area	Nitrogen loads			Phosphorus loads			Nitrogen export			Phosphorus export		
	km ²	Total (kg.)	Average (kg/km ²)	%	Total (kg.)	Average (kg/km ²)	%	Total (kg.)	Average (kg/km ²)	%	Total (kg.)	Average (kg/km ²)	%
Urban and built-up area (UR)	36.50	84,921.63	2,326.62	13.04	4,747.69	130.07	3.47	10,810.83	296.19	11.54	604.48	16.56	3.00
Paddy field (PD)	211.82	698,547.48	3,297.88	18.48	190,488.08	899.30	24.02	94,989.26	448.45	17.47	25,906.16	122.30	22.14
Field crop (FC)	22.69	75,037.16	3,306.83	18.53	20,462.01	901.74	24.09	11,988.06	528.30	20.58	3,269.47	144.08	26.08
Para rubber (RB)	27.57	82,640.42	2,996.99	16.79	24,788.89	898.98	24.02	12,238.63	443.84	17.29	3,671.59	133.15	24.10
Perennial tree and orchard (PO)	96.77	290,688.28	3,003.93	16.83	87,195.10	901.06	24.07	43,576.52	450.31	17.54	13,072.96	135.09	24.46
Forest land (FO)	404.03	218,133.46	539.90	3.03	1,332.86	3.30	0.09	32,143.36	79.56	3.10	196.43	0.49	0.09
Water body (WB)	40.58	12.17	0.30	0.00	12.17	0.30	0.01	2.90	0.07	0.00	2.90	0.07	0.01
Rangeland (RL)	32.72	19,579.86	598.32	3.35	107.68	3.29	0.09	2,428.77	74.22	2.89	13.36	0.41	0.07
Wetland (WL)	15.10	9,042.51	598.80	3.36	75.34	4.99	0.13	352.82	23.36	0.91	2.94	0.19	0.04
Miscellaneous land (ML)	3.57	4,200.04	1,177.22	6.60	1.05	0.29	0.01	793.99	222.55	8.67	0.20	0.06	0.01
Total	891.35	1,482,803.01		100.00	329,210.86		100.00	209,325.14		100.00	46,740.48		100.00

Table 7.27 Contribution of nutrient (nitrogen and phosphorus) load and export by LULC classes in 2029 under Scenario I.

LULC types	Area	Nitrogen loads			Phosphorus loads			Nitrogen export			Phosphorus export		
	km ²	Total (kg.)	Average (kg/km ²)	%	Total (kg.)	Average (kg/km ²)	%	Total (kg.)	Average (kg/km ²)	%	Total (kg.)	Average (kg/km ²)	%
Urban and built-up area (UR)	36.90	85,894.64	2,327.60	13.04	4,802.84	130.15	3.48	11,001.97	298.14	11.55	615.16	16.67	3.00
Paddy field (PD)	210.84	695,589.01	3,299.14	18.48	189,711.03	899.79	24.03	94,685.94	449.09	17.40	25,823.44	122.48	22.01
Field crop (FC)	22.81	75,312.48	3,301.86	18.50	20,540.30	900.53	24.05	12,143.56	532.40	20.63	3,311.88	145.20	26.09
Para rubber (RB)	28.45	85,344.75	2,999.34	16.80	25,604.09	899.83	24.03	12,808.26	450.13	17.44	3,842.48	135.04	24.27
Perennial tree and orchard (PO)	98.75	296,739.54	3,005.05	16.84	89,024.18	901.54	24.08	44,712.64	452.80	17.54	13,413.79	135.84	24.41
Forest land (FO)	400.39	216,235.73	540.06	3.03	1,321.48	3.30	0.09	31,910.69	79.70	3.09	195.01	0.49	0.09
Water body (WB)	41.35	12.42	0.30	0.00	12.42	0.30	0.01	2.97	0.07	0.00	2.97	0.07	0.01
Rangeland (RL)	33.36	19,971.65	598.72	3.35	109.85	3.29	0.09	2,485.70	74.52	2.89	13.67	0.41	0.07
Wetland (WL)	14.82	8,872.27	598.63	3.35	73.94	4.99	0.13	343.78	23.20	0.90	2.86	0.19	0.03
Miscellaneous land (ML)	3.68	4,333.26	1,179.03	6.61	1.08	0.29	0.01	812.35	221.03	8.56	0.20	0.06	0.01
Total	891.35	1,488,305.75		100.00	331,201.20		100.00	210,907.86		100.00	47,221.47		100.00

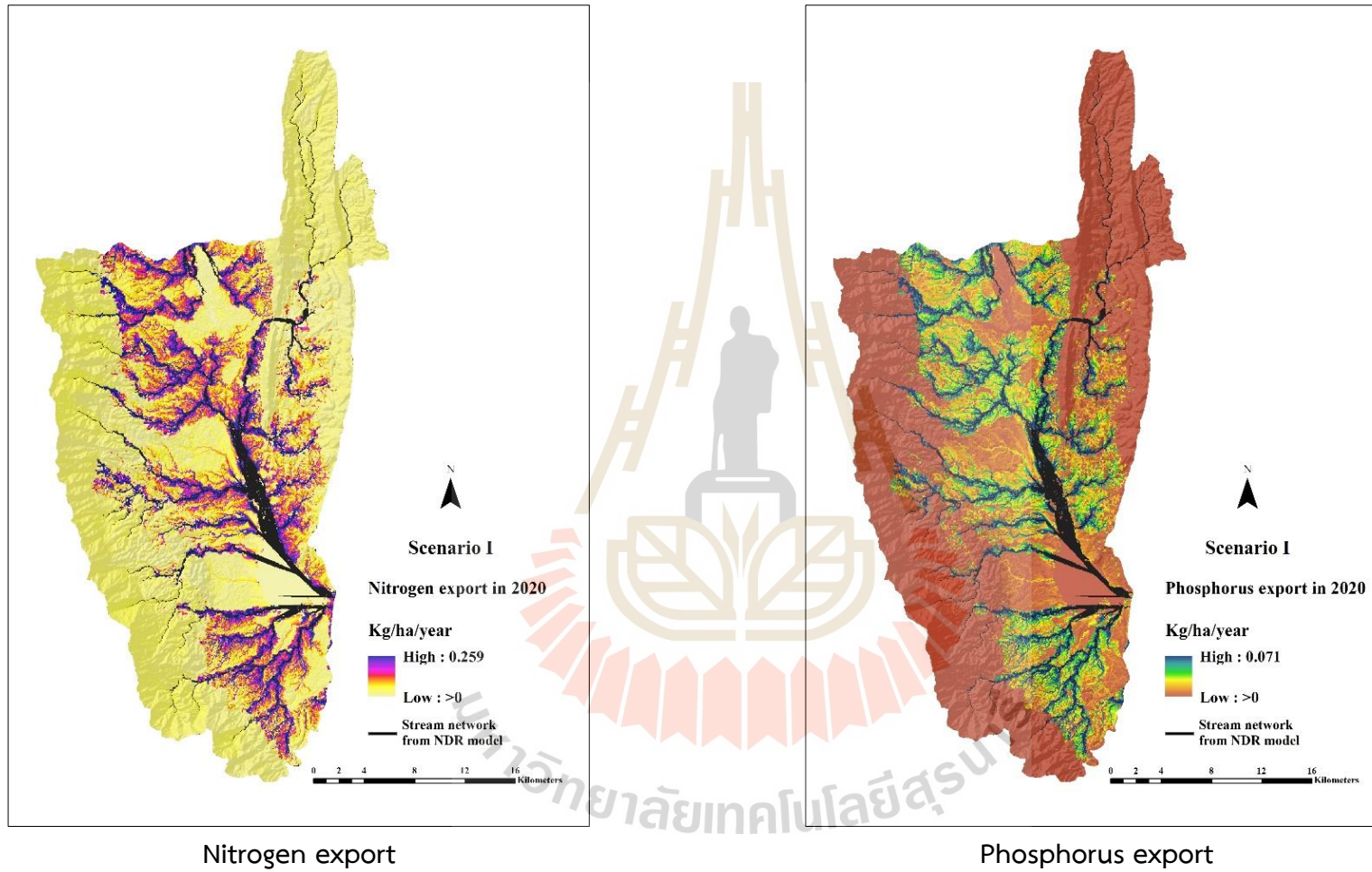


Figure 7.11 Spatial distribution of nitrogen and phosphorus export in 2020 under Scenario I.

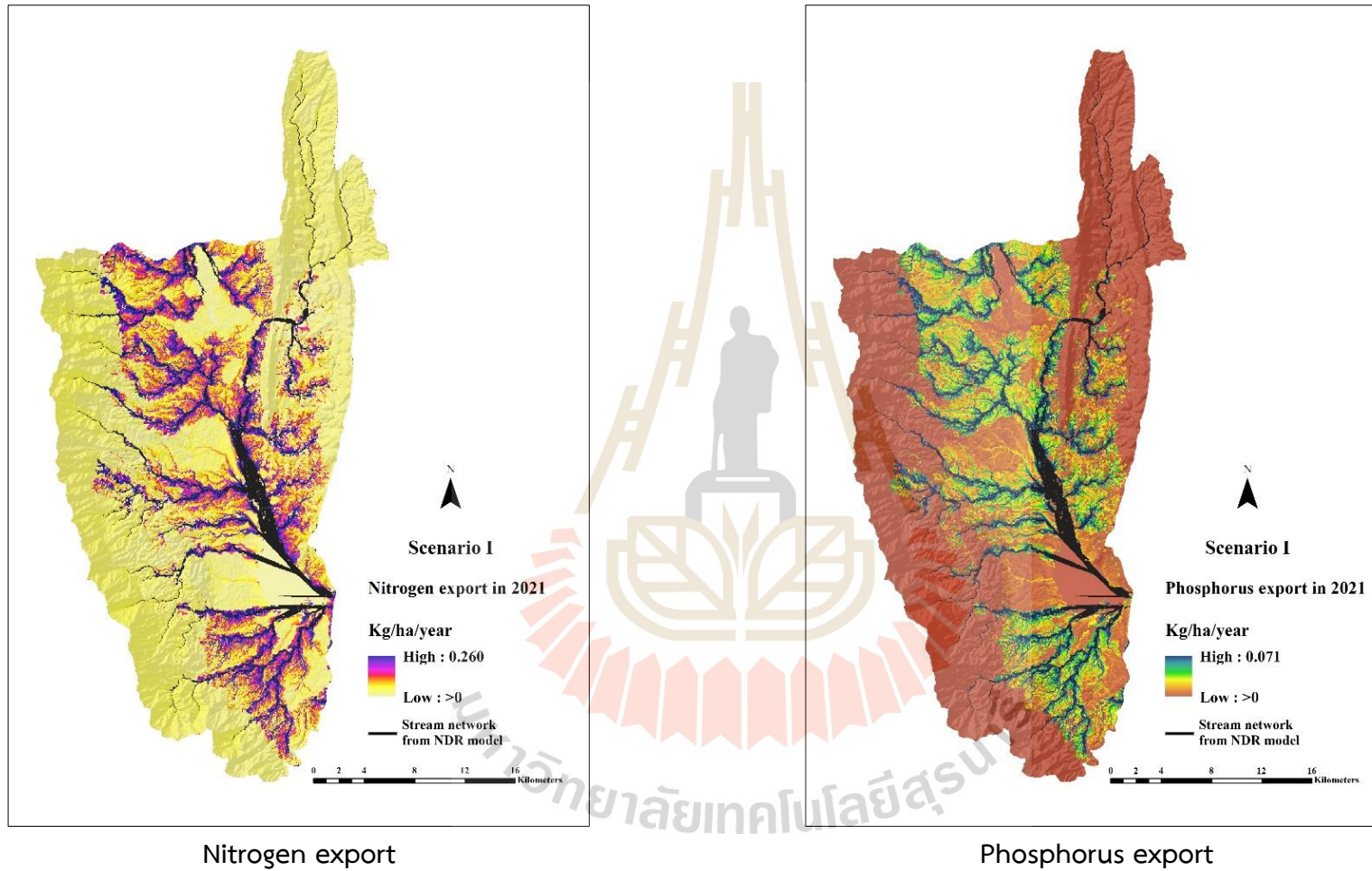


Figure 7.12 Spatial distribution of nitrogen and phosphorus export in 2021 under Scenario I.

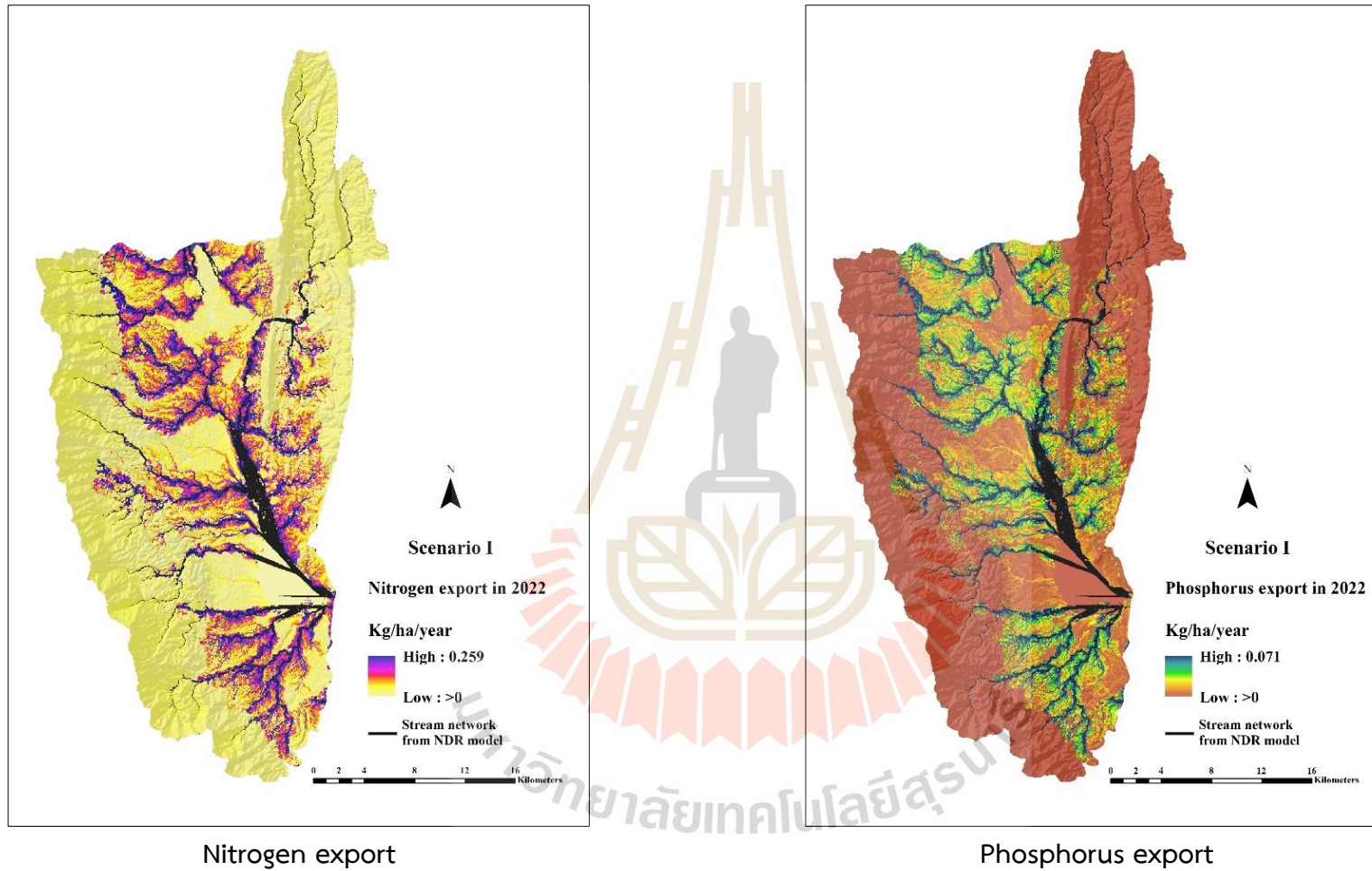


Figure 7.13 Spatial distribution of nitrogen and phosphorus export in 2022 under Scenario I.

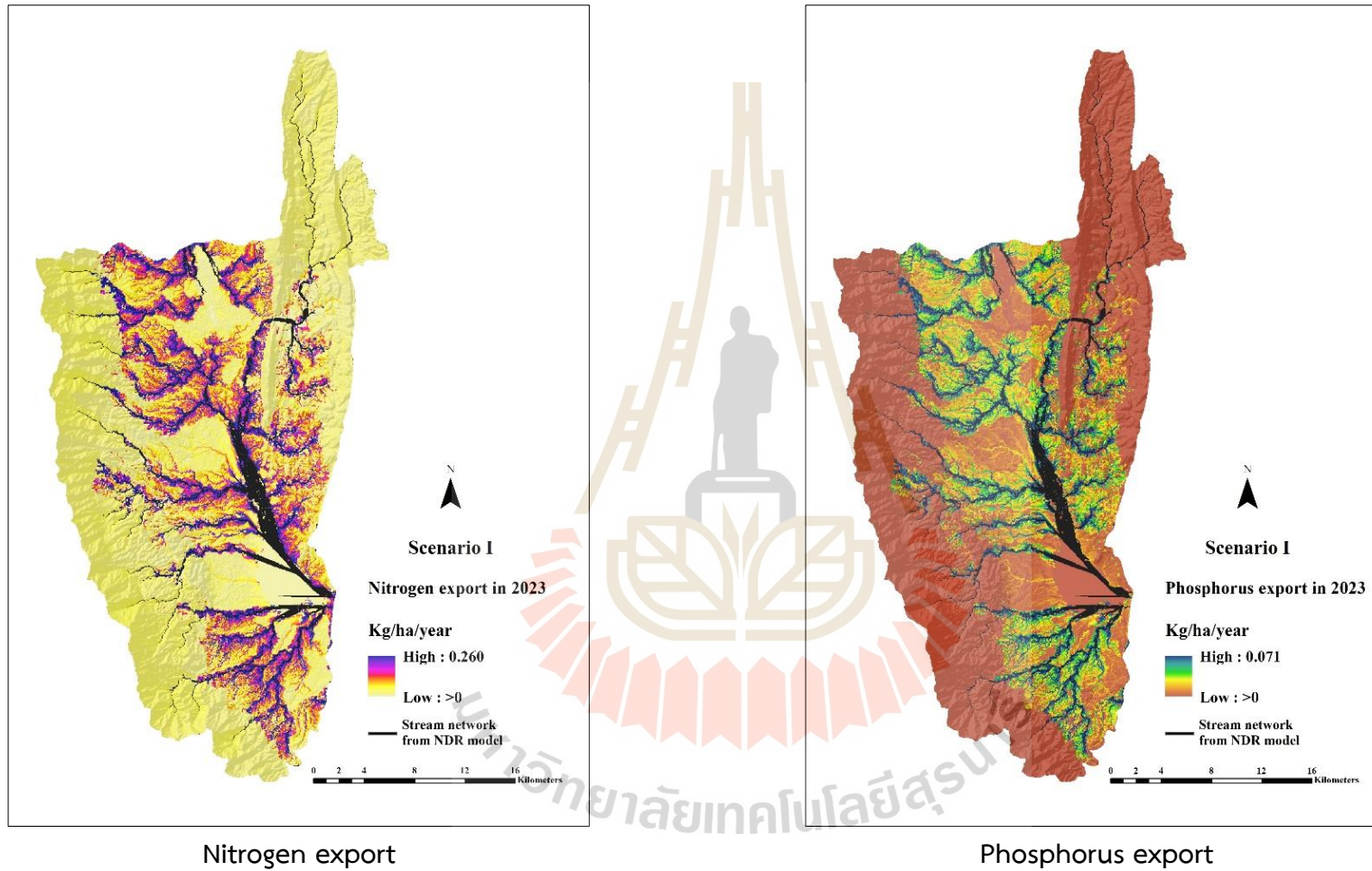


Figure 7.14 Spatial distribution of nitrogen and phosphorus export in 2023 under Scenario I.

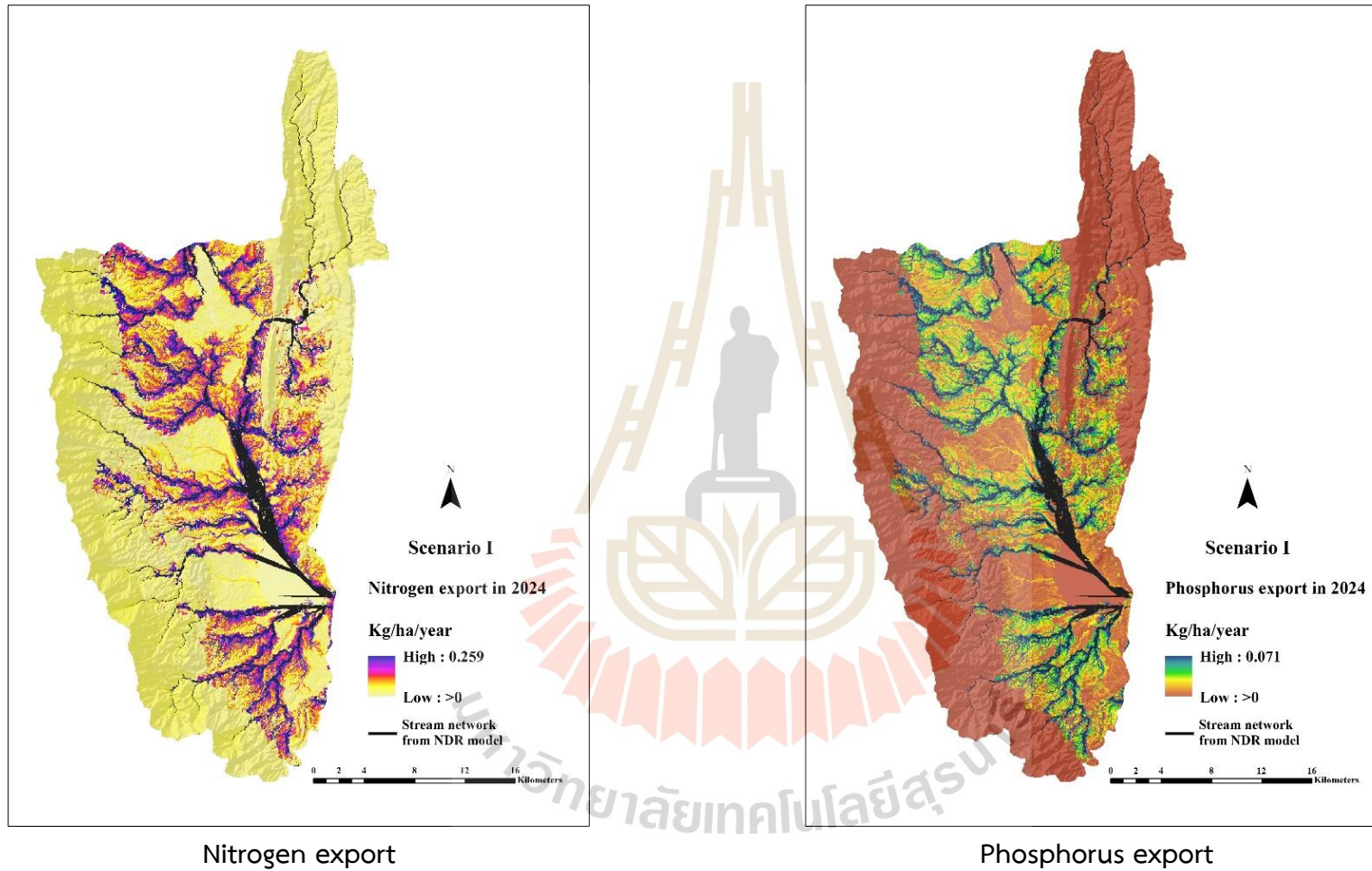


Figure 7.15 Spatial distribution of nitrogen and phosphorus export in 2024 under Scenario I.

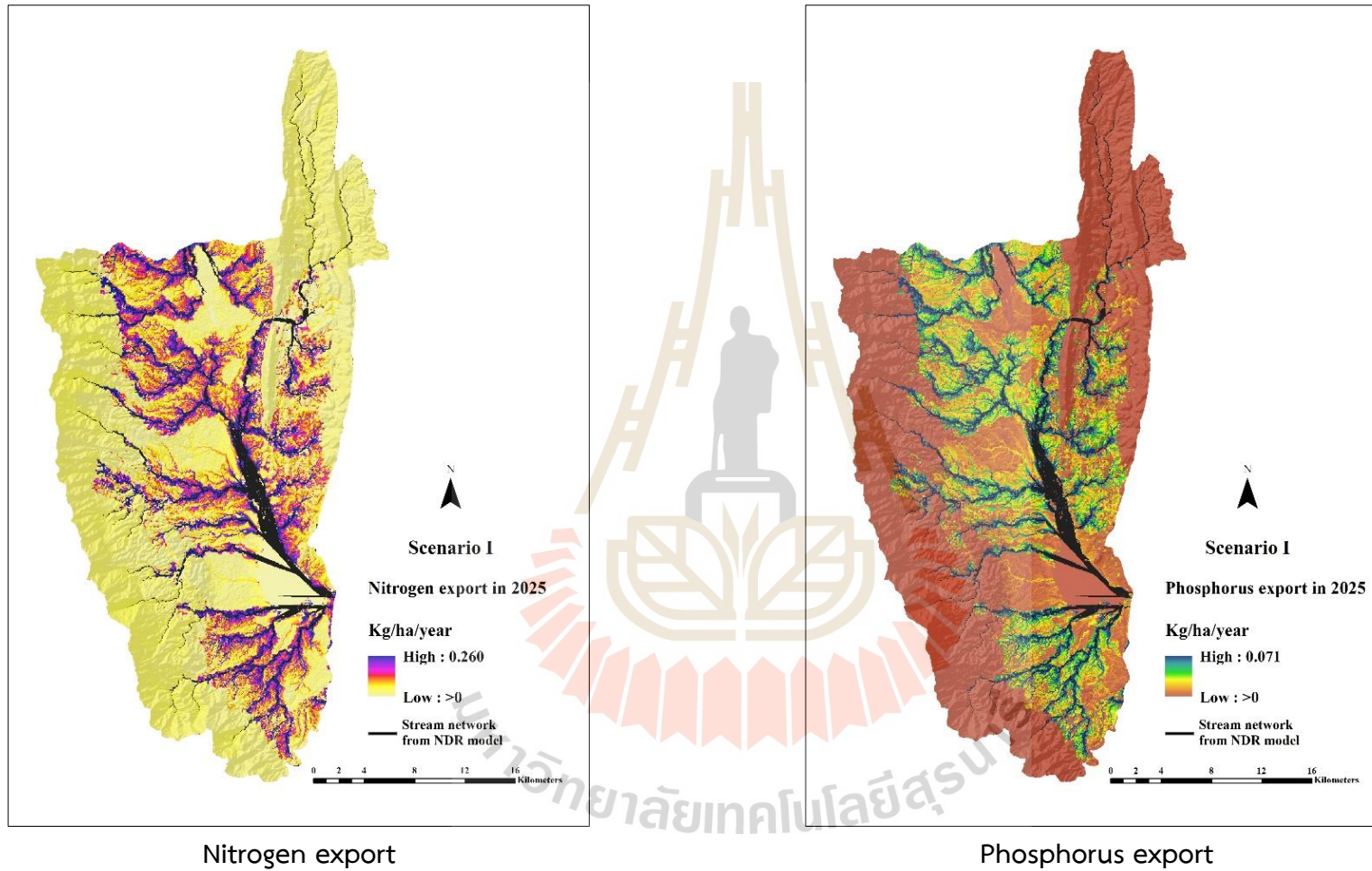


Figure 7.16 Spatial distribution of nitrogen and phosphorus export in 2025 under Scenario I.

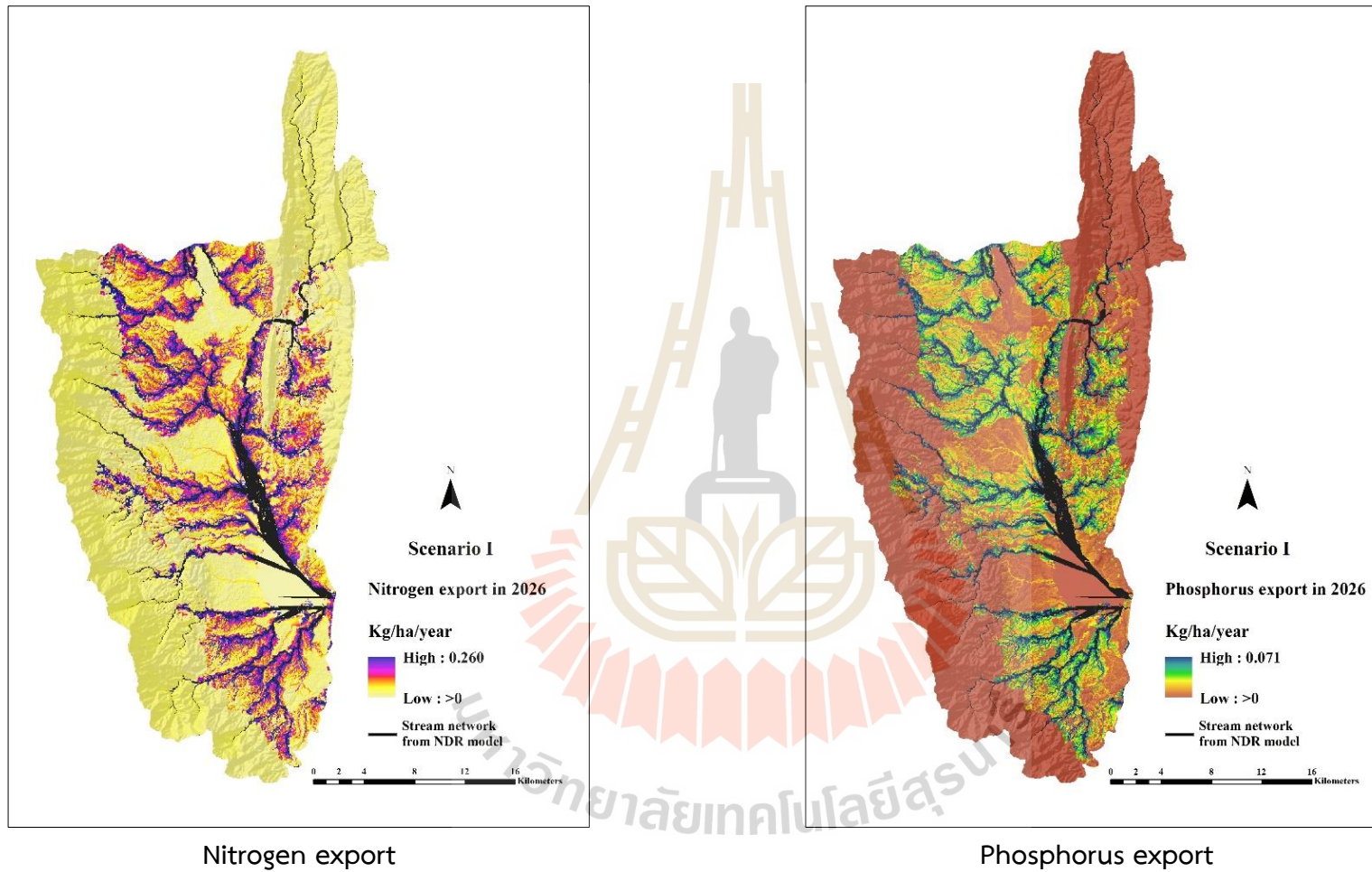


Figure 7.17 Spatial distribution of nitrogen and phosphorus export in 2026 under Scenario I.

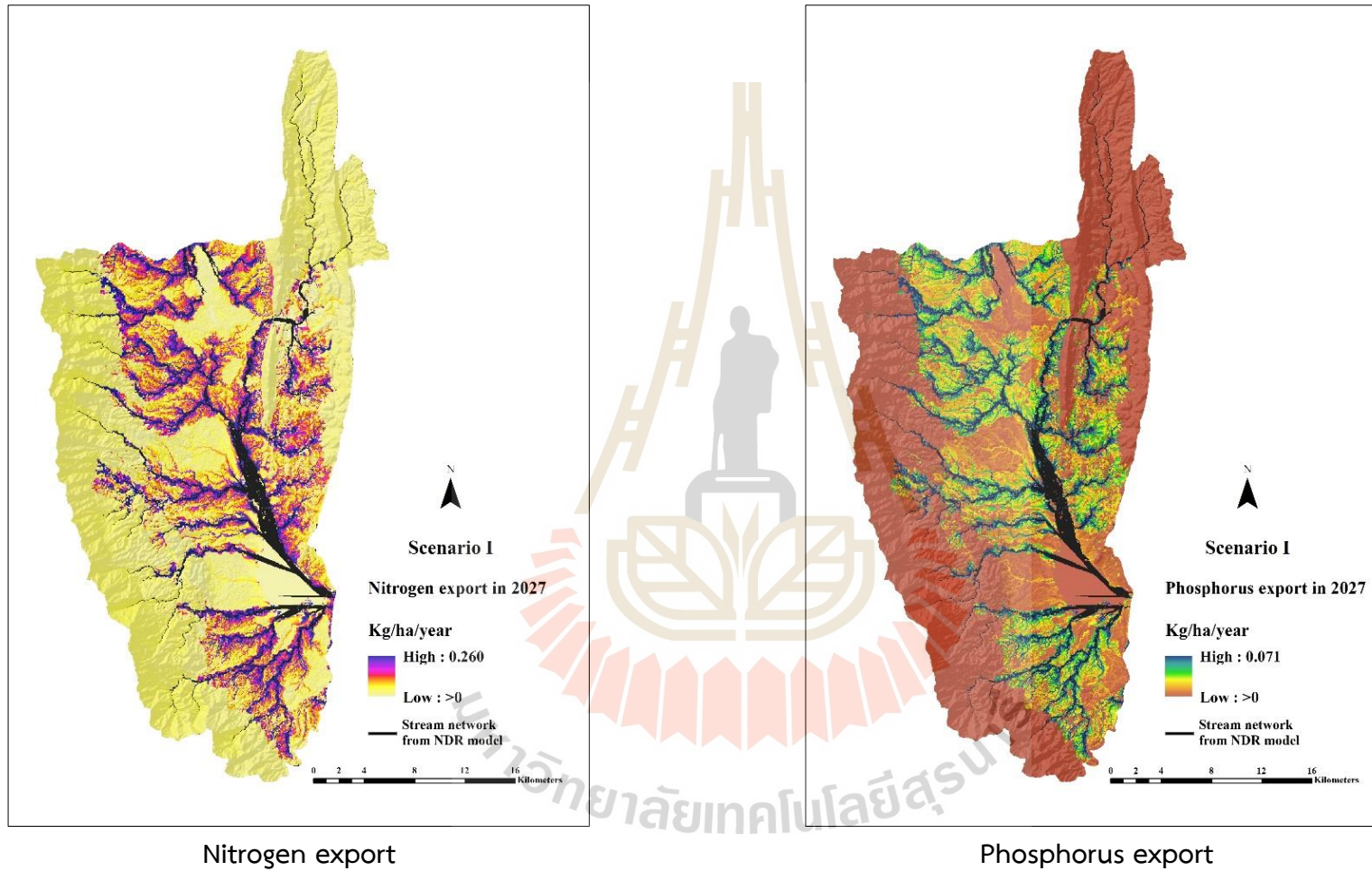


Figure 7.18 Spatial distribution of nitrogen and phosphorus export in 2027 under Scenario I.

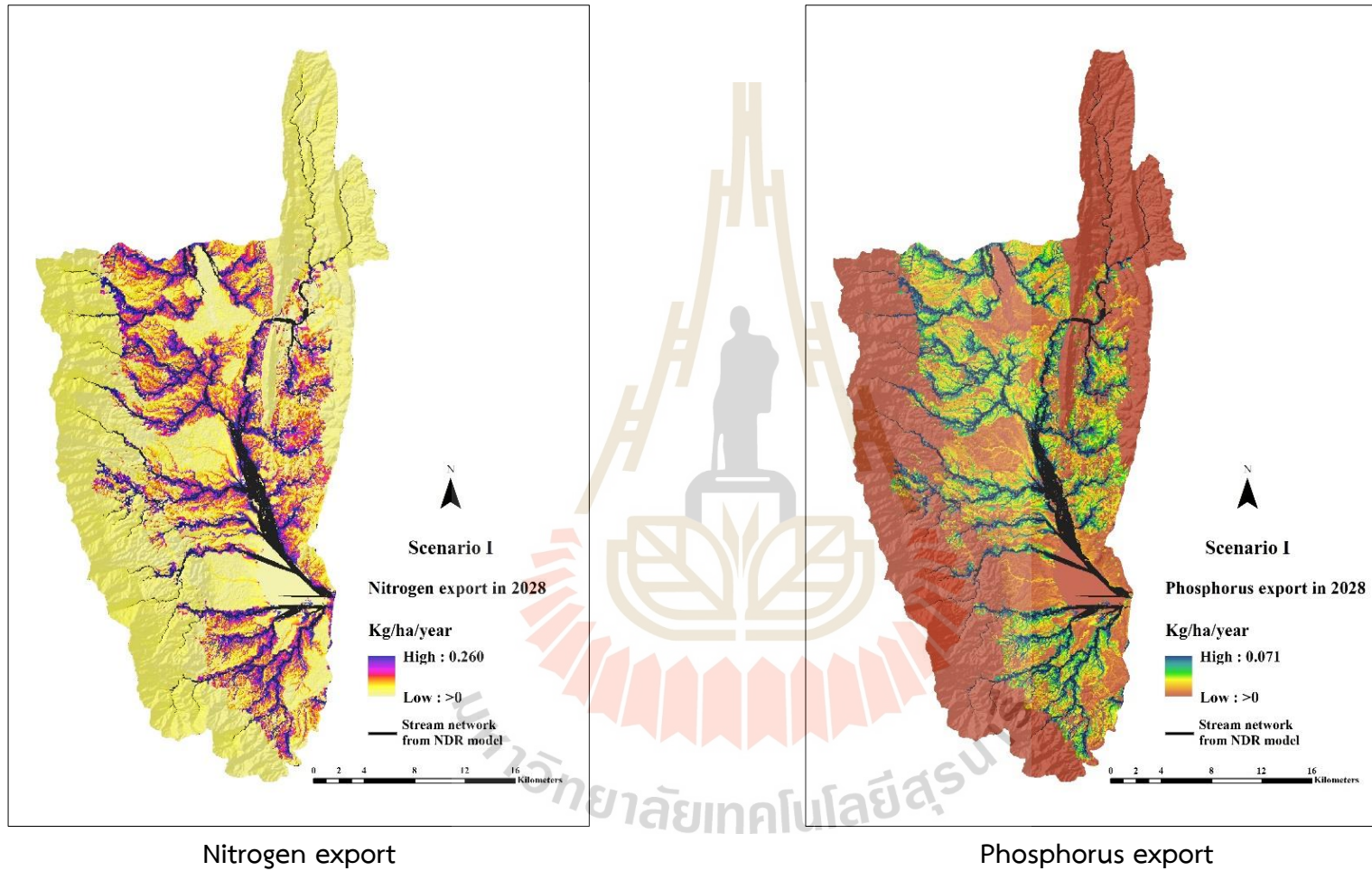


Figure 7.19 Spatial distribution of nitrogen and phosphorus export in 2028 under Scenario I.

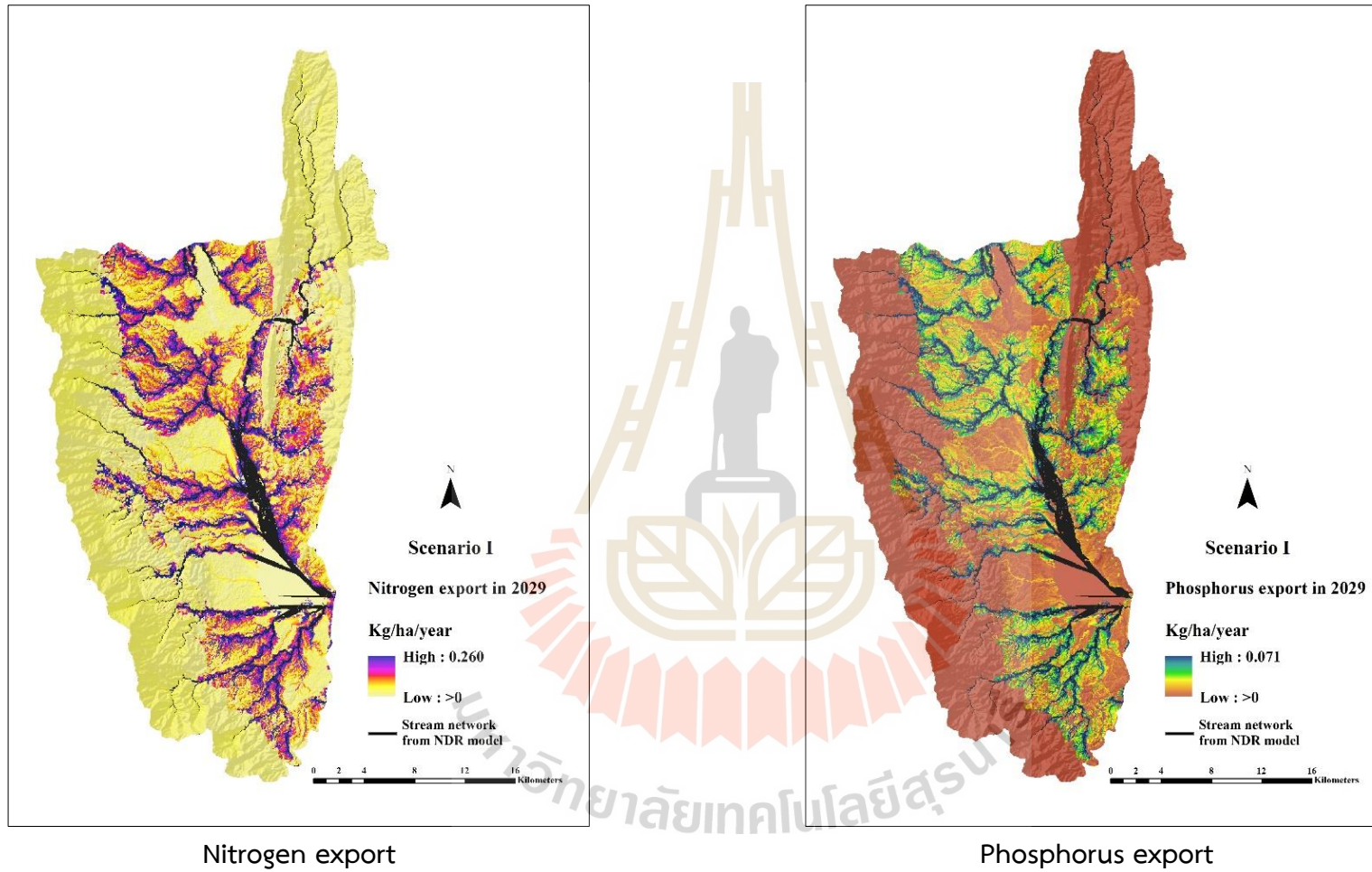


Figure 7.20 Spatial distribution of nitrogen and phosphorus export in 2029 under Scenario I.

As a result of load and export (nitrogen and phosphorus) by LULC classes under Scenario I (Trend of LULC evolution) between 2020 and 2029 (Tables 7.18 to 7.27), the highest total nutrient load was found on the paddy field with a value of nitrogen between 724,853.82 kg. (3,298.91 kg/km²) in 2020 and 695,589.01 kg. (3,299.14 kg/km²) in 2029, and the value of phosphorus between 197,705.89 kg. (899.79 kg/km²) in 2020 and 189,711.03 kg. (899.79 kg/km²) in 2029. However, the highest average nitrogen load appears on field crop with values between 3,312.27 kg/km² (18.55%) in 2023 and 3,301.86 kg/km² (18.50 %) in 2029, while the highest average phosphorus load appears on field crops and perennial trees and orchards between 2020 and 2029. In contrast, the lowest total nitrogen load occurs on the waterbody, with a value between 10.26 kg. (0.30 kg/km²) in 2020 and 12.42 kg. (0.30 kg/km²) in 2029, while the lowest total phosphorus load occurs on miscellaneous land with a value between 0.82 kg. (0.30 kg/km²) in 2020 and 1.08 kg. (0.29 kg/km²) in 2029.

In the meantime, the highest total nutrient export appears on the paddy field with a nitrogen value between 98,331.00 kg. (447.52 kg/km²) in 2020 and 94,685.94 kg. (449.09 kg/km²) in 2029, and the value of phosphorus between 26,817.54 kg. (122.05 kg/km²) in 2020 and 25,823.44 kg. (122.48 kg/km²) in 2029. Conversely, the lowest total nitrogen export occurs on the water body with a value between 2.39 kg. (0.07 kg/km²) in 2020 and 2.97 kg. (0.07 kg/km²) in 2029, while the lowest total phosphorus export occurs on miscellaneous land with a value between 0.15 kg. (0.05 kg/km²) in 2020 and 0.20 kg. (0.06 kg/km²) in 2029. This result agrees with Yang et al. (2019), who indicated that the highest nitrogen and phosphorus exports occurred on cultivated land. However, there are very few nitrogen and phosphorus exports on forest land, water areas, and unused land.

This finding suggests that the change in LULC types associated with the biophysical table parameters affects nitrogen and phosphorus export. Even though the LULC data of Scenario I (Trend of LULC evolution) is simulated based on the annual rate of LULC change from the transition area matrix between 2009 and 2019 using the Markov Chain model, which does not represent dramatic change under this scenario, the minor change of area also changes the amount load and export of nutrient.

7.5 Nutrient export estimation of predictive LULC of Scenario II

Estimation of total and average nitrogen and phosphorus export of predictive LULC between 2020 and 2029 under Scenario II (Maximization of ecosystem service values) is presented in Table 7.28.

Table 7.28 Estimation of nitrogen and phosphorus export between 2020 and 2029 under Scenario II.

Year	Area km ²	Nitrogen export		Phosphorus export	
		Total (kg)	Average (kg/km ²)	Total (kg)	Average (kg/km ²)
2020	891.35	196,964.74	220.97	43,117.85	48.37
2021	891.35	195,883.51	219.76	42,988.62	48.23
2022	891.35	195,426.12	219.25	42,961.10	48.20
2023	891.35	195,754.01	219.62	43,137.70	48.40
2024	891.35	195,641.77	219.49	43,160.14	48.42
2025	891.35	195,988.64	219.88	43,334.48	48.62
2026	891.35	195,915.15	219.80	43,415.07	48.71
2027	891.35	196,276.87	220.20	43,540.77	48.85
2028	891.35	196,689.44	220.66	43,714.70	49.04
2029	891.35	196,815.34	220.81	43,797.81	49.14

As a result, it was found that the highest total and average nitrogen export under Scenario II (Maximization of ecosystem service values) are 196,964.74 kg. and 220.97 kg/km² occurring in 2020, while the lowest total and average nitrogen export are 195,426.12 kg. and 219.25 kg/km² occurring in 2022. Conversely, the highest total and average phosphorus export under this scenario are 43,797.81 kg. and 49.14 kg/km² occurring in 2029, while the lowest total and average phosphorus export are 42,961.10 kg. and 48.20 kg/km² occurring in 2022. These results indicate that the change of LULC types and areas affects parameters in the biophysical table, which leads to different nitrogen and phosphorus export.

The contribution of the predictive LULC of Scenario II (Maximization of ecosystem service values) on nutrient (nitrogen and phosphorus) load and export between 2020 and 2029 is summarized in Tables 7.29 to 7.38. The spatial distribution of nitrogen and phosphorus export of the predictive LULC between 2020 and 2029 of Scenario II (Maximization of ecosystem service values) is displayed in Figures 7.20 to 7.30.



Table 7.29 Contribution of nutrient (nitrogen and phosphorus) load and export by LULC classes in 2020 under Scenario II.

LULC types	Area	Nitrogen loads			Phosphorus loads			Nitrogen export			Phosphorus export		
	km ²	Total (kg.)	Average (kg/km ²)	%	Total (kg.)	Average (kg/km ²)	%	Total (kg.)	Average (kg/km ²)	%	Total (kg.)	Average (kg/km ²)	%
Urban and built-up area (UR)	33.36	77,628.98	2,326.67	13.02	4,340.95	130.11	3.47	9,541.47	285.97	11.89	533.50	15.99	3.12
Paddy field (PD)	219.74	724,975.98	3,299.28	18.47	197,739.23	899.89	24.01	98,056.33	446.24	18.56	26,742.63	121.70	23.74
Field crop (FC)	21.85	72,157.15	3,302.91	18.49	19,681.06	900.88	24.04	10,090.38	461.88	19.21	2,751.92	125.97	24.57
Para rubber (RB)	20.67	62,159.41	3,007.75	16.84	18,649.57	902.41	24.08	8,256.81	399.53	16.61	2,477.04	119.86	23.38
Perennial tree and orchard (PO)	81.16	243,987.03	3,006.22	16.83	73,202.96	901.95	24.07	34,638.08	426.78	17.75	10,391.42	128.04	24.97
Forest land (FO)	434.86	234,900.83	540.18	3.02	1,435.64	3.30	0.09	33,593.33	77.25	3.21	205.29	0.47	0.09
Water body (WB)	33.57	10.08	0.30	0.00	10.08	0.30	0.01	2.33	0.07	0.00	2.33	0.07	0.01
Rangeland (RL)	25.87	15,506.36	599.35	3.35	85.29	3.30	0.09	1,808.61	69.91	2.91	9.95	0.38	0.07
Wetland (WL)	17.72	10,585.14	597.31	3.34	88.22	4.98	0.13	434.07	24.49	1.02	3.62	0.20	0.04
Miscellaneous land (ML)	2.56	3,026.95	1,184.63	6.63	0.76	0.30	0.01	543.33	212.64	8.84	0.14	0.05	0.01
Total	891.35	1,444,937.91		100.00	315,233.76		100.00	196,964.74		100.00	43,117.85		100.00

Table 7.30 Contribution of nutrient (nitrogen and phosphorus) load and export by LULC classes in 2021 under Scenario II.

LULC types	Area	Nitrogen loads			Phosphorus loads			Nitrogen export			Phosphorus export		
	km ²	Total (kg.)	Average (kg/km ²)	%	Total (kg.)	Average (kg/km ²)	%	Total (kg.)	Average (kg/km ²)	%	Total (kg.)	Average (kg/km ²)	%
Urban and built-up area (UR)	33.84	78,738.79	2,326.81	13.03	4,402.69	130.10	3.47	9,273.52	274.04	11.69	518.52	15.32	3.03
Paddy field (PD)	218.73	721,407.84	3,298.16	18.47	196,751.61	899.52	24.01	97,280.15	444.75	18.97	26,530.95	121.30	23.99
Field crop (FC)	21.82	72,177.91	3,307.27	18.52	19,685.29	902.00	24.08	9,822.71	450.09	19.20	2,678.92	122.75	24.28
Para rubber (RB)	21.50	64,522.72	3,001.54	16.81	19,357.21	900.48	24.04	8,514.05	396.07	16.90	2,554.21	118.82	23.50
Perennial tree and orchard (PO)	83.12	249,752.84	3,004.88	16.82	74,927.38	901.48	24.07	34,953.59	420.54	17.94	10,486.08	126.16	24.96
Forest land (FO)	432.77	233,732.10	540.08	3.02	1,428.39	3.30	0.09	33,396.65	77.17	3.29	204.09	0.47	0.09
Water body (WB)	33.57	10.07	0.30	0.00	10.07	0.30	0.01	2.33	0.07	0.00	2.33	0.07	0.01
Rangeland (RL)	24.51	14,690.96	599.34	3.36	80.80	3.30	0.09	1,707.68	69.67	2.97	9.39	0.38	0.08
Wetland (WL)	19.07	11,408.12	598.10	3.35	95.07	4.98	0.13	482.47	25.30	1.08	4.02	0.21	0.04
Miscellaneous land (ML)	2.42	2,862.16	1,183.85	6.63	0.72	0.30	0.01	450.37	186.28	7.95	0.11	0.05	0.01
Total	891.35	1,449,303.53		100.00	316,739.23		100.00	195,883.51		100.00	42,988.62		100.00

Table 7.31 Contribution of nutrient (nitrogen and phosphorus) load and export by LULC classes in 2022 under Scenario II.

LULC types	Area	Nitrogen loads			Phosphorus loads			Nitrogen export			Phosphorus export		
	km ²	Total (kg.)	Average (kg/km ²)	%	Total (kg.)	Average (kg/km ²)	%	Total (kg.)	Average (kg/km ²)	%	Total (kg.)	Average (kg/km ²)	%
Urban and built-up area (UR)	34.22	79,619.62	2,326.54	13.04	4,450.85	130.06	3.48	9,167.06	267.87	11.59	512.57	14.98	2.99
Paddy field (PD)	217.75	717,876.57	3,296.79	18.47	195,740.75	898.92	24.02	96,535.74	443.33	19.19	26,327.93	120.91	24.10
Field crop (FC)	21.82	72,120.13	3,305.00	18.52	19,664.73	901.16	24.08	9,786.24	448.47	19.41	2,668.98	122.31	24.38
Para rubber (RB)	22.37	67,110.08	3,000.13	16.81	20,128.52	899.84	24.04	8,777.21	392.38	16.98	2,633.16	117.71	23.46
Perennial tree and orchard (PO)	85.05	255,327.58	3,002.23	16.82	76,581.15	900.47	24.06	35,330.98	415.43	17.98	10,599.29	124.63	24.84
Forest land (FO)	430.71	232,496.12	539.80	3.02	1,420.49	3.30	0.09	33,315.03	77.35	3.35	203.59	0.47	0.09
Water body (WB)	33.57	10.07	0.30	0.00	10.07	0.30	0.01	2.32	0.07	0.00	2.32	0.07	0.01
Rangeland (RL)	23.16	13,865.68	598.58	3.35	76.24	3.29	0.09	1,591.58	68.71	2.97	8.75	0.38	0.08
Wetland (WL)	20.42	12,196.29	597.38	3.35	101.61	4.98	0.13	528.80	25.90	1.12	4.41	0.22	0.04
Miscellaneous land (ML)	2.29	2,698.65	1,180.95	6.62	0.67	0.30	0.01	391.17	171.18	7.41	0.10	0.04	0.01
Total	891.35	1,453,320.78		100.00	318,175.10		100.00	195,426.12		100.00	42,961.10		100.00

Table 7.32 Contribution of nutrient (nitrogen and phosphorus) load and export by LULC classes in 2023 under Scenario II.

LULC types	Area	Nitrogen loads			Phosphorus loads			Nitrogen export			Phosphorus export		
	km ²	Total (kg.)	Average (kg/km ²)	%	Total (kg.)	Average (kg/km ²)	%	Total (kg.)	Average (kg/km ²)	%	Total (kg.)	Average (kg/km ²)	%
Urban and built-up area (UR)	34.60	80,506.69	2,326.62	13.03	4,501.44	130.09	3.47	9,311.82	269.11	11.70	520.66	15.05	3.00
Paddy field (PD)	216.77	715,023.91	3,298.53	18.48	195,006.26	899.60	24.01	96,036.20	443.03	19.25	26,191.69	120.83	24.13
Field crop (FC)	21.81	72,270.75	3,313.42	18.56	19,710.18	903.66	24.12	9,727.68	445.99	19.38	2,653.00	121.63	24.29
Para rubber (RB)	23.23	69,731.88	3,001.27	16.81	20,919.53	900.38	24.03	9,118.58	392.46	17.06	2,735.57	117.74	23.51
Perennial tree and orchard (PO)	87.01	261,277.19	3,002.80	16.82	78,383.05	900.84	24.04	36,064.15	414.48	18.01	10,819.24	124.34	24.83
Forest land (FO)	428.65	231,516.53	540.10	3.03	1,414.82	3.30	0.09	33,099.39	77.22	3.36	202.27	0.47	0.09
Water body (WB)	33.57	10.07	0.30	0.00	10.07	0.30	0.01	2.33	0.07	0.00	2.33	0.07	0.01
Rangeland (RL)	21.78	13,035.91	598.42	3.35	71.70	3.29	0.09	1,467.43	67.36	2.93	8.07	0.37	0.07
Wetland (WL)	21.76	13,021.33	598.30	3.35	108.51	4.99	0.13	571.56	26.26	1.14	4.76	0.22	0.04
Miscellaneous land (ML)	2.15	2,519.70	1,171.87	6.56	0.63	0.29	0.01	354.86	165.04	7.17	0.09	0.04	0.01
Total	891.35	1,458,913.97		100.00	320,126.20		100.00	195,754.01		100.00	43,137.70		100.00

Table 7.33 Contribution of nutrient (nitrogen and phosphorus) load and export by LULC classes in 2024 under Scenario II.

LULC types	Area	Nitrogen loads			Phosphorus loads			Nitrogen export			Phosphorus export		
	km ²	Total (kg.)	Average (kg/km ²)	%	Total (kg.)	Average (kg/km ²)	%	Total (kg.)	Average (kg/km ²)	%	Total (kg.)	Average (kg/km ²)	%
Urban and built-up area (UR)	34.99	81,371.82	2,325.74	13.03	4,548.80	130.01	3.47	9,427.61	269.46	11.77	527.14	15.07	3.03
Paddy field (PD)	215.78	711,410.81	3,296.89	18.48	193,977.37	898.95	24.01	95,286.36	441.58	19.30	25,987.19	120.43	24.21
Field crop (FC)	21.81	72,157.22	3,308.97	18.54	19,674.81	902.24	24.10	9,599.71	440.22	19.24	2,618.10	120.06	24.13
Para rubber (RB)	24.09	72,276.78	3,000.07	16.81	21,678.14	899.82	24.04	9,420.42	391.02	17.09	2,826.12	117.31	23.58
Perennial tree and orchard (PO)	88.96	267,037.08	3,001.89	16.82	80,093.06	900.36	24.05	36,616.74	411.63	17.99	10,985.02	123.49	24.82
Forest land (FO)	426.61	230,307.14	539.85	3.03	1,407.12	3.30	0.09	33,003.59	77.36	3.38	201.69	0.47	0.10
Water body (WB)	33.57	10.07	0.30	0.00	10.07	0.30	0.01	2.32	0.07	0.00	2.32	0.07	0.01
Rangeland (RL)	20.43	12,193.84	596.89	3.35	67.05	3.28	0.09	1,340.38	65.61	2.87	7.37	0.36	0.07
Wetland (WL)	23.10	13,815.76	598.17	3.35	115.11	4.98	0.13	611.50	26.48	1.16	5.10	0.22	0.04
Miscellaneous land (ML)	2.02	2,369.47	1,174.37	6.58	0.59	0.29	0.01	333.14	165.11	7.21	0.08	0.04	0.01
Total	891.35	1,462,949.99		100.00	321,572.11		100.00	195,641.77		100.00	43,160.14		100.00

Table 7.34 Contribution of nutrient (nitrogen and phosphorus) load and export by LULC classes in 2025 under Scenario II.

LULC types	Area	Nitrogen loads			Phosphorus loads			Nitrogen export			Phosphorus export		
	km ²	Total (kg.)	Average (kg/km ²)	%	Total (kg.)	Average (kg/km ²)	%	Total (kg.)	Average (kg/km ²)	%	Total (kg.)	Average (kg/km ²)	%
Urban and built-up area (UR)	35.39	82,423.93	2,328.69	13.04	4,608.99	130.22	3.48	9,604.17	271.34	11.91	537.01	15.17	3.06
Paddy field (PD)	214.77	708,509.65	3,298.92	18.47	193,243.95	899.77	24.02	94,870.98	441.73	19.39	25,873.90	120.47	24.31
Field crop (FC)	21.86	72,362.38	3,310.03	18.53	19,736.63	902.80	24.10	9,488.64	434.03	19.05	2,587.81	118.37	23.88
Para rubber (RB)	24.98	74,873.83	2,997.44	16.78	22,463.78	899.30	24.01	9,762.12	390.81	17.16	2,928.63	117.24	23.65
Perennial tree and orchard (PO)	90.81	272,757.77	3,003.48	16.82	81,833.28	901.11	24.06	37,307.58	410.81	18.03	11,192.28	123.24	24.86
Forest land (FO)	424.52	229,323.92	540.19	3.02	1,401.53	3.30	0.09	32,766.04	77.18	3.39	200.24	0.47	0.10
Water body (WB)	33.70	10.12	0.30	0.00	10.12	0.30	0.01	2.34	0.07	0.00	2.34	0.07	0.01
Rangeland (RL)	19.14	11,441.44	597.66	3.35	62.93	3.29	0.09	1,232.30	64.37	2.83	6.78	0.35	0.07
Wetland (WL)	24.27	14,542.15	599.08	3.35	121.19	4.99	0.13	650.01	26.78	1.18	5.42	0.22	0.05
Miscellaneous land (ML)	1.89	2,238.17	1,182.57	6.62	0.56	0.30	0.01	304.46	160.87	7.06	0.08	0.04	0.01
Total	891.35	1,468,483.36		100.00	323,482.95		100.00	195,988.64		100.00	43,334.48		100.00

Table 7.35 Contribution of nutrient (nitrogen and phosphorus) load and export by LULC classes in 2026 under Scenario II.

LULC types	Area	Nitrogen loads			Phosphorus loads			Nitrogen export			Phosphorus export		
	km ²	Total (kg.)	Average (kg/km ²)	%	Total (kg.)	Average (kg/km ²)	%	Total (kg.)	Average (kg/km ²)	%	Total (kg.)	Average (kg/km ²)	%
Urban and built-up area (UR)	35.42	82,504.36	2,329.48	13.04	4,613.66	130.26	3.48	9,607.36	271.26	12.06	537.19	15.17	3.08
Paddy field (PD)	213.82	705,541.11	3,299.62	18.47	192,441.51	900.00	24.02	94,394.33	441.46	19.63	25,743.91	120.40	24.44
Field crop (FC)	21.85	72,269.49	3,308.05	18.52	19,712.03	902.30	24.09	9,307.13	426.02	18.94	2,538.31	116.19	23.59
Para rubber (RB)	25.87	77,610.05	3,000.08	16.80	23,285.58	900.12	24.03	10,142.82	392.08	17.43	3,042.85	117.62	23.88
Perennial tree and orchard (PO)	92.90	279,043.44	3,003.81	16.82	83,722.26	901.24	24.06	37,797.59	406.88	18.09	11,339.28	122.06	24.78
Forest land (FO)	422.49	228,231.06	540.21	3.02	1,394.90	3.30	0.09	32,597.75	77.16	3.43	199.21	0.47	0.10
Water body (WB)	33.70	10.12	0.30	0.00	10.12	0.30	0.01	2.34	0.07	0.00	2.34	0.07	0.01
Rangeland (RL)	17.72	10,606.02	598.66	3.35	58.34	3.29	0.09	1,112.27	62.78	2.79	6.12	0.35	0.07
Wetland (WL)	25.82	15,452.33	598.36	3.35	128.78	4.99	0.13	698.19	27.04	1.20	5.82	0.23	0.05
Miscellaneous land (ML)	1.77	2,095.82	1,183.99	6.63	0.52	0.30	0.01	255.38	144.27	6.41	0.06	0.04	0.01
Total	891.35	1,473,363.79		100.00	325,367.71		100.00	195,915.15		100.00	43,415.07		100.00

Table 7.36 Contribution of nutrient (nitrogen and phosphorus) load and export by LULC classes in 2027 under Scenario II.

LULC types	Area	Nitrogen loads			Phosphorus loads			Nitrogen export			Phosphorus export		
	km ²	Total (kg.)	Average (kg/km ²)	%	Total (kg.)	Average (kg/km ²)	%	Total (kg.)	Average (kg/km ²)	%	Total (kg.)	Average (kg/km ²)	%
Urban and built-up area (UR)	36.17	84,166.86	2,327.30	13.03	4,705.03	130.10	3.48	9,863.06	272.72	12.25	551.48	15.25	3.11
Paddy field (PD)	212.74	701,369.59	3,296.76	18.46	191,238.93	898.91	24.03	93,780.13	440.81	19.80	25,576.40	120.22	24.49
Field crop (FC)	21.84	72,118.70	3,302.66	18.49	19,664.24	900.52	24.07	9,186.62	420.70	18.90	2,505.44	114.74	23.37
Para rubber (RB)	26.74	80,196.96	2,998.93	16.79	24,053.59	899.47	24.04	10,499.69	392.63	17.63	3,149.91	117.79	23.99
Perennial tree and orchard (PO)	94.81	284,578.03	3,001.51	16.81	85,353.91	900.25	24.06	38,482.70	405.89	18.23	11,544.81	121.77	24.80
Forest land (FO)	420.45	226,938.44	539.75	3.02	1,386.53	3.30	0.09	32,530.87	77.37	3.48	198.80	0.47	0.10
Water body (WB)	33.70	10.11	0.30	0.00	10.11	0.30	0.01	2.34	0.07	0.00	2.34	0.07	0.01
Rangeland (RL)	16.35	9,785.66	598.65	3.35	53.81	3.29	0.09	993.71	60.79	2.73	5.47	0.33	0.07
Wetland (WL)	26.93	16,101.46	597.86	3.35	134.15	4.98	0.13	729.72	27.09	1.22	6.08	0.23	0.05
Miscellaneous land (ML)	1.62	1,936.51	1,195.30	6.69	0.48	0.30	0.01	208.03	128.41	5.77	0.05	0.03	0.01
Total	891.35	1,477,202.33		100.00	326,600.78		100.00	196,276.87		100.00	43,540.77		100.00

Table 7.37 Contribution of nutrient (nitrogen and phosphorus) load and export by LULC classes in 2028 under Scenario II.

LULC types	Area	Nitrogen loads			Phosphorus loads			Nitrogen export			Phosphorus export		
	km ²	Total (kg.)	Average (kg/km ²)	%	Total (kg.)	Average (kg/km ²)	%	Total (kg.)	Average (kg/km ²)	%	Total (kg.)	Average (kg/km ²)	%
Urban and built-up area (UR)	36.47	84,898.17	2,327.89	13.03	4,746.38	130.14	3.48	10,006.34	274.37	12.35	559.49	15.34	3.12
Paddy field (PD)	211.81	698,490.33	3,297.65	18.46	190,472.80	899.24	24.02	93,295.01	440.46	19.82	25,444.09	120.12	24.47
Field crop (FC)	21.86	72,180.42	3,301.71	18.48	19,683.03	900.35	24.05	9,188.36	420.30	18.92	2,505.92	114.63	23.35
Para rubber (RB)	27.56	82,739.86	3,001.96	16.81	24,818.76	900.47	24.06	10,883.13	394.86	17.77	3,264.94	118.46	24.13
Perennial tree and orchard (PO)	96.70	290,370.93	3,002.67	16.81	87,100.05	900.68	24.06	39,095.60	404.28	18.20	11,728.68	121.28	24.70
Forest land (FO)	418.34	225,849.76	539.87	3.02	1,380.02	3.30	0.09	32,381.30	77.40	3.48	197.89	0.47	0.10
Water body (WB)	33.70	10.11	0.30	0.00	10.11	0.30	0.01	2.34	0.07	0.00	2.34	0.07	0.01
Rangeland (RL)	14.97	8,958.24	598.27	3.35	49.26	3.29	0.09	876.83	58.56	2.64	4.82	0.32	0.07
Wetland (WL)	28.44	17,003.06	597.76	3.35	141.67	4.98	0.13	777.12	27.32	1.23	6.48	0.23	0.05
Miscellaneous land (ML)	1.48	1,765.30	1,194.71	6.69	0.44	0.30	0.01	183.41	124.12	5.59	0.05	0.03	0.01
Total	891.35	1,482,266.19		100.00	328,402.53		100.00	196,689.44		100.00	43,714.70		100.00

Table 7.38 Contribution of nutrient (nitrogen and phosphorus) load and export by LULC classes in 2029 under Scenario II.

LULC types	Area	Nitrogen loads			Phosphorus loads			Nitrogen export			Phosphorus export		
	km ²	Total (kg.)	Average (kg/km ²)	%	Total (kg.)	Average (kg/km ²)	%	Total (kg.)	Average (kg/km ²)	%	Total (kg.)	Average (kg/km ²)	%
Urban and built-up area (UR)	36.94	85,976.37	2,327.30	13.03	4,807.41	130.13	3.48	10,204.97	276.24	12.50	570.60	15.45	3.15
Paddy field (PD)	210.78	695,319.69	3,298.80	18.47	189,637.70	899.70	24.03	92,700.60	439.80	19.90	25,281.98	119.94	24.50
Field crop (FC)	21.80	71,890.91	3,297.90	18.47	19,607.13	899.45	24.03	9,146.26	419.57	18.98	2,494.43	114.43	23.37
Para rubber (RB)	28.46	85,490.68	3,004.21	16.82	25,647.89	901.29	24.07	11,222.78	394.38	17.84	3,366.83	118.31	24.17
Perennial tree and orchard (PO)	98.68	296,372.73	3,003.31	16.82	88,914.19	901.02	24.07	39,578.91	401.08	18.15	11,873.67	120.32	24.58
Forest land (FO)	416.34	224,863.62	540.10	3.02	1,374.20	3.30	0.09	32,224.45	77.40	3.50	196.93	0.47	0.10
Water body (WB)	33.70	10.12	0.30	0.00	10.12	0.30	0.01	2.34	0.07	0.00	2.34	0.07	0.01
Rangeland (RL)	13.57	8,127.03	598.74	3.35	44.70	3.29	0.09	755.26	55.64	2.52	4.15	0.31	0.06
Wetland (WL)	29.72	17,783.44	598.37	3.35	148.20	4.99	0.13	818.67	27.55	1.25	6.82	0.23	0.05
Miscellaneous land (ML)	1.36	1,620.11	1,191.18	6.67	0.41	0.30	0.01	161.10	118.45	5.36	0.04	0.03	0.01
Total	891.35	1,487,454.71		100.00	330,191.95		100.00	196,815.34		100.00	43,797.81		100.00

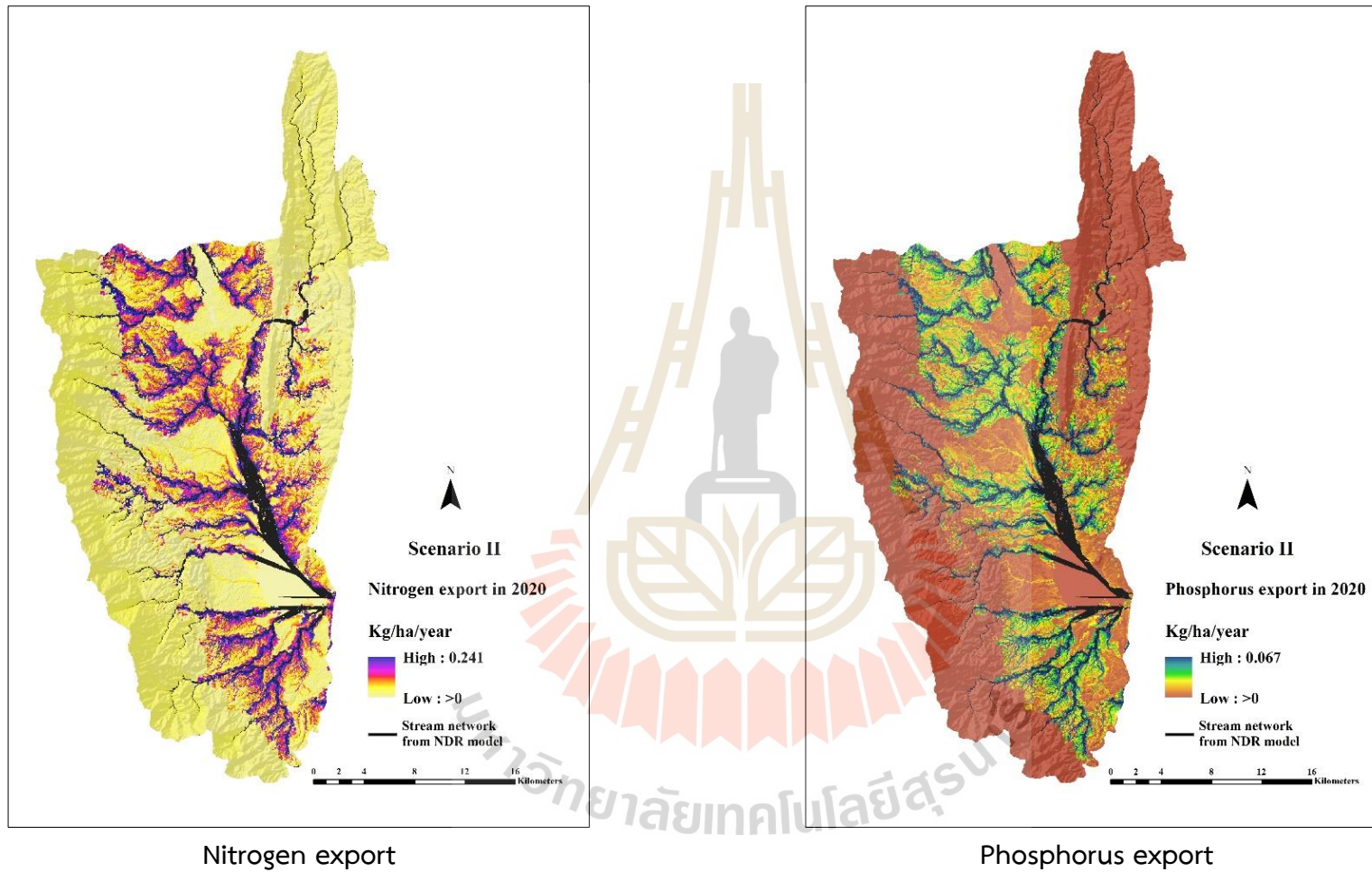


Figure 7.21 Spatial distribution of nitrogen and phosphorus export in 2020 under Scenario II.

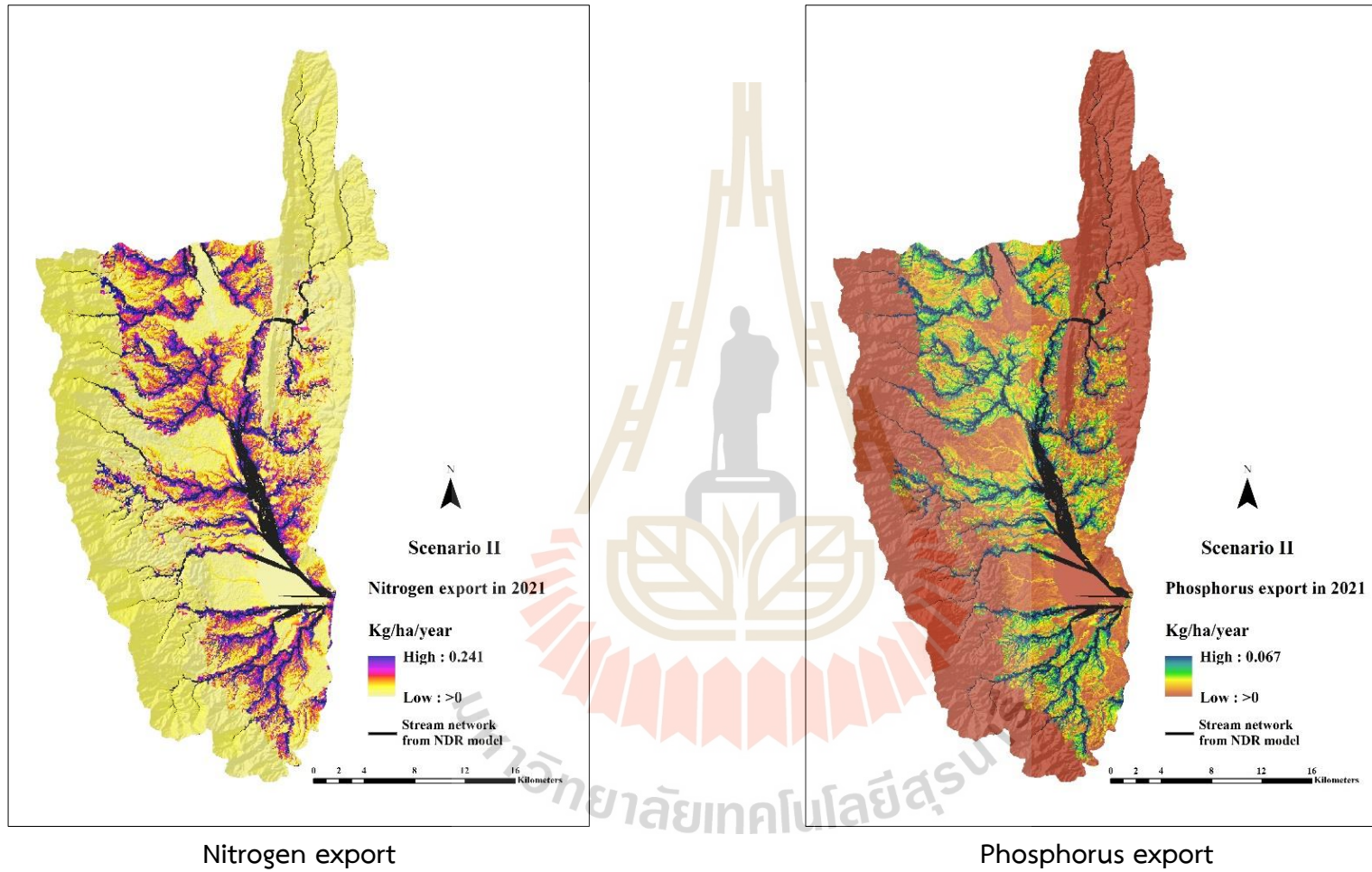


Figure 7.22 Spatial distribution of nitrogen and phosphorus export in 2021 under Scenario II.

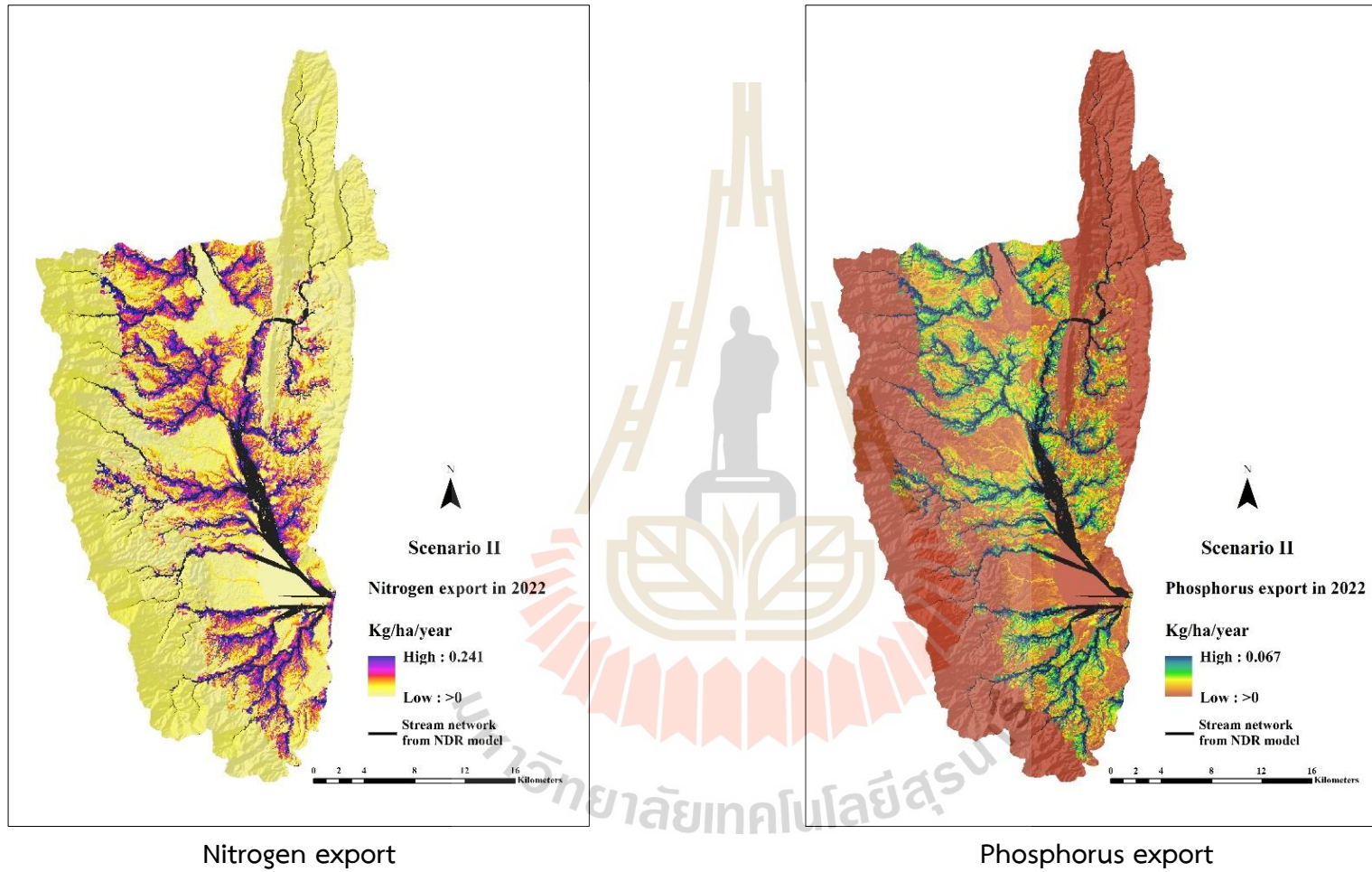


Figure 7.23 Spatial distribution of nitrogen and phosphorus export in 2022 under Scenario II.

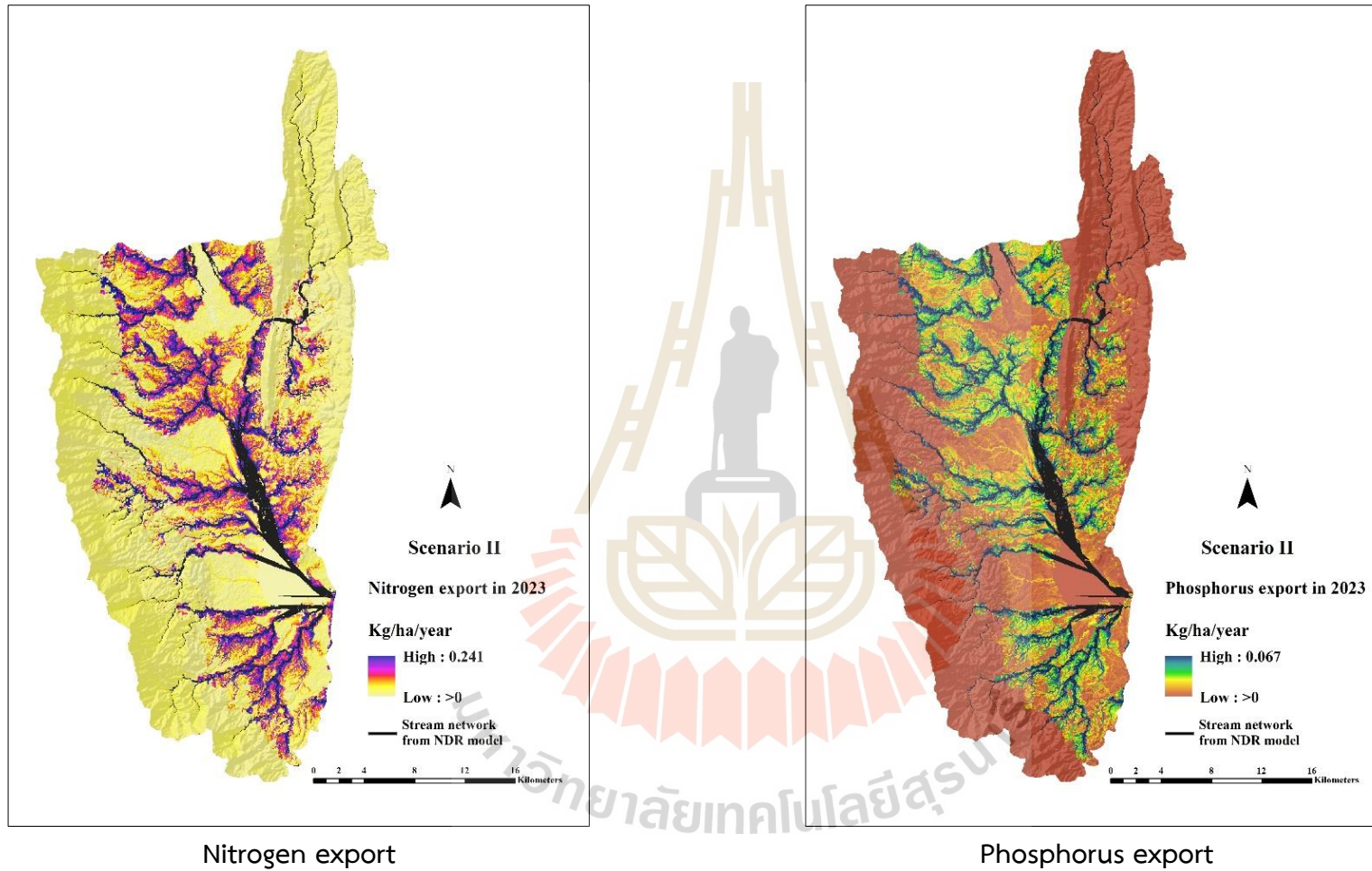


Figure 7.24 Spatial distribution of nitrogen and phosphorus export in 2023 under Scenario II.

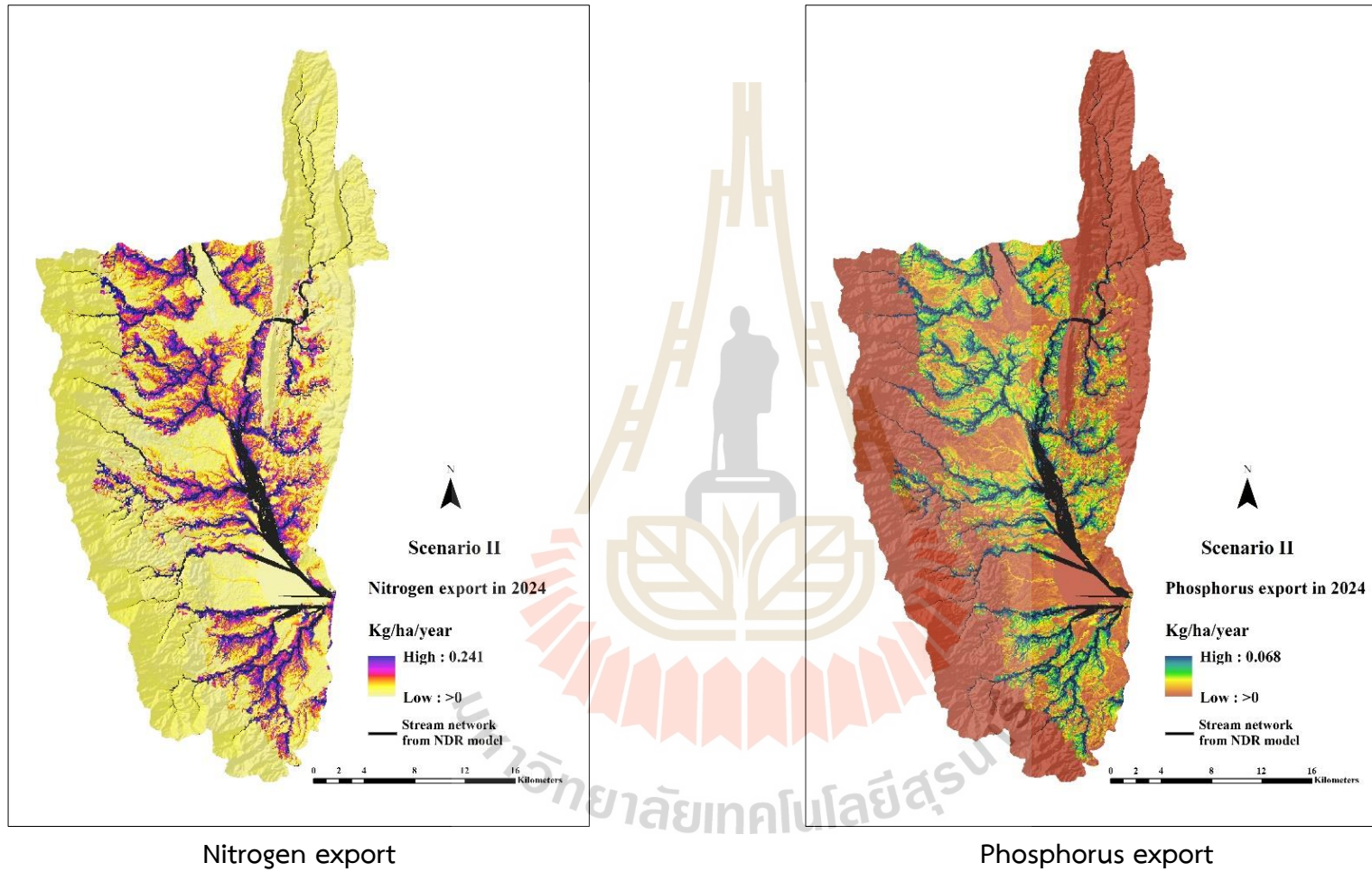


Figure 7.25 Spatial distribution of nitrogen and phosphorus export in 2024 under Scenario II.

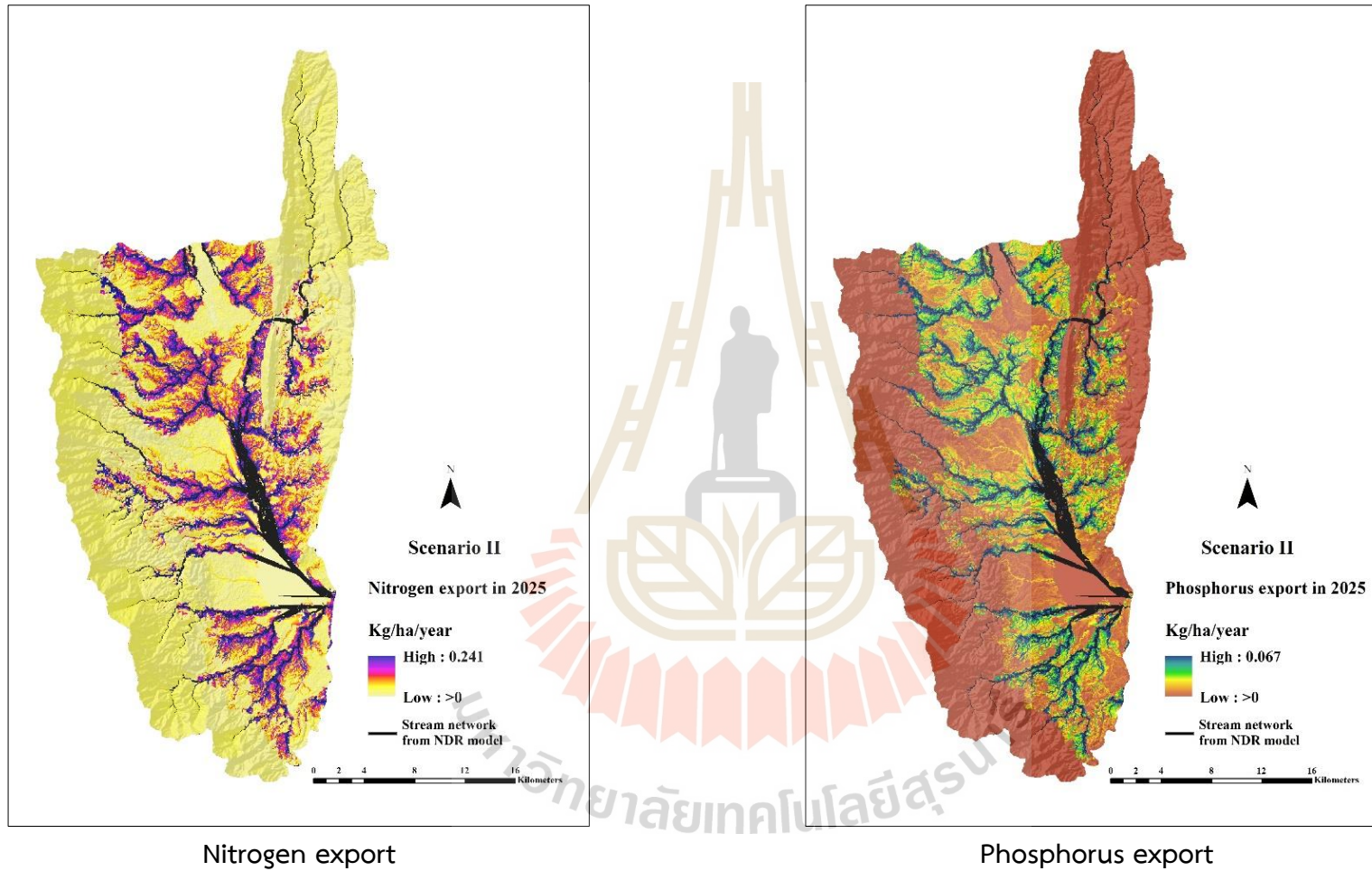


Figure 7.26 Spatial distribution of nitrogen and phosphorus export in 2025 under Scenario II.

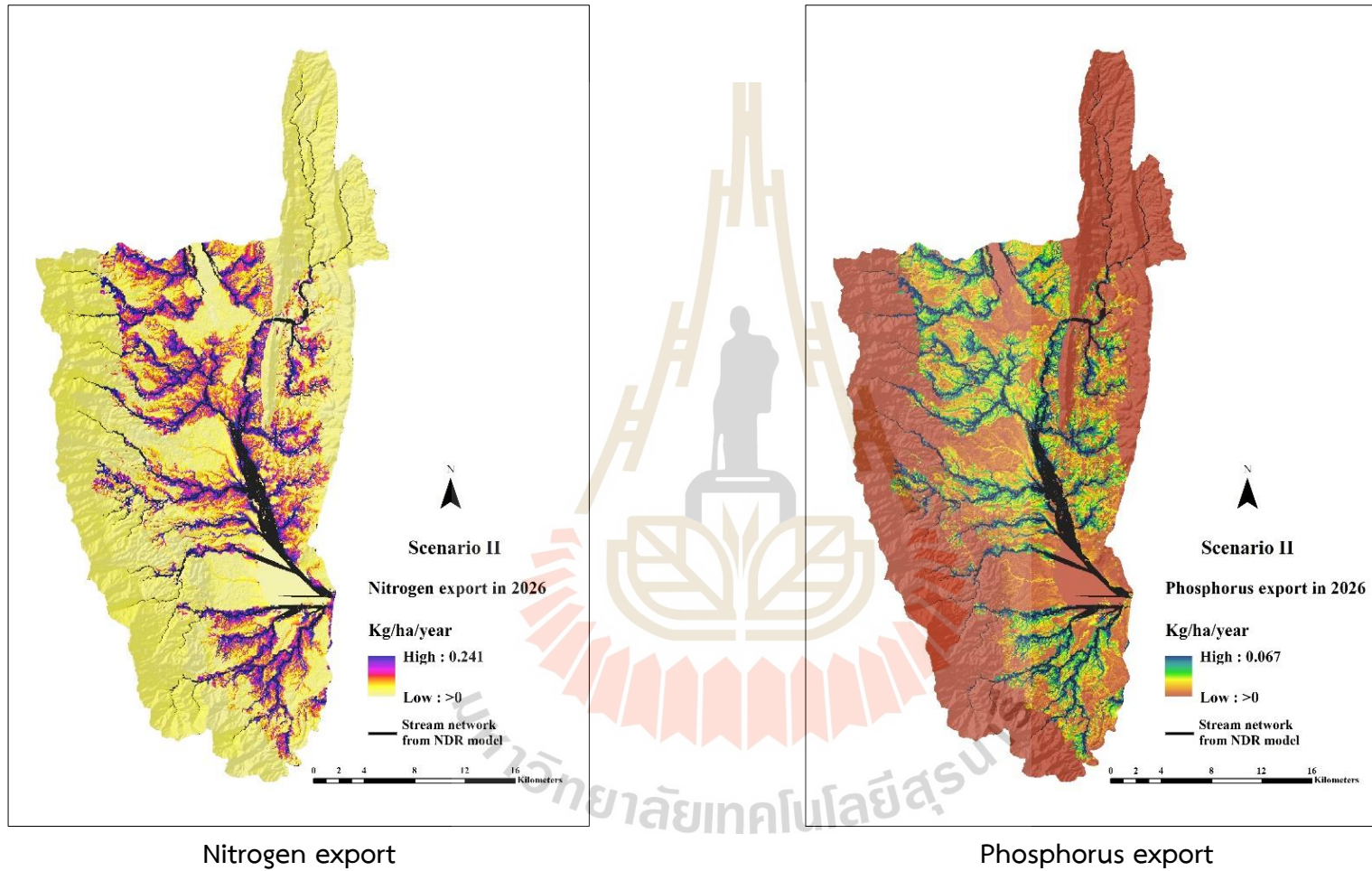


Figure 7.27 Spatial distribution of nitrogen and phosphorus export in 2026 under Scenario II.

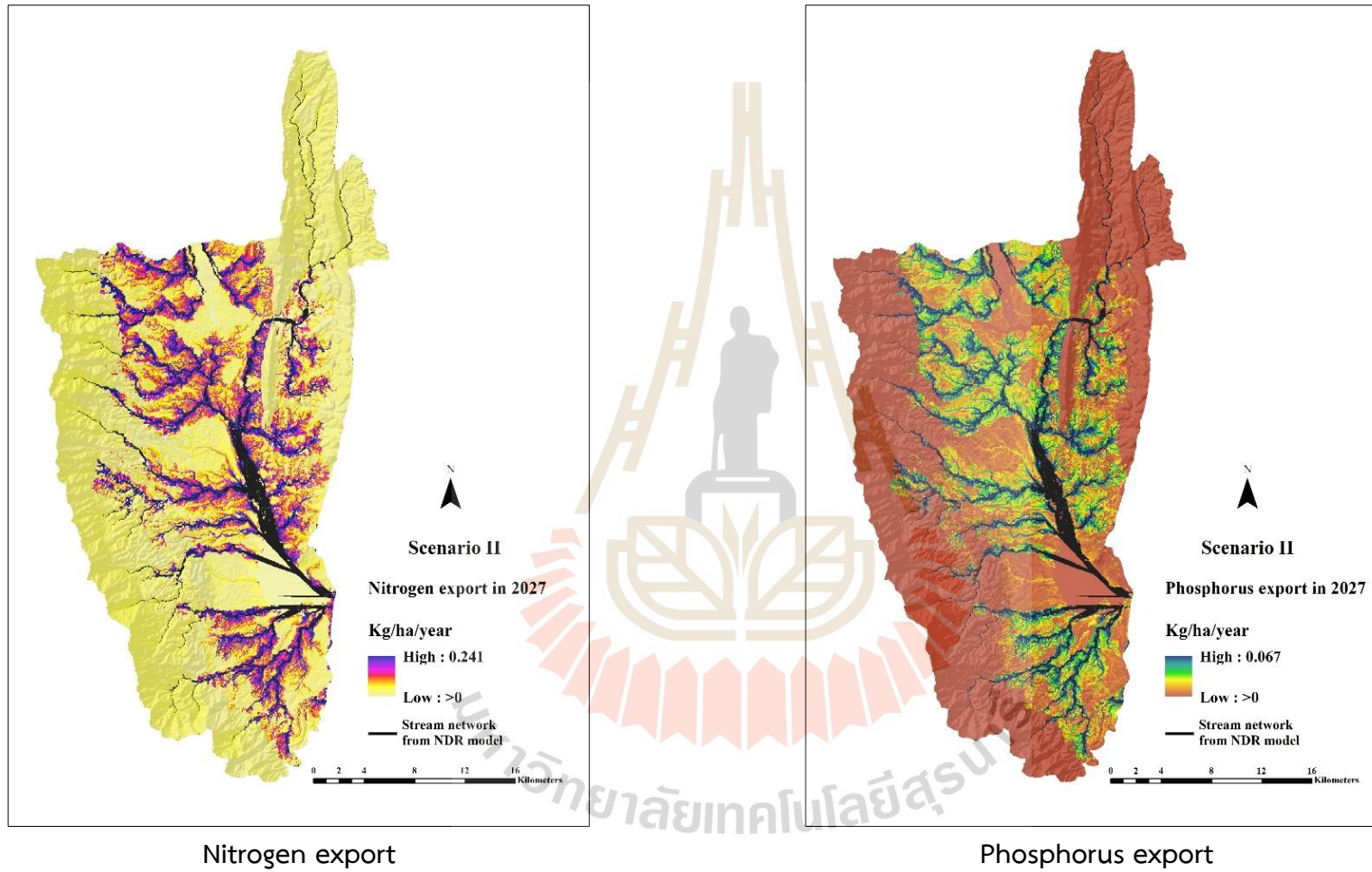


Figure 7.28 Spatial distribution of nitrogen and phosphorus export in 2027 under Scenario II.

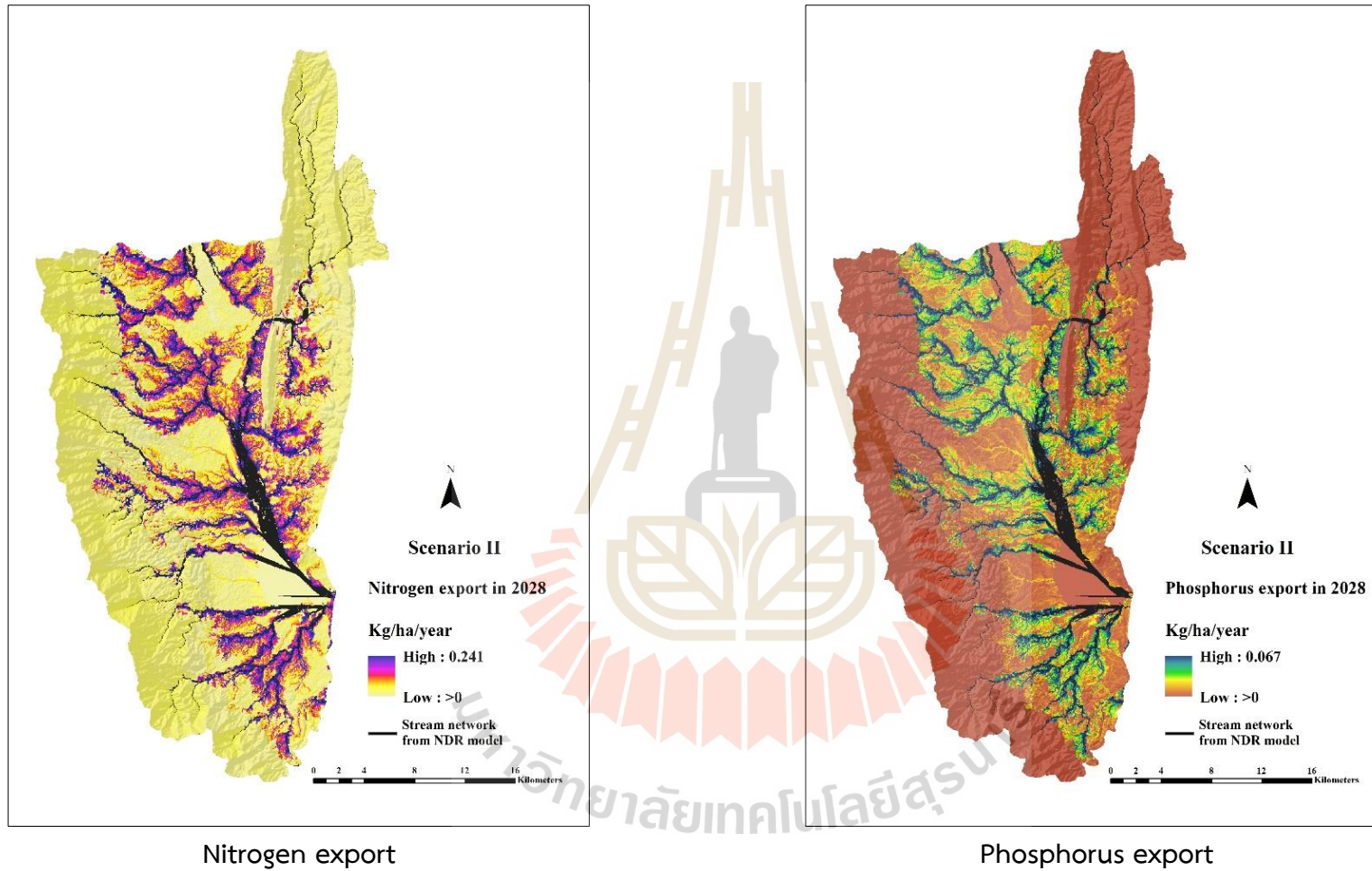


Figure 7.29 Spatial distribution of nitrogen and phosphorus export in 2028 under Scenario II.

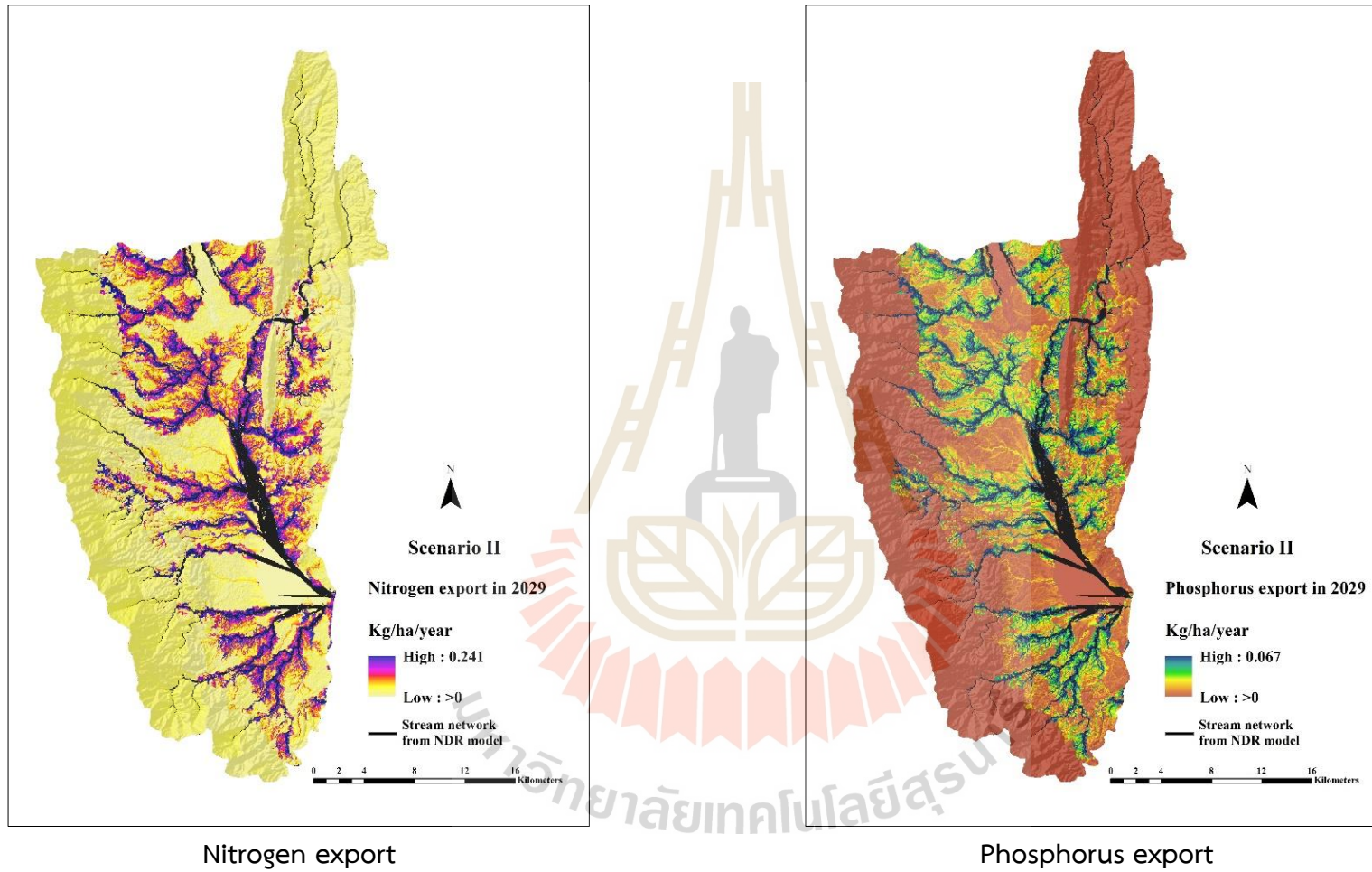


Figure 7.30 Spatial distribution of nitrogen and phosphorus export in 2029 under Scenario II.

As a result of load and export (nitrogen and phosphorus) by LULC classes under Scenario II (Maximization ecosystem service values) between 2020 and 2029 (Tables 7.29 to 7.38), the highest total nutrient load is found on the paddy field with a nitrogen value between 724,975.98 kg. (3,299.28 kg/km²) in 2020 and 695,319.69 kg. (3,298.80 kg/km²) in 2029, and the value of phosphorus between 197,739.23 kg. (899.89 kg/km²) in 2020 and 189,637.70 kg. (899.70 kg/km²) in 2029. However, the highest average nitrogen load appears on field crop with values between 3,313.42 kg/km² (18.56 %) in 2023 and 3,297.90 kg/km² (18.47 %) in 2029, while the highest average phosphorus load appears on several LULC classes, namely field crop, para rubber, and perennial tree and orchard between 2020 and 2029. In contrast, the lowest average nitrogen load occurs on the water body with a value of 0.30 kg/km² from 2020 to 2029, while the lowest total phosphorus load occurs on miscellaneous land with a value between 0.41 kg. (0.30 kg/km²) in 2029 and 0.76 kg. (0.30 kg/km²) in 2020.

In the meantime, the highest total nutrient export appears on the paddy field, with a value of nitrogen between 98,056.33 kg. (446.24 kg/km²) in 2020 and 92,700.60 kg. (439.80 kg/km²) in 2029, and a value of phosphorus between 26,742.63 kg. (121.70 kg/km²) in 2020 and 25,281.98 kg. (119.94 kg/km²) in 2029. Conversely, the lowest total nitrogen export occurs on the water body with a value of 0.07 kg/km² from 2020 to 2029, while the lowest total phosphorus export occurs on miscellaneous land, with a value between 0.04 kg (0.03 kg/km²) in 2029 and 0.14 kg. (0.05 kg/km²) in 2020. This result is similar to Han, Reidy, and Li (2021). They analyzed nutrient load and delivery from different scenarios and found cultivated crops' biggest load rate per unit area and very low retention efficiency. Besides, agriculture is the main cause of nutrient release in the watershed from different LULC scenarios.

This finding suggests that the change in LULC types associated with the biophysical table parameters affects nitrogen and phosphorus export. Notably, the LULC data under this scenario has influences nutrient export due to the LULC data of Scenario II (Maximization ecosystem service values) simulated based on the annual rate of LULC change from transition area matrix between 2009 and 2019 for some LULC types and the linear programming to maximize ecosystem service values by reducing the area of rangeland and miscellaneous land and increasing the area of

wetland. Therefore, it shows significant LULC change under this scenario due to the change of area and the amount load and export of nutrients.

7.6 Nutrient export estimation of predictive LULC of Scenario III

Estimating total and average nitrogen and phosphorus export of predictive LULC between 2020 and 2029 under Scenario III: Economic crop zonation is presented in Table 7.39.

Table 7.39 Estimation of nitrogen and phosphorus export between 2020 and 2029 under Scenario III.

Year	Area km ²	Nitrogen export		Phosphorus export	
		Total (kg)	Average (kg/km ²)	Total (kg)	Average (kg/km ²)
2020	891.35	200,387.36	224.81	43,956.03	49.31
2021	891.35	204,228.36	229.12	44,919.41	50.39
2022	891.35	207,404.15	232.69	45,715.39	51.29
2023	891.35	210,923.54	236.63	46,580.29	52.26
2024	891.35	213,774.11	239.83	47,267.91	53.03
2025	891.35	217,498.34	244.01	48,206.67	54.08
2026	891.35	220,573.44	247.46	48,942.83	54.91
2027	891.35	223,621.85	250.88	49,650.28	55.70
2028	891.35	226,714.19	254.35	50,389.99	56.53
2029	891.35	229,756.13	257.76	51,149.42	57.38

As a result, it was found that the highest total and average nitrogen export under Scenario III (Economic crop zonation) are 229,756.13 kg. and 257.76 kg/km² occurring in 2029, while the lowest total and average nitrogen export are 200,387.36 kg. and 224.81 kg/km² occurring in 2020. Likewise, the highest total and average phosphorus export under this scenario are 51,149.42 kg. and 57.38 kg/km² occurring in 2029, while the lowest total and average phosphorus export are 43,956.03 kg. and 49.31 kg/km² occurring in 2020. These results indicate that the change of LULC types and areas affects parameters in the biophysical table, which leads to different nitrogen

and phosphorus export like Scenario I and II.

The contribution of the predictive LULC of Scenario III (Economic crop zonation) on nutrient (nitrogen and phosphorus) load and export between 2020 and 2029 is summarized in Tables 7.40 to 7.49, and the spatial distribution of nitrogen and phosphorus export of the predictive LULC between 2020 and 2029 of Scenario III (Economic crop zonation) is displayed in Figures 7.31 to 7.40.



Table 7.40 Contribution of nutrient (nitrogen and phosphorus) load and export by LULC classes in 2020 under Scenario III.

LULC types	Area	Nitrogen loads			Phosphorus loads			Nitrogen export			Phosphorus export		
	km ²	Total (kg.)	Average (kg/km ²)	%	Total (kg.)	Average (kg/km ²)	%	Total (kg.)	Average (kg/km ²)	%	Total (kg.)	Average (kg/km ²)	%
Urban and built-up area (UR)	33.20	77,271.55	2,327.47	13.03	4,320.98	130.15	3.47	9,409.09	283.41	11.65	526.10	15.85	3.05
Paddy field (PD)	226.72	747,941.81	3,298.95	18.47	204,003.82	899.80	24.02	103,451.12	456.29	18.76	28,213.94	124.44	23.93
Field crop (FC)	23.08	76,221.65	3,301.91	18.49	20,789.73	900.61	24.04	10,912.50	472.73	19.43	2,976.14	128.93	24.79
Para rubber (RB)	19.78	59,421.27	3,003.52	16.81	17,828.10	901.14	24.06	7,869.31	397.76	16.35	2,360.79	119.33	22.94
Perennial tree and orchard (PO)	74.06	222,682.58	3,006.88	16.83	66,811.22	902.15	24.08	32,190.51	434.67	17.87	9,657.15	130.40	25.07
Forest land (FO)	433.30	234,078.81	540.22	3.02	1,430.62	3.30	0.09	33,574.02	77.48	3.19	205.17	0.47	0.09
Water body (WB)	34.34	10.31	0.30	0.00	10.31	0.30	0.01	2.39	0.07	0.00	2.39	0.07	0.01
Rangeland (RL)	27.86	16,668.31	598.35	3.35	91.68	3.29	0.09	1,990.24	71.44	2.94	10.95	0.39	0.08
Wetland (WL)	16.22	9,712.87	598.96	3.35	80.95	4.99	0.13	389.14	24.00	0.99	3.24	0.20	0.04
Miscellaneous land (ML)	2.79	3,308.92	1,185.91	6.64	0.83	0.30	0.01	599.04	214.69	8.83	0.15	0.05	0.01
Total	891.35	1,447,318.09		100.00	315,368.24		100.00	200,387.36		100.00	43,956.03		100.00

Table 7.41 Contribution of nutrient (nitrogen and phosphorus) load and export by LULC classes in 2021 under Scenario III.

LULC types	Area	Nitrogen loads			Phosphorus loads			Nitrogen export			Phosphorus export		
	km ²	Total (kg.)	Average (kg/km ²)	%	Total (kg.)	Average (kg/km ²)	%	Total (kg.)	Average (kg/km ²)	%	Total (kg.)	Average (kg/km ²)	%
Urban and built-up area (UR)	33.78	78,638.48	2,327.80	13.03	4,397.08	130.16	3.47	9,657.61	285.88	11.48	540.00	15.98	2.99
Paddy field (PD)	232.67	767,235.71	3,297.47	18.46	209,250.61	899.33	24.00	107,527.56	462.14	18.56	29,325.70	126.04	23.55
Field crop (FC)	24.26	80,328.17	3,310.90	18.53	21,908.15	902.99	24.10	12,398.13	511.02	20.53	3,381.31	139.37	26.04
Para rubber (RB)	19.83	59,570.75	3,003.48	16.81	17,871.61	901.06	24.05	7,998.18	403.26	16.20	2,399.46	120.98	22.61
Perennial tree and orchard (PO)	68.78	206,594.02	3,003.48	16.81	61,979.54	901.06	24.05	30,172.33	438.65	17.62	9,051.70	131.59	24.59
Forest land (FO)	429.61	232,029.93	540.09	3.02	1,417.99	3.30	0.09	33,394.96	77.73	3.12	204.08	0.48	0.09
Water body (WB)	34.93	10.49	0.30	0.00	10.49	0.30	0.01	2.43	0.07	0.00	2.43	0.07	0.01
Rangeland (RL)	28.46	17,059.56	599.43	3.35	93.83	3.30	0.09	2,066.05	72.60	2.92	11.36	0.40	0.07
Wetland (WL)	16.10	9,634.14	598.54	3.35	80.29	4.99	0.13	386.24	24.00	0.96	3.22	0.20	0.04
Miscellaneous land (ML)	2.92	3,459.43	1,185.67	6.64	0.86	0.30	0.01	624.86	214.16	8.60	0.16	0.05	0.01
Total	891.35	1,454,560.68		100.00	317,010.45		100.00	204,228.36		100.00	44,919.41		100.00

Table 7.42 Contribution of nutrient (nitrogen and phosphorus) load and export by LULC classes in 2022 under Scenario III.

LULC types	Area	Nitrogen loads			Phosphorus loads			Nitrogen export			Phosphorus export		
	km ²	Total (kg.)	Average (kg/km ²)	%	Total (kg.)	Average (kg/km ²)	%	Total (kg.)	Average (kg/km ²)	%	Total (kg.)	Average (kg/km ²)	%
Urban and built-up area (UR)	33.94	78,952.86	2,326.43	13.04	4,413.38	130.04	3.48	9,783.35	288.28	11.40	547.03	16.12	2.96
Paddy field (PD)	238.65	786,471.20	3,295.44	18.47	214,434.48	898.52	24.02	111,292.00	466.33	18.44	30,352.36	127.18	23.33
Field crop (FC)	25.54	84,239.54	3,298.11	18.48	22,968.24	899.24	24.04	13,618.36	533.18	21.08	3,714.10	145.41	26.67
Para rubber (RB)	19.85	59,580.70	3,001.34	16.82	17,869.41	900.16	24.06	8,103.23	408.19	16.14	2,430.97	122.46	22.46
Perennial tree and orchard (PO)	63.62	191,079.76	3,003.36	16.83	57,308.52	900.77	24.08	28,166.67	442.72	17.51	8,450.00	132.82	24.36
Forest land (FO)	425.98	229,917.44	539.73	3.02	1,404.67	3.30	0.09	33,270.78	78.10	3.09	203.32	0.48	0.09
Water body (WB)	35.73	10.72	0.30	0.00	10.72	0.30	0.01	2.48	0.07	0.00	2.48	0.07	0.01
Rangeland (RL)	29.06	17,469.16	601.20	3.37	96.05	3.31	0.09	2,141.57	73.70	2.91	11.78	0.41	0.07
Wetland (WL)	15.97	9,559.79	598.47	3.35	79.64	4.99	0.13	382.76	23.96	0.95	3.19	0.20	0.04
Miscellaneous land (ML)	3.00	3,536.15	1,179.62	6.61	0.88	0.29	0.01	642.94	214.48	8.48	0.16	0.05	0.01
Total	891.35	1,460,817.32		100.00	318,586.00		100.00	207,404.15		100.00	45,715.39		100.00

Table 7.43 Contribution of nutrient (nitrogen and phosphorus) load and export by LULC classes in 2023 under Scenario III.

LULC types	Area	Nitrogen loads			Phosphorus loads			Nitrogen export			Phosphorus export		
	km ²	Total (kg.)	Average (kg/km ²)	%	Total (kg.)	Average (kg/km ²)	%	Total (kg.)	Average (kg/km ²)	%	Total (kg.)	Average (kg/km ²)	%
Urban and built-up area (UR)	34.56	80,493.13	2,328.75	13.05	4,500.62	130.21	3.48	10,164.81	294.08	11.46	568.35	16.44	2.97
Paddy field (PD)	244.54	806,812.86	3,299.25	18.48	220,036.54	899.78	24.03	115,572.97	472.60	18.41	31,519.90	128.89	23.29
Field crop (FC)	26.74	88,198.15	3,298.13	18.48	24,053.68	899.48	24.02	14,528.13	543.27	21.16	3,962.22	148.17	26.78
Para rubber (RB)	19.87	59,665.30	3,002.57	16.82	17,899.32	900.76	24.06	8,221.49	413.74	16.12	2,466.45	124.12	22.43
Perennial tree and orchard (PO)	58.31	175,313.04	3,006.49	16.84	52,593.12	901.93	24.09	26,145.32	448.37	17.47	7,843.59	134.51	24.31
Forest land (FO)	422.30	228,052.81	540.03	3.03	1,393.63	3.30	0.09	33,030.11	78.22	3.05	201.85	0.48	0.09
Water body (WB)	36.43	10.94	0.30	0.00	10.94	0.30	0.01	2.53	0.07	0.00	2.53	0.07	0.01
Rangeland (RL)	29.68	17,772.69	598.82	3.35	97.75	3.29	0.09	2,193.60	73.91	2.88	12.06	0.41	0.07
Wetland (WL)	15.78	9,441.47	598.47	3.35	78.68	4.99	0.13	377.86	23.95	0.93	3.15	0.20	0.04
Miscellaneous land (ML)	3.14	3,694.72	1,177.52	6.60	0.92	0.29	0.01	686.72	218.86	8.53	0.17	0.05	0.01
Total	891.35	1,469,455.10		100.00	320,665.19		100.00	210,923.54		100.00	46,580.29		100.00

Table 7.44 Contribution of nutrient (nitrogen and phosphorus) load and export by LULC classes in 2024 under Scenario III.

LULC types	Area	Nitrogen loads			Phosphorus loads			Nitrogen export			Phosphorus export		
	km ²	Total (kg.)	Average (kg/km ²)	%	Total (kg.)	Average (kg/km ²)	%	Total (kg.)	Average (kg/km ²)	%	Total (kg.)	Average (kg/km ²)	%
Urban and built-up area (UR)	34.76	80,910.82	2,327.54	13.04	4,522.66	130.10	3.48	10,286.05	295.90	11.29	575.13	16.54	2.94
Paddy field (PD)	250.55	825,981.36	3,296.70	18.47	225,198.49	898.83	24.02	119,105.09	475.38	18.14	32,483.21	129.65	23.06
Field crop (FC)	27.93	92,103.87	3,297.73	18.48	25,111.53	899.11	24.03	15,715.19	562.67	21.47	4,285.96	153.46	27.30
Para rubber (RB)	19.89	59,700.93	3,001.34	16.82	17,904.78	900.13	24.06	8,338.71	419.21	15.99	2,501.61	125.76	22.37
Perennial tree and orchard (PO)	53.13	159,633.33	3,004.65	16.83	47,875.30	901.12	24.08	24,008.38	451.89	17.24	7,202.51	135.57	24.11
Forest land (FO)	418.60	225,944.90	539.76	3.02	1,380.35	3.30	0.09	32,898.41	78.59	3.00	201.05	0.48	0.09
Water body (WB)	37.07	11.12	0.30	0.00	11.12	0.30	0.01	2.57	0.07	0.00	2.57	0.07	0.01
Rangeland (RL)	30.61	18,325.30	598.73	3.35	100.76	3.29	0.09	2,287.74	74.75	2.85	12.58	0.41	0.07
Wetland (WL)	15.63	9,337.24	597.35	3.35	77.79	4.98	0.13	372.69	23.84	0.91	3.11	0.20	0.04
Miscellaneous land (ML)	3.18	3,768.14	1,184.87	6.64	0.94	0.30	0.01	759.30	238.76	9.11	0.19	0.06	0.01
Total	891.35	1,475,717.02		100.00	322,183.70		100.00	213,774.11		100.00	47,267.91		100.00

Table 7.45 Contribution of nutrient (nitrogen and phosphorus) load and export by LULC classes in 2025 under Scenario III.

LULC types	Area	Nitrogen loads			Phosphorus loads			Nitrogen export			Phosphorus export		
	km ²	Total (kg.)	Average (kg/km ²)	%	Total (kg.)	Average (kg/km ²)	%	Total (kg.)	Average (kg/km ²)	%	Total (kg.)	Average (kg/km ²)	%
Urban and built-up area (UR)	35.41	82,561.08	2,331.58	13.05	4,616.71	130.38	3.48	10,526.63	297.28	11.13	588.59	16.62	2.90
Paddy field (PD)	256.39	845,872.92	3,299.19	18.47	230,712.05	899.86	24.04	123,526.96	481.80	18.04	33,689.17	131.40	22.95
Field crop (FC)	29.15	95,715.09	3,283.59	18.38	26,106.31	895.60	23.92	17,140.01	588.00	22.02	4,674.55	160.36	28.01
Para rubber (RB)	19.89	59,757.29	3,003.80	16.82	17,928.70	901.22	24.07	8,419.35	423.21	15.85	2,525.81	126.96	22.18
Perennial tree and orchard (PO)	47.91	144,435.05	3,014.82	16.88	43,334.16	904.52	24.16	21,701.02	452.97	16.96	6,510.31	135.89	23.74
Forest land (FO)	414.93	224,123.85	540.15	3.02	1,369.76	3.30	0.09	32,647.61	78.68	2.95	199.51	0.48	0.08
Water body (WB)	37.96	11.40	0.30	0.00	11.40	0.30	0.01	2.62	0.07	0.00	2.62	0.07	0.01
Rangeland (RL)	30.94	18,536.43	599.07	3.35	101.96	3.30	0.09	2,335.68	75.49	2.83	12.85	0.42	0.07
Wetland (WL)	15.43	9,227.70	597.99	3.35	76.90	4.98	0.13	368.46	23.88	0.89	3.07	0.20	0.03
Miscellaneous land (ML)	3.34	3,968.70	1,189.93	6.66	0.99	0.30	0.01	829.99	248.86	9.32	0.21	0.06	0.01
Total	891.35	1,484,209.51		100.00	324,258.95		100.00	217,498.34		100.00	48,206.67		100.00

Table 7.46 Contribution of nutrient (nitrogen and phosphorus) load and export by LULC classes in 2026 under Scenario III.

LULC types	Area	Nitrogen loads			Phosphorus loads			Nitrogen export			Phosphorus export		
	km ²	Total (kg.)	Average (kg/km ²)	%	Total (kg.)	Average (kg/km ²)	%	Total (kg.)	Average (kg/km ²)	%	Total (kg.)	Average (kg/km ²)	%
Urban and built-up area (UR)	35.75	83,344.43	2,331.15	13.04	4,660.65	130.36	3.48	10,705.50	299.43	11.04	598.59	16.74	2.89
Paddy field (PD)	262.42	865,961.06	3,299.89	18.46	236,198.03	900.07	24.01	127,655.67	486.45	17.94	34,815.18	132.67	22.94
Field crop (FC)	30.40	100,232.24	3,297.42	18.45	27,339.17	899.40	24.00	18,409.02	605.62	22.34	5,020.64	165.17	28.56
Para rubber (RB)	19.89	59,736.71	3,003.90	16.81	17,923.05	901.27	24.05	8,470.36	425.94	15.71	2,541.11	127.78	22.09
Perennial tree and orchard (PO)	42.65	128,639.99	3,015.97	16.88	38,596.38	904.89	24.14	19,165.48	449.34	16.57	5,749.64	134.80	23.31
Forest land (FO)	411.24	222,145.03	540.19	3.02	1,357.71	3.30	0.09	32,437.75	78.88	2.91	198.23	0.48	0.08
Water body (WB)	38.71	11.62	0.30	0.00	11.63	0.30	0.01	2.66	0.07	0.00	2.66	0.07	0.01
Rangeland (RL)	31.56	18,854.96	597.34	3.34	103.71	3.29	0.09	2,456.05	77.81	2.87	13.51	0.43	0.07
Wetland (WL)	15.29	9,153.07	598.49	3.35	76.28	4.99	0.13	364.35	23.82	0.88	3.04	0.20	0.03
Miscellaneous land (ML)	3.44	4,077.16	1,186.86	6.64	1.02	0.30	0.01	906.61	263.91	9.73	0.23	0.07	0.01
Total	891.35	1,492,156.27		100.00	326,267.62		100.00	220,573.44		100.00	48,942.83		100.00

Table 7.47 Contribution of nutrient (nitrogen and phosphorus) load and export by LULC classes in 2027 under Scenario III.

LULC types	Area	Nitrogen loads			Phosphorus loads			Nitrogen export			Phosphorus export		
	km ²	Total (kg.)	Average (kg/km ²)	%	Total (kg.)	Average (kg/km ²)	%	Total (kg.)	Average (kg/km ²)	%	Total (kg.)	Average (kg/km ²)	%
Urban and built-up area (UR)	36.10	84,062.03	2,328.75	13.04	4,698.94	130.17	3.48	10,941.66	303.11	11.04	611.79	16.95	2.91
Paddy field (PD)	268.46	885,091.14	3,296.90	18.46	241,321.38	898.91	24.00	131,852.88	491.14	17.89	35,959.88	133.95	23.02
Field crop (FC)	31.62	104,585.14	3,307.33	18.52	28,515.29	901.75	24.08	19,359.88	612.22	22.30	5,279.97	166.97	28.70
Para rubber (RB)	19.88	59,657.47	3,000.67	16.80	17,892.26	899.95	24.03	8,527.50	428.92	15.63	2,558.25	128.68	22.11
Perennial tree and orchard (PO)	37.46	112,692.92	3,008.14	16.84	33,798.48	902.19	24.09	16,743.61	446.94	16.28	5,023.08	134.08	23.04
Forest land (FO)	407.57	219,971.39	539.72	3.02	1,343.90	3.30	0.09	32,313.82	79.28	2.89	197.47	0.48	0.08
Water body (WB)	39.48	11.84	0.30	0.00	11.83	0.30	0.01	2.69	0.07	0.00	2.69	0.07	0.01
Rangeland (RL)	32.14	19,194.12	597.25	3.34	105.54	3.28	0.09	2,531.12	78.76	2.87	13.92	0.43	0.07
Wetland (WL)	15.11	9,031.73	597.69	3.35	75.24	4.98	0.13	357.45	23.66	0.86	2.98	0.20	0.03
Miscellaneous land (ML)	3.53	4,186.92	1,186.01	6.64	1.05	0.30	0.01	991.22	280.78	10.23	0.25	0.07	0.01
Total	891.35	1,498,484.70		100.00	327,763.91		100.00	223,621.85		100.00	49,650.28		100.00

Table 7.48 Contribution of nutrient (nitrogen and phosphorus) load and export by LULC classes in 2028 under Scenario III.

LULC types	Area	Nitrogen loads			Phosphorus loads			Nitrogen export			Phosphorus export		
	km ²	Total (kg.)	Average (kg/km ²)	%	Total (kg.)	Average (kg/km ²)	%	Total (kg.)	Average (kg/km ²)	%	Total (kg.)	Average (kg/km ²)	%
Urban and built-up area (UR)	36.65	85,385.38	2,329.91	13.05	4,773.48	130.25	3.48	11,196.60	305.52	11.03	626.05	17.08	2.92
Paddy field (PD)	274.37	904,867.58	3,297.96	18.47	246,743.16	899.30	24.02	136,427.60	497.24	17.95	37,207.53	135.61	23.18
Field crop (FC)	32.79	108,074.73	3,295.74	18.45	29,470.28	898.70	24.00	20,117.90	613.49	22.15	5,486.70	167.32	28.60
Para rubber (RB)	19.59	58,790.60	3,000.46	16.80	17,634.40	900.00	24.04	8,469.49	432.25	15.61	2,540.85	129.68	22.17
Perennial tree and orchard (PO)	32.17	96,927.17	3,012.99	16.87	29,073.57	903.75	24.14	14,374.42	446.83	16.13	4,312.33	134.05	22.91
Forest land (FO)	403.96	218,084.18	539.87	3.02	1,332.53	3.30	0.09	32,103.90	79.47	2.87	196.19	0.49	0.08
Water body (WB)	40.47	12.13	0.30	0.00	12.13	0.30	0.01	2.75	0.07	0.00	2.75	0.07	0.01
Rangeland (RL)	32.78	19,628.90	598.72	3.35	107.94	3.29	0.09	2,616.99	79.82	2.88	14.39	0.44	0.08
Wetland (WL)	14.96	8,946.13	598.06	3.35	74.54	4.98	0.13	352.96	23.60	0.85	2.94	0.20	0.03
Miscellaneous land (ML)	3.61	4,283.04	1,186.35	6.64	1.07	0.30	0.01	1,051.59	291.28	10.52	0.26	0.07	0.01
Total	891.35	1,504,999.84		100.00	329,223.10		100.00	226,714.19		100.00	50,389.99		100.00

Table 7.49 Contribution of nutrient (nitrogen and phosphorus) load and export by LULC classes in 2029 under Scenario III.

LULC types	Area	Nitrogen loads			Phosphorus loads			Nitrogen export			Phosphorus export		
	km ²	Total (kg.)	Average (kg/km ²)	%	Total (kg.)	Average (kg/km ²)	%	Total (kg.)	Average (kg/km ²)	%	Total (kg.)	Average (kg/km ²)	%
Urban and built-up area (UR)	36.96	86,150.49	2,331.06	13.04	4,817.17	130.34	3.48	11,329.76	306.56	10.97	633.49	17.14	2.91
Paddy field (PD)	280.20	924,496.58	3,299.39	18.46	252,143.21	899.86	24.01	140,538.09	501.56	17.95	38,328.57	136.79	23.23
Field crop (FC)	34.11	112,856.57	3,308.37	18.51	30,780.01	902.31	24.07	21,438.94	628.48	22.49	5,846.98	171.40	29.11
Para rubber (RB)	19.78	59,396.35	3,003.02	16.80	17,819.45	900.93	24.04	8,631.81	436.42	15.61	2,589.54	130.92	22.24
Perennial tree and orchard (PO)	26.94	81,057.37	3,008.60	16.83	24,317.96	902.61	24.08	11,784.30	437.40	15.65	3,535.29	131.22	22.29
Forest land (FO)	400.22	216,153.51	540.08	3.02	1,320.98	3.30	0.09	31,873.94	79.64	2.85	194.79	0.49	0.08
Water body (WB)	41.11	12.34	0.30	0.00	12.34	0.30	0.01	2.80	0.07	0.00	2.80	0.07	0.01
Rangeland (RL)	33.44	19,956.11	596.73	3.34	109.76	3.28	0.09	2,683.90	80.25	2.87	14.76	0.44	0.07
Wetland (WL)	14.85	8,898.79	599.10	3.35	74.16	4.99	0.13	351.07	23.64	0.85	2.93	0.20	0.03
Miscellaneous land (ML)	3.73	4,439.13	1,190.83	6.66	1.11	0.30	0.01	1,121.52	300.86	10.76	0.28	0.08	0.01
Total	891.35	1,513,417.24		100.00	331,396.15		100.00	229,756.13		100.00	51,149.42		100.00

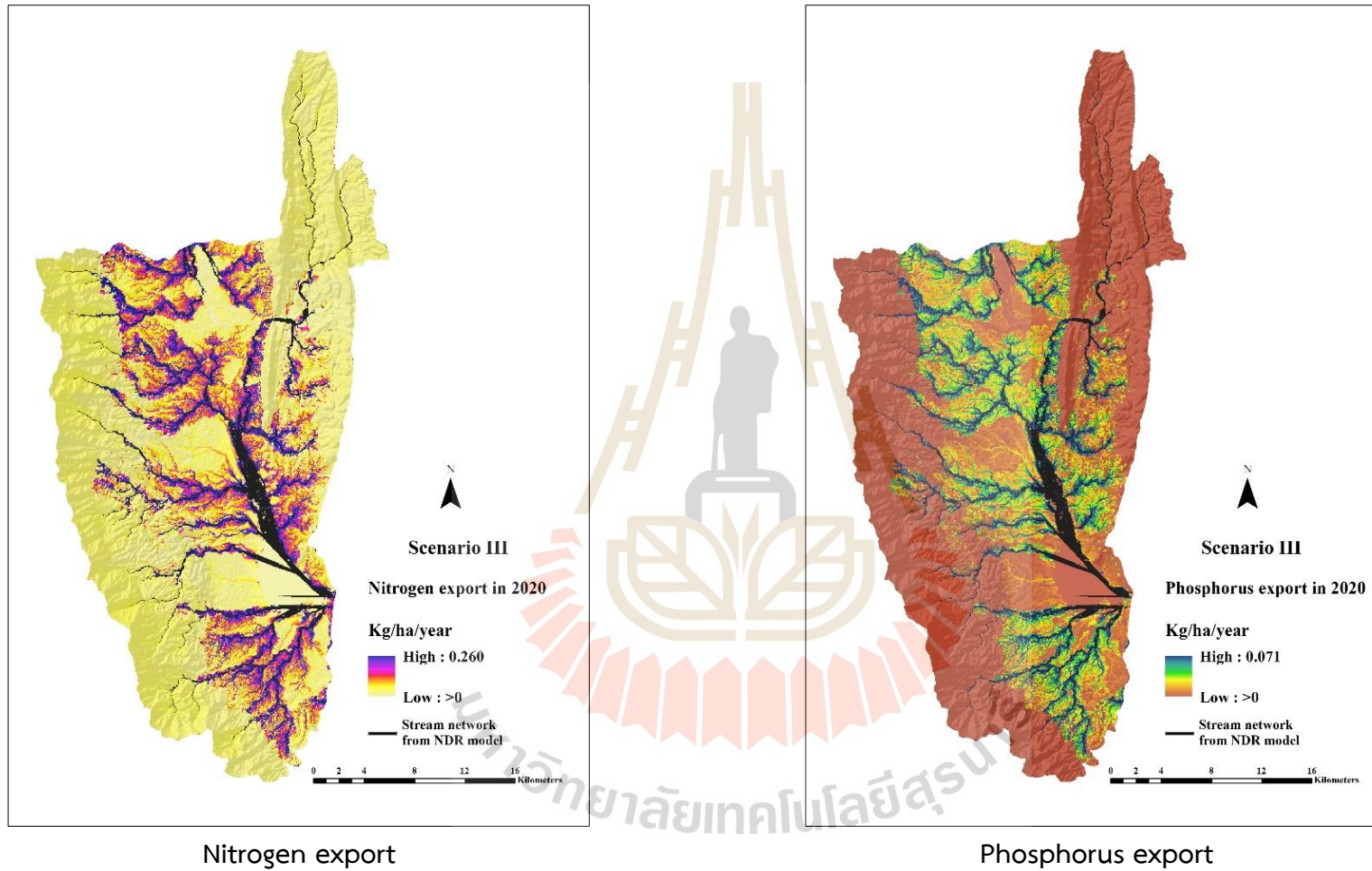


Figure 7.31 Spatial distribution of nitrogen and phosphorus export in 2020 under Scenario III.

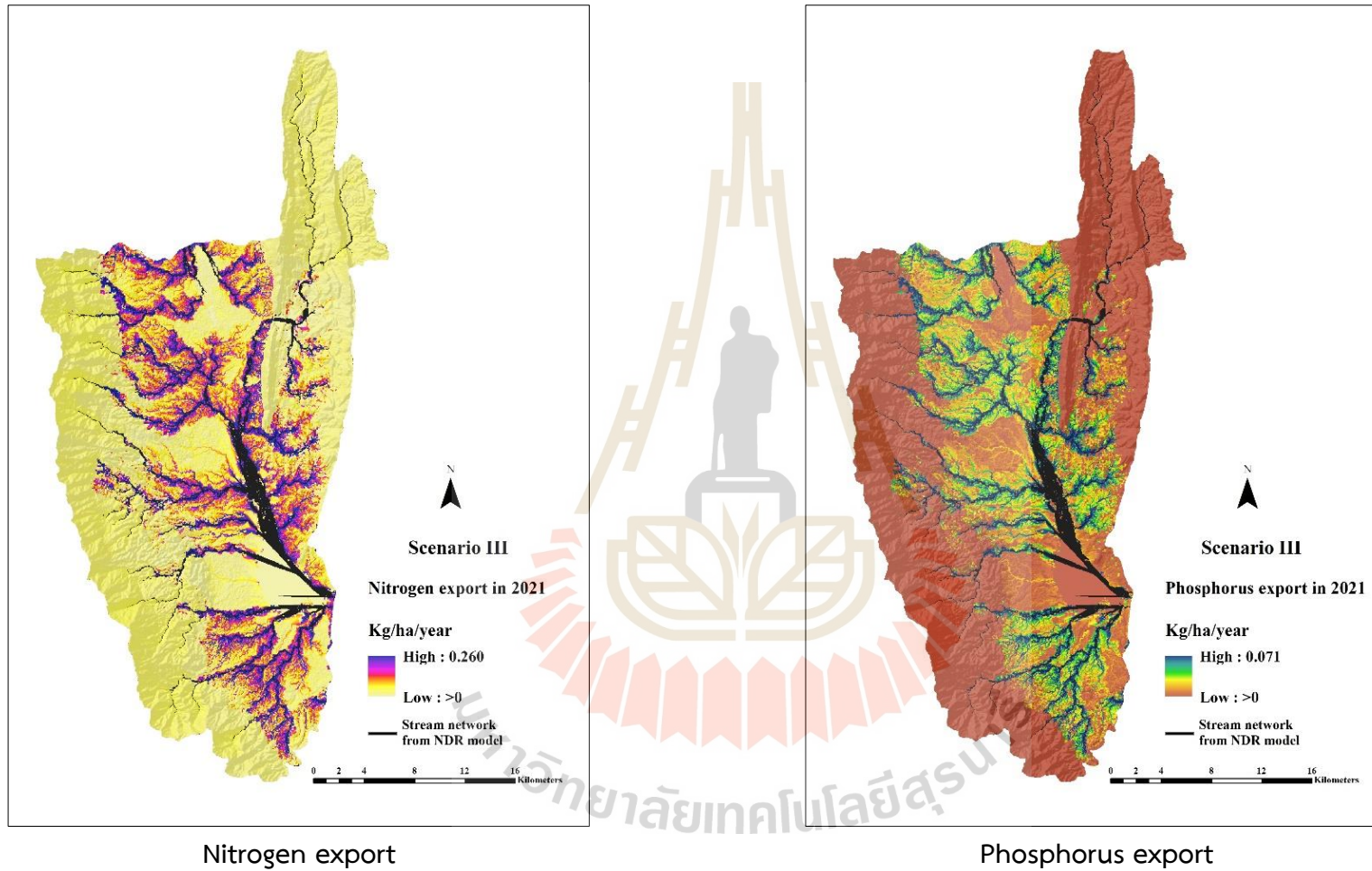


Figure 7.32 Spatial distribution of nitrogen and phosphorus export in 2021 under Scenario III.

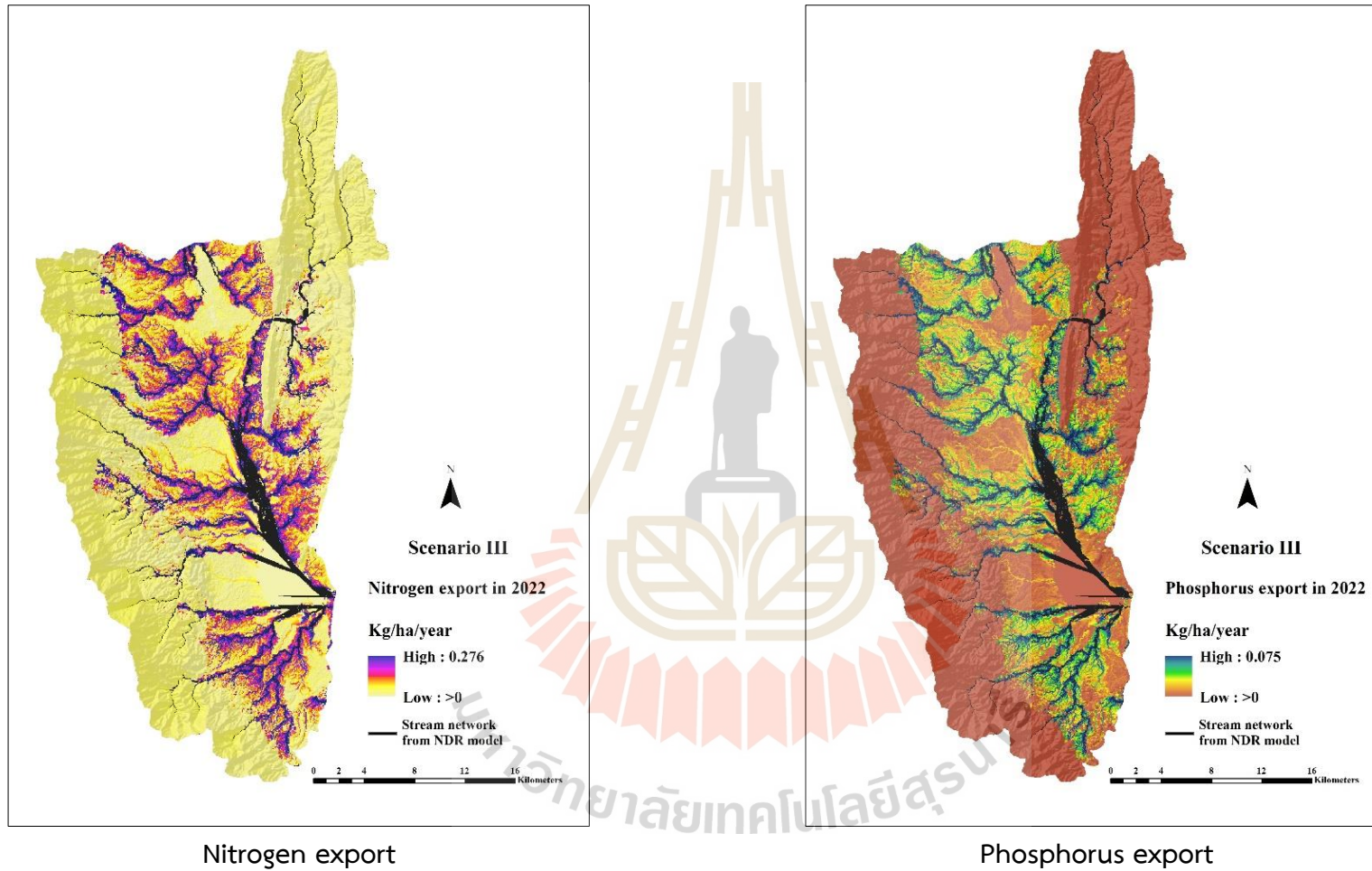


Figure 7.33 Spatial distribution of nitrogen and phosphorus export in 2022 under Scenario III.

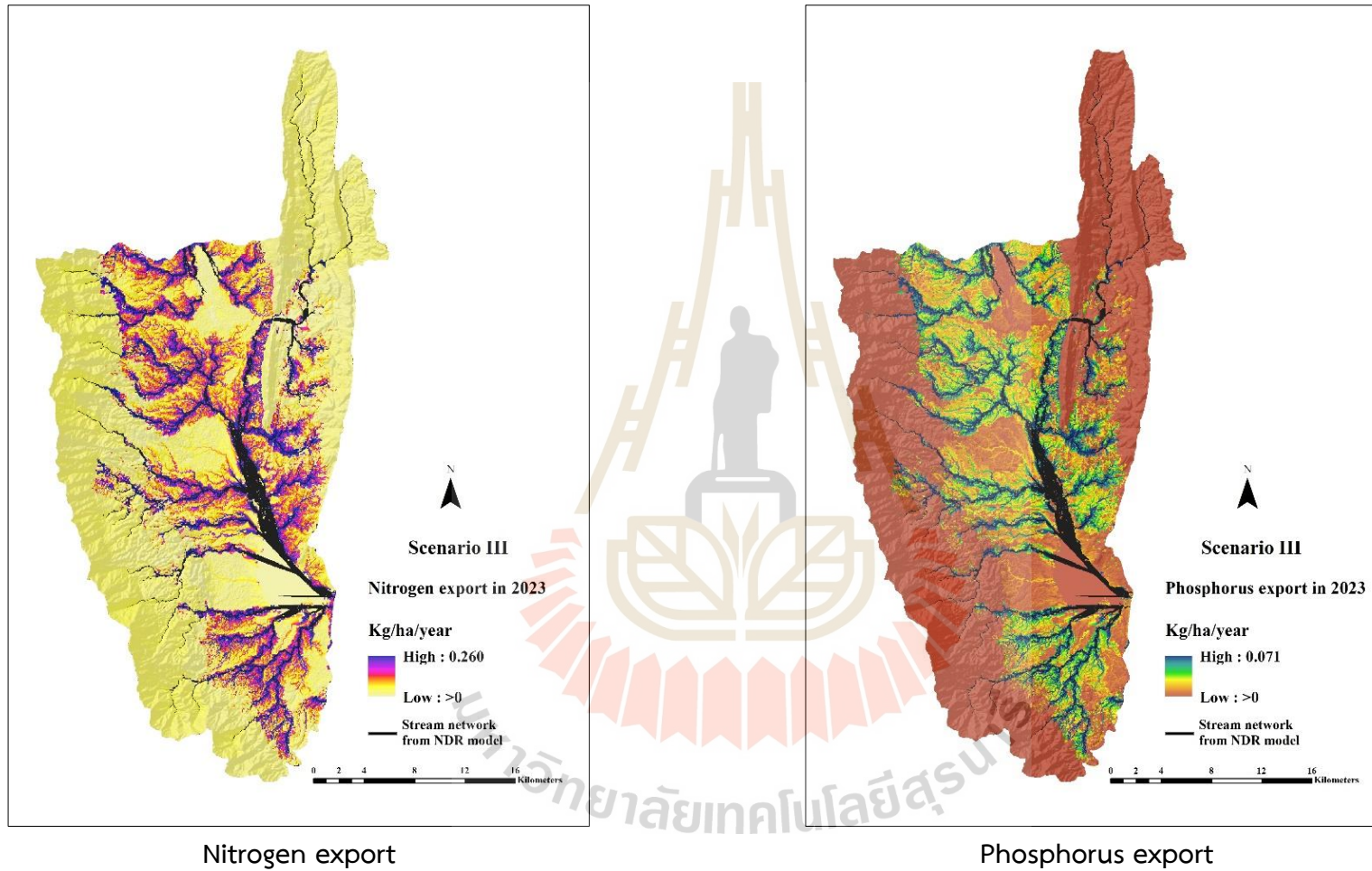


Figure 7.34 Spatial distribution of nitrogen and phosphorus export in 2023 under Scenario III.

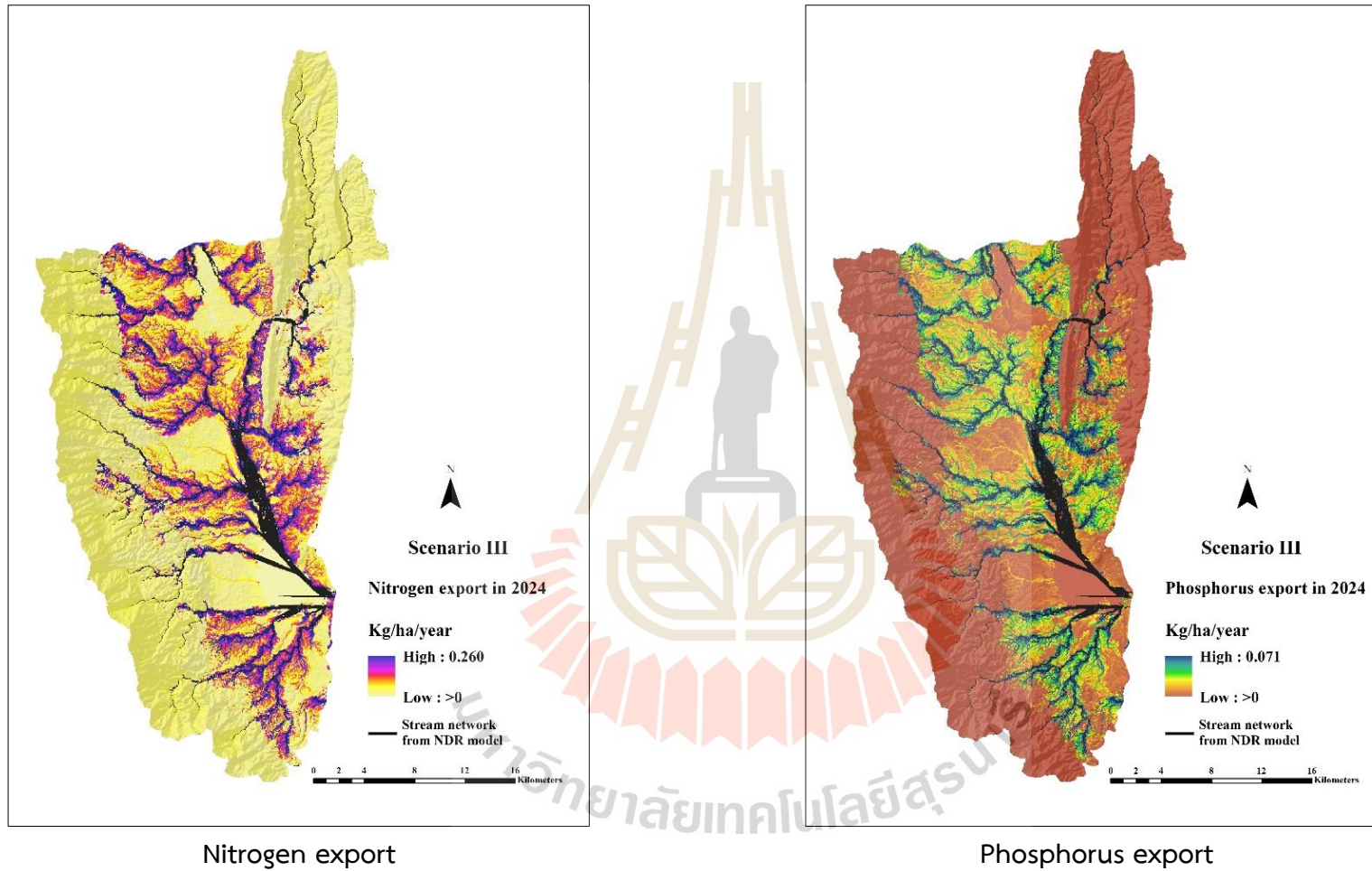


Figure 7.35 Spatial distribution of nitrogen and phosphorus export in 2024 under Scenario III.

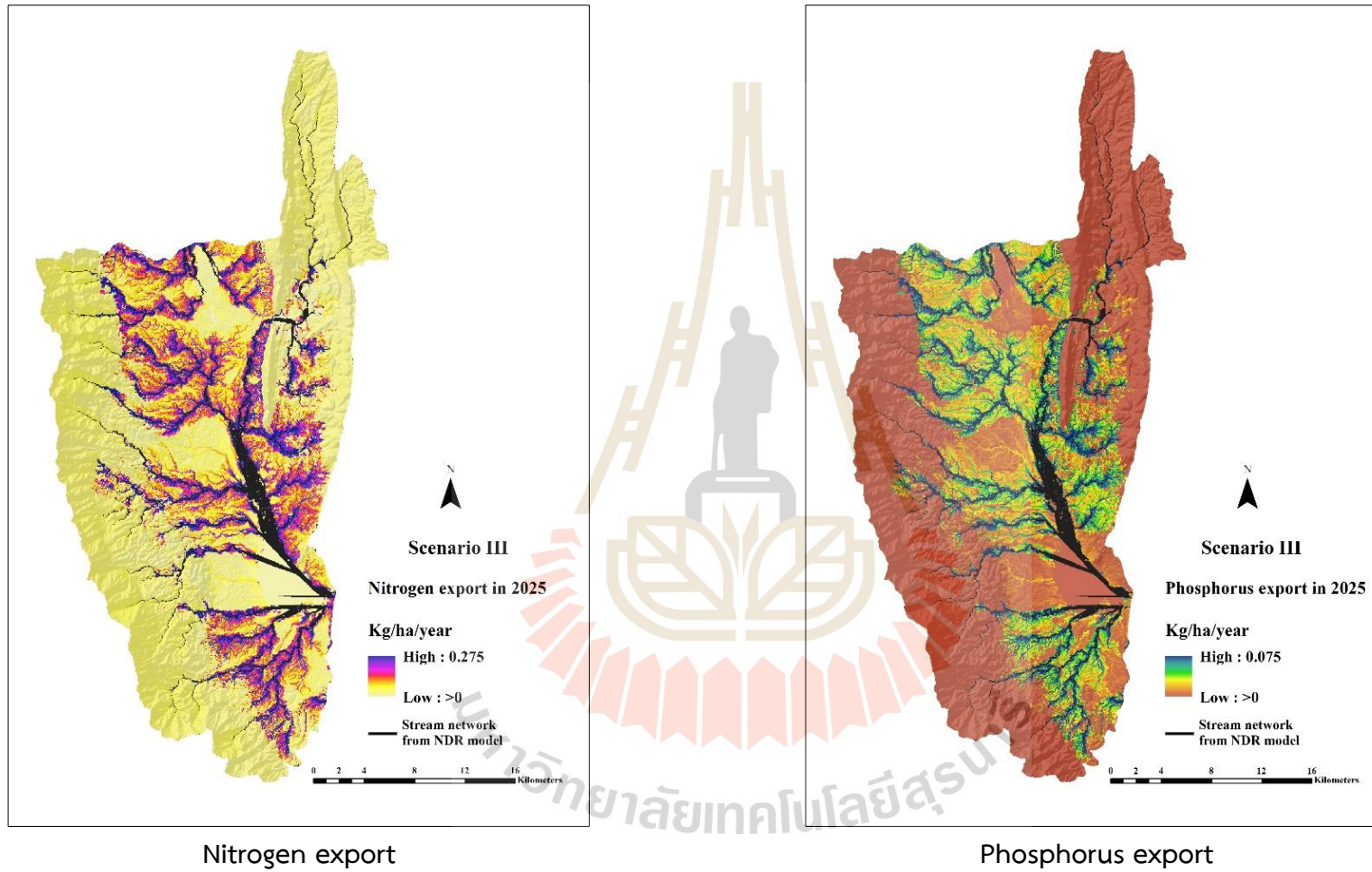


Figure 7.36 Spatial distribution of nitrogen and phosphorus export in 2025 under Scenario III.

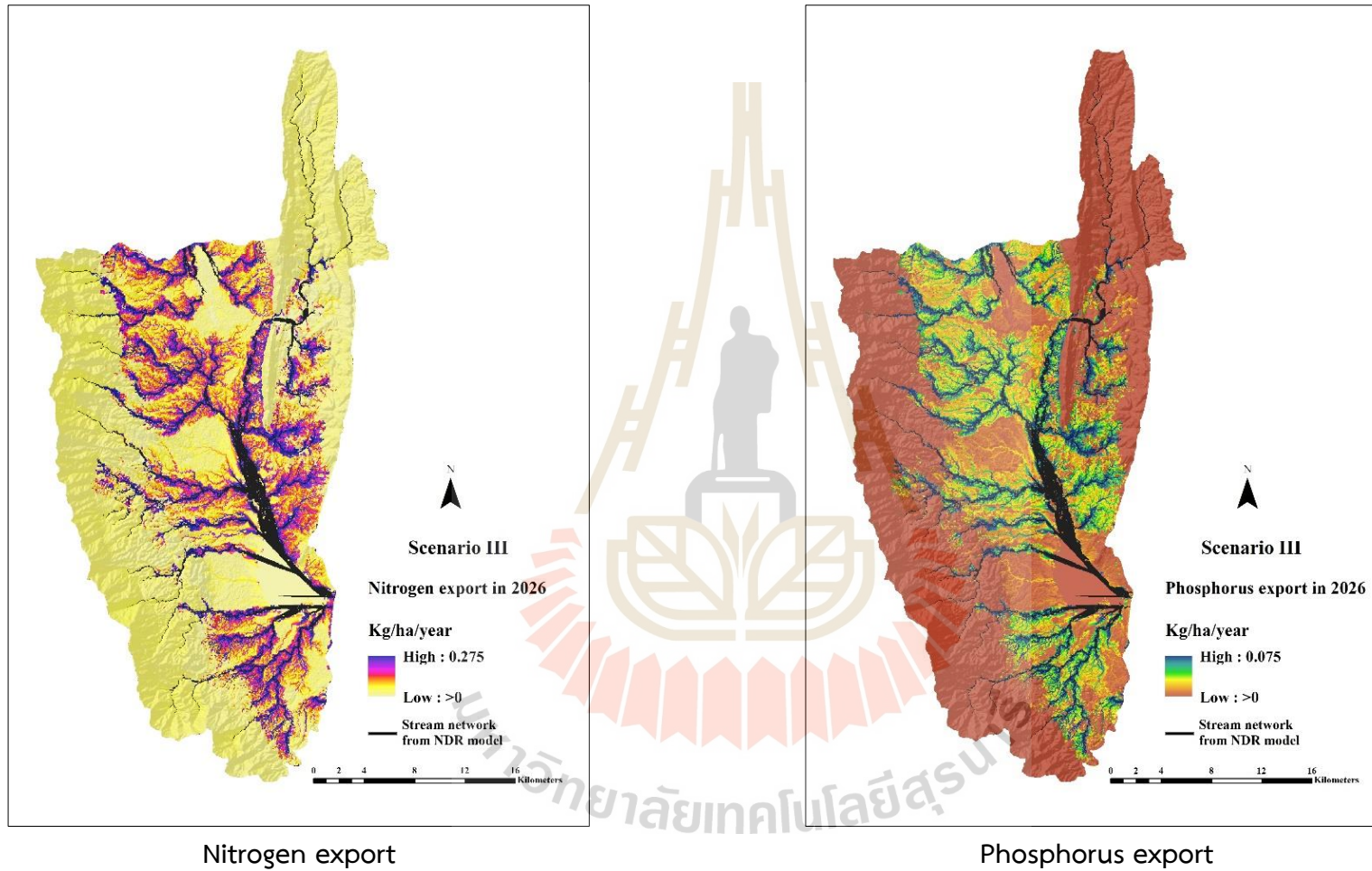


Figure 7.37 Spatial distribution of nitrogen and phosphorus export in 2026 under Scenario III.

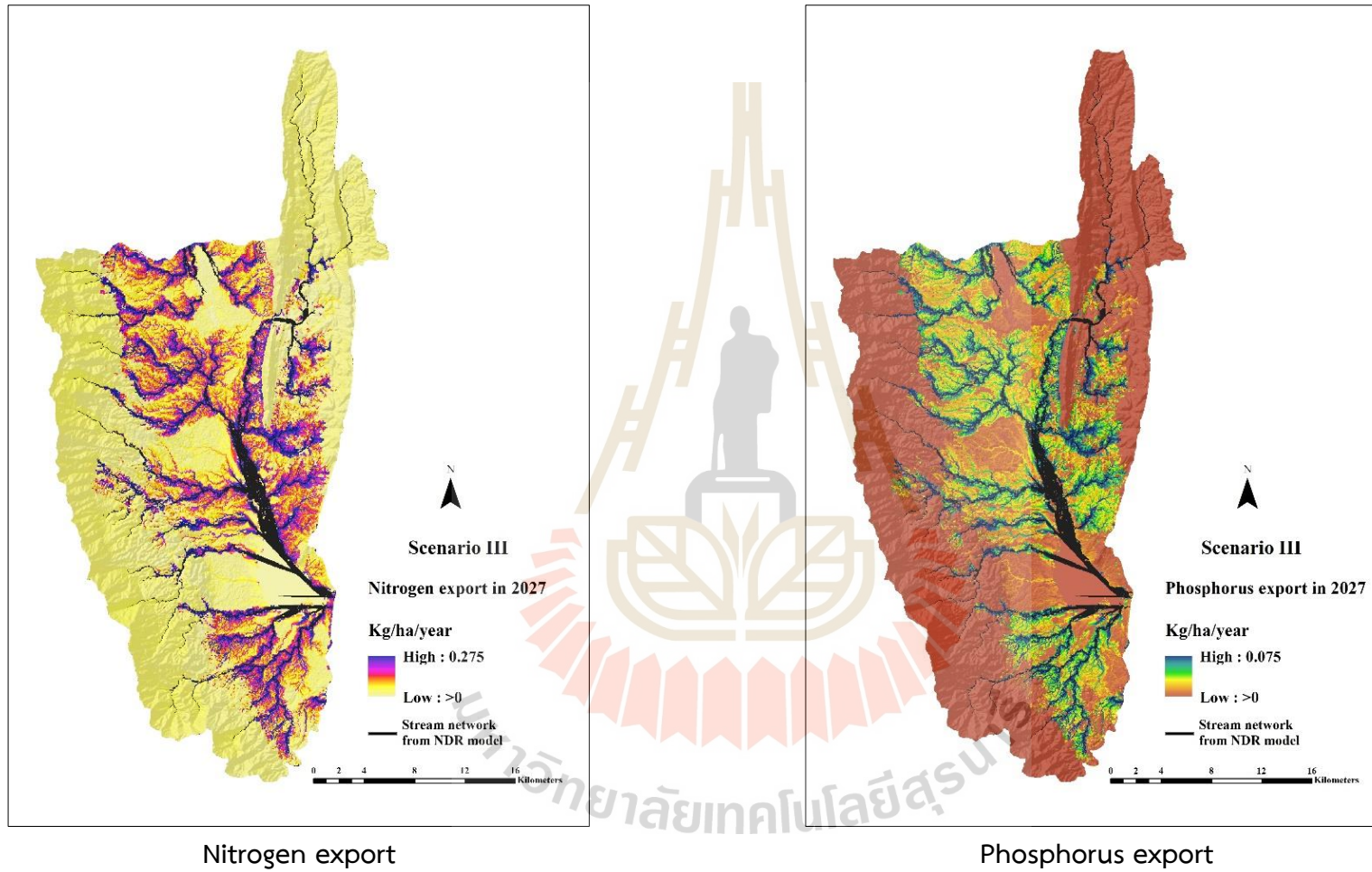


Figure 7.38 Spatial distribution of nitrogen and phosphorus export in 2027 under Scenario III.

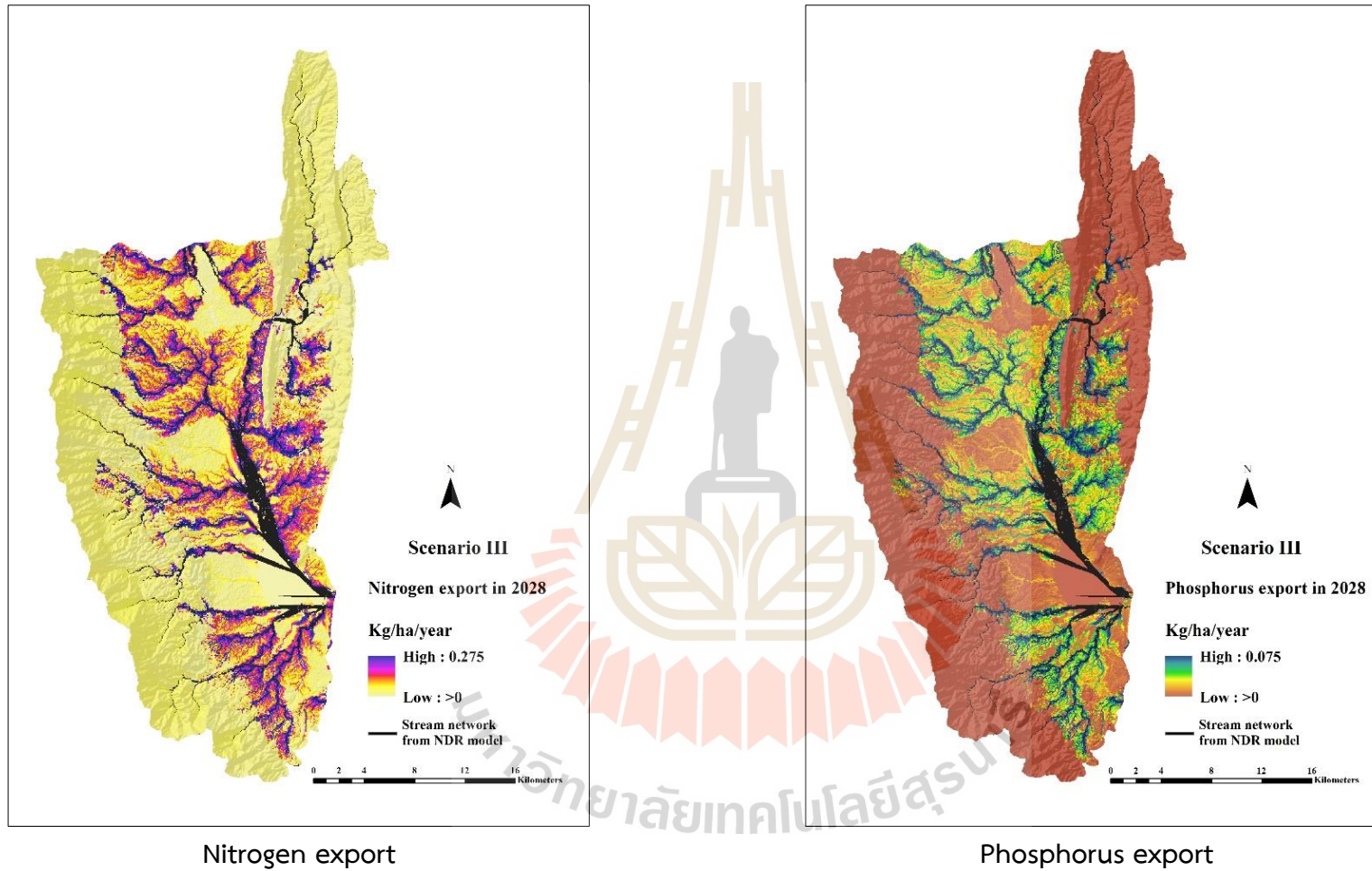


Figure 7.39 Spatial distribution of nitrogen and phosphorus export in 2028 under Scenario III.

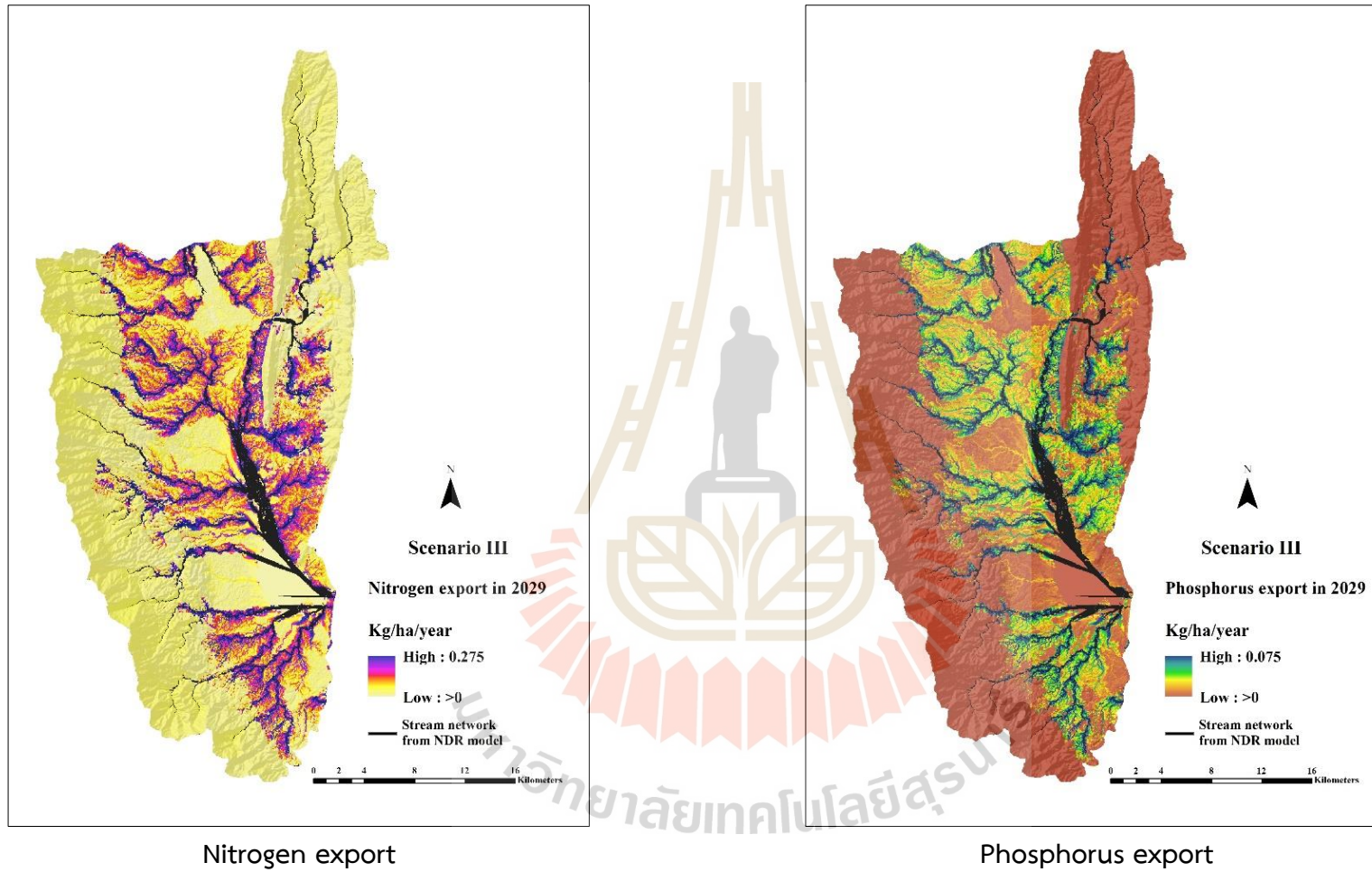


Figure 7.40 Spatial distribution of nitrogen and phosphorus export in 2029 under Scenario III.

As a result of load and export (nitrogen and phosphorus) by LULC classes under Scenario III (Economic crop zonation) between 2020 and 2029 (Tables 7.40 to 7.49), the highest total nutrient load is found on the paddy field, with a nitrogen value between 747,941.81 kg. (3,298.95 kg/km²) in 2020 and 924,496.58 kg. (3,299.39 kg/km²) in 2029, and the value of phosphorus between 204,003.82 kg. (899.80 kg/km²) in 2020 and 252,143.21 kg. (899.86 kg/km²) in 2029. In contrast, the lowest total nitrogen load occurs on the waterbody, with a value between 10.31 kg. (0.30 kg/km²) in 2020 and 12.34 kg. (0.30 kg/km²) in 2029, the lowest total phosphorus load occurs on miscellaneous land, with a value between 0.83 kg. (0.30 kg/km²) in 2020 and 1.11 kg. (0.30 kg/km²) in 2029. However, the highest average nitrogen load appears on field crop and paddy field between 2020 and 2029. The highest average phosphorus load appears on field crops and perennial trees and orchards between 2020 and 2029.

In the meantime, the highest total nutrient export appears on the paddy field, with a nitrogen value between 103,451.12 kg. (456.29 kg/km²) in 2020 and 140,538.09 kg. (501.56 kg/km²) in 2029, and the value of phosphorus between 28,213.94 kg. (124.44 kg/km²) in 2020 and 38,328.57 kg. (136.79 kg/km²) in 2029. Conversely, the lowest total nitrogen export occurs on the waterbody, with a value between 2.39 kg. (0.07 kg/km²) in 2020 and 2.80 kg. (0.07 kg/km²) in 2029, while the lowest total phosphorus export occurs on miscellaneous land, a value between 0.15 kg. (0.05 kg/km²) in 2020 and 0.28 kg. (0.08 kg/km²) in 2029. This result is similar to Raji, Odunuga, and Fasona (2020), who found that cropland and agroforestry influenced roughly 90% of the nutrient exported while water bodies were identified as sinks.

This finding suggests that the change in LULC types associated with the biophysical table parameters affects nitrogen and phosphorus export. In particular, The LULC data under this scenario has influences nutrient export due to the LULC data of Scenario III (Economic crop zonation) simulated based on the annual rate of LULC change from transition area matrix between 2009 and 2019 for some LULC types and the economic crop zonation, particularly the increase of paddy field and field crop areas and decrease of the perennial tree and orchard areas, which represent dramatic change under this scenario, which lead to changes the amount load and export of

nutrient. Hence, it shows significant LULC change under this scenario.

7.7 Comparison of nutrient export estimation among three different scenarios

The summary on nitrogen and phosphorus export between 2020 and 2029 of three different scenarios was compared and discussed under this section. Table 7.50 summarizes the average nitrogen and phosphorus export between 2020 and 2029 of three scenarios and is displayed in Figures 7.41 and 7.42.

As a result, it disclosed that the predictive LULC between 2020 and 2029 of Scenario II (Maximization of ecosystem service values) delivers the lowest annual nitrogen and phosphorus export than Scenario I and III, with an average value of 220.04 kg/km² and 48.60 kg/km² due to the allocation area from linear programming to maximize the ecosystems service values by increasing areas of wetland. In addition, the increases in wetland areas such as wetland restoration and constructed riparian wetlands can reduce nitrogen export (Yan et al., 2018) and phosphorus (Nitin K Singh et al., 2019) that enter water bodies. Besides, based on the biophysical table, wetland provides the highest maximum retention efficiency and gives a small load in nitrogen and phosphorus.

Moreover, the paddy field area decreased, affecting the nutrient export because this LULC type supplies the highest nitrogen and phosphorus load with low maximum retention efficiency. Whereas scenario III (Economic crop zonation) generates the highest nutrient export than other scenarios since the paddy field and field crop areas increase according to their suitability classes by the LDD, these areas provide the highest nitrogen and phosphorus load but low maximum retention efficiency. This result agrees with Mei, Kong, Ke, and Yang (2017), who applied the NDR model to calculate nutrient export under two different scenarios. They found that the cropland balance policy negatively impacts water purification by increasing nitrogen export, which is 8.36% higher than the No strict cropland protection scenario.

Table 7.50 Average nitrogen and phosphors export (kg/km^2) between 2020 and 2029 of three different scenarios.

Year	Nitrogen export			Phosphorus export		
	Scenario I	Scenario II	Scenario III	Scenario I	Scenario II	Scenario III
2020	222.10	220.97	224.81	48.64	48.37	49.31
2021	223.91	219.76	229.12	49.18	48.23	50.39
2022	225.34	219.25	232.69	49.58	48.20	51.29
2023	226.93	219.62	236.63	50.06	48.40	52.26
2024	228.19	219.49	239.83	50.43	48.42	53.03
2025	230.18	219.88	244.01	51.04	48.62	54.08
2026	231.94	219.80	247.46	51.57	48.71	54.91
2027	233.12	220.20	250.88	51.91	48.85	55.70
2028	234.84	220.66	254.35	52.44	49.04	56.53
2029	236.62	220.81	257.76	52.98	49.14	57.38
Average	229.32	220.04	241.75	50.78	48.60	53.49

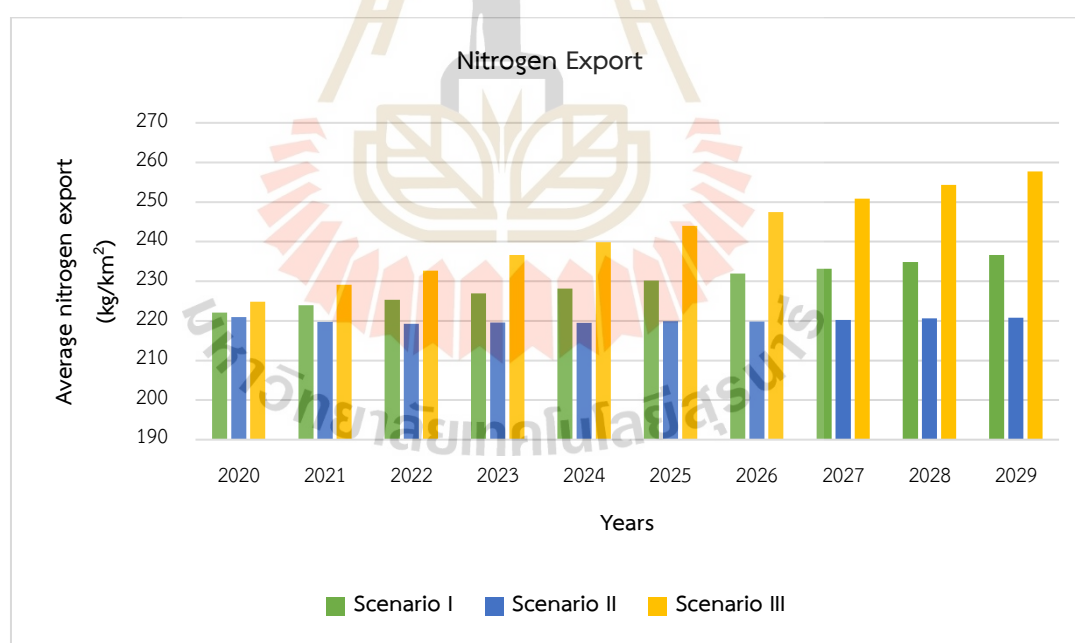


Figure 7.41 Comparison of nitrogen export between 2020 and 2029 of three different scenarios.

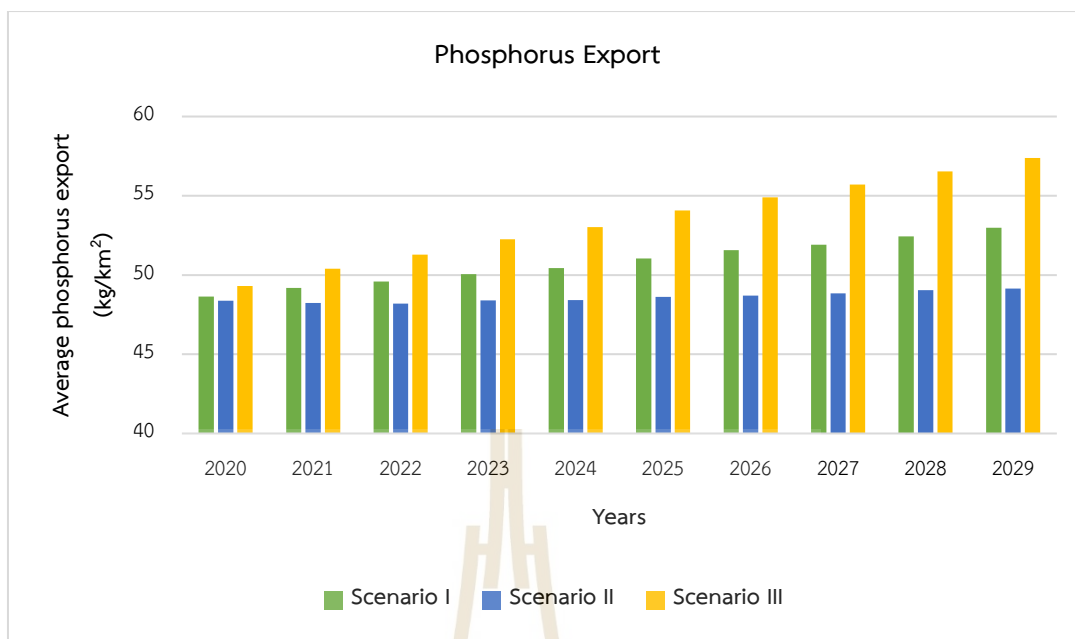


Figure 7.42 Comparison of phosphorus export between 2020 and 2029 of three different scenarios.



CHAPTER VIII

SUITABLE LAND USE AND LAND COVER ALLOCATION SCENARIOS TO MINIMIZE SEDIMENT AND NUTRIENT EXPORTS

This chapter presents the results of the fifth objective focusing on the suitable LULC allocation from three scenarios to minimize sediment and nutrient exports using ecosystems services change index (ESCI). The main results consist of (1) suitable LULC allocation scenarios to minimize sediment export, (2) suitable LULC allocation scenarios to minimize nutrient export, and (3) suitable LULC allocation scenarios to minimize sediment and nutrient export are here described and discussed in detail.

The ecosystems services change index (ESCI), as proposed by Leh, Matlock, Cummings, and Nalley (2013), was applied to assess the ecosystem services states (ES). The ESCI represents the relative gain or loss of each ecosystem service. It ranges from negative 1 to positive 1, with an ESCI of 0 indicating no change in ecosystem services. In contrast, a negative 1 ESCI indicates a loss of all the ecosystem services relative to baseline. Thus, the ESCI provides the state of change in particular services, i.e., sediment and nutrient export due to LULC change.

In this study, to quantify the cumulative impacts on all ecosystem services, the ESCI was first calculated from estimated sediment and nutrient export at the watershed level using SDR and NDR models based on the actual LULC data in 2019 and the predictive LULC data of three different scenarios using the CLUE-S model and simulated rainfall data of the NCAR between 2020 and 2029. Then, the derived ESCI, the lowest value, was further applied to identify suitable LULC allocation scenarios for minimizing sediment and nutrient exports into Kwan Phayao Lake, Upper Ing watershed.

8.1 Suitable LULC allocation scenario to minimize sediment export

Under this section, the characteristics of ESCI of sediment export from three different scenarios are evaluated and compared to identify a suitable LULC allocation scenario for minimizing sediment export in terms of ecosystem service change.

8.1.1 Ecosystem service change on sediment export of Scenario I

Ecosystem service change on sediment export of Scenario I (Trend of LULC evolution) and its ESCI is summarized in Table 8.1 and comparative displayed in Figure 8.1.

As a result, it discloses that the lowest sediment export of Scenario I will occur in 2022 with the value of 32,373.49 tons, and the highest sediment export will occur in 2026 with the value of 58,797.97 tons. An average sediment export between 2020 and 2029 was 43,723.02 tons. Moreover, all predictive sediment export of Scenario I in this period is higher than sediment export of base year in 2019. This result indicates that the increasing sediment export of Scenario I during 2020 and 2029 affects ecosystem service in terms of low retention capacity compared with sediment export of base year data in 2019.

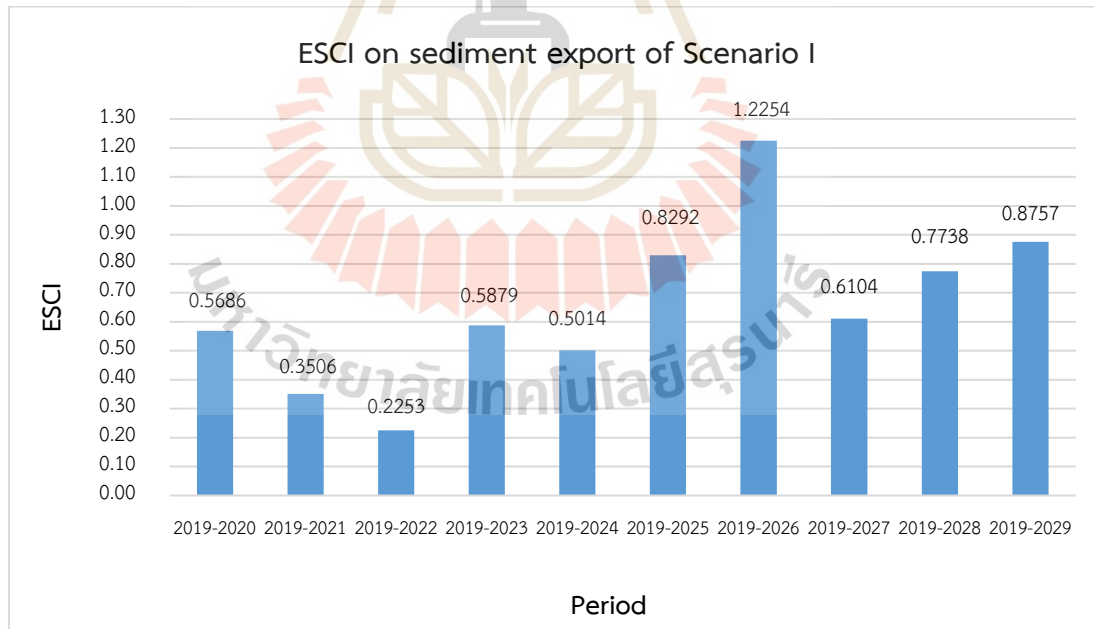
In addition, the ecosystem service change index (ESCI) identifies that the lowest cumulative ecosystem services gain from sediment export under this scenario from 2019 to 2029 will occur in 2022, with a value of 0.2253. On the contrary, the highest cumulative ecosystem service gain from sediment export will occur in 2026, with a value of 1.2254. The average ESCI of sediment export in this scenario was 0.6548.

The significant driver of these findings is LULC change in the future based on the historical trend using the Markov Chain model. Additionally, predictive rainfall data of the RCPs 8.5 simulation model of NCAR, which characterizes the impact of climate change on water yield (Riahi, Grubler and Nakicenovic, 2007), play a significant role in rainfall erosivity calculation. These factors directly affect estimated sediment export between 2020 and 2029. (See detail more in Section 6.4 of Chapter 6). However, the value of ESCI is assessed from the value of sediment export, which means that the high value of ESCI under Scenario I, represents the low sediment retention capability for water purification.

Table 8.1 Ecosystem service on sediment export and its ESCI value under Scenario I.

Year	Sediment export (tons)	ESCI	Period
2019	26,421.41		
2020	41,445.02	0.5686	2019-2020
2021	35,685.45	0.3506	2019-2021
2022	32,373.49	0.2253	2019-2022
2023	41,954.52	0.5879	2019-2023
2024	39,669.68	0.5014	2019-2024
2025	48,329.18	0.8292	2019-2025
2026	58,797.97	1.2254	2019-2026
2027	42,549.03	0.6104	2019-2027
2028	46,867.05	0.7738	2019-2028
2029	49,558.85	0.8757	2019-2029
Average	43,723.02*	0.6548	

Note: * The average value from data between 2020 and 2029.

**Figure 8.1** Ecosystem service on sediment export and its ESCI value under Scenario I.

8.1.2 Ecosystem service change on sediment export of Scenario II

Ecosystem service change on sediment export of Scenario II (Maximization ecosystem service values) and its ESCI is summarized in Table 8.2 and comparative displayed in Figure 8.2.

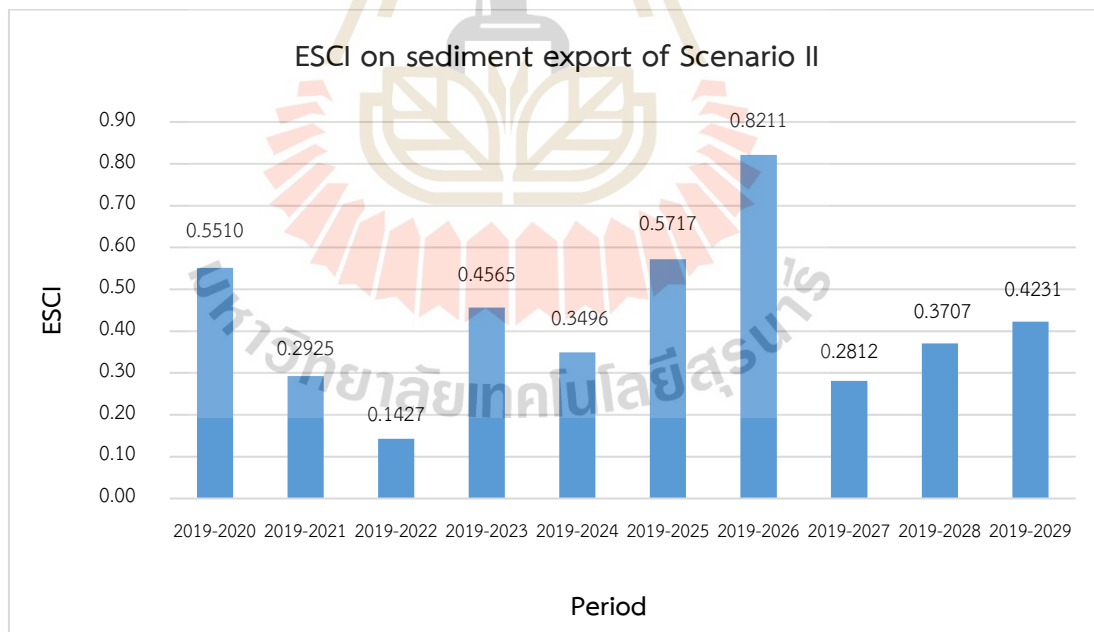
As a result, it reveals that the lowest sediment export of Scenario II will occur in 2022 with the value of 30,190.61 tons, and the highest sediment export will occur in 2026 with the value of 48,115.01 tons. The average sediment export of this scenario between 2020 and 2029 was 37,677.19 tons. Moreover, all predictive sediment export between 2020 and 2029 of Scenario II is higher than sediment export of base year in 2019. This result indicates that the increasing sediment export of Scenario II during 2020 and 2029 affects ecosystem service in terms of low retention capacity compared with sediment export of base year data in 2019.

In addition, the ecosystem service change index (ESCI) identifies that the lowest cumulative ecosystem services gain from sediment export under this scenario from 2019 to 2029 will occur in 2022, with a value of 0.1427. On the contrary, the highest cumulative ecosystem service gain from sediment export will occur in 2026, with a value of 0.8211. The average ESCI of sediment export in this scenario was 0.4260. These findings show the effect of predictive rainfall erosivity and LULC change on sediment export prediction under this scenario, as mentioned earlier under Section 8.1.1 and in Section 6.5 of Chapter 6. Although this scenario allocates the areas to reduce sediment export by increasing wetland area and reducing the rangeland and miscellaneous land, it still provides the value of sediment export higher than the base year. Besides, the value of ESCI is evaluated from the value of sediment export, which implies that the high value of ESCI under scenario II represents the low sediment retention capability for water purification.

Table 8.2 Ecosystem service on sediment export and its ESCI value under Scenario II.

Year	Sediment export (tons)	ESCI	Period
2019	26,421.41		
2020	40,979.13	0.5510	2019-2020
2021	34,149.06	0.2925	2019-2021
2022	30,190.61	0.1427	2019-2022
2023	38,483.96	0.4565	2019-2023
2024	35,659.13	0.3496	2019-2024
2025	41,526.64	0.5717	2019-2025
2026	48,115.01	0.8211	2019-2026
2027	33,851.75	0.2812	2019-2027
2028	36,216.79	0.3707	2019-2028
2029	37,599.82	0.4231	2019-2029
Average	37,677.19*	0.4260	

Note: * The average value from data between 2020 and 2029.

**Figure 8.2** Ecosystem service on sediment export and its ESCI value under Scenario II.

8.1.3 Ecosystem service change on sediment export of Scenario III

Ecosystem service change on sediment export of Scenario III (Economic crop zonation) and its ESCI is summarized in Table 8.3 and comparative displayed in Figure 8.3.

As a result, it exposes that the lowest sediment export of Scenario III will occur in 2022 with the value of 34,520.48 tons, and the highest sediment export will occur in 2026 with the value of 76,068.33 tons. The average sediment export of this scenario between 2020 and 2029 was 54,568.42 tons. Moreover, all predictive sediment export between 2020 and 2029 of Scenario III is higher than sediment export of base year in 2019. This result indicates that the increasing sediment export of Scenario III during 2020 and 2029 affects ecosystem service in terms of low retention capacity compared with sediment export of base year data in 2019.

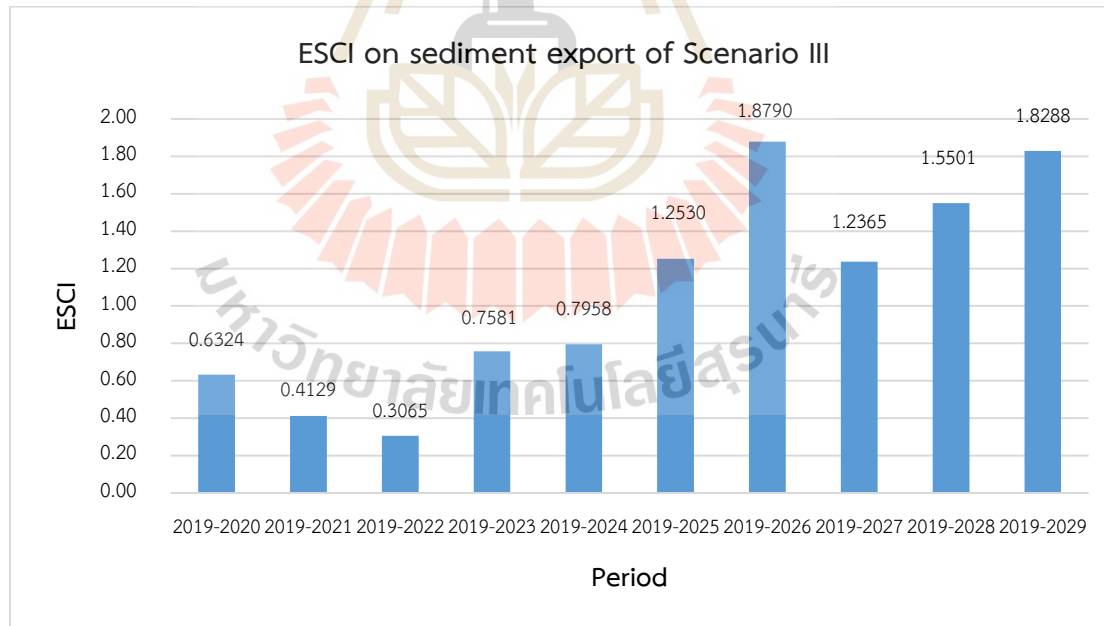
Additionally, the ecosystem service change index (ESCI) identifies that the lowest cumulative ecosystem services gain from sediment export under this scenario from 2019 to 2029 will occur in 2022, with a value of 0.3065. On the contrary, the highest cumulative ecosystem service gain from sediment export will occur in 2026, with a value of 1.8790. The average ESCI of sediment export in this scenario was 1.0653.

These findings show the effect of predictive rainfall erosivity and LULC change on sediment export prediction under this scenario, as mentioned earlier under Section 8.1.1 and in Section 6.6 of Chapter 6. In particular, the increase of economic crop, i.e., paddy field and field crop based on their suitable zonation. Nevertheless, the value of ESCI is estimated from the value of sediment export, which denotes that the high value of ESCI under scenario III represents the low sediment retention capability for water purification.

Table 8.3 Ecosystem service on sediment export and its ESCI value under Scenario III.

Year	Sediment export (tons)	ESCI	Period
2019	26,421.41		
2020	43,130.50	0.6324	2019-2020
2021	37,330.55	0.4129	2019-2021
2022	34,520.48	0.3065	2019-2022
2023	46,451.16	0.7581	2019-2023
2024	47,447.38	0.7958	2019-2024
2025	59,526.42	1.2530	2019-2025
2026	76,068.33	1.8790	2019-2026
2027	59,092.34	1.2365	2019-2027
2028	67,376.26	1.5501	2019-2028
2029	74,740.75	1.8288	2019-2029
Average	54,568.42*	1.0653	

Note: * The average value from data between 2020 and 2029.

**Figure 8.3** Ecosystem service on sediment export and its ESCI value under Scenario III.

8.1.4 Suitable LULC allocation scenario to minimize sediment export

The ESCI values on sediment export and its average from three different scenarios in the Upper Ing watershed were compared to identify a suitable LULC allocation scenario for minimizing sediment export in terms of ecosystem service change, as shown in Table 8.4 and Figure 8.4.

As a result, it was found that LULC of Scenario II (Maximization ecosystem service values) generates the lowest sediment export in every year from 2020 to 2029 among three LULC allocation scenarios, with an average sediment export of 37,677.19 tons. The cumulative ESCI values on sediment export of this scenario are also the lowest, with an average ESCI value of 0.4260. (See detail in Table 8.4). Therefore, LULC allocation of Scenario II (Maximization ecosystem service values) is chosen to minimize sediment export in Kwan Phayao Lake, Upper Ing watershed. Moreover, the average ESCI of three different LULC scenarios has tested the difference of mean using t-Test statistics. The result demonstrates significant differences among average ESCI values on sediment export of three different scenarios at a 95% confidential level, as shown in detail in Table 8.5.

Table 8.4 Sediment export and ESCI value and its average of three different scenarios.

Year	Period	Scenario I		Scenario II		Scenario III	
		Sediment export (tons)	ESCI	Sediment export (tons)	ESCI	Sediment export (tons)	ESCI
2019		26,421.41		26,421.41		26,421.41	
2020	2019-2020	41,445.02	0.5686	40,979.13	0.5510	43,130.50	0.6324
2021	2019-2021	35,685.45	0.3506	34,149.06	0.2925	37,330.55	0.4129
2022	2019-2022	32,373.49	0.2253	30,190.61	0.1427	34,520.48	0.3065
2023	2019-2023	41,954.52	0.5879	38,483.96	0.4565	46,451.16	0.7581
2024	2019-2024	39,669.68	0.5014	35,659.13	0.3496	47,447.38	0.7958
2025	2019-2025	48,329.18	0.8292	41,526.64	0.5717	59,526.42	1.2530
2026	2019-2026	58,797.97	1.2254	48,115.01	0.8211	76,068.33	1.8790
2027	2019-2027	42,549.03	0.6104	33,851.75	0.2812	59,092.34	1.2365
2028	2019-2028	46,867.05	0.7738	36,216.79	0.3707	67,376.26	1.5501
2029	2019-2029	49,558.85	0.8757	37,599.82	0.4231	74,740.75	1.8288
Average		43,723.02*	0.6548	37,677.19*	0.4260	54,568.42*	1.0653

Note: * The average value from data between 2020 and 2029.

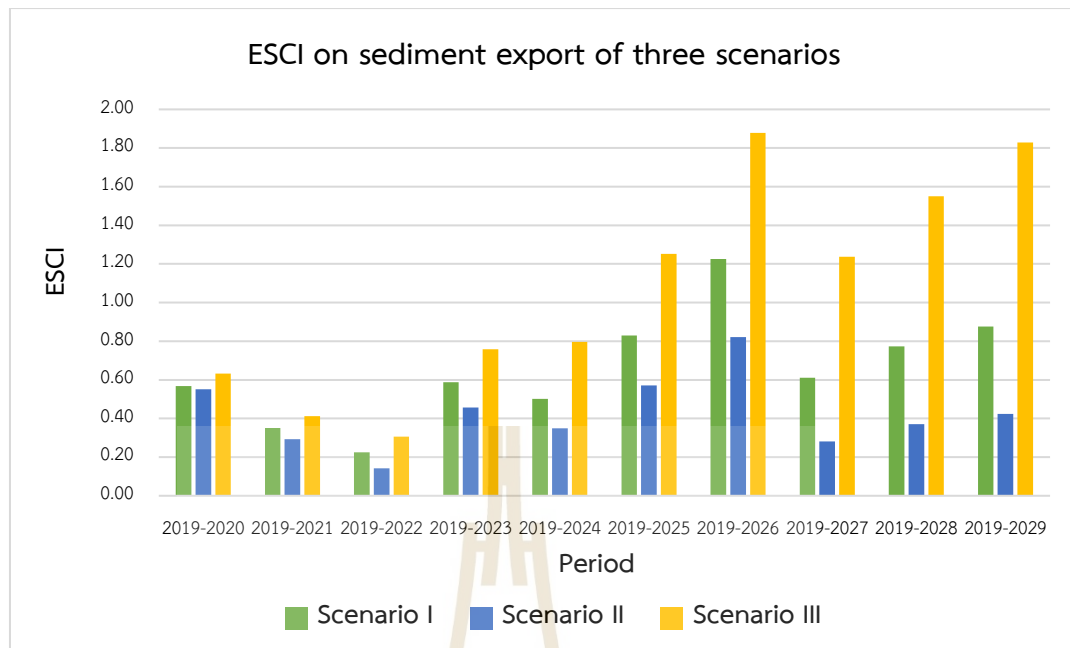


Figure 8.4 Comparison of ESCI on sediment export of three different scenarios.

Table 8.5 Details of t-Test for average ESCI values on sediment export among three different scenarios.

Pairwise of Scenario	Mean		Variance		df	t- Stat	t Critical 2-tail
	Variable 1	Variable 2	Variable 1	Variable 2			
I and II	0.6548	0.4260	0.0815	0.0358	9	4.5002	2.2622
I and III	0.6548	1.0653	0.0815	0.3223	9	-3.9847	2.2622
II and III	0.4260	1.0653	0.0358	0.3223	9	-4.1715	2.2622

8.2 Suitable LULC allocation scenario to minimize nutrient export

Under this section, the characteristics of ESCI of nutrient export from three different scenarios are assessed and compared to identify a suitable LULC allocation scenario for minimizing nutrient export in terms of ecosystem service change.

8.2.1 Ecosystem service change on Nutrient export of Scenario I

Ecosystem service change on nutrient export of Scenario I (Trend of LULC evolution) and its ESCI is summarized in Table 8.6 and 8.7 and displayed in Figures 8.5 and 8.6.

As a result, it discloses that the lowest nitrogen and phosphorus export of Scenario I will occur in 2020 with 197,972.93 kilograms and 43,358.11 kilograms, and the highest nitrogen and phosphorus export will occur in 2029, with a value of 210,907.86 kilograms and 47,221.47 kilograms, respectively. The average nitrogen and phosphorus exports between 2020 and 2029 are 204,402.70 kilograms and 45,265.24 kilograms. Moreover, all predictive nutrient export between 2020 and 2029 of Scenario I are higher than nutrient export of the base year in 2019. This result indicates that the increasing nutrient export of Scenario I during 2020 and 2029 affects ecosystem service in water quality by higher contaminating of nitrogen and phosphorus from the change of LULC compared with nutrient export of base year data in 2019.

In addition, the ecosystem service change index (ESCI) identifies that the lowest cumulative ecosystem services gain from nitrogen and phosphorus export under this scenario from 2019 to 2029 will occur in 2020, with a value of 0.0241 and 0.0329. On the contrary, the highest cumulative ecosystem service gain from nitrogen and phosphorus export will occur in 2029, with a value of 0.0910 and 0.1249. An average ESCI of nitrogen and phosphorus exports in this scenario was 0.0574 and 0.0783, respectively.

These findings show the effect of nutrient loading associated with LULC change on nutrient export prediction under this scenario, as mentioned in Section 7.4 of Chapter 7. Therefore, LULC changes are the main driver for nutrient export on water purification ecosystem services (Chang, 2004). Nutrient exports and retention respond almost exclusively to land cover with high sensitivity to the export coefficients explaining changes in the scenarios (Hoyer and Chang, 2014). However, the value of ESCI is assessed from the value of nutrient export, which means that the high value of ESCI under Scenario I represents the low retention efficiency of that LULC for water purification.

Table 8.6 Ecosystem service on nitrogen export and its ESCI value under Scenario I.

Year	Nitrogen export (kilograms)	ESCI	Period
2019	193,307.56		
2020	197,972.93	0.0241	2019-2020
2021	199,580.02	0.0324	2019-2021
2022	200,858.16	0.0391	2019-2022
2023	202,275.64	0.0464	2019-2023
2024	203,395.90	0.0522	2019-2024
2025	205,172.77	0.0614	2019-2025
2026	206,743.37	0.0695	2019-2026
2027	207,795.18	0.0749	2019-2027
2028	209,32.14	0.0829	2019-2028
2029	210,907.86	0.0910	2019-2029
Average	204,402.70*	0.0574	

Note: * The average value from data between 2020 and 2029.

Table 8.7 Ecosystem service on phosphorus export and its ESCI value under Scenario I.

Year	Phosphorus export (kilograms)	ESCI	Period
2019	41,978.66		
2020	43,358.11	0.0329	2019-2020
2021	43,832.43	0.0442	2019-2021
2022	44,196.29	0.0528	2019-2022
2023	44,619.00	0.0629	2019-2023
2024	44,951.18	0.0708	2019-2024
2025	45,494.30	0.0837	2019-2025
2026	45,966.11	0.0950	2019-2026
2027	46,273.02	0.1023	2019-2027
2028	46,740.48	0.1134	2019-2028
2029	47,221.47	0.1249	2019-2029
Average	45,265.24*	0.0783	

Note: * The average value from data between 2020 and 2029.

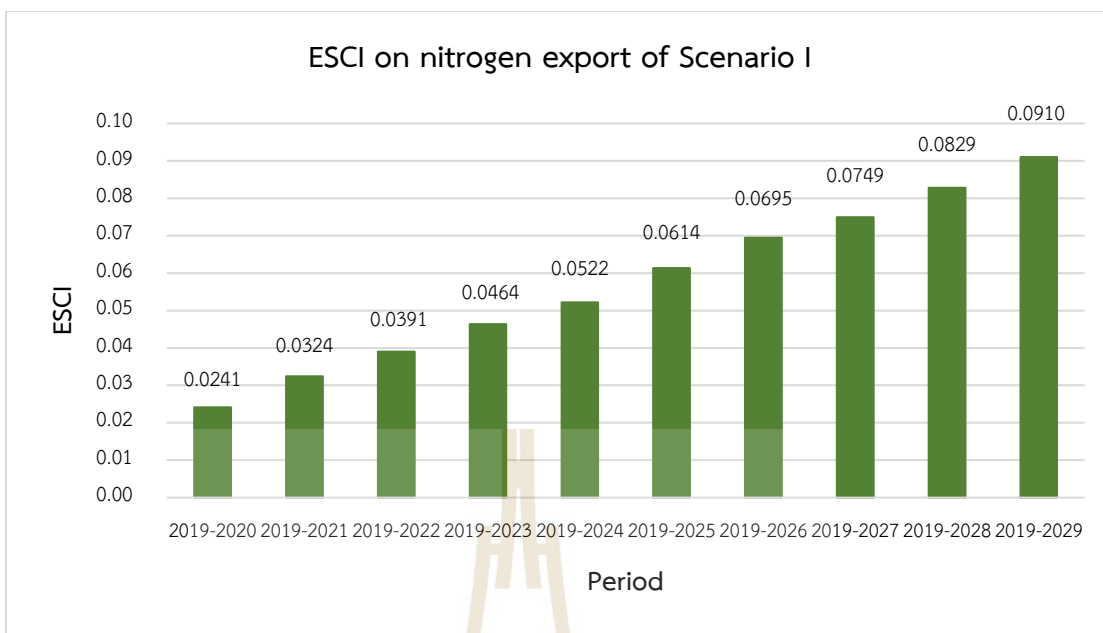


Figure 8.5 Ecosystem service on nitrogen export and its ESCI value under Scenario I.

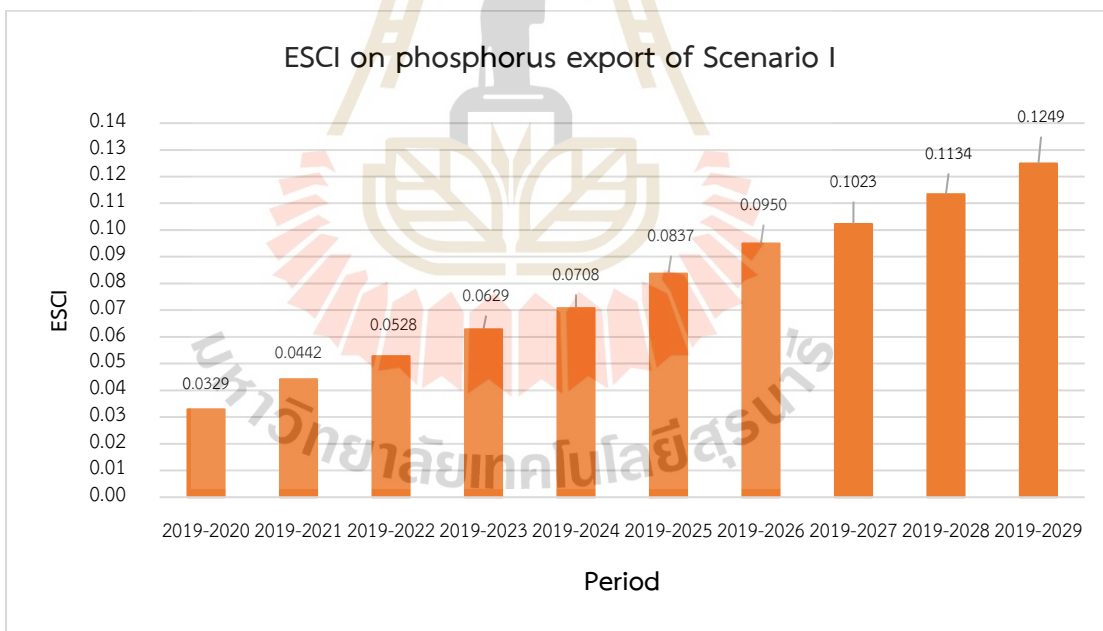


Figure 8.6 Ecosystem service on phosphorus export and its ESCI value under Scenario I.

8.2.2 Ecosystem service change on nutrient export of Scenario II

Ecosystem service change on nutrient export of Scenario II (Maximization ecosystem service values) and its ESCI is summarized in Table 8.8 and 8.9, and comparative displayed in Figure 8.7 and 8.8.

As a result, it reveals that the lowest nitrogen and phosphorus export of Scenario I will occur in 2022 with 195,426.12 kilograms and 42,961.10 kilograms, and the highest nitrogen export will occur in 2020, and the highest phosphorus export will arise in 2029, with a value of 196,964.74 kilograms and 43,797.81 kilograms, respectively. The average nitrogen and phosphorus exports between 2020 and 2029 are 196,135.56 kilograms and 43,316.82 kilograms.

Moreover, all predictive nutrient export between 2020 and 2029 of Scenario II is higher than nutrient export of the base year in 2019. This result indicates that the increasing nutrient export of Scenario II during 2020 and 2029 affects ecosystem service in water quality by higher contaminating of nitrogen and phosphorus from the change of LULC compared with nutrient export of base year data in 2019.

In addition, the ecosystem service change index (ESCI) identifies that the lowest cumulative ecosystem services gain from nitrogen and phosphorus export under this scenario from 2019 to 2029 will happen in 2022, with a value of 0.0110 and 0.0234. On the contrary, the highest cumulative ecosystem service gain from nitrogen export will occur in 2020, and phosphorus export will arise in 2029, with a value of 0.0189 and 0.0433, respectively. An average ESCI of nitrogen and phosphorus exports in this scenario was 0.0146 and 0.0319, respectively.

These findings show the effect of nutrient loading associated with LULC change on nutrient export prediction under this scenario, as mentioned earlier under Section 8.2.1 and in Section 7.5 of Chapter 7. Although this scenario allocates the areas to reduce nutrient export by increasing wetland area and reducing the rangeland and miscellaneous land, it still provides the value of nutrient export higher than the base year. Moreover, the value of ESCI is evaluated from the value of nutrient export, which implies that the high value of ESCI under scenario II represents the low retention efficiency of that LULC for water purification.

Table 8.8 Ecosystem service on nitrogen export and its ESCI value under Scenario II.

Year	Nitrogen export (kilograms)	ESCI	Period
2019	193,307.56		
2020	196,964.74	0.0189	2019-2020
2021	195,883.51	0.0133	2019-2021
2022	195,426.12	0.0110	2019-2022
2023	195,754.01	0.0127	2019-2023
2024	195,641.77	0.0121	2019-2024
2025	195,988.64	0.0139	2019-2025
2026	195,915.15	0.0135	2019-2026
2027	196,276.87	0.0154	2019-2027
2028	196,689.44	0.0175	2019-2028
2029	196,815.34	0.0181	2019-2029
Average	196,135.56*	0.0146	

Note: * The average value from data between 2020 and 2029.

Table 8.9 Ecosystem service on phosphorus export and its ESCI value under Scenario II.

Year	Phosphorus export (kilograms)	ESCI	Period
2019	41,978.66		
2020	43,117.85	0.0271	2019-2020
2021	42,988.62	0.0241	2019-2021
2022	42,961.10	0.0234	2019-2022
2023	43,137.70	0.0276	2019-2023
2024	43,160.14	0.0281	2019-2024
2025	43,334.48	0.0323	2019-2025
2026	43,415.07	0.0342	2019-2026
2027	43,540.77	0.0372	2019-2027
2028	43,714.70	0.0414	2019-2028
2029	43,797.81	0.0433	2019-2029
Average	43,316.82*	0.0319	

Note: * The average value from data between 2020 and 2029.

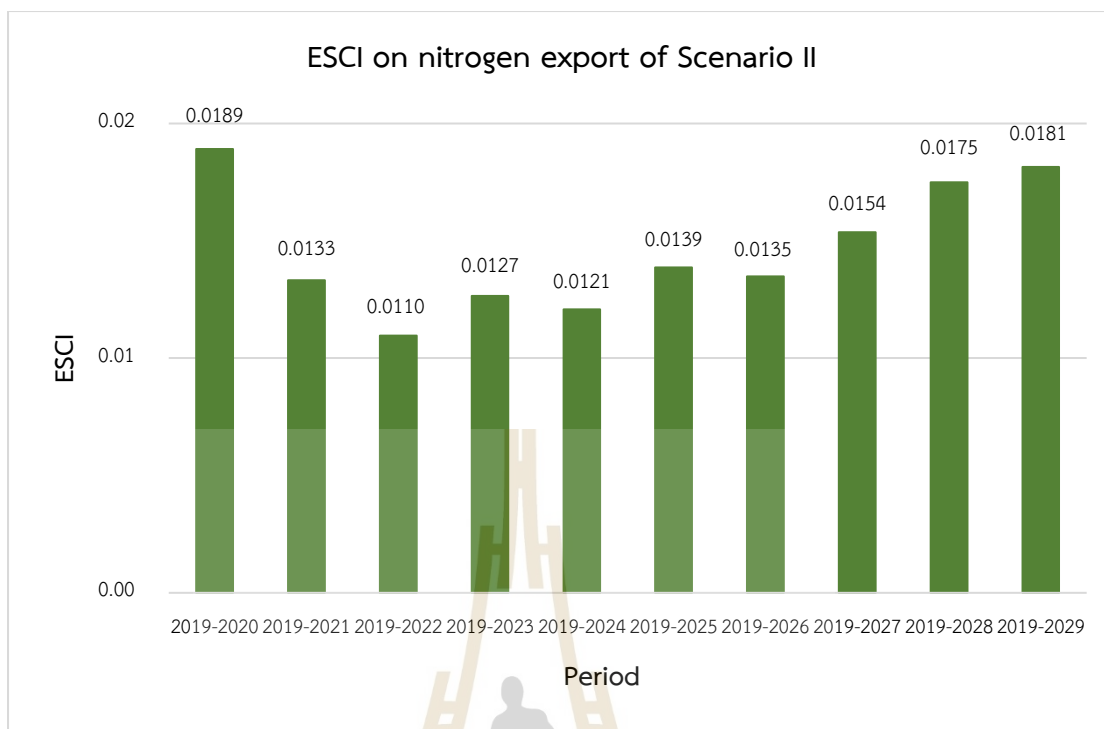


Figure 8.7 Ecosystem service on nitrogen export and its ESCI value under Scenario II.

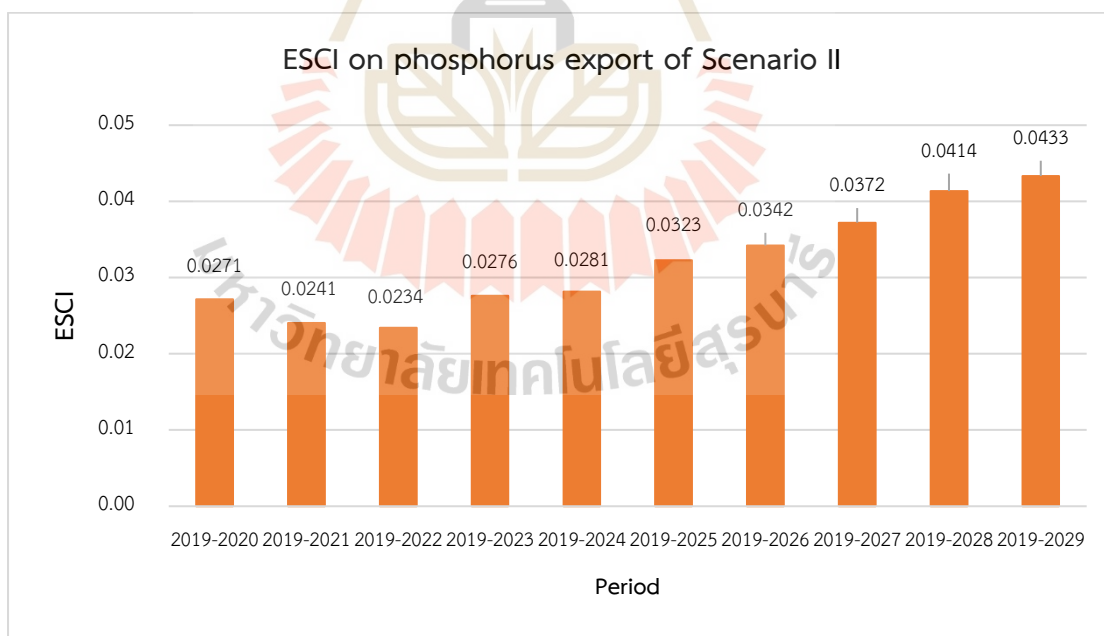


Figure 8.8 Ecosystem service on phosphorus export and its ESCI value under Scenario II.

8.2.3 Ecosystem service change on nutrient export of Scenario III

Ecosystem service change on nutrient export of Scenario III (Economic crop zonation) and its ESCI is summarized in Table 8.10 and 8.11, and comparative displayed in Figure 8.9 and 8.10.

As a result, it discloses that the lowest nitrogen and phosphorus export of Scenario III will occur in 2020 with 200,387.36 kilograms and 43,956.03 kilograms. The highest nitrogen and phosphorus export will occur in 2029, with a value of 229,756.13 kilograms and 51,149.42 kilograms, respectively. Average nitrogen and phosphorus exports between 2020 and 2029 are 215,488.15 kilograms and 47,677.82 kilograms. Moreover, all predictive nutrient export between 2020 and 2029 of Scenario III is higher than nutrient export of the base year in 2019. This result indicates that the increasing nutrient export of Scenario III during 2020 and 2029 affects ecosystem service in water quality by higher contaminating of nitrogen and phosphorus from the change of LULC compared with nutrient export of base year data in 2019.

In addition, the ecosystem service change index (ESCI) identifies that the lowest cumulative ecosystem services gain from nitrogen and phosphorus export under this scenario from 2019 to 2029 will occur in 2020, with a value of 0.0366 and 0.0471. On the contrary, the highest cumulative ecosystem service gain from nitrogen and phosphorus export will occur in 2029, with a value of 0.1886 and 0.2185. An average ESCI of nitrogen and phosphorus exports in this scenario was 0.1147 and 0.1358, respectively.

These findings show the effect of nutrient loading associated with LULC change on nutrient export prediction under this scenario, as mentioned earlier under Section 8.2.1 and in Section 7.6 of Chapter 7. In particular, the increase of economic crop, i.e., paddy field and field crop based on their suitable zonation. However, the value of ESCI is assessed from the value of nutrient export, which denotes that the high value of ESCI under scenario III represents the low retention efficiency of that LULC for water purification.

Table 8.10 Ecosystem service on nitrogen export and its ESCI value under Scenario III.

Year	Nitrogen export (kilograms)	ESCI	Period
2019	193,307.56		
2020	200,387.36	0.0366	2019-2020
2021	204,228.36	0.0565	2019-2021
2022	207,404.15	0.0729	2019-2022
2023	210,923.54	0.0911	2019-2023
2024	213,774.11	0.1059	2019-2024
2025	217,498.34	0.1251	2019-2025
2026	220,573.44	0.1410	2019-2026
2027	223,621.85	0.1568	2019-2027
2028	226,714.19	0.1728	2019-2028
2029	229,756.13	0.1886	2019-2029
Average	215,488.15*	0.1147	

Note: * The average value from data between 2020 and 2029.

Table 8.11 Ecosystem service on phosphorus export and its ESCI value under Scenario III.

Year	Phosphorus export (kilograms)	ESCI	Period
2019	41,978.66		
2020	43,956.03	0.0471	2019-2020
2021	44,919.41	0.0701	2019-2021
2022	45,715.39	0.0890	2019-2022
2023	46,580.29	0.1096	2019-2023
2024	47,267.91	0.1260	2019-2024
2025	48,206.67	0.1484	2019-2025
2026	48,942.83	0.1659	2019-2026
2027	49,650.28	0.1828	2019-2027
2028	50,389.99	0.2004	2019-2028
2029	51,149.42	0.2185	2019-2029
Average	47,677.82*	0.1358	

Note: * The average value from data between 2020 and 2029.

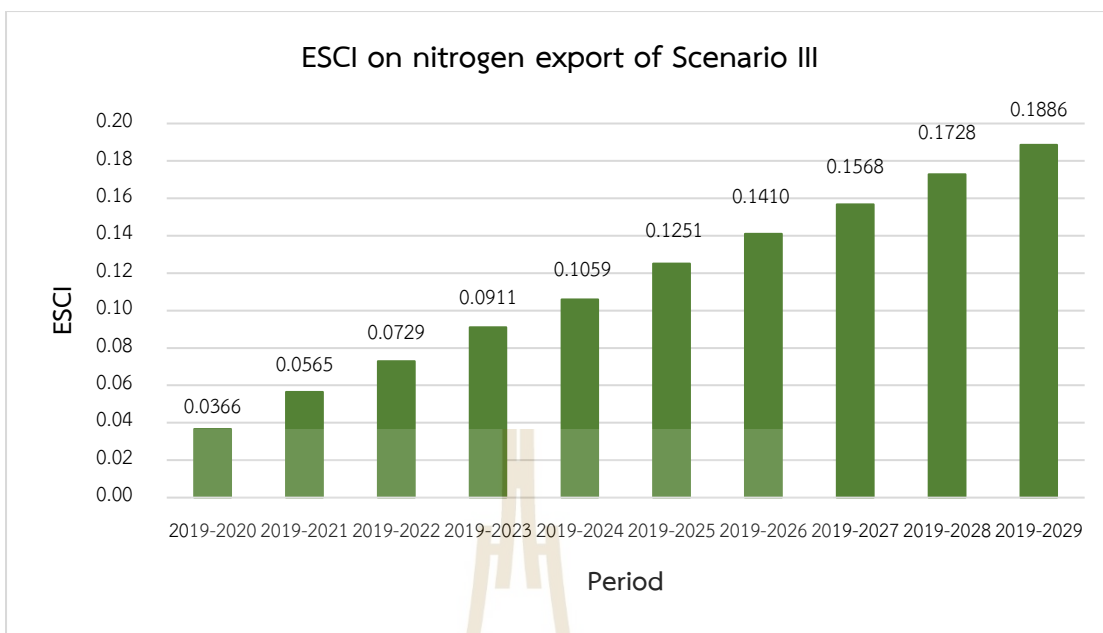


Figure 8.9 Ecosystem service on nitrogen export and its ESCI value under Scenario III.

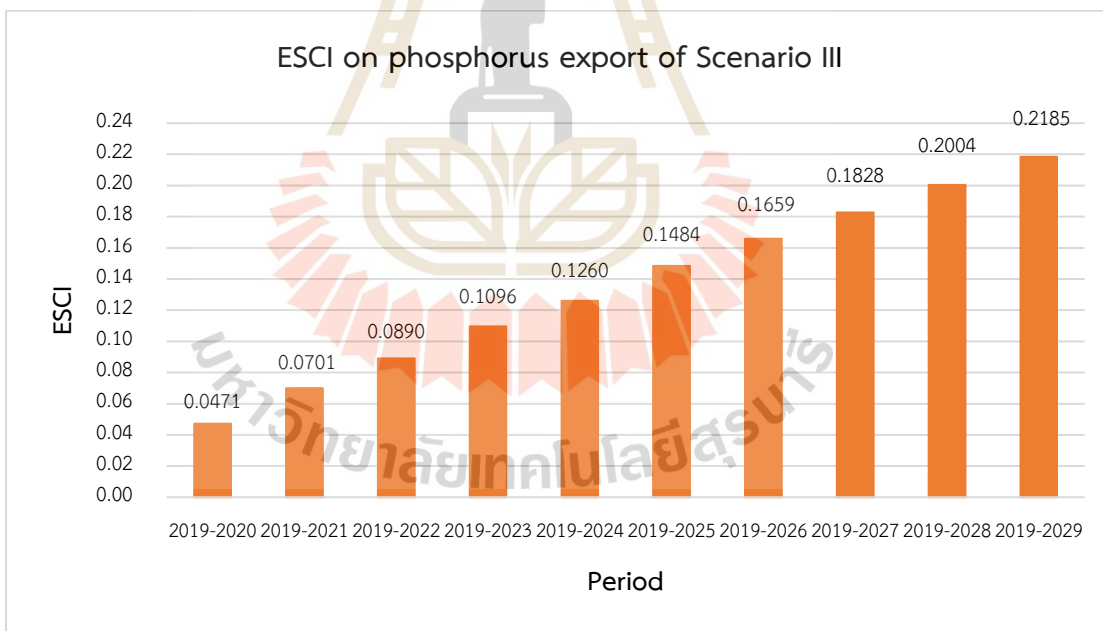


Figure 8.10 Ecosystem service on phosphorus export and its ESCI value under Scenario III.

8.2.4 Suitable LULC allocation scenario to minimize nutrient export

The ESCI values on nutrient export and its average from three different scenarios in the Upper Ing watershed were compared to identify suitable LULC allocation scenario for minimizing nutrient export in terms of ecosystem service change, as shown in Table 8.12 and 8.13, and Figure 8.11 and 8.12.

As a result, it was found that LULC of Scenario II (Maximization ecosystem service values) produces the lowest nutrient (nitrogen and phosphorus) export every year from 2020 to 2029 among three LULC allocation scenarios, with an average value of 196,135.56 kilograms and 43,316.82 kilograms for nitrogen and phosphorus. The cumulative ESCI values on nutrient export of this scenario are also the lowest, with an average ESCI value of nitrogen and phosphorus 0.0146 and 0.0319. (See detail in Tables 8.12 and 8.13). Therefore, LULC allocation of Scenario II (Maximization ecosystem service values) is selected to minimize nutrient export in Kwan Phayao Lake, Upper Ing watershed. Moreover, the average ESCI of three different LULC scenarios has tested the difference of mean using t-Test statistics. The result demonstrates significant differences among average ESCI values on nutrient export of three different scenarios at a 95% confidential level, as shown in detail in Table 8.14.

Table 8.12 Nitrogen export and ESCI value and its average of three different scenarios.

Year	Period	Scenario I		Scenario II		Scenario III	
		Nitrogen export (kg.)	ESCI	Nitrogen export (kg.)	ESCI	Nitrogen export (kg.)	ESCI
2019		193,307.56		193,307.56		193,307.56	
2020	2019-2020	197,972.93	0.0241	196,964.74	0.0189	200,387.36	0.0366
2021	2019-2021	199,580.02	0.0324	195,883.51	0.0133	204,228.36	0.0565
2022	2019-2022	200,858.16	0.0391	195,426.12	0.0110	207,404.15	0.0729
2023	2019-2023	202,275.64	0.0464	195,754.01	0.0127	210,923.54	0.0911
2024	2019-2024	203,395.90	0.0522	195,641.77	0.0121	213,774.11	0.1059
2025	2019-2025	205,172.77	0.0614	195,988.64	0.0139	217,498.34	0.1251
2026	2019-2026	206,743.37	0.0695	195,915.15	0.0135	220,573.44	0.1410
2027	2019-2027	207,795.18	0.0749	196,276.87	0.0154	223,621.85	0.1568
2028	2019-2028	209,325.14	0.0829	196,689.44	0.0175	226,714.19	0.1728
2029	2019-2029	210,907.86	0.0910	196,815.34	0.0181	229,756.13	0.1886
Average		204,402.70*	0.0574	196,135.56*	0.0146	215,488.15*	0.1147

Note: * The average value from data between 2020 and 2029.

Table 8.13 Phosphorus export and ESCI value and its average of three different scenarios.

Year	Period	Scenario I		Scenario II		Scenario III	
		Phosphorus export (kg.)	ESCI	Phosphorus export (kg.)	ESCI	Phosphorus export (kg.)	ESCI
2019		41,978.66		41,978.66		41,978.66	
2020	2019-2020	43,358.11	0.0329	43,117.85	0.0271	43,956.03	0.0471
2021	2019-2021	43,832.43	0.0442	42,988.62	0.0241	44,919.41	0.0701
2022	2019-2022	44,196.29	0.0528	42,961.10	0.0234	45,715.39	0.0890
2023	2019-2023	44,619.00	0.0629	43,137.70	0.0276	46,580.29	0.1096
2024	2019-2024	44,951.18	0.0708	43,160.14	0.0281	47,267.91	0.1260
2025	2019-2025	45,494.30	0.0837	43,334.48	0.0323	48,206.67	0.1484
2026	2019-2026	45,966.11	0.0950	43,415.07	0.0342	48,942.83	0.1659
2027	2019-2027	46,273.02	0.1023	43,540.77	0.0372	49,650.28	0.1828
2028	2019-2028	46,740.48	0.1134	43,714.70	0.0414	50,389.99	0.2004
2029	2019-2029	47,221.47	0.1249	43,797.81	0.0433	51,149.42	0.2185
	Average	45,265.24*	0.0783	43,316.82*	0.0319	47,677.82*	0.1358

Note: * The average value from data between 2020 and 2029.

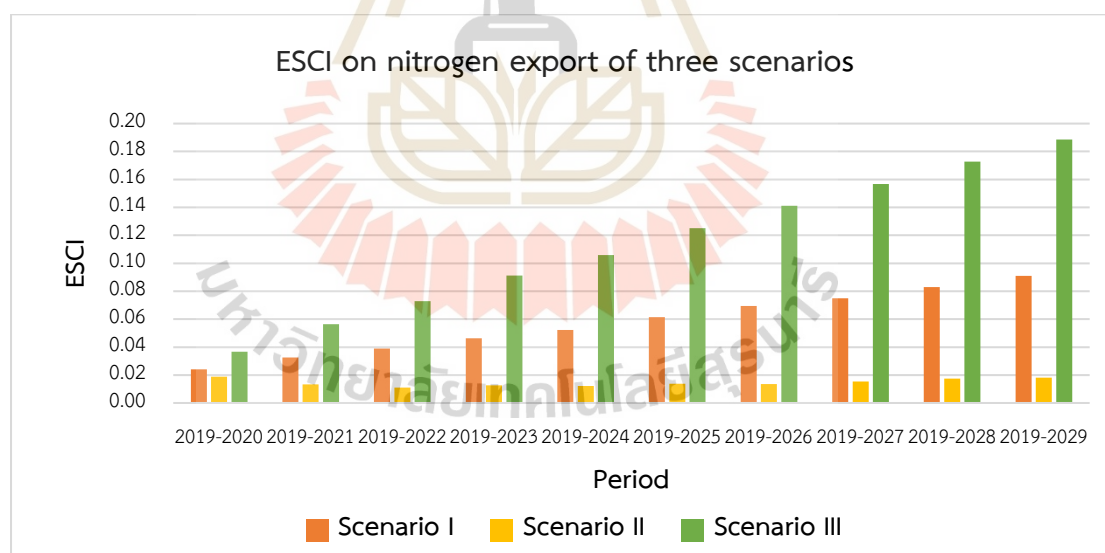


Figure 8.11 Comparison of ESCI on nitrogen export of three different scenarios.

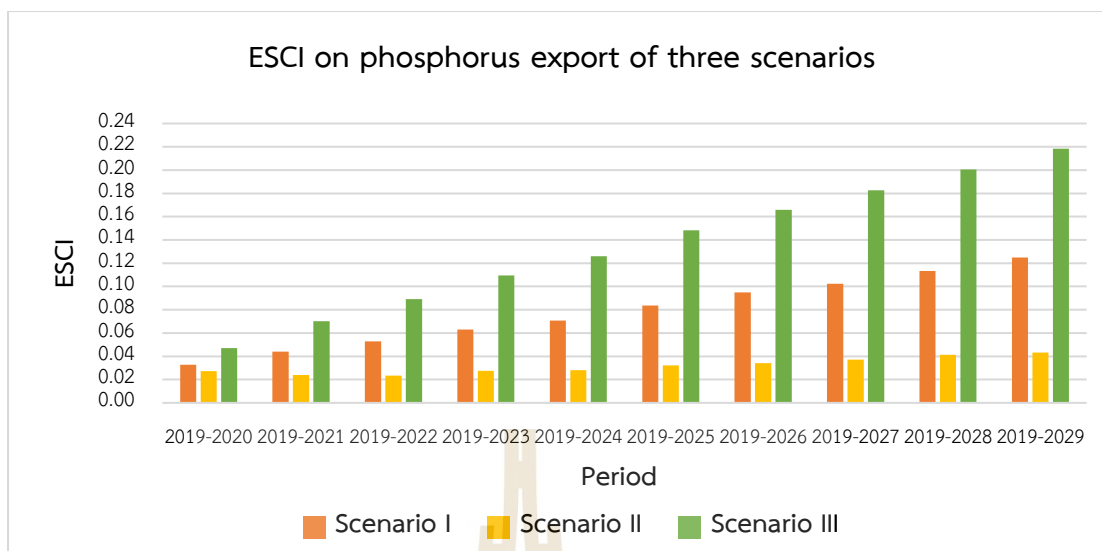


Figure 8.12 Comparison of ESCI on phosphorus export of three different scenarios.

Table 8.14 Details of t-Test for average ESCI values on nitrogen export among three different scenarios.

Pairwise of Scenario	Mean		Variance		df	t- Stat	t Critical 2-tail
	Variable 1	Variable 2	Variable 1	Variable 2			
I and II	0.0574	0.0146	0.0005	0.0000	9	6.2809	2.2622
I and III	0.0574	0.1147	0.0005	0.0026	9	-6.3392	2.2622
II and III	0.0146	0.1147	0.0000	0.0026	9	-6.3214	2.2622

Table 8.15 Details of t-Test for average ESCI values on phosphorus export among three different scenarios.

Pairwise of Scenario	Mean		Variance		df	t- Stat	t Critical 2-tail
	Variable 1	Variable 2	Variable 1	Variable 2			
I and II	0.0783	0.0319	0.0009	0.0000	9	6.0779	2.2622
I and III	0.0783	0.1358	0.0009	0.0033	9	-6.8310	2.2622
II and III	0.0319	0.1358	0.0000	0.0033	9	-6.4782	2.2622

8.3 Suitable LULC allocation scenario to minimize sediment and nutrient export

The average ESCI values of sediment and nutrient (nitrogen and phosphorus) exports from three different LULC allocation scenarios in the Upper Ing watershed were compared to identify suitable LULC allocation scenario to minimize sediment and nutrient export in terms of ecosystem service change, as shown in Figure 8.13 and summary in Table 8.16.

As a result, average cumulative ESCI values of sediment and nutrient export ecosystem services from LULC allocation of Scenario II (Maximization ecosystem service values) can provide the lowest value, with an average ESCI value of 0.1575 among three different LULC scenarios. Additionally, Scenario II creates the lowest yield of sediment, nitrogen, phosphorus exports between 2020 and 2029 among scenarios, with average values of 37,677.19 tons, 196,135.56 kilograms, 43,316.82 kilograms, respectively.

Therefore, LULC allocation of Scenario II (Maximization ecosystem service value) is selected as the suitable LULC allocation scenario to minimize sediment and nutrient exports into Kwan Phayao Lake, Upper Ing watershed. These findings can serve as crucial information to allocate LULC Upper Ing watershed by land use planners, land managers, and decision-makers for minimizing sediment and nutrient loads into Kwan Phayao Lake in the future.

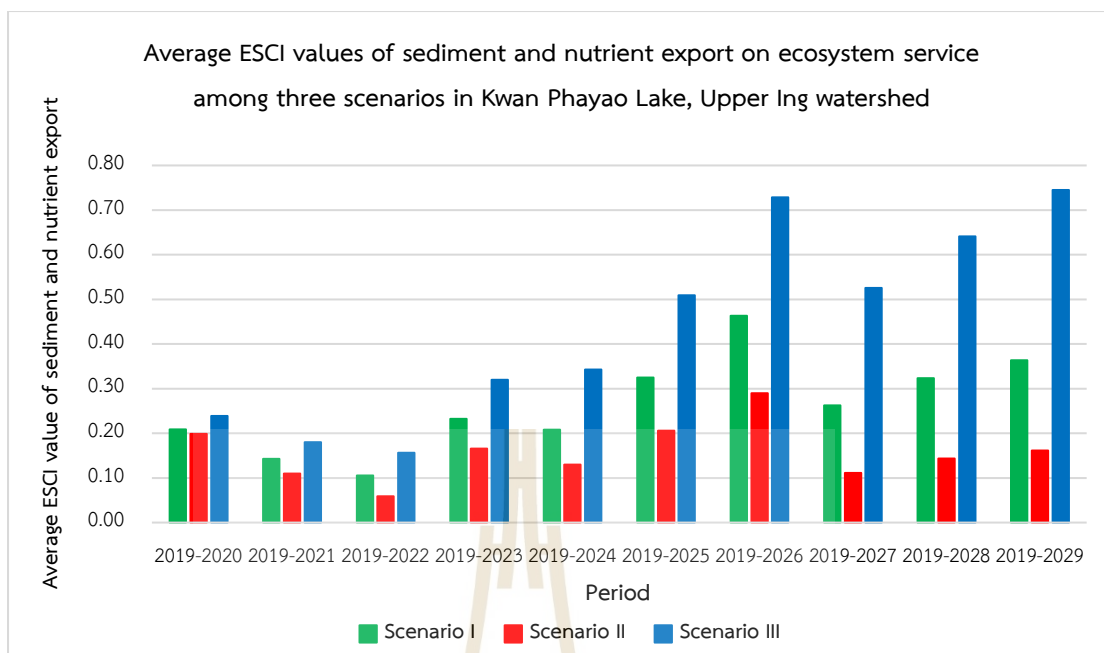


Figure 8.13 Comparison of average ESCI value of sediment and nutrient export on ecosystem service among three scenarios.

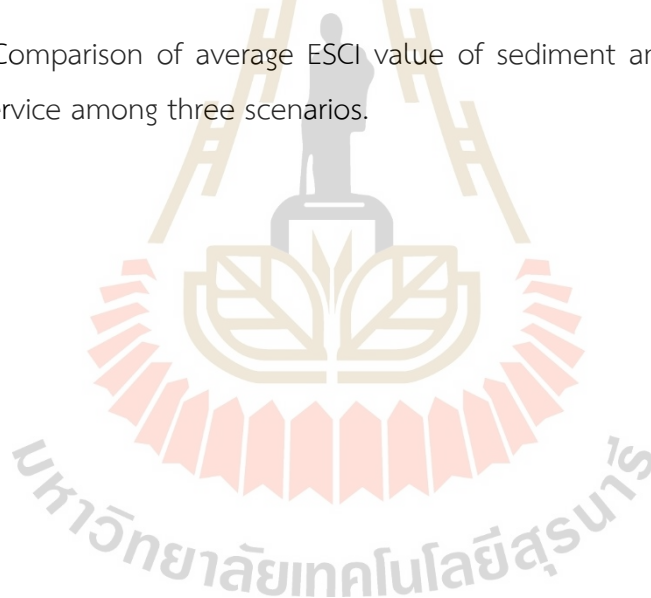


Table 8.16 Average ESCI values of sediment and nutrient export on ecosystem service among three different scenarios.

Period	Scenario I				Scenario II				Scenario III			
	Sediment export (tons)	Nitrogen export (kg.)	Phosphorus export (kg.)	Average	Sediment export (tons)	Nitrogen export (kg.)	Phosphorus export (kg.)	Average	Sediment export (tons)	Nitrogen export (kg.)	Phosphorus export (kg.)	Average
2019-2020	0.5686	0.0241	0.0329	0.2085	0.5510	0.0189	0.0271	0.1990	0.6324	0.0366	0.0471	0.2387
2019-2021	0.3506	0.0324	0.0442	0.1424	0.2925	0.0133	0.0241	0.1100	0.4129	0.0565	0.0701	0.1798
2019-2022	0.2253	0.0391	0.0528	0.1057	0.1427	0.0110	0.0234	0.0590	0.3065	0.0729	0.0890	0.1562
2019-2023	0.5879	0.0464	0.0629	0.2324	0.4565	0.0127	0.0276	0.1656	0.7581	0.0911	0.1096	0.3196
2019-2024	0.5014	0.0522	0.0708	0.2081	0.3496	0.0121	0.0281	0.1299	0.7958	0.1059	0.1260	0.3426
2019-2025	0.8292	0.0614	0.0837	0.3248	0.5717	0.0139	0.0323	0.2060	1.2530	0.1251	0.1484	0.5088
2019-2026	1.2254	0.0695	0.0950	0.4633	0.8211	0.0135	0.0342	0.2896	1.8790	0.1410	0.1659	0.7287
2019-2027	0.6104	0.0749	0.1023	0.2625	0.2812	0.0154	0.0372	0.1113	1.2365	0.1568	0.1828	0.5254
2019-2028	0.7738	0.0829	0.1134	0.3234	0.3707	0.0175	0.0414	0.1432	1.5501	0.1728	0.2004	0.6411
2019-2029	0.8757	0.0910	0.1249	0.3639	0.4231	0.0181	0.0433	0.1615	1.8288	0.1886	0.2185	0.7453
Average				0.2635				0.1575				0.4386

CHAPTER IX

CONCLUSION AND RECOMMENDATIONS

This chapter first presents the conclusion of five main results, which were reported in detail according to research objectives of this study, including (1) land use and land cover evaluation and its change, (2) land requirement estimation of three different scenarios, (3) land use and land cover prediction of three different scenarios, (4) ecosystem service assessment: sediment and nutrient export, and (5) suitable land use and land cover allocation scenario to minimize sediment and nutrient export. Then, some recommendations are suggested for future research and development.

9.1 Conclusion

9.1.1 Land use and land cover evaluation and its change

The major LULC types in 2009 as the historical record and recent LULC data in 2019, which were successfully classified by support vector machines algorithm from Landsat 5 TM and Landsat 8 OLI data, consisted of (1) urban and built-up area, (2) paddy field, (3) field crop, (4) para rubber, (5) perennial trees and orchards, (6) forest land, (7) water body, (8) rangeland, (9) wetland and, (10) miscellaneous land. The dominant increasing areas of LULC types between 2009 and 2019 were perennial trees and orchards, para rubber, and rangeland with an annual change rate of 1.95, 1.64 and 1.05 km², respectively. On the contrary, the major decreasing areas of LULC classes in the same period were forest land and paddy fields with an annual change rate of 3.98 and 2.04 km², respectively. The primary cause of change areas is probably related to deforestation to occupy the land for agriculture. In addition, the overall accuracy and Kappa hat coefficient for accuracy assessment of the thematic LULC map in 2009 and 2019 were 90.86% and 87.00% and 89.59% and 85.85%, respectively.

9.1.2 Land requirement estimation of three different scenarios

Land requirement estimation for Scenario I (Trend of LULC evolution) was calculated based on the annual rate of LULC change from the transition area matrix between 2019 and 2029 using the Markov Chain model. The significant increase of land requirements from LULC types were perennial trees and orchards, para rubber, water body, rangeland, urban and built-up area, field crop, and miscellaneous land. In contrast, the decrease of land requirements from LULC types was forest land, paddy field, and wetland.

Land requirement estimation for Scenario II (Maximization of ecosystem service values) was calculated based on allocated LULC type area to maximize ecosystem service value with a simple benefit transfer method using linear programming. The land requirement characteristics of each LULC type were set based on five categories: historical rate of LULC change (urban and built-up area), unchanged area (water body), decreased area (rangeland and miscellaneous land), increased area (wetland land), and allocated area (paddy fields, field crops, para rubber, perennial trees and orchards, and forest land).

Land requirement estimation for Scenario III (Economic crop zonation) was estimated based on areas of suitability classes for economic crops by the LDD and Markov Chain model. The suitability zonation of four economic crops (paddy field, field crop, para rubber, and perennial tree and orchard) was updated with existing LULC data in 2019 for estimating land requirements. The land requirement characteristics of each LULC type were set based on three categories: historical rate of LULC change (urban and built-up area, forest land, water body, rangeland, wetland, and miscellaneous land), decreased area (para rubber and perennial trees and orchards), increased area (paddy fields and field crops).

9.1.3 Land use and land cover prediction of three different scenarios

The LULC data between 2020 and 2029 were predicted based on LULC type location preference (driving factors), an optimum local parameter (conversion matrix and elasticity), and land requirement of each scenario using the CLUE-S model.

In this study, the conversion matrix was assigned according to the characteristics of each scenario, and elasticity values were assigned according to the transition probability matrix of LULC change between 2019 and 2029 by the Markov Chain model. Also, nine significant driving factors on LULC change included soil drainage, slope, annual rainfall, distance to the road, elevation, population density at the sub-district level, distance to the stream, distance to water body, and distance to village were applied for specific LULC type allocation using the binomial logit regression model. The most significant driving factor for all LULC type allocation in the study area is soil drainage. The derived AUC values vary from 0.79656 (fair fit) to 0.99081 (excellent fit) for each LULC type allocation.

Under Scenario I, the LULC prediction between 2020 and 2029 was dictated by the historical LULC change between 2009 and 2019, representing socio-economic development in the study area. Meanwhile, under Scenario II, the significant LULC types with the increasing area were urban and built-up area, para rubber, perennial trees/orchards, water body, and wetlands but the several LULC types with the decreased area were paddy fields, field crops, forest land, rangeland, and miscellaneous land. The LULC change under this scenario was determined by linear programming to maximize ecosystem services values, remarkably increasing wetland and decreasing rangeland and miscellaneous land. In the meantime, the LULC change under scenario III was dictated by suitability classes for economic crops zonation by Agri-Map, particularly paddy field, field crop, para rubber, and perennial tree and orchard. The significant LULC types with the increasing area were urban and built-up area, paddy field, field crop, water body, rangeland, and miscellaneous land. Conversely, the decreased areas were perennial trees and orchards, forest land, wetland, while the para rubber is stable. Additionally, the deviation values between the required and predicted area of each LULC type from the three scenarios vary from -0.23 km^2 (underestimation) to 0.33 km^2 (overestimation).

Consequently, it can be concluded that the CLUE-S model was an efficient tool for LULC prediction since it could provide good results according to different land requirements in each specific scenario.

9.1.4 Ecosystem service assessment: sediment and nutrient export

This study successfully implemented sediment and nutrient export estimation of actual LULC in 2019 and the predictive LULC of three different scenarios at Upper Ing watershed using the sediment delivery ratio (SDR) model and nutrient delivery ratio (NDR) model under the InVEST software.

(1) Sediment export estimation

In general, the SDR model reports soil erosion, sediment retention, sediment deposition, and sediment export. In this study, only sediment export was selected for ecosystem services in the study area. Sediment export of actual LULC in 2019 and the predictive LULC of three different scenarios were estimated from the amount of annual soil loss and the proportion of soil loss reaching the stream.

The calibration and validation results of sediment export estimation with observed data, calculated from annual TSS and annual surface runoff data, provided a high correlation between the observed and estimated sediment export with R^2 of 0.697 and 0.824, respectively. The *PBIAS* values for calibration provided a good fit for sediment export estimation with a value of -27.03%, whereas the *PBIAS* value for validation result was 65.60%, which provides an unsatisfactory fit.

Sediment export in 2019 was about 29.64 tons/km². The LULC types which delivered high average sediment export were miscellaneous land and field crops, while forest land transported the lowest average sediment export. The highest total sediment export from 2020 to 2029 under Scenario I was 65.97 tons/km², occurring in 2026, while the lowest total sediment export in this period was 36.32 tons/km² occurring in 2022. Likewise, under Scenario II, the highest total sediment export was 53.98 tons/km², occurring in 2026, while the lowest total sediment export was 33.87 tons/km², occurring in 2022. Similarly, under Scenario III, the highest total sediment export was 85.34 tons/km², occurring in 2026, while the lowest total sediment export was 38.73 tons/km², occurring in 2022. These results indicate the primary influence of LULC types and the RUSLE model, particularly rainfall erosivity (*R*), that affects soil loss as the sediment eroded was exported to the stream. Under three different scenarios, the LULC types that delivered the high average sediment

export were miscellaneous land and field crops, while forest land transported the lowest average sediment export.

Comparison of sediment export estimation among three scenarios showed that the predictive LULC between 2020 and 2029 of Scenario II delivered the lowest annual sediment export, with an average value of 42.27 tons/km². This scenario was increased wetland and decreased areas of rangeland and miscellaneous land, which were caused by linear programming to maximize the ecosystem service values. In contrast, the predictive LULC of Scenario III delivered the highest annual sediment export than other scenarios since the paddy field and field crop areas increased according to their suitability classes by the LDD. This comparison indicated that minor change areas of miscellaneous land affect soil loss and sediment export. The increased agriculture areas and decreased forest land cause higher soil loss and sediment export.

(2) Nutrient export estimation

In the NDR model, nitrogen and phosphorus exports as selected ecosystem services in this study. Nutrient export of actual LULC in 2019 and the predictive LULC of three scenarios were estimated from nutrient sources from watersheds and their transport to the stream.

The calibration and validation results of nutrient export estimation with observed data, calculated from annual TN, annual TP, and annual surface runoff data. In the case of nitrogen export, calibration and validation results provided a high correlation between the observed and estimated nitrogen export with R^2 of 0.575 and 0.895, respectively. The *PBIAS* values for calibration and validation provided a very good fit and a good fit for nitrogen export estimation with a value of -20.42% and 33.39%, respectively. Meanwhile, calibration and validation results of phosphorus export provided a high correlation between the observed and estimated phosphorus export with R^2 of 0.828 and 0.643, respectively. The *PBIAS* values for calibration and validation provided a very good fit and a good fit for phosphorus export estimation with a value of 12.57% and 30.21%, respectively.

The total nitrogen and phosphorus export in 2019 was 216.87 kg/km² and 47.10 kg/km², respectively. The LULC types which delivered the highest average nitrogen export were field crops, and the highest average phosphorus export were

perennial trees and orchards. In contrast, water bodies transported the lowest average nitrogen export while miscellaneous land generated the lowest phosphorus export. The highest total nutrient export from 2020 to 2029 under Scenario I was 236.62 kg/km² for nitrogen and 52.98 kg/km² for phosphorus, occurring in 2029, while the lowest total nutrient export was 222.10 kg/km² for nitrogen and 48.64 kg/km², occurring in 2020. Likewise, under Scenario II, the highest total nitrogen export was 220.97 kg/km² occurring in 2020, while the highest total phosphorus export was 49.14 kg/km² occurring in 2029. Conversely, the lowest total nutrient export was 219.25 kg/km² for nitrogen and 48.20 kg/km² for phosphorus, occurring in 2022. Similarly, under Scenario III, the highest total nutrient export was 257.76 kg/km² for nitrogen and 57.38 kg/km² for phosphorus, occurring in 2029, while the lowest total nutrient export was 224.81 kg/km² for nitrogen and 49.31 kg/km², occurring in 2020. These results indicate that the change of LULC types and areas affects parameters in the biophysical table, which leads to different nitrogen and phosphorus export. As the results of three scenarios, the LULC types which delivered the high average nutrient export were paddy field, field crops, para rubber, and perennial trees and orchard. On the contrary, water bodies generated the lowest average nitrogen export while miscellaneous land caused the lowest average phosphorus export.

Comparison of nutrient export estimation among three scenarios showed that the predictive LULC between 2020 and 2029 of Scenario II delivered the lowest annual nitrogen and phosphorus export, with an average value of 220.04 kg/km² and 48.60 kg/km² since this scenario was allocated area by linear programming to maximize the ecosystem service values, mainly, increasing area of wetland that provided the highest maximum retention efficiency and gave a small load in nitrogen and phosphorus. In contrast, the predictive LULC of Scenario III delivered the highest annual nutrient export than other scenarios since the paddy field and field crop areas increased according to their suitability classes by the LDD. These areas provide the highest nitrogen and phosphorus load but low maximum retention efficiency. This comparison indicated that increased agriculture areas and loss of vegetation such as forest land and wetland cause higher nutrient export.

9.1.5 Suitable land use and land cover allocation scenario to minimize sediment and nutrient export

Ecosystem service change on sediment export of three different scenarios during 2020 and 2029 disclosed that all three scenarios increased sediment export which affected ecosystem service in terms of low sediment retention capability for water purification compared with sediment export of base year data in 2019. Consequently, predictive rainfall erosivity and LULC change play a significant role in sediment export prediction under different scenarios.

At the same time, ecosystem service change on nutrient export of three different scenarios in the same period revealed that all three scenarios increased nutrient export which affected ecosystem service in water quality by higher contaminating of nitrogen and phosphorus from the change of LULC compared with nutrient export of base year data in 2019. Therefore, under different scenarios, the effect of nutrient loading associated with LULC change plays a critical role in nutrient export prediction.

According to average cumulative ESCI values of sediment and nutrient export ecosystem service from three different scenarios, LULC allocation of Scenario II (Maximization ecosystem service values) provided the lowest average ESCI value of 0.1575 among three different scenarios. Therefore, LULC allocation of Scenario II (Maximization ecosystem service value) is chosen as the suitable LULC allocation scenario to minimize sediment and nutrient exports into Kwan Phayao Lake, Upper Ing watershed.

In conclusion, integration of remote sensing with advanced classification method (support vector machine classifier), GIS data with linear programming and geospatial models (CLUE-S model, sediment and nutrient delivery ratio models of InVEST software suite) can be used as an efficient tool to identify a suitable LULC allocation scenario to minimize sediment and nutrient export. Additionally, the derived results can serve as crucial inputs to allocate LULC Upper Ing watershed by land use planners, land managers, and decision-makers for reducing sediment and nutrient loads into Kwan Phayao Lake in the future.

9.2 Recommendations

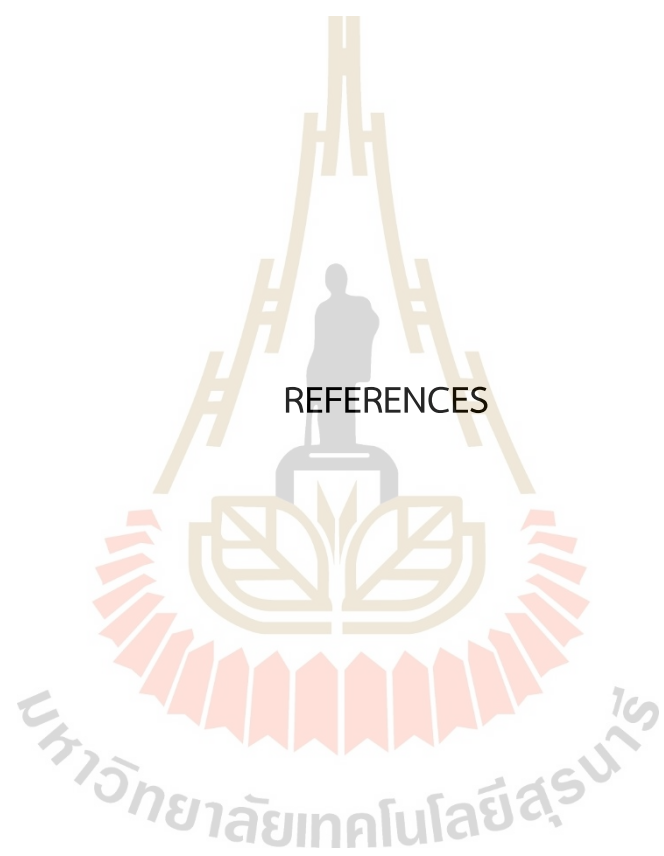
Many objectives were investigated in this study, including LULC evaluation and its change, land requirement estimation of three different scenarios, LULC prediction of three different scenarios, sediment and nutrient export estimation, and suitable LULC allocation to minimize sediment and nutrient export in the Upper Ing watershed, Phayao province. Therefore, the possible expected recommendations and implications could be made for further studies as follows.

(1) For future study, a very high spatial resolution of remotely sensed data (Sentinel-2A) should be considered to apply for LULC classification because the classified LULC data play a vital role in LULC evaluation and its change, land requirement estimation, prediction in the CLUE-S model, and sediment and nutrient export estimate.

(2) According to the land requirement estimation of scenario-II (Maximization ecosystem service values), future areas as a constraint in the linear programming model should consult with local government agencies and communities for ecological balancing.

(3) Based on the sediment delivery ratio (SDR) model, the cover management (C) and support practice (P) factors should be collected from the local area or adjusted C and P factors in the calibration process. These parameters are related to the RUSLE, which affects soil loss and sediment export.

(4) Based on the nutrient delivery ratio (NDR) model, the loads and maximum retention efficiency of nitrogen and phosphorus should be collected from the local area because the model shows a high sensitivity to these inputs, affecting nutrient export. Also, subsurface NDR representing nutrients transported by groundwater should be regarded in future studies.



REFERENCES

REFERENCES

- Al-doski, J., Mansor, S. B., & Shafri, H. Z. M. (2013, 7-9 April 2013). *Support vector machine classification to detect land cover changes in Halabja City, Iraq*. Paper presented at the 2013 IEEE Business Engineering and Industrial Applications Colloquium (BEIAC).
- Alcamo, J., & Bennett, E. M. (2003). *Ecosystems and Human Well-being: A Framework for Assessment*. Washington, DC: Island Press.
- Anderson, J. R., Hardy, E. E., Roach, J. T., & Witmer, R. E. (1976). *A land use and land cover classification system for use with remote sensor data*. Retrieved from <http://pubs.er.usgs.gov/publication/pp964>
- Arunyawat, S., & Shrestha, R. P. (2016). Assessing Land Use Change and Its Impact on Ecosystem Services in Northern Thailand. *Sustainability.*, 8(8), 1-22.
- Ballatore, T. J., & Muhandiki, V. S. (2002). The case for a World Lake Vision. *Hydrological Processes.*, 16(11), 2079-2089.
- Benez-Secanho, F. J., & Dwivedi, P. (2019). Does Quantification of Ecosystem Services Depend Upon Scale (Resolution and Extent)? A Case Study Using the InVEST Nutrient Delivery Ratio Model in Georgia, United States. *environments*, 6(5), 52.
- Bogdan, S.-M., Pătru-Stupariu, I., & Zaharia, L. (2016). The assessment of regulatory ecosystem services: the case of the sediment retention service in a mountain landscape in the Southern Romanian Carpathians. *Procedia Environmental Sciences*, 32(2016), 12-27.
- Borselli, L., Cassi, P., & Torri, D. (2008). Prolegomena to sediment and flow connectivity in the landscape: A GIS and field numerical assessment. *Catena*, 75(3), 268-277.
- Bouaziz, M., Eisold, S., & Guermazi, E. (2017). Semiautomatic approach for land cover classification: a remote sensing study for arid climate in southeastern Tunisia. *Euro-Mediterranean Journal for Environmental Integration*, 2(1), 24.

- Bouguerra, S., Jebari, S., & Tarhouni, J. (2019). An analysis of sediment production and control in Rmel river basin using InVEST Sediment Retention model. *Journal of new sciences, Agriculture and Biotechnology*, 66(4), 4170-4181.
- Chang, H. (2004). Water Quality Impacts of Climate and Land Use Changes in Southeastern Pennsylvania. *The Professional Geographer*, 56(2), 240-257.
- Chen, H., Zhang, W., Gao, H., & Nie, N. (2018). Climate Change and Anthropogenic Impacts on Wetland and Agriculture in the Songnen and Sanjiang Plain, Northeast China. *Remote Sensing*, 10, 356.
- Chuvieco, E. (1993). Integration of Linear Programming and GIS for Land-use Modelling. *International Journal of Geographical Information Systems*, 7(1), 71-83.
- Cohen, J. (1988). *Statistical power analysis for the behavioral sciences*. Hillsdale, N.J.: L. Erlbaum Associates.
- Congalton, R., & Green, K. (2009). *Assessing the Accuracy of Remotely Sensed Data: Principles and Practices, Third Edition*.
- Coppin, P., Jonckheere, I., Nackaerts, K., Muys, B., & Lambin, E. (2004). Digital Change Detection Methods in Ecosystem Monitoring: A Review. *International Journal of Remote Sensing - INT J REMOTE SENS*, 25, 1565-1596.
- Cortes, C., & Vapnik, V. (1995). Support-Vector Networks. *Mach. Learn.*, 20, 273-297.
- Costanza, R., d'Arge, R., de Groot, R., Farber, S., Grasso, M., Hannon, B., Limburg, K., Naeem, S., O'Neill, R. V., Paruelo, J., Raskin, R. G., Sutton, P., & van den Belt, M. (1997). The value of the world's ecosystem services and natural capital. *Nature*, 387(6630), 253-260.
- Cristianini, N., & Shawe-Taylor, J. (2000). *An introduction to support Vector Machines: and other kernel-based learning methods*. Cambridge: Cambridge University Press.
- Department of Public Works and Town & Country Planning. (2010). *Eradication of Water Hyacinth and Aquatic Weeds's Report*. Retrieved from [http://www.dpt.go.th/gtop/download/Eradication of water hyacinth.pdf](http://www.dpt.go.th/gtop/download/Eradication%20of%20water%20hyacinth.pdf)
- Desmet, P. J. J., & Govers, G. (1996). A GIs procedure for automatically calculating the USLE LS factor on topographically complex landscape units. *Journal of Soil and Water Conservation*, 51(5), 427-433.

- Editorial. (2004). Modelling land use change and environmental impact. *Journal of Environmental Management*, 72(2004), 1-3.
- Forest Land Management Bureau. (2019). Forest statistics data 2019. Retrieved from <http://forestinfo.forest.go.th/55/Content.aspx?id=1>
- Fu, B., Zhang, L., Xu, Z., Zhao, Y., Wei, Y., & Skinner, D. (2015). Ecosystem services in changing land use. *Journal of Soils and Sediments*, 15(4), 833-843.
- Griffin, R., Vogl, A., Wolny, S., Covino, S., Monroy, E., Ricci, H., Sharp, R., Schmidt, C., & Uchida, E. (2020). Including Additional Pollutants into an Integrated Assessment Model for Estimating Nonmarket Benefits from Water Quality. *Land Economics*, 96(4), 457-477.
- Guang Liu, Qingwen Jin, Jingyi Li, Lei Li, Chengxin He, Yuqing Huang, & Yuefeng Yao. (2017). Policy factors impact analysis based on remote sensing data and the CLUE-S model in the Lijiang River Basin, China. *Catena*, 158(2017), 286-297.
- Guesri, M., Megnounif, A., & Ghenim, A. N. (2020). Rainfall erosivity and sediment yield in Northeast Algeria: K'sob watershed case study. *Arabian Journal of Geosciences*, 13(7), 299.
- Gurung, K., Yang, J., & Fang, L. (2018). Assessing Ecosystem Services from the Forestry-Based Reclamation of Surface Mined Areas in the North Fork of the Kentucky River Watershed. *Forests*, 9(10), 1-23.
- Han, B., Reidy, A., & Li, A. (2021). Modeling nutrient release with compiled data in a typical Midwest watershed. *Ecological Indicators*, 121, 107213.
- Han, H., Yang, C., & Song, J. (2015). Scenario Simulation and the Prediction of Land Use and Land Cover Change in Beijing, China. *Sustainability*, 2015(7), 4260-4279.
- Heathcote, A. J., Filstrup, C. T., & Downing, J. A. (2013). Watershed Sediment Losses to Lakes Accelerating Despite Agricultural Soil Conservation Efforts. *PLoS ONE*, 8(1), 1-4.
- Homklin, S., Jakrawatana, N., Thanawong, K., Khitka, B., Kannika, K., Ngammuangtueng, P., Saikown, T., & Thoaran, J. (2019). *The participatory water quality management project of Kwan Phayao Phase 2*. Retrieved from University of Phayao and The Thailand Research Fund (ABC60A03).

- Hoyer, R., & Chang, H. (2014). Assessment of freshwater ecosystem services in the Tualatin and Yamhill basins under climate change and urbanization. *Applied Geography*, 53, 402-416.
- Hua, A. K. (2017). Land Use Land Cover Changes in Detection of Water Quality: A Study Based on Remote Sensing and Multivariate Statistics. *Journal of Environmental and Public Health*, 2017, 1-12.
- Huang, J., Zhan, J., Yan, H., Wu, F., & Deng, X. (2013). Evaluation of the Impacts of Land Use on Water Quality: A Case Study in The Chaohu Lake Basin. *The Scientific World Journal*, 2013, 1-7.
- Iamchuen, N., & Thepwong, W. (2020). Relationship between Physical Factors and Land Use for the Future Land Use Prediction. *JARS*, 17(2), 79-92.
- ILEC. (2005). *Managing Lakes and their Basin for Sustainable Use: A Report for Lake Basin Managers and Stakeholders*. International Lake Environment Committee Foundation: Kusatsu, Japan.
- Inland Fisheries Research and Development Regional Center 1 (Phayao) Department of fisheries. (2020). *Kwan Phayao*. Retrieved from Department of fisheries: https://www4.fisheries.go.th/local/pic_activities/202002171317301_pic.pdf
- Jensen, J. R. (2015). *Introductory Digital Image Processing: A Remote Sensing Perspective*: Prentice Hall Press.
- JIA, K., LIU, J., TU, Y., LI, Q., SUN, Z., WEI, X., YAO, Y., & ZHANG, X. (2019). Land use and land cover classification using Chinese GF-2 multispectral data in a region of the North China Plain. *Frontiers of Earth Science*, 13(2), 327-335.
- Kaewsri, K., & Traichaiyaporn, S. (2012). Monitoring on water quality and algae diversity of Kwan Phayao, Phayao Province, Thailand. *Journal of Agricultural Technology*, 8(2), 537-550.
- Kamwi, J. M., Cho, M. A., Kaetsch, C., Manda, S. O., Graz, F. P., & Chirwa, P. W. (2018). Assessing the Spatial Drivers of Land Use and Land Cover Change in the Protected and Communal Areas of the Zambezi Region, Namibia. *Land*, 7(4), 131.

- Kavzoglu, T., & Colkesen, I. (2009). A kernel functions analysis for support vector machines for land cover classification. *International Journal of Applied Earth Observation and Geoinformation*, 11(2009), 352-359.
- Kreoungsanu, C., & Suksard, S. (2014). Opinions of Para Rubber Tree Growers on their Enterprise in Phayao Province. *Thai J. For.*, 33(2), 123-130.
- Land Development Department. (2000). *Soil erosion in Thailand (In Thailand)*. Ministry of Agriculture and Cooperatives. Bangkok: Thailand.
- Land Development Department. (2017,2018). *Agri-Map*. Office of Land Use Policy and Plan, Ministry of Agriculture and Cooperatives: Bangkok, Thailand.
- Leh, M. D. K., Matlock, M. D., Cummings, E. C., & Nalley, L. L. (2013). Quantifying and mapping multiple ecosystem services change in West Africa. *Agriculture, Ecosystems & Environment*, 165, 6-18.
- Liu, S., Huang, S., Xie, Y., Leng, G., Huang, Q., Wang, L., & Xue, Q. (2018). Spatial-temporal changes of rainfall erosivity in the loess plateau, China: Changing patterns, causes and implications. *Catena*, 166, 279-289.
- Mamat, A., Halik, Ü., & Rouzi, A. (2018). Variations of Ecosystem Service Value in Response to Land-Use Change in the Kashgar Region, Northwest China. *Sustainability*, 10(1), 200-218.
- Mandal, S., & Saha, A. (2018). Support vector machines for monitoring land use dynamicity and temporal variation of land surface temperature in Kurseong and surrounding of Darjeeling Himalaya. *Modeling Earth Systems and Environment*, 4(2), 659-672.
- Mantero, P., Moser, G., & Serpico, S. B. (2005). Partially Supervised Classification of Remote Sensing Images Through SVM-Based Probability Density Estimation. *IEEE Transactions on Geoscience and Remote Sensing*, 43(3), 559-570.
- Mayer, P. M., Jr., S. K. R., McCutchen, M. D., & Canfield, T. J. (2007). Meta-Analysis of Nitrogen Removal in Riparian Buffers. *J. Environ. Qual.*, 36(4), 1172-1180.
- McDill, M. E. (1999). *Forest Resource Management*.
- Me, W., Abell, J. M., & Hamilton, D. P. (2015). Effects of hydrologic conditions on SWAT model performance and parameter sensitivity for a small, mixed land use catchment in New Zealand. *Hydrol. Earth Syst. Sci.*, 19(10), 4127-4147.

- Mei, Y., Kong, X., Ke, X., & Yang, B. (2017). The Impact of Cropland Balance Policy on Ecosystem Service of Water Purification—A Case Study of Wuhan, China. *Water*, 9(8), 620.
- Mekong River Commission. (2017). *Basin-wide Assessments of Climate Change Impacts on Water and Water-related Resources and Sector in Lower Mekong Basin, Technical Report: Ecosystem Component, Sub-component II: Basin-wide Impacts of Climate Change on Ecosystem Services in the Lower Mekong Basin* (Version: 1st Draft). Retrieved from Mekong River Commission Planning Division, Mekong River Commission For Sustainable Development:
- Moriasi, D., Arnold, J., Liew, M., Bingner, R., Harmel, R. D., & Veith, T. (2007). Model Evaluation Guidelines for Systematic Quantification of Accuracy in Watershed Simulations. *Transactions of the ASABE*, 50(3), 885-900.
- Mountrakis, G., Im, J., & Ogole, C. (2011). Support vector machines in remote sensing: A review. *ISPRS Journal of Photogrammetry and Remote Sensing*, 66(2011), 247-259.
- Mushtaq, F., & Pandey, A. C. (2013). Assessment of land use/land cover dynamics vis-à-vis hydrometeorological variability in Wular Lake environs Kashmir Valley, India using multitemporal satellite data. *Arab J Geosci*, 2014(7), 4707-4715.
- Nalepa, J., & Kawulok, M. (2019). Selecting training sets for support vector machines: a review. *Artificial Intelligence Review*, 52(2), 857-900.
- NCAR GIS Program. (2012). Climate System Model, June 2004 version 3.0. Retrieved from <http://www.gisclimatechange.org>
- Nikkami, D., Shabani, M., & Ahmadi, H. (2009). Land Use Scenarios and Optimization in a Watershed. *Journal of Applied Sciences*, 9(2), 287-295.
- Ongsomwang, S., & lamchuen, N. (2015). Integration of geospatial models for optimum land use allocation in three different scenarios. *Suranaree J. Sci. Technol.*, 22(4), 377-396.
- Patle, A., & Chouhan, D. S. (2013). *SVM Kernel Functions for Classification*. Paper presented at the 2013 International Conference on Advances in Technology and Engineering (ICATE), Mumbai, India.

- Pedregal, P. (2004). *Introduction to Optimization*. 175 Fifth Avenue, New York, NY 10010, USA: Springer-Verlag New York, Inc.
- Pedro, C., Clément, F., Harold, L., Mélodie, C., & Damien, B. (2016). Assessing the impact of land-cover changes on ecosystem services: A first step toward integrative planning in Bordeaux, France. *Ecosystem Services*, 22, 318-327.
- Peerapornpisal, Y., Suphan, S., Ngearnpat, N., & Pekkoh, J. (2008). Distribution of chlorophytic phytoplankton in Northern Thailand. *Biologia*, 63(6), 852-858.
- Pokhrel, B. K., & Paudel, K. P. (2019). Assessing the Efficiency of Alternative Best Management Practices to Reduce Nonpoint Source Pollution in a Rural Watershed Located in Louisiana, USA. *Water*, 11(8), 1-14.
- Prasad, S. V. S., Savithri, T. S., & Krishna, I. V. M. (2017). Comparison of Accuracy Measures for RS Image Classification using SVM and ANN Classifiers *International Journal of Electrical and Computer Engineering (IJECE)*, 7(3), 1180-1187.
- Raji, S. A., Odunuga, S., & Fasona, M. (2020). Spatiotemporal Modeling of Nutrient Retention in a Tropical Semi-Arid Basin. *Environmental Research and Technology*, 3(4), 225-237.
- Rattanadaeng, P., Panboon, K., & Soe-been, S. (2015). *Structure and Distribution of Fish Community in Kwan Phayao, Phayao Province* (53-0577-53033-002). Sukhothai Inland Fisheries Research and Development Center Inland Fisheries Research and Development Division. Retrieved from <http://elib.fisheries.go.th/libcab/drawers/abs/data0001/00001395.pdf>
- Redhead, J. W., May, L., Oliver, T. H., Hamel, P., Sharp, R., & Bullock, J. M. (2018). National scale evaluation of the InVEST nutrient retention model in the United Kingdom. *Science of the Total Environment*, 610-611, 666-677.
- Renard, K. G., & Freimund, J. R. (1994). Using monthly precipitation data to estimate the R-factor in the revised USLE. *Journal of Hydrology*, 157(1-4), 287-306.
- Riahi, K., Grubler, A., & Nakicenovic, N. (2007). Scenarios of long-term socio-economic and environmental development under climate stabilization. *Technological Forecasting and Social Change*, 74, 887-935.

- Rosenfield, G. H., & Fitzpatrick-Lins, K. (1986). A coefficient of agreement as a measure of thematic classification accuracy. *Photogrammetric Engineering and Remote Sensing*, 52(2), 223-227.
- Royal irrigation department. (2017). *Natural development planing*. Retrieved from http://water.rid.go.th/hwm/wmoc/planing/natural_development_planing2560-05-03.pdf
- Rubber Division Department of Agriculture. (2020). Thailand Rubber Statistics. Retrieved from <https://www.doa.go.th/rc/suratthani/wp-content/uploads/2019/05/statistics-2563-1.pdf>
- Salata, S., Garnero, G., Barbieri, C. A., & Giaino, C. (2017). The Integration of Ecosystem Services in Planning: An Evaluation of the Nutrient Retention Model Using InVEST Software. *Land*, 6(3), 48.
- Scott, D. A. (1989). *A directory of Asian wetlands*. Slimbridge Gloucester GL2 7BX U.K.: IUCN Publication.
- Sharp, R., Douglass, J., Wolny, S., Arkema, K., Bernhardt, J., Bierbower, W., Chaumont, N., Denu, D., Fisher, D., Glowinski, K., Griffin, R., Guannel, G., Guerry, A., Johnson, J., Hamel, P., Kennedy, C., Kim, C.K., Lacayo, M., Lonsdorf, E., Mandle, L., Rogers, L., Silver, J., Toft, J., Verutes, G., Vogl, A. L., Wood, S., & Wyatt, K. (2020). *InVEST 3.8.9.post0+ug.gc993a4f.d20201118 User's Guide*. The Natural Capital Project: Stanford University, University of Minnesota, The Nature Conservancy, and World Wildlife Fund.
- Shicheng, L., Zhaofeng, W., & Yili, Z. (2017). Crop cover reconstruction and its effects on sediment retention in the Tibetan Plateau for 1900–2000. *Journal of Geographical Sciences*, 27(7), 786-800.
- Shoyamaa, K., Kamiyamaa, C., Morimotob, J., Oobac, M., & Okurod, T. (2017). A review of modeling approaches for ecosystem services assessment in the Asian region. *Ecosystem Services*, 26(2017), 316-328.
- Singh, N. K., Gourevitch, J. D., Wemple, B. C., Watson, K. B., Rizzo, D. M., Polasky, S., & Ricketts, T. H. (2019). Optimizing wetland restoration to improve water quality at a regional scale. *Environmental Research Letters*, 14(6), 064006.

- Sokouti, R., & Nikkami, D. (2017). Optimizing land use pattern to reduce soil erosion. *Eurasian J Soil Sci*, 6(1), 75-83.
- Srichaichana, J., Trisurat, Y., & Ongsomwang, S. (2019). Land Use and Land Cover Scenarios for Optimum Water Yield and Sediment Retention Ecosystem Services in Klong U-Tapao Watershed, Songkhla, Thailand. *Sustainability*, 11(10), 1-22.
- Statistical Office Phoyao Province. (2017). *The 2017 Industrial Census Basic Information Phoyao Province*. Retrieved from National Statistical Office, Ministry of Digital Economy and Society:
- Sun, X., Zhang, Y., Shen, Y., Randhir, T. O., & Cao, M. (2019). Exploring ecosystem services and scenario simulation in the headwaters of Qiantang River watershed of China. *Environmental Science and Pollution Research*, 2019, 1-19.
- Taati, A., Sarmadian, F., Mousavi, A., Pour, C. T. H., & Shahir, A. H. E. (2015). Land Use Classification using Support Vector Machine and Maximum Likelihood Algorithms by Landsat 5 TM Images. *Walailak Journal of Science and Technology*, 12(8), 681-687.
- Tolessa, T., Senbeta, F., & Kidane, M. (2017). The impact of land use/land cover change on ecosystem services in the central highlands of Ethiopia. *Ecosystem Services*, 23(2017), 47-54.
- Traore, A., & Watanabe, T. (2017). Modeling Determinants of Urban Growth in Conakry, Guinea: A Spatial Logistic Approach. *Urban Science*, 1(2), 12.
- Ustuner, M., Sanli, F. B., & Dixon, B. (2015). Application of Support Vector Machines for Landuse Classification Using High-Resolution RapidEye Images: A Sensitivity Analysis. *European Journal of Remote Sensing*, 48, 403-422.
- Van der Linden, S., Rabe, A., Held, M., Jakimow, B., Leitão, P. J., Okujeni, A., Schwieder, M., Suess, S., & Hostert, P. (2015). The EnMAP-Box—A Toolbox and Application Programming Interface for EnMAP Data Processing. *Remote Sensing*, 7(9), 11249-11266.
- Van der Linden, S., Rabe, A., Held, M., Wirth, F., Suess, S., Okujeni, A., & Hostert, P. (2014). *imageSVM Classification, Manual for Application: imageSVM version 3.0*. Humboldt-Universität zu Berlin, Germany.

- Vapnik, V. N. (1999). An Overview of Statistical Learning Theory. *IEEE Transactions on Neural Networks.*, 10(5), 988-999.
- Verburg, P. H., & Lesschen, J. P. (2014). Practical: Explorative modeling of future land use for the Randstad region of the Netherlands.
- Verburg, P. H., & Overmars, K. P. (2007). *Dynamic Simulation of Land-Use Change Trajectories with the Clue-S Model*. The GeoJournal Library, vol 90: Springer, Dordrecht.
- Vigiak, O., Borselli, L., Newham, L. T. H., McInnes, J., & Roberts, A. M. (2012). Comparison of conceptual landscape metrics to define hillslope-scale sediment delivery ratio. *Geomorphology*, 138 (2012), 74–88.
- Wang, L., Jia, Y., Yao, Y., & Xu, D. (2019). Accuracy Assessment of Land Use Classification Using Support Vector Machine and Neural Network for Coal Mining Area of Hegang City, China. *Nature Environment and Pollution Technology An International Quarterly Scientific Journal*, 18(1), 335-241.
- Wischmeier, W. H., & Smith, D. D. (1978). *Predicting Rainfall Erosion Losses. A Guide to Conservation Planning*. The USDA Agricultural Handbook No. 537: Maryland.
- Xu, L., Li, Z., Song, H., & Yin, H. (2013). Land-Use Planning for Urban Sprawl Based on the CLUE-S Model: A Case Study of Guangzhou, China. *Entropy*, 15, 3490-3506.
- Yan, Y., Guan, Q., Wang, M., Su, X., Wu, G., Chiang, P., & Cao, W. (2018). Assessment of nitrogen reduction by constructed wetland based on InVEST: A case study of the Jiulong River Watershed, China. *Marine Pollution Bulletin*, 133, 349-356.
- Yang, X., Ji, G., Wang, C., Zuo, J., Yang, H., Xu, J., & Chen, R. (2019). Modeling nitrogen and phosphorus export with InVEST model in Bosten Lake basin of Northwest China. *PLoS ONE.*, 14(7), 1-17.
- Yao, X., Yu, J., Jiang, H., Sun, W., & Li, Z. (2016). Roles of soil erodibility, rainfall erosivity and land use in affecting soil erosion at the basin scale. *Agricultural Water Management*, 174, 82-92.
- Ying, Z., Hongqi, Z., Dongying, N., & Wei, S. (2012). Agricultural Land Use Optimal Allocation System in Developing Area: Application to Yili Watershed, Xinjiang Region. *Chin. Geogra. Sci.*, 22(2), 232-244.

- Yuan, F. (2008). Land-cover change and environmental impact analysis in the Greater Mankato area of Minnesota using remote sensing and GIS modelling. *International Journal of Remote Sensing*, 29(4), 1169-1184.
- Zare, M., Samani, A. A. N., Mohammady, M., Salmani, H., & Bazrafshan, J. (2017). Investigating effects of land use change scenarios on soil erosion using CLUE-s and RUSLE models. *Int. J. Environ. Sci. Technol.*, 2017(14), 1905-1918.
- Zhang, L., Zhang, S., Huang, Y., Cao, M., Huang, Y., & Zhang, H. (2016). Exploring an Ecologically Sustainable Scheme for Landscape Restoration of Abandoned Mine Land: Scenario-Based Simulation Integrated Linear Programming and CLUE-S Model. *International Journal of Environmental Research and Public Health*, 13(4), 354.
- Zhang, R., Tang, C., Ma, S., Yuan, H., Gao, L., & Fan, W. (2011). Using Markov chains to analyze changes in wetland trends in arid Yinchuan Plain, China. *Mathematical and Computer Modelling*, 54(3), 924-930.
- Zhang, X., Liu, X., Zhang, M., Dahlgren, R. A., & Eitzel, M. (2010). A review of vegetated buffers and a meta-analysis of their mitigation efficacy in reducing nonpoint source pollution. *J. Environ. Qual.*, 39, 76-84.
- Zhang, X., & Song, Q. (2015). A multi-label learning based kernel automatic recommendation method for support vector machine. *PLOS ONE*, 10(3), 1-30.
- Zhou, M., Deng, J., Lin, Y., Belete, M., Wang, K., Comber, A., Huang, L., & Gan, M. (2019). Identifying the effects of land use change on sediment export: Integrating sediment source and sediment delivery in the Qiantang River Basin, China. *Science of the Total Environment*, 686, 38-49.
- Zhu, G., & Blumberg, D. G. (2002). Classification using ASTER data and SVM algorithms; The case study of Beer Sheva, Israel. *Remote Sensing of Environment*, 80(2002), 233-240.

CURRICULUM VITAE

Name Miss. Jiraporn Kulsoontornrat

Date of Birth November 20, 1986

Place of Birth Prachuap Khiri khan

Education Background:

2008: Bachelor of Science in Geography,
School of Agriculture and Natural Resources, Naresuan
University, Phayao campus, Thailand.

2012: Master of Science in Remote Sensing and Geographic
Information Systems, School of engineering and
technology, Asian Institute of technology, Thailand.

Work Experiences:

2012-Present: Lecturer,
Department of Geographic Information Science,
School of Information and Communication Technology,
University of Phayao.

มหาวิทยาลัยเทคโนโลยีสุรนารี